マイクロフィルム用

ISSD 0386-5878
Technical Memorandum of PWRI No. 3815

UJNR

TSUKUBA 1999

PROCEEDINGS OF THE 31ST JOINT MEETING OF U.S. - JAPAN PANEL ON WIND AND SEISMIC EFFECTS UJNR

May 11 - 14, 1999
Tsukuba, Japan

Public Works Research Institute
Ministry of Construction

Copyright © (1999) by P.W.R.I

All rights reserved. No part of this book may be reproduced by any means, nor transmitted, nor translated into a machine language without the written permission of the Director General of P.W.R.I.

この報告書は、土木研究所長の承認を得て刊行したものである。したがって、本報告書の全部又は一部の転載、複製は、土木研究所長の文書による承認を得ずしてこれを行ってはならない。

Technical Memorandum
of PWRI NO. 3653

PROCEEDINGS OF THE 31ST JOINT MEETING OF U.S.-JAPAN PANEL ON WIND AND SEISMIC EFFECTS, UJNR

Edited by

Michio Okahara, Secretary-General
Japan-side Panel on Wind and Seismic Effects

Synopsis:
This publication contains the Proceedings of the 31st Joint Meeting of the U.S.-Japan Panel on Wind and Seismic Effects, UJNR, which was held at the Public Works Research Institute, Tsukuba, during 11-14 May 1999. Forty-seven papers were written, 23 by U.S. members and 24 by Japanese members. Thirty-Five papers were presented orally; 17 by the U.S. -side and 18 by the Japan-side. The papers were organized into five themes: Wind Engineering; Earthquake Engineering; Storm Surge and Tsunamis; Summary of Joint Cooperative Research Programs; and Seismic Information Systems.

Key words: Wind Engineering, Earthquake Engineering, Joint Cooperative Research, U J N R

CONTENTS

PREFACE 1

AGENDA OF JOINT MEETING AND TECHNICAL SITE VISITS 5

LIST OF PANEL MEMBERS 21

LIST OF TASK COMMITTEE MEMBERS 39

RESOLUTIONS 47

PAPERS 53

THEME 1. Wind Engineering

Wind Properties for Design of Highway Bridges
Hiroshi SATO, Ken-ichi OGI (PWRI) 57

The Fujita Tornado Intensity Scale: A Reassessment from Structural Engineering Perspective
Long T. Phan, and Emil Simiu (NIST) (Presented by H.S.Lew, NIST) 71

Research Project on Propriety and Reliability of Designing Wind Load and Wind Pressure Coefficients
Hisashi OKADA, Hitomitsu KIKITSU (BRI),
Yukio TAMURA (Tokyo Institute of Polytechnics),
Yasushi UEMATSU (Tohoku University) 79

A Probabilistic Tornado Wind Hazard Model for the Continental United States
Quazi Hossain (LLNL), Richard Mensing (LLNL), Jean Savy (LLNL),
Jeffery Kimball (DOE) 86

10km Scale Wind Speed Fluctuation Observed in Typhoon Area
Yoshinobu TANAKA (MRI) 93

THEME 2. Earthquake Engineering

Recent Projects at PWRI for Improvement of Seismic Performance of Civil Infrastructures
Masahiko YASUDA (PWRI) 103

Comparison of U.S. and Japanese Highway Bridge Seismic Retrofitting Measures
W. Phillip Yen (FHWA) and Shigeki UNJOH (PWRI) 114

Model Experiments on Characteristics of Motions of Continuous Pontoon Type and Separate Support Type Elastic Floating Bodies in Waves
Haruo YONEYAMA, Satoru SHIRAISHI and Go ISHIMI (PHRI) ·····126

Development of a Probabilistic Seismic Hazard Analysis for Offshore Facilities in the Santa Barbara Channel
Charles E. Smith (MMS) and Robert Murray (LLNL) ·····140

GPS in Dynamic Monitoring of Long-period Structures
Mehmet Çelebi (USGS) ·····156

Real-time Hybrid Vibration Experiments with a 2-Dimensional and 3-Degrees-of-Freedom Model
Keiichi TAMURA, Hiroshi KOBAYASHI (PWRI) ·····167

Integrated Surface and Borehole Strong-Motion, Soil-Response Arrays in San Francisco, California
R.D. Borcherdt, H.P. Liu, R.E. Westerlund, C. Ditel, J.F. Gibbs,
and R.E. Warrick (USGS) ·····179

Three Dimensional Shaking Table Tests on Seismic Behavior of Isolators for Houses
Masanori IIBA, Mitsumasa MIDORIKAWA , Hiroyuki YAMANOUCHI (BRI)
and Bujar Myslimaj (Univ. of Tsukuba) ·····191

Application of Advanced Technologies in Seismic Protection of Critical Facilities An MCEER Program
George Lee (Univ. of New York at Buffalo)
Michel Bruneau, Masanobu Shinozuka, and Kathleen Tierney (MCEER) ·····204

A Study on the Behavior of a Seismic Isolation Device Using Full-scale Dynamic Push-over Experimental Equipment
Takashi SATOU, Hiroshi MITAMURA (CERI),
Akio HAYASHI (Pacific Consultants)
and Toshihiko BESSYO (The Japan Steel Works) ·····214

Investigations of Active Faults for Dam Construction - The Present State at The Ministry of Construction -
Yasuhiko WAKIZAKA (PWRI) ·····231

Present and Future Roles of Nonlinear Numerical Procedures in the Seismic Analysis of Concrete Dams
Robert L. Hall (WES),
Enrique E. Matheu (Virginia Polytechnic Institute and State University) ·····245

Dynamic Response and Failure Mechanism of a Pile Foundation During Soil Liquefaction under Shaking Table Test Using a Large-scale Laminar Shear Box
Shuji TAMURA, Chikahiro MINOWA (NIED),
Yasutsugu SUZUKI (Kajima Corporation),
Michio SUGIMOTO (Takenaka Corporation), Shunji FUJII (Taisei Corporation)
and Takaaki KAGAWA (Wayne State University) ····· 252

Equivalent-Linear Ground-Response Calculations with Frequency-Dependent Damping
William B. Joyner (USGS) ····· 258

Development of Smart Structure System
Shunsuke OTANI (University of Tokyo), Hisahiro HIRAISHI,
Mitsumasa MIDORIKAWA, Masaomi TESHIGAWARA (BRI) ····· 265

Development of the FEMA-273 Document-Guidelines for the Seismic Rehabilitation of Buildings
A. Gerald Brady (ATC) ····· 274

Population-based Survey on Indirect Health Effects after the 1995 Great Hanshin-Awaji Earthquake
Keiko OGAWA, Ichirou TSUJI, Shigeru HISAMICHI (Tohoku University),
Keishi SHIONO (Nagaoka Technical College) ····· 278

Revisiting the public health consequences of natural disasters through an epidemiologic perspective
Josephine Malilay (CDC) ····· 288

THEME 3. Storm Surge and Tsunamis

Outline and Performance of New Tsunami Forecast Service In the Japan Meteorological Agency
Yasuo SEKITA, Hidee TAKAHATA, Tsuneaki ANAMI
and Takashi KADOWAKI (JMA) ····· 299

Affordable Tsunami Mitigation
Michael E. Blackford (NOAA) ····· 303

Large-scale Experiment on Dynamic Response of Sand Bed around a Cylinder Due to Tsunami
Fuminori Kato, Shinji SATO (PWRI), Harry Yeh (Univ. of Washington) ····· 307

Storm Surge in Ise and Mikawa Bay Caused by Typhoon
Hiroyasu KAWAI (PHRI) ····· 320

THEME 4. Seismic Information Systems

Seismic Information System for National Land Management
Hideki SUGITA, Tomofumi NOZAKI (PWRI) ····335

Change Detection Using Geospatial Analysis
William Roper (TEC) ····345

Hurricane Mitch Recovery
William Roper (TEC) ····365

Early Estimation System for Earthquake Disasters
Takaharu KIRIYAMA, Kazuo OKAYAMA (NLA) ····379

THEME 5. Joint Cooperative Research Programs

30-Year Accomplishments and Future Challenges of the Panel on Wind and Seismic Effects
Yasutake INOUE, and Michio OKAHARA (PWRI) ····391

U.S.- Japan Cooperative Earthquake Research Program on Composite and Hybrid Structures - U.S.- side Progress
Subash C. Goel (Univ. of Michigan) (Presented by Charles Roeder Univ. of Washington) ····418

U.S.- Japan Cooperative Earthquake Engineering Research Program on Composite and Hybrid Structures — Japanese side research accomplishments —
Isao NISHIYAMA, Hiroyuki YAMANOUCHI, Hisahiro HIRAISHI (BRI) ····422

MANUSCRIPTS AUTHORED FOR PANEL MEETING BUT NOT PRESENTED ORALLY

Perforated Shear Walls with Conventional and Innovative Base Restraint Connection
Jay Crandell, P.E. (NAHB) William Freeborne (HUD)
Shawn McKee (NAHB) ····433

The New FHWA/MCEER Seismic Vulnerability Study of Highway Systems:
Loss Estimation Methodology and the Seismic Design and Retrofitting of Long Span Bridges
Ian M.Friedland, P.E. (MCEER)
W. Phillip Yen, John D. O'Fallon (FHWA) ····452

Development of Test Guidelines for Passive Energy Dissipation Devices
Michael A. Riley (NIST) and Fahim Sadek (Southern Methodist Univ.) ····461

A Liquefaction Evaluation Procedure Based on Shear Wave Velocity
Ronald D. Andrus (NIST)
and Kenneth H. Stokoe, II (Univ.of Texas at Austin) ·····469

Influence of Confining Stress on Liquefaction Resistance
Mary Ellen Hynes & Richard S. Olsen (WES) ·····475

State-of the-art of Stability Assessment of Underground Structures during Liquefaction
Osamu MATSUO and Tetsuya SASAKI (PWRI) ·····485

Development of Seismic Performance Evaluation Procedures in Building Code of Japan
Hisahiro HIRAISHI, Mitsumasa MIDORIKAWA, Izuru OKAWA
Masanori IIBA, Masaomi TESHIGAWARA, and Hiroshi ISODA (BRI) ·····499

Seismic Performance of an Existing RC Frame Retrofitted by Preacast Prestressed Concrete Shear Walls
Mizuo INUKAI, Takashi KAMINOSONO (BRI) ·····513

Construction of GSI's Nationwide GPS Array
Shin-ichi MIYAZAKI (GSI) ·····518

APPENDIX

TASK COMMITTEE REPORTS ·····531
TECHNICAL SITE VISITS ·····555

PREFACE

This publication is the proceedings of the 31st Joint Meeting of the U.S.-Japan Panel on Wind and Seismic Effects. The meeting was held at the Public Works Research Institute, Tsukuba, Japan, during May 11-14. 1999. The proceedings include the program, list of members, panel resolutions, task committee reports and technical papers submitted to the Joint Panel Meeting, and summary of the technical site visits.

BACKGROUND

Responding to the need for improving engineering and scientific practices through exchange of technical
data and information, research personnel, and research equipment, the United States and Japan in 1961 created the U.S.-Japan Cooperative Science Program. Three collateral programs comprise the Cooperative Science Program. The U.S.-Japan Cooperative Program in Natural Resources (UJNR), one of the three, was created in January 1964. The objective of UJNR is to exchange information on research results and exchange scientists and engineers in the area of natural resources for the benefit of both countries. UJNR is composed of 18 Panels each responsible for specific technical subjects.

The Panel on Wind and Seismic Effects was established in 1969. Seventeen U.S. and seven Japanese agencies participated with representatives of primate sector organizations to develop and exchange technologies aimed at reducing damage from high winds, earthquakes, storm surge, and tsunamis. This work is produced through collaboration between U.S. and Japanese member researchers working in eleven task committees. Each task committee focuses on specific technical issues, e.g., earthquake strong motion data. The Panel provides the vehicle to exchange technical data and information on design and construction of civil engineering lifelines, buildings and waterfront structures, and to exchange high wind and seismic measurement records. Annual meetings alternate between Japan and United States (odd numbered years in Japan; even numbered years in U.S.). These one-week technical meetings provide the forum to discuss ongoing research and research results; they are followed by a one-week series of technical site visits.

The National Institute of Standards and Technology (NIST) provides the U.S.-side chairman and secretary-general. The Public Works Research Institute (PWRI), Japan, provides the Japan-side chairman and secretary-general.

Annual meetings provide the mechanism for interaction with the U.S. and Japanese researchers in wind and seismic engineering which provides opportunities to gain valuable information and to engage in cooperative research. Through these opportunities, the Panel member organizations have realized important advances in building and structures technology. The

Panel's activities have resulted in improved building and structures codes and standards in both countries, for example:

- created and exchanged digitized earthquake records used as the basis of design and research for Japan and the United States;
- transferred earthquake engineering information and strong-motion measurement techniques for use by seismically active countries, e.g., Australia, Canada, Italy, Mexico, Peru. Taiwan, Turkey, and North Africa;
- produced data that advanced design and construction of bridge structures;
- produced large-scale testing data that advanced the seismic design standards for buildings;
- improved in-situ measurement methods for soil liquefaction and stability under seismic loads;
- created a database on storm surge and tsunamis and verified mathematical models of tsunami and storm surge warning systems;
- established a library resource of current research on wind and earthquake engineering and on storm surge and tsunamis;
- published proceedings of Panel meeting, Task Committee Workshops, and special publications such as List of Panel Publications and translated two-volume series on earthquake resistant construction using base isolation systems;
- provided earthquake science and technology expertise to the U.S.-Japan Natural Disaster Reduction Initiative of the U.S.-Japan Framework for New Economic Partnership (Common Agenda);
- created a Web Site for promoting the Panel's activities widely.

The Panel's efforts are exemplary of effective joint research and of technology delivery between researchers from the U.S. and Japan. Since its creation, more than I 800 papers were presented in 29 Joint Meetings and more than 55 Task Committee Workshops and over 200 guest researchers were exchanged. The Panel provides important information about the U.S. and Japan's civil engineering thrusts which influence both countries' research and provide the basis for improvements in building and structures codes and standards.

HIGHLIGHTS OF THE 31st JOINT PANEL Meeting

Thirty-five papers were presented orally. The papers were organized into five themes: Wind Engineering; Earthquake Engineering; Storm Surge and Tsunamis; Summary of Joint Cooperative Research Programs; and Seismic Imformation Systems.

Highlights include:

- Technical presentations:
  - Important knowledge was exchanged for research and practice, e.g., analytical and experimental research results on wind engineering; seismic design of bridges, dams and buildings; disaster prevention information systems and risk assessment using GIS; and

research in public health following natural disasters.
- Information was exchanged about extensive U.S. I Japanese public works projects, civil engineering research, and their applications into practice.

- Excellent projects are being performed by both sides in intelligent and smart materials and systems technologies.

- Task Committee activities grow in strength. The TIC structure is an extremely effective vehicle to explore in depth the technologies and methods being used by both countries.
  - Five Task Committee Workshops were held in the past year and seven Workshops/Committee Meetings are planed for the coming year.
  - Desirability to create a new T/C on Seismic Imformation Systems was recognized.

- Cooperative Research Programs continue to be productive.
  - Composite and hybrid structures,
  - Soil liquefaction and countermeasures, and
  - Smart materials.

Michio Okahara, Secretary - General
Japan- side Panel on Wind and Seismic Effects

Agenda of Joint Meeting and Technical site Visits

AGENDA OF THE 31ST JOINT MEETING ON WIND AND SEISMIC EFFECTS

TECHNICAL MEETING

May 11 (Tue)

10:30 Opening Ceremonies [8F Conference Room]
Call to order by Michio OKAHARA, Secretary-General, Japan- Side

Opening remarks by Nobuhiko SATO, Vice-Minister of Construction for Engineering, Ministry of Construction

Remarks by James H. Hall, Minister-Counselor, Embassy of the United States of America

Remarks by Youichirou OHTSUKA, Director, International Affairs Division, Science and Technology Promotion Bureau, Science and Technology Agency

Remarks by Yasutake INOUE, Chairman, Japan-Side Panel on Wind and Seismic Effects, Director-General, Public Works Research Institute, Ministry of Construction

Remarks by S. Shyam Sunder, Chairman, U.S.-Side Panel on Wind and Seismic Effects, Chief, Structures Division, National Institute of Standards and Technology, Department of Commerce

Introduction of Japan-side Members by Japan-side Panel Chairman

Introduction of U.S.-side Members by U.S.-side Panel Chairman

Elect Joint Meeting Chairman

Adopt Agenda

Adjourn

11:45 Group Photograph

12:00 Lunch hosted by BRI [1F Conference Room]

13:30 Session 1 (Joint Cooperative Research Programs) Chairman - S. Shyam Sunder

13:30 30-Year Accomplishments and Future Challenges of the Panel on Wind and Seismic Effects
Yasutake INOUE, and Michio OKAHARA (PWRI)

13：45 U.S.-Japan Cooperative Earthquake Research Program on Composite and Hybrid Structures - U.S.-side Progress

Subash C. Goel (Univ. of Michigan)

(Presented by Charles Roeder Univ.of Washington)

14：00 U.S.- Japan Cooperative Earthquake Engineering Research Program on Composite and Hybrid Structures — Japanese side research accomplishments —

Isao NISHIYAMA, Hiroyuki YAMANOUCHI, Hisahiro HIRAISH (BRI)

14：15 Discussion

14：50 Break

15：10 Task Committee Meetings

A: Strong-Motion Data and Applications [5F Room 524]

B: Design Testing and Evaluation Procedures for Building Systems [5F Room 526]

G: Seismic Information Systems [5F Room 534]

I: Storm Surge and Tsunami [5F Room 531A]

F: Disaster Prevention Methods for Lifelines Systems [6F Room 610]

K:Wind and Earthquake Engineering for offshore and Coastal Facilities [6F Room 617]

18：30 Reception hosted by the Vice-Minister of Construction for Engineering
(Hotel Grand Shinonome, Tel. 0298-56-2211)

May 12 (Wed)

9 : 0 0 Session 2 (Earthquake Engineering 1) Chairman - Yasutake INOUE

9 : 0 0 Recent Projects at PWRI for Improvement of Seismic Performance of Civil Infrastructures
Masahiko YASUDA (PWRI)

9 : 1 5 Comparison of U.S. and Japanese Highway Bridge Seismic Retrofitting Measures
W. Phillip Yen (FHWA) and Shigeki UNJOH (PWRI)

9 : 3 0 Model Experiments on Characteristics of Motions of Continuous Pontoon Type and Separate Support Type Elastic Floating Bodies in Waves
Haruo YONEYAMA, Satoru SHIRAISHI and Go ISHIMI (PHRI)

9 : 4 5 Development of a Probabilistic Seismic Hazard Analysis for Offshore Facilities in the Santa Barbara Channel
Charles E. Smith (MMS) and Robert Murray (LLNL)

1 0 : 0 0 Discussion

1 0 : 4 0 Break

1 1 : 0 0 Session 3 (Earthquake Engineering 2) Chairman - Yasutake INOUE

1 1 : 0 0 GPS in Dynamic Monitoring of Long-period Structures
Mehmet Çelebi (USGS)

1 1 : 1 5 Real-time Hybrid Vibration Experiments with a 2-Dimensional and 3-Degrees -of-Freedom Model
Keiichi TAMURA, Hiroshi KOBAYASHI (PWRI)

1 1 : 3 0 Integrated Surface and Borehole Strong-Motion, Soil-Response Arrays in San Francisco, California
R. D. Borcherdt, H.P. Liu, R.E. Westerlund, C. Ditel,
J.F. Gibbs, R.E. Warrick (USGS)

1 1 : 4 5 Discussion

1 2 : 2 0 Lunch hosted by MRI [1F Conference Room]

1 3 : 2 0 Session 4 (Wind Engineering) Chairman - Yasutake INOUE

1 3 : 2 0 Wind Properties for Design of Highway Bridges
Hiroshi SATO, Ken-ichi OGI (PWRI)

1 3 : 3 5 The Fujita Tornado Intensity Scale: A Reassessment from Structural Engineering Perspective
Long T. Phan, and Emil Simiu (NIST) (Presented by H.S.Lew, NIST)

1 3 : 5 0 Research Project on Propriety and Reliability of Designing Wind Lord and Wind Pressure Coefficients
Hisashi OKADA, Hitomitsu KIKITSU (BRI), Yukio TAMURA (Tokyo Institute of Polytechnics), Yasushi UEMATSU (Tohoku University)

1 4 : 0 5 A Probabilistic Tornado Wind Hazard Model for the Continental United States
Quazi Hossain (LLNL) , Richard Mensing (LLNL)
Jean Savy (LLNL), Jeffery Kimball (DOE)

14:20 10km Scale Wind Speed Fluctuation Observed in Typhoon Area
Yoshinobu TANAKA (MRI)

14:35 Discussion

15:30 Break

15:50 Task Committee Meetings

C: Evaluation and Improvement of Structures [5F Room 526]
E: Design for Wind and Wind Hazard Mitigation [6F Room 610]
D: Earthquake Engineering for Dams [5F Room 534]
H: Soil Behavior and Stability During Earthquakes [6F Room 617]
J: Wind and Earthquake Engineering for Transportation Systems [5F Room 531A]

18:30 Dinner Hosted by Director-General of Public Works Research Institute
(Tsukuba University Hall, Tel. 0298-58-0939)

May 13 (Thu)

9 : 0 0 Session 5 (Storm Surge and Tsunamis) Chairman - S. Shyam Sunder

9 : 0 0 Outline and Performance of New Tsunami Forecast Service In the Japan Meteorological Agency
Yasuo SEKITA, Hidee TAKAHATA, Tsuneaki ANAMI
Takashi KADOWAKI (JMA)

9 : 1 5 Affordable Tsunami Mitigation
Michael Blackford (NOAA)

9 : 3 0 Large-scale Experiment on Dynamic Response of Sand Bed around a Cylinder Due to Tsunami
Fuminori Kato, Shinji SATO (PWRI), Harry Yeh (Univ. of Washington)

9 : 4 5 Storm Surge in Ise and Mikawa Bay Caused by Typhoon
Hiroyasu KAWAI (PHRI)

1 0 : 0 0 Discussion

1 0 : 4 0 Break

1 0 : 5 0 Session 6 (Earthquake Engineering 3) Chairman - S. Shyam Sunder

1 0 : 5 0 Three Dimensional Shaking Table Tests on Seismic Behavior of Isolators for Houses
Masanori IIBA, Mitsumasa MIDORIKAWA
Hiroyuki YAMANOUCHI (BRI) and Bujar Myslimaj (Univ.of Tsukuba)

1 1 : 1 0 Application of Advanced Technologies in Seismic Protection of Critical Facilities -An MCEER Program
George Lee (Univ. of New York at Buffalo)
Michel Bruneau, Masanobu Shinozuka, and Kathleen Tierney (MCEER)

1 1 : 3 0 A Study on the Behavior of a Seismic Isolation Device Using Full-scale Dynamic Push-over Experimental Equipment
Takashi SATOU, Hiroshi MITAMURA (CERI), Akio HAYASHI (Pacific Consultants), Toshihiko BESSYO (The Japan Steel Works)

1 1 : 5 0 Discussion

1 2 : 1 0 Lunch hosted by CERI [1F Conference Room]

1 3 : 1 0 Session 7 (Earthquake Engineering 4) Chairman - S. Shyam Sander

1 3 : 1 0 Investigations of Active Faults for Dam Construction - The Present State at The Ministry of Construction
Yasuhiko WAKIZAKA (PWRI)

1 3 : 2 5 Present and Future Roles of Nonlinear Numerical Procedures in the Seismic Analysis of Concrete Dams
Robert L. Hall (WES), Enrique E. Matheu (Virginia Polytechnic Institute and State University)

1 3 : 4 0 Dynamic Response and Failure Mechanism of a Pile Foundation During Soil Liquefaction under Shaking Table Test Using a Large-scale Laminar Shear Box
Shuji TAMURA, Chikahiro MINOWA (NIED), Yasutsugu SUZUKI

(Kajima Corporation), Michio SUGIMOTO (Takenaka Corporation), Shunji FUJII (Taisei Corporation), Takaaki KAGAWA (Wayne State University)

13：55 Equivalent-Linear Ground-Response Calculations with Frequency-Dependent Damping
William B. Joyner (USGS)

14：10 Discussion

14：40 Break

14：50 Session 8 (Earthquake Engineering 5) Chairman - S. Shyam Sunder

14：50 Development of Smart Structure Systems
Shunsuke OTANI (University of Tokyo), Hisahiro HIRAISHI, Mitsumasa MIDORIKAWA, Masaomi TESHIGAWARA (BRI)

15：05 Development of the FEMA-273 Document-Guidelines for the Seismic Rehabilitation of Buildings
A. Gerald Brady (ATC)

15：20 Population-based Survey on Indirect Health Effects after the 1995 Great Hanshin-Awaji Earthquake
Keiko OGAWA, Ichirou TSUJI, Shigeru HISAMICHI (Tohoku University), Keishi SHIONO (Nagaoka Technical College)

15：35 Revisiting the public health consequences of natural disasters through an epidemiologic perspective
Josephine Malilay (CDC)

15：50 Discussion

16：20 Break

16：30 Workshop Reports

17：30 Adjourn

18：30 Individually Hosted Dinner

May 14 (Fri)

9 : 0 0	Session 9 (Seismic Information Systems) Chairman - Yasutake INOUE
9 : 0 0	Seismic Information System for National Land Management Hideki SUGITA, Tomofumi NOZAKI (PWRI)
9 : 1 5	Change Detection Using Geospatial Analysis William Roper (TEC)
9 : 3 0	Hurricane Mitch Recovery William Roper (TEC)
9 : 4 5	Early Estimation System for Earthquake Disasters Takaharu KIRIYAMA, Kazuo OKAYAMA (NLA)
1 0 : 0 0	Discussion
1 1 : 0 0	Break
1 1 : 1 0	Report of Task Committees 1
1 2 : 0 0	Lunch hosted by NIED [1F Conference Room]
1 3 : 0 0	Report of Task Committees 2
1 4 : 0 0	Break
1 4 : 2 0	Adoption of Final Resolutions
1 6 : 0 0	Break
1 6 : 2 0	Closing Ceremonies Call to Order by Michio OKAHARA, Secretary -General, Japan- side Panel Closing Remarks by S. Shyam Sunder, Chairman U.S. - Side Panel Closing Remarks by Yasutake INOUE, Chairman Japan - Side Panel Conclusion of 31st Joint Panel Technical Sessions Reception Hosted by U.S. Members (Tsukuba Dai-ichi Hotel, Tel. 0298-52-1112)

OPENING CEREMONIES

May 11(Tue) 10:30 ~ 12:00

10:30 OPENING CEREMONIES

Call to order by Michio OKAHARA, Secretary-General, Japan- Side

Opening remarks by Nobuhiko SATO, Vice-Minister of Construction for Engineering, Ministry of Construction

Remarks by James H. Hall, Minister-Counselor, Embassy of the United States of America

Remarks by Youichirou OHTSUKA, Director, International Affairs Division, Science and Technology Promotion Bureau, Science and Technology Agency

Remarks by Yasutake INOUE, Chairman, Japan-Side Panel on Wind and Seismic Effects, Director-General, Public Works Research Institute, Ministry of Construction

Remarks by S.Shyam Sunder, Chairman, U.S.-Side Panel on Wind and Seismic Effects, Chief, Structures Division, National Institute of Standards and Technology, Department of Commerce

Introduction of Japan-side Members by Japan-side Panel Chairman

Introduction of U.S.-side Members by U.S.-side Panel Chairman

Elect Joint Meeting Chairman

Adopt Agenda

Adjourn

11:45 Group Photograph

CLOSING CEREMONIES

May 14(Fri) 16:20 ～ 16:50

16：20 CLOSING CEREMONIES

Call to Order by Michio OKAHARA, Secretary - General, Japan - Side Panel

Closing Remarks by S. Shyam Sunder, Chairman U.S. - Side Panel

Closing Remarks by Yasutake INOUE, Chairman Japan - Side Panel

TECHNICAL SITE VISITS

Monday 10 May

9:50	Depart from Kenshu Kaikan by bus
10:00-13:00	Visit to Geographical Survey Institute
13:20	Leave Geographical Survey Institute by bus
13:30-15:20	Visit to National Research Institute for Earth Science and Disaster Prevention
15:20	Leave National Research Institute for Earth Science and Disaster Prevention by bus
15:30	Arrive at Kenshu Kaikan
	Stay at Kenshu Kaikan

Tuesday 11 May -Friday 14 May Joint Panel Meeting

Stay at Kenshu Kaikan

Saturday 15 May

9:20	Depart from Kenshu Kaikan by bus
10:00	Arrive at Tsuchiura JR Station
10:21	Depart from Tsuchiura JR Station by Express Train (Fresh Hitachi #16)
11:04	Arrive at Ueno JR Station. Move to Tokyo JR Station by Yamanote Line
11:45	Depart from Tokyo JR Station by Super Express Train (Hikari #159)
12:45	Arrive at Shizuoka JR Station. Move to Sumata Area by bus
15:00-17:00	Visit to Sumata Area (Sight-seeing)
17:30	Arrive at Sumata Hot Spring Area
	Stay at Hotel Suiko-en

Sunday 16 May

9:00	Depart from Hotel by bus
9:30-13:00	Visit to Construction Site of Nagashima Dam by Oigawa train (Apt type train)
13:00-15:00	Visit to Sessokyo Area by bus
15:00	Move to Kakegawa JR Station by bus
17:01	Depart from Kakegawa JR Station by Super Express Train (Kodama #425)
18:04	Arrive at Nagoya JR Station
	Stay at Hotel Sunroute Nagoya

Monday 17 May

9:00	Depart from Hotel by bus
10:00-15:00	Visit to Construction Site of 2nd Tomeishin (Tokyo-Nagoya-Kobe) Highway (Meiko Bridges, Ibigawa Bridge, Kisogawa Bridge etc.)
16:00	Arrive at Nagoya JR Station by bus
16:29	Depart from Nagoya JR Station by Super Express Train (Hikari #137)
17:55	Arrive at Shin-Kobe JR Station
	Stay at Green Hill Hotel Annex

Tuesday 18 May

9:00	Depart from Hotel by bus
9:10-10:00	Visit to Hyogo Prefectural Government (Phoenix Disaster Prevention Center)
10:00	Move to Awaji Service Area through Akashi Kaikyo Birdge by bus
11:00-12:00	Visit to Awaji Service Area (Largest Service Area in Japan)
12:20-12:50	Visit to Fault of Nojima-Danso by bus
13:10-14:30	Visit to Akashi Kaikyo Bridge, Top of 3P Tower (Move 4A to 3P by foot)
15:30	Arrive at Shin-Kobe JR Station by bus
16:00	Depart from Shin-Kobe JR Station by Super Express Train (Hikari #118)
19:14	Arrive at Tokyo JR Station
20:00	Arrive at Tokyo Prince Hotel by JR Line or Subway
	Stay at Tokyo Prince Hotel

Wednesday 19 May

9:00	Depart from Tokyo Prince Hotel by bus
10:30-12:00	Visit to Fire Prevention Research Institute
13:00	Move to Yamaguchi Water Reservoir by bus
15:00-17:00	Visit Yamaguchi Water Reservoir
18:30	Arrive at Tokyo Prince Hotel by bus
	Stay at Tokyo Prince Hotel

Thursday 20 May

8:30	Depart from Tokyo Prince Hotel by Foot
9:00	Depart from Sengakuji Station by Keihin Express Train (Kurihama Line)
10:00	Arrive at Oppama Station
10:10-11:30	Visit to Mega Float Structure
11:50-14:00	Visit to Port and Harbor Research Institute
14:20	Move to Kamakura by bus
15:00-18:00	Visit to Kamakura Area (Historic Area)
19:00	Arrive at Tokyo JR Station by train (JR Yokosuka Line)
19:30	Arrive at Tokyo Prince Hotel by JR Line or Subway
	Stay at Tokyo Prince Hotel

Friday 21 May US delegation Depart from Narita/Tokyo

List of panel members

UNITED STATES-SIDE PANEL ON WIND AND SEISMIC EFFECTS MEMBERSHIP LIST

Dr. S. Shyam Sunder
Chairman, U.S.-side Panel
Chief, Structures Division
Building and Fire Research Laboratory
National Institute of Standards and Technology
100 Bureau Drive, Stop 8611
Gaithersburg, MD 20899-8611
301-975-6061 FAX:301-869-6275
e-mail:sunder@nist.gov

Dr. John Gross
Secretary-General, U.S.-side Panel
Leader, Structural Systems and Design Group
Building and Fire Research Laboratory
National Institute of Standards and Technology
100 Bureau Drive, Stop 8611
Gaithersburg, MD 20899-8611
301-975-6068 FAX:301-869-6275
e-mail:john.gross@nist.gov

Dr. Daniel P. Abrams
Director, Mid-America Earthquake Center
Hanson Engineers Professor of Civil Engineering
University of Illinois
1241 Newwark Laboratory
205 North Mathews Avenue
Urbana, IL 61801
217-244-6302 FAX:217-333-3821
email:d-abrams@uiuc.edu

Dr. Kharaiti L. Abrol
Principal Structural Engineering Consultant
Room 475
Department of Veterans Affairs
810 Vermont Avenue, NW
Washington, DC 20420
202-565-5579 FAX:202-565-5478
email:abrkha@hq.med.va.gov

Dr. John Ake
Geophysicist
Seismotectonics and Geophysics Section
Code D-8330
P.O. Box 25007
Bureau of Reclamation
U.S. Department of the Interior
Denver, CO 80225
303-236-4195 x276 FAX:303-236-9127
e-mail:jake@seismo.usbr.gov

Dr. William Anderson
Hazard Reduction Program
National Science Foundation
Room 545
Arlington, VA 22230
703-306-1361 FAX:703-306-0291
e-mail:Wanderson@nsf.gov

Mr. John Baals
Seismic Safety Coordinator
P.O. Box 25007 (D-8110)
Bureau of Reclamation
U.S. Department of the Interior
Denver, CO 80225
303-236-3999 x534 FAX:303-236-9099
e-mail:jbaals@do.usbr.gov

Dr. Celso S. Barrientos
Supervisory Physical Scientist
National Environmental Satellite Data
Information Service - Code E/RA28
National Oceanic and Atmospheric Administration
U.S. Department of Commerce
5200 Auth Road
Camp Springs, MD 20746
301-763-8102 FAX:301-763-8020
e-mail:cbarrientos@nesdis.noaa.gov

Dr. Eddie N. Bernard
Director, Pacific Marine Environmental Laboratory
National Oceanic and Atmospheric Administration
U.S. Department of Commerce
7600 Sand Point Way, NE
BIN C15700/Building 3
Seattle, WA 98115-0070
206-526-6800 FAX:206-526-6815
e-mail:bernard@pmel.noaa.gov

Mr. Mike Blackford
IOC-NWS/INTERNATIONAL
Director, International Tsunami Information Center
737 Bishop Street, Suite 2200
Honolulu, HI 96813-3213
808-532-6423 or 6422 FAX:808-532-5576
e-mail:mike@itic.noaa.gov

Dr. David M. Boore
U.S. Geological Survey
345 Middlefield Road MS 977
Menlo Park, CA 94025
650-329-5616 FAX:650-329-5163
e-mail:boore@samoa.wr.usgs.gov

Dr. Roger D. Borcherdt
Branch of Seismology

U.S. Geological Survey
U.S. Department of the Interior
345 Middlefield Road, MS 977
Menlo Park, CA 94025
650-329-5619 FAX:650-329-5163
e-mail:borcherdt@samoa.wr.usgs.gov

Dr. Mehmet K. Celebi
Research Civil Engineer
Branch of Earthquake and Geomagnetic Information
U.S. Geological Survey
U.S. Department of the Interior
345 Middlefield Road, MS 977
Menlo Park, CA 94025
650-329-5623 FAX: 650-329-5163
email:celebi@samoa.wr.usgs.gov

Mr. Harish Chander
U.S. Dept. of Energy (EH-31),
CXXI, Room 2016 (GTN)
19901 Germantown Road
Germantown, MD 20874-1290
301-903-6681 FAX:301-903-8693
e-mail:harish.chander@hq.doe.gov

Dr. Ken P. Chong
Director, Mechanics & Materials
Directorate of Engineering
National Science Foundation
4201 Wilson Boulevard - Room 545
Arlington, VA 22230
703-306-1361 FAX:703-306-0291
e-mail:KChong@NSF.gov

Mr. James D. Cooper
Chief, Structures Division, HNR-10
Federal Highway Administration
U.S. Department of Transportation
6300 Georgetown Pike
McLean, VA 22101
703-285-2060 FAX:703-285-2766
e-mail:jim.cooper@fhwa.dot.gov

Mr. William Freeborne
Housing and Urban Development
Room 8132
451 Seventh Street, SW
Washington, D.C. 20410
202-708-4370 x5725 FAX:202-708-5873
e-mail:william_e._freeborne@hud.gov

Mr. Joseph H. Golden
NOAA/OAR/USWRP
1315 East-West Highway
Room 11554
Silver Spring, MD 20910
301-713-0460 x123 FAX:301-713-1459
202-482-1584
e-mail:joe.golden@noaa.gov

Mr. Peter E. Gurvin
Director, Building Design and Engineering Division
Foreign Building Operations
Building SA-6, Room 335
U.S. Department of State
Washington, D.C. 20520
703-875-6117 FAX:703-875-6204
e-mail:peter.e.gurvin@dos.us-state.gov

Dr. Robert L. Hall
Chief, Structural Analysis Group
U.S. Army Engineer Waterways Experiment Station
3909 Halls Ferry Road
Vicksburg, MS 39180-6199
601-634-2567 FAX:601-634-3412
e-mail:hallr3@mail.wes.army.mil

Dr. Walter W. Hays
Earthquake Hazards Reduction Program
U.S. Geological Survey
905 National Center
12201 Sunrise Valley Drive
Reston, VA 20192
703-648-6711 FAX:703-648-6747
e-mail:whays@usgs.gov

Dr. Allen M. Hittelman
Chief, Solid Earth Geophysics Division
E/GC1, National Geophysical Data Center
NOAA, NESDIS
325 Broadway
Boulder, CO 80303-3328
303-497-6591 FAX:303-497-6513
e-mail:allen.m.hittelman@noaa.gov

Mr. Larry C. Hultengren
Senior Structural Engineer
Office of Civil/Structural Engineering
Foreign Building Operations
Building SA-6, Room 346
U.S. Department of State
Washington, D.C. 20520
703-875-6194 FAX:703-875-6204
email:hultengrenlc@state.gov

Dr. Mary Ellen Hynes
Chief, Earthquake Engineering and Geophysics Branch
Geotechnical Laboratory
USACE-CEWES-GG-H
3909 Halls Ferry Road
U.S. Army Waterways Experiment Station
Vicksburg, MS 39180
601-634-2280 FAX:601-634-3453
email:hynesm@ex1.wes.army.mil

Dr. William B. Joyner
Geophysicist
Branch of Seismology
U.S. Geological Survey
U.S. Department of the Interior
345 Middlefield Road, MS 977
Menlo Park, CA 94025
650-329-5640 FAX:650-329-5163
e-mail:joyner@samoa.wr.usgs.gov

Mr. Roger M. Kenneally
Structural Engineer
Structural and Seismic Engineering Branch
Mail Stop T10-L1
U.S. Nuclear Regulatory Commission
Washington, D.C. 20555
301-415-6303 FAX:301-415-5074
e-mail:rmk@nrc.gov

Dr. George Lee
Director, Multidisciplinary Center for Earthquake Engineering Research (MCEER)
State University of New York at Buffalo
Red Jacket Quadrangle
Buffalo, NY 14261
716-645-3391 FAX:716-645-3399
email:gclee@acsu.buffalo.edu

Dr. H.S. Lew
Structures Division
Building and Fire Research Laboratory
National Institute of Standards and Technology
100 Bureau Drive Stop 8611
Gaithersburg, MD 20899-861
301-975-6060 FAX:301-869-6275
e-mail:hai.lew@nist.gov

Dr. Shih-Chi Liu
Program Director, Structural Systems
Division of Biological and Critical Systems
National Science Foundation
4201 Wilson Boulevard - Room 545
Arlington, VA 22230
703-306-1362 FAX:703-306-0291
e-mail:sliu@nsf.gov

Dr. Josephine Malilay
Disaster Assessment and Epidemiology Section
National Center for Environmental Health
F-46 Center for Disease Control and Prevention
4770 Buford Highway, NE
Atlanta, GA 30341
770-488-7295 FAX: 770-488-7335
e-mail:jym7@cchdch1.em.cdc.gov

Dr. Francis G. McLean
Value Engineering Program Manager
Code D-8170
P.O. Box 25007
Bureau of Reclamation
U.S. Department of the Interior
Denver, CO 80225
303-445-3091 FAX:303-6475
e-mail:FMCLEAN@do.usbr.gov

Dr. Raymond E. Meyer
Department of State
SA14/Room 1705
USAID/Washington, D.C. 20523-1443
202-712-1078 FAX: 202-216-3707
e-mail:Rmeyer@usaid.gov

Dr. Jack Moehle
Director, Pacific Earthquake Engineering Research Center (PEER)
1301 South 46th Street
Richmond, CA 94804-4698
510-231-9554 FAX: 510-231-9471
email:moehle@eerc.berkeley.edu

Mr. Ugo Morelli
Policy Manager
Federal Emergency Management Agency
500 C Street, SW
Washington, D.C. 20472
202-646-2810 FAX:202-646-2577
e-mail:UMorelli@fema.gov

Mr. Howard D. Nickerson
Earthquake Engineering and Weapons Specialist
Naval Facilities Engineering Command
Hoffman Building #2, Room 12S63,
Code 04B2
200 Stovall Street
Alexandria, VA 22332
202-433-8599 FAX: 202-433-8777
e-mail:howard.d.nickerson@esc61@navfac.nfesc

Dr. Stuart Nishenko
Federal Emergency Management Agency
500 C Street, SW
Washington, D.C. 20472
202-646-3945 FAX:202-646-4596
e-mail:stuart.nishenko@fema.gov

Mr. Tom Post
Chief, Earthquake Engineering Division
California Department of Transportation
(CALTRANS)
P.O. Box 942873
Sacramento, CA 95814
916-227-8728 FAX: 916-227-8898
email:tpost@trmx3.dot.ca.gov

Dr. William E. Roper
Director, U.S. Army Topographic Engineering Center
7701 Telegraph Road
Alexandria, VA 22315-3864
703-428-6600 FAX:703-428-8154
email:wroper@tec.army.mil

Dr. Charles E. Smith
Research Program Manager
Offshore Minerals Management
Technology Assessment and Research Branch
Minerals Management Service
U.S. Department of the Interior
381 Elden Street, MS 4800
Herndon, VA 20170-4817
703-787-1561 FAX:703-787-1555
e-mail:smithc@smtp.mms.gov

Mr. Stanley Strickland
Chief, Air Base Systems Branch
Stop 37, WL/FIVC/OL, Bldg. 1120
139 Barnes Drive, STE 2
Tyndall AFB, FL 2403-6001
904-283-3709 FAX:904-283-3722
e-mail:stan@mail.interoz.com

Dr. Phillip Yen
Federal Highway Administration
6300 Georegetown Pike
McLean, VA 22101
703-285-2315 FAX:703-285-2766
e-mail:wen-huei.yen@fhwa.dot.gov

ALTERNATE MEMBERS

Dr. Clifford J. Astill
Program Director
Division of Biological and Critical Systems
National Science Foundation
4201 Wilson Boulevard - Room 545
Arlington, VA 22230
703-306-1361 FAX:703-306-0291
email:castill@nsf.gov

Mr. Michael Changery
Chief, Global Analysis Branch
National Climatic Data Center
National Oceanic and Atmospheric Administration
U. S. Department of Commerce
Federal Building
Ashville, NC 28801
704-271-4765 FAX:704-271-4246
email:mchangry@ncdc.noaa.gov

Dr. C.Y. Chen
Senior Civil/Geotechnical Engineer
Office of Foreign Buildings
Department of State
Code SA-6, Rm. 347
Washington, D.C. 20520
703-875-6207 FAX:703-875-6204
email:chency@state.gov

Mr. Vincent P. Chiarito
Research Structural Engineer
Structural Mechanics Division
Structures Laboratory
U.S. Army Engineer Waterways Experiment Station
3909 Halls Ferry Road
Vicksburg, MS 39180-6199
601-634-2714 FAX:601-634-3412
email: chiariv@ex1.wes.army.mil

Dr. James F. Costello
Senior Structural Engineer
Structural and Geological Engineering Branch
Office of Nuclear Regulatory Research
U.S. Nuclear Regulatory Commission
Mail Stop T10-L1
Washington, D.C. 20555
301-415-6009 FAX:301-415-5074
email:jfc2@nrc.gov

Dr. James R. Houston
Director, Coastal Engineering Research Center
U.S. Army Engineer Waterways Experiment
Station/WESCV-Z
3909 Halls Ferry Road
Vicksburg, MS 39180-6199
601-634-2000 FAX:601-634-2055
e-mail:houston@coafs1.wes.army.mil

Mr. James Lander
Geophysicist
Cooperative Institute for Research in
Environmental Sciences
University of Colorado
Campus Box 449, Room 152 RL3
3100 Marine Street
Boulder, CO 80309
303-497-6446 FAX: 303-497-6513
email:jlander@ngdc.noaa.gov

Mr. Tingley K. Lew
Research Structural Engineer
Structures Division
Naval Facilities Engineering Service Center - Code
C62
1110 23rd Ave.
Port Hueneme, CA 93043-4370
805-982-1234 FAX:805-982-1418
email:tlew@nfesc.navy.mil

Mr. Michael Mahoney
Physical Scientist
Federal Emergency Management Agency
500 C Street, SW
Washington, D.C. 20472
202-646-2794 FAX:202-646-4387
e-mail:mike.mahoney@fema.gov

Dr. Martin C. Miller
Chief, Coastal Oceanograhy Branch
USAE, Waterways Experiment Station
Coastal and Hydraulics Laboratory (CEWES-CR-O)
3909 Halls Ferry Road
Vicksburg, MS 39180
601-634-3999 FAX:601-634-4314
e-mail:m.miller@cerc.wes.army.mil

Dr. Erdal Safak
Research Structural Engineer
U.S. Geological Survey
Box 25046, MS 966
Denver Federal Center
Denver, CO 80225
303-273-8593 FAX:303-273-8600
email:safak@usgs.gov

Dr. John B. Scalzi
Program Director, Structures and Building Systems
National Science Foundation
4201 Wilson Blvd. - Room 545
Arlington, VA 22230
703-306-1361 FAX:703-306-0291
e-mail:jscalzi@nsf.gov

JAPAN-SIDE PANEL ON WIND AND SEISMIC EFFECTS MEMBERSHIP LIST

STEERING COMMITTEE MEMBERS

Dr. Yasutake Inoue
Chairman, Japan-side Panel on Wind and Seismic Effects
Director-General, Public Works Research Institute
Ministry of Construction
1, Asahi, Tsukuba-shi, Ibaraki-ken 305-0804
Tel: 0298-64-2211
Fax: 0298-64-2148
E-mail: y-inoue@pwri.go.jp

Dr. Michio Okahara
Secretary-General, Japan-side Panel on Wind and Seismic Effects
Director, Structure and Bridge Department
Public Works Research Institute
Ministry of Construction
1, Asahi, Tsukuba-shi, Ibaraki-ken 305-0804
Tel: 0298-64-2211
Fax: 0298-64-0565
E-mail: okahara@pwri.go.jp

Mr.Yoshitoki Hashimoto
Director, Disaster Countermeasure Office
Coast Administration Disaster Prevention Division
Ports and Harbors Bureau
Ministry of Transport
2-1-3, Kasumigaseki, Chiyoda-ku, Tokyo 100-0013
Tel: 03-3580-7021
Fax: 03-5511-8280

Dr. Hisahiro Hiraishi
Director, Structural Engineering Department
Building Research Institute
Ministry of Construction
1, Tatehara, Tsukuba-shi, Ibaraki-ken 305-0802
Tel: 0298-64-6633
Fax: 0298-64-6773
E-mail: hiraishi@kenken.go.jp

Dr. Susumu Iai
Director, Earthquake Disaster Prevention Laboratory
Port and Harbour Research Institute
Ministry of Transport
3-1-1, Nagase, Yokosuka-shi, Kanagawa-ken
239-0826
Tel: 0468-44-5030
Fax: 0468-44-0839
E-mail: iai@ipc.phri.go.jp

Dr. Keishi Ishimoto
Director, Structure Department
Civil Engineering Research Institute
Hokkaido Development Bureau
Prime Minister's Office
1-3, Hiragishi, Toyohira-ku, Sapporo-shi
Hokkaido 062-0931
Tel: 011-841-5175
Fax: 011-820-2714
E-mail: ishimoto@ceri.go.jp

Dr. Toshio Iwasaki
President, Civil Engineering Research Laboratory
1-18 Kandasuda-cho
Chiyoda-ku, Tokyo 101-0041
Tel: 03-3254-9481
Fax: 03-3254-9448

Dr. Takashi Kaminosono
Associate Director for International Codes and Standards
Codes and Evaluation Research Center
Building Research Institute
Ministry of Construction
1, Tatehara, Tsukuba-shi, Ibaraki-ken 305-0802
Tel:0298-64-6665
Fax:0298-64-6774
E-mail: kamino@kenken.go.jp

Dr. Kazumasa Kato
Director, Hydraulic Engineering Division
Port and Harbour Research Institute
Ministry of Transport
3-1-1, Nagase, Yokosuka-shi, Kanagawa-ken
239-0826
Tel: 0468-44-5009
Fax: 0468-41-3888

Mr. Shirou Kato
Director, Road Disaster Prevention Section
Road Bureau
Ministry of Construction
2-1-3, Kasumigaseki, Chiyoda-ku, Tokyo 100-0013
Tel: 03-3580-4311
Fax: 03-5251-1949
E-mail: katou0zv@road.hs.moc.go.jp

Prof. Kazuhiko Kawashima
Professor, Department of Civil Engineering
Tokyo Institute of Technology
2-12-1, O-okayama, Meguro-ku, Tokyo 152-0033
Tel: 03-5734-2922
Fax: 03-3729-0728
E-mail: kawasima@cv.titech.ac.jp

Mr. Osamu Matsuo
Head, Soil Dynamics Division
Earthquake Disaster Prevention Research Center
Public Works Research Institute
Ministry of Construction
1, Asahi, Tsukuba-shi, Ibaraki-ken 305-0804
Tel: 0298-64-2933
Fax: 0298-64-2576
E-mail: matsuo@pwri.go.jp

Mr. Chikahiro Minowa
Cooperative Research Officer
National Research Institute for Earth Science and Disaster Prevention
3-1, Tennodai, Tsukuba-shi, Ibaraki-ken 305-0006
Tel: 0298-51-1611
Fax: 0298-51-5658
E-mail: minowa@geo.bosai.gov.jp

Mr. Toshitaka Miyata
Director, International Affairs Division
Economic Affairs Bureau
Ministry of Construction
2-1-3, Kasumigaseki, Chiyoda-ku, Tokyo 100-0013
Tel: 03-3580-4311
Fax: 03-3502-3955
E-mail: miyat01e@econ.hs.moc.go.jp

Mr. Nobuo Nagai
Director, Geographic Department
Geographical Survey Institute
Ministry of Construction
1, Kitasato, Tsukuba-shi, Ibaraki-ken 305-0811
Tel:0298-64-1111
Fax:0298-64-1804

Dr. Nobuyuki Narita
President, Japan Steel Structure Corporation
3-3-1, Marunouthi, Chiyoda-ku, Tokyo 100-0005
Tel: 03-3212-0875
Fax: 03-3212-0878

Mr. Kazuhiro Nishikawa
Head, Bridge Division
Structure and Bridge Department
Public Works Research Institute
Ministry of Construction
1, Asahi, Tsukuba-shi, Ibaraki-ken 305-0804
Tel: 0298-64-2905
Fax: 0298-64-0565
E-mail: knishikawa@pwri.go.jp

Dr. Isao Nishiyama
Head, Housing Construction Division
Production Department
Building Research Institute
Ministry of Construction
1, Tatehara, Tsukuba-shi, Ibaraki-ken 305-0802
Tel: 0298-64-2151
Fax: 0298-64-6774
E-mail: isao@kenken.go.jp

Mr. Fumiaki Nomura
Office for Disaster Prevention Research
Research and Development Bureau
Science and Technology Agency
Prime Minister's Office
2-2-1, Kasumigaseki, Chiyoda-ku, Tokyo 100-0013
Tel: 03-3503-8164
Fax: 03-3503-8169

Mr. Tomiyoshi Ogawa
Director, Building Disaster Prevention Section
Housing Bureau
Ministry of Construction
2-1-3, Kasumigaseki, Chiyoda-ku, Tokyo 100-0013
Tel: 03-3580-4311
Fax: 03-3580-7050
E-mail: ogawa0a2@house.hs.moc.go.jp

Mr. Keiichi Ohtani
Director, Disaster Prevention Research Division
National Research Institute for Earth Science and Disaster Prevention
Science and Technology Agency
3-1, Tennodai, Tsukuba-shi, Ibaraki-ken 305-0006
Tel: 0298-51-1611 ex.321
Fax: 0298-52-8512
E-mail: ohtani@knetgk.k-net.bosai.go.jp

Dr. Hisashi Okada
Associate Director for Composite Structures
Structural Engineering Department
Building Research Institute
Ministry of Construction
1, Tatehara, Tsukuba-shi, Ibaraki-ken 305-0802
Tel: 0298-64-6641
Fax: 0298-64-6773
E-mail: okada@kenken.go.jp

Prof. Tsuneo Okada
Professor, Department of Architecture and Building Engineering
Shibaura Institute of Technology
3-9-14 Shibaura, Minato-ku, Tokyo 108-0023
Tel: 03-5476-2452
Fax: 03-5476-2446

Dr. Izuru Ohkawa
Head, Construction Techigues Division
Production Department
Building Research Institute
Ministry of Construction
1, Tatehara, Tsukuba-shi, Ibaraki-ken 305-0802
Tel: 0298-64-2151
Fax: 0298-64-6777
E-mail: okawa@kenken.go.jp

Mr. Kazuo Okayama
Director, Earthquake Disaster Countermeasure Division
Disaster Prevention Bureau
National Land Agency
1-2-2, Kasumigaseki, Chiyoda-ku, Tokyo 100-0013
Tel: 03-3593-3311
Fax: 03-3501-5199

Dr. Hiroshi Sato
Head, Structure Division
Structure and Bridge Department
Public Works Research Institute
Ministry of Construction
1, Asahi, Tsukuba-shi, Ibaraki-ken 305-0804
Tel: 0298-64-2874
Fax: 0298-64-0565
E-mail: hsato@pwri.go.jp

Dr. Takahiro Sugano
Chief, Structural Dynamics Laboratory
Structural Engineering Division
Port and Harbour Research Institute
Ministry of Transport
3-1-1, Nagase, Yokosuka-shi, Kanagawa-ken
239-0826
Tel: 0468-44-5029
Fax: 0468-44-0839
E-mail: macsuga@ipc.phri.go.jp

Dr. Hideki Sugita
Head, Earthquake Disaster Prevention Technology Division
Earthquake Disaster Prevention Research Center
Public Works Research Institute
Ministry of Construction
1, Asahi, Tsukuba-shi, Ibaraki-ken 305-0804
Tel: 0298-64-3245
Fax: 0298-64-0598
E-mail: sugita@pwri.go.jp

Mr. Kenichi Takahashi
International Cooperation Coordinator, International Affairs Division,
Science and Technology Promotion Bureau
Science and Technology Agency
2-2-1, Kasumigaseki, Chiyoda-ku, Tokyo 100-0013
Tel: 03-3593-0362
Fax: 03-3501-5909
E-mail: katakaha@sta.go.jp

Mr. Masaaki Takeuchi
Senior Assistant for Disaster Prevention Planning Division
Administration Department
Japan Meteorological Agency
1-3-4, Ohte-machi, Chiyoda-ku, Tokyo 100-0013
Tel: 03-3212-8341
Fax: 03-3212-2453

Dr. Keiichi Tamura
Head, Ground Vibration Division
Earthquake Disaster Prevention Research Center
Public Works Research Institute
Ministry of Construction
1, Asahi, Tsukuba-shi, Ibaraki-ken 305-0804
Tel: 0298-64-2926
Fax: 0298-64-0598
E-mail: tamura@pwri.go.jp

Dr. Masaomi Teshigawara
Head, Structure Division
Department of Structural Engineering
Building Research Institute
Ministry of Construction
1, Tatehara, Tsukuba-shi, Ibaraki-ken 305-0802
Tel: 0298-64-6753
Fax: 0298-64-6773
E-mail: teshi@kenken.go.jp

Mr. Kenichi Torii
Head, Coast Division
River Department
Public Works Research Institute
Ministry of Construction
1, Asahi, Tsukuba-shi, Ibaraki-ken 305-0804
Tel: 0298-64-2211
Fax: 0298-64-1168
E-mail: torii@pwri.go.jp

Dr. Takaaki Uda
Director, River Department
Public Works Research Institute
Ministry of Construction
1, Asahi, Tsukuba-shi, Ibaraki-ken 305-0804
Tel: 0298-64-2211
E-mail: uda@pwri.go.jp

Mr. Tsuneo Uesaka
Director, Dam Department
Public Works Research Institute
Ministry of Construction
1, Asahi, Tsukuba-shi, Ibaraki-ken 305-0804
Tel: 0298-64-2211
Fax: 0298-64-2688
E-mail: t_uesaka@pwri.go.jp

Dr. Shigeki Unjoh
Head, Earthquake Engineering Division
Earthquake Disaster Prevention Research Center
Public Works Research Institute
Ministry of Construction
1, Asahi, Tsukuba-shi, Ibaraki-ken 305-0804
Tel: 0298-64-4966
Fax: 0298-64-4424
E-mail: unjoh@pwri.go.jp

Dr. Tatsuo Uwabe
Director, Structural Engineering Division
Port and Harbour Research Institute
Ministry of Transport
3-1-1, Nagase, Yokosuka-shi, Kanagawa-ken
239-0826
Tel: 0468-44-5027
Fax: 0468-44-4095
E-mail: uwabe@ipc.phri.go.jp

Dr. Makoto Watabe
2-25-5, Tokiwadai, Itabashi-ku, Tokyo 174-0071
Tel: 03-3960-0374

Mr. Shoin Yagi
Director, Typhoon Research Department
Meteorological Research Institute
Japan Meteorological Agency
1-1, Nagamine, Tsukuba-shi, Ibaraki-ken 305-0052
Tel: 0298-53-8663
Fax: 0298-53-8735

Dr. Hiroyuki Yamanouchi
Director, Codes and Evaluation Research Center
Building Research Institute
Ministry of Construction
1, Takehara, Tsukuba-shi, Ibaraki-ken 305-0802
Tel: 0298-64-6688
Fax: 0298-64-67701
E-mail: yamanoch@kenken.go.jp

Mr. Joji Yanagawa
Director, Disaster Management Division
River Bureau
Ministry of Construction
2-1-3, Kasumigaseki, Chiyoda-ku, Tokyo 100-0013
Tel: 03-3580-4311 Ext. 3431
Fax: 03-5251-1946
E-mail: yanag0an@river.hs.moc.go.jp

Dr. Masahiko Yasuda
Director, Earthquake Disaster Prevention Research
Center
Public Works Research Institute
Ministry of Construction
1, Asahi, Tsukuba-shi, Ibaraki-ken 305-0804
Tel: 0298-64-2829
Fax: 0298-64-0598
E-mail: m-yasuda@pwri.go.jp

Dr. Akio Yoshida
Director, Seismology and Volcanology
Research Department
Meteorological Research Institute
Japan Meteorological Agency
1-1, Nagamine, Tsukuba-shi, Ibaraki-ken 305-0052
Tel: 0298-53-8675
Fax: 0298-53-8735

Mr. Hitoshi Yoshida
Head, Fill-type Dam Division
Dam Department
Public Works Research Institute
Ministry of Construction
1, Asahi, Tsukuba-shi, Ibaraki-ken 305-0804
Tel: 0298-64-2413
Fax: 0298-64-0164
E-mail: h-yshida@pwri.go.jp

SECRETARIES COMMITTEE MEMBERS

Dr. Michio Okahara
Secretary-General, Japan-side Panel on Wind and Seismic Effects
Director, Structure and Bridge Department
Public Works Research Institute
Ministry of Construction
1, Asahi, Tsukuba-shi, Ibaraki-ken 305-0804
Tel: 0298-64-2211
Fax: 0298-64-0565
E-mail: okahara@pwri.go.jp

Mr. Jiro Fukui
Head, Foundation Engineering Division
Structure and Bridge Department
Public Works Research Institute
Ministry of Construction
1, Asahi, Tsukuba-shi, Ibaraki-ken 305-0804
Tel: 0298-64-2211
Fax: 0298-64-0565
E-mail: fukui @pwri.go.jp

Dr. Hisahiro Hiraishi
Director, Structural Engineering Department
Building Research Institute
Ministry of Construction
1, Tatehara, Tsukuba-shi, Ibaraki-ken 305-0802
Tel: 0298-64-6633
Fax: 0298-64-6773
E-mail: hiraishi@kenken.go.jp

Dr. Susumu Iai
Chief, Geotechnical Earthquake Engineering Laboratory
Port and Harbour Research Institute
Ministry of Transport
3-1-1, Nagase, Yokosuka-shi, Kanagawa-ken 239-0826
Tel: 0468-44-5030
Fax: 0468-44-0839
E-mail: iai@cc.phri.go.jp

Dr. Masanori Iiba
Head, Aerodynamics Division
Structural Engineering Department
Building Research Institute
Ministry of Construction
1, Tatehara, Tsukuba-shi, Ibaraki-ken 305-0802
Tel: 0298-64-6654
Fax: 0298-64-6773
E-mail: iiba@kenken.go.jp

Mr. Kenji Ikeda
Director, Structures Division
Structures Department.
Civil Engineering Research Institute
Hokkaido Development Bureau
Prime Minister's Office
1-3, Hiragishi, Toyohira-ku, Sapporo-shi
Hokkaido 062-0931
Tel: 011-841-1111
Fax: 011-820-2714
E-mail: ikedak@ceri.go.jp

Prof. Kazuhiko Kawashima
Professor, Department of Civil Engineering
Tokyo Institute of Technology
2-12-1 O-okayama, Meguro-ku Tokyo 152-0033
Tel: 03-5734-2922
Fax: 03-3729-0728
E-mail: kawasima@cv.titech.ac.jp

Mr. Hiromichi Maruyama
Head, Planning Division
Geographic Department
Geographical Survey Institute
Ministry of Construction
1, Kitasato, Tsukuba-shi, Ibaraki-ken 305-0811
Tel: 0298-64-1111
Fax: 0298-64-1804
E-mail: maruyama@gsi-mc.go.jp

Mr. Osamu Matsuo
Head, Soil Dynamics Division
Earthquake Disaster Prevention Research Center
Public Works Research Institute
Ministry of Construction
1, Asahi, Tsukuba-shi, Ibaraki-ken 305-0804
Tel: 0298-64-2933
Fax: 0298-64-2576
E-mail: matsuo@pwri.go.jp

Mr. Chikahiro Minowa
Cooperative Research Officer
National Research Institute for Earth Science and Disaster Prevention
3-1, Tennodai, Tsukuba-shi, Ibaraki-ken 305-0006
Tel: 0298-51-1611
Fax: 0298-51-5658
E-mail: minowa@geo.bosai.gov.jp

Mr. Akiyoshi Mukai
Head, Testing and Evaluation Division
Codes and Evaluation Research Center
Building Research Institute
Ministry of Construction
1, Tatehara, Tsukuba-shi, Ibaraki-ken 305-0802
Tel: 0298-64-6643
Fax: 0298-64-6770

Mr. Kazuhiro Nishikawa
Head, Bridge Division
Structure and Bridge Department
Public Works Research Institute
Ministry of Construction
1, Asahi, Tsukuba-shi, Ibaraki-ken 305-0804
Tel: 0298-64-2905
Fax: 0298-64-0565
E-mail: knishika@pwri.go.jp

Dr. Nobuyuki Ogawa
Head, Earthquake Engineering Laboratory
National Research Institute for Earth Science and Disaster Prevention
Science and Technology Agency
3-1, Tennodai, Tsukuba-shi, Ibaraki-ken 305-0006
Tel: 0298-51-1611
Fax: 0298-51-5658
E-mail: ogawa@geo.bosai.go.jp

Mr. Keiichi Ohtani
Director, Disaster Prevention Research Division
National Research Institute for Earth Science and Disaster Prevention
Science and Technology Agency
3-1, Tennodai, Tsukuba-shi, Ibaraki-ken, 305-0006
Tel: 0298-51-1611 Ext. 321
Fax: 0298-52-8512
E-mail: ohtani@knetgk.k-net.bosai.go.jp

Dr. Hisashi Okada
Associate Director for Composite Structures
Structural Engineering Department
Building Research Institute
Ministry of Construction
1, Tatehara, Tsukuba-shi, Ibaraki-ken 305-0802
Tel: 0298-64-6641
Fax: 0298-64-6773
E-mail: okada@kenken.go.jp

Mr. Masami Okada
Head, The First Research Laboratory
Seismology and Volcanology Research Department
Meteorological Research Institute
Japan Meteorological Agency
Ministry of Transport
1-1, Nagamine, Tsukuba-shi, Ibaraki-ken 305-0052
Tel: 0298-51-3730
Fax: 0298-53-8735

Dr. Hiroshi Sato
Head, Structure Division
Structure and Bridge Department
Public Works Research Institute
Ministry of Construction
1, Asahi, Tsukuba-shi, Ibaraki-ken 305-0804
Tel: 0298-64-2874
Fax: 0298-64-0565
E-mail: hsato@pwri.go.jp

Mr. Masaya Sato
Director, Research Planning and Coordination Section, Administration Division
Civil Engineering Research Institute
Hokkaido Development Bureau
Prime Minister's Office
1-3, Hiragishi, Toyohira-ku, Sapporo-shi
Hokkaido 062-0931
Tel: 011-841-1111
Fax: 011-820-2714

Dr. Takahiro Sugano
Chief, Structural Dynamics Laboratory
Structural Engineering Division
Port and Harbour Research Institute
Ministry of Transport
3-1-1, Nagase, Yokosuka-shi, Kanagawa-ken
239-0826
Tel: 0468-44-5029
Fax: 0468-44-0839
E-mail: macsuga@ipc.phri.go.jp

Dr. Hideki Sugita
Head, Earthquake Disaster Prevention Technology Division
Earthquake Disaster Prevention Research Center
Public Works Research Institute
Ministry of Construction
1, Asahi, Tsukuba-shi, Ibaraki-ken 305-0804
Tel: 0298-64-3245
Fax: 0298-64-0598
E-mail: sugita@pwri.go.jp

Dr. Keiichi Tamura
Head, Ground Vibration Division
Earthquake Disaster Prevention Research Center
Public Works Research Institute
Ministry of Construction
1, Asahi, Tsukuba-shi, Ibaraki-ken 305-0804
Tel: 0298-64-2926
Fax: 0298-64-0598
E-mail: tamura@pwri.go.jp

Mr. Kenichi Torii
Head, Coast Division
River Department
Public Works Research Institute
Ministry of Construction
1, Asahi, Tsukuba-shi, Ibaraki-ken 305-0804
Tel: 0298-64-2327
Fax: 0298-64-1168
E-mail: sato@pwri.go.jp

Mr. Nobuyuki Tsuneoka
Head, International Cooperation Division
Planning and Research Administration Department
Public Works Research Institute
Ministry of Construction
1, Asahi, Tsukuba-shi, Ibaraki-ken 305-0804
Tel: 0298-64-4412
Fax: 0298-64-4322
E-mail: tsuneoka@pwri.go.jp

Dr. Shigeki Unjoh
Head, Earthquake Engineering Division
Earthquake Disaster Prevention Research Center
Public Works Research Institute
Ministry of Construction
1, Asahi, Tsukuba-shi, Ibaraki-ken 305-0804
Tel: 0298-64-4966
Fax: 0298-64-4424
E-mail: unjoh@pwri.go.jp

Dr. Masahiko Yasuda
Director, Earthquake Disaster Prevention Research Center
Public Works Research Institute
Ministry of Construction
1, Asahi, Tsukuba-shi, Ibaraki-ken 305-0804
Tel: 0298-64-2829
Fax: 0298-64-0598
E-mail: yokoyama@pwri.go.jp

Mr. Hitoshi Yoshida
Head, Fill-type Dam Division
Dam Department
Public Works Research Institute
Ministry of Construction
1, Asahi, Tsukuba-shi, Ibaraki-ken 305-0804
Tel: 0298-64-2413
Fax: 0298-64-0164
E-mail: h-yshida@pwri.go.jp

TEMPORARY MEMBERS

Mr. Fuminori Kato
Research Engineer
Coast Division, River Department
Public Works Research Institute
Ministry of Construction
1, Asahi, Tsukuba-shi, Ibaraki-ken 305-0804
Tel: 0298-64-3163
Fax: 0298-64-1168
E-mail: kato@pwri.go.jp

Mr. Hiroyasu Kawai
Senior Research Engineer
Hydraulic Engineering Division
Port and Harbour Research Institute
Ministry of Transport
3-1-1, Nagase, Yokosuka-shi, Kanagawa-ken
239-0826
Tel: 0468-44-5063
Fax: 0468-41-3888

Mr. Hitomitu Kikitsu
Research Engineer
Aerodynamic Division
Structural Department
Building Research Institute
Ministry of Construction
1, Tatehara, Tsukuba-shi, Ibaraki-ken 305-0802
Tel: 0298-64-6623
Fax: 0298-64-6773

Mr. Takaharu Kiriyama
Deputy Director
Earthquake Disaster Countermeasure Division
Disaster Prevention Bureau
National Land Agency
1-2-2, Kasumigaseki, Chiyoda-ku, Tokyo 100-8972
Tel: 03-3593-3311
Fax: 03-3501-5199

Mr. Mitsumasa Midorikawa
Director, International Institute of Seismology and
Earthquake Engineering
Building Research Institute
Ministry of Construction
1, Tatehara, Tsukuba-shi, Ibaraki-ken 305-0802
Tel: 0298-64-6648
Fax: 0298-64-6777

Mr. Takashi Satou
Engineer
Structures Section
Structures Division
Civil Engineering Research Institute
Hokkaido Development Bureau
1-3, Hiragishi, Toyohira-ku, Sapporo,
062-8602 Japan
Tel: 011-841-1111
Fax: 011-820-2714

Dr. Keishi SHIONO
Assistant Professor
Nagaoka National College of Technology
888 Nishikatagaicyou, Nagaoka-shi, Niigata-ken,
940-8432 Japan
Tel: 0258-32-6435
Fax: 0258-34-9700
E-mail: kshiono@nagaoka-ct.ac.jp

Mr. Yasuo Sekita
Assistant Director
Earthquake and Tsunami Observations Division,
Seismological and Volcanological Department,
Japan Meteorological Agency
1-3-4, Otemachi, Chiyoda-ku, Tokyo, 100-8122
Japan
Tel: 03-3211-8341 Ext. 4555
Fax: 03-3215-2963
E-mail: sekita@met.kishou.go.jp

Mr. Shuji Tamura
Engineer
Disaster Prevention Research Division
National Research Institute for Earth Science and
Disaster Prevention
Science and Technology Agency
3-1, Tennodai, Tsukuba-shi, Ibaraki-ken 305-0006
Tel: 0298-51-1611
Fax: 0298-52-8512

Mr. Yoshinobu Tanaka
The Second Research Division
Typhoon Research Department
Meteorological Research Institute
Japan Meteorological Agency
1-1, Nagamine, Tsukuba-shi, Ibaraki-ken 305-0052
Tel: 0298-53-8663
Fax: 0298-53-8735

Mr. Yasuhiko Wakizaka
Head, Geology Division,
Environment Department
Public Works Research Institute
Ministry of Construction
1, Asahi, Tsukuba-shi, Ibaraki-ken, 305-0804
Tel: 0298-64-2245
Fax: 0298-64-7183

Mr. Haruo Yoneyama
Senior Research Engineer
Structural Engineering Division
Port and Harbour Research Institute
Ministry of Transport
3-1-1, Nagase, Yokosuka-shi, Kanagawa-ken
239-0826
Tel: 0468-44-5032
Fax: 0468-44-4161

ASSOCIATE MEMBERS

Dr. Minoru Fujiwara
President, Strait Crossing Highway Research Association
1-4-13, kyobashi, chuo-ku,Tokyo 104-0031
Tel: 03-3245-9840
Fax: 03-3245-9844

Dr. Masami Fukuoka
President, Management Systemassessment Center,
2-17-7, Kyoubashi, Chuo-ku
Tokyo 104-0031
Tel:03-3535-4021
Fax: 03-3535-4024

Dr. Masaya Hirosawa
Professor, Kogakuin University
1-24-2-91, Nishi-shinjuku, Shinjuku-ku, Tokyo 163-0023
Tel: 03-3342-1211
Fax: 03-3340-0149

Dr. Shiro Ibukiyama
President, Kogyokusha College of Technology5-14-2, Nishigotanda, Shinagawa-ku
Tokyo 141-0031
Tel: 03-3493-5671
Fax: 03-3495-4071

Dr. Kaoru Ichihara
Adviser, Central Consul Tant Inc.
2-16-2, Minami-Kamata, Ohta-ku
Tokyo 144-0035
Tel:03-5703-6161
Fax:03-5703-6151

Dr. Ryuichi Iida
President, Japan Dam Engineering Center
2-4-5, Azabudai, Minato-ku, Tokyo 106-0041
Tel: 03-3433-7811
Fax: 03-3432-6204

Dr. Takashi Iijima
President, Sekisui-jushi Co., Ltd.
1-11-1, Kaigan, Minato-ku, Tokyo 105-0022
Tel: 03-5400-1801
Fax: 03-5400-1805

Dr. Toshio Iwasaki
President, Civil Engineering Research Laboratory
1-18 Kandasuda-cho,Chiyoda-ku, Tokyo 101-0041
Tel: 03-3254-9481
Fax: 03-3254-9448

Mr. Shunichiro Kamijo
President, Mitsui Construction Corporation,
1-2-3, Ohte-machi, Chiyoda-ku,
Tokyo 100-0004
Tel: 03-5223-3915
Fax: 03-5223-3920

Mr. Kenji Kawakami
Adviser, Kubota Corporation
3-1-3, Nihonbashi-muromachi, Cyuoh-ku, Tokyo 103-0022
Tel: 03-3245-3660
Fax: 03-3245-3454

Prof. Eiichi Kuribayashi
Professor, Toyohashi University of Technology
1-1, Hibarigaoka, Tenpaku-cho, Toyohashi-shi
Aichi-ken 441-8122
Tel: 0532-44-6967
Fax: 0532-44-6831

Mr. Mitsuru Nagao
President, Japan Construction Mechanization Association
3-5-8, Shibakoen, Minato-ku, Tokyo 105-0011
Tel: 03-3433-1501
fax: 03-3432-0289

Prof. Kiyoshi Nakano
979-66, Kumada, Minaminasu-machi, Nasu-gun, Tochigi-ken
Tel: 0287-88-0022

Dr. Kazuto Nakazawa
President, Regional Development Consultants Inc.
2-7-6, Higashi-Ueno, Taitou-ku,
Tokyo 110-0015
Tel: 03-3831 -2916
Fax: 03-3836-4048

Dr. Nobuyuki Narita
President, Japan Steel Structure Corporation
3-3-1, Marunouthi, Chiyoda-ku,
Tokyo 100-0005
Tel: 03-3212-0875
Fax: 03-3212-0878

Dr.Setuo Noda
President, Coastal Development Institute of Technology
3-16, Hayabusa-cho, Chiyoda-ku, Tokyo 102-0092
TEl: 03-3234-5861
fax: 03-3234-5877

Dr. Shin Okamoto
Central Research Institute for Construction Tehchnology
Japan Association of Representative General Contractors
1-6-34, Kounan, Minato-ku, Tokyo 108-0075
Tel: 03-3458-1011
Fax: 03-3458-6321

Mr. Yoshijiro Sakagami
Receive, Japan Development Construction Corporation,
4-9-9, Akasaka, Minato-ku, Tokyo 107-0052
Tel: 03-5410-5730
Fax: 03-3403-9039

Dr. Tadahiko Sakamoto
President, Japan Dam Engineering Center
2-4-5, Azabudai, Minato-ku, Tokyo 106-0041
Tel: 03-3433-7811
Fax: 03-3432-6204

Prof. Yasushi Sasaki
Professor, Department of Civil and Environmental Engineering
Hiroshima University
1-4-1, Kagamiyama, Higashihiroshima-shi,
Hiroshima-ken 739-0046
Tel: 0824-24-7783
Fax: 0824-24-7783
E-mail: ysasaki@ue.ipc.hiroshima-u.ac.jp

Dr. Yukihiko Sumiyoshi
Executive Counselor, Nippon Steel Co., Ltd.
2-6-3, Ohte-machi, Chiyoda-ku,
Tokyo 100-0004
Tel: 03-3275-5868
Fax:03-3275-5636

Mr. Jiro Taguchi
President, Construction Research Institure
11-8, Ohdenma-chou, Nihonbashi, Chuo-ku,
Tokyo 103-0011
Tel: 03-3663-2411
Fax: 03-3633-2417

Dr. Hiroshi Takahashi
4-22-1, Nishihara-machi, Fuchuu-shi, Tokyo
183-0046
Tel: 0425-72-3227

Dr. Masateru Tominaga
President, Public Works Research Center
1-6-4, Taito, Taito-ku, Tokyo 110-0016
Tel: 03-3835-3609
Fax: 03-3275-5648

Dr. Hajime Tsuchida
Executive Counselor, Nippon Steel Co., Ltd.
2-6-3, Ohte-machi, Chiyoda-ku, Tokyo 100-0004
Tel: 03-3275-5894
Fax: 03-3275-5648

Mr.Seizo Tsuji
Adviser, Road Management Technology Center
2-3-21, Kouraku, Bunkyou-ku,Tokyo 112-0004
Tel: 03-5803-7011
Fax: 03-5803-7020

Dr. Makoto Watabe
2-25-5, Tokiwadai, Itabashi-ku, Tokyo 174-0071
Tel: 03-3960-0374

Prof. Kouichi Yokoyama
Professor, Urban and Civil Engineering
Faculty of Engineering, Ibaraki University
4-12-1, Nakanarisawa-machi, Hitachi-shi,
Ibaraki-ken 316-8511
Tel: 0294-38-5161
Fax: 0294-35-8146

List of Task Committee Members

TASK COMMITTEE MEMBERSHIP LIST

TASK COMMITEE	U.S. Side	Japan Side
A. Strong-Motion Data and Applications Applications	*R. D. Borcherdt	*S. Iai
	C. J. Astill	Y. Ichii
	M. K. Celebi	M. Miyata
	W. B. Joyner	E. Mochizuki
	F. G. Mclean	N. Nagai
	C. S. Barrientos	Y. Nakao
	T. K. Lew	I. Okawa
	E. Safak	K. Ohtani
	J. Kimball	M. Satoh
	J. Hunt	K. Tamura
	W. Freeborne	H. Yamanouchi
	J. Ake	
B. Testing and Evaluation Procedures for Building Systems	*H. S. Lew	*K. Ohtani
	V. P. Chiarito	T. Fukuda
	J. E. Sabadell	T. Kaminosono
	C. E. Smith	T. Morino
	K. Abrol	S. Nakata
	S. Sweeney	I. Nishiyama
	W. Freedorne	H. Noguchi
		A. Tanaka
		A. Wada

C. High Performance Structural Systems and Auto-Adaptive Medis	*G. Lee	*H. Hiraishi
	#M. Bruneau	H. Fukuyama
	H. S. Lew	T. Kaminosono
	T. K. Lew	A. Mukai
	H. D. Nickerson	M. Nakajima
	D. H. Oh	K. Nishikawa
	M. A. Phipps	I. Nishiyama
	J. B. Scalzi	S. Otani
	S. Woodson	M. Okahara
	S. A. Asar	H. Shiobara
	M. K. Celebi	M. Teshigawara
	K. L. Abrol	S. Unjoh
	R. L. Hall	A. Wada
	K. Mutreja	
	P. Brady	
	W. Freeborne	
	S. C. Liu	
D. Earthquake Engineering for Dams	*R. L. Hall	*H. Yoshida
	W. E. Roper	T. Fujono
	F. G. Mclean	M. Sumitani
	L. G. Guthrie	J. Inomata
	R. Davidson	T. Iwashita
	M. E. Hynes	J. Kashiwai
	A. G. Franklin	I. Nagayama
	R. Navidi	S. Nakamura
	L. Von Thun	T. Ohmachi
	W. Allerton	Y. Ohne
		T. Sasaki
		S. Takasu
		J. Tamura
		M. Toyata
		T. Uesaka
		Y. Wakisaka
		K. Watanabe
		T. Wadanabe
		A. Yamaguchi
		Y. Yamaguchi

E. Design for Wind and Wind Hazard Mitigation	*J. Golden	*T. Okada
	B. Bienkiewicz	*H. Satoh
	H. Bousch	N. Furuya
	G. Chiu	H. Kikitsu
	W. Freeborne	Y. Kimura
	A. Kareem	N. Kinoshita
	H. S. Lew	T. Mabuchi
	K. Mehta	G. Naitoh
	D. Reed	H. Shirado
	T. Reinhold	T. Tamura
	C. Smith	Y. Tamura
	P. Tertell	Y. Uematsu
	A. Chiu	H. Yamada
	M. Mahoney	M. Yagi
F. Disaster Prevention Methods for Lifeline Systems	C. J. Astill	*M. Yasuda
	M. K. Celebi	M. Hamada
	#J. D. Cooper	J. Hoshikuma
	G. Al-Chaar	K. Fujihashi
	T. K. Lew	Y. Inoue
	J. B. Scalzi	Y. Kajiya
	S. Wu	H. Kameda
	S. Sommer	T. Katayama
		A. Kinoshita
		O. Matsuo
		K. Miyamoto
		Y. Nakao
		N. Ogawa
		M. Ozaki
		K. Shimamura
		S. Takada
		K. Tamura
		J. Tohma
		S. Unjoh
		T. Uwabe
		H. Sugita
		K. Yokoyama

G. Seismic Information Systems	*S. Nishenko	*K. Okayama
	*W. Roper	*H. Sugita
	H. Benz	H. Itoh
	R. Borcherdt	I. Okawa
	M. Celebi	K. Ohtani
	R. Eisner	A. Kimura
	W. Ellsworth	T. Kiriyama
	W. Hays	A. Nagai
	H. S. Lew	T. Nozaki
	P. Ward	A. Nozu
	T. Ahern	H. Masaharu
	R. Eguchi	H. Yamanouchi
	J. Goltz	T. Yokoi
	S. Lawson	K. Ogawa
	D. Simpson	Y. Murakami
H. Soil Behavior and Stability During Earthquakes	*M. E. Hynes	*O. Matsuo
	C. J. Astill	J. Fukui
	R. D. Borcherdt	S. Iai
	C. Y. Chen	M. Iiba
	F. G. Mclean	H. Kobayashi
	C. E. Smith	J. Koseki
	R. M. Chung	C. Minowa
	#M. Sharp	J. Nishikawa
		M. Okamura
		T. Sugano
		H. Suzuki
		K. Tamura
		I. Tohata
		J. Tohma
		K. Fujihashi
		S. Yasuda
		K. Yokoyama
		H. Yoshida
		K. Zen

I. Storm Surge and Tsunami	*M. Blackford	*K. Torii
	C. J Astill	T. Hayashi
	C. S. Barrientos	T. Gotoh
	E. N. Bernard	S. Iwasaki
	J. Lander	K. Kawata
	W. E. Roper	T. Onishi
	A. M. Hittelman	T. Nagai
		T. Nakayama
		K. Katoh
		M. Okada
		K. Satake
		N. Syutoh
		T. Yamashita
J. Wind and Earthquake Engineering for Transportation Systems	*J. D. Cooper	*K. Nishikawa
	J. B. Scalzi	Y. Fujino
	J. H. Gates	N. Furuya
	H. S. Lew	J. Fukui
	W. P. Yen	K. Ikeda
	H. R. Bosch	K. Kawashima
		M. Kitazawa
		T. Moritani
		Y. Nakao
		M. Okahara
		H. Satoh
		T. Sumitani
		H. Takano
		Y. Tanaka
		K. Tamura
		S. Unjoh
		M. Yasuda

K. Wind and Earthquake Engineering for Offshore and Coastal Systems	*C. E. Smith	*T. Sugano
	C. S. Barrientos	J. Fukui
	W. E. Roper	S. Iai
	J. E. Sabadell	M. Kazama
	M. C. Miller	S. Noda
	M. K. Celebi	A. Notsu
		M. Okada
		H. Shiojiri
		H. Tsuchida
		T. Uwabe
		Y. Yoshida

* Chairman

\# Acting Task Committee Chairman for the 31st Joint Meeting

Resolutions

RESOLUTIONS OF THE THIRTY-FIRST JOINT MEETING
U.S.-JAPAN PANEL ON WIND AND SEISMIC EFFECTS (UJNR)
Public Works Research Institute, Tsukuba, Japan
11-14 May 1999

The following resolutions are hereby adopted:

1. The Thirty-First Joint Panel Meeting provided the forum to exchange valuable technical information that is beneficial to both countries. In view of the importance of cooperative programs on the subject of wind and seismic effects, the continuation of Joint Panel Meetings is considered essential. Both sides agreed to explore new ideas and areas to strengthen cooperative activities in support of the Panel's mission.

2. The following activities have been conducted since the Thirtieth Joint Meeting:

a. Technology Exchanges. Technical experts, technical documents, and applications of the electronic media have been exchanged. These exchanges have contributed to the development of new research programs and enhanced ongoing research in both countries.

b. Task Committee Workshops. The Panel held eight workshops, symposia, or committee meetings; approximately 400 specialists from both countries participated in these activities:

1. Task Committee (A), 1st U.S.-Japan Workshop on Soil-Structure Interaction, 22-23 September 1998, Menlo Park, CA, USA.
2. Task Committee (B&C), 20-year Commemoration Symposium on Cooperative Earthquake Engineering Research, 9 October 1998, Tokyo, Japan.
3. Task Committee (B&C), 5th U.S.-Japan Joint Technical Coordinating Committee Meeting on Composite and Hybrid Structural Systems, 5-7 October 1998, Tokyo, Japan.
4. Task Committee (B&C), U.S.-Japan Workshop on Auto-Adaptive Media (Smart Structural Systems), 17-20 May 1998, Sonoma, CA, USA.
5. Task Committee (D), 2nd Workshop on Earthquake Engineering for Dams, 7-8 May 1999, Tokyo, Japan.
6. Task Committee (H), 5th U.S.-Japan Workshop on Geotechnical Earthquake Engineering, 28-29 September 1998, Tsukuba, Japan.
7. Task Committee (I), 5th Tsunami Workshop, 9-11 July 1998, Sapporo, Japan.
8. Task Committee (J), 14th Bridge Workshop, 3-4 November 1998, Pittsburgh, PA, USA.

c. Common Agenda. The Panel recognizes the importance of providing earthquake science and technology expertise to the 17 April 1996 U.S.-Japan Natural Disaster Reduction Initiative of the U.S.-Japan Framework for New Economic Partnership (Common Agenda). Panel members organized and participated in the First High-Level U.S.-Japan Earthquake Policy Cooperation Forum, 20-22 October, 1998, Seattle, Washington, USA. The Panel will

continue to provide, in close cooperation with the Earthquake Disaster Mitigation Partnership, technical leadership and participation in the Second High-Level Forum Meeting that will address four themes: 1. Use of Early Transmission and Gathering Systems for Earthquake and Earthquake-damage Information; 2. Programs to reduce Earthquake Damage to Structures; 3. Post-Earthquake Emergency Response Activities; 4: Long-Term Recovery Strategies and Programs. Appropriate Task Committees will respond to the Common Agenda in planning their work.

3. The Panel approved the Task Committee reports presented during the 31st Joint Panel Meeting. Each report included objectives, scope of work, accomplishments, future plans, and other information. The Panel will continue to review the Task Committees' progress toward meeting their objectives; consolidating, eliminating, and/or creating Task Committees as desirable.

4. The Panel endorses the following eight (8) proposed Task Committee Workshops or Committee Meetings during the coming year:
   a. Task Committee (B), 6th U.S.-Japan Joint Technical Coordinating Committee Meeting on Composite and Hybrid Structural Systems, August 1999, San Francisco, USA.
   b. Task Committee (B), U.S.-Japan Workshop on Test Procedure, Documentation, Retrieval of Test Data, and Experimental Facilities, in conjunction with the 32nd Joint Panel Meeting, USA.
   c. Task Committee (C), 1st U.S.-Japan Technical Coordinating Committee Meeting on Auto-Adaptive Media (Smart Structural Systems), Fall 1999, USA.
   d. Task Committee (E), 2nd U.S.-Japan Workshop on Design for Wind and Wind Hazard Mitigation, 24-26 May 1999, Tsukuba, Japan.
   e. Task Committee (F), upon appointment of the U.S. - side Chair, plan and conduct the 8th Workshop on Earthquake Disaster Prevention for Lifeline Systems
   f. Task Committee (G), 1st U.S.-Japan Workshop on Seismic Information Systems, Fall 1999, Japan
   g. Task Committee (J), 15th U.S.-Japan Bridge Workshop, November 1999, Tsukuba, Japan.
   h. Task Committee (K), 3rd Workshop on Wind and Earthquake Engineering for Offshore and Coastal Facilities, 5-6 December, 1999, Yokosuka, Japan.

In the event that T/C co-chairs deem it essential to conduct a joint meeting or workshop that is not included in this endorsement, the T/C co-chairs will make such a request through their respective Secretary-General for approval by the U.S. and Japan Joint Panel Chairmen.

Scheduling for the Workshops will be done by the U.S. and Japan Chairmen of the Task Committees with concurrence of the Joint Panel Chairmen. Both sides' Secretaries-General will be kept informed of the planning, conduct and results of workshops or committee meetings including resolutions and reports. Results of each activity conducted before the 32nd Joint Panel Meeting will be presented at the 32nd Joint Panel Meeting.

5. The Panel recognizes the importance of continued exchange of personnel, technical information, research results, and recorded data that lead to mitigating losses from strong winds and earthquakes. The Panel also recognizes the importance of using available large-scale testing facilities and complementary capabilities in both countries. Thus, these activities should be continued, strengthened, and expanded. Further, the Panel will study the feasibility of establishing a network for live transmission of experimental testing, including data, models, and simulation tools.

6. The Panel recognizes the importance of continuing its joint research programs on Soil Liquefaction and Countermeasures and on Auto-Adaptive Media (Smart Structural Systems).

7. The Panel recognizes the importance of conducting research in the following areas and recommends the subjects be featured in the 32nd Joint Panel Meeting.
   a. Research on the use of information technology to land management and to natural disaster prevention countermeasures
   b. Research on performance-based design methods with and without the integration of structural control devices
   c. Research on science, application and public policy for public health following natural disasters

8. The Panel recognizes the significant vulnerability of residential construction to natural hazards and believes that reduction of life and property losses in the housing sector is critical for both sides and in other parts of the world. The panel affirms the need to make disaster-resistant housing a priority and to strengthen activities in support of this objective in the future.

9. The Panel recognizes the importance to continue to seek means to contribute to the International Organization for Standardization (ISO) through participation of its members and related agencies in appropriate ISO Technical Committees. The Panel also recognizes the importance of continuing the related information exchange to contribute to the ISO.

10. The Panel will continue to transfer technical information obtained through the Panel and Task Committee activities including technology transfer on wind and seismic effects to developing countries.

11. The Panel published its sixth newsletter issue, *Wind and Seismic Effects*, Winter 1999. The newsletter featured articles on the 30th Joint Panel Meeting; highlights of recent T/C workshops (T/C: J, H and A); spotlights on US member agencies including Agency for International Development and the U.S. Department of Energy Natural Phenomena Hazards Programs; and spotlight on Japan-side member agencies including Geographical Survey Institute and Meteorological Research Institute. The Panel endorses continuing the publication of the Panel's newsletter. The Japan-side will publish the seventh newsletter during the winter of 1999-2000.

12. The National Institute of Standards and Technology (NIST) will continue to maintain the

Panel's Web Site on an interim basis. Links will be added to web pages of major U.S. and Japan agencies. The Panel encourages all members from both sides to use electronic media, as much as possible, in communicating Panel findings and summaries of its activities. The Web Site URL address is: http://www.bfrl.nist.gov/info/ujnr/ujnr1.html.

13. The Thirty-Second Joint Panel Meeting of the UJNR Panel on Wind and Seismic Effects will be held at the National Institute of Standards and Technology, Gaithersburg, MD, USA in May 2000. Dates, program, and itinerary will be proposed by the U.S.-side with concurrence of the Japan-side Panel.

Papers

Theme 1

Wind Engineering

WIND PROPERTIES FOR DESIGN OF HIGHWAY BRIDGES

by

Hiroshi SATO[1] and Ken-ichi OGI[2]

ABSTRACT

In wind resistant design of highway bridges, it is necessary to clarify characteristics of strong wind. The Wind Resistant Design Manual for Highway Bridges [1] provides design wind speed and turbulence properties for plane-like terrains, but the effects of local topography were not included. In this paper, described are the effects of valleys on wind properties. Wind tunnel studies for real valley models and simplified valley models are described first. Then CFD is applied to wind properties in the simplified valley models.

KEYWORDS: wind properties, topographic effects, valley, Computational Fluid Dynamics

1. INTRODUCTION

In wind resistant design of highway bridges, it is necessary to clarify characteristics of strong wind, such as basic wind speed and turbulence intensity. In Japan, these characteristics can be decided according to "the Wind Resistant Design Manual for Highway Bridges"[1] (hereinafter referred as to 'the Manual') as follows.

1) Category of surface roughness

Wind properties were modeled fundamentally according to Davenport [2][3], namely, lower mean wind speed but higher turbulence in rough terrian and low altitude, and higher mean wind speed but lower turbulence in smooth terrian and high altitude. The terrians are classified into four, namely rough sea (Terrain I), open farmland(Terrain II), suburbs(Terrain III) and city centers(Terrain IV).

2) Basic wind speed U10

The basic wind speed U10 is defined as the mean wind speed over open farmland(Terrain II)at an elevation of 10m, averaged over a period of 10minutes. Using the meteorological data at weather stations in Japan, extreme wind speeds were estimated. The probability that the annual maximum mean wind speed exceeds the basic wind speed is 40% in a 50-year period. The basic wind speeds were classified into 4 categories, namely 35m/s, 40m/s, 45m/s and 50m/s. It is shown in Fig.1.

3) The design wind speed Ud

The design wind speed for dynamic design can be obtained from the following formula.

Ud=U10*E1

where, E1: correction factor for altitude and terrains

The model of design wind speed profiles are shown in Fig.2.

4) Turbulence properties

Typical values for turbulence properties such as turbulence intensities and power spectal density functions are provided in the Manual. Turbulence intensity Iu is shown in Fig.3.

---

1) Head, Structure Division, Structure and Bridge Department, Public Works Research Institute, Ministry of Construction

2) Research Engineer, Structure Division, ditto

The geographical features of Japan are steep and complicated because of many high mountains and valleys, and sometimes affect characteristics of strong wind. It is difficult to predict the characteristics of strong wind at complicated topographic conditions. Several studies were conducted for simple and typical topographic conditions, such as terraces, independent peaks, ridges, valleys and so on. For example, it was found that wind speed increases considerably, when wind direction is along an open valley [4]. The details of this channelling effect, however, are not so clear.

The local topographic effects on strong wind are not considered in 'the Manual'. When a bridge is conducted at a complicated topographic site, some correction will be required for design wind properties. The most accurate way of investigating local wind properties is field survey at the site, but it would take much cost and time. Another way is to conduct wind tunnel test using topographical models. The CFD (Computational Fluid Dynamics), which has been developed remarkably, will be one of the possible prediction methods in near future.

In this paper, described are wind tunnel studies on the topographic effects. Models of the real valley and the simplified valley were used. Furthermore, CFD technique was applied to the simplified model.

2. WIND TUNNEL STUDY FOR THE REAL VALLEY MODELS. [5]

The valley was facing the Sea of Japan and its depth was about 70 meters (Fig.4). The traffic accident occurred on the bridge across the valley because of the strong wind [6]. The wind-rose shows that wind along the valley is distinguished, and wind from sea is stronger than wind from land (Fig.5).

2.1 Experimental Conditions

2 models (photo 1,2) were used. Their scale ratios were 1/600 and 1/1,500. Wider area was modeled in case of scale ratio 1/1,500 (Fig. 6). The test was conducted in the Gottingen type wind tunnel (cross-section is 2.5m×4m) of the Public Works Research Institute. The profile of approaching flow is shown in Fig.7. Wind speed and turbulence intensity were measured in the sections A,B and C (Fig.4).

2.2 Characteristics of the Strong Wind in the Valley

The measured wind speed was divided by the wind speed of the approaching flow at the same altitude as the measuring point, and the ratios are shown in Fig8.

The approaching flow is increased at the section B, where cross sectional area becomes smallest, and decreased at the section C (Fig.8 (a)-(c)). In the cross section of the valley, wind speed ratio becomes maximum near the slope of the valley (Fig.8(b),(d)), not in the center of cross section.

2.3 Influence of the Model Scale and Range

Although details of topographic features were reproduced in case of the 1/600 model, the modeled range was narrower than 1/1,500 model. For example, the mountain whose altitude was about 300m and the cape around the valley were not included in 1/600 model. The wind speed ratio distribution of the two models are, however, almost similar (Fig.8 (b),(d)). It seems that wind properties are strongly influenced by local geographical condition rather than surrounding geographical condition in case of valleys like this.

2.4 Influence of the Model Roughness

Sponge-like resin was stuck on the surface of the 1/600 model, and influence of surface roughness was investigated. In the case of rough surface model, the turbulence intensity is stronger and the wind speed ratio is smaller than the smooth-surface model near the slope (Fig.8(b),(e),(f),(g)). It seems that the surface condition should be simulated properly to represent wind properties near the slope of valleys.

3. WIND TUNNEL STUDY FOR SIMPLIFIED VALLEY MODELS [5]

3.1 Experimental Conditions

Simplified valley models were used to investigate parametrically the effects of width and slope of the valley. The models and experimental conditions are shown in Fig.9 and Table 2, respectively. Two types of approaching flow were used, and their vertical profiles are shown in Fig.10. Mean wind speed and turbulence intensity were measured at the section I and II as are shown in Fig.9, and the wind speed ratios were calculated.

3.2 Wind Speed Distribution

In the Section I along wind direction, the wind speed ratio becomes maximum around the entrance of the valley, and it gradually decreases along the valley (Fig.11). Turbulence intensity shows reverse tendency (Fig.12). In the cross section II the wind speed becomes maximum near the slope of the valley, but not at center of the valley (Fig.13). This tendency is similar to the result of the real valley model.

3.3 Influence of Valley Width

The maximum value of the wind speed ratio increases, as the valley width becomes narrower as is shown in cases 2 to 5 in Table 2.

3.4 Influence of Valley Slope

Among three slope angles, 45deg, 60deg and 90deg, the wind speed ratio became maximum at the slope of 60deg (Cases 1 to 3 and 6 to 8 in Table 2). It seems that slope angle affected both cross section area of the valley and separation of the flow, and that these effects resulted in the maximum wind speed ratio at the 60deg slope.

3.5 Influence of Vertical Profile of Approaching Flow

Between the two kinds of approaching flow, vertical profiles of mean wind speed were almost same, but vertical profiles of turbulence intensity were not. Turbulence intensity at the height of the valley (H=100mm) of approaching flow 1 was about 3%, and that of approaching flow 2 was about 8%. The maximum value of the wind speed ratio for approaching flow 1 was around 1.2. The maximum value was increased in case of approaching flow 2, which was more turbulent (Cases 1 to 3 and 6 to 8 in Table2).

4 APPLICATION OF COMPUTATIONAL FLUID DYNAMICS TO THE SIMPLIFIED VALLEY MODELS [7]

CFD technique was applied to the Cases 1 to 3 of the simplified valley models. The analysis area is shown in Fig.14. The number of meshes was $60 \times 40 \times 50$, and the interval of mesh was narrower around the entrance of the valley than the other area. As for the turbulence model, standard K-ε model was used. The wind speed profile near the ground was assumed to accord with power law (n=1/6), whose power was the same as the approaching flow 1

The maximum value of the wind speed ratio was a little larger than the result of the wind tunnel test (Table 2 and Table 3). The difference becomes large near the ground (Fig.11 and Fig.15). It seems that the boundary conditions near the ground should be improved for this calculation. In qualitative point of view, however, CFD results agreed fairly well with the experimental results, namely wind speed increased near the entrance of the valley, and decreased along the valley. These result suggests that CFD would be applicable to the prediction of wind properties in near future.

5. CONCLUDING REMARKS

The effects of valleys on wind properties were studied by wind tunnel tests and CFD. The major findings are as follows.

Wind tunnel study for real valley models:

1) The approaching flow was increased at the smallest section, and decreased along the valley.

2) In the cross section of the valley, wind speed ratio became maximum near the slope of the valley, not in the center of cross section.

3) Wind properties were strongly influenced by local topographical condition rather than surrounding geographical condition in the valleys.

4) Surface condition should be simulated properly to represent wind properties near the slope of valleys.

Wind tunnel study for simplified valley models:

5) The maximum value of the wind speed ratio increased as the valley width becomes narrower.

6) Among three slope angles, 45deg, 60deg and 90deg, the wind speed ratio became maximum at the slope of 60deg.

7) Vertical profiles of turbulence intensity of approaching flow affected the maximum value of the wind speed ratio.

CFD study for simplified valley models:

8) CFD results agreed qualitatively well with the experimental results. In the future CFD would be applicable to the prediction of wind properties.

6. REFERENCES

[1] The Wind Resistant Design Manual, Japan Road Association, 1991

[2] Davenport A.G., Wind structure and wind climate, Safety of Structures under Dynamic Loading, TAPIR, 1978

[3] Davenport A.G., The interaction of wind and structures, Engineering Meterology, Elservier, 1982

[4] ESDU, Strong winds in the atmospheric boundary layer, Part1: mean-hourly wind speeds,1982

[5] Sato H., Ohgi K., Matufuji H. and Matsuno Y., Study on the effects of local topography on wind characteristics, Technical Memorandum of PWRI No.3632, 1999

[6]Soma S., Car accidents caused by high winds, Proceedings of 7th National Symposium of Wind Engineering, 1982

[7] Sato H., Ohgi K., Matufuji H. and Matsuno Y., Study on the prediction of wind characteristics taking local topography into consideration, Proceedings of 15th National Symposium of Wind Engineering, 1998

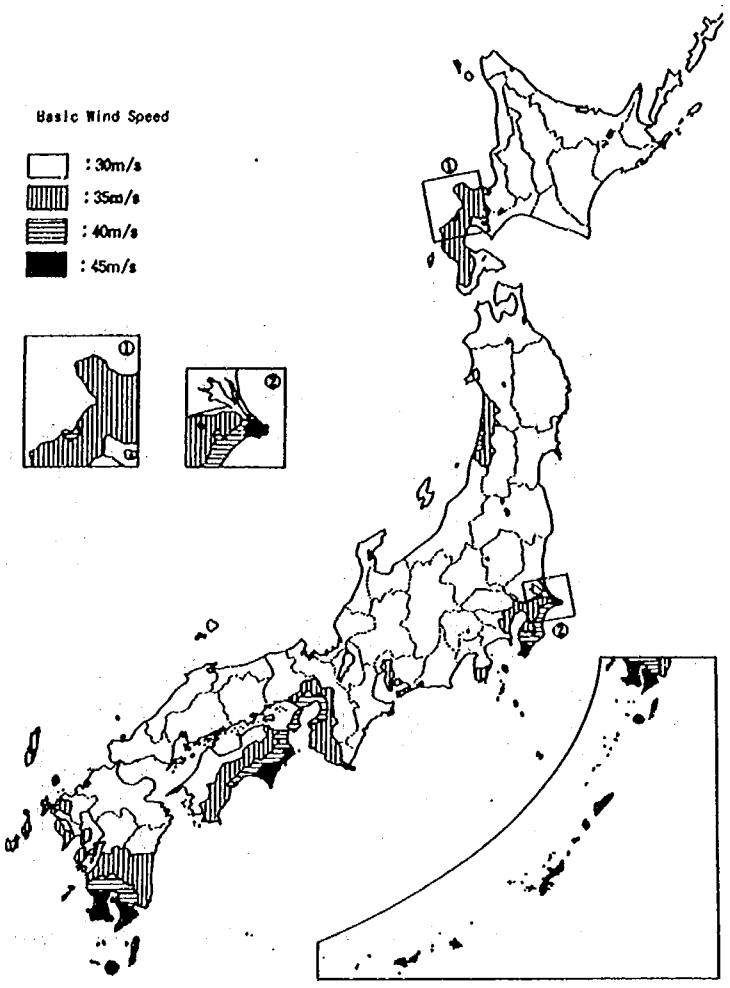


Fig.1 Basic Wind Speed

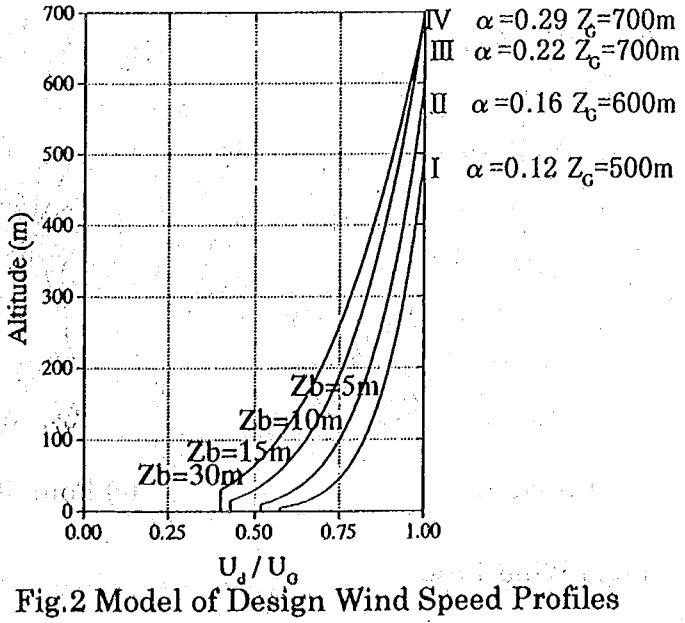


Fig.2 Model of Design Wind Speed Profiles

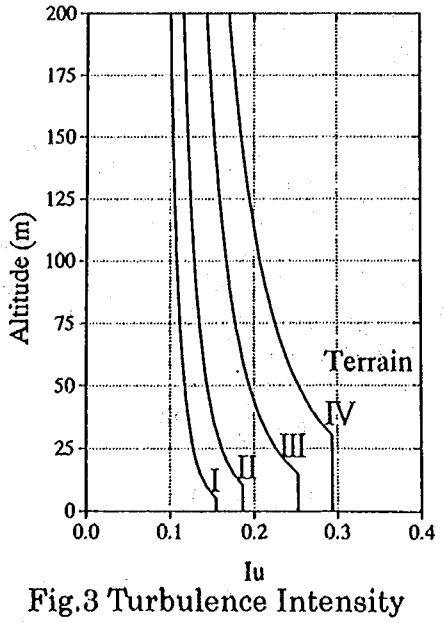
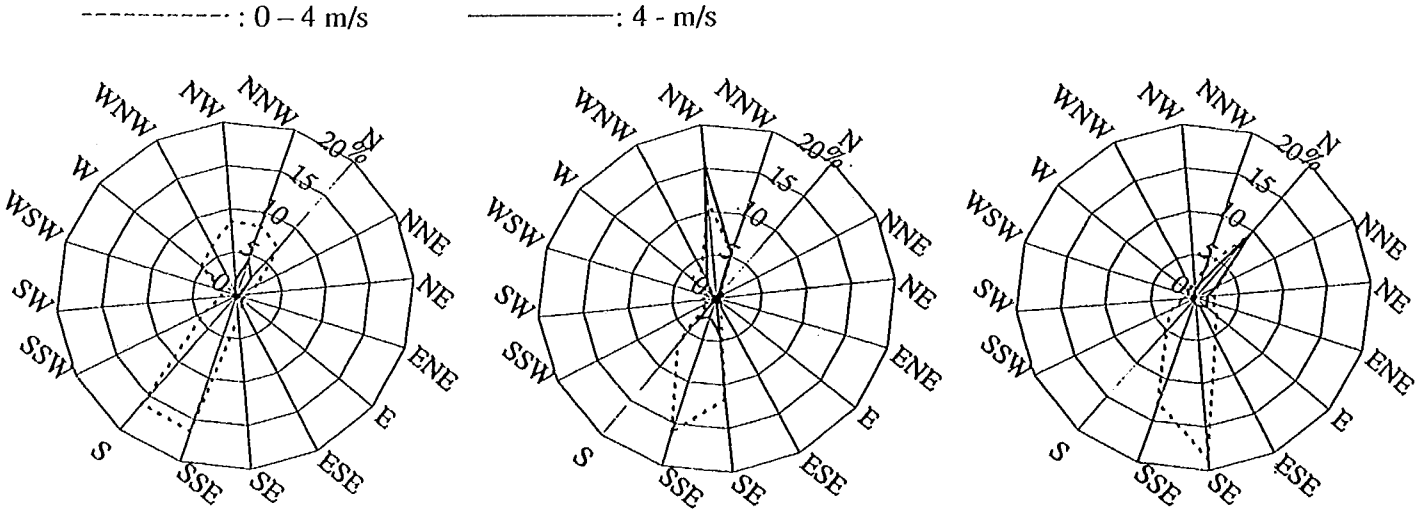


Fig.3 Turbulence Intensity



Fig.4 Measurement Sections and Observation Points



(a) Point 1 (b) Point 2 (c) Point 3

Fig.5 Wind Rose

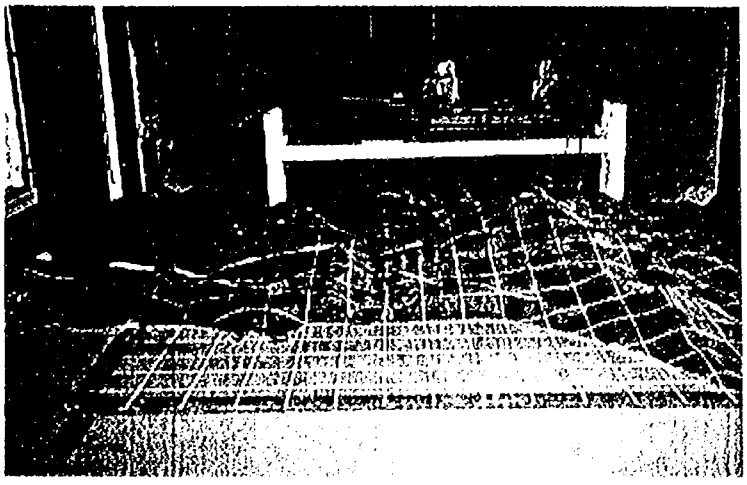


Photo 1　1/1,500 Model

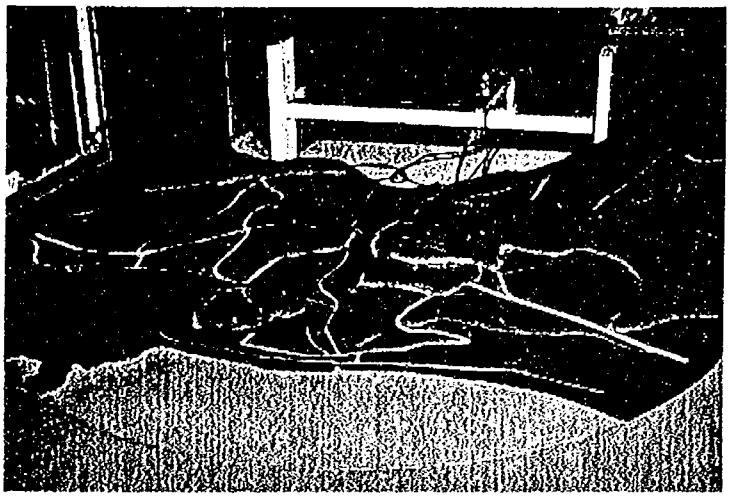


Photo 2　1/600 Model

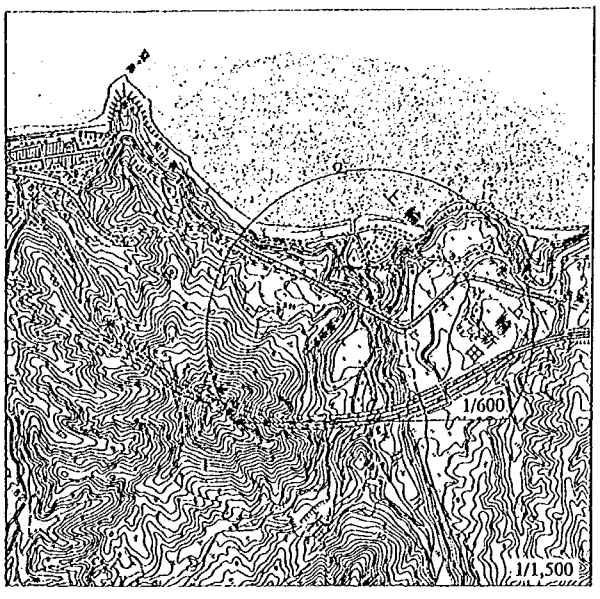


Fig.6　Range of Models

Table 1 Conditions of Wind Tunnel Study for Real Valley

	scale	wind direction	surface roughness	approaching flow
CASE1	1/600	NW	ignored	flow 1
CASE2	1/1,500	NW	ignored	flow 2
CASE3	1/600	NW	considered	flow 1

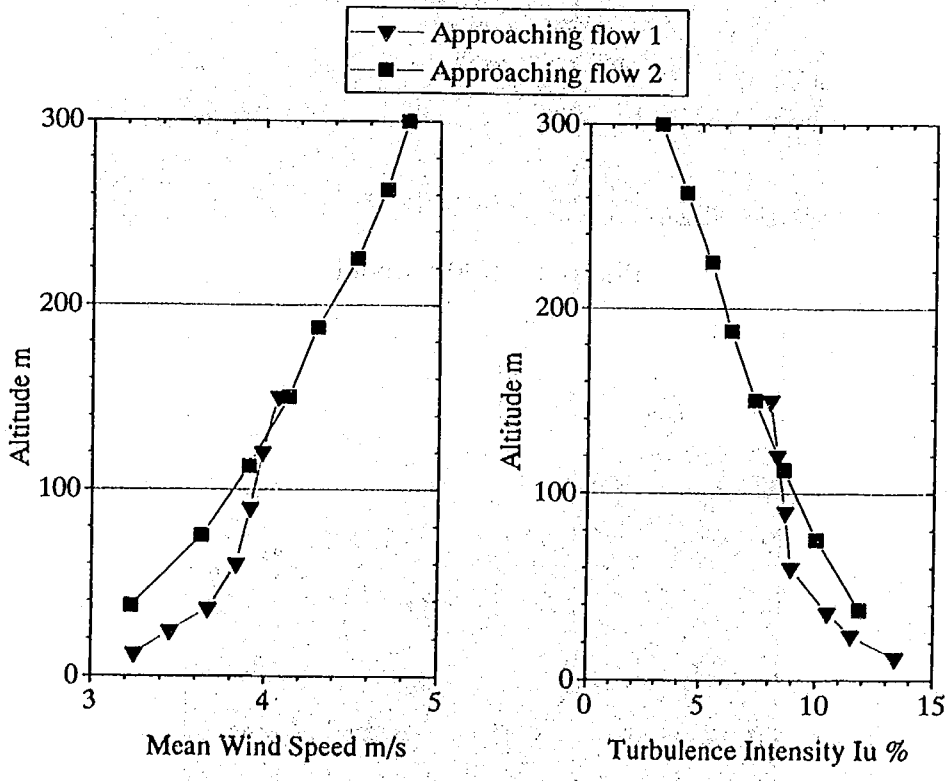
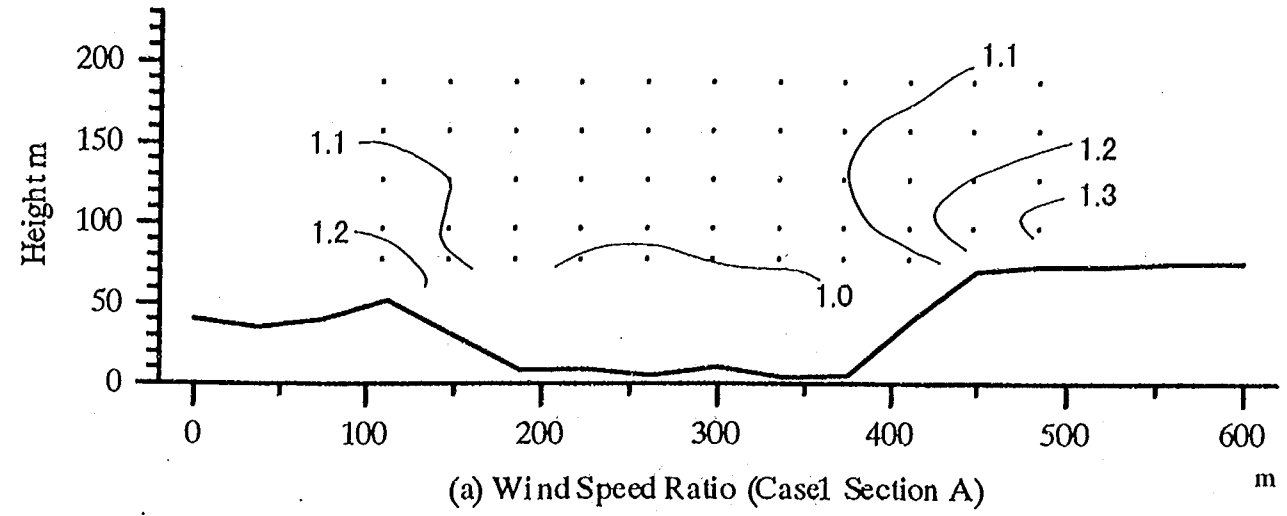
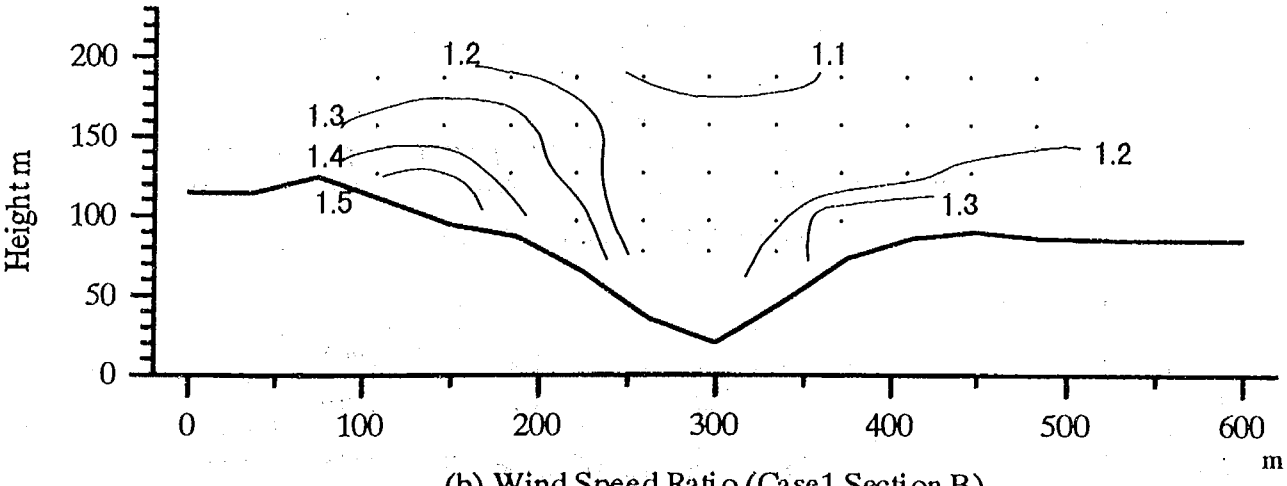


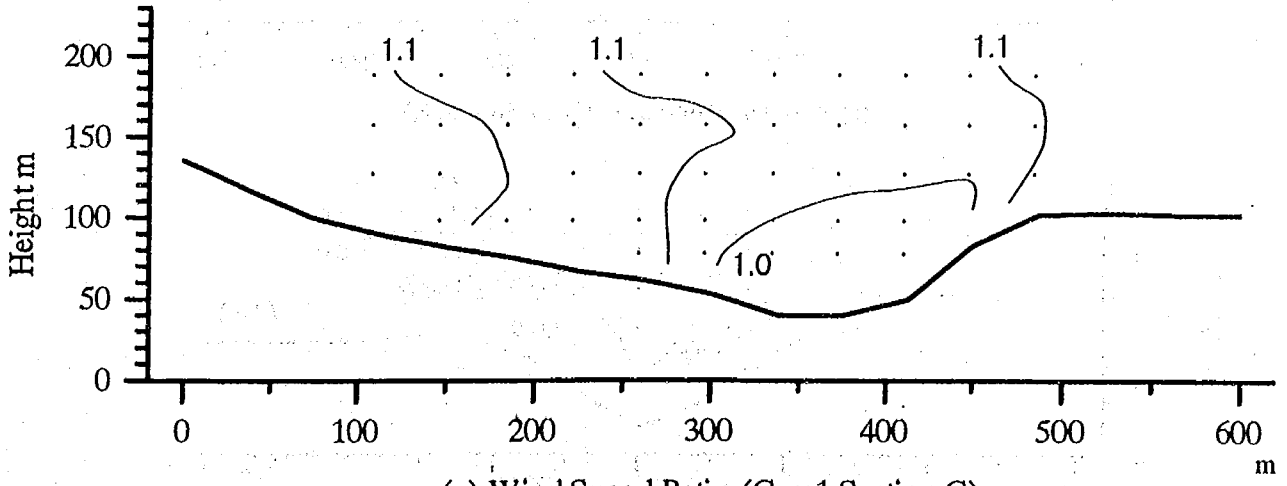
Fig. 7 Profile of Approaching Flow



(a) Wind Speed Ratio (Case1 Section A)

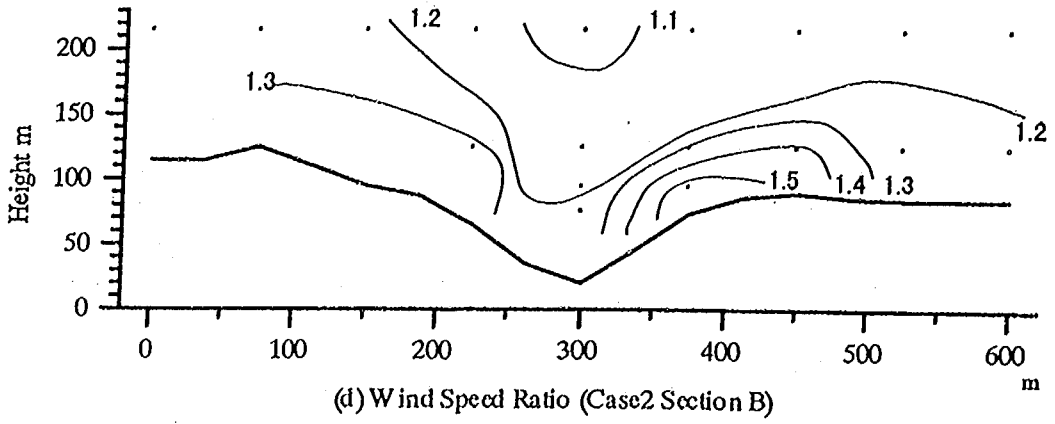


(b) Wind Speed Ratio (Case1 Section B)

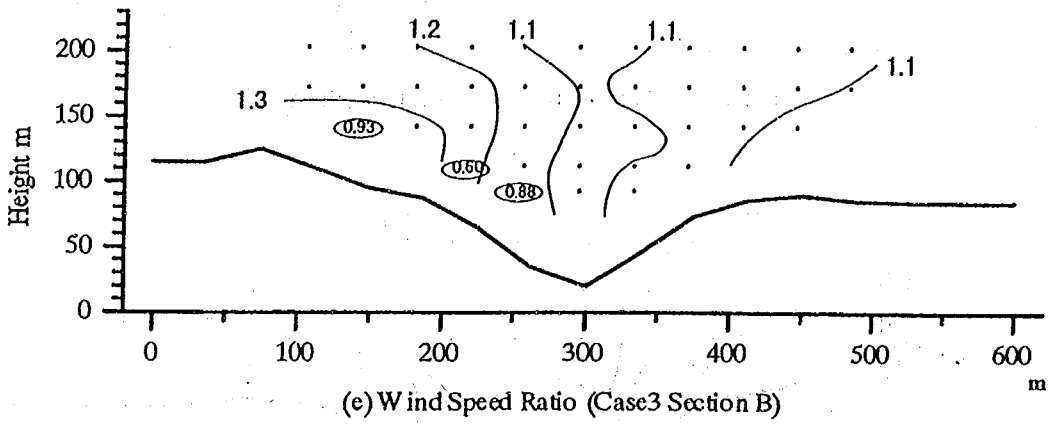


(c) Wind Speed Ratio (Case1 Section C)

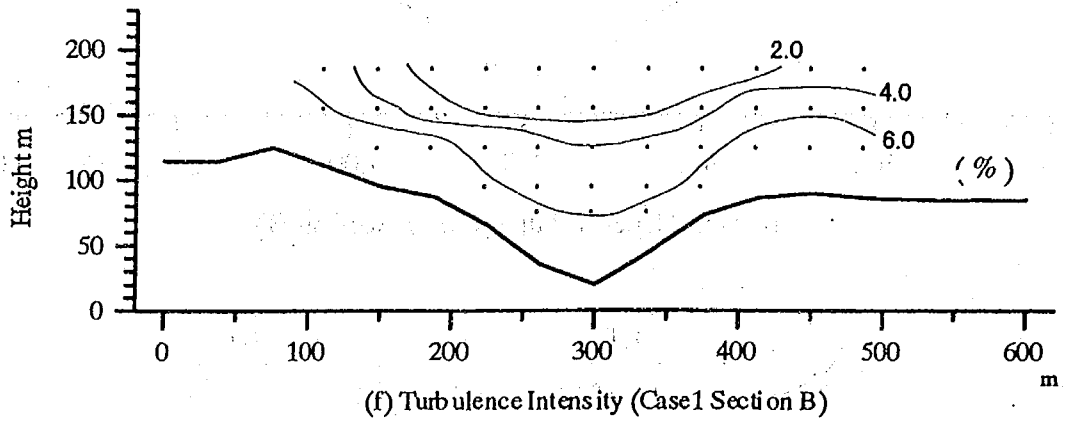
Fig.8 Results of Wind Tunnel Study for the Real Valley



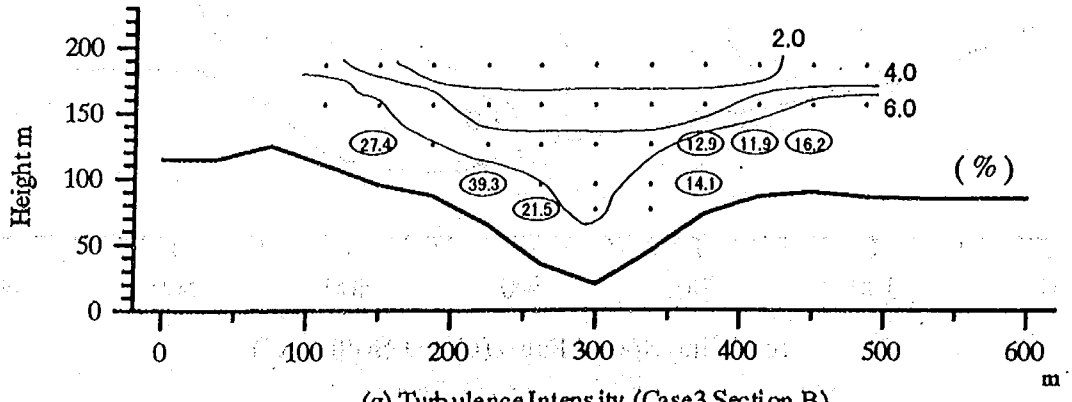
(d) Wind Speed Ratio (Case2 Section B)



(e) Wind Speed Ratio (Case3 Section B)



(f) Turbulence Intensity (Case1 Section B)



(g) Turbulence Intensity (Case3 Section B)

Fig. 8 Results of Wind Tunnel Test for the Real Valley (continued)

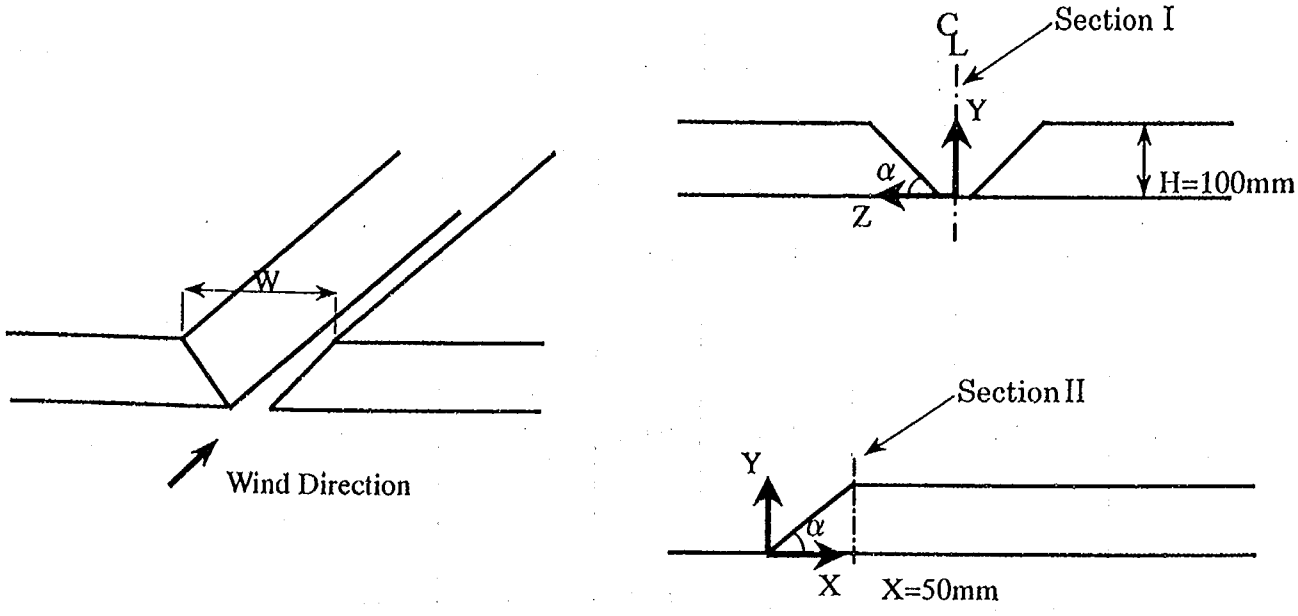


Fig.9 Simplified Valley Model

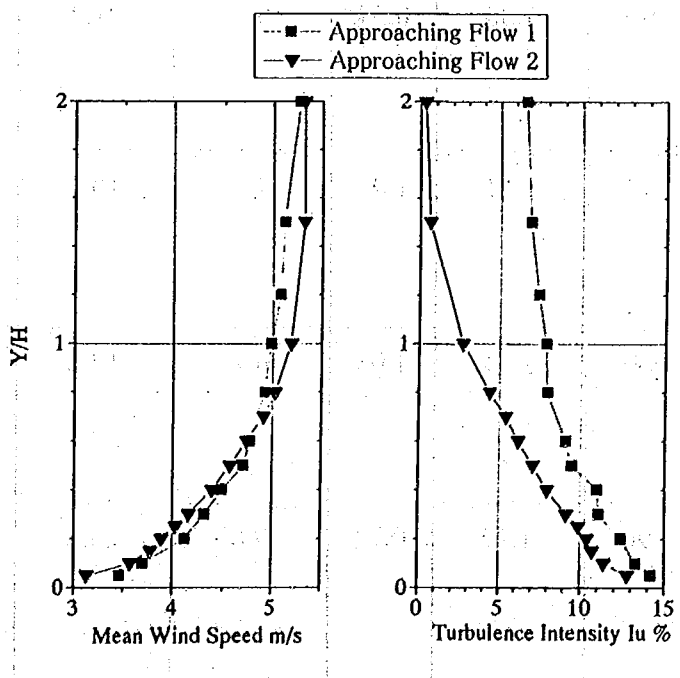
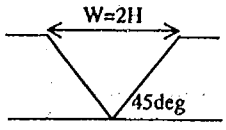
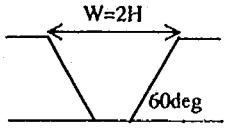
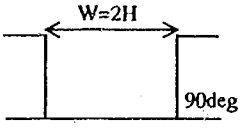
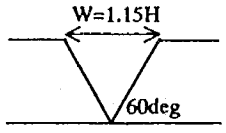
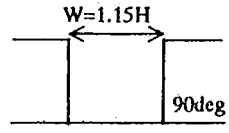
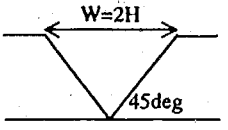
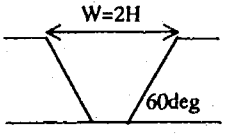
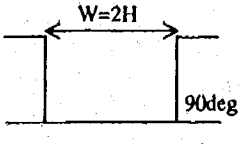


Fig. 10 Profile of Approaching Flow

Table 2 Wind Tunnel Study for the Simplified Valley

CASE	Approaching Flow	Width of Valley W	Slope Angle α (deg.)	Maximum Value of Wind Speed Ratio	Wind Speed Ratio *1	Minimum Value of Turbulence Intensity *2 (%)	Turbulence Intensity *1 (%)	Shape of Cross Section
1	1	W=2H	45	1.18	0.92	5.5	7.6	
2	1	W=2H	60	1.22	0.87	5.1	10.1	
3	1	W=2H	90	1.19	0.58	5.9	21.8	
4	1	W=1.15H	60	1.36	0.79	5.0	10.4	
5	1	W=1.15H	90	1.30	0.54	5.8	21.7	
6	2	W=2H	45	1.24	1.02	7.2	10.6	
7	2	W=2H	60	1.34	1.03	6.7	12.2	
8	2	W=2H	90	1.29	0.72	7.6	25.8	

*1 X=5.5H , Y=0.75H *2 Y=0.75H

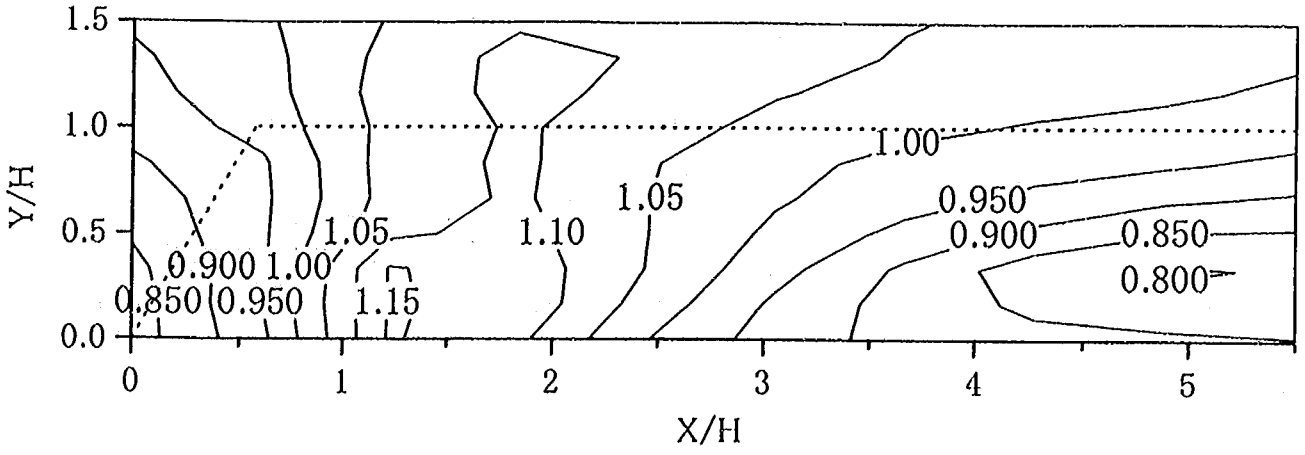


Fig.11 Distribution of Wind Speed Ratio (Case 2 Section I)

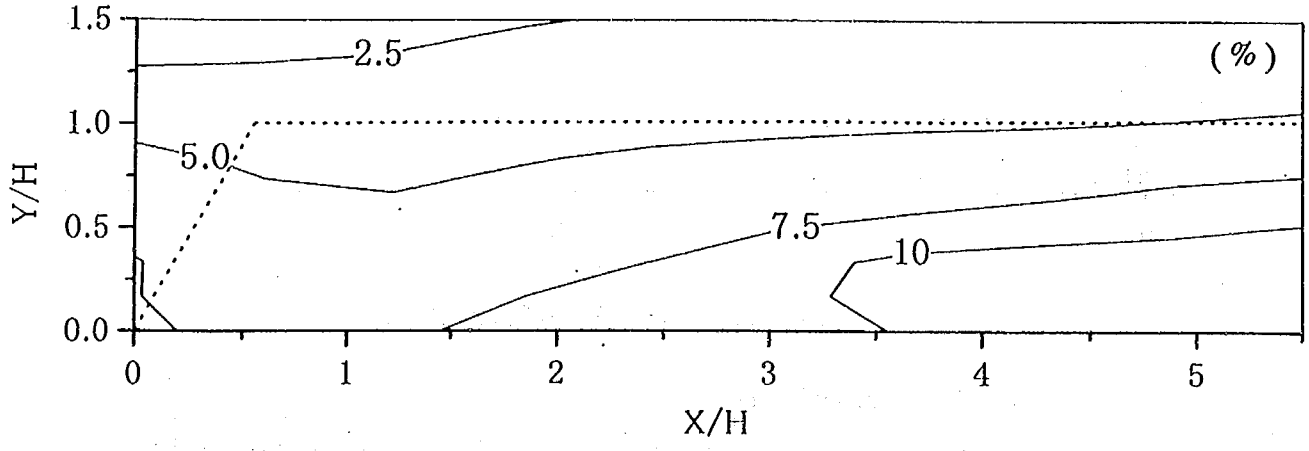


Fig.12 Distribution of Turbulence Intensity (Case 2 Section I)

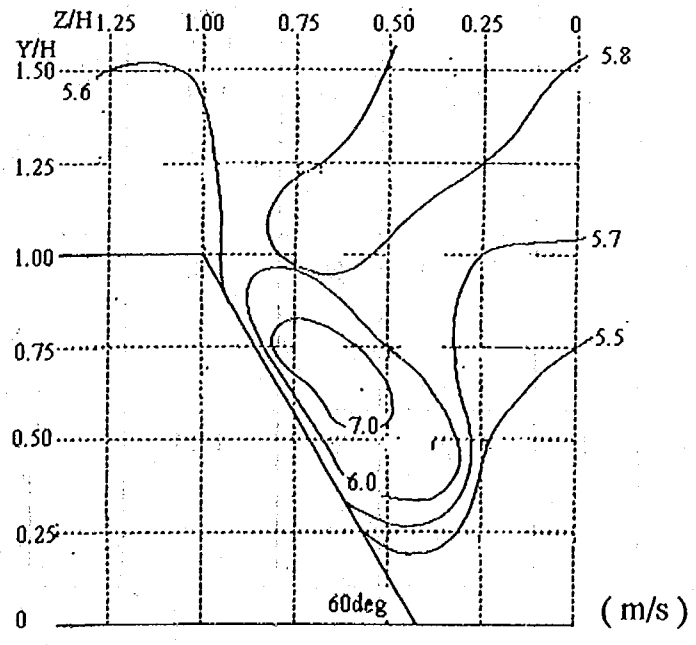
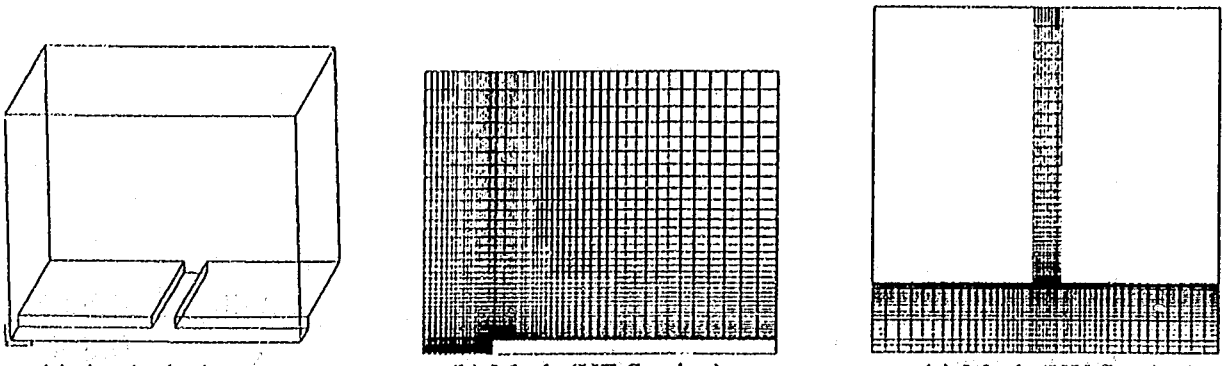


Fig.13 Distribution of Wind Speed (Case 2 Section II)



(a) Analysis Area (b) Mesh (XZ Section) (c) Mesh (XY Section)

Fig. 14 Analysis Area

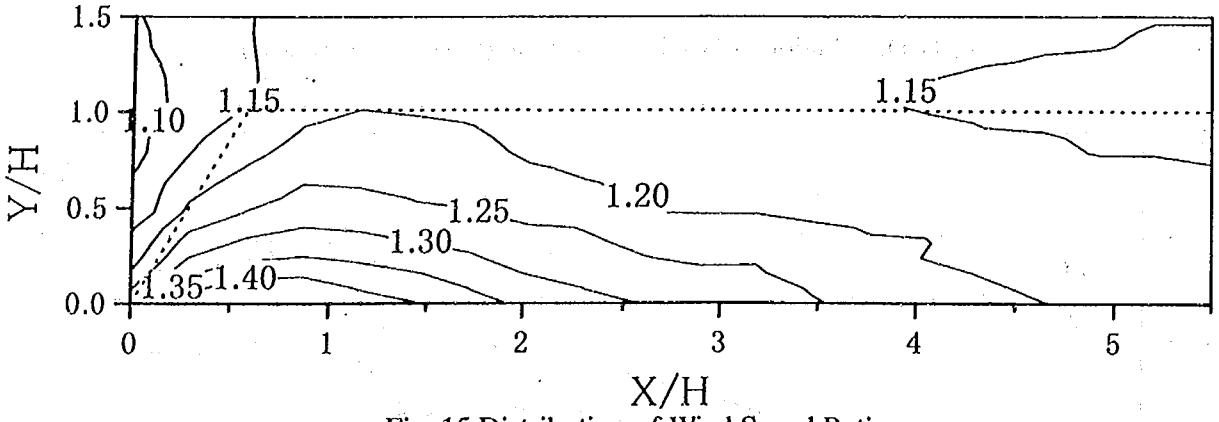
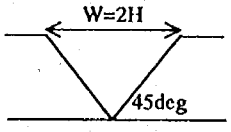
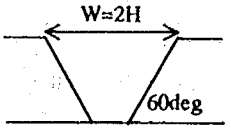
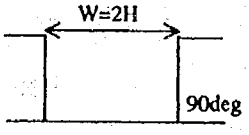


Fig. 15 Distribution of Wind Speed Ratio

Table 3 Results of CFD

CASE	Approaching Flow	Width of Valley W	Slope Angle α	Maximum Value of Wind Speed Ratio	Shape of Cross Section
1	1	W=2H	45	1.36	
2	1	W=2H	60	1.45	
3	1	W=2H	90	1.40	

The Fujita Tornado Intensity Scale: A Reassessment from Structural Engineering Perspective

by

Long T. Phan[1] and Emil Simiu[2]

ABSTRACT

On May 27, 1997 the town of Jarrell in central Texas, and on May 30, 1998 the town of Spencer in South Dakota were hit by two violent tornadoes. We evaluated the structural damage caused by the Jarrell tornado and concluded that the worst damage can be explained by wind speeds corresponding to an F3 rating on the Fujita tornado intensity scale (wind speeds of 71 m/s to 92 m/s). An F4 (93 m/s to 116 m/s) rating, or the F5 (117 m/s to 142 m/s) rating officially issued by the National Weather Service (NWS), need not be assumed to explain that damage. We also present assessments of damage in the Spencer tornado, and suggest there is an inconsistency between the NWS ratings of the Jarrell and Spencer tornadoes. We ascribe the NWS ratings to the failure of the Fujita scale to account explicitly for the dependence of wind speeds causing specified types of damage upon two structural engineering factors: (1) the basic design wind speed at the geographical location of interest, and (2) quality of construction, defined as degree of conformity to applicable standards requirements. We address the need for a stronger involvement of the structural engineering profession in nationwide efforts to develop an improved tornado classification scale and a more realistic tornado windspeed database.

KEYWORDS: Building technology; Fujita tornado intensity scale; meteorology; standards; structural engineering; wind engineering; tornadoes.

[1] Research Structural Engineer, National Institute of Standards and Technology, Gaithersburg, MD 20899

[2] NIST Fellow, National Institute of Standards and Technology, Gaithersburg, MD 20899

1. INTRODUCTION

On May 27, 1997 a violent tornado swept through a housing area on the outskirts of Jarrell, Texas (population 410) in Williamson County, approximately 60 km north of Austin, Texas, destroying about 40 single family residences and killing 27 people. A year later, on May 30, 1998 a violent tornado struck the town of Spencer, South Dakota, a small farm community approximately 72 km west of Sioux Falls, leaving 6 dead, more than 150 injured, and nearly 90 percent of a total 195 structures in the six-by-seven blocks community destroyed. Immediately following the passages of these tornadoes, structural engineers of the National Institute of Standards and Technology (NIST), in collaboration with meteorologists of the National Weather Service (NWS), conducted post-storm inspections to document structural damage and to assess tornado intensities. (Both NIST and NWS are agencies of the U.S. Department of Commerce.) This paper (1) describes the most severe structural damage observed for the Jarrell and Spencer tornadoes, which served as the basis for the NWS official rating of F5 and F4, respectively (see Appendix I); and (2) assesses the tornado wind speeds in Jarrell based on engineering considerations. From this assessment it was concluded that the damage caused by the Jarrell tornado may be explained by wind speeds corresponding to an F3 rating. An F4 rating, or the F5 ratings officially issued by the NWS, need not be assumed to explain that damage. The apparent misclassification of the Jarrell tornado can be ascribed to two shortcomings inherent in the current Fujita tornado intensity scale. The first shortcoming is that the damage descriptors for tornado categories F3 to F5 include ambiguous terms referring to construction quality, such as "well constructed houses," "structures with weak foundation," and "strong frame houses." These

descriptions are open to subjective interpretations and can lead to inconsistent field applications, especially by non-engineers who normally cannot be expected to have the requisite technical knowledge needed for ascertaining whether or not houses destroyed by tornadoes were well-constructed or strong. Evidence of subjective application of the Fujita tornado intensity scale is further illustrated by comparing the damage caused the Spencer tornado and that of the Jarrell tornado. While similar damage to similar structures was observed in Spencer and Jarrell, the Spencer tornado was rated as an F4 tornado instead of F5, as was the case for the Jarrell tornado. The second shortcoming is that the Fujita tornado intensity scale does not reflect the dependence of the tornado wind speeds causing various types of damage upon the design wind speed specified for the zone of interest. For example, a tornado wind speed that tears down the roofs of well constructed houses may be assumed to be larger by a factor of roughly 1.6 for zones in which the design wind speed is 63 m/s than for zones where the design wind speed is 40 m/s; that is, damage that in a 63 m/s zone could be attributed to an F5 tornado could be explained in a 40 m/s zone by F3 tornado winds.

2. THE JARRELL TORNADO

2.1 Post-storm Survey

Shortly before 3:45 PM CDT on May 27, 1997, the Jarrell tornado first struck areas of Bell County causing minor damage to trees and the roofs of a few residences. The tornado then crossed the Bell/Williamson county line into Williamson County where the town of Jarrell was located. The locations where the tornado crossed county roads were clearly marked by strips of scoured asphalt road surface. The top layer of the asphalt pavement was about 20 mm thick. The scouring of asphalt road surface is ascribed to differences between the atmospheric pressure in pockets of air trapped underneath the asphalt and the lower atmospheric pressure at the tornado center. The tornado path length was estimated to be 12.2 km and the maximum path width was measured to be approximately 1.2 km. Witnesses estimated that the Jarrell tornado was moving at a slow speed of between 2 m/s and 4 m/s.

The NIST-NWS post-storm survey team conducted ground surveys, on May 29 and June 1, 1997, and two aerial surveys: one on May 30, 1997 using a fixed wing aircraft flying between 760 m and 910 m, and the second on May 31, 1997 using a helicopter flying between 150 m and 300 m. A commercial Global Positioning System (GPS) was used to obtain the coordinates defining the tornado path.

2.2 Main Damage Observations

The first structural damage in Jarrell occurred at the corner of County Road 305 and County Road 307, where a culvert plant collapsed in place (Figure 1). The plant was a light steel frame construction with non-reinforced masonry and steel tube columns supporting steel pipe, gable roof trusses. The steel tube columns were cast into a concrete mat foundation on grade. The roofing, supported by wood purlins, consisted of corrugated sheet metal. An identical plant located approximately 15 m away from the collapsed culvert plant, and a mobile home located about 150 m north-northwest of the plant sustained only very minor damage. As the tornado continued its track south-southwestward, a barn located just southwest of the culvert plant and just north of the Double Creek Estates subdivision in Jarrell was destroyed. The tornado then moved through the Double Creek Estates subdivision and the surrounding areas, where the destructive path widened to its maximum of 1.2 km and the tornado became most deadly.

Figure 2 shows a portion of what remained of Double Creek Estates subdivision after the tornado passage. The structures in the subdivision consisted mainly of single family residences built over the last 15 years or so, of the typical slab-on-grade construction type. Owing to the presence of a limestone bedrock most houses had no basements or underground shelters. The houses, which consisted mainly of wood frame construction, were completely swept off the concrete foundations. Inspections of the concrete

slab-on-grade foundations performed during the ground surveys revealed that, in many cases, even the sill plates that connect the wood frames to the concrete slab-on-grade foundations were blown away (see Figure 3). There was evidence that the sill plates had been connected to the foundations by explosive-driven nails. Figure 4 shows a nail that remained in the foundation but pulled through the sill plate. Figure 5 shows nails, spaced 0.9 m apart, that pulled out of the foundation. The Council of American Building Officials (CABO): One and Two Family Dwelling Code and other nationally recognized model codes require that sill plates of exterior walls for wood-frame construction be anchored to the foundation by anchor bolts not more than 1.83 m apart, but no evidence of anchor bolts was found by the team. It should be noted that Williamson County *has not adopted a building code*, even though Jarrell was also hit by a tornado on May 17, 1989.

3. THE SPENCER TORNADO

3.1 Post-storm Survey

The Spencer tornado struck at 8:38 pm CDT on May 30, 1998 and moved through the town of Spencer at a speed of approximately 15-20 m/s. The tornado left a ground track about 34 km long and close to 1.5 km wide at its broadest. An aerial survey using fixed wing aircraft flying at between 760 m to 910 m was conducted on the following day, and was followed by a ground survey one day later.

Based on surveys of the most severe structural damage, the NWS assigned it an F4 rating. Reportedly, a Doppler-On-Wheels (DOW) radar, operated by the School of Meteorology of the University of Oklahoma as part of the Radar Observations of Tornadoes and Thunderstorms Experiments (ROTATE-98) program, was able to record wind speeds of this tornado and indicated wind speeds of up to 110 m/s. These measurements, if validated, would be consistent with the wind speed range associated with an F4 tornado (93-116 m/s).

3.2 Main Damage Observations

Figure 6 shows an overview of the town of Spencer after the tornado passage. Within the town of Spencer, the observed damage ranged from total disintegration of structures in the direct path of the tornado, to light damage to envelopes of structures in the outlying areas. The structures affected varied in age and structural systems. Completely destroyed structures included one and two-story wood-frame, heavy timber, and engineered metal frame constructions. Among these were wood-frame constructions that were either poorly connected or totally unconnected (i.e., relying on gravity alone) to the concrete or brick foundations. However, structures that were totally destroyed also included some (post office, fire department, gas station, antique and other stores) that were properly anchored to the concrete slab-on-grade foundations by 12.7 mm (½-in) anchor bolts with proper spacing as required by CABO (1995) and other nationally recognized model codes (see Figures 7 (a) and (b)). Many heavy trucks, some reportedly fully loaded, used in transporting grains to and from the town's grain processing and storage warehouses, were lifted and carried more than 30 m away by the wind. Trucks and houses exhibited widespread evidence of missile impacts from broken wooden power poles, tree branches, and other debris.

4. TORNADO INTENSITY ESTIMATES

The Jarrell and Spencer tornadoes offered an opportunity to assess subjective tornado intensity estimates based on Fujita scale damage descriptions. Our assessments are based on structural engineering considerations.

The basic peak gust wind speed specified in the ASCE 7-95 Standard (1995) for the design of buildings in central Texas is 40 m/s. Building designs for central Texas before 1995 should be roughly compatible with this basic speed. Design and construction practices of buildings such as those destroyed by the Jarrell tornado are normally based on experience and judgment rather than formal engineering calculations. When they are sound, such practices are consistent with the

requirement that buildings should be capable of withstanding wind speeds higher than the basic design wind speed, with a safety margin with respect to wind loading of at most 1.5 to 2. Assume that in areas with a 40 m/s basic design wind speed buildings would collapse under winds loads twice as large as the loads induced by the 40 m/s speed. It follows from the proportionality of the wind loads to the square of the wind speeds that those buildings would be expected to collapse under wind speeds in excess of $40 \times (2)^{1/2} = 56.6$ m/s. The expectation would be even stronger that wind speeds corresponding to wind loads 3 times as large as those induced by the 40 m/s speed (i.e., 69 m/s wind speeds) would leave no buildings standing, especially if the construction is mediocre or poor, as appears to have been the case for buildings destroyed by the Jarrell tornado.

Speeds assigned to F3 tornadoes in the Fujita classification are about 72 m/s to 94 m/s. For a building to resist such speeds its safety margin with respect to wind loads would on average have to be about 3.1 to 5.5. There is no reason to believe that any of the buildings destroyed by the Jarrell tornado were that strong. We note that 90 m/s wind speeds, which in the Fujita classification are associated with F3 tornadoes, would likely destroy residential homes not only in a 40 m/s basic design wind speed zone, but in hurricane-prone areas with 63 m/s basic design wind speeds as well.

In fact, based on evidence that code compliance with respect to the connections between the upper wood frame and the concrete foundation was better in Spencer than in Jarrell, one may conclude that buildings that were completely destroyed were stronger in Spencer than in Jarrell. Nevertheless, the NWS tornado ratings were F5 and F4 for the Jarrell and Spencer tornadoes, respectively. In our opinion this is a clear indication of possible inconsistencies inherent in subjective tornado speed assessments by non-engineers.

5. CONCLUSIONS

Our conclusions are:

1. The strongest damage caused by the Jarrell tornado can be explained by wind speeds corresponding to an F3 rating (i.e., 71 m/s to 92 m/s).

2. The Fujita tornado intensity scale has two major shortcomings that can lead to misclassification of tornadoes by non-engineers:

(a) It does not reflect the dependence of the tornado wind speeds causing various types of damage upon the design wind speed specified for the zone of interest.

(b) The damage descriptions include ambiguous descriptions of structural quality such as "well-constructed houses" and "strong frame houses." Non-engineers normally cannot be expected to have the requisite technical knowledge needed for ascertaining whether or not houses destroyed by tornadoes were well-constructed or strong.

These conclusions are of significance insofar as:

1. Tornado misclassification corrupts the database used to develop design criteria for structures whose performance must be unaffected by strong tornadoes.

2. Ascribing failures to unrealistically high wind speeds when the actual speeds are in fact lower discourages the application and enforcement of standards, such as ASCE 7, that are capable of reducing loss of life and property caused by most tornadoes.

3. A stronger contribution of the structural engineering profession to efforts aimed at assessing tornado wind speeds could help improve the knowledge needed to protect the public from tornado-induced losses.

For these reasons, we recommend the followings:

1. Engineers, meteorologists, disaster relief workers, and representatives of standards organizations, regulatory bodies and the insurance industry should work together to develop a tornado intensity classification scale wherein damage descriptions make specific reference to basic design wind speeds and to quality of construction as defined by degree of conformity to standards requirements. As a basis for discussion, it is suggested that wind speed ranges included in tornado intensity classifications be affected by numerical factors related to the basic design wind speeds and to quality of construction. Factors related to quality of construction could be specified in accordance with matrices of the type considered for development by insurance companies, wherein conformity to various standards requirements is estimated both qualitatively and quantitatively.

2. ASCE, in collaboration with other interested parties, should consider organizing and training local ASCE chapter volunteer engineering teams that could join in expeditiously with local NOAA and other specialized personnel, and promptly record from the strength of their professional knowledge significant evidence on tornado intensities. This recommendation is based on experience which shows that evidence of tornado effects is often removed from the site less than a day after a tornado occurrence, that is, *before* survey teams can reach the site.

3. The documentation for the approximately 150 tornadoes (about 0.5% of the total number of recorded tornadoes in the U.S.) that were classified as F5 should be revisited in an attempt to reassess their classification. Such reassessment would involve a relatively small effort and would, even if only partly successful, allow some updating of the database from which probability distributions of tornado wind speeds have been estimated so far. This recommendation follows a proposal by K. Mehta of Texas Tech University.

4. Continuing efforts to develop procedures for obtaining direct, scientific tornado wind speed measurements should be encouraged. On the one hand such measurements would add valuable data to the database, even though the effect of such addition to the more than 25,000 data currently available would be small: many years of data would have to be collected for that effect to be significant. On the other hand, scientific measurements can help to assess estimates of tornado wind speeds based on observations of damage. This would in turn help to effect corrections to the existing database by allowing the use of Bayesian or other updating techniques.

6. REFERENCES

ASCE 7-95, Minimum Design Loads for Buildings and Other Structures, ASCE Standard, American Society of Civil Engineers, New York, New York.

The Council of American Building Officials, *CABO One and Two Family Dwelling Code,* 1995 edition, Falls Church, Virginia.

Long T. Phan and Emil Simiu, *The Fujita Tornado Intensity Scale: A Critique Based on Observations of the Jarrell Tornado of May 27, 1997,* NIST Technical Note 1426, National Institute of Standards and Technology, July, 1998.

Long T. Phan and Emil Simiu, *Tornado Aftermath: Questioning the Tools,* ASCE Civil Engineering Magazine, December, 1998.

APPENDIX I. FUJITA TORNADO INTENSITY SCALE

Category-Definition-Effects

F0 Gale tornado (Approximate wind speeds 18-32 m/s (40-72 mph)): Light damage. Some damage to chimneys; break branches off trees; push over shallow rooted trees; damage sign boards.

F1 Moderate tornado (Approximate wind speeds 33-50 m/s (73-112 mph)): Moderate damage. Lower limit is the beginning of hurricane wind speed; peel surface off roofs; mobile homes pushed off foundations or overturned; moving autos pushed off the roads.

F2 Significant tornado (Approximate wind speeds 51-70 m/s (113-157 mph)): Considerable damage. Roofs torn off frame houses; mobile homes demolished; boxcars pushed over; large trees snapped or uprooted; light-object missiles generated.

F3 Severe tornado (Approximate wind speeds 71-92 m/s (158-206 mph)): Severe damage. Roofs and some walls torn off well-constructed houses; trains overturned; most trees in forests uprooted; heavy cars lifted off ground and thrown.

F4 Devastating tornado (Approximate wind speeds 93-116 m/s (207-260 mph)): Devastating damage Well constructed houses leveled; structures with weak foundation blown off some distance; cars thrown and large missiles generated.

F5 Incredible tornado (Approximate wind speeds 117-142 m/s (261-318 mph)): Incredible damage Strong frame houses lifted off foundations and carried considerable distance to disintegrate; automobile-sized missiles fly through the air in excess of 100 yards; trees debarked; incredible phenomena will occur.

(From National Post-storm Data Acquisition Plan, Federal Coordinator for Meteorological Services and Supporting Research, National Oceanic and Atmospheric Administration.)

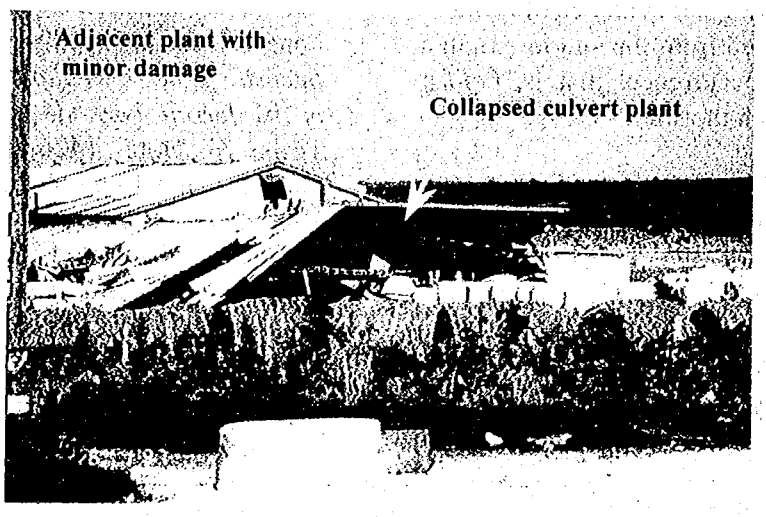


Figure 1. Ground view of collapsed culvert plant.

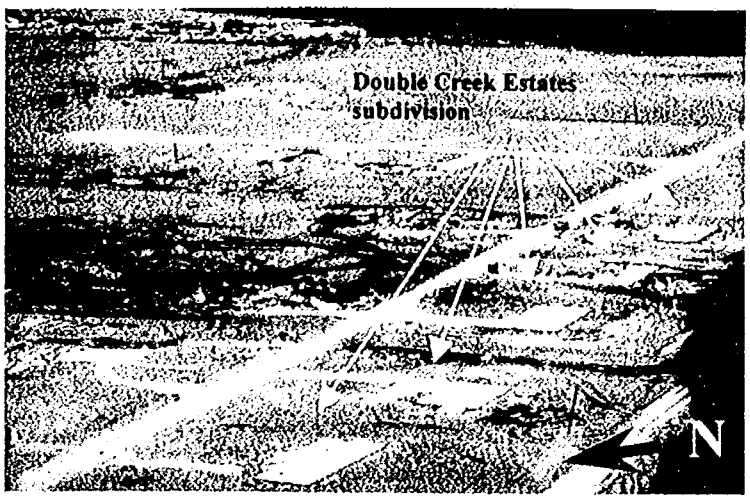


Figure 2. Aerial view of portion of the Double Creek Estates subdivision after tornado passage

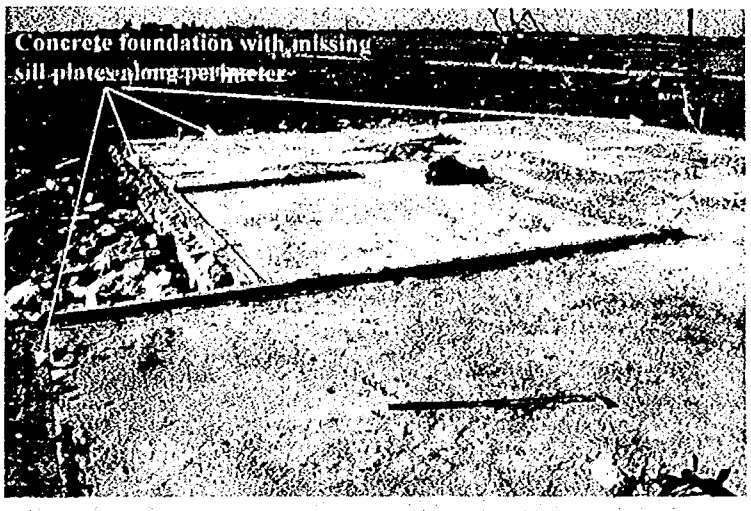


Figure 3. Close-up view of a typical slab-on-grade foundation of houses in Jarrell. Only one sill plate remains connected to the concrete foundation.

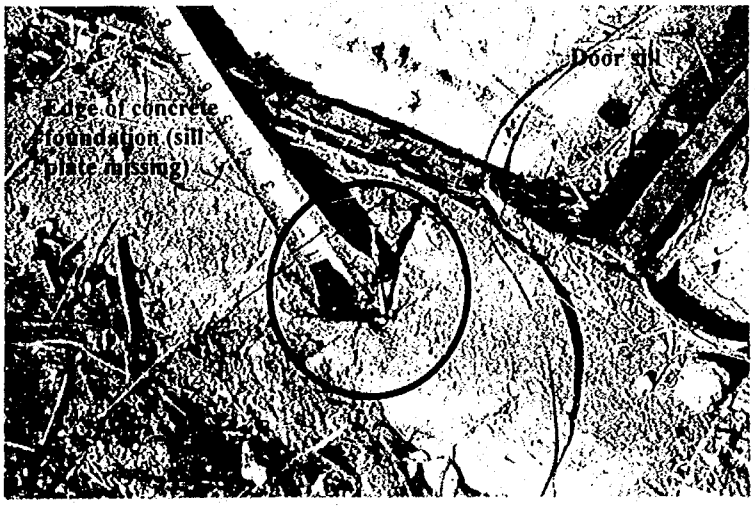


Figure 4. Evidence of nail that was used for connecting sill plate to concrete foundation.

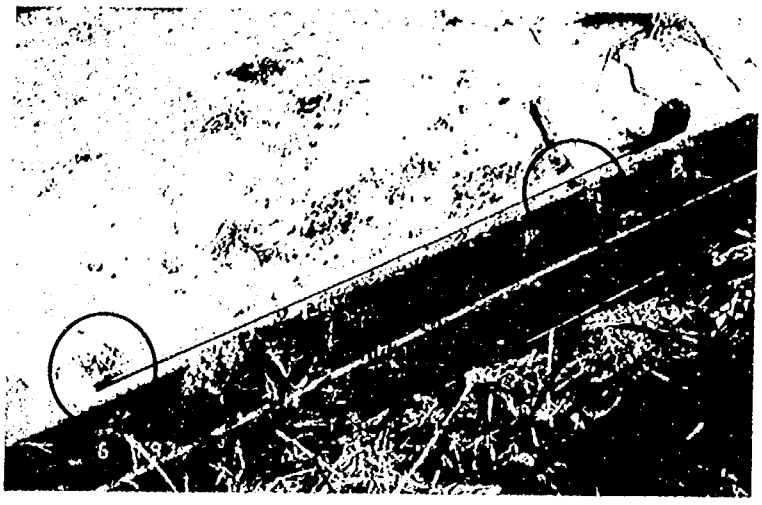
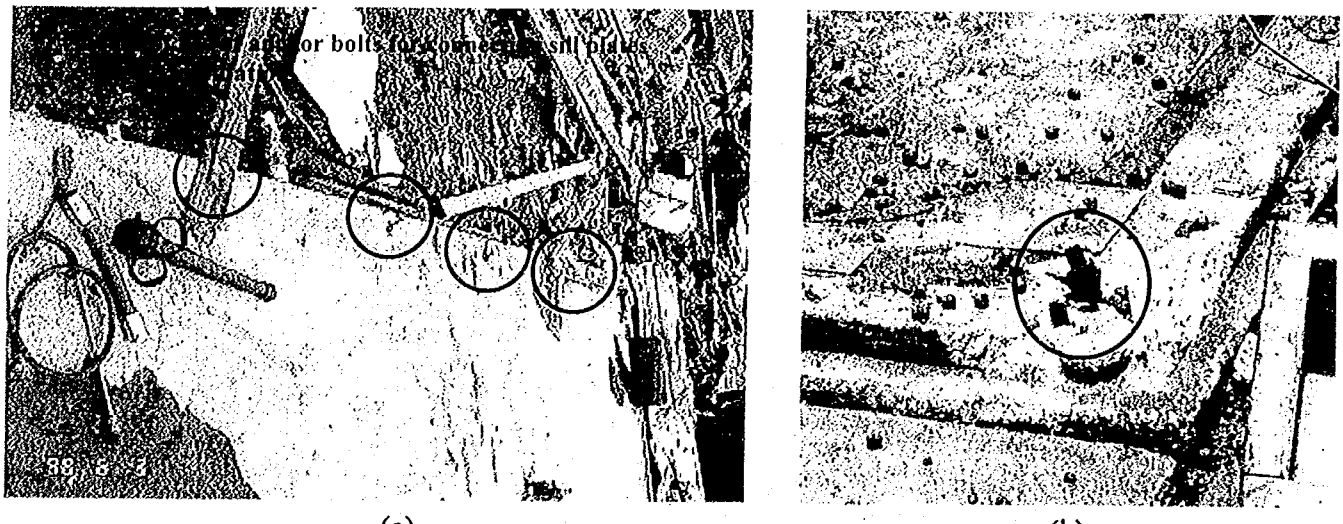


Figure 5. Evidence of pullout of nails used to fasten sill plates to concrete foundation.



Figure 6. Aerial view of portion of the town of Spencer, South Dakota, after tornado passage.



(a) (b)

Figures 7 (a) and (b). Evidence of anchor bolts used to connect upper structure to concrete slab-on-grade foundation in Spencer, South Dakota.

RESEARCH PROJECT ON PROPRIETY AND RELIABILITY OF DESIGNING WIND LOAD AND WIND PRESSURE COEFFICIENTS

Comparison of gust effect factors and wind pressure coefficients between several codes and standards

Hisashi OKADA[1], Yukio TAMURA[2], Yasushi UEMATSU[3] and Hitomitsu KIKITSU[4]

ABSTRACT

This paper describes the outline of the research projects carried out in a committee since 1998, which is composed of Japanese academic people and researchers in charge of wind tunnel experiments. The main work is a comparison of products of gust effect factors and wind pressure coefficients between current codes and standards used in several nations. In this study, these products were adjusted based on consistent concept for the comparison, since each provision does not always use the same averaging time of basic wind velocity and reference height. This paper shows the results about gable roof and vaulted roof as examples and points out the difference of the design concepts.

Key Words: Reliability, Wind pressure coefficient, Gust effect factor

1. Introduction

Wind pressure coefficients and gust effect factors are essential for evaluation of wind loads on whole buildings and their claddings. Structural designers usually get those data by carrying out wind tunnel experiments, or otherwise by referring standards or guidebooks. Therefore, the wind tunnel experiments should be carried out carefully and the data listed in those sources should be reliable. And information of the reliability or statistical data such as mean and variable pressure coefficients should be needed for the reliability analysis. However, very few information of the reliability has been offered so far. While structural design is now oriented toward the performance-based design, it is necessary to make clear how wind pressure coefficients are reliable, which discussion of the wind resistant performance is based on.

From 1998, Building Research Institute (BRI) has launched the research project for evaluation of wind pressure coefficients' reliability, where the main purposes are as below:

- Survey on the reliability of wind pressure coefficients regulated in current codes and standards used in several nations
- Survey on the reliability of experimental data derived from wind tunnel experiments

Based on the former purpose, last year we organized a committee in the Building Center of Japan (chairperson: Prof. Takeshi OHKUMA, Kanagawa Univ.). The committee is composed of the academic people and researchers in charge of wind tunnel experiments in research institutes of the private sectors. The names of the working members are listed in the section 4.

As the initial activity, we carried out the comparison of wind pressure coefficients and gust effect factors between various codes and standards. Holmes[1] did the similar survey and highlighted the large difference between them. We would like to make clear the reason why

1) Assoc. Director for Composite Structures, Building Research Institute, MOC, Dr. Eng.
2) Professor, Dept. of Architectural Engineering, Faculty of Engineering, Tokyo Institute of Polytechnics, Dr. Eng.
3) Assoc. Professor, Dept. of Architecture and Building Science, Tohoku Univ., Dr. Eng.
4) Research Eng., Building Research Institute, MOC, M. Eng.

such large difference exists. This survey has just initiated and now is ongoing. This paper describes the procedure of the comparison and preliminary report of the results.

2. Comparison of Products of Gust Effect Factors and Wind Pressure Coefficients

2.1 Procedure of Comparison

Gust effect factor is important as well as wind pressure coefficient to evaluate the wind load. Some codes and standards regulate the products of gust effect factor and wind pressure coefficient, not them separately. Therefore, the product of them must be considered to understand and compare their design concepts. Codes and standards concerned in this study are the following:

(1) ISO International Standard, ISO/DIS 4354[2]
(2) EUROCODE 1, ENV 1991-2-4[3]
(3) ASCE Standard, ANSI/ASCE 7-95[4]
(4) SAA Loading Code Part 2, AS1170.2[5]
(5) National Building Code of Canada[6]
(6) Swiss Standard[7]

These codes and standards regulate internal pressure coefficients and several patterns of external pressure coefficients for enclosed buildings as shown in Table 1.

This study focuses on the comparison of the internal pressure and the external pressure effects on claddings. From these lists, we selected several pressure coefficients as examples for comparison, which are internal pressure coefficients and five external pressure coefficients for frat roof, gable roof, shed roof, vaulted roof and walls. And the comparisons of pressure coefficients were applied for two types of enclosed rectangular buildings with these roof shapes as below:

- Type 1: Span 20m x Ridge 30m x Mean roof height 10m
- Type 2: Span 60m x Ridge 60m x Mean roof height 10m

Table 1. Lists of Wind Pressure Coefficients regulated for Enclosed Buildings

Codes and Standards	Regulated Wind Pressure Coefficients	
ISO4354	Frat roof * Gable roof * Vaulted roof and doom * Sphere	Cylinder, Chimney and Tank Wall * Internal pressure *
EURO CODE ENV-1991	Frat roof * Gable roof * Shed roof * Hipped roof Multi-span roof	Vaulted roof and doom * Sphere Wall * Internal pressure *
ASCE 7-95	Frat roof * Gable roof * Shed roof * Hipped roof Multi-span roof	Stepped roof Vaulted roof and doom * Chimney Wall * Internal pressure *
AS1170.2	Frat roof * Gable roof * Shed roof * Multi-span roof Vaulted roof and doom *	Mansard roof Circular bin, Silo and Tank Wall * Internal pressure *
NBCC 1990	Frat roof * Gable roof * Shed roof * Vaulted roof and doom *	Sphere Cylinder, Chimney and Tank Wall * Internal pressure *
SWISS Standard	Frat roof * Gable roof * Shed roof * Multi-span roof Mansard roof	Roof with ventilated ridges Cylinder, Chimney and Tank Wall * Internal pressure *

*) Wind pressure coefficients considered in this study

The mean roof height is the same each other. Type 1 is the general size of the low-rise building for evaluating internal pressure coefficients and external pressure coefficients except vaulted roof. Type 2 is the size of the gymnasium for evaluating external pressure coefficient of vaulted roof.

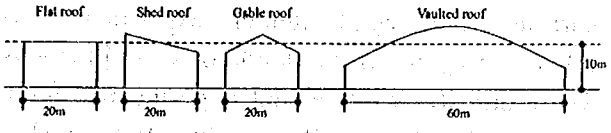


Figure 1. Concerned Patterns of Roof Shapes and Spans

Generally, different codes and standards may

define different averaging time or different reference height for the reference wind pressure as shown in Table 2. For example, the reference wind pressure in ISO 4354 corresponds to the mean wind pressure with averaging time of 10 minutes and its reference height is higher one, mean roof height or 6m, for designing claddings. On the other hand, AS 1170.2 defines the maximum 2-3 seconds gust as the basic design gust speed and its reference height is the same as height of the building. Therefore, before comparing the products of gust effect factor and pressure coefficient, it is necessary to take such conceptual differences into consideration and introduce consistent reference wind pressure. In this study, the consistent reference pressure q_{II} is defined as below:

- Averaging time : 10 minutes
- Reference height H : mean roof height
- Roughness condition : open terrain

For simplification, structural importance multiplier and effects of local topographic condition such as hills and escarpments are neglected.

Table 2. Definitions of Averaging Time and Reference Height

Codes and Standards	Averaging time	Reference height
ISO4354	10 minutes	Mean roof height, or 6m
EUROCODE ENV-1991	10 minutes	Height of the building
ASCE 7-95	3 seconds	Mean roof height
AS1170.2	2-3 seconds	Height of the building
NBCC1990	1 hour	Mean roof height, or 6m
SWISS Standard	2-3 seconds	Height of the building

In the codes or standards concerned, the equation for external pressure w can be generally expressed as below:

$$w = q_{ref}(G_{pe}C_{pe}) \qquad (1)$$

Where q_{ref} and $(G_{pe}C_{pe})$ denote the reference wind pressure and the product of gust effect factor and wind pressure coefficient provided in the code or standard, respectively. Based on the consistent reference pressure q_{II}, the following equation can be substituted for Eq.(1).

$$w = q_{II}\left[\frac{q_{ref}}{q_{II}}(G_{pe}C_{pe})\right] = q_{II}(G_{pe}C_{pe})^{*} \qquad (2)$$

Where $(G_{pe}C_{pe})^*$ denotes converted product of gust effect factor and wind pressure coefficient.

Table 3. Converted Products of Gust Effect Factor and External Pressure Coefficient

Codes and Standards	$(GpeCpe)^*$
ISO4354 (Simplified Method of Analysis)	$2.5\left(\frac{z}{H}\right)^{0.28} C_{pe}$ z : Mean roof height or 6.0m, whichever is greater
EURO CODE ENV-1991	$\left\{\frac{C_r(z)}{C_r(H)}\right\}^2\left\{1+\frac{1.3}{C_r(z)}\right\}C_{pe}$ C_r : Roughness coefficient z : Height of the building (Mean roof height for vaulted roofs)
ASCE 7-95	$1.7C_{pe}$
AS1170.2 (Static Analysis)	$2.0\left\{\frac{M_{(z,cat)}}{M_{(H,cat)}}\right\}^2 K_1 C_{pe}$ $M_{(*,cat)}$: Gust wind speed multiplier K_1 : Local pressure factor z : Height of the building
NBCC 1990 (Simple Procedure)	$2.2\left(\frac{z}{H}\right)^{0.2} C_{pe}$ z : Mean roof height roof or 6.0m, whichever is greater
SWISS Standard	$2.0\left\{\frac{C_h(z)}{C_h(H)}\right\}C_{red}C_{pe}$ C_{red} : Reduction coefficient C_h : Height coefficient z : Height of the building

Table 3 shows the converted products of them in the codes and standards concerned, where Cpe is external pressure coefficient regulated in the code or standard. Fig.C6-1 in ASCE 7-95 Commentary[4] is utilized for converting averaging time into 10 minutes.

2.2 Result of Comparison

This section shows examples of the converted products $(G_{pe}C_{pe})^*$ about claddings of gable roof and vaulted roof. The compared values are based on wind pressure effects on the effective wind area of $1.0m^2$.

2.2.1 Gable roof

The external pressure coefficients for the gable roof are regulated in all the codes and standards. Applied building model following the size of type 1 is shown in Figure 2. Wind direction is perpendicular to the ridge.

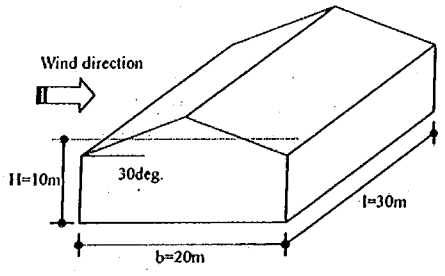


Figure 2. Building Model with Gable Roof

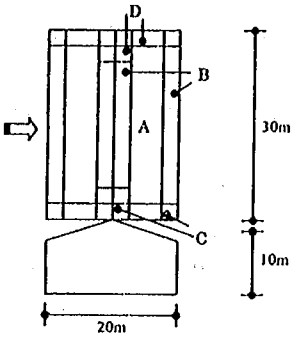
The converted products are shown in Tables 4-9. All the codes and standards take into consideration negative pressure due to suction at corners or ridge of the roof, but the results as shown below are different one another.

In ISO4354, ASCE7-95 and NBCC1990, they regulate negative value of around -4.0~-7.0, while AS1170.2 and Swiss Standard regulate not so conservative values. As for ISO4354 and NBCC1990, the regulated gust effect factors and external pressure coefficients themselves are the same each other, but the converted products (GpeCpe)* result in being different each other and the values in ISO4354 seem to be more conservative. It is seen that negative values in ASCE 7-95 have tendency to be more conservative than those in others.

(1) ISO 4354(Simplified Method of Analysis)

Table 4. (GpeCpe) for gable roof in ISO 4354*

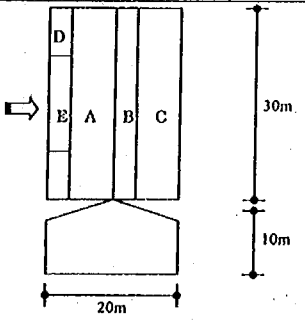
Area	A	B	C	D
(GpeCpe)*	-1.6	-2.0	-4.1	-3.1



(2) EUROCODE ENV 1991-2-4

Table 5. (GpeCpe) for gable roof in ENV1991-2-4*

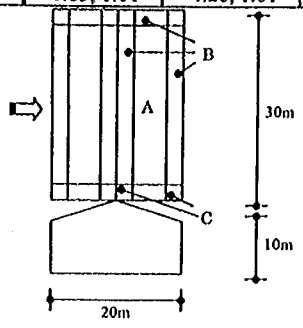
Area	A	B	C	D
(GpeCpe)*	-0.4, 0.8	-1.0	-0.8	-3.0, 1.4



(3) ASCE 7-95

Table 6. (GpeCpe) for gable roof in ASCE7-95*

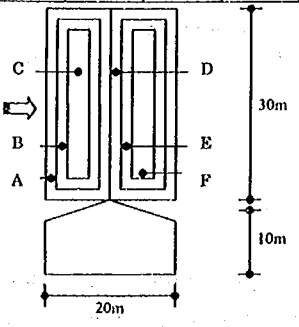
Area	A	B	C
(GpeCpe)*	-1.83, 1.01	-4.26, 1.01	-7.51, 1.01



(4) AS1170.2(Static Analysis)

Table 7. (GpeCpe) for gable roof in AS1170.2*

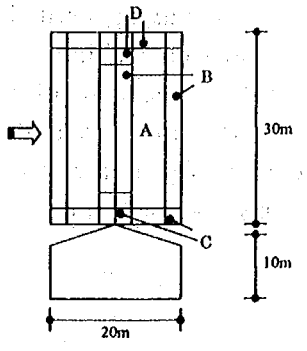
Area	A	B	C	D	E	F
(GpeCpe)*	-0.75 0.75	-0.56 0.56	-0.37 0.37	-2.24	-1.68	-1.12



(5) NBCC 1990(Simple Procedure)

Table 8. (GpeCpe) for gable roof in NBCC1990*

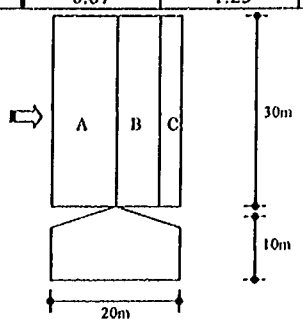
Area	A	B	C	D
(GpeCpe)*	-1.4	-1.75	-3.58	-2.70



(6) Swiss Standard

Table 9. (GpeCpe) for gable roof in Swiss Standard*

Area[m]	A	B	C
(GpeCpe)*	0.67	-1.23	-1.45



2.2.2 Vaulted roof

The external pressure coefficients for the vaulted roof are regulated in all the codes and standards except Swiss Standard. Applied building model following the size of type 2 is shown in Figure 3, and in this case, wind direction is also perpendicular to the ridge.

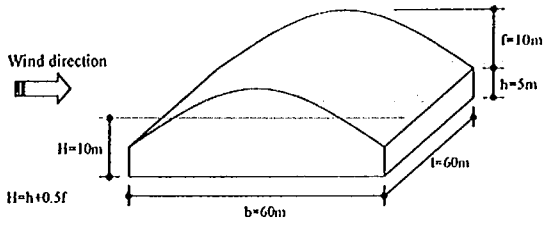


Figure 3. Building Model with Vaulted Roof

The converted products are shown in Tables 10–14. On the whole, converted values in AS1170.2 are the most conservative than others.

High suction observed at separation area is of great concern for the cladding design and it is necessary to regulate more conservative coefficient at such areas. With regard to this important point, it is found out that the concerned area is different in the codes and standards. AS1170.2 and ASCE 7-95 regard windward corner as the most conservative area, while ISO4354, EUROCODE and NBCC1990

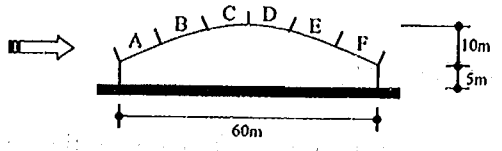
do top roof area. The reason of this discrepancy should be investigated.

As being pointed out in section 2.2.1, the values in ISO4354 are also more conservative than those in NBCC1990.

(1) ISO 4354(Simplified Method of Analysis)

Table 10. (GpeCpe) for vaulted roof in ISO 4354*

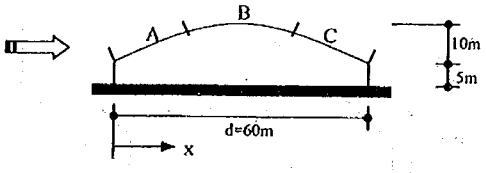
Area	A	B	C	D	E	F
(GpeCpe)*	-0.25	-1.25	-2.00	-2.00	-1.00	-0.25



(2) EUROCODE ENV 1991-2-4

Table 11. (GpeCpe) for vaulted roof in ENV1991-2-4*

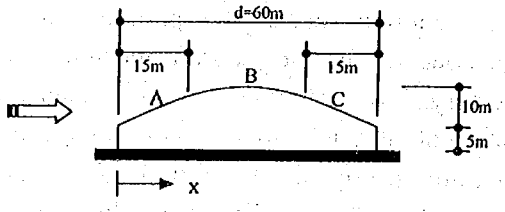
Area [m]	A 0<x<15 (=d/4)	B 15<x<45 (=3d/4)	C 45<x<60 (=d)
(GpeCpe)*	0.04	-2.00	-0.93



(3) ASCE 7-95

Table 12. (GpeCpe) for vaulted roof in ASCE7-95*

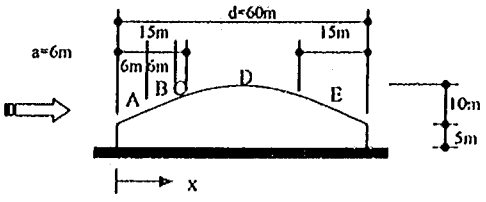
Area [m]	A 0<x<15 (=d/4)	B 15<x<45 (=3d/4)	C 45<x<60 (=d)
(GpeCpe)*	-1.34	-1.29	-0.74



(4) AS1170.2(Static Analysis)

Table 13. (GpeCpe) for vaulted roof in AS1170.2*

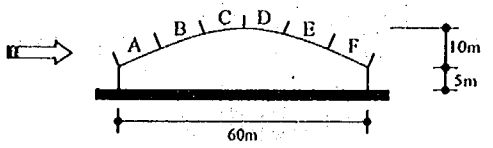
Area [m]	A 0<x<6 (=a/2)	B 6<x<12 (=a)	C 12<x<15 (=d/4)	D 15<x<45 (=3d/4)	E 45<x<60 (=d)
(GpeCpe)*	-4.00	-3.00	-2.00	-1.90	-1.10



(5) NBCC 1990(Simple Procedure)

Table 14. (GpeCpe) for vaulted roof in NBCC1990*

Area	A	B	C	D	E	F
(GpeCpe)*	-0.22	-1.09	-1.74	-1.74	-0.87	-0.22



3. Conclusion

This paper presented the outline of our committee's ongoing works, which is the comparison of products of gust effect factors and wind pressure coefficients between current codes and standards used in several nations.

From this study, it was proved that there are differences of wind pressure level and concept between each code and standard. The work will be continued, and after making clear causes that lead to such differences, some of the results will be refereed in the revised works of Recommendations for Loads on Buildings in Architectural Institute of Japan.

4. Committee Members

Prof. Takeshi OKUMA
Kanagawa University
Prof. Yukio TAMURA
Tokyo Institute of Polytechnics
Assoc. Prof. Yasushi UEMATSU
Tohoku University
Dr. Hisashi OKADA
Building Research Institute
Mr. Akihisa KAWAGUCHI
Obayashi Corporation
Mr. Hiroshi NODA
Mitsui Construction Co., Ltd.
Mr. Hisao MARUKAWA
Izumi Sohken Engineering Co., Ltd.
Dr. Kazuki HIBI
Shimizu Corporation
Dr. Kazuo OTAKE
Takenaka Corporation
Dr. Ken'ichi SUDA
Sato Kogyo Co., Ltd.
Mr. Koji KONDO
Kajima Technical Research Institute
Dr. Kunio FUJII
Wind Engineering Institute Co., Ltd.
Dr. Masanao NAKAYAMA
Fujita Corporation
Dr. Morimasa WATAKABE
Toda Corporation
Dr. Nobuo KATO
Tokyu Construction Co., Ltd.
Dr. Ryuichiro YOSHIE
Maeda Corporation
Dr. Saburo KAWABATA
Nippon Sheet Glass D & G System Co., Ltd.
Mr. Yutaka ASAMI
Taisei Corporation
Mr. Hitomitsu KIKITSU
Building Research Institute

References

[1] J.D.Holmes, Wind Loading of Large Roofs – the Code and Beyond, International Seminar on Loading Standards for Structural Design, The Institution of Engineers, Singapore, 1998.

[2] Internal Organization for Standardization, ISO International Standard – Wind Actions on Structures, ISO/DIS 4354, 1997.

[3] European Committee for Organization (CEN), Draft Eurocode 1: Basis of Design and Actions on Structures, Part 2.4: wind actions, ENV-1991-2-4, 1995.

[4] American Society of Civil Engineers, Minimum Design Loads for Buildings and Other Structures, ASCE Standard, ANSI/ASCE 7-95, 1995.

[5] Standard Australia, SAA Loading Code Part 2: Wind loads, AS1170.2-1989.

[6] Associate Committee on the National Building Code, National Research Council of Canada, National Building Code of Canada, 1990.

[7] Swiss Society of Engineers and Architects, Swiss Standard, Actions on Structures, 1991.

A Probabilistic Tornado Wind Hazard Model for the Continental United States

By

Quazi Hossain[1], Richard Mensing[2], Jean Savy[1], and Jeffery Kimball[3]

ABSTRACT

A probabilistic tornado wind hazard model for the continental United States (CONUS) is described. The model incorporates both aleatory (random) and epistemic uncertainties associated with quantifying the tornado wind hazard parameters. The temporal occurrences of tornadoes within the continental United States (CONUS) is assumed to be a Poisson process. A spatial distribution of tornado touchdown locations is developed empirically based on the observed historical events within the CONUS. The hazard model is an aerial probability model that takes into consideration the size and orientation of the facility, the length and width of the tornado damage area (idealized as a rectangle and dependent on the tornado intensity scale), wind speed variation within the damage area, tornado intensity classification errors (i.e.,errors in assigning a Fujita intensity scale based on surveyed damage), and the tornado path direction. Epistemic uncertainties in describing the distributions of the aleatory variables are accounted for by using more than one distribution model to describe aleatory variations. The epistemic uncertainties are based on inputs from a panel of experts. A computer program, TORNADO, has been developed incorporating this model; features of this program are also presented.

[1]Lawrence Livermore National Laboratory, Livermore, California, 94550
[2]Consultant, Lawrence Livermore National Laboratory, Livermore, California, 94550
[3]United States Department of Energy, Germantown, Maryland, 20874

KEYWORDS: tornado hazard; probabilistic hazard model; epistemic and aleatory uncertainties; Fujita scale; tornado intensity; intensity classification error.

1. INTRODUCTION

For designing critical and hazardous facilities, the tornado wind hazard at a facility is generally described in terms of a probabilistic hazard curve. This curve quantifies the hazard in terms of the expected frequency, per year, that tornado wind speeds at a facility exceed a given velocity, over a range of velocities. The hazard curve is used to estimate the expected frequency or occurrence interval for a specific wind speed or, conversely, to assess a design-basis wind speed for a specified hazard level. Two types of tornado wind hazard models are commonly used: point-strike models or aerial models. A point-strike model treats the target as a point (unit area), so the hazard is described at a point or unit area. Examples of point-strike models are the Thom (1963), Abbey and Fujita (1975, 1979), Ramsdell (Ramsdell, et. al., 1986) and McDonald (1980, 1996) models. Unlike a point-strike model, an aerial model considers the dimensions and orientation of the facility in determining the wind hazard at a facility. Hazard assessments using aerial models can be based on assessing the probability that a specified wind speed occurs somewhere within the facility area (union definition of a tornado strike) or the entire facility experiences a specified wind speed (intersection definition of a tornado strike). Examples of aerial models are the Twisdale (1978) and Reinhold and Ellingwood (1982) models. Almost all of these models assume that tornado touchdowns occur uniformly throughout a relevant area surrounding the facility.

The model described in this paper is an aerial model that considers tornado touchdowns

occurring non-uniformly throughout the CONUS. The model is designed for site-specific risk assessments at sites anywhere in the CONUS. It is based on probabilistic risk assessment methodologies, which have been used to estimate the risks and/or hazards of other natural hazards, e.g., earthquakes, hurricanes, floods, as well as technological risks, e.g., aircraft crashes, production and other operational accidents. The existence of a credible database of the touchdown locations of historical tornadoes throughout the CONUS is essential. The United States Storm Prediction Center (SPC) database is used in the computer program TORNADO, developed to implement the model. Also crucial to the model is the availability of estimates of the following model 'parameters':

- Expected number of tornadoes per year, i.e. tornado occurrence rate.
- Distribution of F-scale intensity (Developed by Theodore Fujita of the University of Chicago, F-scale is the most widely used method of classifying a tornado based on observed/surveyed damage. Each F-scale intensity has been assigned a wind speed range).
- Misclassification matrix (that probabilistically quantifies the errors in each of the seven F-scale intensities).
- F-scale to wind speed relation (Since the damage assessment for intensity classification is subjective, wind-speed assigned to a F-scale has uncertainties associated with it).
- Distribution of the tornado heading, i.e. direction (This would account for any directional bias that tornadoes may have).
- Distribution of the tornado damage area length and width (This would account for the variation in the length and width of the area damaged by tornadoes of different intensities).
- Variation in wind speeds within the damage area.

These parameters are used to describe the aleatory (random) variability of tornado occurrences and characteristics. The model recognizes that the available information regarding these parameters is based on observations and analyses of the historic tornadoes, hence represents only an estimate of reality. Further, in order to account for the fact that some of the tornado characteristics (e.g., occurrence rates or F-scale intensity distributions) are not uniform throughout the CONUS, the model recognizes epistemic, (modeling) uncertainty as well. This is included by allowing for alternatives 'values' of the model parameters and a measure of relative confidence in the adequacy/goodness/reality of each of the alternatives.

2. TORNADO WIND HAZARD MODEL

The tornado wind hazard model is based on treating tornado occurrences and the characteristics of tornadoes as aleatory variables. The temporal occurrence of tornadoes throughout the CONUS is assumed to be a stationary Poisson process. Given a site of interest, and letting λ denote the occurrence rate (per year) of tornadoes in an appropriate area surrounding the site, the expected frequency (per year) of wind speeds exceeding v mph at the site, i.e., the tornado wind hazard at the site, is

$$EF(V>v) = \lambda\, P(V>v|\text{a tornado})$$

The conditional probability, given a tornado touches down, that the wind speeds at the site exceeds v, $P(V>v|\text{a tornado})$, depends on the intensity of the tornado. The model uses the standard F-scale intensity classification, F0 through F5, of tornadoes. Given the F-scale intensity distribution, $P(Fj)$, $j=0,1,..\ 5$, the tornado wind hazard at the site is

$$EF(V>v) = \lambda \sum_i P(V>v|\, Fi)\, P(Fj)$$

The model allows for the potential misclassification of tornado intensities due to random encounter of structures and human errors in classification. These sources of variability/uncertainty are treated as a random

(aleatory) uncertainty based on the following rationale: Given a tornado, there is a maximum wind speed associated with it, generally unknown. This wind speed has the capability of producing a given amount of damage (e.g., F3 intensity damage) provided the opportunities to produce damage exist. The existence of opportunities is a function of the touchdown location, the tornado path, and the number and locations of structures, trees, vehicles, etc. within the damage area. These are issues of the state of nature and the world, thus, classification errors due to the existence of opportunities is considered an aleatory variable. Since tornado intensity classification involves human judgement there is also a source of epistemic uncertainty in the intensity classification process. However, it is assumed that the aleatory variability is the dominant source of uncertainty. Let p_{ij} denote the probability that the true intensity is Fi, given that the recorded intensity is Fj. Accounting for classification errors, the tornado wind hazard is

$$EF(V>v) = \lambda \sum_i P(V>v|\, Fi)\ (\sum_j p_{ij} P_R(Fj))$$

$$= \lambda \sum_i P(V>v|\, Fi)\ P_T(Fi)$$

where, $P_T(Fi) = \sum_j p_{ij}\ P_R(Fj)$

If it is assumed that touchdown locations are uniformly distributed within a region of interest, the probability that the wind speed exceeds v mph at an arbitrary point in the region, $P(V>v|Fi)$, is proportional to the size of the sub-area of the tornado damage area in which the wind speed exceeds v. An estimate of this probability is $A(v|\, Fi)/A$, where A is the area of the region of interest and $A(v|\, Fi)$ is the average size of the sub-area in which wind speeds exceed v, given an Fi level tornado. Applying the usual quantification of the variability of wind speeds within the damage area in terms of 'local intensities', the estimate of this probability is

$$P(V>v|Fi) = \sum_{j \le i} P(V>v|\, Fj, Fi)\ A(Fj|\, Fi)/A$$

The term $P(V>v|\, Fj, Fi)$ recognizes that wind speeds associated with local intensity Fj vary within a range of speeds. The model assumes that the wind speeds are uniformly distributed within the range. Inserting this into Equation (4), the tornado wind hazard is

$$EF(V>v) = \lambda \sum_i (\sum_{j \le i} P(V>v|\, Fj, Fi)\ A(Fj|\, Fi)/A)\ P_T(Fi)$$

The revised model extends this model in two ways, (1) the site or facility is treated as an area rather then a point and (2) a non-uniform distribution of tornado touchdown locations within the affective region around the site is used. To estimate the tornado wind hazard when the site is an area, it is necessary to identify the 'tornado origin area' (Twisdale, 1978). Using the union definition of a tornado strike, this area is the set of tornado touchdown locations for which wind speeds at some point at the facility are greater then v mph. To identify the 'tornado origin area', it is necessary to model the tornado damage area. The model approximates the damage area as a rectangular area (Twisdale, 1978). The length and width of the damage area are considered aleatory variables. The joint distribution of length and width depends on the F-scale intensity of the tornado. It is also necessary to consider wind speed variation within the damage area. Areas of increasing 'local intensity' are modeled as included rectangles, centered, lengthwise, at the center of the damage area. Along the width of the damage area the included rectangles are offset from the storm center track to the right in recognition of the existence of suction vortices rotating about the parent tornado (Abbey and Fujita, 1979). The tornado origin area depends on the dimensions and orientation of the facility and the direction of the tornado path, as well as the characteristics of the damage area.

Mathematically, allowing for a non-uniform distribution of tornado touchdown locations and an aerial model, the term $A(Fj|\, Fi)/A$ changes to the integral of the density function of the

distribution of touchdown locations within the tornado origin area corresponding to Fj local intensity. The location and dimensions of this area depend on the tornado F-scale intensity, Fi; the direction of the tornado path,θ; the length and width, $(L, W)_i$, of the damage area; and the proportion of the damage area involving winds of local intensity Fj. The lengths and widths of the local intensity areas are expressed as fractions, (δ_L, $\delta_W)_{ij}$, of the damage area lengths and widths respectively. The revised mathematical expression for the wind hazard is

$$EF(V>v) = \lambda \sum_i P_T(Fi) \{\sum_j P(V>v| Fj, Fi) \int_{A(Sij)} dF(x, y) \}$$

where, F(x, y) denotes the distribution function of the tornado touchdown locations and Sij denotes the parameters { θ, $(L,W)_i$, (δL, $\delta W)_{ij}$ } which define the local intensity areas. Since the parameters are aleatory variables, the calculation averages over the probability distributions of these aleatory variables. In the model, distributions are used for the tornado path direction and damage area length and width; singular values, dependent on the local intensity and F-scale intensity, are assumed for the dimensions of the local intensity areas. Adding this to the model, the mathematical expression for the tornado wind hazard is

$$EF(V>v) = \lambda \sum_i P_T(FI) \{ \sum_j P(V>v| Fj,Fi) \int_0 \int_{(L,W)i} \int_{A(Sij)} dF(x,y)\, dG(\theta)\, dH(L,W)\} \quad (8)$$

This is the basic model in the TORNADO code that has been developed to create the tornado wind hazard curves.

3.0 COMPUTER PROGRAM TORNADO

The tornado wind hazard model described in Section 2 forms the basis for the computer program TORNADO that is used to develop site-specific tornado wind hazard curves. The program assumes that the facilities at the site can be approximated by a set of convex polygons. The inputs into the program are:

1. The location of the site, given by the (latitude, longitude) of the site. This is treated as the center of an (x, y) coordinate system for defining the dimensions of the facility.

2. The (x, y) coordinates of the corners of the convex polygon(s) identifying the facility.

Also required are data on the locations and characteristics of tornadoes, specifically:

a. A database of the historical tornado touchdown locations within the CONUS. Included in the current version of the code is a database of locations based on the Storm Prediction Center's (SPC) database of tornadoes for 1950-1995.

b. Alternative estimates, with epistemic uncertainties, of the model parameters identified in Section 1.

Central to the wind hazard calculations is the development of a probability distribution of the touchdown locations of tornadoes throughout the CONUS. Given the database of touchdown locations of the historical tornadoes, a 2-dimensional normal kernel density estimator is used to estimate the distribution of tornado locations throughout the CONUS

$$f(x_1, x_2) = \frac{1}{2\pi n h_1 h_2} \sum_{i=1}^{n} Exp\left\{ -\frac{1}{2} \sum_{j=1}^{2} \left(\frac{x_j - x_{ij}}{h_j} \right)^2 \right\}$$

where, (x1,x2) and (x_{i1}, x_{i2}), i= 1,...,n are the (latitude, longitude) of an arbitrary location in the CONUS and the touchdown locations of the historical tornadoes respectively. The smoothing parameters, h_1, h_2, used in the current version of TORNADO are a fraction of $\sigma_i n^{-1/6}$, where, n is the number of tornadoes in the touchdown location database and the σ_i are estimates of the standard deviations of the recorded latitudes and longitudes. The smoothing parameters reflect the variability of future tornado locations relative to the locations of the historical events.

Given the sets of values of the model parameters and the site-specific location and facility dimensions, the program identifies a site specific tornado effect area (SSTEA). The SSTEA is defined by the locust of touchdown locations from which a tornado could start and have the potential to affect the facility. It is based on the potential longest tornado path length. Given the SSTEA and the database of historical tornado locations, the program conceptually estimates a site- specific occurrence rate and a conditional location distribution over the SSTEA. This forms the basis for the site-specific hazard calculations.

The output of TORNADO is an estimate of the tornado wind hazard curve for the site. Since the model includes epistemic uncertainty, the estimate is a set of hazard curves representing envelopes of hazard fractiles produced by the epistemic uncertainties.

4.0 TREATMENT OF UNCERTAINTY

Since the true values of the model parameters listed in Section 1 are not known exactly and can only be estimated, a very important aspect of the model is the inclusion of epistemic uncertainties reflecting the current state of knowledge about parameters. This is included in the model by allowing for alternative values of the model parameters along with a measure of the relative confidence that each of the alternatives approximates the true value of the parameter. The credibility of the estimated tornado wind hazard curves depends on the credibility of the values of the model parameters. Thus, it is important that the values be derived with direct interaction and involvement of industry experts in the field. A panel of experts was formed to elicit input about the model parameters. A discussion of the information elicited is included in the following subsections.

4.1 Occurrence Rate of Tornadoes

An obvious source of an estimate for the occurrence rate is a database of historical tornadoes, such as the SPC database. Depending on the years selected, the estimated occurrence rate can vary between approximately 650 and 1200 per year. Estimated rates for several periods were provided to the experts. They were asked to provide their estimate of a lower and upper bound for the rate and their relative confidence that the rate does not exceed several intermediate values. From this input, a 'consensus' uncertainty distribution of the occurrence rate will be developed.

4.2 F-scale Intensity Distribution

Since an F-scale intensity is assigned to all recorded tornadoes, the obvious source of estimates for the probability distribution of the recorded F-scale intensity is the database of historical tornadoes. Since the parameter is a probability distribution instead of a single-valued parameter, the credibility of an estimate depends on the number of years used as well as the time period. Thus, several time periods of varying length were provided to the experts and they were asked to provide their relative confidence in each. The expert's inputs will be combined to develop a 'consensus' weighting of the various time periods, hence, weighting of the estimated recorded F-scale intensity distributions.

4.3 Probabilities Associated with Classification Errors: Misclassification Matrix

The misclassification matrix provides a means of accounting for errors in the F-scale classification of tornadoes. Misclassification is quantified in terms of the conditional probability, p_{ij}, that the true intensity of a tornado is Fi, given that the recorded intensity is Fj. The misclassification matrix is the matrix of the probabilities, p_{ij}, used to assess the distribution of true F-scale intensity, given the distribution of recorded intensity. Based on a review of the tornado literature, most estimates of misclassification matrices include both evaluation and random dispersion uncertainty. The aleatory aspects of these uncertainties are assumed to be the dominant sources of error. Several alternative estimates of the misclassification matrix, based

primarily on the work of Twisdale (1978, 1981, 1983) and Reinhold and Ellingwood (1982) were provided to the experts. They were asked to provide their relative confidence in each alternative.

4.4 F-scale Intensity to Wind Speed Relation

Several models for associating wind speeds to each of the F-scale intensities have been developed. One is the original association of wind speeds and damage developed by Fujita (1973). Two other relations in the literature were developed by Twisdale (1978) based on a Bayesian analysis of the range of wind speeds associated with the F-scale intensities. One assumes a uniform uncertainty on the upper bounds of the wind speed intervals related to each F-scale intensity level. The second assumes a linearly increasing uncertainty on the upper bound. Another relation was developed by Dames and Moore (Beebe, et. al, 1975). The experts were asked to provide their relative confidences in each of these alternative relations.

4.5 Distribution of Tornado Path Direction

Elicitation of uncertainties in estimates of the distribution of tornado path direction was done in the same way as that for the distribution of F-scale intensity.

4.6 Distribution of Damage Area Length and Width

The damage area of a tornado is modeled as a rectangle with specified length and width. Aleatory variation in the damage area is represented by a joint probability distribution of length and width, conditional on the F-scale intensity of the tornado. Data from the database of historical tornadoes is the basis for estimating the joint distribution. Epistemic uncertainty was quantified by having the experts provide their relative confidence in using data from several alternative time periods to estimate the joint probability distribution.

4.7 Variation in Wind Speeds Within the Damage Area

Cascading rectangular sub-areas of diminishing size within the damage area are used to model the wind speed variation within the damage area. The lengths and widths of these included sub-areas, specified as fractions of the length and width of the damage area, are functions of the F-scale intensity. The fractions for each of the higher intensities (e.g., F2 and F1 for an F2 intensity tornado) are model parameters. Several alternative sets of values for the length fractions, including those by Fujita(1978), MacDonald(1980), Twisdale(1981), and Reinhold and Ellingwood(1982) were considered. Similarly, several alternative sets of values for the width fractions were developed for inputs. These included fractions based on the Dapple values developed by Abbey and Fujita (Abbey & Fujita, 1979) and on values based on the work of Garson, et. al(1975), Reinhold & Ellingwood,(1982) and McDonald(1983). Combinations of sets of length and width fractions were provided to the experts for their assessment of their relative confidence in each combination.

5.0 CONCLUSIONS

The TORNADO code is presently undergoing modification to develop site-specific tornado intensity distributions. Once the modification is completed, the code is expected to provide a comprehensive tool for developing a site-specific probabilistic tornado hazard curve at any site within the CONUS. The program allows easy modification of the model parameter values to account for new data and new interpretations of existing data.

6.0 REFERENCES

Abbey, R.F., Jr., "Research Efforts in Severe Storms Applied to Nuclear Reactors", Second U.S. National Conference on Wind Engineering Research, Ft. Collins, CO, 1975.

Abbey, R.F. and Fujita, T.T., "The DAPPLE Method for Computing Tornado Hazard Probabilities: Refinements and Theoretical Considerations, " 11th Conference on Severe Local Storms," American Meteorological Society, Boston, 1979.

Fujita, T.T., 'Workbook of Tornadoes and High Winds for Engineering Applications," SMRP Research Paper 165, Department of the Geophysical Sciences, the University of Chocago, September 1978.

Fujita, T.T. and A.D. Pearson, "Results of FPP Classification of 1971 and 1972 Tornadoes," Paper presented at the Eighth Conference on Severe Local Storms, 1973.

Garson, R.C., J.M. Catalan, and C.A. Cornell, "Tornado Design Winds based on Risk, " Journal of the Structural Division, ASCE, Vol. 101, No.9, September 1975.

McDonald, J.R., "A Methodology for Tornado Hazard Probability Assessment," Institute for Disaster Research, Texas Tech University, Lubbock, Texas, 1980.

McDonald J.R., "The Modified IDR Model - Short Course Notes," Engineering for Extreme Winds: 1996, Texas Tech University, February 1996.

Ramsdell, J.V. and G.L.Andrews, "tornado Climatology of the Contiguous United States," Pacific Northwest Laboratory, prepared for the US Nuclear Regulatory Commission, NUREG/CR-4461, May 1986.

Reinhold, T. and B. Ellingwood, "Tornado Damage Risk Assessment," National Bureau of Standards, NUREG/CR-2944, 1982.

Twisdale, L.A. and W.L. Dunn, "Tornado Missile Simulation and Design Methodology," Research Triangle Institute, NP-2005, Vol. 1, 1981.

Twisdale, L.A., W.L. Dunn and J. Chu, "Tornado Missile Risk Analysis", EPRI Reports NP-768 and NP-769, Electric Power Research Institute, Palo Alto, 1978.

Twisdale, L.A. et al., "Probabilistic Analysis of Tornado Wind Risk," ASCE Journal of Structural Engineering, Vol. 109, No. 2, February 1983.

10km Scale Wind Speed Fluctuation Observed in Typhoon Area.

by

Yoshinobu Tanaka[1]

ABSTRACT

Typhoon VIOLET approached Kanto district on September 22nd, 1996, and heavy rain and strong wind was brought. 10km scale linear echoes took their rise in the north-west quadrant region of the typhoon. The linear echoes had an orientation of NNE to SSW and spreaded wavely. They had a intensive variation of 5 to 10 m/s at doppler velocity. They moved from west to east with variation of wind during 3 hours. The wind speed fluctuation of the scale under 1km was also observed by the radar in the except for the title. Although the author is researching the mechanism of these phenomena, other studies say that they are the roll convection in the boundary layer.

Such small scale intensive fluctuation of wind speed, which the measurment in the past could not observe, will affect the detailed prediction of wind and the architecture design about wind endurance.

KEY WORDS: tropical cyclone ; typhoon ; hurricane ; gale ; rainband ; boundary layer ; mesoscale ; radar

1 INTRODUCTION

Typhoon VIOLET had approached Kanto district nearest in recent years Typhoon, and it gave most ruin.

1996, the second operational doppler RADAR in Japan was deployed (the following Narita radar) at New Tokyo Aviation Local Meteorological Observatry (NARITA Air-port). Typhoon VIOLET was the first typhoon approached the Narita radar.

Since ,in Japan, there was no operational instrment that could catch wind speed in the high density spatially and time-related under the strong wind like the typhoon, the data of the Narita radar is precious. The author is investigating the mesoscale phenomenon in the typhoon, and , as the initial stage, analyzed the data of Narita radar . As the result, in the typhoon VIOLET the 10km scale raind band was found.

Still, it is utilized for the understanding of the mechanism by classifying the weather phenomenon in the order of the dimension, in the meteorology. The 'mesoscale' phenomenon indicates the one in the order of several kiro-meter to several hundred kirometer, and it can be also classified into three scales from α scale to γ scale.

2 TYPHOON PATH AND THE DAMAGES

The tropical cyclone arose in the Philippines east open sea on Septermber 11th, 1996 became with typhoon VIOLET at 13th. It passed Minami-Daito Island , Hachijo Island, approached in Kanto district on 22nd at closest range, and by passing the Hokkaido east open sea, it changed in the extratropical cyclone at the Chishima Islands on 23rd.

[1]Typhoon Research Department, Meteorological Research Institute, Japan Meteorological Agency

On 15 o'clock September 22nd 1996 (all of the followig times is local time), on which the typhoon approached in Kanto district at closest range, the center of it located at 31.5 degree latitude ,141.0 degree longitude, which is the location 50km away from the east coast of Boso peninsula. At this time, the typhoon kept large and the strong power so that the pressure of center was 960 hPa, the maximum of wind speed was 35 m/s. Then, around the south of Kanto district, the record precipitaion and wind were observed, and the damages occured.

At Choshi , the maximum instantaneous wind speed 51.9 m/s and the maximum wind speed 36.3m/s ware recorded, and at Hachijo Island , the maximum instantaneous wind speed 51.5 m/s and the maximum wind speed 28.8m/s were recorded. At Nijima(Niijima village, Tokyo), all of the amount of precipitation was 387mm, at Kurobara(Ootaki town, Chiba) it was 365mm , and at Sakahata(Kmizu city, Chiba) it was 363mm.

The major dameges were the 12 deads , the 73 injureds , the 8 full broken houses, the 891 half broken houses, the 2,612 houses inundated over floor, the 9,614 houses inundated under floor, the 612 road dameges , the 61 ships , the 10.95 billion yen costs of aglicultture and the traffics stop and delay, the damage of the infrastractures related with life. Mobara city and Musuzawa town , Chiba , had the 3000 houses inundated over or under floor, and the disaster saving law was administered.

3 DATA ACQUISITION

The Narita radar has the high resolution that is 0.7 degree in azimuth direction and 150m in rudius direction, within low elevation, has the time resolution of about 1 minute and 20 seconds. The maximum range of detection is 120km.

Since the Narita radar caught the most usuful data of the typhoon VIOLET from 13 to 17 o'cklock 22nd, the data of this time was used for analysis.

4 RESULT OF ANALYSIS 1 — 10KM SCALE FLUCTUATION

(1) DISTRIBUTION OF THE REFLECTIVITY AND THE DOPPLER VELOCITY

As the first stage of the analysises, the time sequence of the radar reflectivity and the doppler velocity was made. At this time, the reflectivity and the doppler velocity were superimposed for seeing the relation of position of each other. As the region of analysis, Ibaraki prefecture and its east open sea were took note of.

At the analysis time , from 13 to 17 o'clock 22nd, the center of the typhoon located on the Boso peninsula's east open sea, the analysis region located at north-west quadrant of the center of the typhoon, and was the north or north-east place 50km away from the Narita radar.

Indicated by the solid air-line in the figure 1, in this region, the several part of the strong reflectivity which run from NNE to SSW was found. That is to say, the several linear part of heavy rainfall paralleled.

Then, it is found that the contour of doppler velocity was lifted up along the rainband.

In this region, the reflectivity and doppler veolcity ranged wavely, and the phases of both were synchronized. That is to say, the ridge of the filed of the reflectivity and the ridge of the field of the doppler velocity was concurrent, and the trough of the filed of the reflectivity and the trough of the field of the doppler velocity also did.

The distribution of both like this ocuured from 13 to 16 o'clock during the analysis time, it moved continuously from west to east keeping the synchronization of the phase like the propagation of wave.

It was from 15 to 16 o'clock that the situation appeared most distinctly. Before 15

o'clock, the interval between rainbands was about 10km, from 15 to 16 o'clock, that was about 20km. The amplitude of the fluctuation of the doppler velocity was $5 \sim 8m/s$, the moving speed of the echoes was about 30 m/s.

Although the fluctuation of the reflecticvity indicates the one of the rainfall intensity, only one radar can not resolve whether did the fluctuation of the doppler velocity indicate the one of the wind speed, the wind direction , or both of the speed and the direction.

(2) VERTICAL STRUCTURE OF THE REFLECTIVITY AND THE DOPPLER VELOCITY

The figure 2 shows the vertical cross section on the circle of the 80 km radius from the Narita radar. The structure of the synchronization of the fluctuation of the reflectivity and the doppler velocity reaches the altitude $5 \sim 6$ km from low level altitude.

Because the average of the wind speed becomes stronger as level lower, it is found that the addition of the preceding fluctuation to the average makes the wind speed stronger instantaneously, or the wind direction strong.

5 RESULT OF ANALYSIS 2 — UNDER 1 KM SCALE FLUCTUATION

The smaller scale fluctuation of velocity was also found in this typhoon.

The figure 3 shows the reflectivity and the doppler velocity in the area within 5km east , west , north and south each direction from the Narita radar. The striping was found in the figure of the doppler velocity. The stripes run NE to SW, and the interval of stripes is less than 1 km. There is the wave which has wavelength less than 1 km in the doppler velocity field. The amplitude of the wave is about 5 m/s. On the other hand, the reflectivity has no such flactuation. Differing from the section 4, This wave of the doppler velocity has no relation with the reflectivity Because the ovservation cycle of the radar was not enough fine to find the change of the wave of this scale, the moving speed of the wave could not be took.

Next, a comparison between the doppler velocity of 6 elevations from 0.7 degree to 17.0 degree was made. As the elevation became higher, the region in which the wave appeared distinctly became closer to the radar site, and the wave disapeared in the region more distant from the site. It is to say that the wave was generated only in the low altitude. Since the region in which the wave apeared spreaded within $2 \sim 3$ km from site at the elevation 5.1 degree, the wave reached to only the altitude lower then 1km from the ground level.

6 EXAMINATION

(1) 10 KM SCALE FLUCTUATION

In the boundary layer near of the center of typhoon , the friction between the surface generates the convergence of wind and the ascend flow. The boundary layer means the low stratum of the atmosphere which is affected by the heat and the friction stress between surface , and it is usually the stratum from surface to $1 \sim 2$ km. Since the air of the boundary layer of the typhoon is humid and unstable, the ascend flow generates cumulus (eye wall) and the condensation heat is released. This heat increases the wind of the typhoon and reinforces the convergence of the wind in the doundary layer. The eye wall of the typhoon is generated with the mechanism , so called Conditional Instability of the Second Kind (CISK) that is the effect the instablility of atmospheric stratiform layer and the frictional convergence on the surface are combined.

On the other hand, it is considered that the rainband outside of the typhoon is generatede by the mechanism different from CISK and

the gravity wave plays an important role. In the stable stratiform layer, when the air block moves to vertical direction it is oscillated by the gravity which plays an role as restoring force, and this oscillation propagetes far away as wave. In meteorology , the wave is called 'gravity wave'.

Gall. et al(1998) observed 10 km scale rainbands near the eye wall. They considered that it was same as the roll convection in the boundary layer and not the gravity wave. One of the famous examples of the roll convection in the boundary layer is the cloud streets occuring on Japan sea or Bering sea at winter. When the lower of the boundary layer having no wind becomes unstable *Reyleigh-Bénard* convection occurs. But if the wind having vertical shear blows , it is structured to the horizontal roll vortex. Usually, the roll vortex in the boundary layer has 2 $\sim$ 20 km wave length and 1 $\sim$ 2 km vertical width.

Since the rainband observed by them was the convection having 5 $\sim$ 6 km height, it was taller than the usuall roll convection. They suggested that it was because the unstable layer of the atmosphere was much deep.

It is not known whether the 10 km scale rainband of typhoon VIOLET described at the section 4 is the roll convection or the gravity wave, because the analysis has not proceeded yet. At all events, this rainband had the structure of the much wind speed change or the much direction change, and it is considered that it is not a little important for the prediction and the estimation of the effect of the wind of typhoon.

(2) UNDER 1 KM SCALE FLUCTUATION

This scale fluctuation did not appear on the reflectivity field, and it appeared only on the doppler velocity field. It was not the convection with the generation of the precipitation breaking the thermal unstable.

Wurman and Winslow(1998) got the result of the observation like the typhoon VIOLET in the hurricane Fran, and considerd that it was because the wind structure was same as the one of the roll convection in boundary layer. Although the roll convection in boundary layer usually occurs in the convective unstable layer, because of the obscurely unstable layer in thier observation they could not manifest the origin of the phenomenon.

Since the phenomenon of typhoon VIOLET was same as the thier observation with regard to both of the horizontal scale and the vertical distribution, perhaps, it had the same wind structure with the roll convection in the boundary layer.

7 CONCLUSION

Tow scale wave like fluctuations were observed on the typhoon VIOLET.

10 km scale fluctuation had 5 $\sim$ 10 m/s amplitude of doppler velocity and 10 $\sim$ 20 km wavelength. This phenomenon continued during more than three hours when the typhoon approached in Kanto district at closest range, and it had 5 $\sim$ 6 km height. The typhoon had the mesoscale precipitation system which had the structure that the fluctuation of wind and rainfall synchronized.

Under 1 km scale fluctuation had under 1 km wavelength and under 1 km height.

8 ACKNOWLEDGEMENT

Data used in this study provided by New Tokyo Aviation Local Meteorological Observatry.

APPENDIX

The doppler radar measures the reflectivity and the doppler velocity.

The reflectivity is the quantity that indicates how intensely the power of the sent radio wave is reflected by the precipitation particles, and it is considered to be univalently correspondent with the precipitation intensity.

When the precipitation particles move to the radar, the frequency of the recieved radio wave changes from the one of the sent wave by Doppler effect. The doppler radar provides the precipitation's speed equivalent with the doppler shift , that is , the wind speed (so called doppler velocity). The doppler velocity is the sight line component of the wind speed. If the wind blows perpendicularly to the direction of antenna, the doppler velocity becomes zero. The doppler velocity becomes positive when the wind blows away from the site, and it becomes negative when the wind approaches to the site.

References

[1] Okada,K., 1997: Typhoon No.17 which brought about the storm in the capital territory. *Meteorology,* 480, 14862-14864.

[2] Gall,R.,J.Tuttle, and P. Hildebrand, 1998: Small-Scale Spiral Bands Observed in Hurricanes Andrew,Hugo,and Erin. *Mon. Wea. Rev.,* 126, 1749-1766.

[3] Wurman,J., and J. Winslow, 1998: Intense Sub-Kilometer-Scale Boundary Layer Rolls Observed in Hurricane Fran. *Sci. Mag.,* 280, 555-557.

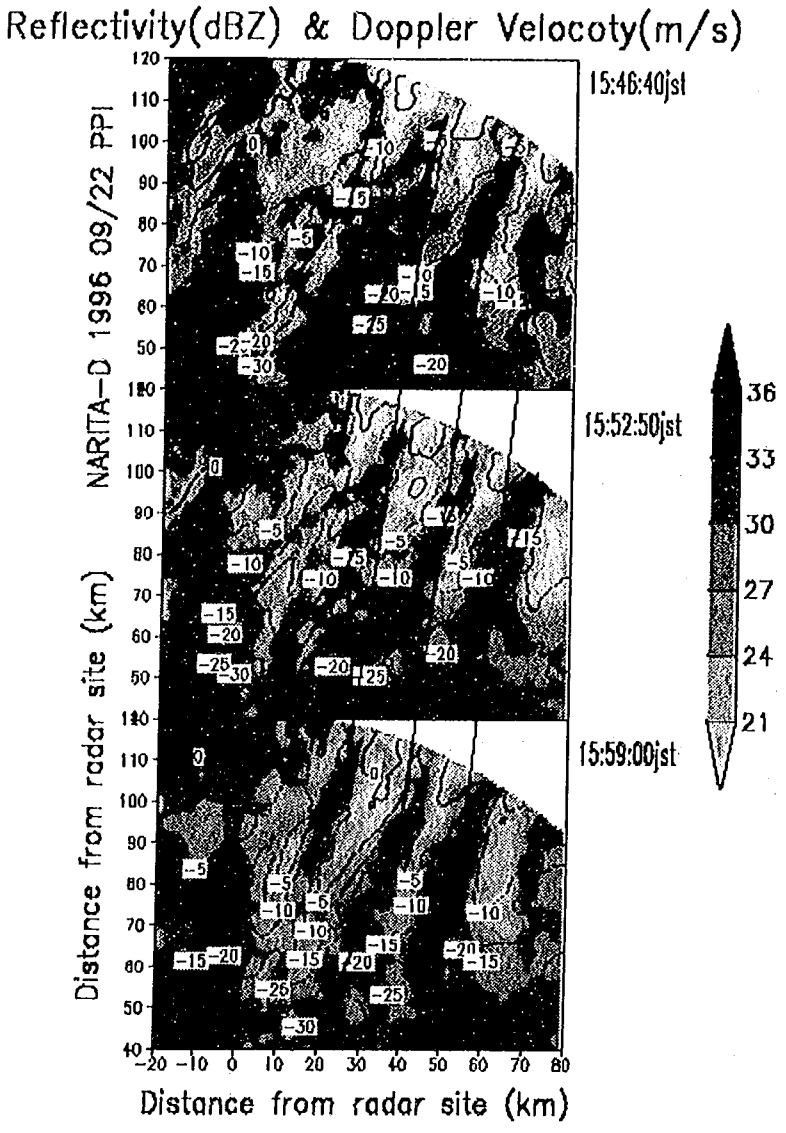


Figure 1: The reflectivity(shade:dBZ) and the doppler velocity (broken line: component approaching to the radar site thin solid line: component away from site m/s) of Narita radar at 15:46JST,15:52JST and 15:59JST, 22nd. The axis of abscissas indicates the distance of east direction from the radar site, the one of ordinates indicates the distance of north direction. The thick solid straight lines indicate the location of the remarked rainbands. The thin solid straight lines indicate the motion of the rainbands. On the remarked rainbands, the doppler velocity became large, and it is found that the rainbands moved keeping the positoin. The rainbands had about 20 km interval and about 30 m/s moving speed.

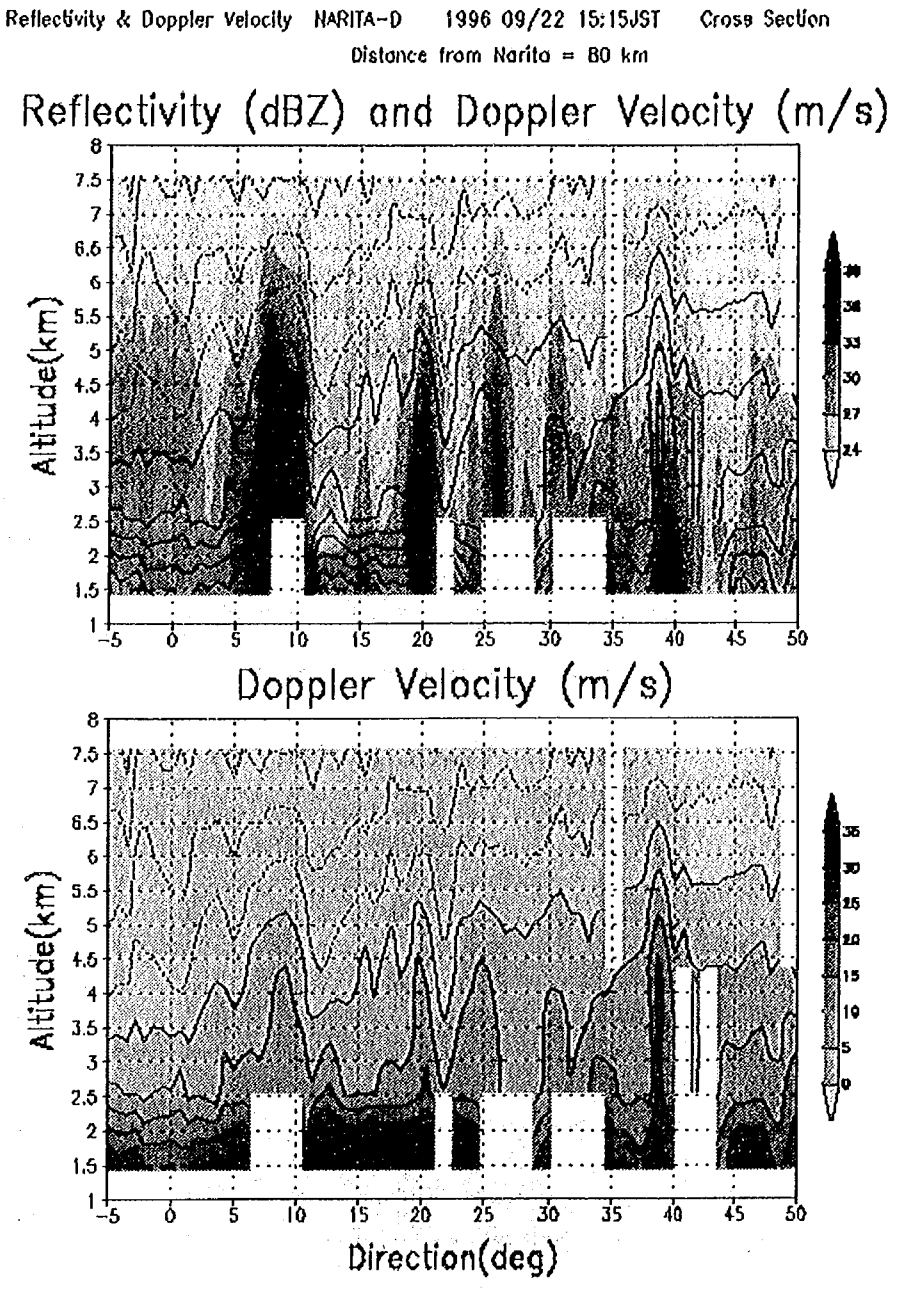


Figure 2: The vertical cross section at 15:15JST,22nd on the circle whose radius is 80 km from Narita radar. Upper figure indicates the reflectivity(shade:dBZ) and the doppler velocity(contour: m/s). Lower indicates the doppler velocity(shade:m/s). The axis of abscissas indicates the azimuth(north is zero), and the one of ordinates indicates the altitude. The synchronization of the reflectivity and the doppler velocity extended to $5 \sim 6$ km altitude.

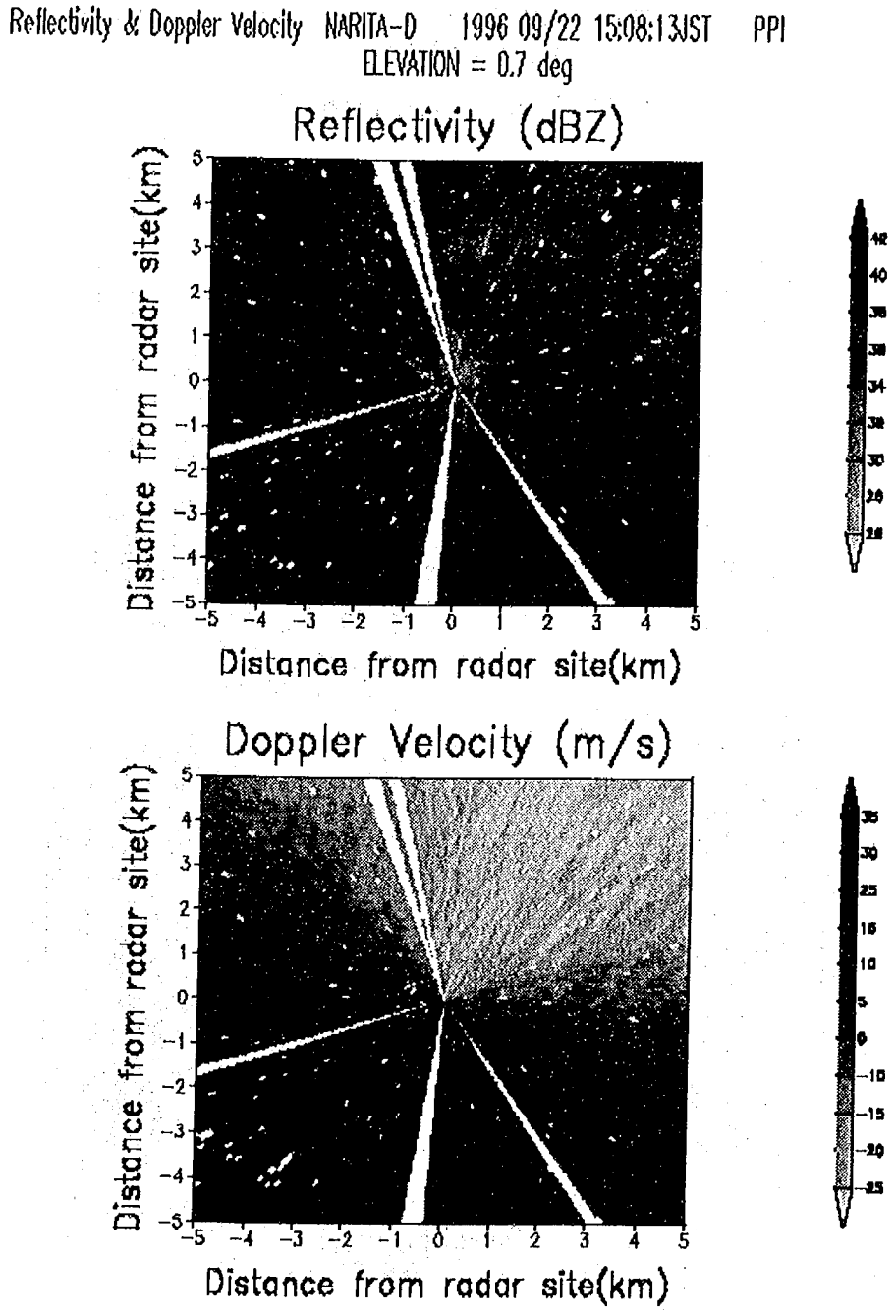


Figure 3: The reflectivity(upper:dBZ) and the doppler velocity(lower:m/s) near of Narita radar at 15:08JST, 22nd. The striping which runs from NE to SW was found in the figure of the doppler velocity. There was not anything correspondent with it in the reflectivity.

Theme 2

Earthquake Engineering

RECENT PROJECTS AT PWRI FOR IMPROVEMENT OF SEISMIC PERFORMANCE OF CIVIL INFRASTRUCTURES

by

YASUDA Masahiko[1)]

1. INTRODUCTION

Since the Hyogo-ken Nanbu Earthquake four years ago, seismic performance of civil infrastructures has been improved through revising the seismic codes for newly constructed facilities and nationwide retrofit for existing facilities. However, there still exist many problems in order for farther improvement of their seismic performance. This paper describes the recent projects that are especially propelled by Public Works Research Institute (PWRI) to cope with some of the problems. Those include,

(1) Rational Methodology to Determine Seismic Potential of Civil Infrastructures
(2) Very Strong Design Ground Motions with Direct Consideration for Source Faults
(3) Development of Seismic Design Methodology for Bridges
(4) Earthquake Resistance Design for Soil Structures

2. RATIONAL METHODOLOGY TO DETERMINE SEISMIC POTENTIAL OF CIVIL INFRASTRUCTURES

The question that has been posted since the Hyogo-ken Nanbu earthquake is that if the seismic performance between different types of infrastructures or between different structures of same types is consistent. Because each facility is designed based on its own code and because the performance is required respectively, the seismic performance between different types of facilities may have imbalance in their damages and their societal effects. Also the seismic performance of facilities may deviate affecting the functions of the system such as a highway network composed of those facilities. In such cases, validity of earthquake resistant investment needs to be examined carefully by taking the seismic performance of the facilities in the earthquake. Therefore, the methodology to determine the well-balanced seismic potential for the facilities in an area by counting their seismic performance realized in the earthquakes (Fig. 2.1).

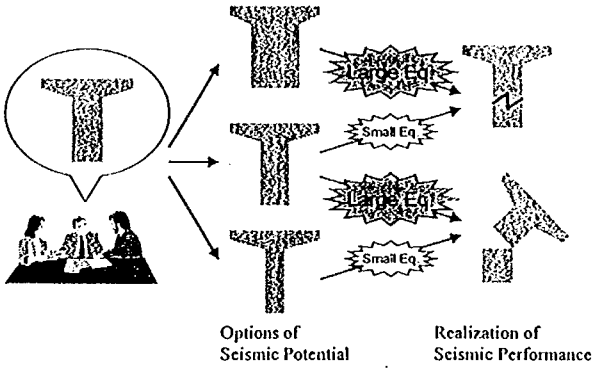


Fig. 2.1 Seismic Potential, Input Earthquake Level and Seismic Performance

Many countries are trying to revise their design codes to performance based expressions. An example of such attempt is the performance matrix proposed by the VISION 2000 committee of SEAOC, U.S.. It shows the lines indicating demanded seismic potentials corresponding to the importance of facilities in

1)Director, Earthquake Disaster Prevention Research Center, Public Works Research Institute, Ministry of Construction, Tsukuba Ibaraki 305-0804, Japan

the rectangle area provided by the input earthquake strong motion levels and the performance levels. Here, the lines mean the seismic potential that must be satisfied in the design, and their importances are supposed to be given by externally. In this sense this potential matrix can be referred as the "demanded performance matrix" (DPM), (Fig. 2.2).

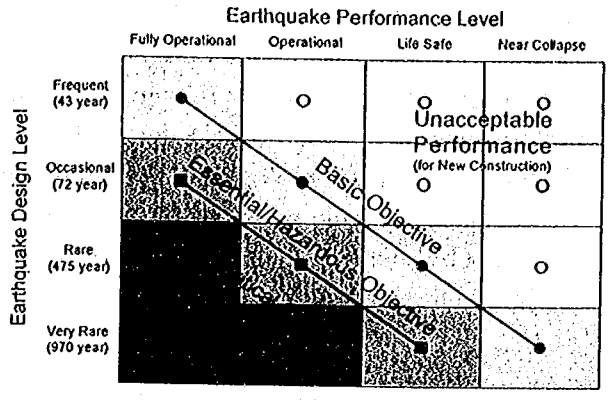


Fig. 2.2 Performance Matrix

In contrast, when a structure is designed, a seismic performance is determined from an input strong motion level dependently. Thus, the potential line that can be actually drawn corresponding to the specific design does not necessarily agree with that of conventional DPM. The performance matrix shown by this actual potential line can be referred as the "realized performance matrix" (RPM). When one consider the investment assigning plan for more than one facilities in the area, it needs to maximize the area's satisfactory by taking RPM of each structure into account.

In this research the idea of RPM is extended to the "input-output-cost curve" (IOC curve), in which the cost for structural earthquake resistant measure is displayed in addition to the input strong motion level and the seismic performance level in three dimensional space (Fig. 2.3). Given this IOC curve, decision makers can compare the earthquake resistant investment plans.

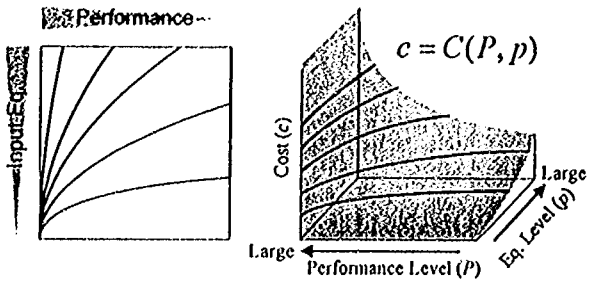


Fig. 2.3 IOC curve

Besides proposing and showing the example of the RPM and IOC curve, this research deals with a methodology to select the seismic potentials of more than one structure so that the combination of their potentials maximizes the satisfactory of the area. Assuming that there are two structures in the area, let us set the objective to maximize the quantitatively derived community's satisfactory under the several constraints such as the limit of the budget.

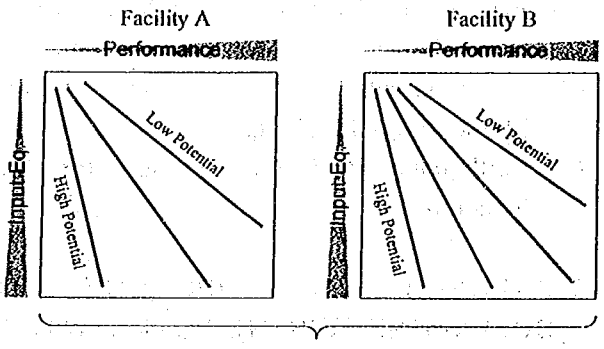


Fig. 2.4 Selecting Seismic Potentials

When the satisfactory is measured as the expected utility (EU), the problem is written as equations below.

$$\max_{P_{11},P_{12},P_{21},P_{22}} \quad p_1 U(P_{11}, P_{21}) + p_2 U(P_{12}, P_{22})$$

$$\text{s.t.} \quad C_1(P_{11}, p_1) = C_1(P_{12}, p_2)$$
$$C_2(P_{21}, p_1) = C_2(P_{22}, p_2)$$
$$C_1(P_{11}, p_1) + C_2(P_{21}, p_1) = c$$

where, p_e : occurrence probability of level e strong motion (e = 1, 2), P_{se} : seismic performance level of structure s (s = 1, 2) revealed when it experiences the strong motion of level e, $C_s(P_{se}, p_e)$: cost for such seismic potential that performance P_{se} realizes at the input level of e with the probability p_e, ; i.e., IOC function, and c* : the limit of total cost. The equations were solved analytically by assuming the unique function forms for U and C_s. In addition, an IOC function was tentatively derived for various levels of seismic potentials of the bridge under a given condition.

The concept in this paper is expected to be utilized in the regional earthquake resistant plans in the future, and is related to the seismic codes of various facilities. To apply the methodology to the practical planning and design, several problems must be solved; i.e., expressing the facility's seismic performance in adequate manners and determining the objective function forms of the net benefit or the representative utility as the objective function.

3. VERY STRONG DESIGN GROUND MOTIONS WITH DIRECT CONSIDERATION FOR SOURCE FAULTS

Numerous valuable strong motion records were obtained by various organizations during the 1995 Hyogo-ken Nanbu earthquake and it has been found that the earthquake generated extremely strong ground motion that had rarely been recorded in Japan. Design ground motions for public works, in general, had been based on the ground motions in rather far field due to large interplate earthquakes such as the 1923 Kanto earthquake, whereas those in near field due to earthquakes by inland active faults such as the Hyogo-ken Nanbu earthquake had not been taken into account. The Hyogo-ken Nanbu earthquake triggered revision of various seismic design codes based on its strong motion records and previous researches. However, because of lack of strong motion records obtained in near field, characteristics of near field ground motion still leave much room for discussion.

To study and grasp the characteristics of near field ground motions, in addition to the conventional techniques making use of strong motion records and attenuation relations, ground motion estimation techniques based on fault models have been developed and investigated. According to the techniques, the fault plane of a target event is divided into subfaults and the ground motion of the target event is synthesized by superimposing ground motions generated by each subfault.

The techniques can be applied to estimation of near field ground motion, which may be beyond the application of the conventional attenuation relations, because the extent and rupture process of the source fault are taken into account. On the other hand, the techniques require various source parameters, such as the location, extent,

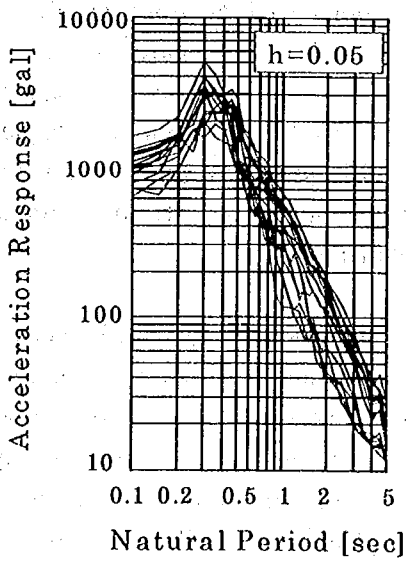


Fig. 3.1 Acceleration Response Spectra for the Estimated Ground Motions at JMA Kobe

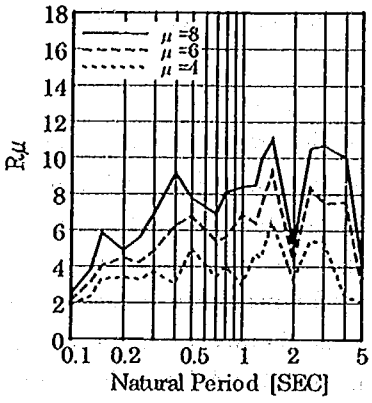
and rupture process, most of which are difficult to be determined accurately. Moreover, those parameters have noticeable effects on estimated ground motions as shown in Fig. 3.1. Fig. 3.1 compares acceleration response spectra (damping ratio h=0.05) of estimated ground motions at JMA Kobe during the Hyogo-ken Nanbu earthquake with various source parameters. We can see that the largest acceleration response may be more than 5 times as large as the smallest one at certain natural periods.

Currently, the ground motion estimation techniques based on fault models have been developed and expected to be practical for seismic design along with surveys of inland active faults. Researches on attenuation relations for near field ground motion using strong motion records due to earthquakes by inland active faults and seismic hazard analyses considering active faults and regional characteristics of seismicity have also been carried out.

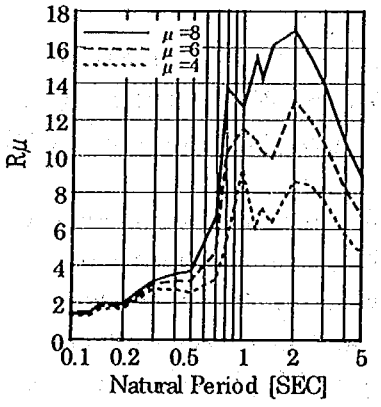
For rational seismic design against very strong ground motions, such as those generated by the Hyogo-ken Nanbu earthquake, energy absorption capacity should be improved by ensuring allowable appropriate displacement ductility. Because structures cannot withstand such ground motions only by strengthening structural members.

In order to evaluate the differences in the inelastic behavior of structures due to ground motion characteristics, strength reduction factor $R\mu$ can be used. $R\mu$ indicates the possible reduction of the strength of a structure when a certain displacement ductility is allowed. $R\mu$ can be calculated for arbitrary natural period and therefore it makes spectrum, namely strength reduction factor spectrum ($R\mu$ spectrum).

Fig. 3.2 shows $R\mu$ spectra for Kaihoku Bridge record and JMA Kobe record. Kaihoku Bridge record is ground motion from the Miyagi-ken Oki Earthquake, inter-plate earthquake, and JMA Kobe record is ground motion from the Hyogo-ken Nanbu eartquake, intra-plate earthquake. Both records were obtained on the stiff ground. The Fig. 3.2 shows that non-linear response of the structure varies depending on the ground motion characteristics.



(a) Kaihoku Bridge Record



(b) JMA Kobe Record

Fig. 3.2 Strength Reduction Factor Spectra

The effects of ground motions on inelastic behavior of structures are studied using strength reduction factor spectra and the ground motion characteristics. The ground motion characteristics affecting the inelastic response of structures should be considered when design

forces and design ground motions are discussed.

4. DEVELOPMENT OF SEISMIC DESIGN METHODOLOGY FOR BRIDGES

4.1 Future Scopes for Development of Seismic Design Methodology

1) Performance-based Design

The use of the performance-based design has been recently suggested in terms of the better-cost performance of construction, the promotion of new technology and the activation of international trade. To clarify the seismic performance demand and satisfy above demands, it is needed to describe seismic performance criteria and limit states of civil engineering infrastructures and establish the performance-based approach for the seismic design. The analytical and experimental verification systems would be also required to evaluate the performance capability of the structures and to prove an applicability of new technology. Moreover, development of social system to accept the performance-based engineering would be also required

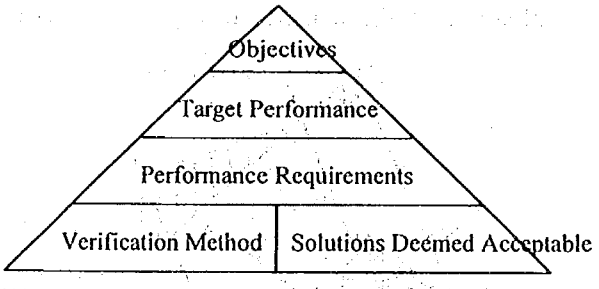
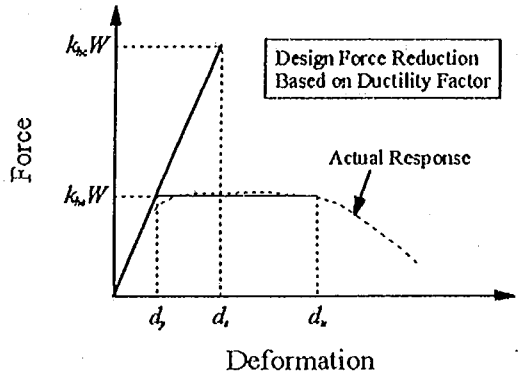


Fig. 4.1 Framework of Performance-based Design

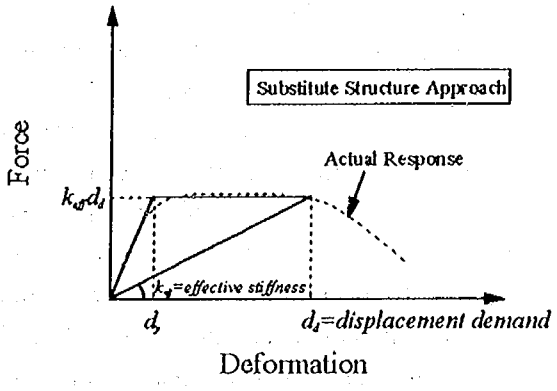
2) Displacement-based Design

Current seismic design is one of the force-based approaches in nature. Although the current force-based design approach involves allowance for inelastic damage during major earthquakes, it does not directly address the inelastic nature of a system during the earthquakes. Furthermore it requires the use of the controversial reduction factors which are based on an energy conservation assumption or displacement conservation assumptions. Seismic damage can be easily described by the deformation of the structures so that the alternative design approach using displacement as a reliable indicator of the structural damage.

The displacement-based design is a response spectra based methodology to design a structure to achieve a specified level of displacement in incorporated with the substitute structure approach. The substitute structure approach is a design approach whereby an inelastic system can be modeled using equivalent elastic properties such as the effective stiffness K_{eff} and the effective damping ξ as shown in Fig. 4.2.



(a) Force-Based Design



(b) Displacement-Based Design

Fig. 4.2 Design Concepts of Force-Based and Displacement-Based Design

3) Capacity Design and Reliability-based Design

The capacity design is a design methodology with the concept that the collapse mechanisms are clearly identified. In other words, an appropriate strength difference should be made between the plastic hinges and capacity-protected members. The concept of capacity design is illustrated in Fig. 4.3, where a ring 1 is strong enough to protect its capacity, while a ring 2 has a well-ductile property. In this system, the ring 1 cannot be subjected to its yield force or more and the ring 2 must exhibit an inelastic response when a large force is applied to the system. In order to achieve the capacity design process, the maximum feasible flexural strength for the plastic hinge regions should be adequately evaluated with considering over-strength and variation of materials using reliability based approach.

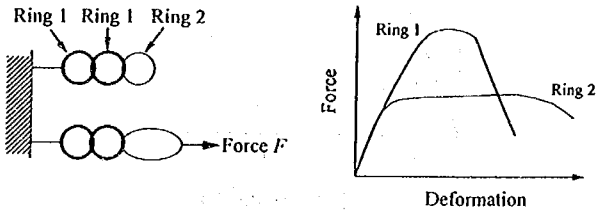


Fig. 4.3 Concept of Capacity Design

4) Strength and Ductility

It is one of options to increase a section or steel percent so as to increase the flexural strength of columns. On the other hand, the significant increase in the flexural strength causes design of a big column and thus results in high construction cost. Therefore, it may be unreasonable to design the column with high flexural strength. However, the design of well-ductile column can reduce a seismic force but causes a large displacement response and then significant residual displacement may be developed after excitation. Furthermore, P-Δ effects are not ignored if the column exhibits such large inelastic response during the earthquake. Accordingly, an appropriate balance between the flexural strength and ductility should be given to the column to satisfy the seismic performance demand.

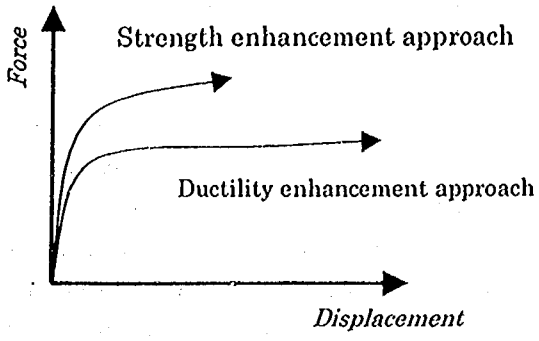


Fig. 4.3 Seismic Design Approach

5) Directional Uncertainty

Seismic forces have been applied to structures in both longitudinal and transverse directions independently, according to the current design code of highway bridges in Japan, except complicated structures such as the long-span bridges. In the United States, on the other hand, the directional uncertainty has been considered in evaluation of the seismic design forces. An

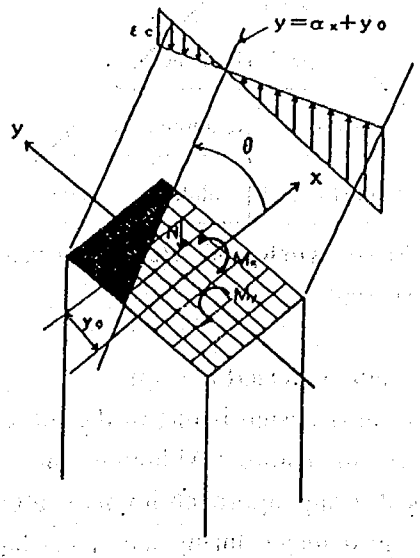


Fig. 4.4 Schematic Image of Bi-axial Bending

additional lateral force corresponding to 30% of the design force in the orthogonal direction is taken into account. Since the actual seismic force acts to the structures in two- or three-dimensional direction, the directional uncertainty effect on the structural response should be investigated.

4.2 Future Research Topics on Development of Evaluation Methodology of Structure Limit States

1) Studies on Failure Mechanisms and Inelastic Response Properties

Lack of the study on the failure mechanisms for members subjected to high axial load, variable axial load, bi-axial bending during an earthquake is a constraint against developing the seismic design based on the structure limit states. The failure mechanism of overall structure systems and their structural members should be studied through loading tests and shaking table tests with use of large-scaled units.



Photo 4.1 Shaking Table Test using Large Scale Unit

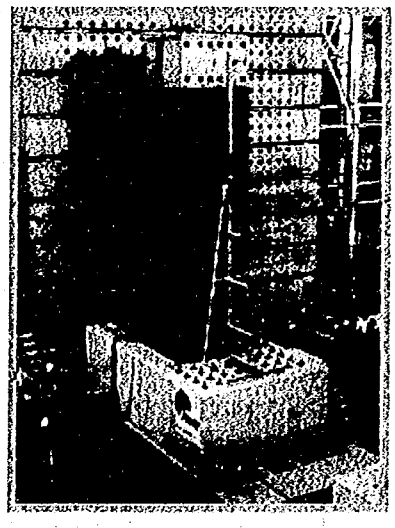


Photo 4.2 Cyclic Loading Test using a Real Scale Specimen

2) Determination of Limit States

There are several useful limit states of structural response in the seismic design process. In terms of the reinforced concrete members, four limit states may be determined, that is, cracking limit state, yield limit state, spalling limit state and ultimate limit state. The overall structure limit states can also be determined as serviceability limit state, damage-control limit state and survival limit state. These limit states may be defined based on the strength and ductility of the structures. Therefore, it is required to clarify the relation between the strength/ductility response and damage level at the plastic hinge.

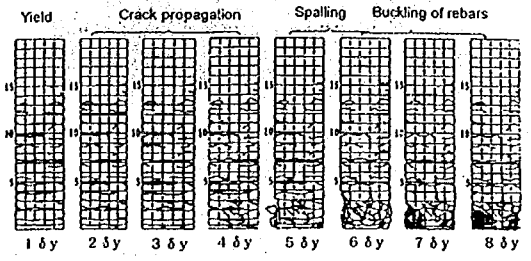


Fig. 4.6 Common Damage Progress of Reinforce Concrete Column

3) Modeling and Analysis

Nonlinear hysteresis models, in which the fundamental dynamic properties such as the stiffness and the damping of structures can be incorporated adequately, are required in the limit state design process with convenient analytical tools applicable to the dynamic response analysis.

4.3 Use of Advanced Technology

By using the interlocking steel with spiral and advanced materials such as the high strength concrete and the high performance steel, the columns would exhibit more ductile behavior than the conventional reinforced concrete structures. Development of new earthquake protective systems such as seismic isolation devices is also expected, to reduce the seismic effects.

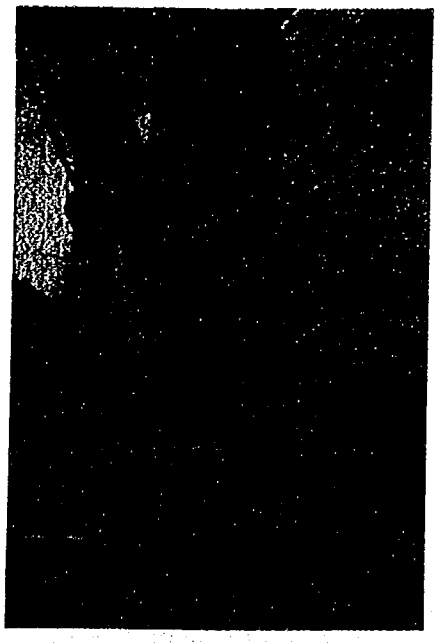


Photo 4.3 Carbon Fiber Retrofit Technology (Sakawa Bridge)

5. SEISMIC DESIGN FOR SOIL STRUCTURES

(1) Improvement of the Conventional Pseudo-static Analysis Procedure

The conventional pseudo-static analysis procedure which is based on the combined use of the limit equilibrium theory and the seismic coefficient method is considered the out-of-date technique. However, there do not exist alternative procedures to be used in the field practice with satisfactory reliability. Thus, the conventional procedure should be used until more rational and practical alternatives are developed. The use of the pseudo-static analysis procedure, which yields only a factor of safety, is justified only if there exists any correlation between the safety factor and the extent of deformation. Fig. 5.1 shows the correlation between the peak ground acceleration and the seismic coefficient to be used in the circular sliding method, which was obtained by back-analysis of damaged/non-damaged case records. The dotted line in the figure well separates both cases. This may indicate a potential of the method to predict the extent of deformation, although further study is needed to verify the procedure.

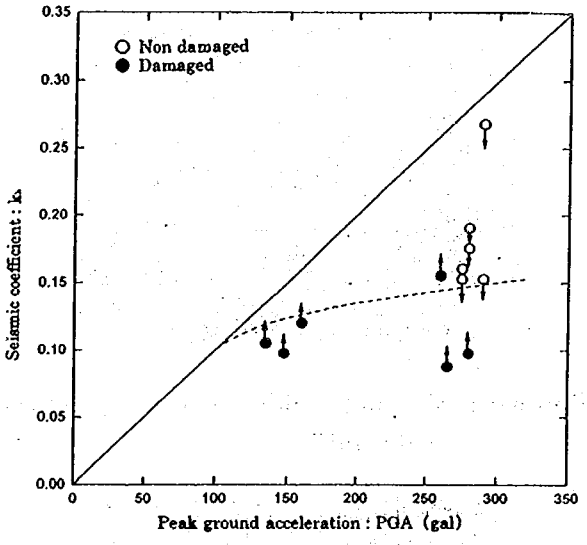


Fig.5.1 Correlation between the peak ground acceleration and the seismic coefficient to be used in the circular sliding method

(2) Development of the Deformation Analysis

Prediction of earthquake-induced deformation is usually needed when the very strong earthquake is considered in the design, as in the case of the other structures. Several methods which can predict deformation have been proposed so far, but none of the methods has reached in the level of wide practical use. Among these, the most rational and potential

method would be the elasto-plastic finite element analysis method. In order to introduce the procedure into practice, more research work should be done to verify the capability through a number of case studies.

Fig.5.2 shows an example result of such case study using the elasto-plastic finite element method for a river bank which was damaged by the Hyogo-ken Nanbu earthquake. The predicted crest settlement was 2.9 m, while the measured one was 2.7 m. Although this example shows a very good agreement, if this type of analyses is established in the level of practical use, introduction of performance-based design into soil structures would be realized.

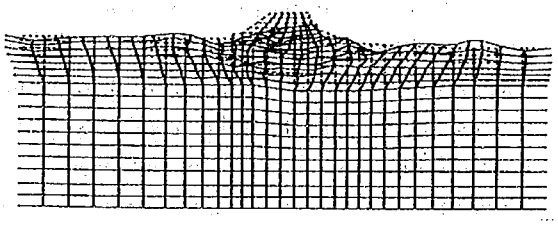


Fig.5.2 Result of the simulation, at Yodo river left bank, Torishima

(3) Development of the Rational Counter-measures Against Earthquakes

A wide variety of countermeasures such as ground improvements and soil reinforcements have been proposed to date. But the effectiveness of these countermeasures under very strong earthquake has not been evaluated quantatively, and consequently the seismic design procedures have not yet been established. Thus, further research is needed. In particular, prediction procedures of permanent deformation of soil structures with any countermeasure will play a very important role in elaborating the design methods.

Another aspect is that the cost of seismic countermeasures for the existing structures is expensive as compared with the construction cost of the soil structure itself. The cost may be sometimes as much as or more than that of the soil structure, unlike in the case of reinforcement of reinforced concrete or steel structures. Therefore to make it economical, a method or procedure which aims at making the damage to be within the allowable limit rather than preventing the damage has to be developed.

(4) Development of the Simple and Practical Soil Surveying Methods

As was mentioned before, seismic performance of soil structures is strongly affected by the ground conditions. Therefore, the ground surveying and evaluation of the data play an important role in predicting seismic stability of soil structures. On the other hand, the soil structures are typical as embankments are usually large in size and in length. To grasp the soil profile along the soil structure, a number of sounding must be executed, resulting in very expensive cost. The standard penetration test has been widely used to identify the soil profile and to assess liquefaction potential of the soils. However, this is not cost-effective. One of the potential sounding techniques which can substitute the SPT and are more economical would be the piezometric cone penetration test. The advantage of this test is listed below as compared with the standard penetration test.

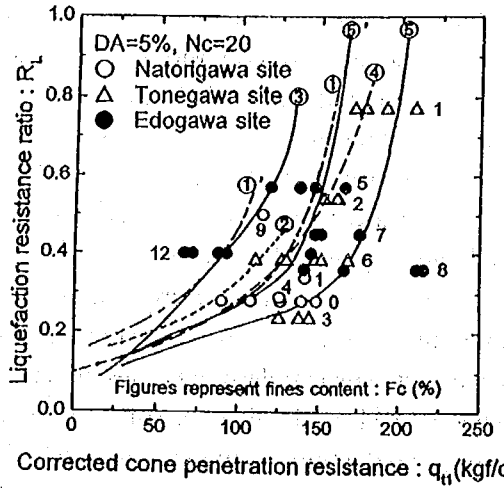
- cost for a unit length is about one third
- continuous data can be acquired along the vertical direction

Defects are as follows:

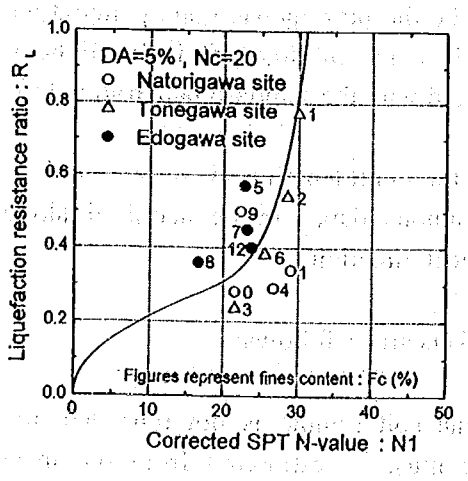
- as the soil sample is not retrieved, the soil type must be estimated from the measured value
- it cannot be penetrated into the gravelly soil, etc.

Fig.5.3(a) shows the relationship between the

cone tip resistance and the liquefaction resistance that was obtained by the field tests. Result of the standard penetration test is also presented in Fig. 5.5(b) for comparison. Judging from these two figures, the cone penetration test has almost the same accuracy as the standard penetration test. Reliability of the testing method would be enhanced by further accumulating the field data.



(a) cone penetration test



(b) standard penetration test

Fig.5.3 Relationship between the penetration resistance and the liquefaction resistance

6. CONCLUSIONS

(1) As a rational methodology to determine the seismic potential of civil infrastructure, the new concepts of the realized performance matrix (RPM) and the IOC curve was proposed. Also, the example of optimization of the earthquake resistant investment was introduced. Such approaches from the planning point of view will become important to thrust the earthquake disaster prevention measures with the consensus in the near future.

(2) The researches regarding the rational methods to determine the very strong design ground motion were introduced. The estimation of near field ground motions makes it feasible to take region specific active faults into account in the process to determine the very strong design ground motion. The strength reduction factor spectrum can be used to evaluate inelastic behavior of structures for rational seismic design against such very strong ground motion.

(3) Future scopes for development of seismic design methodology were presented and the future research needs were also discussed. Among all the research topics stated in this paper, development of the performance-based design method is one of the needed projects to be finished within a few years in Japan. The five-year project was already launched in 1998 to establish the performance-based seismic design method and to improve the related performance evaluation methods.

(4) For most of the soil structures typically as soil embankments, seismic design had not

been mandatory until the Hyogo-ken Nanbu earthquake took place. But now, very strong earthquake should be considered in the design of very important structures. Major researches that need to be focused on would be development of the new design procedure based on the allowable deformation, improvement of the conventional pseudo-static analysis procedure and development of cost-effective countermeasures.

REFERENCES

Seismic Retrofitting Manual for Highway Bridges, U.S. DOT, Federal Highway Administration, May 1995

VISION 2000 - Performance Based Seismic Engineering of Buildings, Structural Engineers Association of California Vision 2000 Committee, April 1995

Tamura, K. and Nakao, Y.: Strong ground motion estimation based on source modeling and semi-empirical Green's function technique, 14th U.S.-Japan Bridge Engineering Workshop, UJNR, 1998.

Miranda, E. and Bertero, V. V.: Evaluation of strength reduction factors for earthquake-resistant design, Earthquake Spectra, Vol. 10, 357-379, 1994.

M.J.N. Priestley, F. Seible, G.M. Calvi: Seismic Design and Retrofit of Bridges, 1996

CALTRANS: Bridges Design Specifications, 1990

Transit New Zealand: Bridge Manual, 1995

P. E. Pinto: Eurocode 8, Part 2, Earthquake Resistant Design of Bridges, Proc. of the First Japan-Italy Workshop on Seismic Design of Bridges, 1995

Matsuo, M. and T. Tsutsumi: Evaluation of Cone Penetration Testing as an in situ Liquefaction Resistance Measurement, Proc. 1st Intl. Conf. On Site Characterization-ISC'98/ Atlanta/ Georgia/ USA/ 19-22 April 1998, pp. 1309-1315.

Comparison of U.S. and Japanese Highway Bridge Seismic Retrofitting Measures

By

W. Phillip YEN[1] and Shigeki UNJOH[2]

ABSTRACT

This paper presents comparisons between the philosophy and methods used for seismic retrofitting of highway bridges in Japan and United States. Similarities and differences between the fundamental philosophies, retrofitting process and retrofitting measures in different bridge components are discussed, including a comparison of the fundamental retrofitting procedure and design criteria.

KEYWORDS: Earthquake Engineering, Seismic Retrofitting, Highway Bridges.

1. INTRODUCTION

1.1 Background

There are about 596,000 bridges in the U.S., of which 70 percent were constructed prior to 1971 with little or no consideration given to seismic resistance. Japanese bridge design specifications first included seismic design provisions following the 1923 Kanto earthquake. Similarly Ministry of Construction of Japan (MOC) of Japan made several seismic inspections of highway bridges through out the country since 1971, and successfully retrofitted and strengthened many bridges. In the 1991's national-wide inspection, about 18,000 out of 60,000 bridges were subjected to seismic retrofitting. [Unjoh, et al. 1997]. Recently, three large destructive earthquakes have occurred in the United States and Japan. These earthquakes, the Loma Prieta earthquake in 1989, the Northridge earthquake in 1994, and the Kobe earthquake in 1995, have severely damaged a number of highway bridges, and have cost many lives and billions of dollars. Among those damaged bridges, most of them were designed and constructed prior to the implementation of modern seismic design codes, significant damage also occurred in some bridges built to more recent codes. Most of these damaged or collapsed bridges were due to inadequate seat width for the superstructure, insufficient ductility and shear reinforcement for bridge piers, or foundation failure caused by soil liquefaction or large movement. Seismic retrofitting of vulnerable bridges to reduce their hazards to earthquake damage becomes an important issue. In lieu of the new findings on highway bridge performance under earthquakes, the Public Works Research Institute (PWRI) of Japan and the Federal Highway Administration (FHWA) of US initiated a cooperative research to further investigate the current seismic retrofitting methods, and to develop a more efficient and cost-effective method(s).

[1] Research Structural Engineer, Office of Infrastructure R&D
Turner-Fairbank Highway Research Center, FHWA
6300 Georgetown Pike, McLean, VA 22101, USA
[2] Division Head, Earthquake Engineering Division
Public Works Research Institute, MOC
Tsukuba Science City, 305 Japan

This initiation was agreed at the 7th FHWA/MOC Bridge Engineering Workshop in Pittsburgh, PA in November, 1998.

In the United States, *Seismic Retrofitting Guidelines for Highway Bridges* was first issued in 1983, and was refined in 1987 as a national manual, *Seismic Design and Retrofitting for Highway Bridges.* In 1995, FHWA updated this manual with more currently knowledge and practical technology. This revision is to reflect recent changes in seismic design philosophy and performance criteria that was proposed to American Association of State Highway and Transportation Officials (AASHTO) in 1995. The guidance (or specification) of Japanese seismic retrofitting are most covered in Japan Road Association's (JRA) seismic design specifications, and are generally updated while codes are revised. The other important reference, *JRA's Manual for Earthquake Disaster Prevention of Road Facilities,* was published in 1988 [Note: this is also called as *Pre-earthquake Countermeasures*]. In 1996, the latest JRA seismic design code was issued. This revision has taken in consideration of the findings from the Kobe earthquake. A new guideline, *Reference Manual of Seismic Retrofitting for Existing Highway Bridges,* was also published which including new retrofitting requirements for reinforced concrete (RC) bridges piers and steel piers.

Seismic design and retrofitting philosophy and specification in both countries have become more rigorous and rational over time, as subsequent damaging earthquakes have occurred and educated bridge engineers worldwide. It seems that every earthquake provides an opportunity to improve the understanding of the performance and behavior of structures of all kinds, both through reconnaissance studies and research. In the latter case, observed behavior is often used to calibrate and/or refine theoretical models, which in turn may lead to changes in construction details and analysis methods.

1.2 Objective

The objective of this paper is to review and study those comparisons between the seismic retrofitting philosophies and design criteria for highway bridges as contained in the Japanese and United States' retrofitting specifications and manuals. This review is based on current seismic retrofitting manuals or codes being used in the two countries: In US, the FHWA's Seismic Retrofitting Manual for Highway Bridges published in 1995: In Japan, JRA Bridge Design Specification, Vol. V (Seismic), published in 1996; and Reference Manual of Seismic Retrofitting for Existing Highway Bridges of JRA, issued in 1997. Several technical papers [Kawashima, et al, 1993 and Zelinski 1996] were also reviewed. This review will present the different approaches used for seismic design through a comparison of fundamental philosophies, retrofitting process and retrofitting measures.

2. RETROFITTING PHILOSOPHIES

In order to understand the application and intent of a seismic retrofitting manual or specifications, it is important to have an understanding of the underlying philosophy on which the manual is based. In both the United States and Japan, because of the difficulty and cost involved in strengthening an existing bridge to new design standards, it is usually not economically justifiable to do so. The general goal of retrofitting is to prevent unacceptable failure. However, the interpretation of the "unacceptable" failure may not be the same in both countries. In the US, this implies that a considerable amount of structural damage during a major earthquake is acceptable as long as bridge

collapsed is prevented. However, for important bridges such as lifeline system, the capability of the bridges to carry out emergency transportation immediately following an earthquake may require a higher level of performance with less structural damage. Thus, the threshold of damage that will constitute unacceptable failure may therefore be defined by the engineer by taking into overall configuration of the structure. In general, the unacceptable damages are the following:

- Serious injury or loss of life
- Collapse of all or part of the bridge.
- Loss of use of a vital transportation route.

In Japan, existing bridges had been expected to prevent critical damage as unseating of the superstrucutres against the maximum creditable events such as 1923 Kanto Earthquake in the past. The existing bridges have been evaluated and retrofitted to meet the criteria through the several inspection and retrofit programs.

However, due to the considerable interruption and damage restoration in the Kobe earthquake, higher level seismic safety requirement for critical bridges are needed to prevent large direct and indirect cost. In the new seismic design specifications [JRA 1996], the bridges are classified into two different categories based on the importance factor. The categories include Type B: important bridges and Type A: standards bridge. The design target for Type B bridges is to recover the transportation function of the bridge as soon as possible after the large earthquake. That of the Type A bridges is to prevent the critical damage such as unseating of the superstructure. This is very similar as US design and retrofitting classification. Performance based design will be the future basis for seismic design and retrofitting criteria. However, the determination of the importance factors and what kind of damage level in terms of immediate function or repairable structures are still debatable in the earthquake communities.

Seismic retrofitting philosophies are very similar in both countries. However, the implementation of this fundamental philosophy is somewhat different in the specifications and manuals of the respective countries, and some of these differences are explored in this paper. In the US, the Retrofitting Manual recommends low-to-moderate seismic zone that retrofitting be considered whenever non-seismic rehabilitation of bridge is planned or when bearing deficiencies exist in structure. But in Japan, since the most of area in the country is in high seismic zone, most of bridges are required for evaluation to meet the new design requirement.

3. RETROFITTING PROCESS

Seismic retrofitting is one solution for mitigating the hazard of existing bridges that are vulnerable to serious damage during an earthquake. Because not all bridges can be retrofitted simultaneously, the most critical bridges should be retrofitted first. The selection of bridges for retrofitting requires an overall evaluation of the whole structure system including seismic risk, economics and social impacts. Thus, the process of the retrofitting bridges involves an assessment of a multiple of variables and requires the use of considerable judgment.

In the US, the process is divided into three different stages:

- Preliminary Screening.
- Detailed Evaluation.
- Design of Retrofitting Measures.

Figure 1 shows the flow chart of the US seismic retrofitting process.

The new JRA seismic design specifications issued in December, 1996 has changed the seismic design criteria in accordance with ground motion characteristics recorded in the Kobe earthquake. The bridge inspection procedure to identify vulnerable bridge is based on the damage experiences during the Kobe earthquake. In the determination of the priority for the retrofitting of the existing bridges, bridge conditions including construction year, ground condition, material, structural member characteristics, etc., and the importance of highway network are considered as shown in Figure 2.

4. RETROFITTING MEASURES

4.1 Retrofitting Strategies

In general, there are two alternative strategies that will allow a design engineer to choose while design in retrofitting a bridge. One is based on conventional strengthening techniques that increase the capacity of structure to meet the demand. The other one is based on reducing the demand on the structure so that the capacity of the existing structure is sufficient to resist earthquake forces. Both countries' retrofitting design guidelines include both strategies to retrofit bridges. The latter approach involves the use of an earthquake protective system, such as base isolation bearing (or called Menshin design) was proven successfully reducing earthquake forces in the Kobe earthquake. Although this approach may not be applicable to all bridge sites, earthquake protective system has been shown to be a cost-effective approach as well.

4.2 Superstructures

Superstructures loss supports at their bearings, seats or expansion joints was found one of the major factors to cause bridge failure in the past earthquakes. Although frequently amazing the results, these failure are relatively simple and inexpensive to prevent by retrofitting. Because of this, most retrofitting efforts to date have been directed toward tying bridges together at their bearings and expansion joints. To prevent this kind of failure, bridge superstructures are tying together at their bearings and expansion joints with restrainers. Restrainers in the US are used in three different purposes when tying the various parts of a bridge together:

- Longitudinal joint restraint.
- Transverse bearing restraint.
- Vertical restraint.

Bearing seat extension, adding shear keys and replacing vulnerable bearings are also used to reduce the seismic vulnerability of bridge superstructures from earthquake damages. After 1971 San Fernando earthquake, US California DOT immediately started to a retrofit program. As a result of that program, seismic resistance of 1260 bridges was improved by the addition of hinge restrainers, seat extensions, and shear keys [Zelinski, 1996].

Superstructures retrofitting are similar in Japan. After the Kobe earthquake 1995, simple supported bridge are tied together to prevent superstructures from falling off their supports in Hanshin Expressway. Generally, steel girders are made continuous up to two or three spans by installing shear and moment plates. The end girders are strengthened with redundant elements such as restrainers, isolation bearings, stoppers, and extended seats.

In comparison with both countries' retrofitting methods in superstructures, restrainers are used very common in both US and Japan. Nevertheless, in Japan more different materials and types of restrainers, such as *Znaidal Flexible Link Restrainer* and *Steel Plate Connector Restrainer* (as shown in Figure 3.) are installed..

4.3 Substructures

Recent destructive earthquakes have re-emphasized the needs to increase seismic resistance of bridge substructures including columns and cap beams. Bridge column failure due to insufficient ductility and inadequate shear reinforcement was found to be the most important factor causing bridge collapse or failure.

In both countries, reinforced concrete (RC) columns are usually retrofitted by adding steel jackets. Although in some cases, columns might be retrofitted with concrete jackets. Composite fiberglass wrapping methods have also been using in certain cases, such as limited working spaces (as shown in the Figure 4). For the rectangular columns, the recommended procedure in the US is to use oval shape jackets (as shown in the Figure 5), which provides a continuous confining action similar to that for a circular column. But in Japan, rectangular columns are retrofitted with steel jackets, and steel plates are welded together around columns. The plastic hinge zone at the bottom of column is confined by H-shaped beams to increase the ductility. The concept to increase the confinement using oval shape jacketing or confined members is similar between US and Japan, the oval shape construction increasing more spaces, which are usually difficult to be applied in most viaduct highways in the urban area of Japan.

In most cases, column retrofitting with steel jackets would not only increase ductility but also enhance certain level of strength capacity to resist earthquake loads in Japan. As recommended by the *Reference Retrofitting Manual* [JRA, 1997], retrofitting for RC column is to enhance ductility as much as possible but not to increase load capacity excessively. So that the foundation would be less effected. However, if the load capacity is not sufficient, enhancing ductility only may cause large residual displacement after earthquake. Thus, it is essential to check the foundation's capacity before retrofitting so that the column strength will not stronger than its foundation. Clearly, the increasing ductility and load capacity should be balanced.

Japan has more steel bridge columns than US has in the high seismicity area due to different soil profiles. They are commonly retrofitted to prevent buckling. In the current *JRA's Seismic Design Specification*, hollow steel columns are recommended to fill with low-strength concrete up to the height where the column's lateral capacity exceeds the earthquake demands. If column is unable to be filled with concrete, welding vertical stiffeners and diaphragms at corners of rectangular tubes is recommended.

Cap beams provide the link in force transfer between superstructure and columns. The US general philosophy is to increase the cap beam flexural strength sufficiently to force plastic hinge into columns. Retrofitting are generally adding vertical and horizontal special joint shear reinforcement and covered by concrete to integrate the joint connections. The other alternative way is to alleviate cap beam problems by adding a new link cap beam below the existing cap beam. However, this method may not be favorable in Japan due to the space underneath the highway might be occupied or used as secondary traffic route.

4.4 Soil and Foundations

Retrofitting of footings or piles may be the most expensive aspect of bridge seismic upgrading. During the past earthquake events, bridge foundations performed fairly well in comparison with bridge columns in both countries. However, the deficiencies

may be found in footing flexural and shear strength, pile capacity and overturning resistance. Retrofitting measures are very alike in both countries. For liquefiable soils, stabilization for site soils such as:

- Lowering of groundwater table.
- Densification of soil by vibro-compaction, vibro-replacement, or compacting grouting
- Vertical network of drains.
- Placement of permeable overburden.
- Particulate or Chemical grouting.

are recommended in the FHWA's retrofitting manual. Structural improvement is the other option to accommodate site soil problem. Foundations are usually retrofitted by enlarging footings or increasing number of piles/ adding batter piles. The new design codes of JRA is using the *Ductility Design Method* for foundation design and the similar retrofitting methods have been studied and developed for vulnerable pile foundations, caisson foundations, footings, and soil liquefaction.

5. SUMMARY AND CONCLUDING REMARKS

This paper has presented a comparison of the philosophies and practical retrofitting measures of seismic retrofitting on highway bridges in both US and Japan. In which the FHWA's *Seismic Retrofitting Manual for Highway Bridges* and JRA new *Seismic Design Codes* and *Reference Manual for Seismic Retrofitting* are based. In comparing with retrofitting measures, the fundamental philosophies and basis are essentially similar. However, due to the different environments and restraints, practical retrofitting methods applied in the site are not the same. For example, although rectangular RC columns retrofitted with oval shapes steel jackets are recognized more efficient than rectangular steel jackets. Applying this measure to a limited-space area, such as an urban area of Japan, may not be practical. Bridge RC column retrofitting in Japan is usually designed for both increasing ductility and strength capacity but not to exceed the limit from foundation's capacity. Other than Japan, column retrofitting are focused on increasing ductility, and retrofitting design criteria are lower than Japan in the low-to-moderate seismicity area. This difference may due to the expectation of the large earthquake occurrence.

Japan has had a long, active history of dealing with earthquakes and designing for them since the 1923 Kanto earthquake. Over the years, Japanese design codes have been upgraded in order to address deficiencies found due to damaging earthquakes (Iemura, 1995). This is also the situation for the United States, especially since 1971 (Buckle, 1995). The recent 1989 Loma Prieta, 1994 Northridge and 1995 Kobe earthquakes have demonstrated the importance of functionality of highway structures for the emergency restoration. Consequently, design criteria for a higher performance should be considered in the codes and manual. Although both countries' current bridge design codes has included bridge importance factor to classify them into a higher category's performance, a more specific performance-based design codes should be developed in the near future. Similar to the new design codes, retrofitting measures should also be moving toward these changes.

Another aspect of seismic retrofitting for the highway structures is to assess the whole impacts of highway system, including other modes of transportation systems, social impacts ... etc from destructive earthquakes. Starting in the fall of 1992, FHWA has been cooperating with the Multidisciplinary Center for Earthquake Engineering Research to work on a comprehensive research program to develop tools to evaluate the

seismic vulnerability of the national highway system in the United States. An important end-product of this program is the development of a seismic evaluation and retrofitting manual for existing highway systems. This manual, which expected in year 2000, is being prepared in three volumes, where Volume I contains the methodologies, procedures, and examples for conducting a seismic risk assessment of highway networks and systems; and Volume II and Volume III contain guidance on seismic vulnerability screening, analysis, and retrofitting of highway bridges, retaining structures, slopes, tunnels, culverts, and pavements. PWRI has also enhanced their research area in the earthquake disaster prevention by adding earthquake information system after the Kobe earthquake.

With the common interests in developing a cost-effective and more efficient method for seismic retrofitting in highway bridges. FHWA and PWRI are looking forward to co-investigating smart device systems and materials that will better retrofit the existing vulnerable bridges.

ACKNOWLEDGMENT

The authors of this paper would like to acknowledge Mr. James D. Cooper and Mr. John D. O'Fallon for their supports and suggestions during the preparation of this paper. The authors also like to thank Mr. Yukio Adachi and Mr. Michio Osumi of PWRI, Japan for providing invaluable information of Japan's seismic design principles of highway bridges.

REFERENCES:

AASHTO, 1995, Interim Revisions to the AASHTO *Standard Specifications for Highway Bridges*, Division I-A: Seismic Design, American Association of State Highway and Transportation Officials, Washington, DC.

Applied Technology Council, 1994, Meeting notes of the ATC-*18 "Seismic Design Criteria Review"* project.

Buckle, I., 1995, "*Influence of Damaging Earthquakes on Bridge Design in the United States of America*," Preprint from the International Bridge Seismic Design Workshop, Tsukuba, Japan.

Buckle, I. And Friedland, I., 1995 "*Seismic Retrofitting Manual for Highway Bridges*", Federal Highway Administration (FHWA), FHWA-RD-94-052, Mclean, VA USA.

Iemura, H., 1995, "*Damage Characteristics of Bridges*," Preprint from the International Bridge Seismic Design Workshop, Tsukuba, Japan.

Japan Road Association, 1996, "*Specifications for Highway Bridges*," Part V: Seismic Design, Japan.

Japan Road Association, 1997, "*Seismic Retrofitting Reference Manual for Existing Highway Bridges*". Japan.

Kawashima, K., 1994, "*Seismic Design Force of Bridges*," Proceedings of the Second International Workshop on Seismic Design of Bridges, Queenstown, New Zealand.

Kawashima, K., and Hasegawa, K., 1994, "*New Design Specification for Highway Bridges in Japan*," Earthquake Spectra, Vol. 10, No. 2.

Kawashima, K. and Unjoh, S., 1992 "*Seismic Strengthening and Retrofitting of Highway Bridges in Japan*", 5th US-Japan Workshop on Earthquake Disaster Prevention for Lifeline System, Tsukuba, Japan.

Kawashima, K., 1990, "*Seismic Strengthening and Repair of Highway Bridges in Japan*", US-Japan Workshop on Seismic Retrofit of Bridges, Tsukuba, Japan.

Unjoh, S., Terayama, T., Adachi, Y. and Hoshikuma, J., 1997, "*Seismic retrofit of Existing Highway Bridges in Japan*", Proceedings of the 29th Joint Meeting of US-Japan Panel on Wind and Seismic Effects, UJNR, May 13-16, Tsukuba, Japan.

Yashinski, M., 1998, "*Bridge Seismic Retrofits After the 1995 Kobe Earthquake*", Periodic of CALTRANS, What's Shakin'.

Zelinski, R. 1996, "*Bridge Retrofit Concepts*", SAMPE Conference, Anaheim, CA.

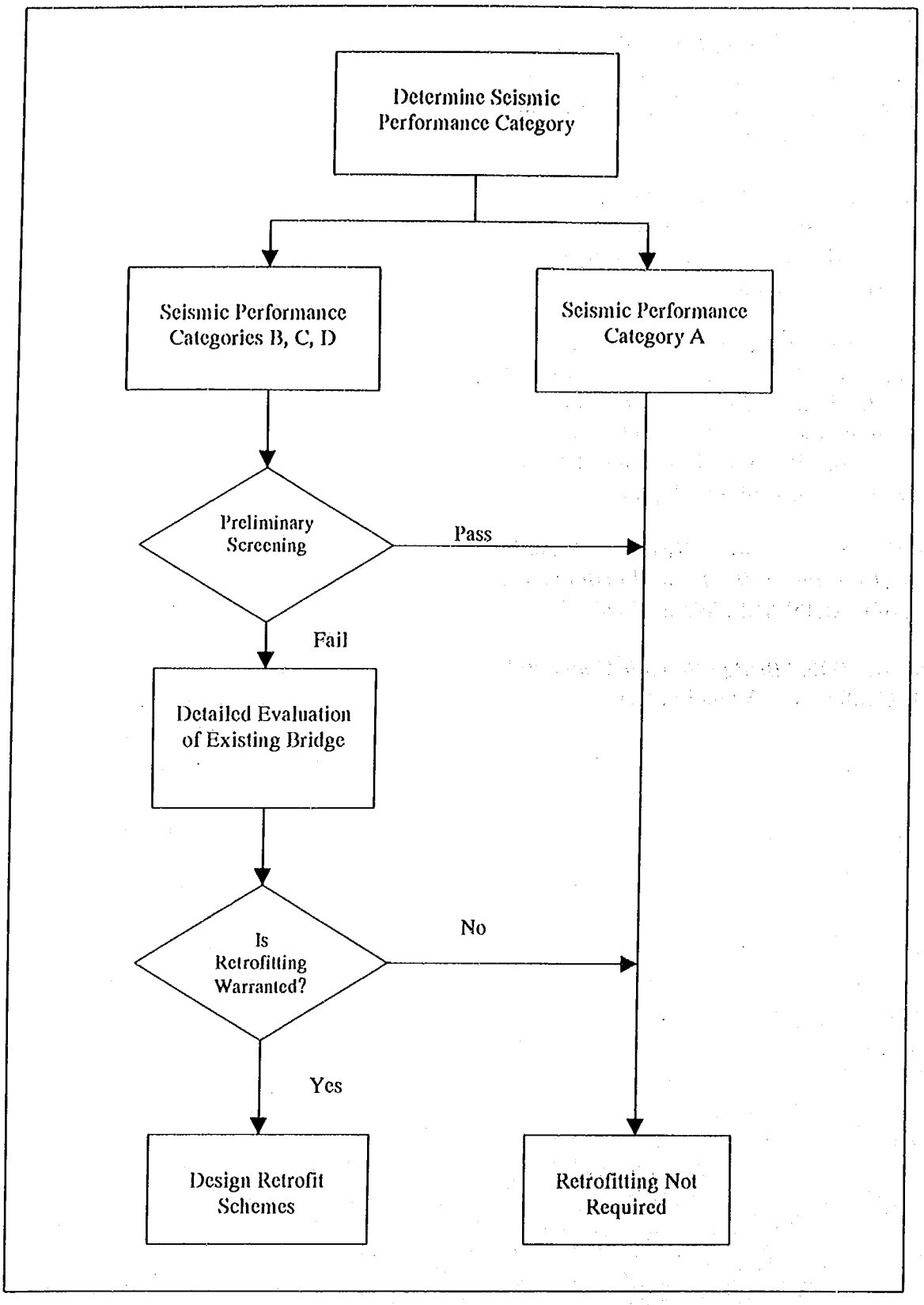


Figure 1 Seismic Retrofitting Process in US
(FHWA Seismic Retrofitting Manual)

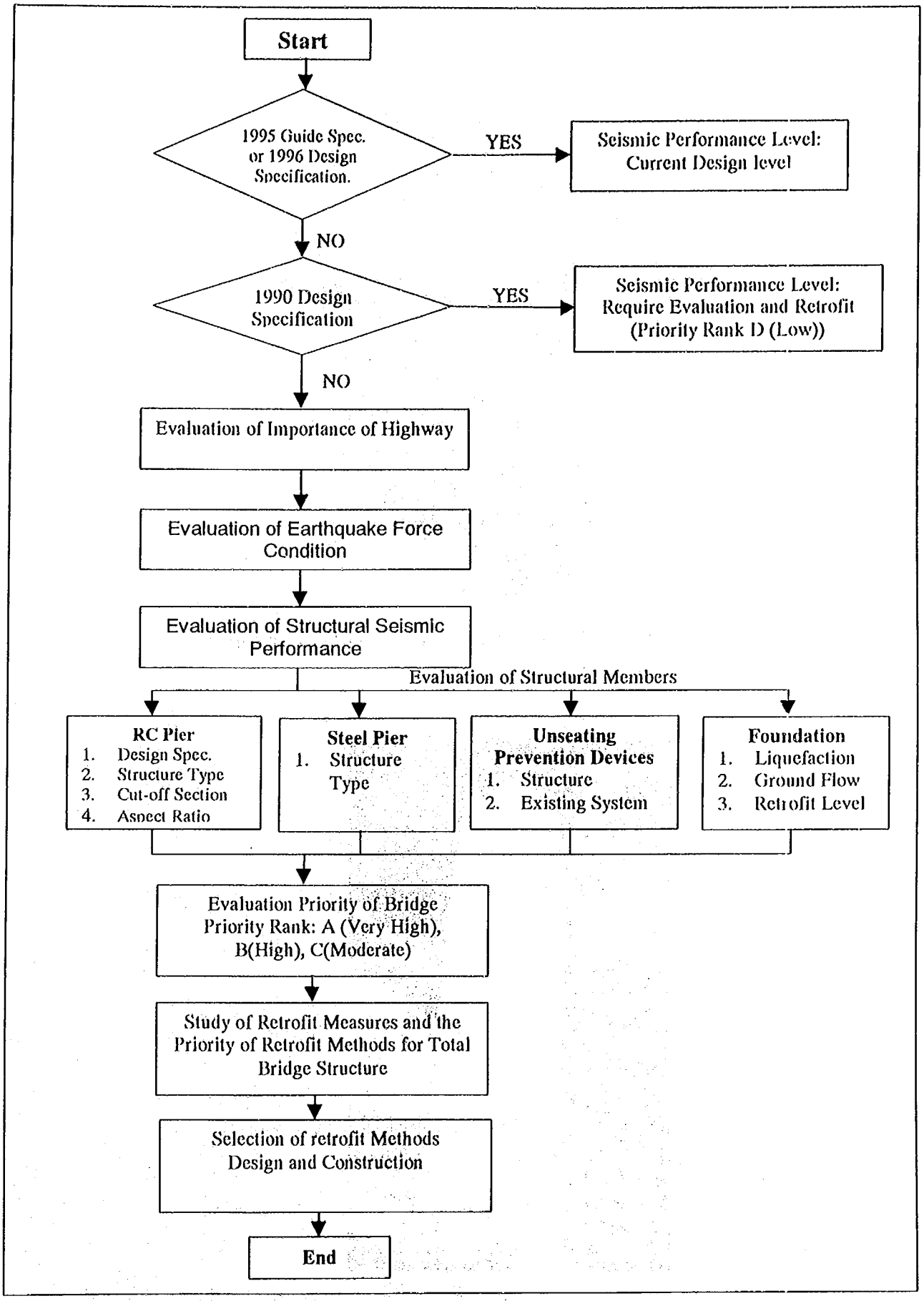


Figure 2 Prioritization Concept of Seismic Retrofit of Highway Bridges in Japan

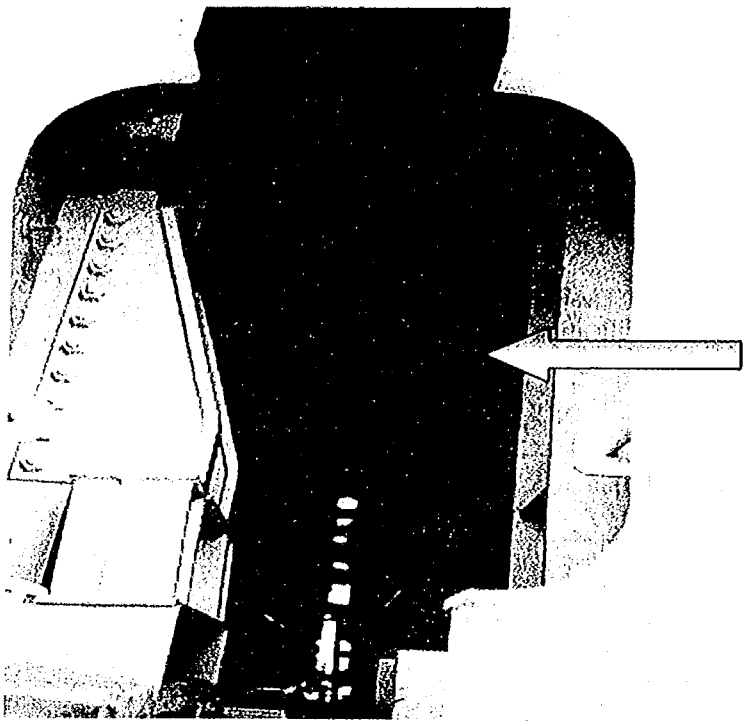


Figure 3 Steel Plate Connector Restrainer Used in Japan

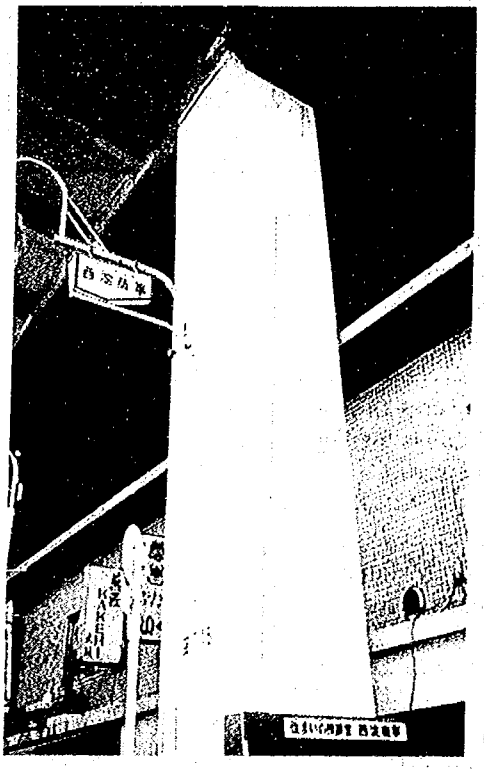


Figure 4 Composite Material (FRP) Wrapping Used in Limited

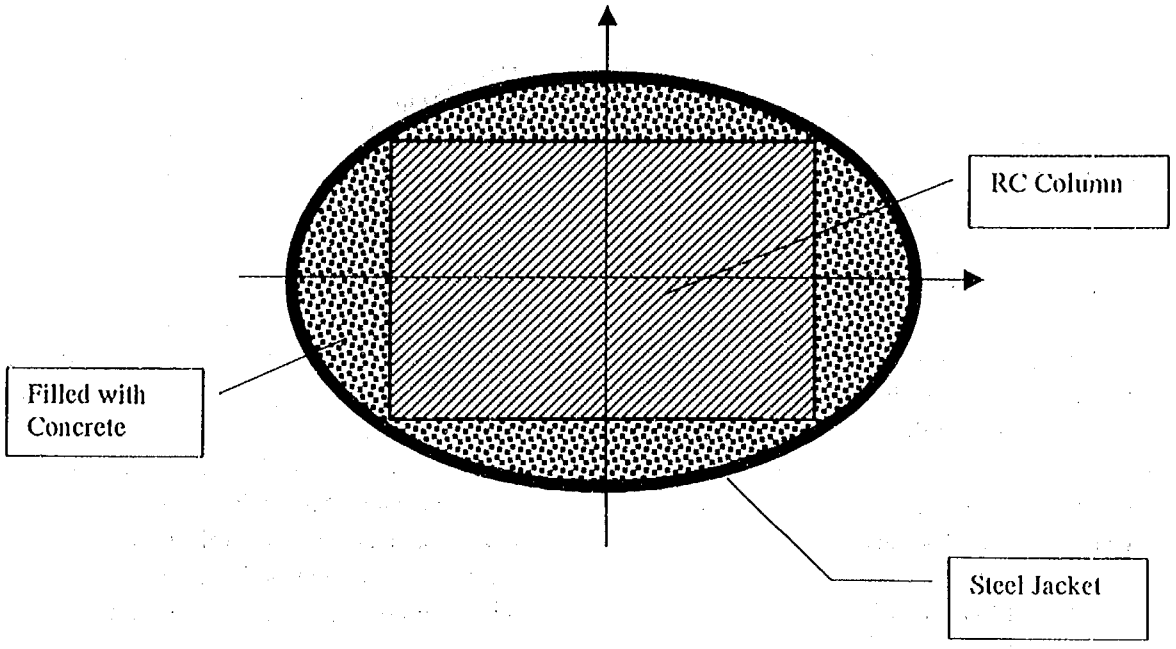


Figure 5 Elliptical (or Oval Shape) Jacket for Rectangular RC Column Retrofit

Model Experiments on Characteristics of Motions of Continuous Pontoon Type and Separate Support Type Elastic Floating Bodies in Waves

by

Haruo YONEYAMA [1], Satoru SHIRAISHI [2] and Go ISHIMI [3]

ABSTRACT

Several floating bridges, which have been recently put to practical use in the United States and Norway, are mainly classified into two types: a continuous pontoon type and a separate support type. It has been well known that long and large beam-like flexible floating structures such as these floating bridges show the characteristics of elastic deformations in waves. In this paper, hydraulic model experiments, which have been carried out to investigate the characteristics of motions of these two types of floating structure, are broadly reported.

KEY WORDS: Floating Bridge
Elastic Deformation
Elastic Floating Body
Rigid Floating body

1. INTRODUCTION

In recent years, various types of floating structure have been planned and constructed for the purpose of effective utilization in coastal areas. Floating structures can be generally considered as rigid floating bodies in estimating their motions in waves because of enough large rigidity of them. On the other hand, long flexible floating structures such as floating bridges have been developed and put to practical use mainly in the United States and Norway (Lwin, 1994; Landet, 1994). Besides, construction of the first floating bridge in Japan has started in Osaka (Maruyama et al., 1998a, 1998b). To evaluate the motions of these types of floating structure, it is improper to regard them as rigid floating bodies because of elastic properties of them. Namely, for dealing with long and large beam-like flexible floating structures such as floating bridges, it becomes necessary to examine the characteristics of their responses due to waves by taking account of elastic deformations of them.

The floating bridges are mainly classified into two types: a continuous pontoon type and a separate support type. The former is the type that consists of several floating box-type pontoons continuously arranged in one row on water surface. Meanwhile, the latter is the type that consists of several floating foundation pontoons arranged at intervals on water surface and a superstructure used as a road surface.

Photograph 1 shows a continuous pontoon type floating bridge called "Evergreen Point Bridge" which was constructed on Lake Washington in Seattle in the United States in 1963. This is one of three Lake Washington Floating Bridges. Since the bridge is composed of 33 prestressed concrete box-type pontoons rigidly connected

1)Senior Research Engineer, Structural Engineering Division, Port and Harbour Research Institute, Ministry of Transport, Nagase 3-1-1, Yokosuka 239-0826, Japan
2)Chief, Offshore Structures Laboratory, Structural Engineering Division, Port and Harbour Research Institute, Ministry of Transport
3)Former Member, Offshore Structures Laboratory, Structural Engineering Division, Port and Harbour Research Institute, Ministry of Transport (The Fifth District Port Construction Bureau, Ministry of Transport)

together, it is a continuous floating structure as a whole. The length of the bridge is 2,310 m, and it has four traffic lanes. Each pontoon is moored to the bottom of the lake by means of stretched anchor cables. This bridge is characterized by a draw span that is provided in the middle of the bridge for a ship navigating the lake.

Photograph 2 shows a separate support type floating bridge named "Bergsφysund Bridge" which was constructed across a fjord in Norway in 1992. This is one of two floating bridges in Norway. The place where the bridge is located has a water depth of about 300m, and a sea state around the bridge is relatively calm. These characteristics are attributed to geographical features of fjords frequently seen in the west coast of Norway. In the place like this, a floating bridge is more economical than any other types of bridge. The superstructure of the bridge is supported by seven high strength lightweight concrete pontoons floating on sea surface. The bridge is also supported by flexible rods and multi-layer rubber bearings at both ends.

Long and large flexible floating structures could be used not only as floating bridges but also as floating port terminals or other applications in the future. To establish design methods for these floating structures, the effects of long and large flexible floating structures on elastic responses of them in waves need to be clarified. This paper reports the results of hydraulic model experiments on the continuous pontoon type and the separate support type elastic floating bodies (Shiraishi et al., 1996, 1997a, 1997b; Ishimi et al., 1999; Shiraishi et al., 1999).

2. CONTINUOUS PONTOON TYPE ELASTIC FLOATING BODY

(1) Hydraulic Model Experiments

a) Models of floating body

A continuous pontoon type elastic floating body in hydraulic model experiments is made of a polyurethane board to reproduce flexible properties of a floating bridge. The purpose of the experiments is to measure the hydraulic characteristics of elastic floating bodies, especially, their deformations and motions.

The view of a model employed here is illustrated in **Fig. 1**. This model is Model-B. The model consists of one thin rectangular floating board and two mooring poles. The floating board has two holes through which the mooring poles are installed to moor the board. The mooring poles are fixed at the bottom of an experimental basin. The board can freely go up and down along the mooring poles subjected to waves.

Table 1 shows six types of floating board. In the table, length, width, thickness, density and Young's modulus of each board are listed. The board length and thickness are 2.0m and 0.02m, respectively. The density and the widths of Model-A, B and C are 98.0 kg/m^3 and 0.1, 0.2 and 0.5m, respectively. The density and the widths of Model-D, E and F are 200.0 kg/m^3 and 0.1, 0.2 and 0.5m, respectively. By using six types of model, the effects of the widths and the elasticity of boards on deflections and motions of them can be examined.

Displacement of the center of each floating board must be measured in air to evaluate rigidity of each floating body. **Photograph 3** shows the situation of deformation measurement of a floating board at the center point of it. The rigidity of floating boards is estimated by use of the measured data. These values are also listed in **Table 1** as Young's moduli. For example, the rigidity of Model-A, B and C is 4.07, 4.10 and 4.03kN/cm^2, respectively. The rigidity of boards before coating on the surface of them is 3.16kN/cm^2. The coating makes the boards waterproof, and this causes the difference between measured rigidity and original one.

b) Method of model experiments

Figure 2 shows the experimental basin and equipment. The basin is 10m in width and about

19m in length. Two irregular wave generators are installed along one side, and wave-absorbing units are arranged along the other three sides. The model of a floating board is set at the center of the basin, and two wave gauges are installed to measure wave heights.

In the model experiments, the motions of a model are measured by use of a laser displacement meter and nine accelerometers. **Photograph 4** shows the arrangement of them around a floating body model in the basin. The laser displacement meter is fixed over the center of the floating board. The nine accelerometers are attached to the points of $+0.4L$, $+0.3L$, $+0.2L$, $+0.1L$, $0.0L$, $-0.1L$, $-0.2L$, $-0.3L$, and $-0.4L$ in the longitudinal direction of the board, respectively, where L is the length of the board. These are named AP-1 to AP-9 in sequence from the incoming direction of waves, respectively. AP-5 is, therefore, located just at the center of the floating body. Strains that are caused by motions of the floating board are also measured. Nine strain gauges named εP-1 to εP-9 are also installed at the same points of the board where the accelerometers are located.

The model scale employed in the model experiments is 1/100. **Tables 2** and **3** show the experimental conditions. Regular waves were adopted in the model experiments. The water depth in the experiments is 0.3m, and the incident wave periods vary from 0.8 to 2.6s at variants of 0.2s. The wave height in the experiments is 0.01m for all types of model. In Model-A, the experiments for the incident wave height of 0.02m were additionally conducted. In addition, the wave direction for all the models is 0degree that means the longitudinal direction of the board. In Model-B, the experiments for three wave directions, which are 0, 30, and 60degrees, were performed.

Photograph 5 shows the overview of the model of a floating body model and all sorts of measuring instruments arranged in the basin. The model shown here is Model-C. Meanwhile, **Photo 6** shows the situation of the model experiment in regular waves. The model is Model-A. It can be clearly seen that waves are coming toward the model from the right of the photograph.

(2) Results of Model Experiments

a) Time histories of accelerations and strains

Figure 3 shows time histories of measured vertical accelerations of Model-A. The wave height, period and direction are 0.01m, 1.0s and 0degree, respectively. The time histories of the accelerations obtained for the time of 100 to 106s are shown here. During this time, the motions of the floating body and incident regular waves keep a steady condition after initial unsteady transient waves decrease. It is easily understood from the figure that the amplitudes of vertical accelerations are different in relation to the points on the board and that there is the phase difference between randomly selected two time histories. High frequency components not corresponding to the incident wave frequency are also seen in the figure. This is considered to be due to the natural frequency components of the floating board. The maximum values of accelerations appear at both ends of the board (AP-1 and AP-9).

Figure 4 shows time histories of measured strains of Model-A. The wave conditions are the same as those in **Fig. 3**. It is found from this figure that the time histories of strains indicate the regular wave profiles and high frequency components cannot be observed. These properties differ from those of the accelerations. Moreover, the maximum strains appear near the center of the board (εP-6).

b) Effects of elasticity of floating body

Figure 5 shows the longitudinal distribution of maximum vertical accelerations of Model-A, B and C, and Model-D, E and F. The wave height, period and direction are 0.01m, 1.0s and 0degree, respectively. The horizontal axis denotes the ratio X/L of the position of the sensor X to the

length of the board L. Meanwhile, the vertical axis denotes the ratio $Amax(X)/H$ of the maximum vertical acceleration at each point ($Amax(X)$, Gal) to the wave height (H, cm). As seen in the figure, the maximum values of the accelerations for all the models have an inclination to appear near both ends of the floating boards (+0.4L and -0.4L). The reason for this is that the vertical motions of the floating bodies become large at these points because of the superposition of heave and pitch motions. From the comparison of Model-A and D that have the same dimensions and different elasticity, it is understood that the maximum vertical accelerations tend to become larger in the floating body with large elasticity.

Figure 6 shows the longitudinal distribution of maximum strains of Model-A, B and C, and Model-D, E and F. The wave conditions are the same as those in **Fig. 5**. The horizontal axis denotes the ratio X/L in the same way as **Fig. 5**. The vertical axis denotes the ratio $\varepsilon max(X)/H$ of the maximum strain at each point ($\varepsilon max(X)$) to the wave height (H, cm). It is obvious from the figure that the maximum values appear at the point of -0.1L for Model-A, B, E and F, and at the points of +0.2L and -0.2L for Model-C and D. From the comparison of Model-A and D that have the same dimensions and different elasticity, it is also recognized that the maximum strains tend to become larger in the floating body with large elasticity.

Figure 7 shows the maximum vertical accelerations at the center point (0.0L) of Model-A, B and C, and Model-D, E and F, for incident wave periods. The horizontal axis denotes the wave period, and the vertical axis denotes the ratio $Amax(0)/H$ of the maximum vertical acceleration at the center point ($Amax(0)$, Gal) to the wave height (H, cm). It is found from the figure that the maximum values of the accelerations appear for the different wave periods in each floating body. Model-C and F have the distinct maximum values of the accelerations near the wave periods of 1.6 and 1.4s, respectively. In these cases, it is supposed that the incident wave periods are close to the natural periods of floating boards. However, it should be noted that the maximum values of the accelerations have an inclination to become large, not at the center of the floating bodies, but at both ends of them.

Figure 8 shows the maximum strains at the center point (0.0L) of Model-A, B and C, and Model-D, E and F, for incident wave periods. The horizontal axis denotes the wave period, and the vertical axis denotes the ratio $\varepsilon max(0)/H$ of the maximum strain at the center point ($\varepsilon max(0)$) to the wave height (H, cm). From this figure, it is understood that the strains show the maximum values near the wave period of 1.2s, and that they become smaller when the wave period becomes longer. Furthermore, the maximum strains of Model-A, B and C with large elasticity are larger than those of Model-D, E and F with small elasticity.

Figure 9 shows the maximum displacements at the center point (0.0L) of Model-A, B and C, and Model-D, E and F, for incident wave periods. The displacements are measured by use of the laser displacement meter. The horizontal axis denotes the wave period, and the vertical axis denotes the ratio $Zmax(0)/H$ of the maximum vertical displacement ($Zmax(0)$, cm) to the wave height (H, cm). It is clearly recognized that the maximum displacements tend to increase when the wave period becomes longer. For instance, the displacements are larger than the wave height, for the wave periods of more than 1.6s in case of Model-A. Moreover, the maximum vertical displacements become smaller when the width of the floating board becomes wider for Model-A, B and C with large elasticity. On the other hand, the effects of the widths cannot be seen for Model-D, E and F with small elasticity.

3. SEPARATE SUPPORT TYPE ELASTIC FLOATING BODY

(1) Hydraulic Model Experiments

a) Models of floating body

A separate support type elastic floating body in hydraulic model experiments is made of a polyurethane board and a few aluminum cylindrical pontoons. The use of the polyurethane board aims at reproducing flexible properties of a superstructure in a floating bridge of this type.

The view of a floating body model employed here is illustrated in **Fig. 10**. This model is composed of one long rectangular board used as a superstructure and two or three cylindrical pontoons used as floating foundations. The length of the board is 1.8 or 2.8m. The pontoons are 0.3m in diameter, 0.3m in height, and 0.25m in draft. There are two mooring poles fixed at the bottom of the experimental basin as well. The mooring system is identical with that of the continuous pontoon type floating body. Namely, the floating body can freely move up and down in the vertical direction along the mooring poles in waves.

Table 4 shows five types of model. Length, width, height, mass, Young's modulus, the number of pontoons, span length between pontoons and the distinction of rigidity of each model are listed in this table. Although the floating body model must be essentially treated as an elastic body, both elastic and rigid floating body models were employed in the experiments to investigate the effects of elasticity of the superstructure on motions and deformations of models. The elastic superstructure is made of polyurethane having a unit weight of 200kg/m^3. Meanwhile, the rigid superstructure is made of an aluminum channel. Model-A and B are rigid floating bodies with two and three pontoons, respectively, while Model-C, D and E are elastic floating bodies with two, three and three pontoons, respectively.

b) Method of model experiments

Hydraulic model experiments were carried out in the same experimental basin as used for continuous pontoon type floating body models. In the experiments, two wave gauges were arranged in the same way.

Tables 5 and **6** show the experimental conditions. Regular waves were adopted in the experiments. The water depth in the model experiments is 0.5m, and the incident wave periods vary from 1.0 to 1.6s at variants of 0.2s. The wave height in the experiments is constant, and it is 0.03m. In addition, the wave directions for all the models are 0 and 30degrees. The wave direction of 0degree coincides with the longitudinal direction of the model. In Model-A, the experiments for the wave direction of 60degrees were additionally conducted. The model experiments were performed based on Froude similitude. Although the floating body models employed in the experiments are not manufactured for specific prototypes, the model scale is assumed to be 1/100.

Photograph 7 shows the arrangement of measuring instruments around a floating body model in the basin. The parameters measured in the model experiments are wave heights, and vertical accelerations, strains and displacements of the superstructure of the model. The vertical accelerations, strains and displacements are obtained by use of accelerometers, strain gauges and two laser displacement meters, respectively. These data are digitally recorded for the duration of 204.8s. For Model-A, B, C and D, seven accelerometers and strain gauges are attached to the points of $+0.35L$, $+0.21L$, $+0.07L$, $0.0L$, $-0.35L$, $-0.21L$, and $-0.07L$ in the longitudinal direction of the board, respectively. Herein, L is the length of the board. These are named AP-1 to AP-7 and εP-1 to εP-7 for accelerometers and strain gauges, respectively. On the other hand, for Model-E, eleven accelerometers and strain gauges are used. Besides, vertical displacements at two pontoon positions are observed by the laser displacement meters at the points of $+0.28L$ and $-0.28L$ for Model-A, B, C and D. These are named LP-1 and LP-2, respectively.

Photograph 8 shows the overview of a floating body model and all sorts of measuring instruments arranged in the basin. This shows the case of Model-E. Next, **Photo 9** shows the situation of deformation of the floating body model subjected to waves. Model-E is the model shown here.

(2) Results of Model Experiments

a) Time histories of accelerations and strains

Figure 11 shows time histories of measured vertical accelerations of Model-D. The wave height, period and direction are 0.03m, 1.6s and 0degree, respectively. The time histories of the accelerations are shown in this figure for the time of 100 to 106s. In the figure, the vertical accelerations at the points near the center of the board (AP-3 to AP-5) are larger than those at the points near both ends of it (AP-1, AP-2 and AP-6) except for the point of AP-7. It is also recognized that high frequency components, which are supposed to be the natural frequency components of the floating body, greatly affect the wave profiles of the accelerations. Therefore, the wave profiles of the accelerations disagree with the incident sinusoidal wave profile.

Figure 12 shows time histories of measured strains of Model-D. The wave conditions are the same as those in **Fig. 11**. It is clear from the figure that the time histories of strains are roughly regarded as sinusoidal wave profiles at the points between two side pontoons (εP-2 to εP-6). In addition, the strain amplitudes at these points are almost the same. The reason for this is that the deformations of the board following the incident regular waves are caused by three pontoons.

b) Effects of elasticity of floating body

Figure 13 shows the longitudinal distribution of maximum vertical accelerations of Model-B and D. The wave height, period and direction are 0.03m, 1.0s and 0degree, respectively. The horizontal axis denotes the ratio X/L of the position of the sensor X to the length of the board L. Meanwhile, the vertical axis denotes the ratio $Amax(X)/H$ of the maximum vertical acceleration at each point ($Amax(X)$, Gal) to the wave height (H, cm). The solid line represents the results of Model-B, while the dotted line represents the results of Model-D. Besides, three vertical solid lines in the figure mean the points where three pontoons are located. It can be obviously seen that the maximum values of the accelerations for these two models tend to appear at both ends of the boards. This is considered to be due to heave motions of three pontoons following the incident waves. Namely, in this case, the heave motions of the pontoons mainly cause the deformations of the boards. From the comparison of Model-B and D, it is also understood that the maximum vertical accelerations are relatively large in the floating body with large elasticity.

Figure 14 shows the longitudinal distribution of maximum strains of Model-B and D. The wave conditions are the same as those in **Fig. 13**. The horizontal axis denotes the ratio X/L, and the vertical axis denotes the ratio $\varepsilon max(X)/H$ of the maximum strain at each point ($\varepsilon max(X)$) to the wave height (H, cm). The lines shown in the figure represent the same ones as shown in **Fig. 13**. It is easily recognized that the maximum strains are large and almost constant at the points between two side pontoons for Model-D. On the other hand, the maximum strains of Model-B are very small as compared with those of Model-D, because of the large rigidity of the board. In other words, the maximum strains tend to become much larger in the floating board with large elasticity.

Figure 15 shows the maximum vertical accelerations at the center point ($0.0L$) of Model-B and D, for incident wave periods. The horizontal axis denotes the wave period, and the vertical axis denotes the ratio $Amax(0)/H$ of the maximum vertical acceleration at the center point ($Amax(0)$, Gal) to the wave height (H, cm). The solid line represents the results of Model-B,

while the dotted line represents the results of Model-D. From the figure, it is clear that the maximum values of the accelerations appear for the wave periods of 1.2 and 1.4s for Model-B and more than 1.2s for Model-D. It is also understood that the accelerations of Model-D with large elasticity are somewhat larger than those of Model-B with small elasticity for almost all the wave periods.

Figure 16 shows the maximum strains at the center point (0.0*L*) of Model-B and D, for incident wave periods. The horizontal axis denotes the wave period, and the vertical axis denotes the ratio $\varepsilon max(0)/H$ of the maximum strain at the center point ($\varepsilon max(0)$) to the wave height (H, cm). The lines shown in the figure represent the same ones as shown in **Fig. 15**. It can be seen from the figure that the maximum strains of Model-B are very small in comparison with those of Model-D in the same way as shown in **Fig. 14**. Moreover, the maximum strain of Model-D becomes larger when the wave period becomes longer. Consequently, the maximum strains of Model-D with large elasticity are larger than those of Model-B with small elasticity.

Figure 17 shows the maximum displacements at the point of LP-1 of Model-B and D, for incident wave periods. The horizontal axis denotes the wave period, and the vertical axis denotes the ratio $Zmax(+0.28L)/H$ of the maximum vertical displacement ($Zmax(+0.28L)$, cm) to the wave height (H, cm). The lines shown in the figure represent the same ones as shown in **Fig. 15**. It is recognized that the maximum vertical displacements are large for the wave periods of 1.2 and 1.4s for both models. Further, the displacements of both models show almost the same tendency for the wave periods. However, in case of Model-D, the displacements are slightly smaller than those of Model-B for the wave periods of more than 1.4s. Accordingly, the elasticity of the floating body models does not have much influence on the maximum displacements of them except for longer wave periods.

c) Effects of number of cylindrical pontoons

Figure 18 shows the longitudinal distribution of maximum vertical accelerations of Model-C and D. The wave height, period and direction are 0.03m, 1.0s and 0degree, respectively. The horizontal axis denotes the ratio X/L, and the vertical axis denotes the ratio $Amax(X)/H$. The solid line represents the results of Model-C with two pontoons, while the dotted line represents the results of Model-D with three pontoons. Besides, two vertical solid lines and three vertical dotted lines in the figure mean the points where two and three pontoons are located, respectively. It is found from the figure that in Model-C with two pontoons, the maximum vertical accelerations near the center of the board are considerably larger than those at both ends of it. Meanwhile, it is understood that in Model-D with three pontoons, the maximum vertical accelerations become larger at both ends of the board. In case of Model-C, since the vertical movements of two pontoons are generated by waves, the vertical deformation of the board becomes large near the center of it, and this causes the increase of the maximum vertical accelerations there. Meanwhile, Model-D has the short span lengths of 0.5m and one pontoon at the center point of the floating body. Namely, the vertical deformation of the board is restricted by the center pontoon, and this results in the decrease of the maximum vertical accelerations near the center of the floating body.

Figure 19 shows the longitudinal distribution of maximum strains of Model-C and D. The wave conditions are the same as those in **Fig. 18**. The horizontal axis denotes the ratio X/L, and the vertical axis denotes the ratio $\varepsilon max(X)/H$. The lines shown in the figure represent the same ones as shown in **Fig. 18**. It can be seen from the figure that the maximum strains have the flat distribution as a whole in case of Model-C with two pontoons. Furthermore, in case of Model-D with three pontoons, the maximum strains are

almost constant at the points between two side pontoons. From the comparison of Model-C and D, it is understood that the maximum strains are large in the floating body with three pontoons in this case.

4. CONCLUSIONS

The results of hydraulic model experiments on the continuous pontoon type and the separate support type elastic floating bodies were described in this paper. This is a fundamental study for realizing construction of long and large flexible floating structures such as floating bridges. The comparison of experimental and numerical results is a main subject to be performed after this.

Major knowledge obtained in the present study is summarized as follows:

(1) The continuous pontoon type floating body

a) In the time histories of vertical accelerations, high frequency components corresponding to the natural frequency components of the floating body are clearly observed. Conversely, the time histories of strains indicate the regular wave profiles.

b) The maximum vertical accelerations and strains tend to become larger in the floating body with large elasticity. The maximum displacements increase when the wave period becomes longer.

(2) The separate support type floating body

a) In the time histories of vertical accelerations, high frequency components corresponding to the natural frequency components of the floating body are recognized. On the other hand, the time histories of strains indicate the regular wave profiles at the points between two side pontoons.

b) The maximum vertical accelerations and strains tend to become larger in the floating body with large elasticity. The maximum displacements become larger for the middle wave periods.

c) The maximum vertical accelerations are remarkably large near the center point in the floating body with two pontoons. The maximum strains become larger in the floating body with three pontoons.

REFERENCES

Lwin,M.M.(1994): "Floating Bridges in the United States", *Proc. of International Workshop on Floating Structures in Coastal Zone, the Port and Harbour Research Institute*, pp.56-73.

Landet, E.(1994): "Planning and Construction of Floating Bridges in Norway", *Proc. of International Workshop on Floating Structures in Coastal Zone, the Port and Harbour Research Institute*, pp.43-45.

Shiraishi,S., Ishimi,G., Yoneyama,H. and M.Kondo(1996): "Experimental Study on Motions of Long Flexible Floating Structures in Waves", *Proc. of International Workshop on Very Large Floating Structures*, pp.265-273.

Shiraishi,S., Ishimi,G. and H.Yoneyama(1997a): "Experiment and Analysis on Motions of Long Flexible Floating Structures in Waves", *Proc. of 21st Joint Meeting UJNR, Marine Facility Panel*, pp.187-194.

Shiraishi,S., Ishimi,G., Yoneyama,H. and M.Kondo(1997b): "Experimental Study on Motions and Forces of Flexible Beam Floating Structures in Waves and Effect of Rigidity of Body", *Proc. of Civil Engineering in the Ocean*, Vol.13, pp.189-194, (in Japanese).

Maruyama,T., Kawamura,Y., Tsuda,T., Kishimoto,T., Tanaka,H. and Y.Yasuda(1998a): "Plan and Design of Yumeshima-Maishima Bridge –Movable Floating Bridge-", *Bridge and Foundation Engineering, Kensetutosyo*, Vol.32, No.2, (in Japanese).

Maruyama,T., Kawamura,Y., Tsuda,T., Takeda,S., Nakaji,E., Oka,S. and M.Tsuchiya(1998b): "Plan and Design of Yumeshima-Maishima Bridge –Movable Floating Bridge-", *Bridge and Foundation Engineering, Kensetutosyo*, Vol.32, No.3, (in Japanese).

Ishimi,G., Shiraishi,S. and H.A.Z.E. Din(1999): "Hydraulic Model Test on Elastic Floating Body Supported by Pontoons", *Technical Note of the Port and Harbour Research Institute*, No.930, (in Japanese).

Shiraishi,S., Ishimi,G. and H.A.Z.E.Din(1999): "Experimental Study on the Motion of Elastic Floating Body Supported by Pontoons", *Proc. of Advances in Structural Engineering and Mechanics*, (in press).

Table 1 Types of floating body model
(continuous pontoon type)

Model	Length (m)	Width (m)	Thickness (m)	Density (kg/m³)	E (kN/cm²)
A	2.0	0.1	0.02	98.0	4.07
B		0.2			4.10
C		0.5			4.03
D		0.1		200.0	16.27
E		0.2			15.59
F		0.5			15.53

Table 2 Experimental conditions (1)
(continuous pontoon type)

	Model	Prototype
Water Depth (m)	0.3	30.0
Wave Period (sec)	0.8, 1.0, 1.2, 1.4, 1.6, 1.8, 2.0, 2.2, 2.4, 2.6	8, 10, 12, 14, 16, 18, 20, 22, 24, 26
Wave Height (m)	0.01, 0.02	1.0, 2.0
Wave Direction (deg)	0, 30, 60	0, 30, 60

Table 3 Experimental conditions (2)
(continuous pontoon type)

Model	Wave Height (m)		Wave Direction (deg)		
	0.01	0.02	0	30	60
A	○	○	○		
B	○		○	○	○
C	○		○		
D	○		○		
E	○		○		
F	○		○		

Table 4 Types of floating body model
(separate support type)

Model	Body	Length (m)	Width (m)	Height (m)	Mass (kg)	E (kN/cm²)	Pontoon	Span Length (m)
A	Rigid	1.8	0.125	0.035 ([type)	5.23	-	2	1.0
B							3	0.5
C	Elastic		0.15	0.02	1.30	14.61	2	1.0
D							3	0.5
E		2.8			1.95	17.61		1.0

Table 5 Experimental conditions (1)
(separate support type)

	Model	Prototype
Water Depth (m)	0.5	50.0
Wave Period (sec)	1.0, 1.2, 1.4, 1.6	10, 12, 14, 16
Wave Height (m)	0.03	3.0
Wave Direction (deg)	0, 30, 60	0, 30, 60

Table 6 Experimental conditions (2)
(separate support type)

Model	Wave Direction (deg)		
	0	30	60
A	○	○	○
B	○	○	
C	○	○	
D	○	○	
E	○	○	

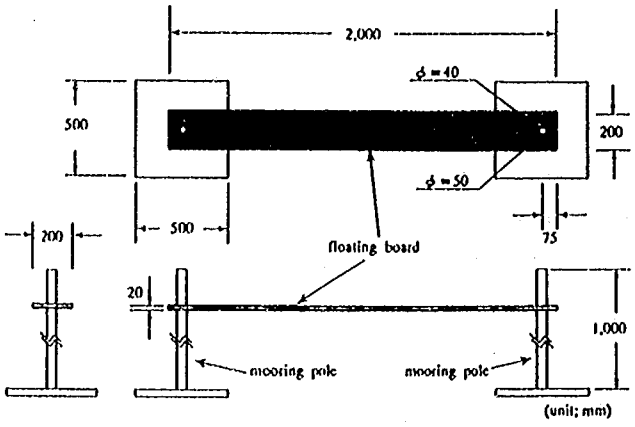


Fig.1 Experimental model
(continuous pontoon type; Model-B)

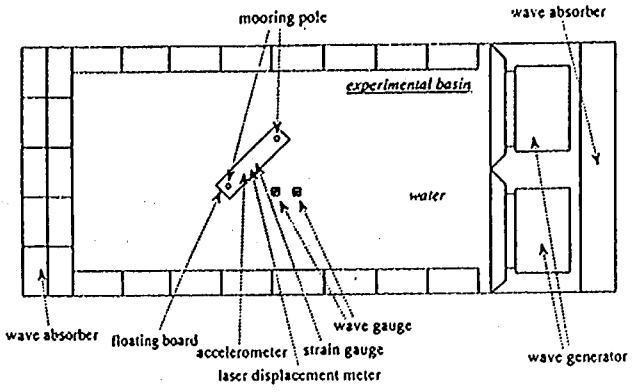


Fig.2 Experimental basin and equipment

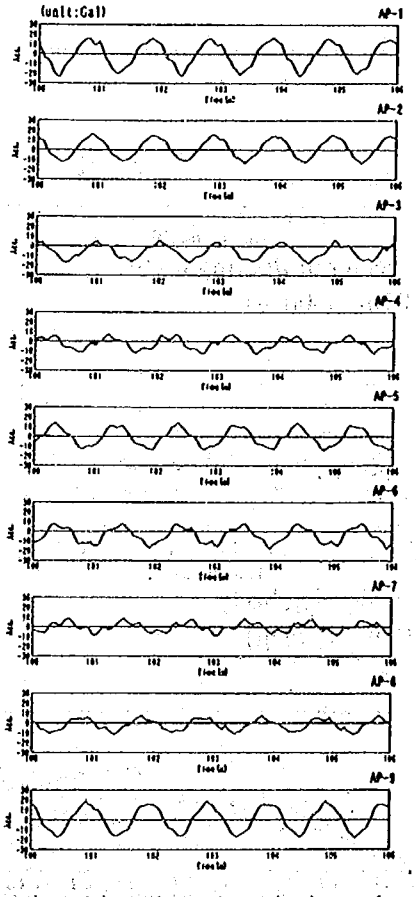


Fig.3 Time histories of vertical accelerations
(Model-A; H=0.01m, T=1.0s, θ=0deg)

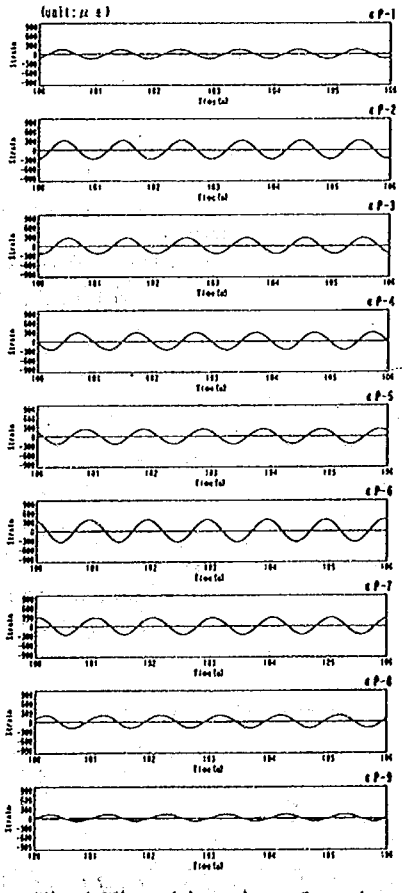


Fig.4 Time histories of strains
(Model-A; H=0.01m, T=1.0s, θ=0deg)

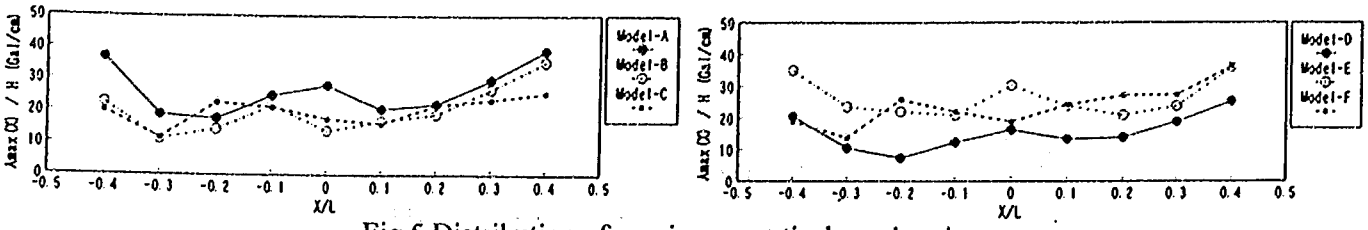


Fig.5 Distribution of maximum vertical accelerations
(Model-A, B, C and D, E, F; H=0.01m, T=1.0s, θ=0deg)

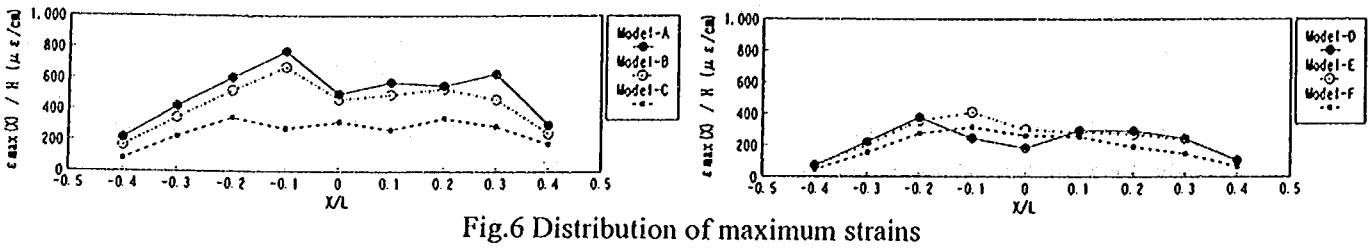


Fig.6 Distribution of maximum strains
(Model-A, B, C and D, E, F; H=0.01m, T=1.0s, θ=0deg)

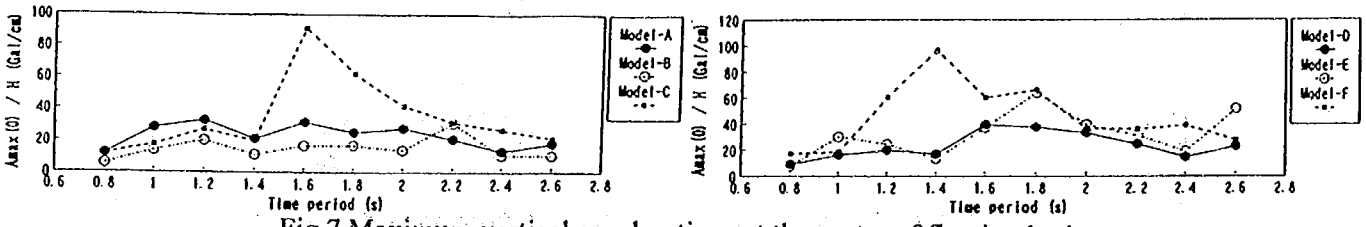


Fig.7 Maximum vertical accelerations at the center of floating body
(Model-A, B, C and D, E, F; H=0.01m, θ=0deg)

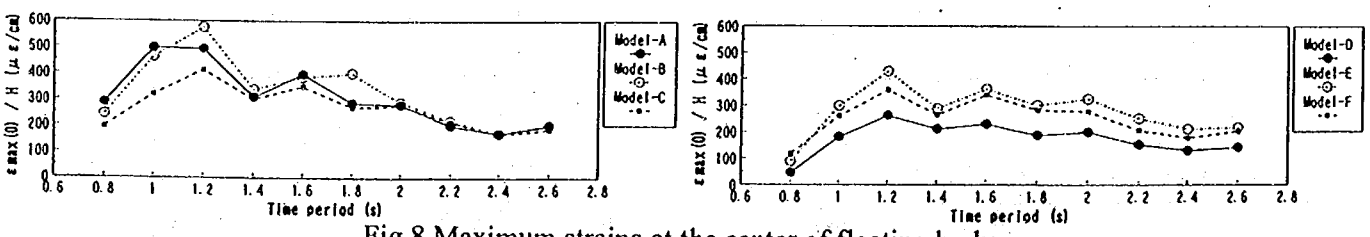


Fig.8 Maximum strains at the center of floating body
(Model-A, B, C and D, E, F; H=0.01m, θ=0deg)

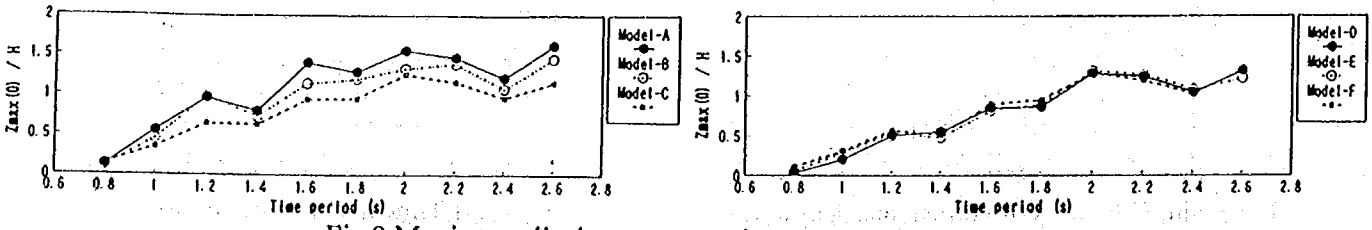


Fig.9 Maximum displacements at the center of floating body
(Model-A, B, C and D, E, F; H=0.01m, θ=0deg)

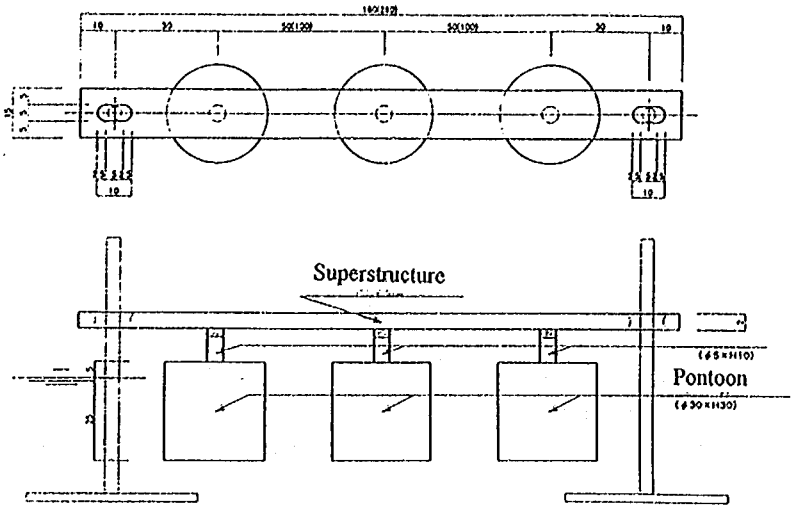


Fig.10 Experimental model (separate support type)

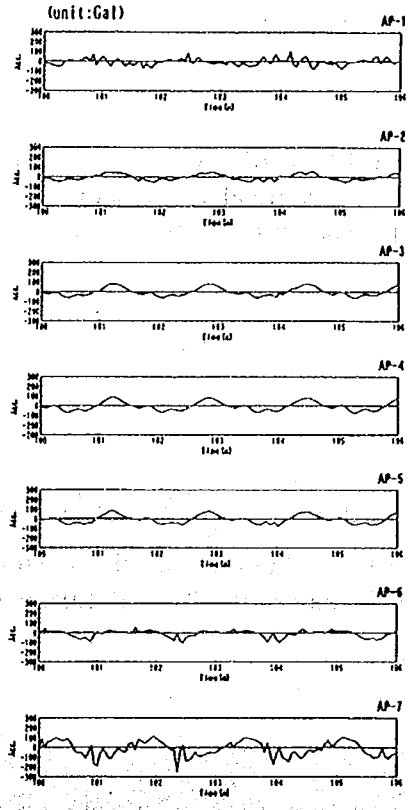


Fig.11 Time histories of vertical accelerations
(Model-D; H=0.03m, T=1.6s, θ=0deg)

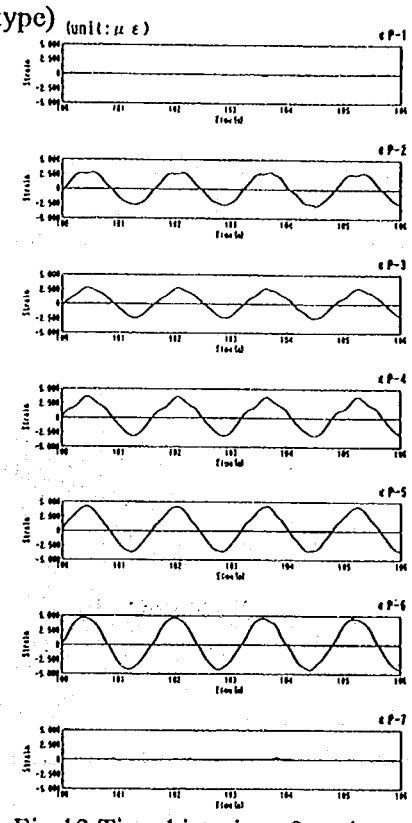


Fig.12 Time histories of strains
(Model-D; H=0.03m, T=1.6s, θ=0deg)

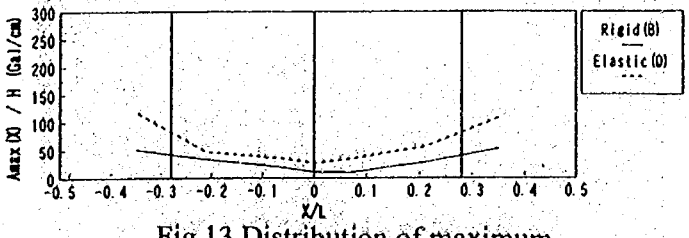


Fig.13 Distribution of maximum vertical accelerations
(Model-B and D; H=0.03m, T=1.0s, θ=0deg)

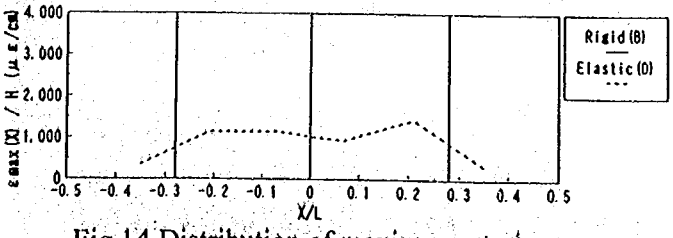


Fig.14 Distribution of maximum strains
(Model-B and D; H=0.03m, T=1.0s, θ=0deg)

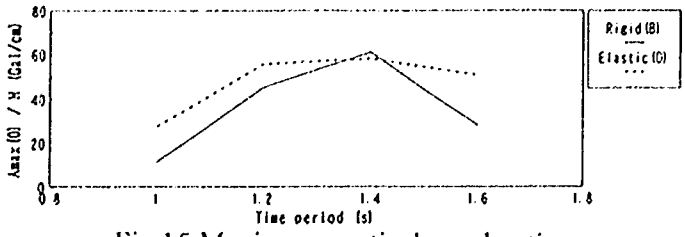


Fig.15 Maximum vertical accelerations at the center of floating body (Model-B and D; H=0.03m, θ=0deg)

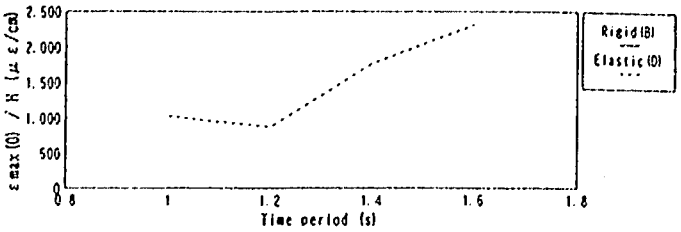


Fig.16 Maximum strains at the center of floating body (Model-B and D; H=0.03m, θ=0deg)

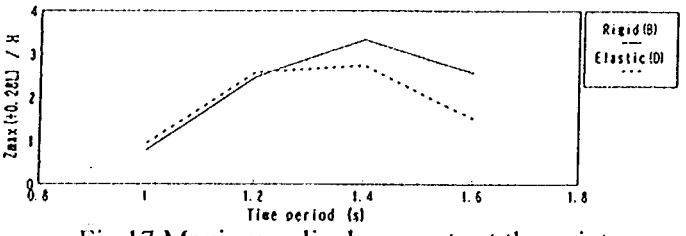


Fig.17 Maximum displacements at the point of LP-1 of floating body (Model-B and D; H=0.03m, θ=0deg)

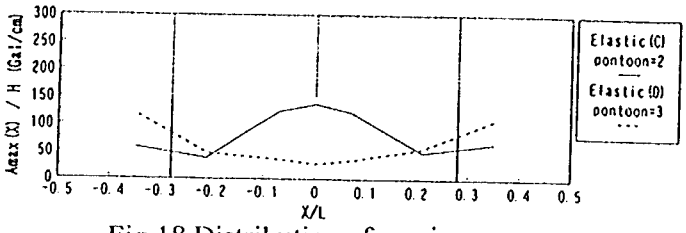


Fig.18 Distribution of maximum vertical accelerations (Model-C and D; H=0.03m, T=1.0s, θ=0deg)

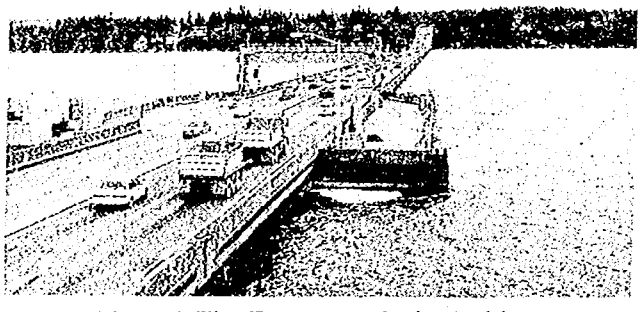


Photo 1 The Evergreen Point Bridge

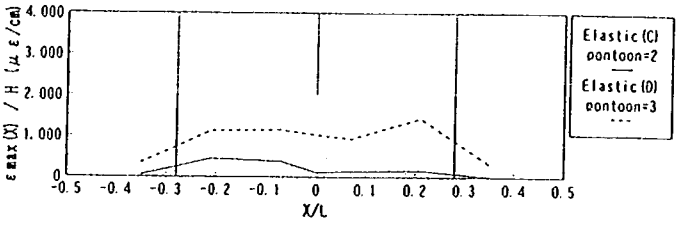


Fig.19 Distribution of maximum strains (Model-C and D; H=0.03m, T=1.0s, θ=0deg)

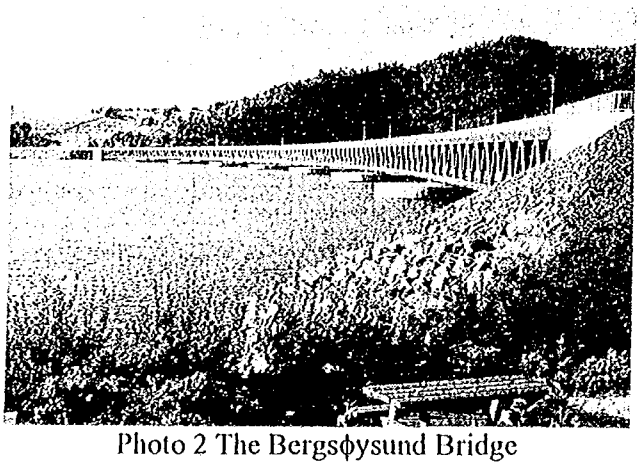


Photo 2 The Bergsϕysund Bridge

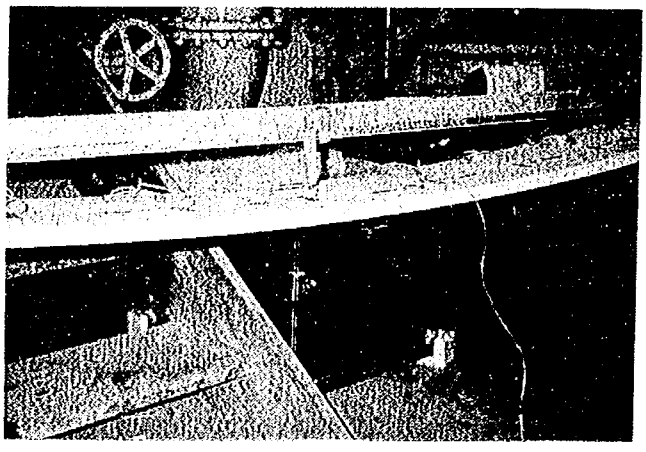


Photo 3 Deformation measurement of a floating board in air

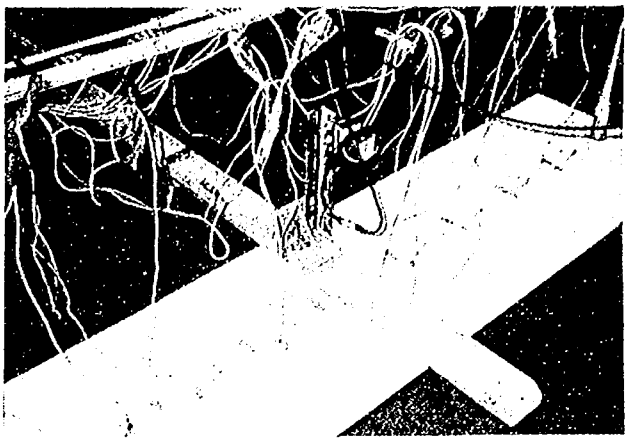


Photo 4 Arrangement of measuring instruments
(continuous pontoon type)

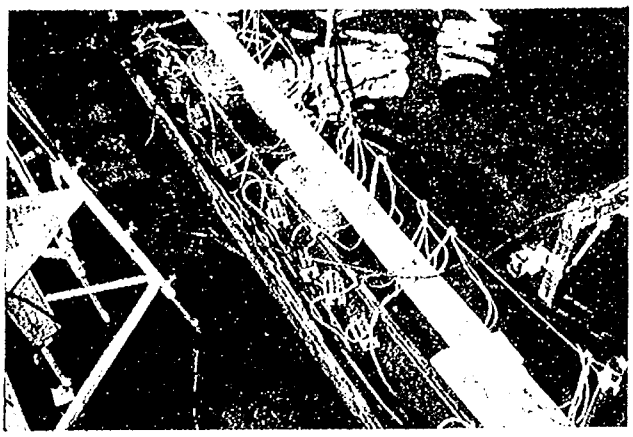


Photo 7 Arrangement of measuring instruments
(separate support type)



Photo 5 Overview of a floating body model
(continuous pontoon type)

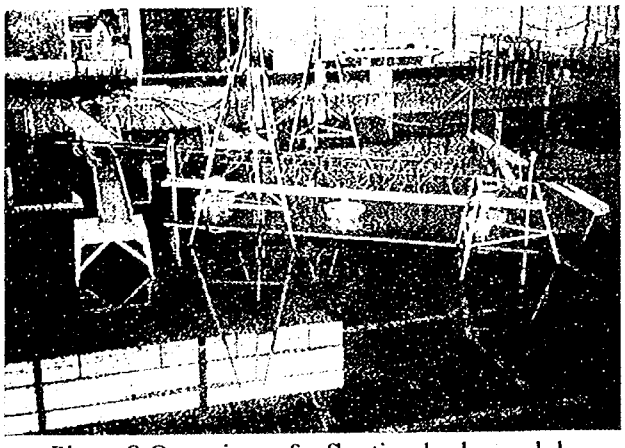


Photo 8 Overview of a floating body model
(separate support type)

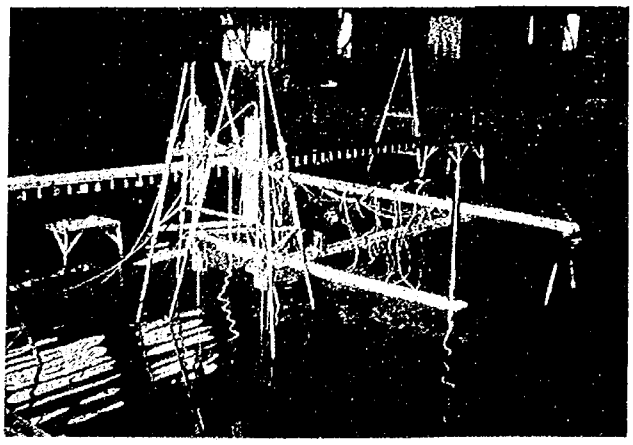


Photo 6 Situation of model experiments
(continuous pontoon type)

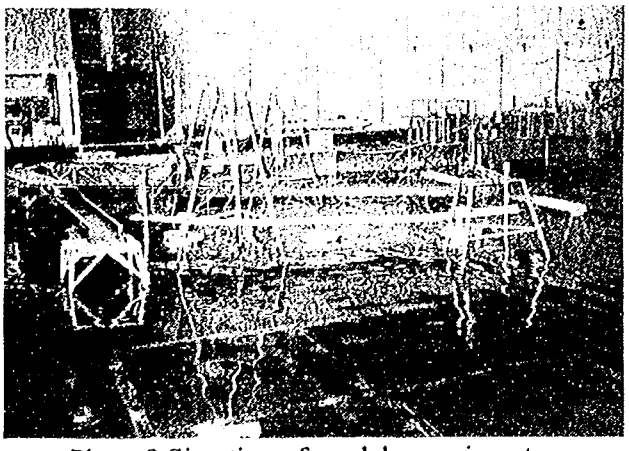


Photo 9 Situation of model experiments
(separate support type)

Development of a Probabilistic Seismic Hazard Analysis for Offshore Facilities in the Santa Barbara Channel

by

Charles E. Smith[1] and Robert Murray[2]

ABSTRACT

This paper summarizes initial efforts to develop a probabilistic seismic hazards analysis (PSHA) for the Santa Barbara Channel conducted by the Lawrence Livermore National Laboratory (LLNL) for the Minerals Management Service (MMS) of the U.S. Department of the Interior. The purpose of the PSHA is to provide a basis for development by MMS of regulations governing evaluation of applications to re-license existing oil platforms in Federal waters within the Channel with respect to seismic loading. The final product of the analysis will be hazard assessments of ground motion parameters at specified probability levels of excedence. This paper summarizes the characterization of local earthquake sources within the Channel and onshore areas of the Western Transverse Ranges, development of a ground motion attenuation model for the region, and presents preliminary hazard results at three selected offshore sites.

KEYWORDS: earthquake ground motions, earthquake source models, offshore platforms, probabilistic seismic hazard analysis, seismological uncertainties.

1. INTRODUCTION

The Minerals Management Service (MMS) of the U.S. Department of the Interior has considered several methodologies with which to re-evaluate the structural design and performance of existing oil-drilling platforms in the Santa Barbara Channel, offshore California. To provide the basis for the seismic loading aspects of these procedures, Lawrence Livermore National (LLNL), in collaboration with the Institute for Crustal Studies (ICS) at the University of California, Santa Barbara was requested to develop procedures to conduct a probabilistic seismic hazards analysis (PSHA) of the Channel.

The Santa Barbara Channel is located within the most seismically active region of the U.S. and can expect to experience moderate to large, and perhaps even great, earthquakes within the lifetimes of some of the existing platforms. Detailed seismic hazard analyses are being conducted onshore based upon an extensive and detailed characterization of earthquake sources by the Southern California Earthquake Center (SCEC). Current efforts are concentrated on the Los Angeles Basin, but the California Division of Mines and Geology (DMG) intends to expand the analyses to include the entire onshore area. An important goal of the MMS is to ensure that the seismic hazard analyses for the Santa Barbara Channel is fully integrated with the onshore analyses by adopting and refining the common SCEC data base and utilizing compatible ground motion attenuation and hazard analysis methodologies.

Phase I of the study concentrated on the eastern half of the Santa Barbara Channel where most of the existing platforms are located. Three levels of detail were used to describe potentially significant earthquake sources: (1) regional-scale faults within 300 km that can generate significant ground motions, including long-period (2 to 5 sec) ground motions, in the study area; (2) a general description of all potentially active faults between 10 and 50 km from the study area and detailed

1. Research Program Manager, Minerals Management Service, Herndon, VA 20170
2. Project Manager, Lawrence Livermore National Laboratory, Livermore, CA 94550

characterization of those capable of generating significant ground motions; (3) detailed characterization of all potentially active structures within 10 km of any platform. Characterizations of regional sources were taken from the SCEC data base and along with other data were used for the Phase II hazard analysis. For specific sites, however, a considerable number of fault sources in categories (2) and (3) above that are not presently characterized in the SCEC data base were considered. In particular, these include offshore faults within the Santa Barbara Channel.

This paper discusses some of the technical issues that may contribute to potential sources of significant uncertainty in the PSHA. These include issues concerning identification and characterization of earthquake sources, as well as issues relative to estimating ground motion offshore. Some of these issues are similar to those addressed in recent onshore studies conducted by the SCEC and DMG, but a number are particularly relevant to the study area and its offshore location. These issues are briefly summarized below.

2. EARTHQUAKE SOURCE CHARACTERIZATION

Major issues concerning identification and characterization of earthquake sources in the vicinity of the Santa Barbara Channel stem from the present poor understanding of the nature of large-scale tectonic deformation within the Western Transverse Ranges tectonic province of which the Channel occupies the southern half. Recent earthquakes, such as the 1994 Northridge event, show that some deformation takes place as moderate to large earthquakes on blind faults. These sources are particularly problematic in that, at present, they cannot be identified or evaluated in advance. Differing interpretations of the fundamental deformation style lead to significantly different characterizations of the blind faults in terms of the characteristic magnitudes they are capable of producing, their geometries relative to surface installations, and estimates of the rates of occurrence of earthquakes generated on them. A blind, shallow-dipping thrust fault, such as the Channel Islands thrust, has been hypothesized to underlie the entire area of the eastern Santa Barbara Channel at mid-crustal depth and has been estimated to be capable of generating earthquakes as large as magnitude 7.4. Several potentially long and active faults have been tentatively identified on the sea floor of the Santa Barbara Channel using seismic and oil well data. Some of these appear to be offshore continuations of major faults known to be active onshore. However, there are conflicting interpretations of certain prominent offshore features, especially features that are in the immediate vicinity of the platforms, which have significantly different implications for offshore seismic hazard analysis.

The SCEC methodology calculates earthquake recurrence intervals by integrating seismic moment rates estimated from geological data for specific faults, geodetic measurements of regional strain rates, and regional seismicity data. Each of these types of data is subject to potentially large uncertainties arising from limited temporal or spatial sampling of past events or long-term deformation and from the accuracy of the measurements. Estimating slip rates for the offshore faults is particularly problematic since, except where these cross the Channel Islands, detailed seismic data are not available. Segmenting long faults into individual rupture segments in an objective way remains a difficult problem even where major faults are mapped in detail. The problems of fault segmentation and slip rate estimation are particularly acute for blind faults and rely on indirect interpretation or modeling of surface observations.

3. STRONG GROUND MOTION

The lack of offshore strong ground motion recordings precludes determination of attenuation relations for offshore areas and investigation of site effects. The few existing offshore recordings for the Santa Barbara Channel are presently being studied, but results to date are not conclusive.[2]

Natural periods of offshore platforms are different from those of typical onshore structures. Steel template-type platforms commonly have natural periods in the range of 1 to 5 seconds. For comparison, residential and commercial structures have natural periods less than 2 seconds. Also, the first vertical modal period of platforms is often in the range of 0.3 to 0.5 seconds. Vertical motion can be important because of cantilevered structures on decks.

The roles of water-saturated sediments and the water itself are not well documented. Unusual characteristics and the generation of different phases and relationships are expected to occur and should be accounted for if onshore attenuation relations are used. There are indications that offshore vertical motions are significantly attenuated relative to similar onshore vertical records. The MMS initiated the Seafloor Earthquake Measurement System (SEMS) some 10 years ago to collect and analyze seismic data measured on the seafloor.

The geometry of the faults in the Santa Barbara Channel and their spatial relationships to the platforms present challenging questions in estimating ground motions. First, platforms may be on the hanging wall of the faults and, therefore, may be subject to large accelerations. Second, platforms may be located near the up-dip extensions of steeply- or moderately-dipping reverse fault planes. This type of geometry maximizes the directivity effect and, therefore, enhances the amplitude of the ground motion, particularly at longer periods. Also, because reverse or thrust faults predominate in the area, the vertical component could be as large as the horizontal.

4. SUMMARY OF PHASE I WORK

In order to properly achieve the intended regulatory basis, the PSHA must account for the uncertainties in characterizing earthquake sources and in ground motion attenuation in the Southern California region and propagate those uncertainties through the analysis to provide estimates of the uncertainty in the hazard in the form of mean estimates and other statistical parameters.[3] These uncertainties include both random uncertainties and uncertainties that arise from our inability, through lack of knowledge, to model the Earth or describe its behavior. Therefore, the primary objective of Phase I of the project was to define and evaluate issues that introduce significant uncertainties into seismic hazard estimation in Southern California in general and to assess in detail the impact of these issues on seismic hazards in the Channel.
As is generally the case in PSHA, the evaluation focused largely on sources of uncertainty. Due to our lack of knowledge, the major issues affecting earthquake source characterization in this region stem from the fundamentally different models of tectonic deformation, "thin-skinned" or "thick-skinned," that have been proposed based upon alternative interpretations of the available data. These issues are currently the focus of intense debate. The main issues affecting ground motion attenuation under the Channel are the absence of a strong motion data base for offshore environments, the effects of sedimentary basins and wedges, and the effects of the water column and saturated soils. Based upon the preliminary characterization of earthquake sources, two preliminary alternative earthquake source maps for the Western Transverse Ranges were developed, which incorporated the geometries and slip rate estimates of the potentially significant faults that form part of each of the proposed alternative tectonic models.

Phase I culminated in a workshop at Stanford University on August 16-17, 1995, in which scientists currently working on key aspects of the tectonics of the Western Transverse Ranges and on ground motion estimation offshore participated. The workshop served as a forum both for dissemination of current data and interpretations and to elicit expert opinion in finalizing earthquake source and ground motion models. Specific objectives were: (1) to ensure that all available data and current tectonic interpretations in forming the major issues were considered and in identifying significant

earthquake sources, (2) to make a comparative evaluation of the evidence supporting the competing tectonic models and specific sources as a basis for weighting the alternatives, (3) using preliminary source maps as "straw men" to develop the basis for a set of maps that fully captures the alternative tectonic hypotheses and accurately represents significant potential sources, and (4) to refine a preliminary ground motion attenuation model and ensure that it is the most suitable form for use offshore. These objectives were successfully achieved during the workshop.

5. SUMMARY OF PHASE II WORK

The results of the workshop, together with comments on the Phase I report received from several reviewers, indicated that the major tectonic interpretations and their variations can be represented by two basic, or "core," earthquake source models corresponding to the thick- (Model 1) and thin-skinned (Model 2) interpretations. Within each of these a considerable number of alternative fault geometries are permitted by the data and need to be included to capture adequately the epistemic uncertainty in source characterization.

Having identified the sources comprising each of the core models, detailed characterization of the models involved: (1) defining the alternative geometries. These alternatives can include ranges of fault dips, possible fault segmentation schemes, and multi-segment rupture scenarios. One source of complexity is the inter-dependence of the down-dip geometries of several of the non-vertical faults, such that alternative geometries for one fault also require alternatives for neighboring faults. Combinations of all the possible fault geometries lead to a large number of alternative source maps for both Models 1 and 2, (2) estimating probability distributions for fault slip rates from the available data, (3) estimating probability distributions for characteristic moment magnitudes (M_W) for each of the fault segments and segment combinations based upon their fault areas. For this, the areas-moment magnitude (M_W) relationship of Wells and Coppersmith[4] were used, and (4) the slip rates and maximum magnitudes were combined to estimate earthquake recurrence rate distributions for a range of magnitudes for each source employing the characteristic earthquake recurrence model of Youngs and Coppersmith[5]. The regional Gutenberg-Richter "b" value of 0.75 ± 0.5 used to construct the recurrence relationships was estimated from the Caltech Western Transverse Ranges earthquake data.

6. SOURCE MODEL 1

Figure 1 is a map of the faults comprising Model 1. Depth sections through the model are shown in Figure 2. Model 1 is based upon the "thick-skinned" tectonic hypothesis proposed primarily by Yeats[6] and Huftile and Yeats[7]. According to this hypothesis, which is based largely upon surface or near-surface observations of fault slip and upon geodetic data, active faults extend into the middle and lower crust at relatively steep dips observed at shallow crustal depths. The model largely comprises surface faults but also includes three blind reverse faults (Figure 1)--a blind extension of the Oak Ridge fault under the Santa Barbara Channel, a major blind thrust fault under the Ojai Valley and Topatopa Mountains and the Northridge fault--the source of the 1994 Northridge earthquake. The Oak Ridge and Ojai blind thrusts have not been observed directly but are inferred from modeling of surface faulting and folding data. For this model, the blind Oak Ridge thrust in particular makes a large contribution to the hazard in the Channel. The Model 1 faults are described in the Phase I report.[1] Fault parameters are given in Table 1 in which data references are identified.

Each possible combination of the alternative characterizations (geometry, including segmentation, and slip rate) of the individual sources forms one source map from which the hazard can be estimated. Alternative characterizations are represented by branches of an event tree, and a source map is compiled by working along a limb formed by connected branches. A subjective weight was assigned to

each branch that expresses degree of confidence both in the existence of that source and that this particular alternative characterization represents the process that generates earthquakes on the source. The weights are based upon assessment of all of the data supporting each interpretation. Weights assigned to multi-segment faults ("cascades") are based upon the subjective estimate of the likelihood that the fault will rupture in that combination of segments relative to other possible combinations and also express qualitatively the estimates of relative frequencies of occurrence of the different segment combinations. The final weight for each map is obtained as the product of the weights of the individual branches that comprise the corresponding limb of the tree. The maps were ranked according to their weights relative to the highest weighted, best estimate, map.

7. SOURCE MODEL 2

Model 2 is shown in Figure 3, with the cross section shown in Figure 4, and is based chiefly upon "thin-skinned" tectonic interpretations by Shaw and Suppe *et al.*[8] Many of the important sources in this model are major blind thrust ramps on regional-scale detachments that are inferred by balanced cross-section modeling. Therefore, the geometries, particularly depths and slip rates of these thrusts, are model-dependent and highly non-unique. This and the possible alternative interpretations of the relationships of surface faults to the detachments (Figure 4) mean that the epistemic uncertainties inherent in this model are large compared with Model 1. The slip rates for Model 2, given in Table 2, are preliminary only.

8. GROUND MOTION ATTENUATION MODEL

Given the state of knowledge about ground motions, the approach to deriving ground motion information for this project was to use Western US ground motion descriptions developed by several experts.

The assumptions underlying this project are:

The ground motion parameter; e.g., peak ground acceleration (PGA), is a lognormal stochastic variable (median = a50, variability = σln).

The median of the ground motion parameter is a function of earthquake magnitude and distance and other source parameters included in ground motion models.

The variability of the ground motion is quantified by the standard deviation of the natural logarithm of the ground motion parameter.

Given these assumptions, the data, data analyses, and the methodologies used to develop the ground motion models were reviewed to assess their adequacy for estimating median ground motion and variability as a function of magnitude and distance.

9. MODEL 1 HAZARD CALCULATIONS

The hazard curves for PGA shown in Figures 5-7 were calculated using the method described in Reference 9 and the Model 1 source characterization. The calculations were performed for three sites: Platforms Houchin, Dos Quadras A, and Pescado A-1, shown in Figures 1 and 3. Five hundred Monte Carlo simulations were performed for each site, one of the Model 1 source maps being selected for each simulation. Rather than sampling the entire source maps, only the 100 highest weighted maps were used to represent the overall map distribution. This procedure was felt justified by the fact that the relative weights of the ranked maps drop rapidly once low weighted alternatives (branches) begin to be included. Therefore, the hazard estimates stabilize at the values that result from a relatively small subset containing the highest weighted maps.

Each simulation sampled one value of the earthquake rate distribution at each magnitude in the range $m \leq m \leq m_u$ and one value of the distribution of m_u to construct the magnitude frequency distribution for each source in the map. The earthquake-site distance distributions were constructed as described in Reference 10. Each simulation sampled one value of the ground motion distribution for each magnitude and distance for each source.

Figures 5-7 show that the mean PGA hazard curves obtained using Model 1 alone are comparable with the results of previous analyses, which fall within the uncertainty bounds of the hazard curves. This is largely because the source models used for those analyses include many of the same local (Western Transverse Ranges) faults as Model 1, although the geometries and rate parameterizations of these faults differ from Model 1 to varying degrees; and significant sources, such as the Oak Ridge blind thrust, are absent from the previous models. It is anticipated that including source Model 2 in the PSHA will widen the uncertainty bounds shown in Figures 5-7. This is first because Models 1 and 2 are based upon fundamentally different tectonic hypotheses, so that including Model 2 in itself introduces significant uncertainty into the source characterization. Second, many of the Model 2 sources that have the potential for making the greatest contribution to the hazard in the Channel are blind thrust faults, which, as discussed earlier, have associated uncertainties that are significantly greater than those associated with most of the Model 1 sources. However, the large epistemic uncertainties associated with Model 2 also mean that this model receives an overall lower weight relative to Model 1, which should significantly mitigate the effect that the Model 2 uncertainties have on the hazard uncertainty. Incorporation of Model 2 into the analyses has not been complete to date due to lack of funding.[1]

10. CONCLUSION

Probabilistic seismic hazard methodologies have been in use for the past 30 years. Such analyses are based on three basic inputs. First, the seismic sources in the study region are identified, and earthquake rates are defined for each fault. Ground motion attenuation relations, which are generally expressed as ground accelerations vs. velocities as a function of magnitude and distance, are then used to model the seismic energy propagation from the source to give the ground motions at the site. An uncertainty analysis is then carried out to incorporate the range of interpretation for each parameter involved in the determination of earthquake recurrences, maximum magnitude, and ground motion attenuation.

The study has demonstrated that these same procedures employed to develop PSHA's for onshore sites can be used for offshore sites. The development of PSHA's can be of great benefit in assessing the structural integrity of offshore facilities with respect to future earthquakes. However, the great uncertainties associated with source models and the lack of historical seafloor seismic data will always lead to discussion on the relative reliability of the data produced.

11. REFERENCES

1. Foxall, W., A. Boisonnade, and L. Hutchings, *Technical Issues Relevant to Seismic Hazard Analysis of the Eastern Santa Barbara Channel*, prepared by Lawrence Livermore National Laboratory for the Minerals Management Service, April 1995.

2. Boore, D.M. and C. E. Smith, *Analysis of Earthquake Recordings Obtained from the Seafloor Earthquake Measurement System (SEMS) Instruments Deployed off the Coast of Southern California*, Bulletin of the Seismological Society of America, Vol. 89, No. 1, pp. 260-274, February 1999.

3. Senior Seismic Hazards Committee (SSHAC), *Recommendations for probabilistic seismic hazard analysis: Guidance on uncertainty and use of experts*, UCRL-ID-122160, Lawrence Livermore National Laboratory, 170 p, 1995.

4. Wells, D.L. and K. J. Coppersmith, *New empirical relationships among magnitude, rupture length, rupture width, rupture area, and surface displacement*, Bulletin of the Seismological Society of America, No. 84, pp. 974-1002, 1994.

5. Youngs, R. R. and K. J. Coppersmith, *Implications of fault slip rates and earthquake recurrence models to probabilistic seismic hazard estimates*, Bulletin of the Seismological Society of America, No. 75, pp. 939-964, 1985.

6. Yeats, R. S., *Converging more slowly*, Nature, 366, pp. 299-301, 1993.

7. Huftile, G. J. and R. S. Yeats, *Convergency rates across a displacement transfer zone in the Western Transverse Ranges, Ventura Basin, California*, J. Geophys. Res., 100, pp. 2043-2067, 1995.

8. Shaw, J. H. and J. Suppe, *Active faulting and growth folding in the eastern Santa Barbara Channel, California*, Geological Society of America Bulletin, Vol. 106, pp. 607-626, 1994.

9. Bernreuter, D. L., J. B. Savy, R.W. Mensing, and J. C. Chen, *Seismic hazard characterization of 69 nuclear plant sites east of the Rocky Mountains*, Report NUREG/CR-1582, Vols. 1-5, prepared by Lawrence Livermore National Laboratory for the U.S. Nuclear Regulatory Commission, 1989.

10. Savy, J. B., UCRL ID 111115, Lawrence Livermore National Laboratory, 1993.

TABLE 1
SANTA BARBARA CHANNEL MODEL 1 SLIP RATES

FAULT	SEGMENT	DIP Deg	SLIP SENSE	V_{min}[a] mm/yr	V_{max}[a] mm/yr	V_{be}[a] mm/yr	Interval[b] Ma	$M_w(A)_u$[c]
Santa Ynez	South Branch	70S	LL-R	0.05[1,2,4]	0.4[1,2,4]	0.1	0.08-.105[1]	6.2
	Lake Cachuma	70S	LL(-R)	0.05	1	1		6.6
	Central	70S	LL-R	0.05[3,4]	6.7[3,4]	1.0	0.01-0.7[3,4]	6.9
	East	70S	LL(-R)	0.05	1	1		6.5
Arroyo Parida-Santa Ana		70S	R(-LL?)	0.3[3,4]	0.4[5]	0.4[5]	0.03-0.04[5,6,7]	6.7
San Cayetano	West	50N	R	0.9[8]	5.8[9]	4.0[8,9]	0.008-0.02[8]	6.6
	East	50N	R	4.4[10]	10.4[10,8]	7.4[10]	0.5[10]	6.5
Northridge		45S	R	1.0[10]	2.5[10]	1.7[10,11]	2.3[10]	6.8
Santa Susana		55/30N	R	2.1[10]	9.8[10]	6.0	0.6-2.3[10,12]	6.75
Santa Rosa Is.		85N	LL(-R)	0.1[13]	1.5[14]	0.75[15,16]		6.9
Santa Cruz Is.	East	85N	LL(-R)	0.1	1.25[16]	0.75[16]		6.9
	West	85N	LL(-R)	0.1	1	0.5[17]		6.9
Malibu Coast		85N	LL(-R)	<0.1[3,4]	1	0.3		6.9
Santa Monica		85N	LL-R	0.3[18]	1	0.6[19]		6.5
Dume		85N	R(-LL?)	0.5	3.5	2		6.9
North Channel Slope		65/35N	R	0.1[20,1]	1.1[21,22]	0.5	0.08-1.8[21]	7.0
Red Mountain	Central	65/35N	R	0.4[7,9]	7.0[9]	1.0[7]	0.045[7]; 0.5[9]	6.6
	East	65/35N	R	0.4[7,9]	7.0[9]	3.5	0.045[7]; 0.5[9]	6.2
	West 1	65/35N	R	0.1	1.1	0.5		
	West 2	65/35N	R	0.1	1.1	0.5		
Ojai Blind T	West	30N	R	6.0[9,23]	6.2[9,23]	6.1	0.5[9]	6.6
	East	30N	R	2.6[9,23]		2.6	0.5[9]	6.6
Blind Oak Ridge	Central	30S	R	4.0[9]	7.5[9]	5.0[9]	0.5[9]	6.9
	East	30S	R	4.0[9]	7.5[9]	5.0[9]	0.5[9]	6.8
	West	30S	R	4.0	7.5	5.0	0.5	
Oak Ridge	West	85/50S	R-LL	4.8[24,25,9]	5.6[24,25]	5.1[24,25]	0.975±.075[9]	6.4
	East	70/50S	R	3.4[10]	5.0[9,26]	4.5	0.5[9,10]	6.6

TABLE 2
SANTA BARBARA CHANNEL MODEL 2 PRELIMINARY SLIP RATES

FAULT	SEGMENT	DIP Deg	SLIP SENSE	V_{min}[a] mm/yr	V_{max}[a] mm/yr	V_{be}[a] mm/yr	Interval[b] Ma
Santa Lucia T.		25NE	R	1.1	2.2	1.6	6-3
Pt. San Luis T.	Tepesquet	23NE	R	1.1	2.1	1.6	6-3
	Figuora	27NE	R	0.6	2.3	1.7	6-3
Black Mtn. T.	NW	15NE	R	1.3	3.1	2.1	6-3
	SE	23NE	R	1.1	3.1	2.3	6-3
Little Pine F.		55NE	R	0.7	1.4	1.0	6-3
Big Pine F.	W	70NNE	R			(1.5)	
	E	70NNE	LL	2	7	4	6-1.8
San Cayetano T.	Pt Conception	20N	R	1.6	5.9	4.4	6-3
	Santa Barbara	20N	R	2.0	7.0	4.5	6-3
	Ojai	30N	R	3.2	7.0	5.1	6-3
	SCT1	20N	R	1.3	5.9	3.6	6-3
	Fillmore	20N	R	5.0	10.0	7.5	6-3
(San Cayetano F.)	SCT2	55NNE	R	0.55	3.7	2.1	6-3
Pico T		40S	R	1.4	1.7	1.6	2.3-2
Channel Is. T.		15N	R			1.3	3
Elysian Park T.	Sa. Monica Mtns.	20N	R	3.0	5.4	4.2	4-2.2
	Sepulveda	20N	R	3.0	5.4	4.2	4-2.2
	Los Angeles	20NE	R	2.5	4.6	3.5	4-2.2
Santa Rosa Is. F.		85N	LL(-R)	0.1	1.5	0.75	
Santa Cruz Is. F.	East	85N	LL(-R)	0.1	1.25	0.75	
	West	85N	LL(-R)	0.1	1	0.5	
Malibu Coast F.		85N	LL(-R?)	<0.1	1	0.3	
Dume F.		70N	R(-LL?)	0.5	3.5	2	
Santa Monica F.		65N	LL-R	0.3	1	0.6	
Sata Ynez F.	South Branch	70S	R	0.05	0.4	0.1	0.08-0.105
	Lake Cachuma	70S	R	0.6	1.2	1.0	6-3

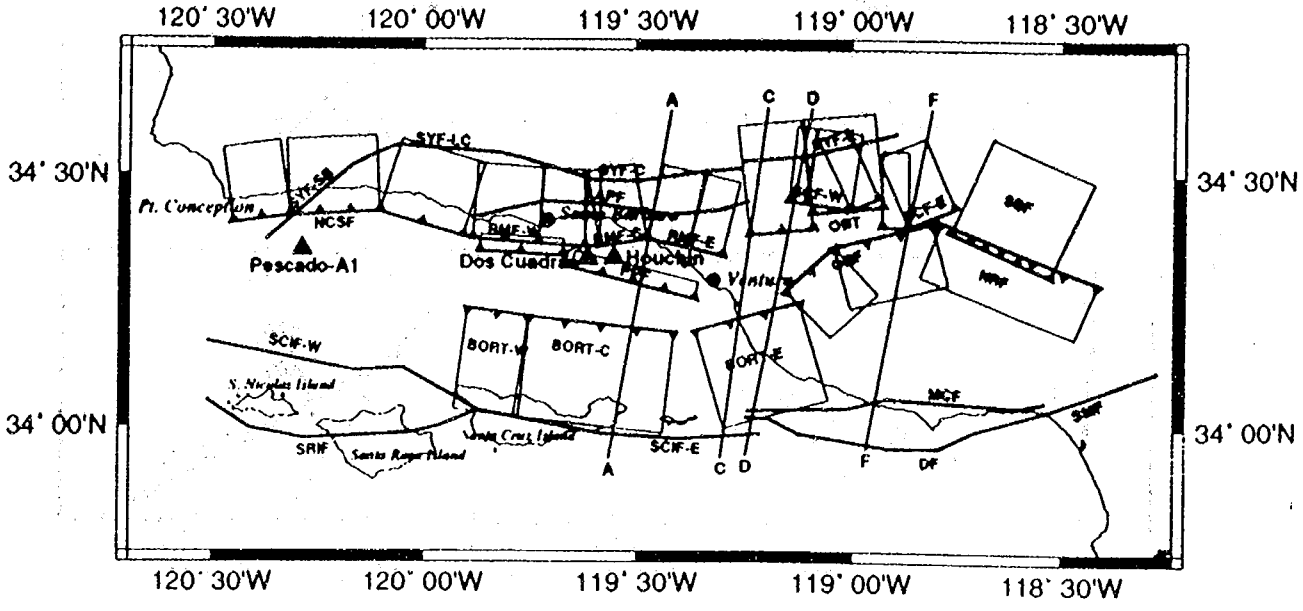


Figure 1: Source Model 1.

Map showing Model 1 fault sources. Surface traces of model faults having dips greater than and less than 65° are shown in red and blue, respectively. Upper edges of blind faults are shown in green. Green and blue rectangles are surface projections of the fault planes of blind faults and shallow-dipping (≤65°) surface faults, respectively. Fault name abbreviations: **SYF-SB, -LC, -C, -E**, Santa Ynez fault, south branch, Lake Cachuma, central, and eastern segments; **NCSF**, North Channel Slope fault; **RMF-E, -C, -W**, Red Mountain fault, eastern, central, west1+west2 segments; **APF**, Arroyo Parida-Santa Ana fault; **PPF**, Pitas Point fault; **SCF-E, -W**, San Cayetano fault, east, west segments; **OBT**, Ojai blind thrust, west+east segments; **SSF**, Santa Susana fault; **NRF**, Northridge blind fault; **ORF**, Oak Ridge fault, west+east segments; **BORT-E, -C, -W**, Oak Ridge blind thrust, east, central, west segments; **SMF**, Santa Monica fault; **MCF**, Malibu Coast fault; **DF**, Dume fault; **SCIF-E, -W**, Santa Cruz Island fault, east, west segments; **SRIF**, Santa Rosa Island fault. Magenta triangles are offshore platform sites.

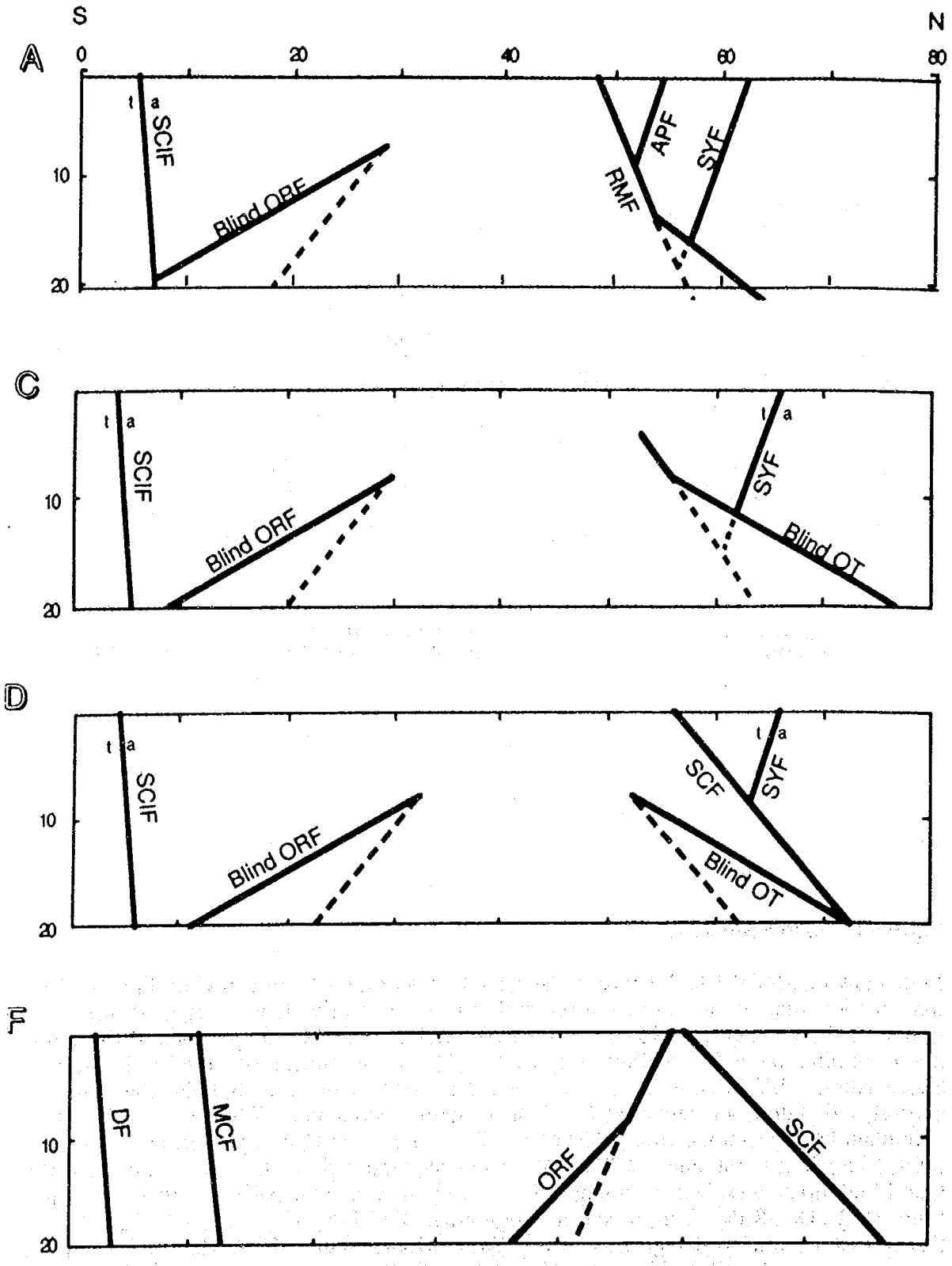


Figure 2: Source Model 1 Cross Sections.

Cross-sections AA, CC, DD, FF (see Figure 1) through source Model 1. Major alternative subsurface geometries shown dashed.

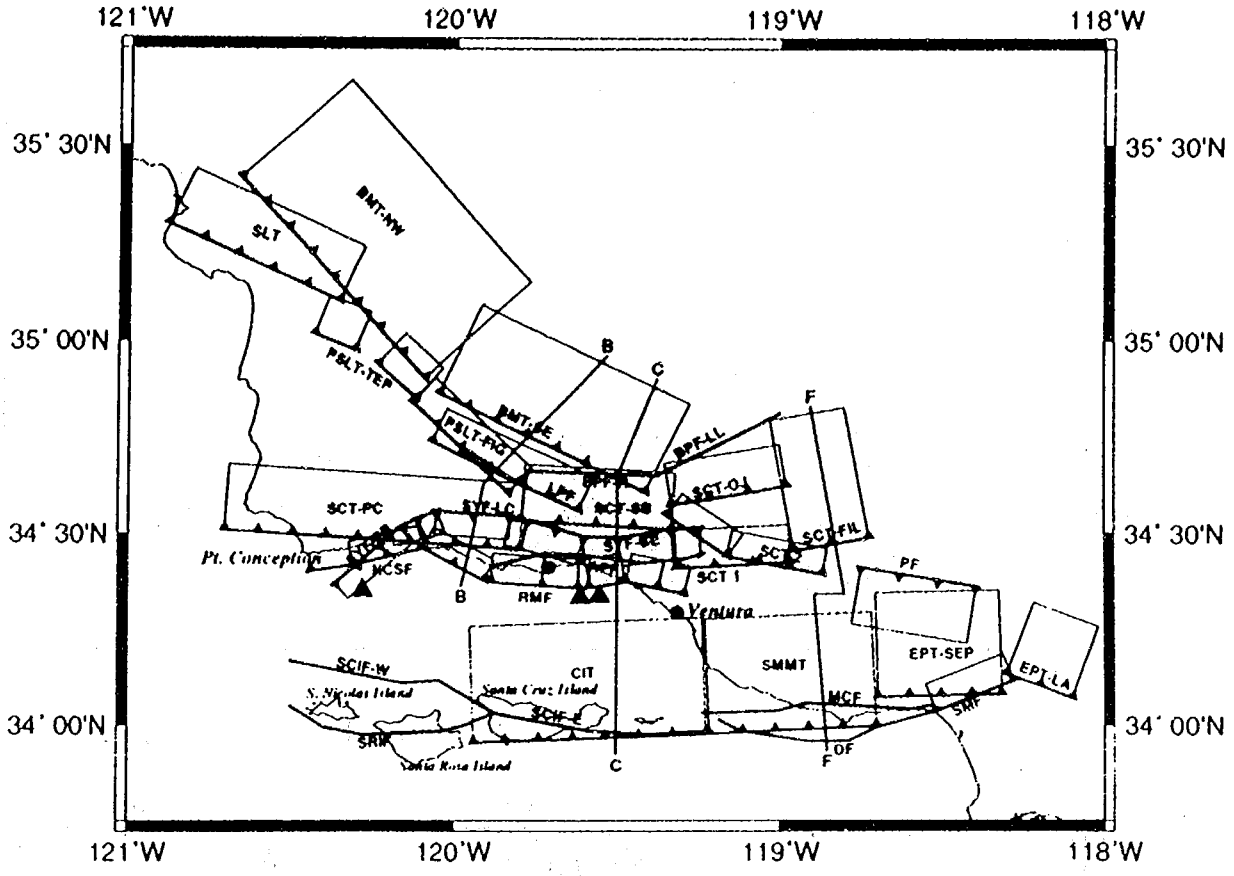


Figure 3: Source Model 2

Map showing Model 2 fault sources. Color coding and symbols the same as Figure 1. Fault abbreviations: **SLT**, Santa Lucia thrust; **BMT-NW**, **-SE**, Black Mountain thrust, northwest, southeast segments; **PSLT-TEP**, **-FIG**, Point San Luis thrust, Tepesquet, Figuora segments; **BPF-LL**, **-R**, Big Pine fault, left-lateral, reverse segments; **LPF**, Little Pine fault; **SCT-PC**,,**-SB**, **-OJ**, **-SCT1**, **-SCT2**, **-FIL**, San Cayetano thrust, Point Conception, Santa Barbara, Ojai,, SCT1; SCT2 (surface San Cayetano fault), Fillmore segments; **SYF-SB**,**-LC**, **-C**, Santa Ynez fault, south branch, Lake Cachuma, central segments; **NCSF**, North Channel Slope fault, **RMF**, Red Mountain fault, [east, central, west1, west2 segments (see Figure 1)]; **APF**, Arroyo Parida-Santa Ana fault; **PF**, Pico fault; **EPT-LA**, **-SEP**, Elysian Park thrust, Los Angeles, Sepulveda segments; **SMMT**, Santa Monica Mountains thrust; **CIT**, Channel Islands thrust; **SMF**, Santa Monica fault; **MCF**, Malibu Coast fault; **DF**, Dume fault; **SCIF-E**, **-W**, Santa Cruz Island fault, east, west segments; **SRIF**, Santa Rosa Island fault.

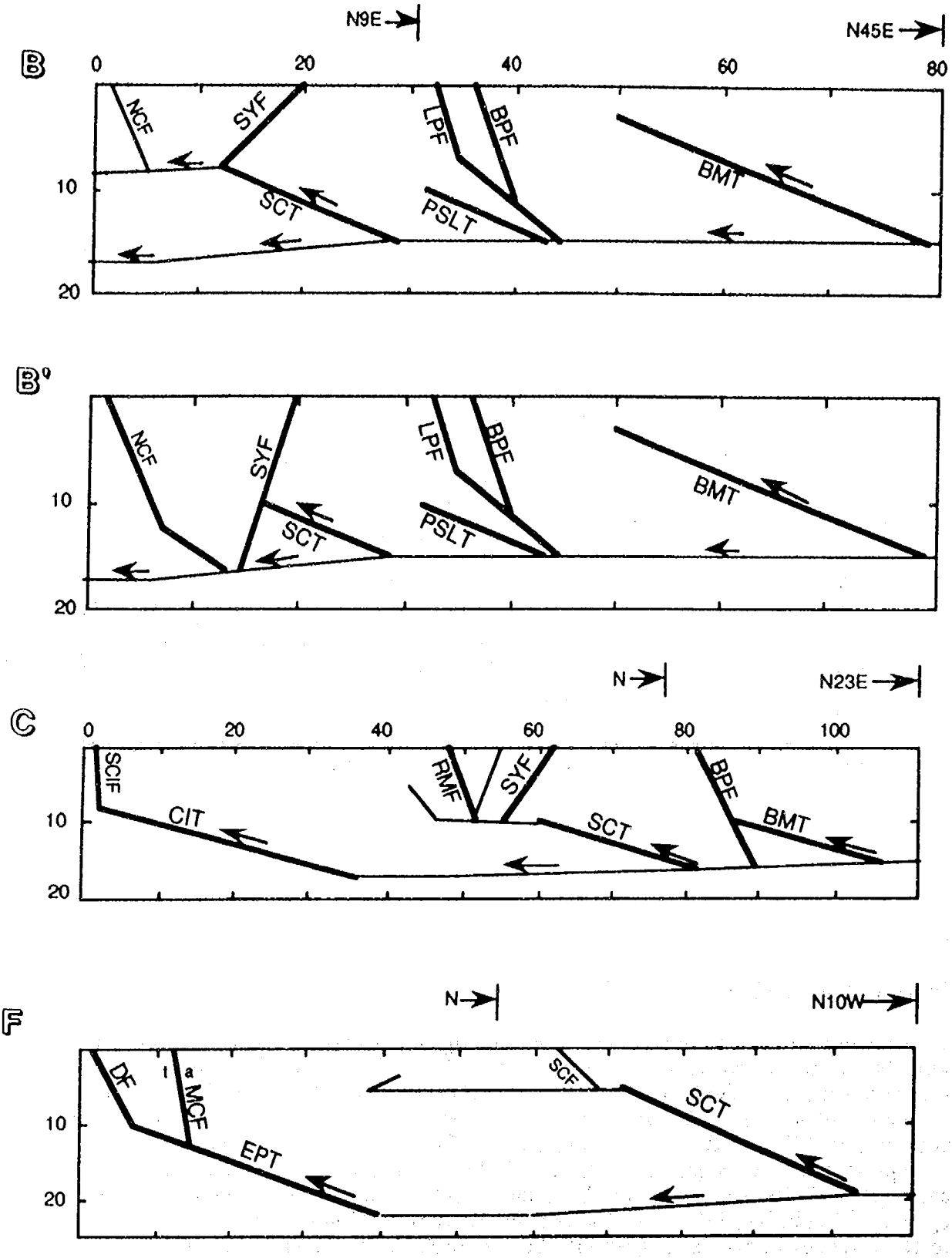


Figure 4: Model 2 Cross Sections

Cross-sections BB, B'B', CC, FF (see Figure 3) through source Model 2. Section B'B' shows a major alternative interpretation to the geometry shown in BB, in which the shallow San Cayetano detachment does not exist.

Figure 5

PLATFORM HOUCHIN HAZARD CURVE

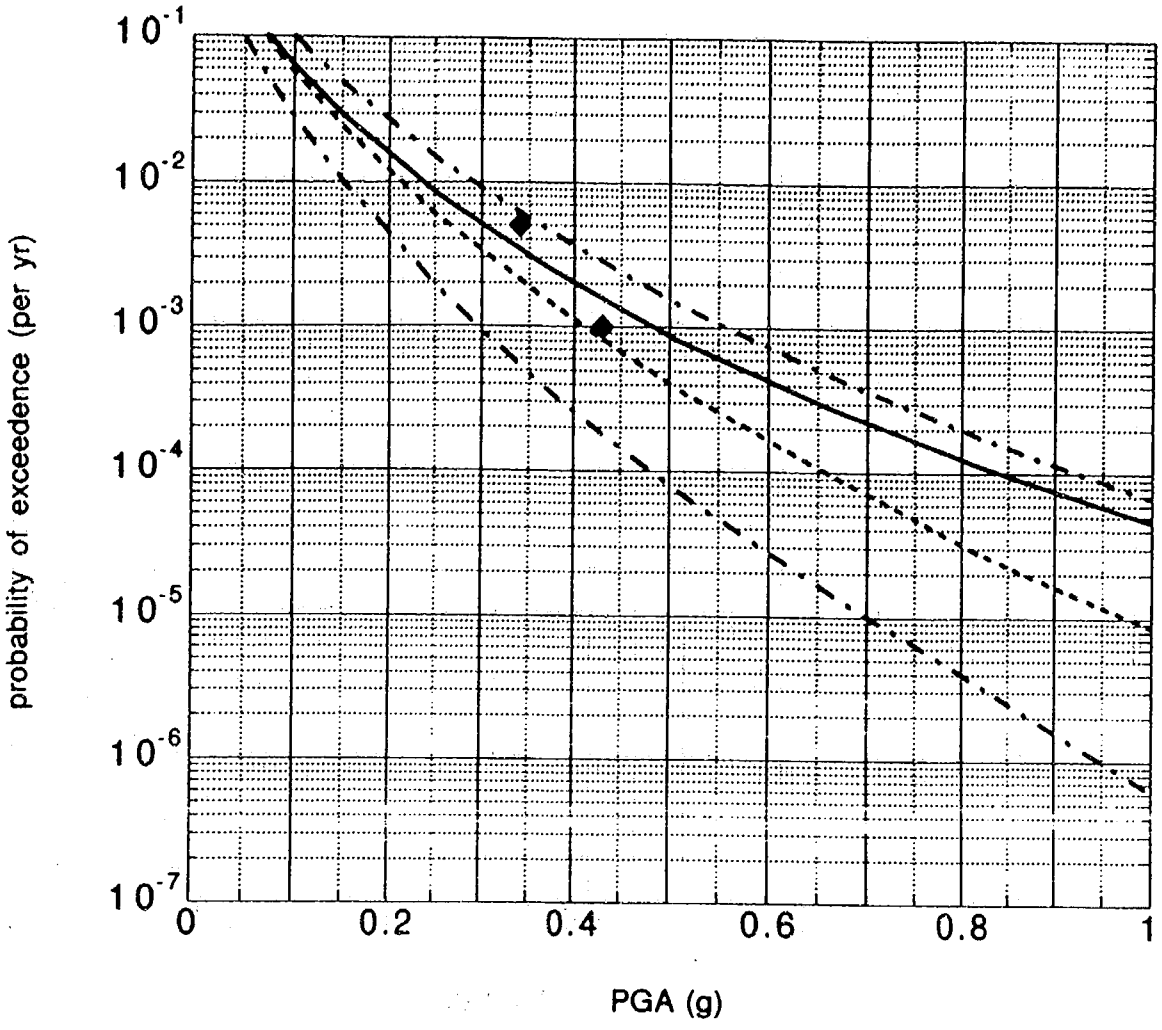


Figure 7

PLATFORM PESCADO-A1 HAZARD CURVE

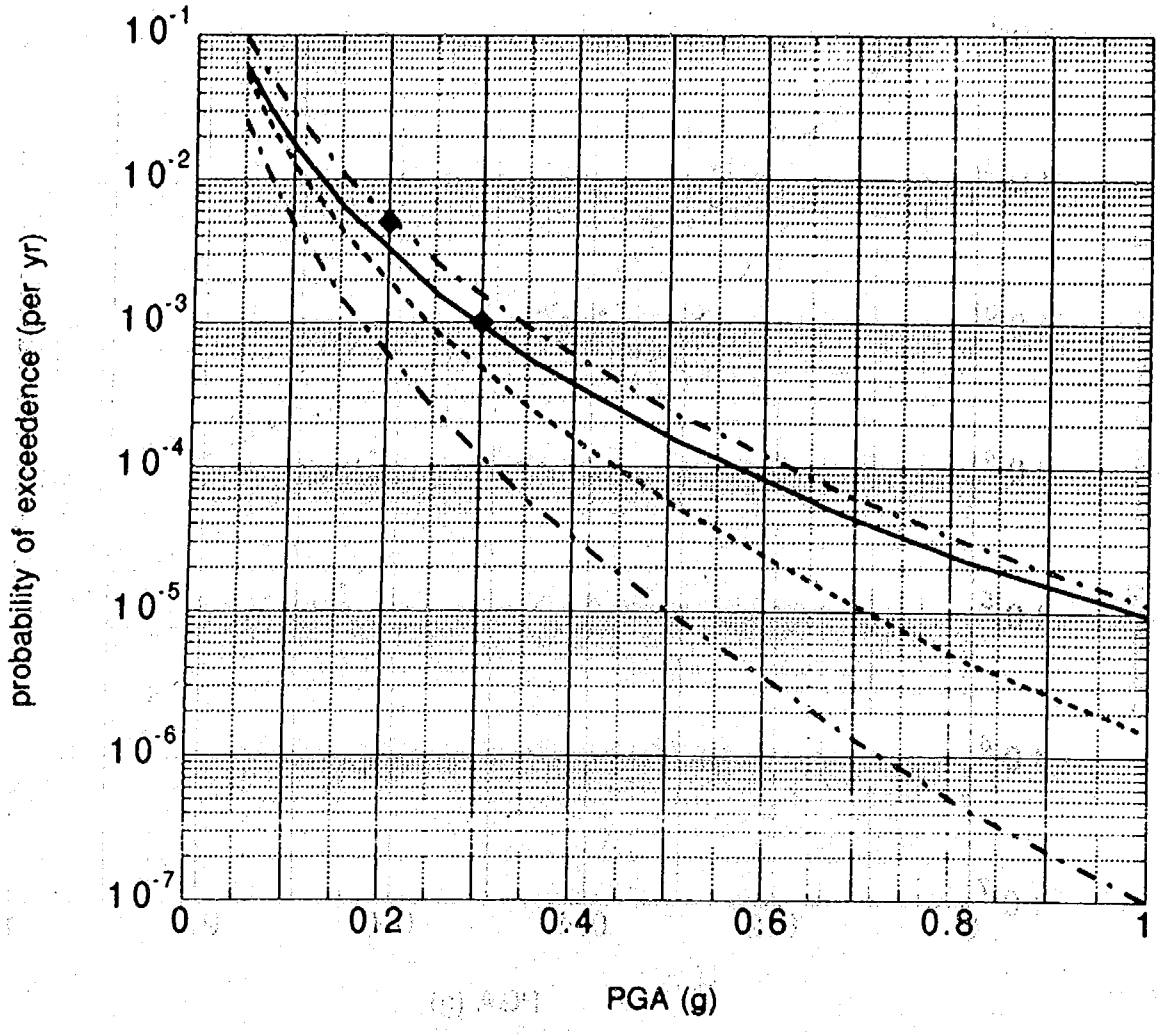
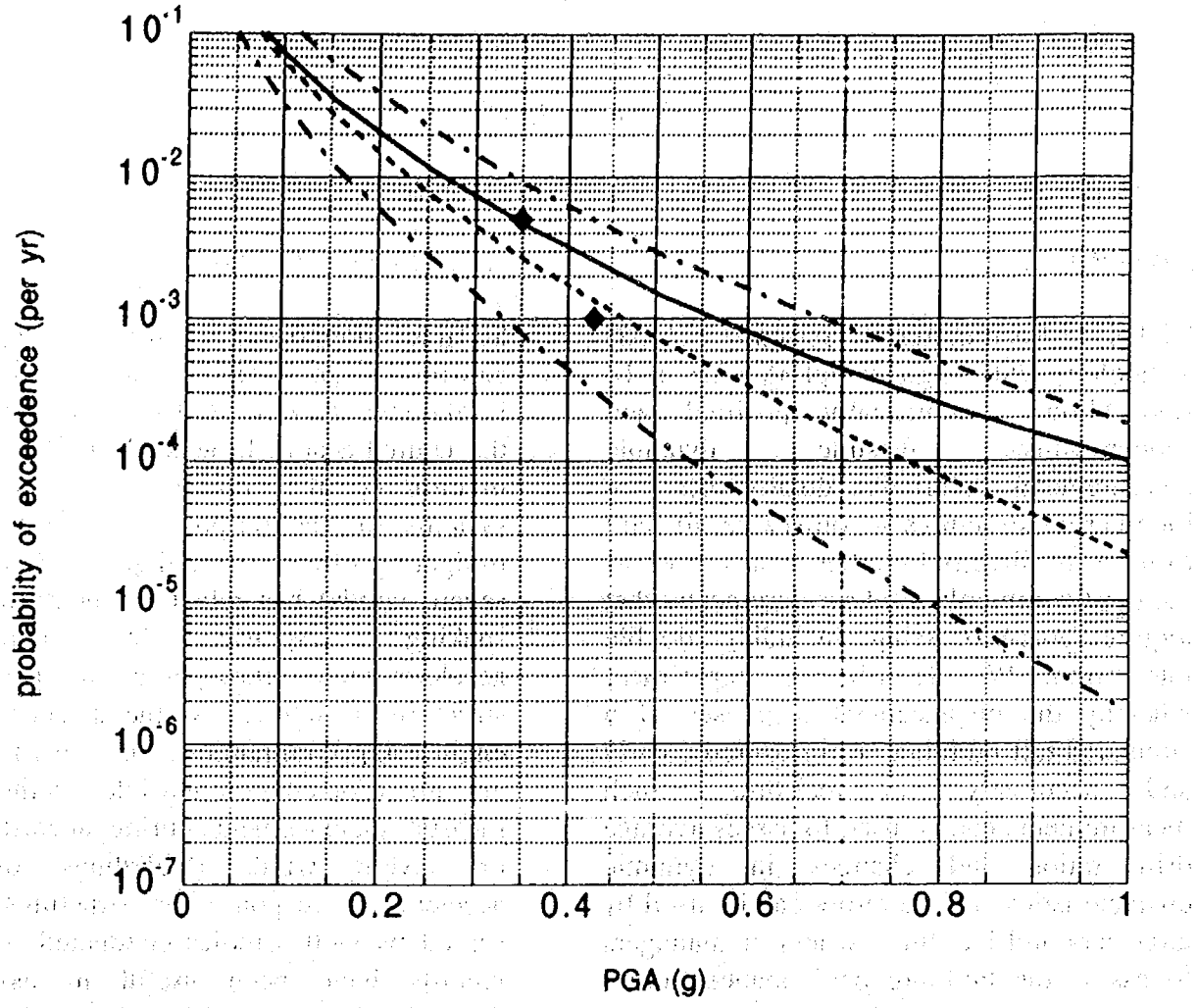


Figure 6

PLATFORM DOS QUADRAS HAZARD CURVE



GPS IN DYNAMIC MONITORING OF LONG-PERIOD STRUCTURES

by

Mehmet Çelebi[1]

ABSTRACT

Global Positioning System (GPS) technology with high sampling rates (~10 sps) allows scientifically justified and economically feasible dynamic measurements of relative displacements of long-period structures --- otherwise difficult to measure directly by other means, such as the most commonly used accelerometers that require post-processing including double integration. We describe an experiment whereby the displacement responses of a simulated tall building are measured clearly and accurately in real-time. Such measurements can be used to assess average drift ratios and changes in dynamic characteristics, and therefore can be used by engineers and building owners or managers to assess the building performance during extreme motions caused by earthquakes and strong winds. By establishing threshold displacements or drift ratios and identifying changing dynamic characteristics, procedures can be developed to use such information to secure public safety and/or take steps to improve the performance of the building.

KEYWORDS: monitoring, GPS, strong-motion, building, structural response, frequency, displacement, acceleration

1. INTRODUCTION

Seismic monitoring of structural systems constitutes an integral part of National Earthquake Hazard Reduction Program of the United States. In general, until recently, monitoring the response of structural systems for the purpose of assessing and mitigating effects of earthquakes (and also severe winds) has relied on measuring the shaking response by deploying accelerometers throughout a particular structure of interest to the scientific and engineering communities. In contrast, there are no efficient or feasible methods to measure displacements during an earthquake or severe wind. Recordings of the acceleration response of structures have served us well. Studies conducted on such records have been useful in assessing design/analysis procedures, improving code provisions, and correlating the response with damage.

Since the M_s=6.7 Northridge (17 January 1994) and M_s=6.8 Kobe (17 January 1995) earthquakes, drift studies and assessment of susceptibility to damage of tall buildings have become important issues, particularly because so many steel-framed buildings were damaged, some severely and some lightly. In the Los Angeles area, for

[1] U.S. Geological Survey, MS 977, 345 Middlefield Rd., Menlo Park, CA 94025

example, following the Northridge event, several hundred steel-framed buildings had to be examined, assessed, and repaired or retrofitted. Only three of these buildings were instrumented prior to the event, providing some limited acceleration response data to be used for interpretation of the widespread damage. Additional data, if available in real-time or near-real-time, could have been very useful for studies and for design of repair and retrofitting projects that followed. Therefore, there is a great need for better and more extensive monitoring of tall buildings.

Relative displacements, which are key to assessing drift and stress conditions of structures, are difficult to measure directly. On the other hand, measuring acceleration response requires a double integration process to arrive at displacements. The integration process is not readily automated because of the nature of signal processing, which requires (a) selection of filters and baseline correction (the constants of integration), and (b) often substantial judgment when anomalies exist in the records. Consequently, this process can lead to errors in the calculation of velocities and displacements. This problem is more acute for permanent displacements. Accelerometer measurements cannot be used to recover the permanent displacements at the centimeter level; and even if they could, it is questionable if it can be done in real-time. That is, the level of accuracy of displacements calculated from accelerations has not been widely verified by observations (e.g., some shake table tests performed to compare the performances of accelerometers and accelerographs have not been directed at checking displacements).

An alternative method to measure relative displacements while monitoring structural systems can be accomplished by using GPS technology, now advanced to record at 10 sps with an accuracy of ± 1 cm horizontally and ± 2cm vertically. This provides a great opportunity to monitor long-period structures reliably (e.g., tall buildings that are 20-40 stories or more). The majority of the tall buildings are flexible steel-framed structures. The fundamental period of such a flexible-framed building can be estimated with the empirical formula[2] , T = 0.1 N, where N is the number of stories of the building. This means that at least 20-40 data points will be recorded for one cycle of motion of a 20-40 story building vibrating at the fundamental period. This provides sufficient accuracy to assess the average drift ratio of a building. Such information can be very useful in assessing the damage to a building. In addition, the main value in using GPS technology to assess the condition of a building is that the displacement measurements can be made directly in real-time and with sufficient precision. As discussed later, we have made preliminary tests to prove the technical feasibility of the application of GPS to monitoring structures.

There is great potential for the application of GPS technology to monitor long-period structures during earthquakes. The application can also be extended to monitoring wind-induced deformation of tall buildings, long-span suspension and cable-stayed bridges, and tall chimneys. Furthermore, with future advances in GPS

[2] For most flexible buildings, the fundamental period (T) is approximated by 0.1N, where N is the number of floors of a building (even though the fundamental period can vary between [0.05-0.15]N depending on the flexibility of the building). Therefore, to simulate a 40-story building, we set the period (frequency) equal to 4 s (0.25 Hz) and proportioned the length, width and thickness of the cantilever.

technology and improvements in sampling capability (e.g., higher than 10 sps), it will be possible to monitor short-period structures as well. Additionally, direct measurements of displacements will enable us to reliably detect structural movement caused by failure of the ground under a structure (e.g., liquefaction).

2. TECHNICAL JUSTIFICATION

In the last few years, there have been numerous studies related to the technical feasibility of using GPS to measure displacements of civil structures. Most of the initial work has been accomplished by aerospace atmospheric researchers. Studies related to the application of GPS for static or dynamic measurements of displacements of structural systems include but not limited to those by Hyzak and others (1997), Teague and others (1995), Guo and Ge (1997), Kondo and Cannon (1995), Lovse and others (1995), Hudnut and Behr (1998), Behr, Hudnut and King (1998) and Stein and others (1997). In our study, we direct the efforts to actual permanent deployment of GPS units alongside accelerometers, and also to use the displacement measurements with GPS as a health monitoring tool.

3. MODEL TESTS SIMULATING A TALL BUILDING

To investigate the feasibility of using GPS technology to monitor tall buildings (and other long-period structures), we conducted two experiments. Figure 1 depicts a photo and the overall set-up for a simple and inexpensive experiment designed by selecting a standard stock steel bar to simulate a 30-40 story flexible building. We selected the length, thickness, and width of the two bar specimens to yield a fundamental period of approximately four seconds in the weak direction. To make

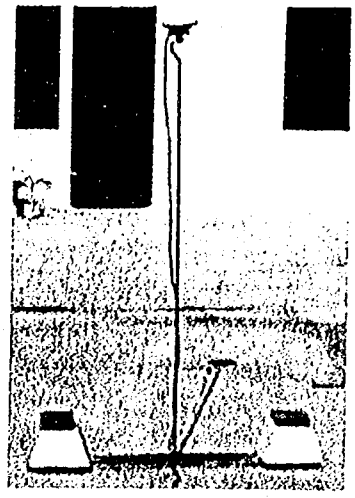


Figure 1a. Photo of test set-up for using GPS for dynamic monitoring of tall buildings.

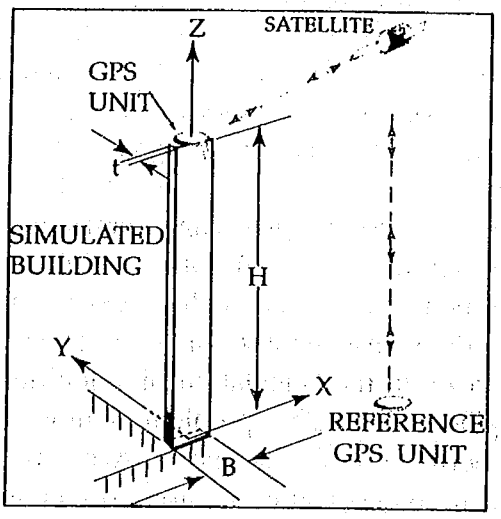


Figure 1b. Schematic of test set-up for using GPS for dynamic monitoring of tall buildings.

things simple, we purposefully selected the width and thickness of each of two bars with an extremely weaker axis in one direction. The width was varied to show the sensitivity of measurements during vibration and at 10 Hz sampling rate. Each bar was fixed at the base and the GPS unit was attached at its tip. By providing an initial displacement (simply by pulling the top of the bar and releasing), each bar was set into free vibration and its

motion was recorded. Results are summarized in Table 1. Figure 2 shows the particle motion and time-history of one of the tests performed. The axes of the bar were at an angle to the NS (and EW) direction. Therefore, the NS and EW components of displacements are identical in phase and proportional in amplitude. Also, since the GPS unit is not symmetrically and concentrically mounted in the weak direction (photo in Figure 1), the amplitudes of positive and negative displacements measured are not the same. The detection of the effect of the eccentric mass adds to the assurance that the measurements are accurate and sensitive. These simple tests and results were and can be duplicated easily and readily.

Figure 3 is a plot of NS components of measured relative displacements and corresponding amplitude spectra of Bars A and B. The figure shows the accuracy and sensitivity of the GPS monitoring technology at ten samples/second. The measurements differentiate between the frequency of the free-vibration response of the two bars with different dynamic characteristics. From the data, the fundamental frequency (period) of the two bars are identified to be 0.245 Hz (4.08 s) and 0.296 Hz (3.38 s) respectively. Also, a damping percentage of approximately 2% is extracted. This simple test shows that sampling at 10 Hz with GPS units provides a clear and accurate displacement response history from which drift ratios and dynamic characteristics of the specimen can be derived (Çelebi et al., 1997, 1999 and Çelebi, 1998). The implications of this go beyond just the measurements. It can be shown that identification of variation of dynamic characteristics can be used to identify not only different structural systems, but also possible nonlinearities that occur during vibration (e.g., due to damage and plastic behavior of the structural members, components and/or joints, or to soil-structure interaction under varying amplitudes of input motions).

4. GPS AMBIENT TEST OF A 44-STORY BUILDING AND STRONG-MOTION ACCELERATION RECORDS

In a second test, we measured ambient vibration (due to winds and traffic noise) of a 44-story building with a GPS unit temporarily deployed on its roof. A reference GPS unit was located within 500 m of the building. The signals were very noisy and amplitudes very small; therefore, most common methods to identify structural characteristics did not work. Only the cross-spectrum of the two orthogonal, horizontal, low-amplitude, ambient displacement recordings (when the signals are coherent and approximately 180° degree out of phase) were used to identify the fundamental frequency of the building at 0.23 Hz (Figure 4), with another frequency at ~ 0.3 Hz. Despite the very small signal, these frequencies appear to be reliable when compared with the 0.23 Hz frequency calculated from accelerations recorded with a triaxial accelerograph on the 38th floor (accepted here as the roof response) during a small earthquake (Figure 5). A comparison of these frequencies is provided in Figure 6.

Despite the small displacements (<1 cm) and low signal to noise ratio of this experiment, the fact that dynamic frequencies could be identified indicates that during larger displacements, better identification of the dynamic characteristics as well as drift ratios can be made with higher confidence.

5. LOOKING TO THE FUTURE: REAL-TIME MONITORING

5.1 Perceived Real-Time Monitoring

Initially, we are planning to deploy the GPS units only on tall buildings that are already instrumented with accelerometers. This will facilitate comparison of absolute and relative displacements measured by GPS and calculated by double integration of accelerations. The GPS units will be configured to provide data to indicate the real-time average drift ratios and changes in the dynamic characteristics of the buildings. This information can be made available to building managers (or interested parties) in real-time or whenever a predetermined displacement threshold is reached. The building managers can assess the response of the buildings according to (a) different threshold displacements (e.g., A, B and C as shown in Figure 7), (b) drift ratios, or (c) changing dynamic characteristics. If a situation is serious, the management can make decisions to evacuate the building for additional inspection. Therefore, one by-product of the effort would be to secure the safety of the occupants and significant contents of the building. Thus, a real-time structural health monitoring environment will be created. At least three GPS units per building are required to monitor a tall building: two of the units should be deployed on the roof to detect translational and torsional response of the building, and the third unit will serve as a reference ground station to evaluate relative displacement. The ground site also needs excellent sky visibility.

Similar deployments are being planned for other types of long-period structures. One project in development at this time is for deploying GPS units on one of the long-period suspension bridges such as the Golden Gate Bridge and Bay Bridge (San Francisco) or Vincent-Thomas Bridge (Los Angeles). As in the case of tall buildings, changes in dynamic characteristics after the displacements at critical locations of a bridge have exceeded predetermined thresholds, can be calculated in near-real-time (Figure 8). When warranted, the management can make decisions to inspect the bridge (e.g., decisions can be made to stop the traffic, thus securing the bridge safety, which is one of the objectives of lifeline earthquake engineering). With the GPS technology, we can furnish time-dependent displacements for the relative movements of critical locations of structures. For example, for the bridges, GPS units placed at pre-selected locations of bridge elements can indicate, in real-time, the amplitude of the displacements of the decks and towers, as well as movements of key bridge elements relative to local bedrock reference points. Thus, movements of the piers relative to the abutments, the top of a tower with respect to its base, or the span with respect to the ground, can be made at a centimeter-level of precision, in real-time. We will recover both the dynamic motions that accompany the earthquake, as well as the static or permanent displacements experienced by the bridge once the shaking has stopped. Such permanent displacements affect the state of stress of a bridge, and provide evidence for distortion or failure of bridge elements or subsidence of piers due to ground compaction induced by earthquake shaking.

5.2 Current Deployments on Tall Buildings

As this paper is being written, deployment of GPS units on the roof of two buildings in

Los Angeles has been completed, and we are in the process of deploying GPS units on the roof of a building in San Francisco. Figure 9 shows the actual deployment on the roof of one of the buildings in Los Angeles. As it happens with field deployments, physical obstacles and constraints necessitate alternate approaches. In this case, the window cleaner machinery on the roof of the 44-story building travels on rails near the parapet and uses the parapet continuously. Therefore, any deployment had to be planned away from the parapet wall. To solve this problem, a stiff auxiliary support frame (Figure 9) was erected. The figure also shows the GPS antenna and the radio antenna to communicate with the reference station so that differential displacements are obtained.

5.3 Requisite Software

Requisite software is being developed to assess and mitigate the two natural hazards (earthquake and severe wind) affecting the structures by using the displacements measured by the GPS units. Figure 10 shows a screen image of software being developed to assess displacements observed with GPS and provide alarm (warning). Such collected information on the response of the structure during strong motion events (or strong winds) can be used to make decisions for further evaluation of the susceptibility to damage of the structure, and future repair/retrofit schemes may be developed.

5.4 Benefits and Other Applications

- The collected information on the response of the structure during strong-motion events (or strong winds) can be used to make decisions for further evaluation of the susceptibility to damage of the structure, and future repair/retrofit schemes may be developed.

- The recorded data can be used to analyze the performance of the structure and such results can be used to improve future analyses/design procedures.

- The data collected can also be used to assess long-term displacements of critical locations of structural systems (e.g., permanent displacements, settlement of foundations, long-term deformations due to change of temperature and the plate tectonic deformation spanning the San Francisco Bay and parts of the Los Angeles Basin) and to develop methodologies on how the findings can be incorporated into useful practical design procedures.

6. CONCLUSIONS

It is shown in this paper that recent advances in sampling rates of GPS technology allow real-time monitoring of long-period structures such as tall buildings and long-span bridges. The advantage over conventional monitoring using accelerometers is that relative displacements can be measured reliably in real-time and with sufficient accuracy to assess potential damage to the structures. The technical feasibility is illustrated through two tests conducted on two vertically cantilevered bars that simulate tall buildings, and an ambient test of a 44-story building. Both approaches show that GPS monitoring of long-period structures provide sufficiently accurate measurements of relative displacements such that dynamic characteristics of the vibrating systems can be accurately identified. This capability can be used for structural health monitoring purposes. Procedures and software are being

developed to permanently deploy GPS units on tall buildings and suspension bridges.

7. REFERENCES

Behr, J. A., Hudnut, K. and King, N., 1998, Monitoring Structural deformation at Pacoima Dam, California using continuous GPS, Proc.11th International Technical Meeting of the Satellite Division of the Institute of Navigation [ION GPS-98; Nashville, TN], pp. 59-68.

Çelebi, M., Prescott, W., Stein, R., Hudnut, K., Behr, J., and Wilson, S., 1999, GPS monitoring of dynamic behavior of long-period structures : ***Earthquake Spectra*** (Journal of EERI), vol. 15, no. 1, pp. 55-66, February 1999.

Çelebi, M., Presscott, W., Stein, R., Hudnut, K., and Wilson, S., 1997, Application of GPS in monitoring tall buildings in seismic areas, Abstract, *AGU Meeting*, San Francisco, CA, Dec. 1997.

Çelebi, M, 1998, GPS and/or strong and weak motion structural response measurements – Case studies, Structural Engineers World Congress-CD-ROM Proceedings, San Francisco, CA.

Guo, J. and Ge, S., 1997, Research on displacement and frequency of tall building under wind loading using GPS, *ION Conference*, Kansas City, MO, (September).

Hudnut, K. W. and Behr, J. A., 1998, Continuous GPS monitoring of structural deformation at Pacoima Dam, California, Seismol. Res. Lett., Vol. 69, No. 4, pp. 299-308.

Hyzak, M., Leach, M. and Duff, K., 1997, Practical application of GPS to bridge deformation monitoring, Permanent Committee Meeting and Symp., Int'l Federation of Surveyors (FIG), (May).

Kondo, H. and Cannon, M. E., 1995, Real-time landslide detection system using precise carrier phase *GPS, ION GPS95 Conference*, The Institute of Navigation, Palm Springs, CA, (September).

Lovse, J.W., Teskey, W. F., Lachapelle, G., and Cannon, M. E., 1995, Dynamic deformation monitoring of a tall structure using GPS technology, *Journal of Surveying Engineering*, ASCE, **121**, 1, 35-40.

Stein, R. S., Hudnut, K. W., Satalich, J., and Hodgkinson, K. M., 1997, Monitoring seismic damage to bridges and highways with GPS: Insights from the 1994 Northridge earthquake, in *Natl. Seismic Confr. on Bridges and Highways*, Sacramento, Fed. Highway Admin. And Calif. Dept. of Transportation, 347-360.

Teague, E. H., How, J. P., Lawson, L. G., and Parkinson, B. W., 1995, GPS as a structural deformation sensor, *Proceedings of the AIAA Guidance, Navigation and Control Conference*, Baltimore, MD, (August).

Table 1. Results of Tests with GPS Units

Specimen	Length [H] ft (m)	Width [B] in.(cm)	Thickness [t] in. (cm)	Measured Frequency [f](Hz)	Measured Period [T](s)	Damping [ξ](%)
BAR A	6 (1.82)	1.5(3.8)	1/8 (0.32)	0.245	4.08	~ 2.0
BAR B	6	2.0(5.0)	1/8	0.296	3.38	~ 2.0

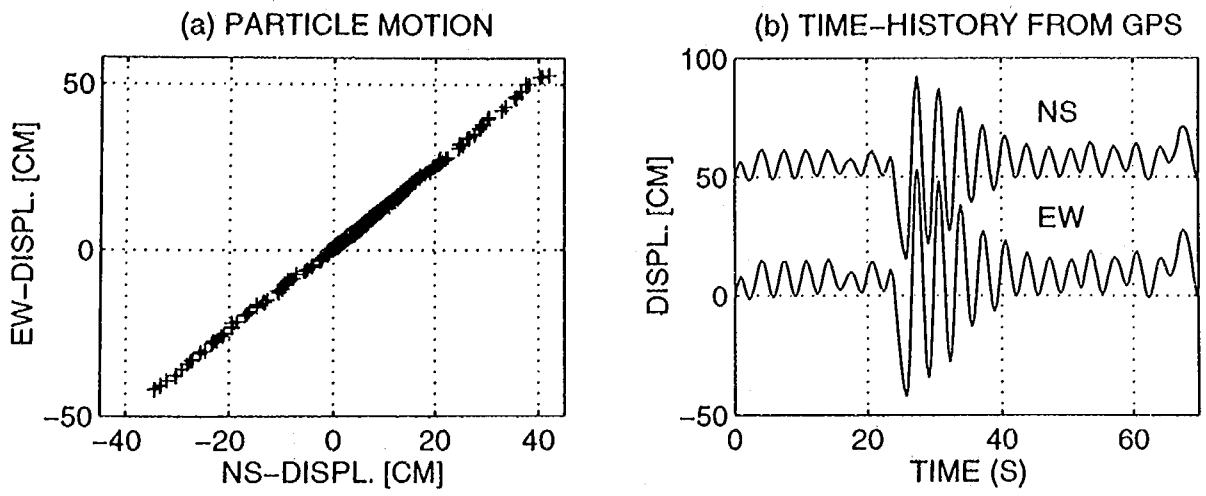


Figure 2. Particle motion and time-history of relative displacements (NS and EW components) of simulated test specimen.

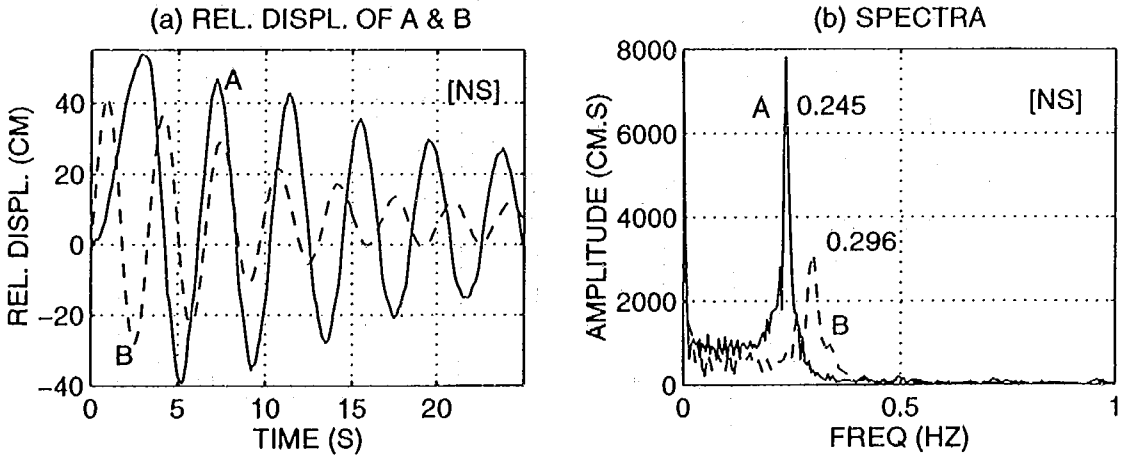


Figure 3. Relative displacements of two test specimens (NS components only) in free-vibration and corresponding amplitude spectra identifying the fundamental frequencies of the test specimens.

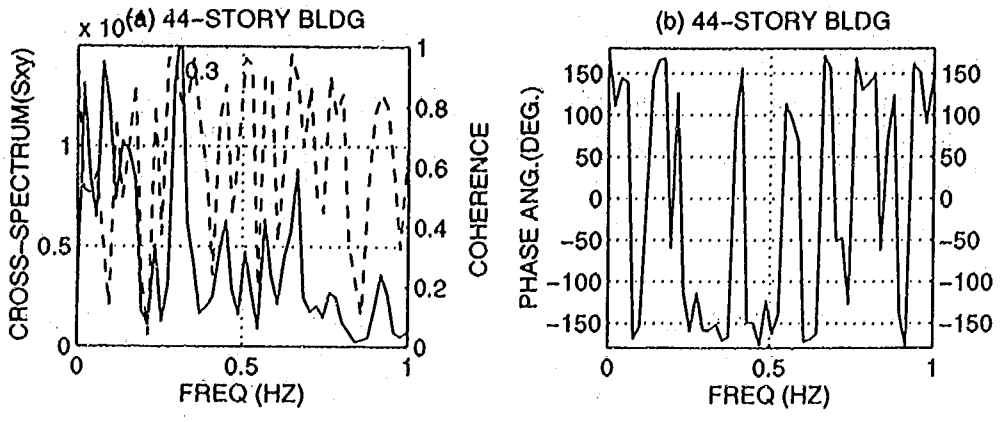


Figure 4. Ambient test of a 44-story building with GPS technology: Cross-spectrum (left-solid), coherence (left-dashed) and phase-angle (right) of two orthogonal horizontal motions.

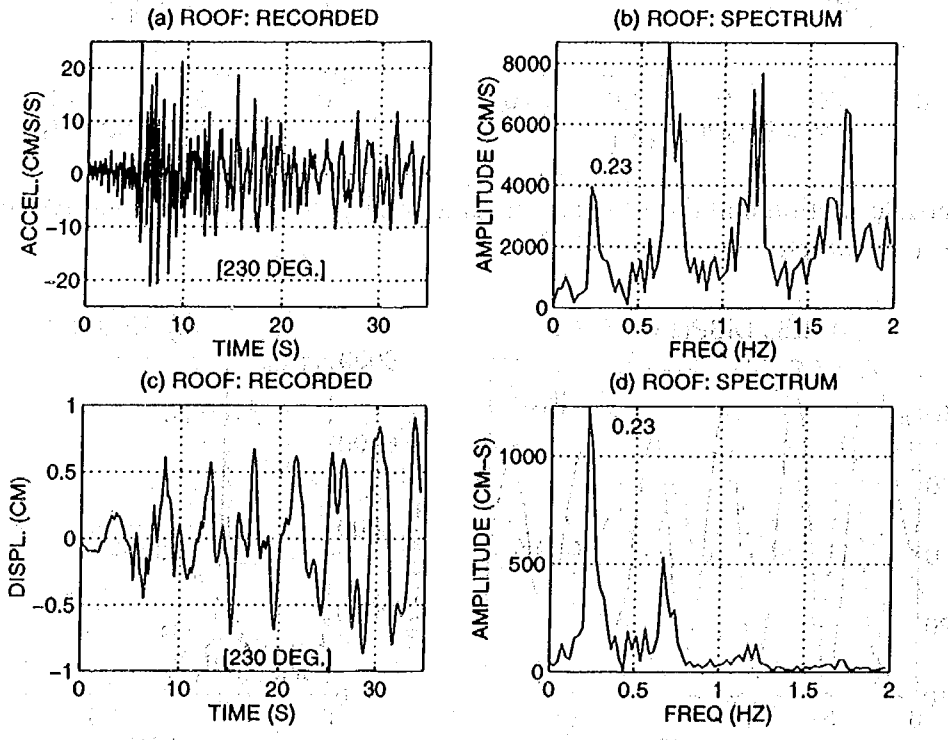


Figure 5. Recorded roof (38th floor accepted in lieu of roof) accelerations of a 44-story building and displacements (derived by double integration) and amplitude spectrum.

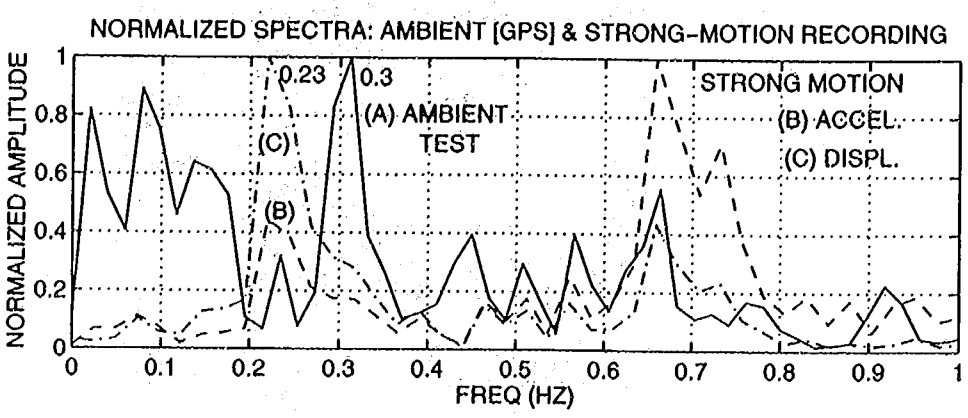


Figure 6. Comparison of normalized frequencies for ambient GPS recording (from cross-spectrum) and strong-motion recording (from amplitude spectrum).

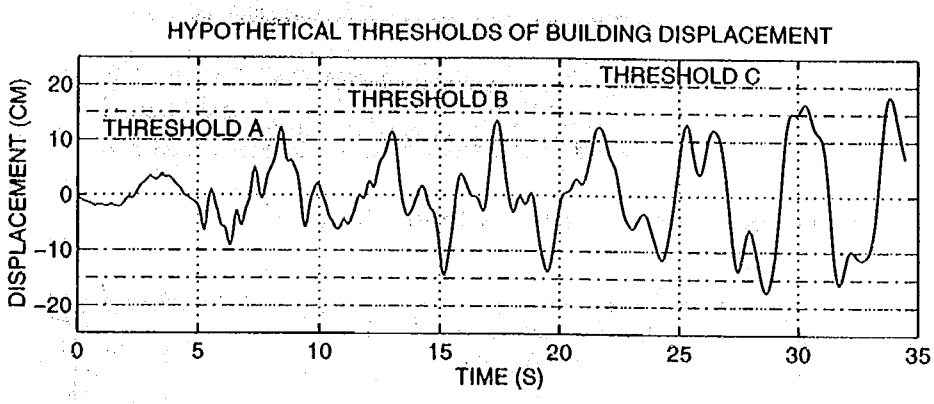


Figure 7. Hypothetical thresholds of displacements. The time-history of displacements shown is actually integrated from accelerations recorded at the 38th floor (accepted in lieu of roof) of a 44-story building. The actual record (in Figure 5) is amplified by 20 times for illustration purposes.

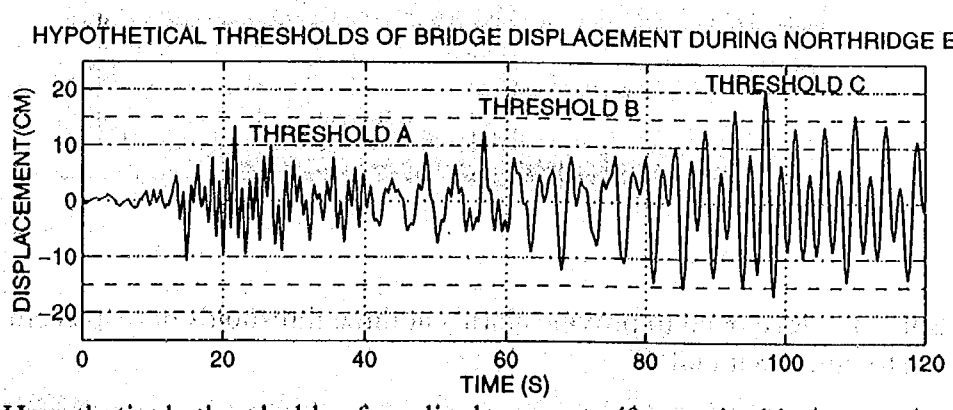


Figure 8. Hypothetical thresholds for displacement (from double-integration of recorded acceleration) of channel 21 (vertical at mid side-span) of Vincent Thomas Bridge (1994 [M=6.7] Northridge earthquake).

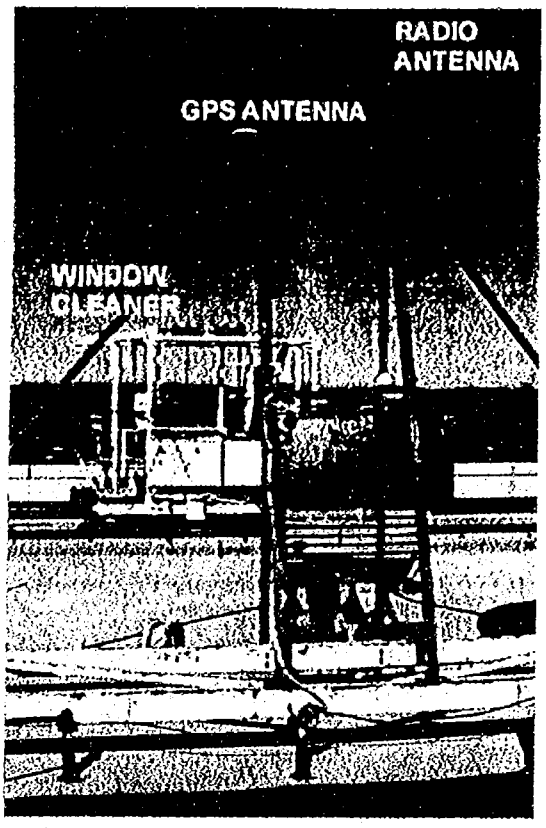


Figure 9. Deployed GPS Unit and Necessary Frame System

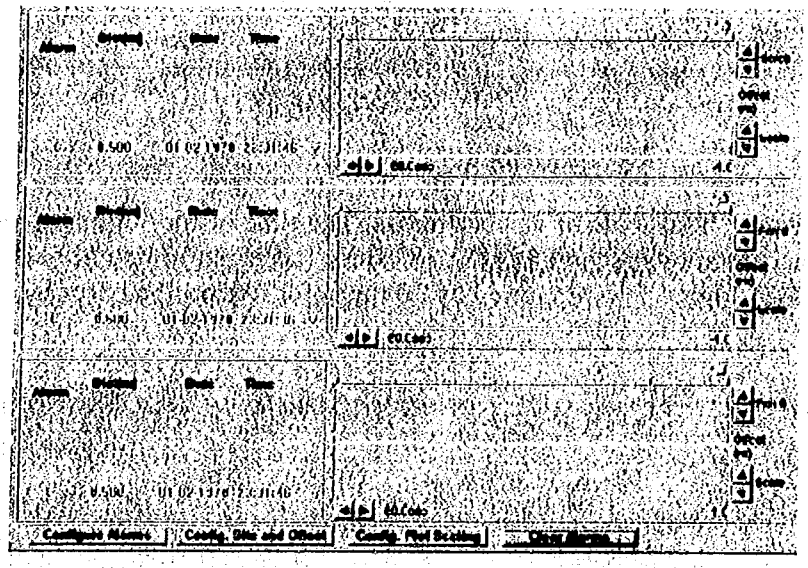


Figure 10. Software developed to provide alarms at three thresholds of displacement of an instrumented structures with GPS.

REAL-TIME HYBRID VIBRATION EXPERIMENTS WITH A 2-DIMENSIONAL AND 3-DEGREES-OF-FREEDOM MODEL

by

Keiichi TAMURA[1] and Hiroshi KOBAYASHI[2]

ABSTRACT

The real-time hybrid vibration experiment is a new concept experiment combining shaking table test and numerical response analysis in real-time. The results of real-time hybrid vibration experiments with a 2 degrees-of-freedom model were reported at the Thirtieth Joint Meeting of U. S. - Japan Panel on Wind and Seismic Effects. In this paper, we have integrated the freedom of control to 2-dimensional and 3-degrees and conducted the real-time hybrid vibration experiments. Results of experiments were compared with those of conventional shaking table tests, and the validity of real-time hybrid vibration experiment is demonstrated.

Key words: real-time hybrid vibration experiment, shaking table test, actuator delay compensation, coil spring

1. INTRODUCTION

Most of the conventional hybrid experiments are pseudo dynamic experiments with an expanded time axis due to limitations of devices, e.g., capability of computation and compensation for actuator delay, and few precedents exist for hybrid vibration experiments using shaking tables. Differing from those conventional techniques, the real-time hybrid vibration experiment is a new concept experiment combining shaking table test and numerical response analysis in real-time.

We have developed a real-time hybrid experiment system at the Public Works Research Institute after the 1995 Kobe Earthquake. At the first stage of experiments, we conducted the real-time hybrid vibration experiment with a 2 degrees-of-freedom model[1]. This model was a 2 storied slab structure supported by rubber bearings. Presented are the results of real-time hybrid vibration experiments with a 2-dimensional and 3 degrees-of-freedom model. Results are compared with those of shaking table tests and the validity of real-time hybrid vibration experiment is demonstrated.

2. OVERVIEW OF REAL-TIME HYBRID VIBRATION EXPERIMENT

As Figure-1 shows, in the real-time hybrid vibration experiment, an original structure is divided into two parts. One is an actual model

[1] Head, Ground Vibration Division, Earthquake Disaster Prevention Research Canter, Public Works Research Institute, Ministry of Construction, 1 Asahi, Tsukuba-shi, Ibaraki-ken, 305-0804, Japan.

[2] Research Engineer, ditto.

specimen of original structure. This specimen is usually taken as a part of structure whose seismic behavior is unknown or complicated. The other is a numerical model for vibration response analysis. This model represents a part of structure whose seismic behavior can be evaluated by numerical analysis.

The numerical model consists of structural elements (mass, damping and stiffness matrices), external force that is calculated from the acceleration of shaking table, and reaction force generated at the boundary of the actual and numerical models. In the numerical analysis, the external and reaction forces are inputted, and the displacement of the actual model for the next time step is calculated. This displacement is realized by actuators. Then, the external and reaction forces are measured and taken into numerical analysis. Iterating these procedures, the seismic behavior of original structure can be accurately simulated.

The equation of motion for numerical analysis is described by

$$M\ddot{x} + C\dot{x} + Kx = p + q \qquad \cdots(1)$$

where

M: Mass matrix
C: Damping matrix
K: Stiffness matrix
x: Relative displacement vector
p: external force (seismic response) vector
q: reaction force vector

Based on eq. (1), the vibration response (displacement vector x) after a short interval Δt is calculated using central difference method from the measured reaction force vector q and the external force vector p.

3. FEATURES OF REAL-TIME HYBRID VIBRATION EXPERIMENT

Vibration Response Analysis (Central Difference Method)

The central difference method is employed in vibration response analysis, because it takes short time to generate actuator signal for the next time step after measuring reaction force. An equation of motion can be written as eq.(2) at time t_i. Subscript i represents the i-th time step.

$$M\ddot{x}_i + C\dot{x}_i + Kx_i = p_i + q_i \qquad \cdots(2)$$

Since the change of motion during calculation time interval Δt is small, we assume constant acceleration over the period between $t_{i-1}=t_i-\Delta t$ and $t_{i+1}=t_i+\Delta t$, as shown in Figure-2. The displacement at t_{i+1} can be expressed by eq. (3) and calculated from the known data at the time t_i. Time required for one cycle process is 2.08ms[2].

$$x_{i+1} = \left(M + \frac{\Delta t}{2}C\right)^{-1} \left\{M(2x_i - x_{i-1}) + \frac{\Delta t}{2}Cx_{i-1} + \Delta t^2(p_i + q_i - Kx_i)\right\} \qquad \cdots(3)$$

Actuator Delay Compensation

Although actuator response delay has unfavorable influence on the real-time hybrid vibration experiment, it is inevitable with a hydraulic actuator. Therefore, a compensation technique is adopted. This technique predicts the displacement of an actuator at the time after actuator delay time[3].

Multi-axial control

Most of conventional hybrid experiments use one-axial control systems. Multi-axial real-time hybrid vibration system[4] is employed in the present study. Figure-3 shows the concept of multi-axial hybrid vibration experiment system. The reaction force F is measured and introduced into vibration response analysis. Then, the displacement at the center of the transfer plate at next step X (x, z, θ) is calculated. In order to realize this displacement, three actuators yield displacements l_1, l_2 and l_3, as shown in Figure-4.

Interlocking Experiment

In the previous study[1], we directly inputted the measured acceleration of the shaking table to the numerical computation part of a hybrid experiment for interlocking the numerical calculation and the shaking table test. This caused divergent phenomenon in some cases because the vibration of the the hybrid experiment apparatus interfered with the control of shaking table. In the present study, we used the control signal of shaking table for numerical analysis instead of the measured acceleration of shaking table.

Inertia Force Modification

To attach a specimen to the hybrid vibration experiment apparatus, it is necessary to install the spacer between the specimen and the three component-force transducer, which results in that the inertia force due to weight of the spacer is included in the measured reaction force. To remove the effect of inertia force of the spacer, the following equation is here introduced.

$$f_{sx}' = f_{sx} - M \times A_{sx} \qquad \cdots(4)$$
$$f_{sz}' = f_{sz} - M \times A_{sz}$$

where, f'_{sx} and f'_{sz} are the modified loads, f_{sx} and f_{sz} are loads measured by the three component-force transducer, A_{sx} and A_{sz} are the acceleration measured by the accelerometer under the three component-force transducer, and M is the weight of spacer.

4. EXPERIMENT MODELS AND CASES

In order to demonstrate the validity of real-time hybrid vibration experiment, both real-time hybrid vibration experiments and conventional experiments with a whole structure model were conducted, and the results were compared.

Two types of original structures were employed in experiments. Type 1 is a concrete slab model which is supported by coil springs. In the experiment, we connected two slabs rigidly to move as one body. Type 2 consists of a 2-story slabs supported by rubber bearings and coil springs. Their conceptual views are presented in Figure-1. The slab part consists of H-shaped beams and infilled concrete. Using coil springs makes the motion of specimen as 2-dimensional and 3-degrees-of-freedom. The stiffness of coil springs and the weight of slabs were determined in advance by numerical analysis to yield the appropriate natural frequency for experiments.

In order to find the fundamental natural frequency of test specimen, both horizontal and vertical random shaking tests were carried out with the original structures. The horizontal and vertical fundamental natural frequencies of type 1 model are 1.32 Hz and 2.10 Hz, and those of type 2 model are 1.17 Hz and 2.05 Hz.

Test cases of hybrid vibration experiments are listed in Table-1 and Table-2. In the hybrid vibration experiment for type 1 model, the mass, stiffness and damping over coil springs were

numerically modeled. In the hybrid vibration experiment for type 2 model, the mass, stiffness and damping of the upper level and the mass of the lower level were numerically modeled, as shown in Figure-5. Besides the hybrid vibration experiments, conventional experiments with the whole structure were also conducted, and the results of hybrid vibration experiments and conventional experiments were compared.

Input motions employed for experiments were five cycles of sinusoidal wave with the frequency that corresponds to the horizontal or vertical fundamental natural frequency of the whole structure, and the strong ground motion recorded in the past as shown Table-1 and Table-2. The maximum peak acceleration was variously changed in experiments.

5. NUMERICAL MODELS FOR HYBRID VIBRATION EXPERIMENTS

5.1 Numerical model

Numerical models for hybrid vibration experiments are shown in Figure-5, and equations of motions for numerical analysis are described for type 1 and type 2 models as follows:

Type 1

$$M\ddot{x}+C\dot{x}+Kx=p+q$$

$$x=\begin{bmatrix} x \\ z \\ \theta_y \end{bmatrix}, M=\begin{bmatrix} m & 0 & -mh \\ 0 & m & 0 \\ -mh & 0 & J \end{bmatrix}, K=\begin{bmatrix} 0 & 0 & 0 \\ 0 & 0 & 0 \\ 0 & 0 & -mgh \end{bmatrix},$$

$$p=\begin{bmatrix} F_x \\ F_z \\ M_y \end{bmatrix}, q=-\begin{bmatrix} m & 0 \\ 0 & m \\ -mh & 0 \end{bmatrix}\begin{bmatrix} \ddot{x}_g \\ g+\ddot{z}_g \end{bmatrix} \quad \cdots(5)$$

Type 2

$$M\ddot{x}+C\dot{x}+Kx=p+q$$

$$x=\begin{bmatrix} x \\ z \\ \theta_y \\ u \end{bmatrix}, M=\begin{bmatrix} m_1+m_2 & 0 & -m_1h_1-m_2h_2 & m_2 \\ 0 & m_1+m_2 & 0 & 0 \\ -m_1h_1-m_2h_2 & 0 & J & -m_2h_2 \\ m_2 & 0 & -m_2h_2 & m_2 \end{bmatrix}$$

$$K=\begin{bmatrix} 0 & 0 & 0 & 0 \\ 0 & 0 & 0 & 0 \\ 0 & 0 & -m_1gh_1-m_2gh_2 & m_2g \\ 0 & 0 & m_2g & k_u \end{bmatrix}$$

$$p=\begin{bmatrix} F_x \\ F_z \\ M_y \\ 0 \end{bmatrix}, q=-\begin{bmatrix} m_1+m_2 & 0 \\ 0 & m_1+m_2 \\ -m_1h_1-m_2h_2 & 0 \\ m_2 & 0 \end{bmatrix}\begin{bmatrix} \ddot{x}_g \\ g+\ddot{z}_g \end{bmatrix} \quad \cdots(6)$$

g in eq (5) and (6) represents the gravitational acceleration, and the mass, damping and stiffness matrices are shown in the following sections.

5.2 Mass Matrix

The mass matrix consists of weight of nurmerical part m, height of the center of gravity h and inertia moment J ($=mh^2+I$, I: inertia moment around the center of gravity), which are shown in eqs. (5) and (6).

Type 1

The weight m_i, the height of the center of gravity h_i and the inertia moment around the center of gravity I_i for each structural part were calculated from the design drawing of the specimen. From the above values m, h and J of the whole numerical mode are obtained as

$$m=\sum m_i$$
$$h=\frac{\sum m_i h_i}{m} \quad \cdots(7)$$
$$J=\sum (m_i h_i^2+I_i)$$

Type 2

In addition to the mass of slabs, that of rubber bearings was also considered.

5.3 Damping Matrix

Type 1

The damping was ignored because the damping of the original structure part that is numerically modeled is small.

Type 2

The damping of rubber bearings were considered. The damping matrix was estimated from the damping ratio to the critical h=0.026, which was obtained by free vibration tests, and the relationship $C=\beta K$($\beta=2h/\omega$).

5.4 Stiffness Matrix

Type 1

m and h were calculated similar to the case of m and h in the mass matrix.

Type 2

The stiffness of rubber bearings were considered. The stiffness coefficient was determined as 2.6×10^{6}N/m based on forced vibration tests.

6. EXPERIMENT RESULTS

Figures-6 and 7 compare acceleration time histories of the control point (Figure-5) in hybrid vibration experiments and conventional shaking table tests with the whole structure. Results are shown for Cases 1, 2, 4, 6, 7 and 9. The hybrid vibration experiment well reproduces both amplitude and phase of acceleration time history. Causes of slight error between real-time hybrid vibration experiments and conventional shaking table tests may exist in:

(1)Detection error by the three component-force transducer:

Since the reaction force generated in the experiments was small and reached several-percent of the rated capacity of transducer, there existed certain error in load measurement.

(2)Difference of the restricting condition

Although the freedom of specimen was 3-dimensional and 6-degrees in conventional shaking table tests, it was restricted to 2-dimensional and 3-degrees-of-freedom in hybrid vibration experiment. For example, slight movement around the vertical axis was generated in conventional shaking table test, and this might affect the experiment result.

7. CONCLUSIONS

We employed actuator delay compensation for the real-time experiment, and contrived multi-axial control for multi-degrees of freedom experiment. The real-time hybrid vibration experiment well reproduces seismic behavior of the 2-dimensional and 3-degrees-of-freedom model and the validity of experiment is confirmed though the degrees-of-freedom are increased.

REFERENCES

1)Keiichi TAMURA and Hiroshi KOBAYASHI, Real-time Hybrid Vibration Experiment with a 2-Degrees-of-Freedom Model, 30th Joint Meeting, Panel on Wind and Seismic Effects, UJNR, 1998

2)Kazuhiro UMEKITA, et al., Development of C Language Library for Super Real-Time Controller (SRC) for Real-Time Hybrid Seismic Testing System with Three-dimensional-in-plane Excitation, 40th Japan Joint Automatic Control Conference, 1997 (in Japanese)

3)Toshihiko HORIUCHI, Masaki NAKAGAWA, Masaharu SUGANO and Takao KONNO, Development of a Real-Time Hybrid Experimental System with Actuator Delay Compensation, 11th World Conference on

Earthquake Engineering, 1996
4)Yasuyuki MOMOI, Toshihiko HORIUCHI, Kazuhiro UMEKITA, Masahiko INOUE and Masaharu SUGANO, Development of Real-Time Hybrid Seismic Experimental System using Multiple-Axis Shaking Device, 5th Symposium on Motion and Vibration Control, JSCE, 1997 (in Japanese)

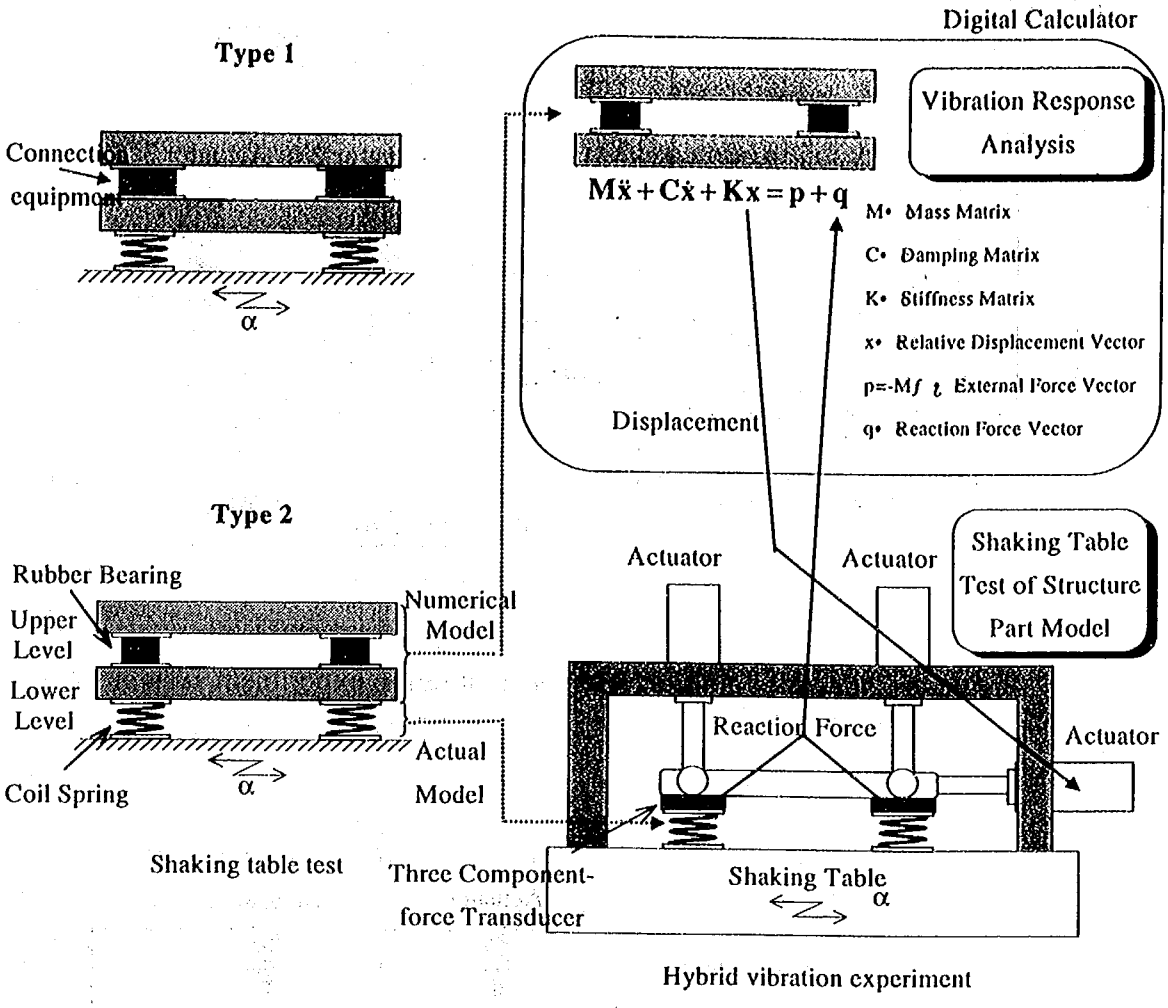


Figure-1 Conceptual view of hybrid vibration experiment

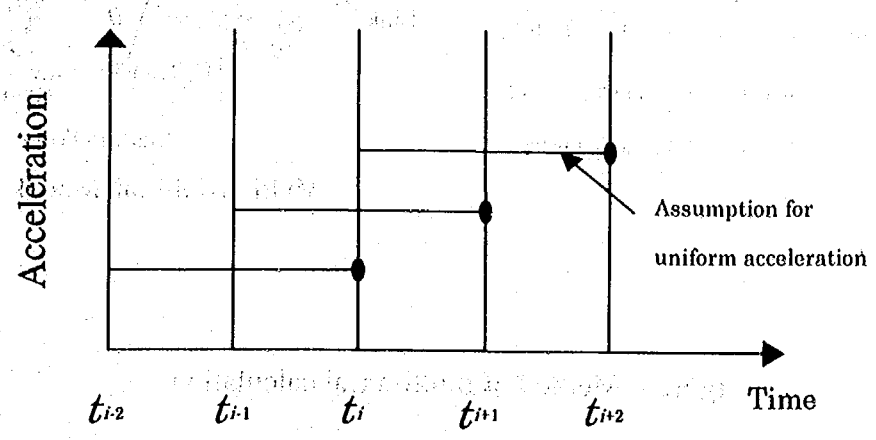


Figure-2 Assumption of acceleration in the central difference method

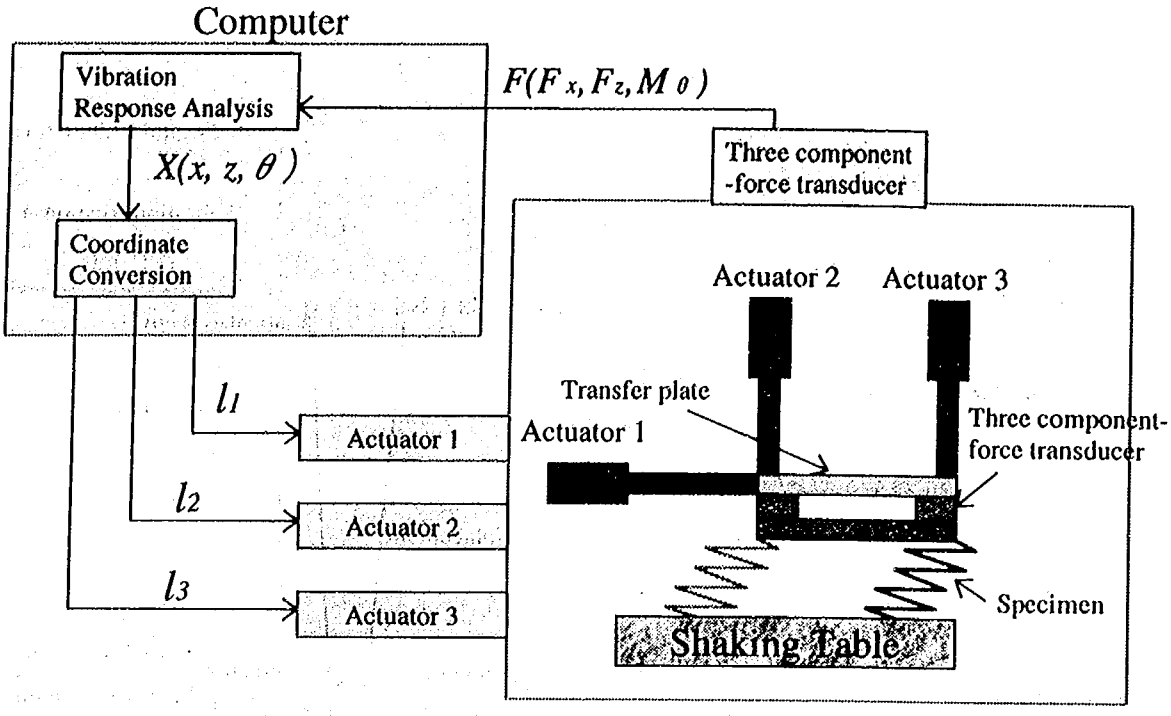


Figure-3 Concept of multi-axial hybrid vibration experiment system

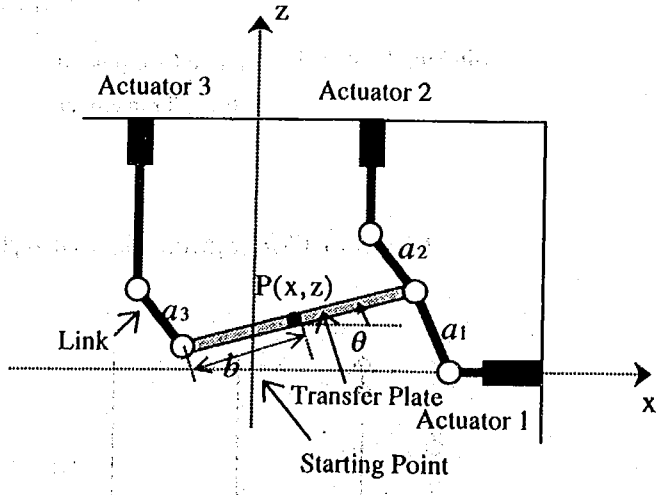
$$l_1 = -(x + b\cos\theta - b) + (a_1 - \sqrt{a_1^2 - (z + b\cos\theta)^2})$$

$$l_2 = -(z + b\sin\theta) + (a_2 - \sqrt{a_2^2 - (x + b\cos\theta - b)^2})$$

$$l_3 = -(z - b\sin\theta) + (a_2 - \sqrt{a_2^2 - (x - b\cos\theta - b)^2})$$

a_1, a_2, a_3: length of link ($a_2 = a_3$)

2b: width of the transfer plate



Multi-Axial Link Model

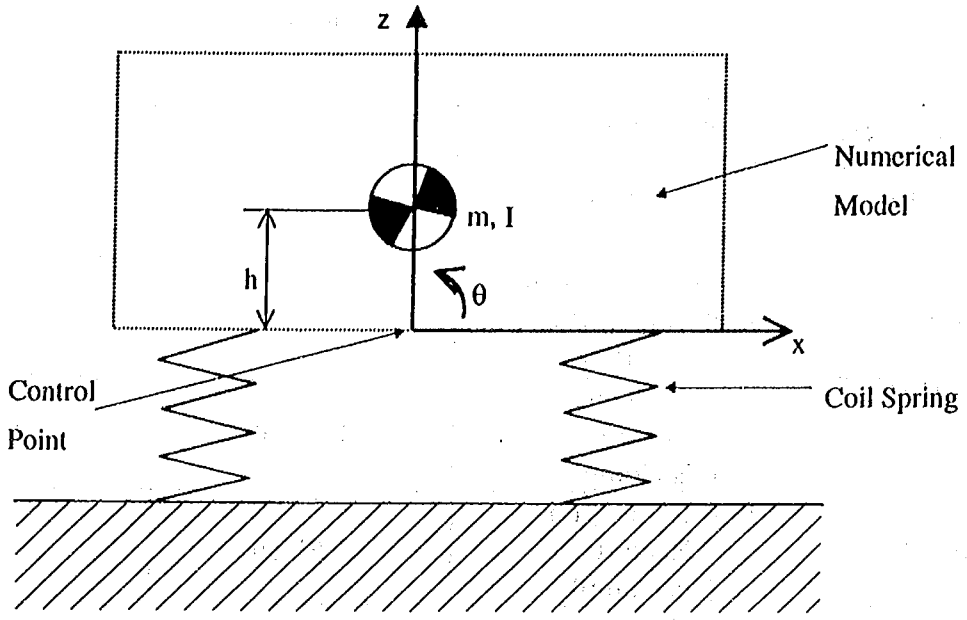
Figure-4 Method of multi-axial calculation

Table-1 Test Cases (Type 1)

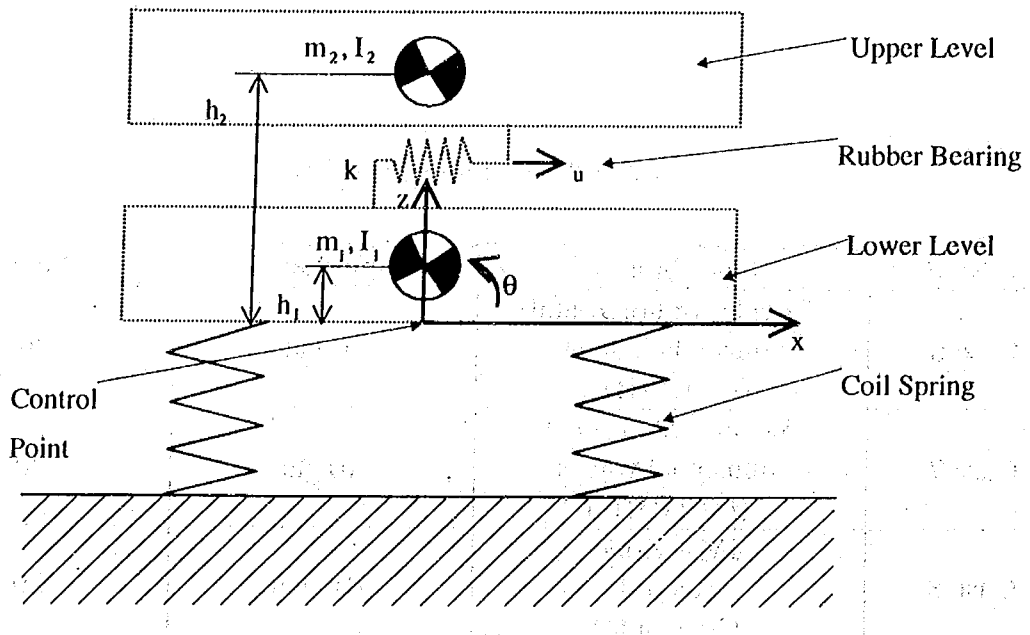
Case Number	Input Motion	Input Level	Duration
Case 1	5 cycles of horizontal sinusoidal waves (f=1.32Hz)	40 gal	20 s
Case 2	5 cycles of vertical sinusoidal waves (f=2.10Hz)	50 gal	20 s
Case 3	JMA Kobe Record (Ns Comp)	150 gal	30 s
Case 4	Port Island Kobe Record (Ns Comp)	120 gal	30 s
Case 5	Elcentro Record (Ns Comp)	120gal	45 s

Table-2 Test Cases (Type 2)

Case Number	Input Motion	Input Level	Duration
Case 6	5 cycles of horizontal sinusoidal waves (f=1.17Hz)	30 gal	20 s
Case 7	5 cycles of vertical sinusoidal waves (f=2.05Hz)	40 gal	20 s
Case 8	JMA Kobe Record (Ns Comp)	100 gal	30 s
Case 9	Port Island Kobe Record (Ns Comp)	100 gal	30 s
Case 10	Elcentro Record (Ns Comp)	100gal	45 s

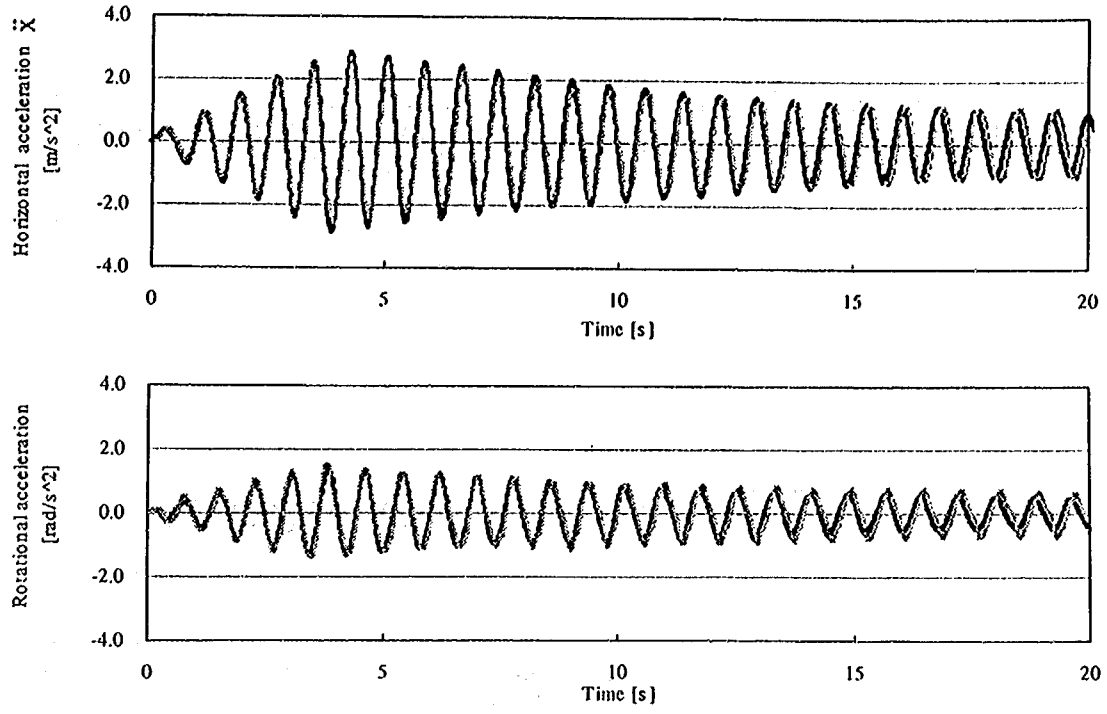


(a) Type 1 model

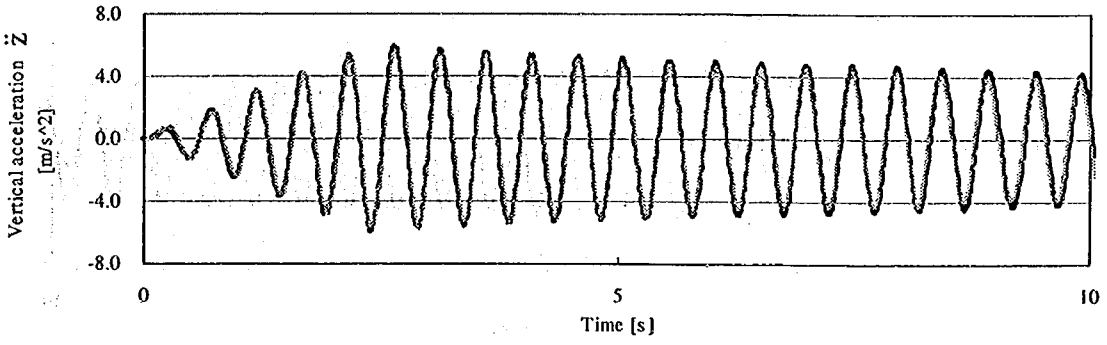


(b) Type 2 model

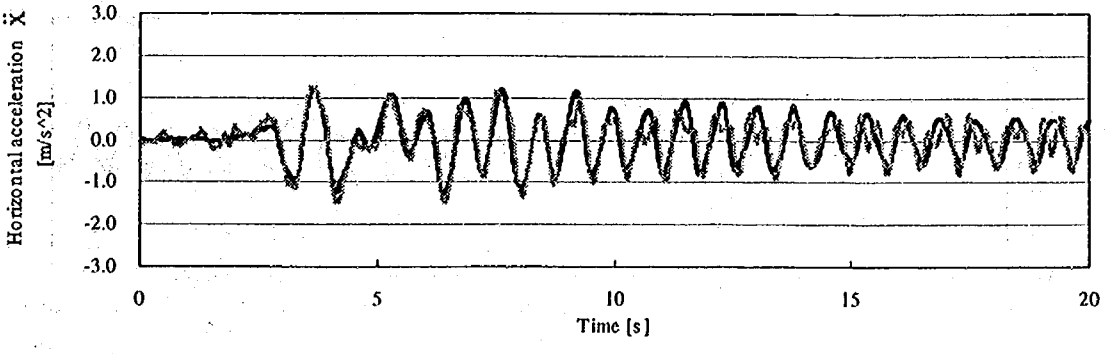
Figure-5 Numerical model for hybrid vibration experiment



(a) Case 1



(b) Case 2

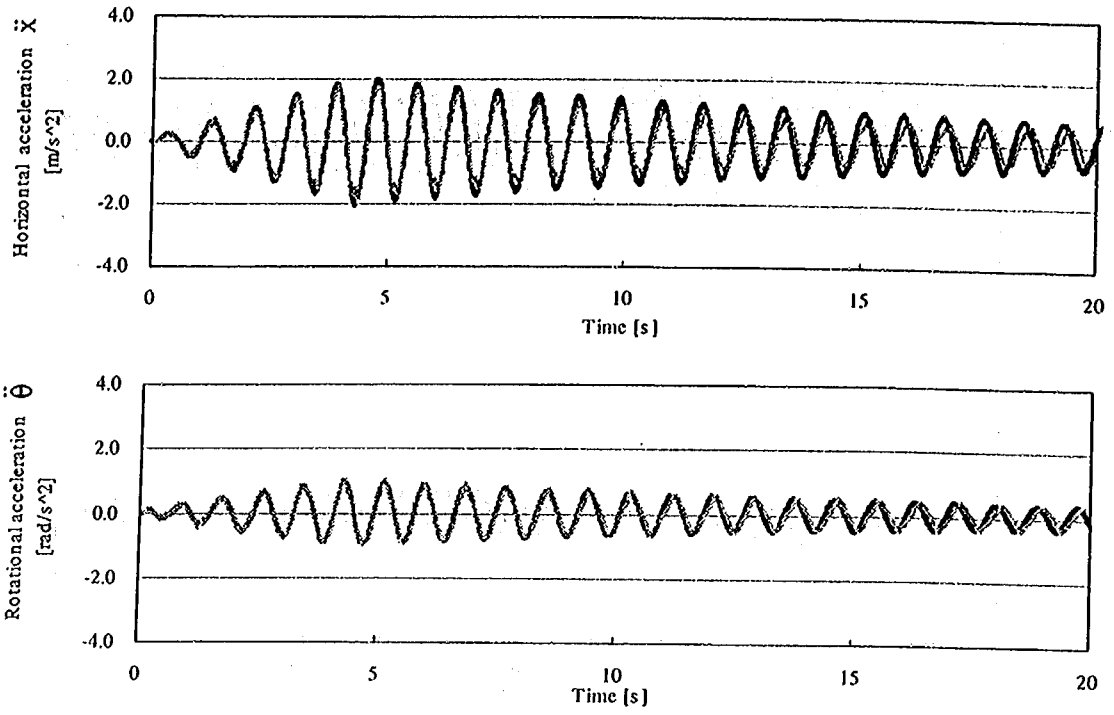


(c) Case 3

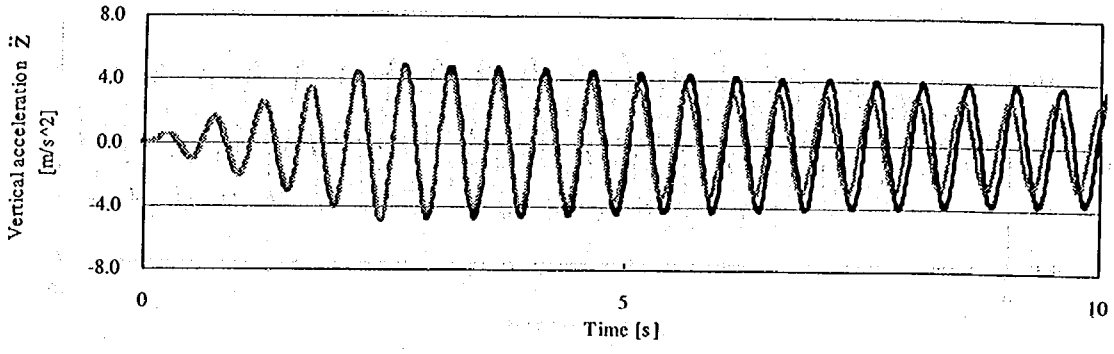
Real-time hybrid vibration experiment

Shaking table test

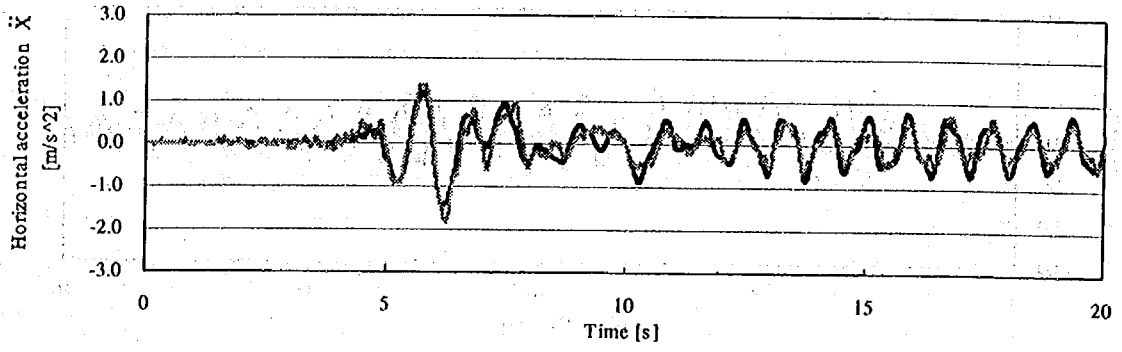
Figure-6 Acceleration time histories of the control point (Type 1 model)



(a) Case 6



(b) Case 7



(c) Case 9

Real-time hybrid vibration experiment

Shaking table test

Figure-7 Acceleration time histories of the control point (Type 2 model)

Integrated Surface and Borehole Strong-Motion, Soil-Response Arrays in San Francisco, California

By

R. D. Borcherdt, H. P. Liu, R. E. Westerlund, C. Dietel, J. F. Gibbs, and R. E. Warrick*

ABSTRACT

An integrated set of four borehole arrays and ten surface installations is installed in the city of San Francisco, California to measure the response of soft-soil deposits to strong earthquake ground motions. The borehole arrays extend through thick layers of soft water-saturated soils of Holocene age and older more consolidated soils of Pleistocene age into bedrock at depths up to 100 m. The surface installations are configured in pairs to provide simultaneous comparative surface measurements of soft soils and nearby rock. The rock locations also permit comparative measurements of rock as observed at the surface and in nearby boreholes. Complementary structural response arrays also are installed near each array.

The arrays are designed to address a wide variety of scientific and engineering issues, and especially the issue of anelastic and nonlinear soil response at high strain levels. Exact anelastic models have been developed to account for contrasts in anelastic properties at boundaries and the resultant inhomogeneity of propagating wave fields. These models predict that significant amounts of energy may be trapped in soil basins with resultant larger amplifications than can be predicted using conventional homogeneous wave-field models with damping. Results of these models are discussed.

* United States Geological Survey
Menlo Park, CA 94025

1. INTRODUCTION

Structural damage and consequent loss of life from earthquakes is often concentrated in areas underlain by soft soils. Damage from modern earthquakes such as those affecting Mexico City (1985), Leninakan, Armenia (1988), San Francisco, California (Loma Prieta 1989), and Kobe, Japan (1995) imply that a major portion of the damage occurred in areas underlain by soft soils. These increased amounts of damage are due to amplification effects of soft soil deposits on certain frequencies of ground shaking and in some cases associated soil failures. Nevertheless, relatively scarce empirical information exists concerning the in-situ response of such deposits. Few strong-motion recordings have been obtained in boreholes necessary to define the actual amplification characteristics as a function of input ground shaking.

In the city of San Francisco, damage from both the great California earthquake of 1906 and the Loma Prieta earthquake of 1989 was concentrated in areas underlain by soft soil deposits. Many of these areas are along the margins of San Francisco Bay and are densely urbanized. However, no in-situ borehole measurements of the response of these deposits have yet been obtained at damaging levels of motion. Such measurements of the next large damaging earthquake will be of

special importance for mitigation of future earthquake losses.

Several important questions exist concerning the in-situ response of soft soil deposits at damaging levels of shaking. A question of particular interest concerns the role of non-linearity in modifying the in-situ amplification characteristics of soft soil deposits as a function of shaking amplitude. This is a major issue yet to be resolved with in-situ evidence. Other questions concerning changes in constitutive properties with duration, ground motion characteristics necessary for the onset of liquefaction, and the influence of basin geometry also are of considerable interest.

This paper describes a set of integrated borehole arrays and surface installations in the city of San Francisco designed to address these questions. It describes the design objectives of the arrays, their location, geologic setting, seismic and geologic information, and instrumentation configuration.

2. GENERAL DESIGN OBJECTIVES

The integrated strong-motion soil response arrays in San Francisco operated by the US Geological Survey are designed to provide comprehensive data on the response of "soft soils" at four different locations in the city underlain by soft water saturated clays, sands, and silts. Major concentrations of damage occurred in these areas during both the 1906 and 1989 earthquakes. Evidence for liquefaction during the earthquakes exists at three of the four sites. Locations of the arrays are shown in Figure 1a. The arrays are located in the vicinity of Embarcadero Plaza (EMB) near lower market street, in Levi Strauss Plaza near the base of Telegraph Hill (LP), at Winfield Scott School in the Marina district (WSS), and at Bessie Charmichael School (BCS) in an area south of Market street. Surface installations with three-component velocity and three-component force-balance accelerometers are installed at 10 additional sites (see Figure 1a).

Measurements in these areas are particularly relevant for purposes of hazard mitigation, because a number of important facilities including high-rise buildings, apartment buildings, rapid transit facilities, bridges, and underground utilities are located in these areas. The arrays are designed to provide new *in-situ* data on the constitutive behavior of soils as a function of strain amplitude and liquefaction-induced failure. They are designed to complement strong-motion data recorded on nearby well-instrumented buildings together with data recorded at surface installations (see Figure 1b).

The arrays are designed to provide an integrated set of data pertinent to addressing a wide variety of scientific and engineering issues. Each array includes sensors located at depths ranging from the surface to below the bedrock interface. Sensors at three of the borehole locations (BCS, LP, EMB) are at four different levels. Sensors at the WSS location are at three different depths. The surface installations permit comparative studies of soil and and rock motions as observed at pairs of closely spaced soil-rock locations. The surface rock locations also permit comparative studies of motions as observed both at the surface and in nearby boreholes at the soil-rock interface. Surface and borehole motions will provide an improved definition of input ground motions for understanding the response of nearby high-rise buildings, bridges, harbor facilities, and a variety of other types of well instrumented structures in San Francisco.

The borehole instrumentation at three of the locations includes pairs of pore-pressure and force-balanced accelerometers (FBA) collocated at two depths. These pairs of sensors provide *in-situ* measurements of the temporal and spatial variations in pressure

and ground displacements. Such collocated measurements using FBAs and dilatometers at other locations in California have been shown (Borcherdt, et al. 1988 and 1989) to provide important new information on *in-situ* material behavior as a function of time not provided by either measurement alone. These studies have shown that simultaneous collocated measurements provide *in-situ* constitutive properties of the surrounding medium as a function of strain amplitude and number of cycles. The extent to which these concepts can be used to help resolve important issues regarding non-linear dynamic soil behavior and its role in influencing ground and structural response is an important design objective of the arrays at three of the locations (BCS, LP, EMB). Each of these arrays also includes two additional FBAs at greater depths including one in bedrock. Installation of an additional velocity transducer is being planned for each site.

One of the arrays is designed with collocated sets of FBAs and velocity transducers (WSS). This array is intended to provide high resolution recordings ranging in amplitude from seismic background noise levels to damaging levels of shaking up to 2g. The array, initially installed with velocity transducers, has provided an extensive data set interpreted by Liu, et al. (1992).

3. GEOLOGIC SETTING

The San Francisco Bay basin is a northwest-trending graben bounded on the northeast and southwest by the active Hayward and San Andreas faults. San Francisco Bay, located in the center of this graben, is bounded by marshlands, alluvial plains, and hills at distances of 1-15 km from the Coast Ranges. A wide variety of geologic units exist in close proximity throughout the region. They range from Mesozoic sedimentary and plutonic rocks in the hills, to Holocene alluvium and estuarine mud near the margins of the bay. Mesozoic and Tertiary rock units form the floor of the graben. This surface is overlain by a sedimentary sequence of which the lower part was initially designated Older bay sediments and the upper part Younger bay mud. Geologic characteristics, physical properties, and seismic shear-wave velocities for the various surficial units in the San Francisco Bay region are summarized in detail by Borcherdt and Glassmoyer (1994).

The Younger bay mud unit is of particular interest, because it yields the largest amplifications of ground motion (Borcherdt 1972, Borcherdt and Gibbs 1976). Thick sections of this unit exist at each of the borehole sites. In general, it is Holocene in age. It is composed of unconsolidated, water-saturated, dark plastic clay and silty clay rich in organic material with local lenses of well-sorted silt and sand and some beds of peat. It attains thickness of 37 meters beneath the bay and thins to vanishing thickness along the margins of the bay. It generally contains more than 50 percent water. It is overlain at each of the borehole array locations by fill, comprised of hydraulically emplaced sands and clays or earth and rock with varying degrees of compaction. Measurements of shear-wave velocity range from 55 to 100 m/s in the depth interval 0 to 10 m and from 100 to 115 m/s in the depth interval 10 to 20 m (Fumal, 1978).

The Older bay sediment unit is in general comprised of Pleistocene deposits ranging in composition from weakly to moderately consolidated, deeply weathered, poorly sorted, irregularly interbedded clay, silt, sand, and gravel to loose, well-sorted, fine- to medium-grained sand with subordinate silt (Helley and Lajoie 1979). This Older Bay Sediment unit reaches overall thickness generally less than 200 m in the northern bay region. Shear-wave velocities range from 150 to 219 m/s for dune sands near the surface to

418 to 749 m/s for coarse-grained, sandy gravels of late Pleistocene age.

The semi-consolidated and consolidated units in the hills of the San Francisco Bay region include plutonic, volcanic, and a wide range of sedimentary rocks. Shear-wave velocities in the top 30 m of these units range from about 425 m/s for soft sandstone to about 1,650 m/s for hard greenstone and fresh granite.

The depths for sensors were chosen to monitor behavior of potentially liquefiable granular layers near the surface, the underlying Holocene bay mud, the underlying Older bay sediment layer, and the underlying bedrock.

4. GEOLOGIC AND SEISMIC LOGS

During the initial drilling a relatively complete set of geologic and seismic logs were obtained at each of the sites (Gibbs, 1994, Kayan, et al., 1990). A summary of the logs for each of the sites is shown in Figures 2, 3, 4, and 5. In addition, undisturbed samples were obtained and tested at the WSS site by Kayan et al. (1990).

The logs at each of the sites shows evidence of a thin compacted layer of fill at the surface overlying deposits of soft clay, silty clay, and silts with the lowest shear wave velocities in the top 20 meters being slightly greater than 100 m/s. In general, the shear velocities increase with depth to values near 350 to 400 m/s then show a significant increase to values from 780 to slightly more than 800 m/s for the underlying bedrock.

5. INSTRUMENTATION

The sensors deployed for direct measurement of acceleration are three component borehole force-balance accelerometers with full scale at $\pm$ 1 or $\pm$ 2 g ($\pm$ 5 volts), and frequency response from dc to 100 Hz, models FBA 13 and FBA 23 DH produced by Kinemetrics, Inc. The velocity transducers with a natural frequency of 2 Hz have been developed for borehole deployment (Liu, et al.,1991). The pore-pressure transducers are wide dynamic range (~140 dB) transducers with digital output proportional to pressure applied to a quartz crystal resonator, model 8DP depth sensor produced by Parascientific, Inc.

Signals from each of the sensors at each location are recorded on site using broadband digital recorders (General Earthquake Observation Systems, GEOS, Borcherdt, et al., 1985) with event derived parameters transmitted and recorded in near real time via GOES satellite (Mueller et al. 1993). Signals from the various sensors are recorded at various gain levels depending on the depth and type of sensor. Gains up to 84dB selectable in 6dB steps are available to permit signals over a dynamic range near 180 dB at frequencies near 1 Hz to be resolved from a variety of sensor types. In general, gains for similar sensors in a single borehole array vary between 6 and 18 dB.

Events are recorded in event triggered mode at 200 samples per second per channel using linear 16-bit linear analog to digital conversion. Absolute time and each of the various recording parameters are recorded simultaneously. Event and instrument parameters are transmitted at a selectable time interval usually chosen to be less than 10 minutes via GOES satellite. Parameters such as trigger time, peak amplitude, time of peak amplitude and duration together with a variety of instrument status parameters are transmitted. The satellite transmissions permit the retrieval of critical event and instrument data in near real time. These data are especially useful in maintaining the array and initial evaluations following a major event.

Sensor and recording system calibrations are recorded before and after each storage media change. Since installation of the array no

earthquakes in the area have generated signals of sufficient strength to be recorded on the FBAs above the relatively high seismic background noise levels. Signals recorded on the velocity transducer array at the WSS site have been analyzed in detail by Liu, et al. (1992).

6. EXACT ANELASTIC MODELS OF SOIL RESPONSE

Damping plays an important role in determining the response of soils. In general, it increases with frequency of shaking. Exact anelastic 2 and 3 dimensional wave-propagation models, which account for damping, show that wave fields, which propagate across anelastic boundaries, must, in general be inhomogeneous. In other words, as energy propagates across soil and soil-rock boundaries, contrasts in damping at the boundaries cause amplitudes to vary along surfaces of constant phase, that is the direction of phase propagation differs from that of maximum attenuation of the wave field. An example showing the directions of propagation and maximum attenuation for an inhomogeneous wave field incident on a soil basin is illustrated in Figure 6.

Inhomogeneity of the wave fields in a soil basin gives rise to a set of physical characteristics for the wave field distinct from those that would be predicted by incorrectly assuming homogeneous wave fields. In particular, exact inhomogeneous models imply two types of inhomogeneous S waves, one with linear particle motions and one with elliptical particle motions. They predict the wave speeds, damping, and other physical characteristics change as the angle of incidence changes. (Borcherdt, 1973, Borcherdt and Wennerberg, 1985, Borcherdt et al., 1986).

Numerical results have been derived using Mathematica for a single layer over a half space based on exact theoretical solutions. The material parameters used to characterize the constitutive characteristics of the material are the velocity ratio (V_R) and damping characterized by twice the reciprocal quality factor (Q^{-1}) for homogeneous waves. Inhomogeneity of the wave fields is denoted by gamma, the angle between the direction of propagation and maximum attenuation. The amplitude response of the layer is shown in Figure 7 for a homogeneous wave as a function of angle of incidence and normalized period. (The period of the wave is normalized by the fundamental period.) Figure 7 shows that as the angle of incidence increases, the amplitude response of the surface layer decreases. This result predicts that for conventional homogeneous wave fields propagating nearly parallel to the surface little or no energy is trapped by the soft surface layer, and hence no amplification occurs.

Results also are calculated for an inhomogeneous wave field incident on a surface layer (Figure 8). These results show that as the angle of incidence increases, the amplitude response of the surface layer may increase significantly. In particular this result predicts that for inhomogeneous wave fields propagating nearly parallel to the surface a significant amount of energy may be trapped by a soft surface layer, and hence give rise to a significant amount of amplification. The propagation of such a wave would correspond to a pseudo surface wave being generated at the margin of a soil basin. This theoretical prediction may help explain significant amplification sometimes observed near basin margins.

7. CONCLUSIONS

The borehole arrays are designed to provide *in-situ* data not previously available on the non-linear response of "soft soils" as a

function of strain amplitude with and without liquefaction-induced failure. Each borehole array includes four three-component forced-balance accelerometers (FBA), two co-located wide dynamic-range pore-pressure transducers, and at least one velocity transducer. The co-located *in-situ* measurements of acceleration and pore pressure are designed to provide estimates of the constitutive properties as a function of time and strain amplitude that cannot be inferred from either measurement alone. A separate borehole array of velocity transducers collocated with FBAs installed at one of the sites (WSS) permits wide dynamic range signals useful for studies of non-linearity to be acquired. Complementary surface bedrock and structural response installations at several nearby sites permit a wide variety of additional scientific and engineering issues to be addressed. Sensor signals are recorded using broadband, wide dynamic range, on-site digital recorders (GEOS). Parameter information for each instrument and each recorded event is transmitted in near-real time via GOES satellite.

Exact theoretical models of anelastic soil response predict that significant amounts of body wave energy being converted to surface waves may be trapped by a layer of soil near the surface giving rise to significant amounts of amplification not predicted by conventional homogeneous wave propagation models. Measurements of strong earthquake ground motions on the integrated arrays will provide empirical evidence to evaluate these and other theoretical model predictions.

REFERENCES

Borcherdt, R.D, 1970, Effects of local geology on ground motion near San Francisco Bay, *Bull. Seismol. Soc. Am.*, **60**, 29-61.

Borcherdt, R.D., 1973, Energy and plane waves in linear viscoelastic media, *Jour. Geoph. Res.*, **78**, 2442-2453.

Borcherdt, R.D, 1994, Estimates of site-dependent response spectra for design (Methodology and Justification), *Earthquake Spectra*, **10**, 617-653.

Borcherdt, R.D. and G. Glassmoyer, 1992, On the characteristics of local geology and their influence on ground motions generated by the Loma Prieta earthquake in the San Francisco Bay region, California. *Bull. Seismol. Soc. Am.*, **82**, 603-641.

Borcherdt, R.D. and G. Glassmoyer, 1994, Influences of local geology on strong and weak ground motions in the San Francisco Bay region, California and their implications for site-specific code provisions, *in* The Loma Prieta earthquake of October 17, 1989 -- strong ground motion, R. D. Borcherdt, *ed., U.S. Geol. Surv. Prof. Paper 1551-A*, 77-108

Borcherdt, R.D., Glassmoyer, G., and Wennerberg, G., 1986, Influence of welded boundaries in anelastic media on energy flow and charac-teristics of general P, S-I and S-II body waves: Observational evidence for inhomogeneous body waves in low-loss solids, *Jour. Geoph. Res.*, **91**, 11,503-11,518.

Borcherdt, R.D., and J. F. Gibbs, J.F., 1976, Effects of local geological conditions in the San Francisco Bay region on ground motions and the intensities of the 1906 earthquake, *Bull. Seismol. Soc. Am*, **66**, 467-500.

Borcherdt, R.D., Fletcher, J. B., Jensen, E. G., Maxwell, G. L., Van Schaack, J. R., Warrick, R. E., Cranswick, E., Johnston, M.J.S., and R. McClearn, 1985, A general earthquake observation system (GEOS). *Bull. Seismol. Soc. Am.*, **75**, 1783-1825.

Borcherdt, R.D, 1988, Volumetric strain and particle displacements for body and surface waves in a general viscoelastic half-space: *Geophys. J. Royal Astr. Soc.*, **93**, 215-228.

Borcherdt, R.D., Johnston, M.J.S., and G. Glassmoyer, 1989, On the use of volumetric strain meters to infer additional characteristics of short-period seismic radiation. *Bull. Seismol. Soc. Am*, **79**, 1006-1023.

Borcherdt, R.D., Fletcher, J.B., Jensen, E.G., Maxwell, G.L., Van Schaack, J.R., Warrick, R.E., Cranswick, E., Johnston, M.J.S., and McClearn, R., 1985, A general earthquake observation system (GEOS), *Bull. Seismol. Soc. Am.*, **75**, 1783-1825.

Borcherdt, R.D., and Wennerberg, L., 1985, General P, type-I S, and type-II S waves in anelastic solids: Inhomogeneous wave fields in low-loss solids, *Bull. Seismol. Soc. Am.*, **75**, 1729-1763.

Fumal, T.E, 1978, Correlations between seismic wave velocities and physical properties of geologic materials in the San Francisco Bay region, California, *U.S. Geol. Surv. Open-File Rept. 78-1067.*

Fumal, T.E., 1991, Shear-wave velocity estimates and site geology for strong-motion recordings sites of the Loma Prieta earthquake of October 17, 1989, *U.S. Geol. Surv. Open-File Rept. 91-311.*

Gibbs, J.F., Fumal, T.E., Borcherdt, R.D. Warrick, R.E., Liu, H.-P., and R.E., Westerlund, 1975, Seismic velocites and geologic logs from boreholes at three downhole arrays in San Francisco, California, *U.S. Geol. Surv. Open-File Rept. 94-706.*

Helley, E.J., and K.R. Lajoie, 1979, Flatland deposits of the San Francisco Bay region, California---their geology and engineering properties, and their importance to comprehensive planning, *U.S. Geol. Surv. Prof. Paper 943.*

Kayan , R.E., H.-P., Liu, Fumal, T.E., Westerlund, R.E., Warrick, R.E., Gibbs, J.F., and H.J. Lee., 1990, Engineering and seismic properties of the soil column at Winfield Scott School, San Francisco, California, *U. S. Geol., Surv., Open-File Rept. 90-253*, G1-G18.

Liu, H.-P., Warrick, R.E., Westerlund, and J.B. Fletcher, 1991, A three-component borehole seismometer for earthquiake seismology. *Bull. Seismol. Soc. Am.* **81**, *2458-2485.*

Liu, H.-P., Warrick, R.E., Westerlund, R.E., Sembera, E.D., and L. Wennerberg, 1992, Observation of local site effects at a downhole -and surface station in the Marina district of San Francisco, *Bull. Seismol. Soc. Am.*, **82**, 1563 - 1591.

Mueller, R.J., Lee, M., Johnston, M.J.S, Borcherdt, R.D., Glassmoyer, G., and Silverman, S., 1993, Near-real time monitoring of seismic events and status of portable digital recorders using satellite telemetry, *Bull. Seismol. Soc. Am.*, **85**, 640-645.

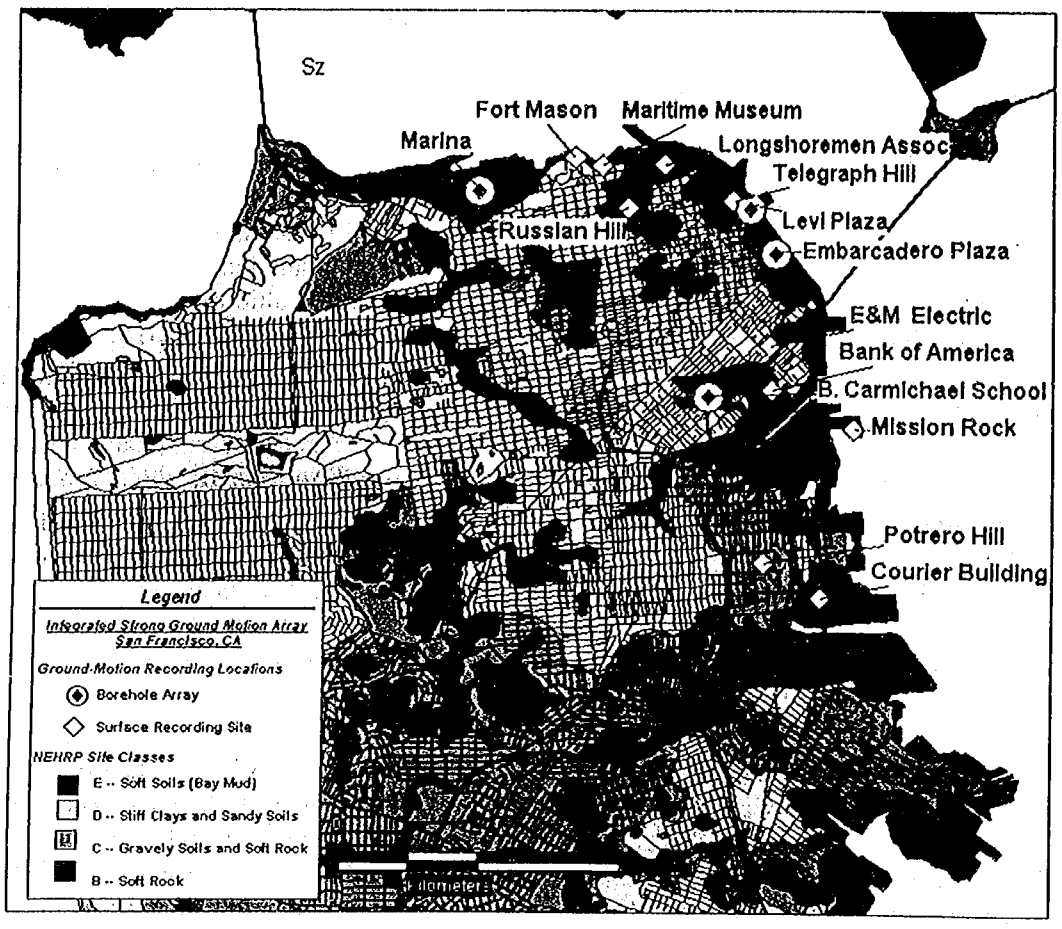


Figure 1a. Map showing location of borehole arrays and complementary surface installations superimposed on map of San Francisco, California showing streets and the NEHRP site classes recently adopted for recommended US building code provisions.

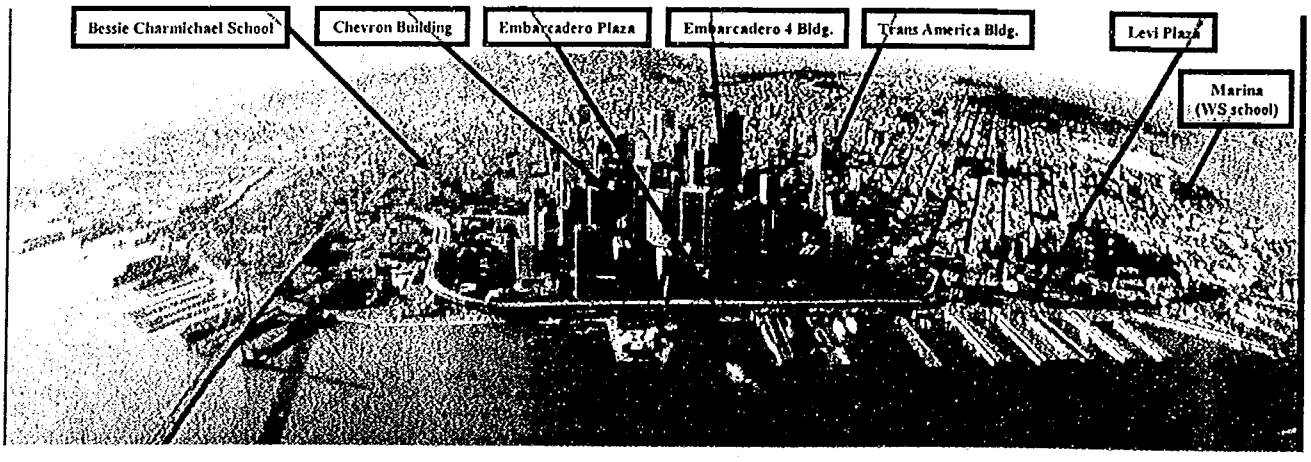


Figure 1b. Map showing location of borehole arrays and nearby structural response arrays superimposed on an areal view of San Francisco, California.

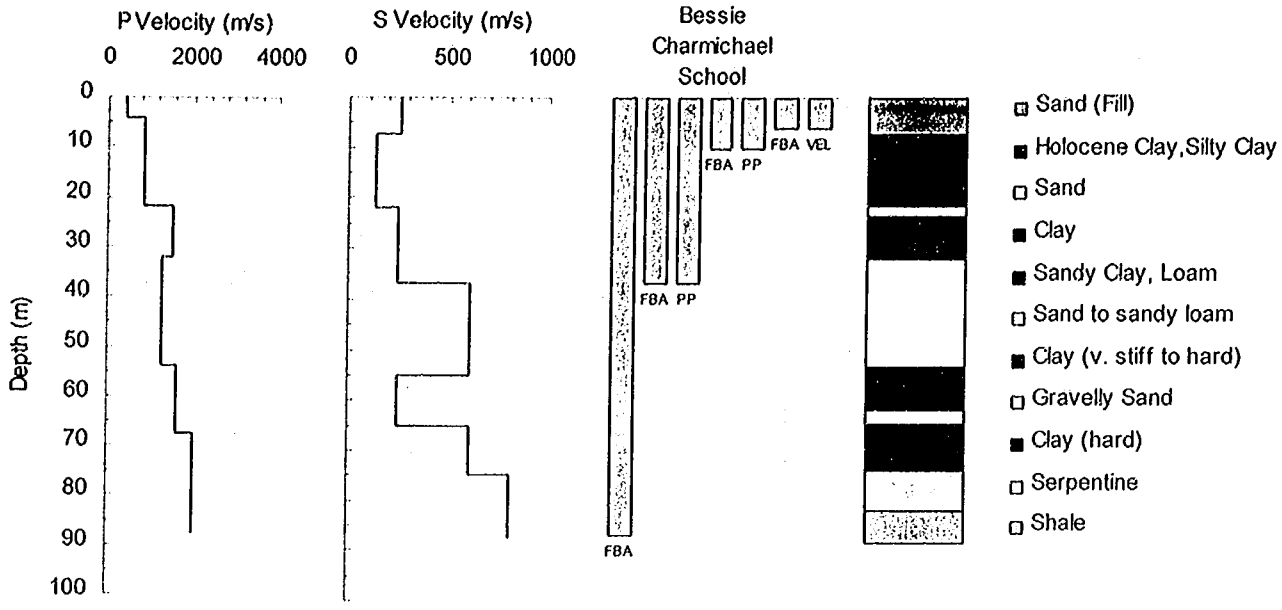


Figure 2. Seismic logs, geologic log, and sensor borehole configuration for the Bessie Charmichael School (BCS) site.

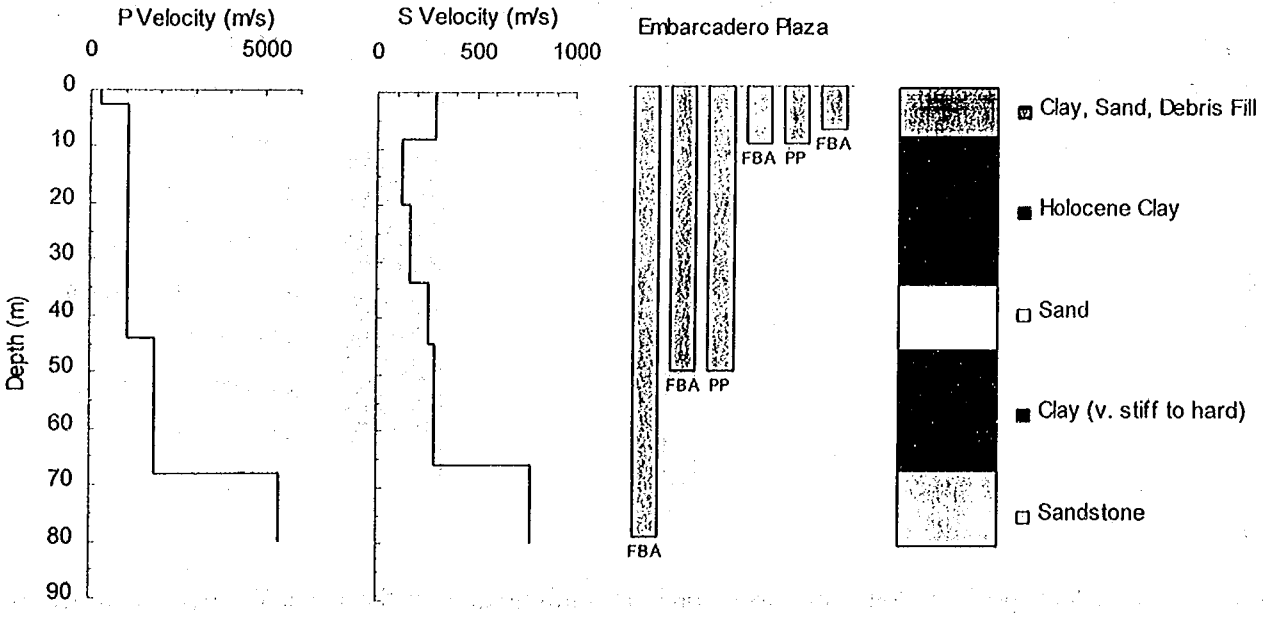


Figure 3. Seismic logs, geologic log, and sensor borehole configuration for the Embarcadero Plaza (EMB) site.

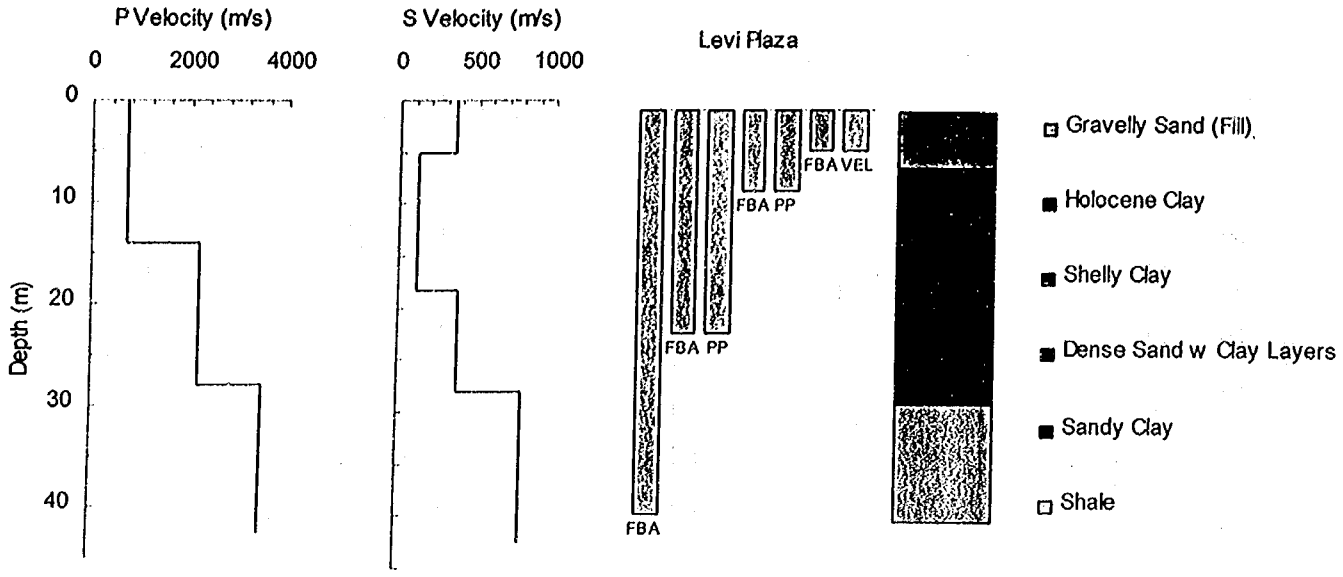


Figure 4. Seismic logs, geologic log, and sensor borehole configuration for the Levi Plaza (LP) site.

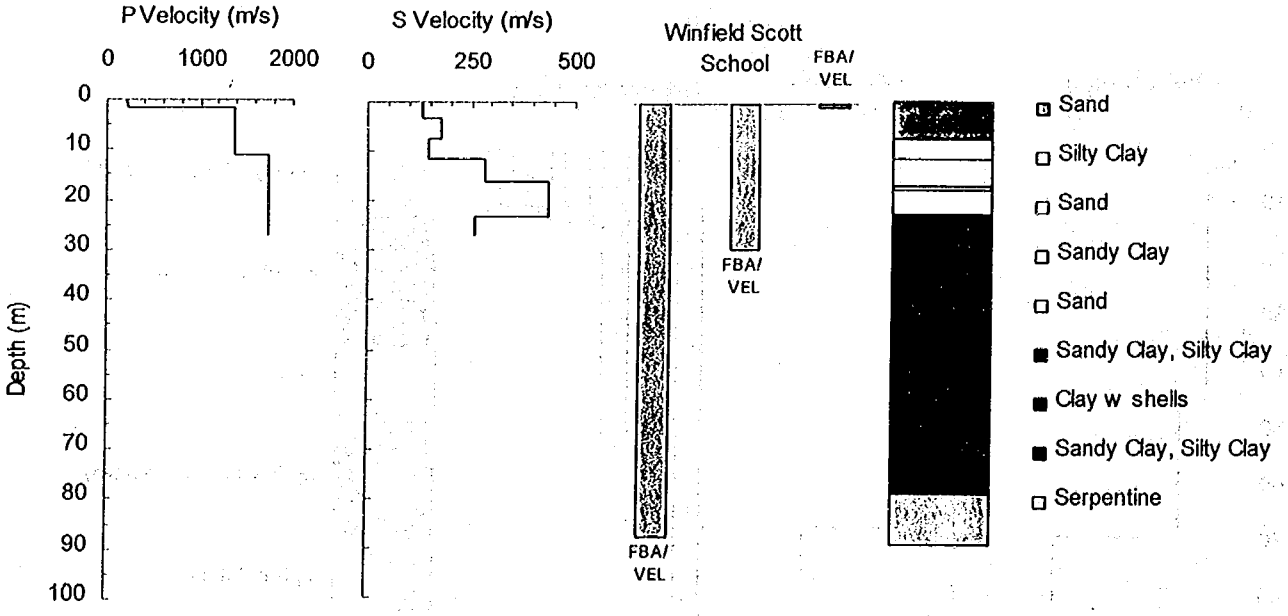


Figure 5. Seismic logs, geologic log, and sensor borehole configuration for the site at Winfield Scott School (WSS) site.

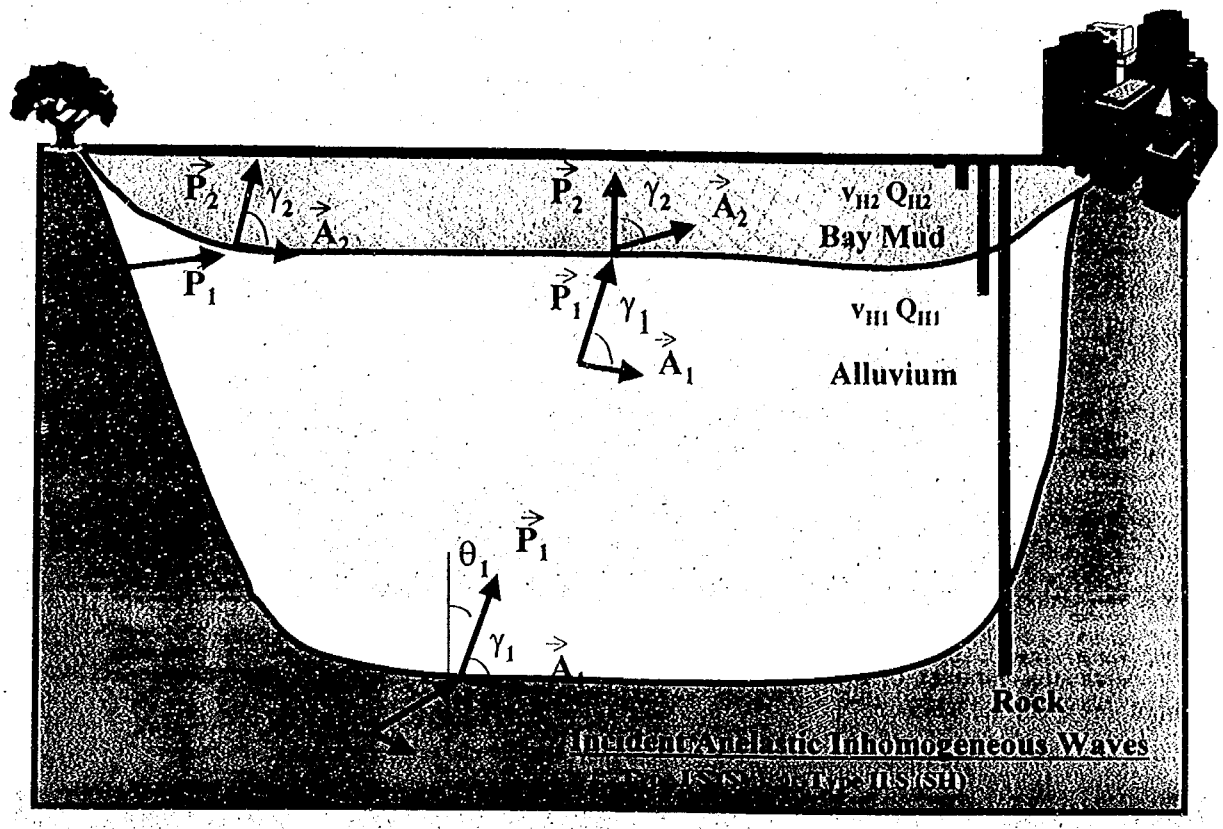


Figure 6. Illustration showing typical configuration for P and S waves in an anelastic soil-rock basin. Configuration illustrates direction of propagation (P) and maximum attenuation (A) for P, SV, and SH waves.

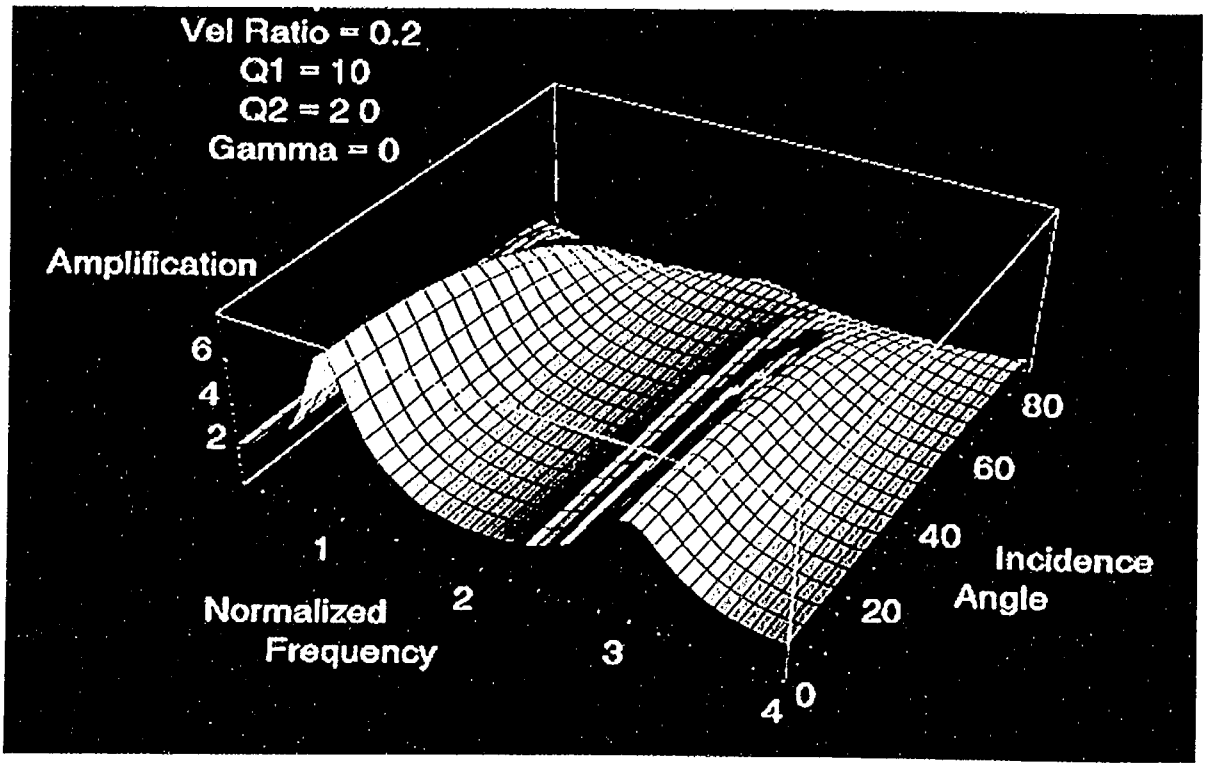


Figure 7 Anelastic response of a soft-soil layer over soft-rock to an incident homogeneous SH wave as a function of angle of incidence.

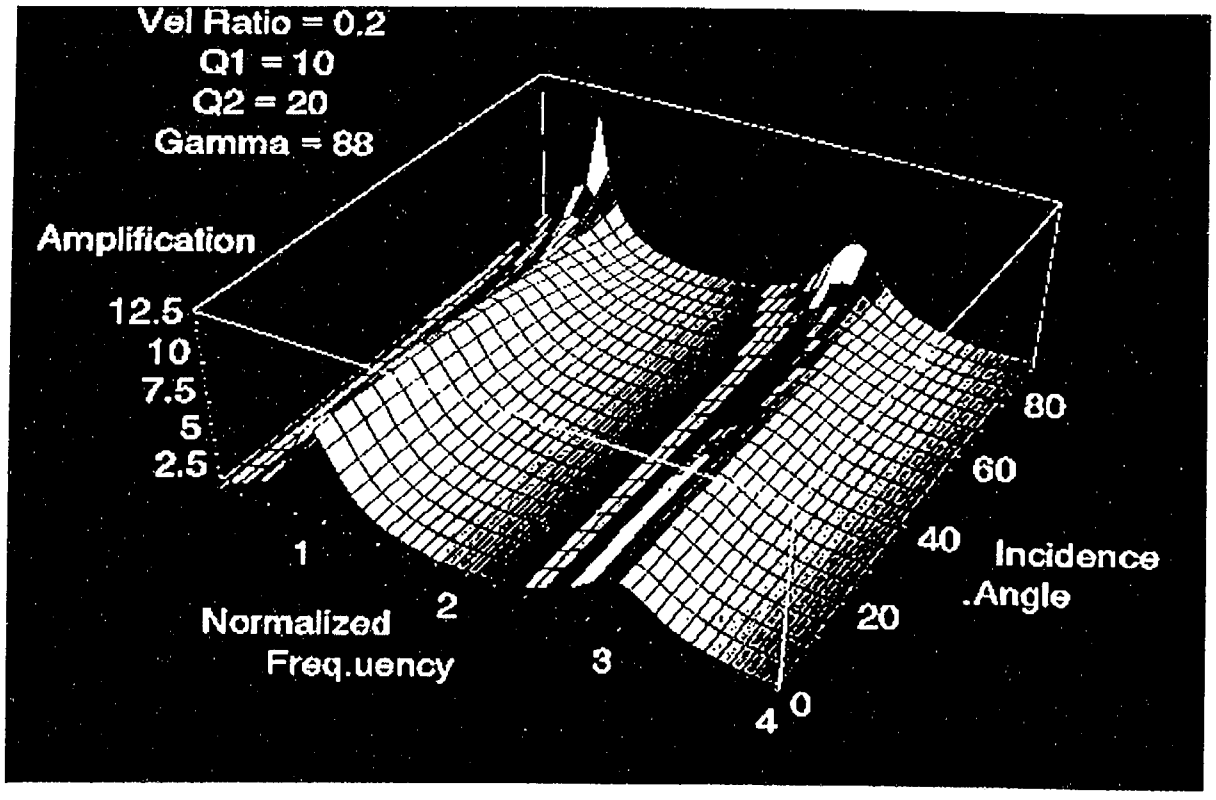


Figure 8. Anelastic response of a soft-soil layer over soft-rock to an incident inhomogeneeous SH wave as a function of angle of incidence.

THREE DIMENSIONAL SHAKING TABLE TESTS ON SEISMIC BEHAVIOR OF ISOLATORS FOR HOUSES

by

Masanori IIBA[1], Mitsumasa MIDORIKAWA[2], Hiroyuki YAMANOUCHI[3] and Bujar MYSLIMAJ[4]

ABSTRACT

Lessons learned from the Hyogo-ken Nanbu Earthquake of January 17, 1995 and the good performance of seismically isolated structures during this destructive earthquake have persuaded structural engineers, isolator makers and housing construction companies to undertake a cooperative research project to investigate the possibility of introducing seismically isolated structures in Japan's private housing sector. Verification of isolators and base-isolated houses behavior under 3-directional recorded earthquake ground motions has been one of the most important objectives of the project. In order to realize that, 3-dimensional shaking table tests on different types of base isolation systems and on a full-scale, two-story base-isolated house model were conducted. In this paper, characteristics of the newly-developed isolators, the outline of the tests and the latest information about the experimental data-processing progress are presented.

KEY WORDS : 3-dimensional
Shaking Table
Isolators
Houses

1. INTRODUCTION

The January 17, 1995 Hyogo-ken Nanbu earthquake, informally called the Kobe earthquake, severely hit one of the most congested urban cities of Japan, unfortunately located near the fault rupture area. It was one of the worst disasters in the second half of this century, almost commensurate with the great Kanto earthquake which Japan experienced in the first half of this century. The earthquake produced severe building damage. Over 5,000 people were killed due to building collapse resulting from the severe shaking. The earthquake was one of the most devastating and costly natural disasters in recent history considering (a) the number of buildings destroyed, (b) the number of people killed and injured, (c) the size of the affected area and (d) the variability, extent and severity of damage. Scientists and engineers involved in earthquake-related disciplines have been shocked by the damage, deaths and injuries that resulted from this earthquake. As a result, important questions have been raised about earthquake preparedness, disaster response, seismic design, upgrading of earthquake-resistant structures and introduction of new technologies which can assure high safety levels against destructive earthquakes.

In this paper, results of 3-dimensional shaking table tests on recently developed base-isolation systems for houses are presented.

---

1) Head, Structural Dynamics Division, Structural Engineering Department, Building Research Institute, Ministry of Construction, Tsukuba-shi, Ibaraki-ken, 305-0802, Japan
2) Director, IISEE, Building Research Institute, Ministry of Construction, Tsukuba-shi, Ibaraki-ken, 305-0802, Japan
3) Director, Codes and Evaluation Research Center, Building Research Institute, Ministry of Construction, Tsukuba-shi, Ibaraki-ken, 305-0802, Japan
4) JSPS Research Fellow, Institute of Engineering Mechanics and Systems, University of Tsukuba, Tsukuba-shi, Ibaraki-ken, 305-8573, Japan

These tests were conducted primarily with the purpose of investigating a) the effect of bi-directional and vertical earthquake motions on characteristics of isolators, b) the effect of mass eccentricity, c) the displacement control device effectiveness and d) the seismic performance of a base-isolated house model.

2. DEVELOPMENT AND POPULARIZATION OF BASE ISOLATION SYSTEMS FOR HOUSES

As in the case of Northridge earthquake of January 17, 1994, during Kobe earthquake as well seismically-isolated structures performed quite well. That was clearly noticed from the observed earthquake response of two base-isolated buildings constructed in Kobe city[1]. In a 6 story steel-encased reinforced concrete base-isolated structure the ratio of maximum acceleration response of first and sixth floor to that of the foundation were 0.35 and 0.34 respectively, demonstrating thus the great effectiveness of base isolation in reducing the acceleration response of structures and consequently the seismic forces acting on them.

The good performance of base-isolated structures during the Kobe earthquake caused a prompt increase in construction of base-isolated buildings [2]. The number of this kind of buildings designed and constructed by the end of 1995 was almost equal to the total number of base-isolated buildings constructed during the period 1985-1994. The year 1996 marked a record. The number of base-isolated structures designed and constructed during this year was more than twice of that reported for the year 1995.

However, base-isolated residential housing is not yet popular in Japan [3,4]. Several factors account for this[4].

a) Relatively Small Weight of Residences

As it is well known, the fundamental principle applied to seismically-isolated structures is the elongation of the natural period in order to reduce the acceleration response and consequently the earthquake forces acting to the structure. This can be achieved either by increasing the weight of the structure or by decreasing its stiffness. The latter is widely applied in mid-rise buildings because of its effectiveness in achieving the goal. Due to the large weight of mid-rise buildings, a slight decrease of the stiffness caused by the installation of laminated rubber bearings at the base of the building structure easily produce considerable period elongation. But this cannot be done so easily in case of light residences. To compensate for their relatively light weight, rather flexible laminated rubber bearings need to be used. In doing so, special attention must be paid to avoid buckling, otherwise other types of isolators (such as sliding or rolling) need to be developed to deal properly with this problem.

b) Habitability During Strong Winds

In case of low, light-weight residences, the impact of earthquake and wind forces have comparable importance on this type of structures. Therefore, besides the reduction of acceleration response through the installation of isolators at the base of the building structure, proper measures need to be taken in order to assure the habitability and comfort during strong winds or typhoons.

c) First Floor and Foundation Reinforcement

In common residential construction (without base-isolation), the weight of building is transferred to the foundation through sills, which are directly laid on the continuous foundation (Fig. 1a). In case of base-isolated residences (Fig. 1b) an additional horizontal frame of girders is needed to carry the weight of the building and transfer it to the foundation through the isolators. Therefore, individual foundation under each isolator, mat foundation or reinforcement of the ordinary continuous foundation is required. This, together with the reinforcement of the first floor, requires extra labor and materials, and consequently lead to additional cost.

d) Cost Performance

Cost performance remains a very important issue. The total cost of base isolation system for residences (isolators plus the reinforcement of the first floor and the foundation) is considerable. Isolator makers and house builders estimate it to be roughly 1/5 - 1/4 of the total cost of ordinary residences without base isolation. Therefore, further efforts are needed to reduce the cost of base isolation systems, including standardization of isolators and simplification of building configuration.

In order to achieve the target performance for the isolators and base-isolated residences, isolators' makers have been focusing on the development of new types of devices which are presented in the following section.

3. FUNDAMENTAL CHARACTERISTICS OF NEWLY-DEVELOPED ISOLATORS

Seven new types of isolators, designated here as R, S, T, U, W V and X, were developed by different makers. Based on the fundamental concepts used for developing each of them, they can be grouped in three systems :

a) - Rubber bearing system : W
b) - Sliding system : S, U
c) - Rolling system : R, T, V, X

Fundamental characteristics of each isolator are shown summarized in Fig. 2.

Rather flexible laminated rubber bearing is used in case of isolator type W (Fig. 2) and in order to prevent buckling phenomena the outer diameter is increased by designing a hollow in the center. Furthermore, in order to achieve a relatively higher equivalent damping oil dampers are added to the system. The two isolators belonging to the sliding system, S and U, are principally designed to absorb the energy through friction, but their mechanical realizations are different. While the former uses the friction between flat surfaces as well as high damping rubber to achieve the desired characteristics, the latter uses a simpler and more compact mechanism : the friction between two spherical surfaces and a sliding cylinder (Fig. 2). In case of isolators belonging to the rolling system, the R and T types are designed on the basis of a combination between ball bearing and high damping laminated rubber, providing an equivalent damping coefficient of 26.9% and 20%, respectively. The isolator V is based on a combination of ball bearing with a spherical surface. Although the isolator type X belongs to the rolling system, the concept used to develop it is different from the isolators R, T and V. In order to achieve its target performance in terms of restoring force characteristic and equivalent damping, curved rail is used in combination with friction resisting shafts and wheels.

4. OUTLINE OF 3-DIMENSIONAL SHAKING TABLE TESTS

Verification of isolators and base-isolated houses behavior under recorded earthquake ground motions has been one of the most important objectives of the project. In order to realize that, 3-dimensional shaking table tests on different types of base isolation systems and on a full-scale, two-story base-isolated house model were conducted.

4.1 Shaking table simulation capabilities

Tests were performed on a large-scale three-dimensional shaking table recently installed at the Public Work Research Institute of Ministry of Construction [5]. This shaking table is specially designed for simulating earthquake ground motions of the same intensity as those ones recorded during the Northridge Earthquake of January 17, 1994 or Kobe Earthquake of January 17, 1995. In order to give a clearer image about the simulation capabilities of this shaking table, its specifications are shown in Table 1 [5].

4.2 Experimental setups and instrumentation

Two experimental setups were used during shaking table tests. The one shown in Fig. 3 was used for testing different types of base-isolation systems under one-, two- and three-directional earthquake excitations, providing thus the experimental data base necessary for the investigation of the effect of bi-directional and vertical earthquake motions on characteristics of isolators, the effect of mass eccentricity and the effectiveness of the displacement control device. The other experimental setup shown in Fig. 4 was used for investigating the seismic performance of a full-scale, two-story base-isolated house model. In Fig. 5 is shown schematically how the experimental setup presented previously in Fig. 4 was rearranged in order to create various conditions of mass/weight distribution in the system, i.e. balanced weight (top), unbalanced weight Case 1 (middle) and unbalanced weight Case 2 (bottom).

The input-output for each of the experimental setup shown in Fig. 3 and Fig. 4, was monitored through 50 and 74 channels, respectively. As it is shown both in Fig. 3 and Fig. 4, accelerometers (strain-gauge type), velocity transducers (servo type) and displacement transducers (servo type, reel type, and laser type) were installed on the specimens.

4.3 Earthquake input motions used

Strong ground motions recorded during the El Centro Earthquake of 1940 and Kobe Earthquake of January 17, 1995 (JMA Kobe Station record) were used as input motions at the shaking table. Based on the peak ground velocity value observed in each record, the input earthquake waves were proportionally adjusted to various intensity levels. The following correspondence between the horizontal components of the recorded motions and the geometrical axes of the specimens (see Figs. 3 and 4) was applied : EW→X and NS→Y. In addition, in order to see the effect of vertical component of earthquake ground motion on the restoring force characteristics of different types of isolators, a special case of three-directional earthquake excitation was also considered, where only the vertical component of input motion was doubled.

4.4 Tests series

Series of tests conducted for each type of isolator are summarized in Table 2. The O sign inside the table cells indicates that for the corresponding type of isolator that category of test was conducted. As it can be seen from this table, two- or three-directional tests and the tests related to the various unbalanced weight conditions were conducted for almost all types of isolators, providing thus a basis for comparing the experimental results obtained from different types of base-isolation systems.

5. RESULTS OF THE TESTS AND DISCUSSION

Results presented hereafter will mainly cover the aspects mentioned previously in section 1. Nevertheless, it is important to mention here that all experimental results obtained from three-dimensional shaking table tests confirmed the beneficial effect of isolators in reducing the acceleration response of base-isolated system. As an illustration, in Fig. 6 are shown the input motion in the Y direction (a) and the corresponding acceleration response wave of base-isolated system (b), for the isolator type U. A remarkable reduction of the acceleration response can be easily noticed.

5.1 Effect of bi-directional and vertical earthquake input motion

In order to investigate the effect of bi-directional and vertical earthquake ground motion on dynamic response characteristics of isolators, one-directional (X,Y), bi-directional (XY,YZ) and three-directional (XYZ,XYZ2) earthquake excitations (El Centro 1940, Kobe JMA 1995) were applied as input motions to the shaking table. The above mentioned symbol

XYZ2 corresponds to a special case of the three-directional excitation, where the vertical component only was doubled.

For convenience, the isolator type T, U and W are referred to in the following results. They are considered as representative types for rolling system, sliding system and rubber bearing system, respectively.

In Fig. 7 are shown the displacement-shear force coefficient relations of Y-direction, for one-directional (Y) (a), bi-directional (XY) (b) and three-directional (XYZ2) (c) Kobe JMA input motion, adjusted to a peak ground velocity of 50cm/s. Comparing first graphs shown in Figs. 7 a) and 7 b), barely any significant difference can be seen between the results obtained by one- and two-directional earthquake excitations. In case of three-directional excitation (Fig. 7 c)), notches superimposed over the main acceleration response can be easily noticed, demonstrating thus the way the vertical component of input motion is expected to affect the restoring force characteristics of newly-developed base-isolation systems for houses.

In order to examine further the effect of vertical component of input motion on the acceleration and displacement response of base-isolation system, peak horizontal acceleration response - peak vertical input acceleration and peak horizontal displacement response - peak vertical input acceleration relationships are drawn in Fig. 8 and Fig. 9, respectively. Peak horizontal acceleration response and peak horizontal displacement response values referred to the vertical axes of Figs. 8 and 9, represent the composed peak response values of acceleration and displacement. Peak vertical input acceleration values referred to the horizontal axes of Figs. 8 and 9, represent the maximum acceleration observed in the vertical component of input motions applied to the shaking table in case of bi-directional (XY) and three-directional (XYZ,XYZ2) Kobe JMA excitations, adjusted to a peak ground velocity of 50cm/s. Looking first at the results shown in Fig. 8, it can be noticed that for the isolator type U and W the increase of vertical input acceleration is associated with a slight increase of horizontal acceleration response. For the isolator type T the same tendency appears to be valid up to a certain level of vertical input acceleration, after that, at a doubled level of vertical input acceleration, the horizontal acceleration response drops slightly. In case of horizontal displacement response (Fig. 9), the increase of vertical input acceleration either doesn't affect at all the displacement response in the horizontal direction (isolator type W) or is associated with a slight drop at a doubled level of vertical input acceleration (isolator type T and U).

5.2 Effect of mass eccentricity

Based on the experimental setup shown previously in Fig. 5, series of tests were conducted (see Table 2) with the purpose of investigating the effect of mass eccentricity on the response of different base-isolation systems. During these tests, El Centro 1940 and Kobe JMA input motions were adjusted to two intensity levels : 25cm/s and 50cm/s.

In Fig. 10 are shown compared the displacement response waves for two extreme cases of weight distribution in the system : balanced weight (ECC0) and unbalanced weight Case 2 (ECC2). Here again, previously mentioned representative types for rolling system, sliding system and rubber bearing system are considered. The first thing which can be noticed from these results is that, for the three types of isolators, the ECC0 response waves are almost similar with those corresponding to the ECC2 case. In addition, in case of unbalanced weight (ECC2) the peak displacement response of the heavier side is larger than that of the lighter side. This can be also noticed from the results shown in Fig. 11, where the horizontal axis is referred to the gravity center location or mass eccentricity ratio, while the vertical one to the maximum displacement response. Larger values of peak displacement response have resulted for the heavier side compared to the lighter one. Furthermore, as the mass eccentricity increases

the difference between the maximum responses of the heavier and lighter side becomes larger, particularly for laminated rubber bearing type and rolling type of isolator. Finally, in order to see the effect of mass eccentricity on the torsional response of the base-isolation system, the maximum torsional angle(MTA) is plotted against mass eccentricity ratio (Fig. 12). From these results it can be noticed that, as the mass eccentricity increases the MTA increases, being this tendency relatively stronger for the rolling type of isolators.

5.3 Effectiveness of displacement control device

An important issue in dealing with base-isolated systems is the displacement control. Certainly, the base-isolation reduces remarkably the acceleration response, but on the other hand it leads to a larger displacement response, which must be kept within the allowable limits determined in accordance with the mechanical characteristics of isolators.

In this section, results obtained from shaking table tests on a base-isolation system (see isolator type W in Fig. 2) additionally equipped with a displacement control device (DCD) are presented. A schematic drawing of DCD is shown in Fig. 13. As it can be noticed from this figure, the contact between the outer cover and the rubber bumper is expected to happen when the displacement response of the base isolation system reaches 150mm. For displacement response values larger than 150mm the isolation-system and DCD will interact together, demonstrating thus the dynamic characteristics of the combined system as a whole, i.e. isolators+DCD. In order to examine the behavior of the combined system at different levels of input motion intensity, three-directional Kobe JMA input motion was adjusted to the following intensity levels : 50, 60, 70, 80 and 90cm/s. For each input level, maximum acceleration and displacement response values in a two-dimensional plan were determined and by making use of respective maximum input acceleration (observed during the tests) the graphs shown in Figs. 14 and 15 could be drawn. For comparison reasons, analytically simulated results for the case of base-isolation system without DCD are also shown. Results presented in both figures indicate that the base-isolation system starts to interact with DCD at the input motion intensity levels higher than 70cm/s (respectively 794gal of maximum input acceleration). At the input motion level of 80cm/s (respectively 936gal), DCD has effectively restraint the displacement response up to an amount of 6mm, without any sudden increase in the acceleration response (Figs. 14 and 15). At the input motion level of 90cm/s (respectively 1089gal), a sharp increase in the acceleration response is observed (Fig. 14), while the displacement response is restraint nearly 12mm (Fig. 15). What was mentioned above for the sharp increase in the acceleration response can be clearly noticed from the acceleration-displacement response relation shown in Fig. 16.

5.4 Seismic performance of a base-isolated house model

Based on the experimental setup shown previously in Fig. 4, two series of tests on a full-scale, two-story non- and base-isolated house model were conducted (see Table 2) with the purpose of investigating the effect of base isolation on the response of superstructure.

In Fig. 17 are shown summarized peak acceleration responses for the non-isolated house model and the base-isolated one due to El Centro 1940 (a) and Kobe JMA (b) input motions, adjusted to a peak ground velocity of 50cm/s. In both cases, a remarkable effect of base-isolation in reducing the acceleration response of superstructure can be noticed.

6. CONCLUDING REMARKS

Three-dimensional shaking table tests on recently developed base-isolation systems for houses and on a full-scale, two-story base-isolated house model were conducted. These tests were primarily conducted with the purpose

of investigating the effect of bi-directional and vertical earthquake motions on characteristics of isolators, the effect of mass eccentricity, the effectiveness of displacement control device and the seismic performance of a base-isolated house model. The most relevant observations made in the previous section are summarized as follows :

1. No significant difference could be observed between the results obtained by one- and two-directional earthquake excitations. Although dependent on the characteristics of isolators, the effect of vertical motion on horizontal responses is not remarkable.

2. As the mass eccentricity increases the difference between the maximum response of the heavier and lighter side of the system becomes larger, particularly for laminated rubber bearing type and rolling type of isolator. The maximum torsional angle response increases with the increasing mass eccentricity, being this tendency relatively stronger for the rolling type of isolators.

3. Displacement control device (DCD) could effectively restrain the displacement response up to an input motion intensity level of 80cm/s. At a higher level of input motion intensity, a sudden increase in the acceleration response was observed, suggesting thus that in the design of DCD-s the effect of input motion intensity should be carefully treated.

4. Two series of tests on a full-scale, two-story non- and base-isolated house model demonstrated clearly the remarkable effect of base-isolation in reducing the acceleration response of superstructure.

7. ACKNOWLEDGMENTS

The authors would like to express their sincere thanks to all the members of the committee on "Development of seismically isolated houses", the chairman of which is Mr. Shoichi Yamaguchi, president of Tokyo Kenchiku Structural Engineers, for providing data and valuable suggestions related to this study. In addition, the kind assistance of Dr. Keiichi Tamura and Mr. Takuo Azuma, respectively Head and Research Engineer of the Ground Vibration Division at the Earthquake Disaster Prevention Research Center of Public Work Research Institute in Tsukuba, in operating the large-scale three-dimensional shaking table is greatly appreciated.

8. REFERENCES

[1] The Building Center of Japan : Base-isolated buildings - Technical development and earthquake motion observation records, Part 2, June 1995 (in Japanese).

[2] Kitagawa Y. : Future view of base-isolated buildings in Japan, The Kenchiku Gijutsu, March 1999, pp. 116-117 (in Japanese).

[3] Yamanouchi H., Midorikawa M. and Iiba M. : Research and development on base-isolation technologies for houses - A survey on the performance based evaluation of base-isolated houses and shaking table tests on model houses, Kenchiku Kenkyu Shiryo, No. 89, March 1997 (in Japanese).

[4] Iiba M. et al. : Research on performance of base-isolated house, Proceedings of the Second World Conference on Structural Control, Kyoto, Japan, June 1998, Volume 2, pp. 1119-1126.

[5] Public Work Research Institute : Large-scale three-dimensional shaking table, Public Work Research Institute, Ministry of Construction, 1997.

Table 1 Specifications of shaking table used

Item	Specifications
Table size	8m x 8m
Loading Capacity	Rated 100tf Max. 300tf
Maximum displacement	Horizontal ±60cm Vertical ±30cm
Maximum velocity	Horizontal ±200cm/s Vertical ±100cm/s
Maximum acceleration*	Horizontal ±2G Vertical ±1G
Exciting frequency	DC～50Hz

* For 100tf loading.

Table 2 Series of tests conducted

Isolator type	Balanced weight		Unbalanced weight	Displacement control device	Triggering device
	2 or 3 directional input motion	*Doubled vertical input motion*			
R	○		○	○	
S	○		○	○	
T	○	○	○	○	○
U	○	○	○		
V	○		○	○	
W	○	○	○	○	
X	○[a]	○		○	
	○[b]				

[a] Test on a base-isolated house model ; [b] Test on a non base-isolated house model

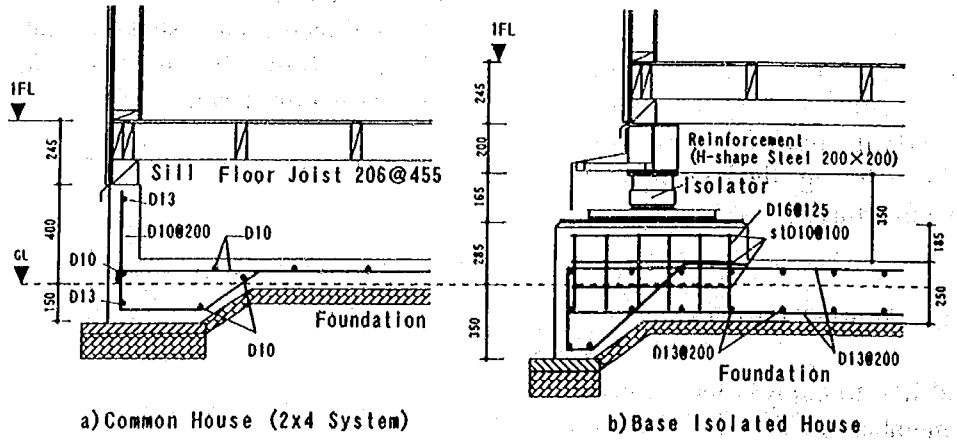
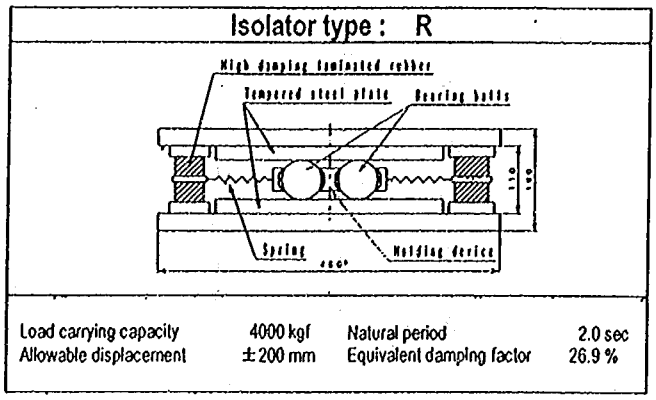
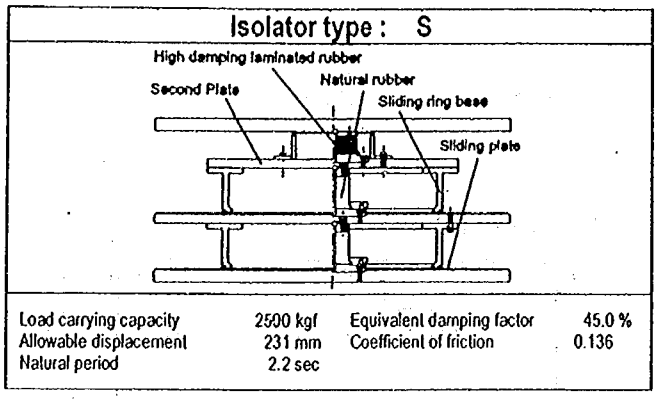
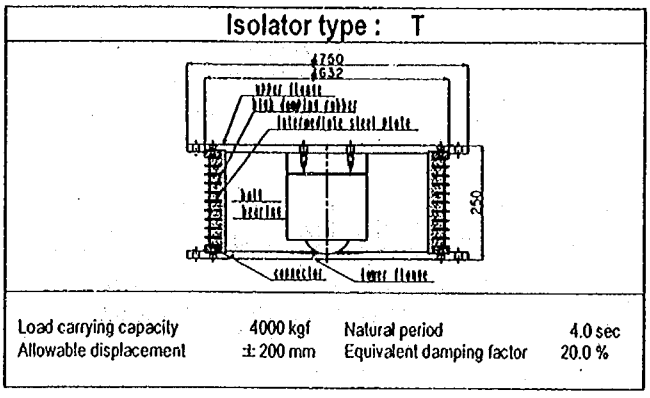
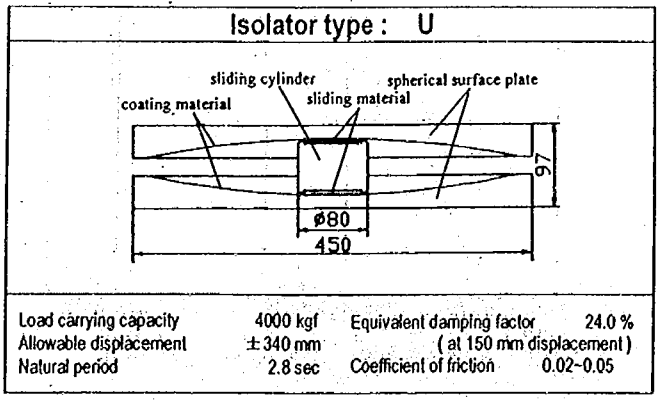


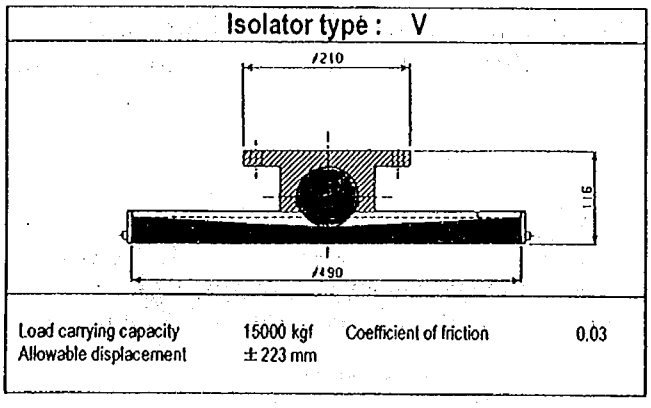
Fig. 1. First floor and foundation design for a common house (a) and a base-isolated one (b).

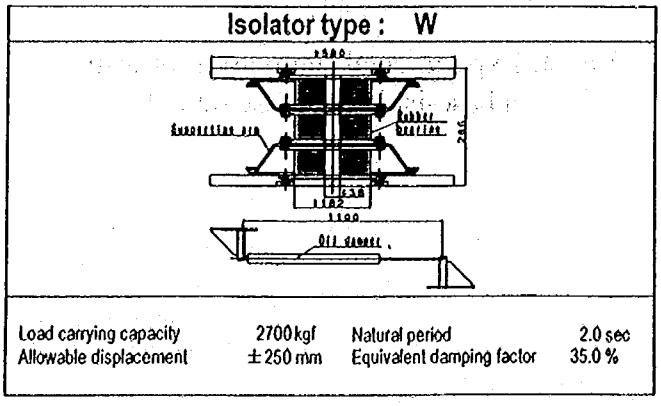












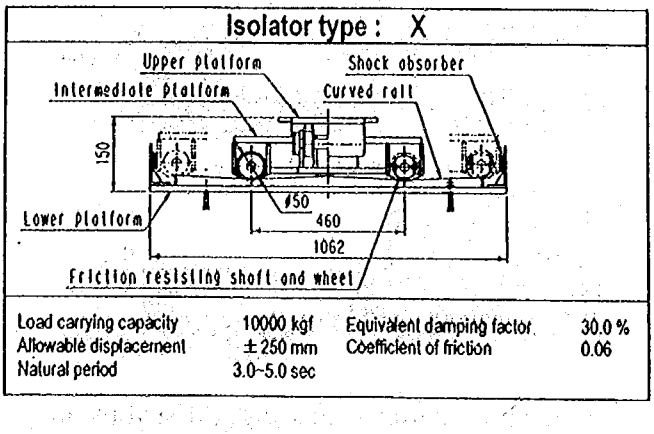


Fig. 2. Fundamental characteristics of newly-developed isolators.

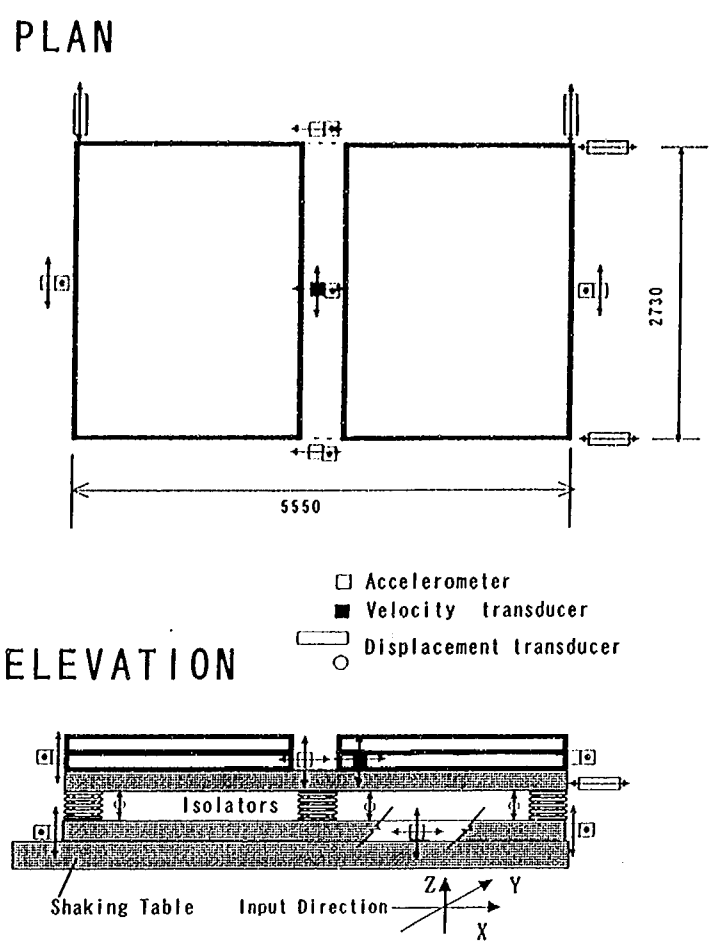


Fig. 3. Experimental setup used for testing different types of base-isolation systems.

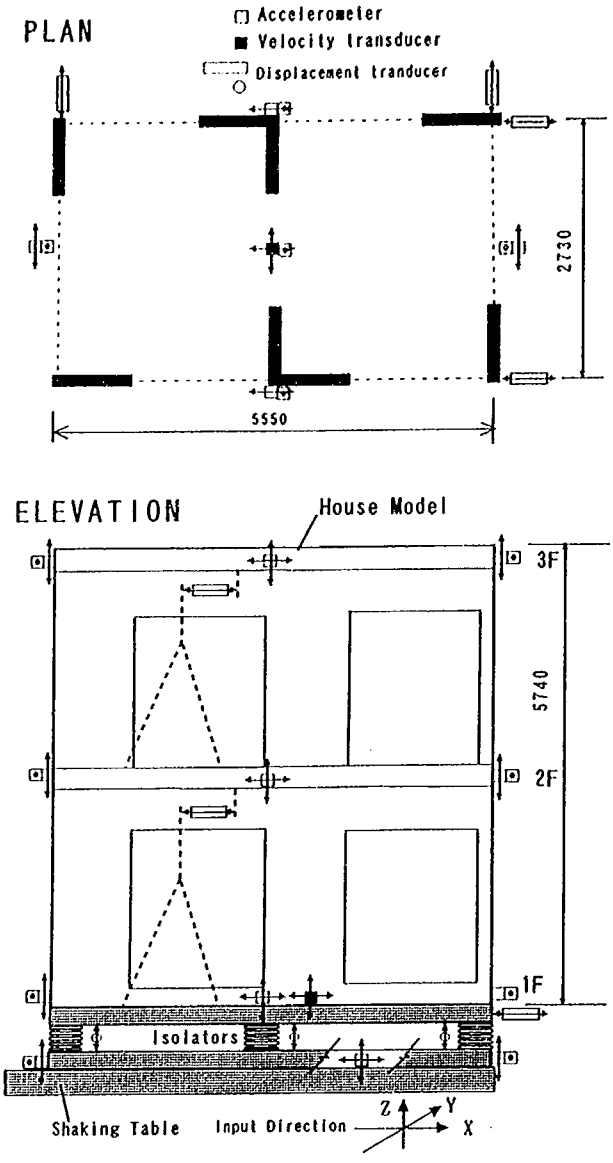


Fig. 4. Experimental setup used for testing a base-isolated house model.

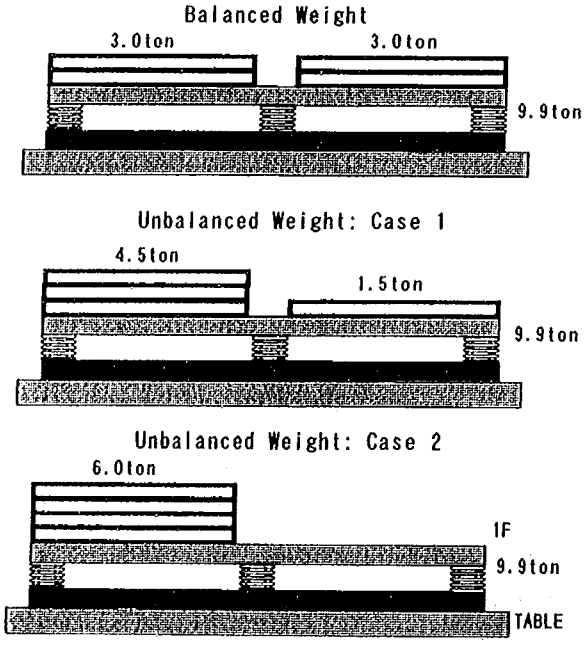
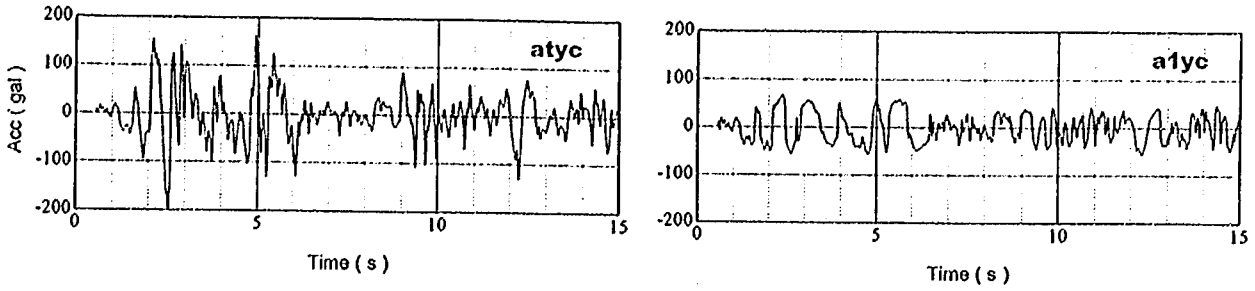
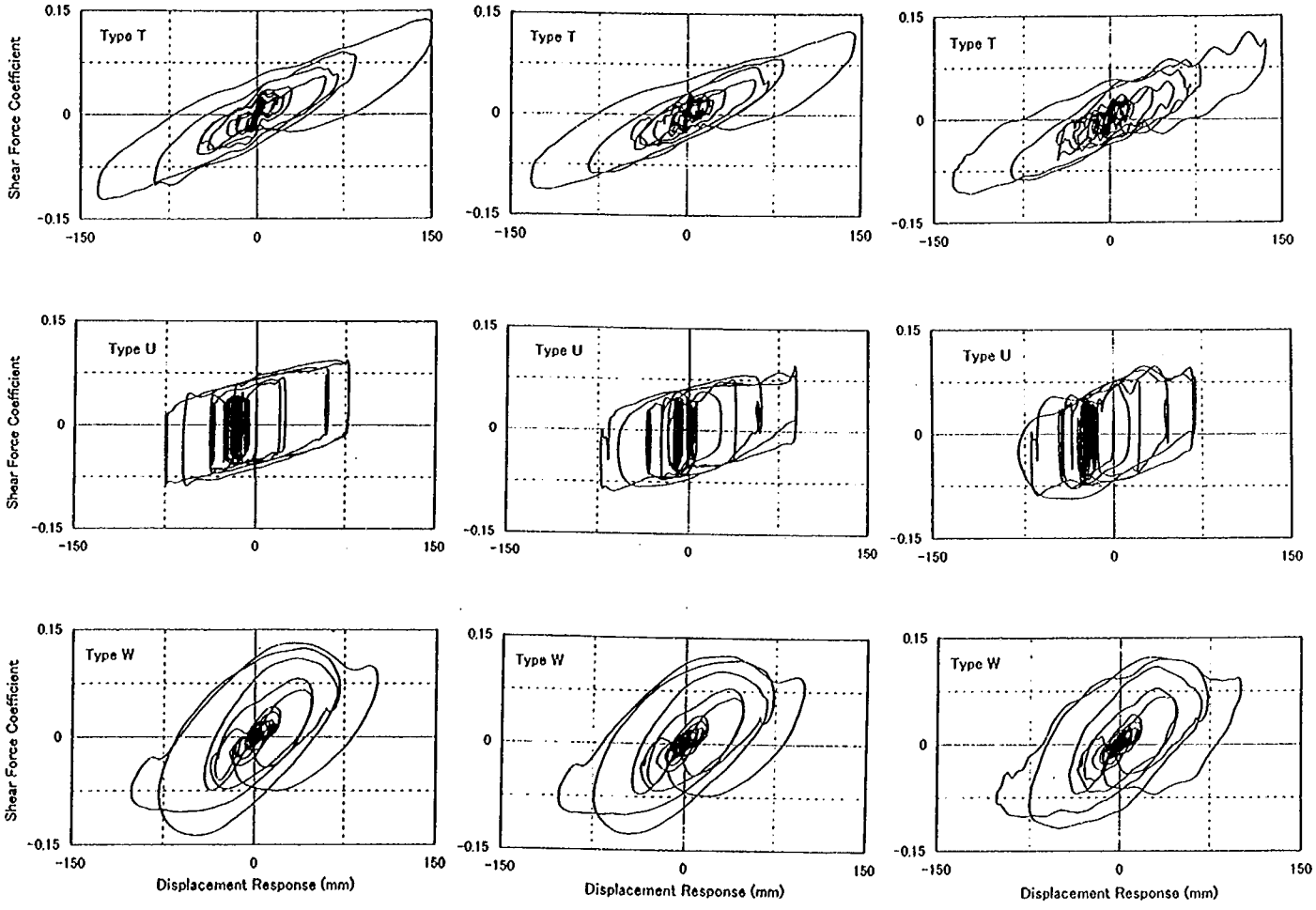


Fig. 5. Three patterns of weight distribution in the system.



a) Input motion. b) Acceleration response wave.

Fig. 6. Input motion in the Y direction (a) and the corresponding acceleration response wave of base-isolated system (b), for the isolator type U.



a) One-directional (Y). b) Two-directional (XY). c) Three-directional (XYZ2).

Fig. 7. Displacement-shear force coefficient relations of Y-direction, for one- (a), two- (b) and three-directional (c) Kobe input motion, adjusted to a peak ground velocity of 50cm/s.

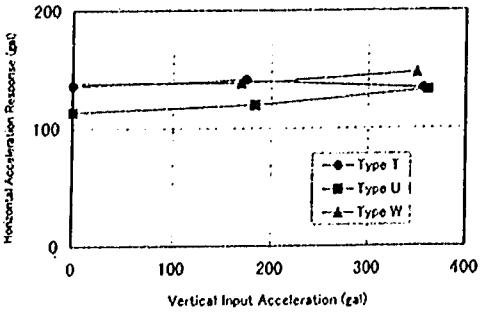


Fig. 8. The relation between peak horizontal acceleration response and peak vertical input acceleration.

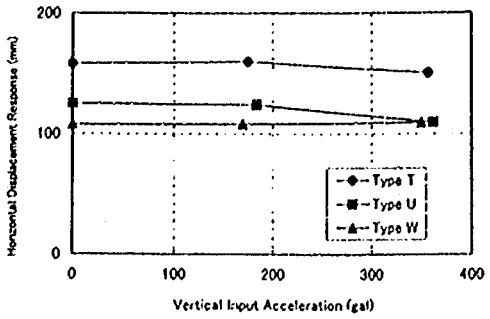


Fig. 9. The relation between peak horizontal displacement response and peak vertical input acceleration.

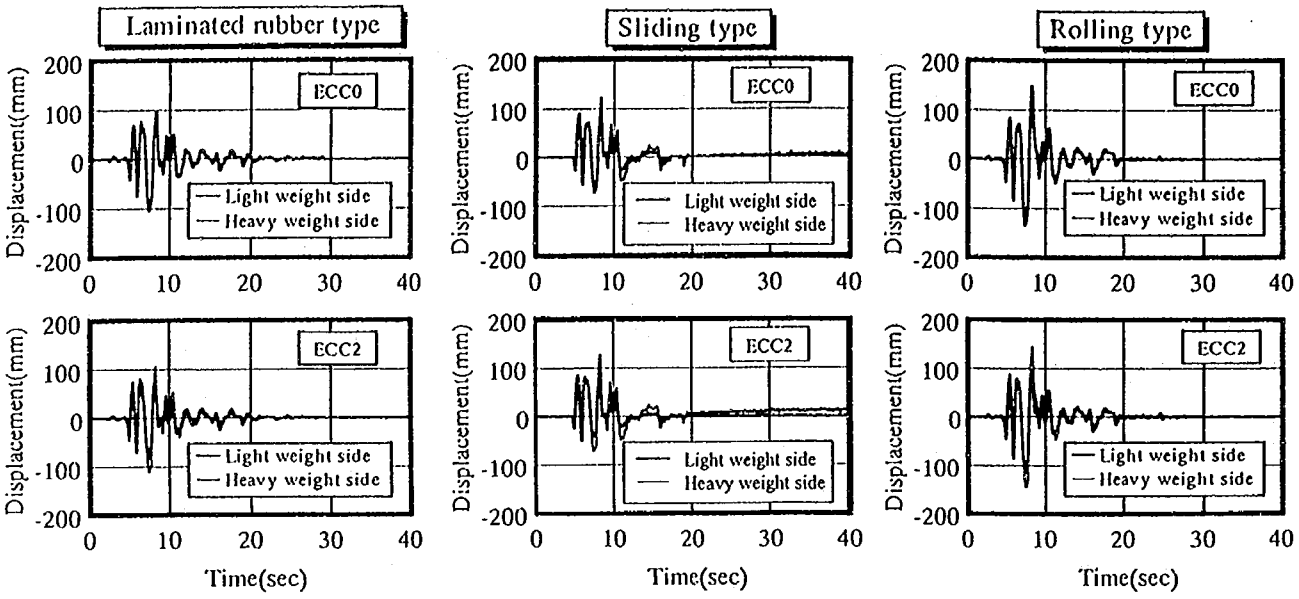


Fig. 10. Displacement response waves for two extreme cases of weight distribution in the system.

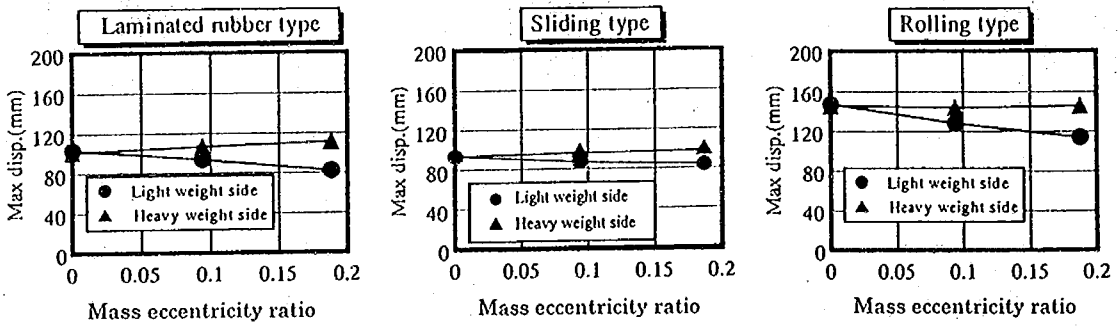


Fig. 11. Maximum displacement response versus mass eccentricity ratio.

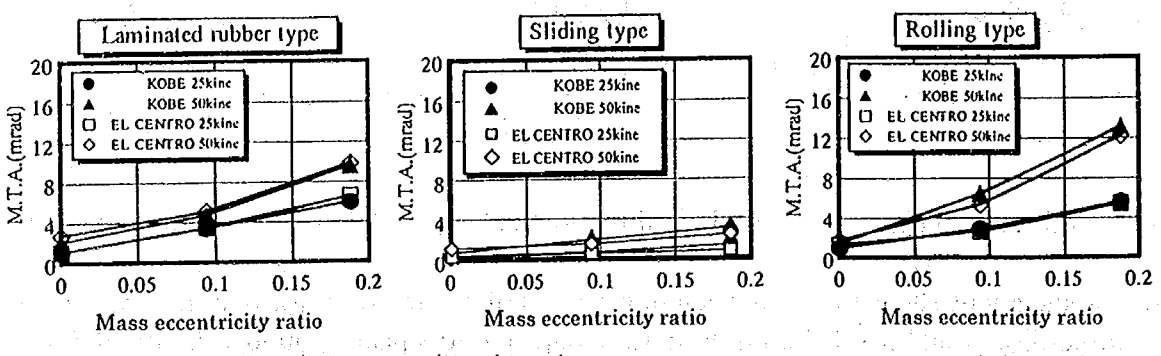


Fig. 12. Maximum torsional angle response versus mass eccentricity ratio.

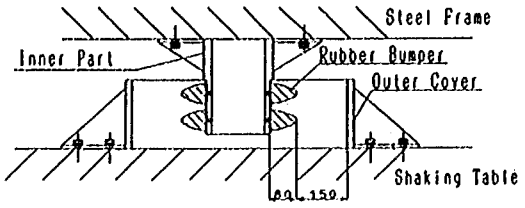


Fig. 13. A schematic drawing of DCD.

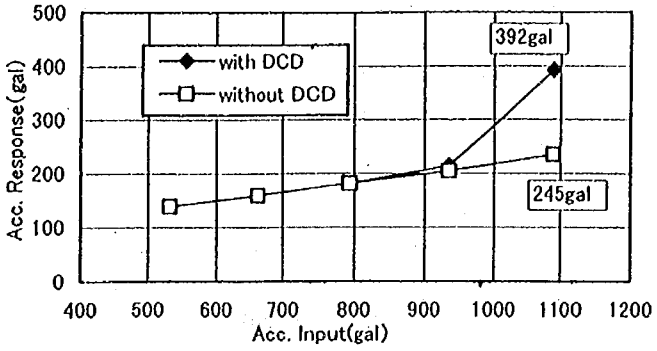


Fig. 14. Effect of DCD on acceleration response variation.

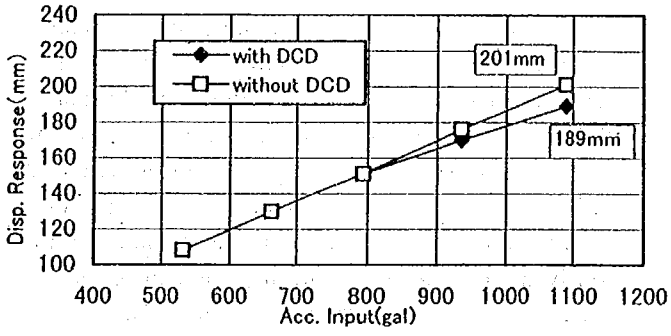


Fig. 15. Effect of DCD on displacement response variation.

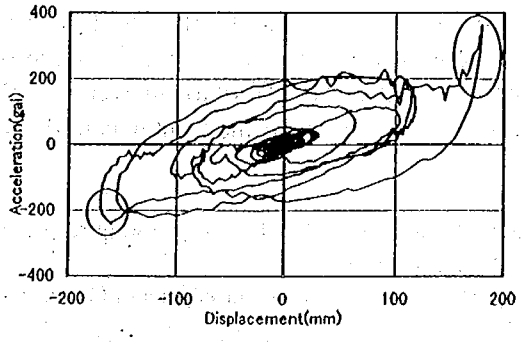
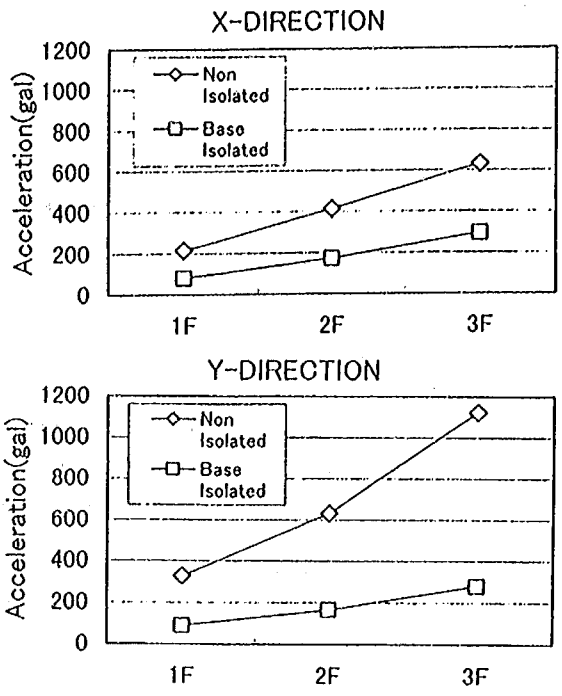
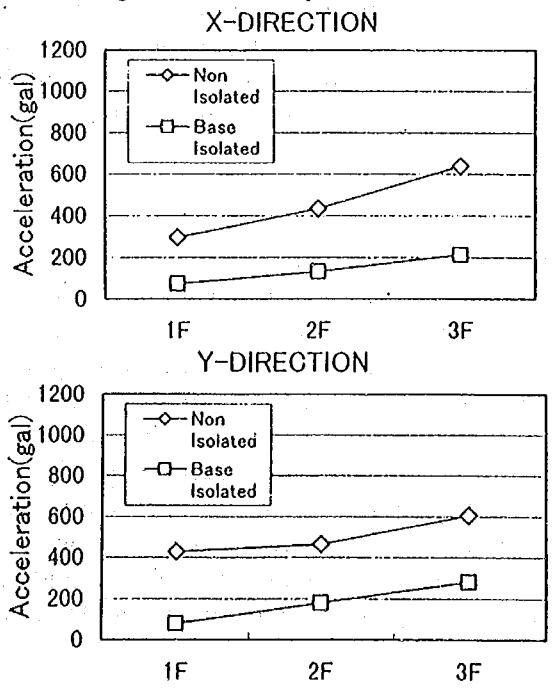


Fig. 16. Displacement-acceleration response relation for Kobe JMA 90cm/s.



a) El Centro 1940 adjusted to a peak ground velocity of 50cm/s.



b) Kobe JMA 1995 adjusted to a peak ground velocity of 50cm/s.

Fig. 17. Peak acceleration responses for the non base -isolated house model and the base-isolated one.

Application of Advanced Technologies in Seismic Protection of Critical Facilities An MCEER Program

by George Lee[1], Michel Bruneau[2], Masanobu Shinozuka[3], and Kathleen Tierney[4]

ABSTRACT

The Multidisciplinary Center for Earthquake Engineering Research (MCEER) has established a coordinated system-integrated research effort to discover, nurture, develop, promote, help implement, and in some instances pilot test, innovative measures and advanced and emerging technologies to reduce losses in future earthquakes in a cost-effective manner. The focus of this research is on critical facilities, such as hospitals, and lifelines. A broad range of technologies are being investigated through this research initiative, and this paper provides a brief overview of some of the technologies currently considered.

KEYWORDS: Advanced technologies, seismic protection, critical facilities, retrofit, loss assessment, emergency preparedness, emergency response, structural engineering, lifeline engineering, geotechnical engineering.

1. INTRODUCTION

Earthquake losses in recent years have exceeded $30 billion in direct costs in California alone and are expected to rise at an escalating rate in future years unless major loss reduction programs are undertaken. Past experience makes it clear that the immediate threat to society lies in existing, seismically vulnerable infrastructure and critical facilities, and that current response and recovery programs are often overwhelmed by unprecedented demands. But rehabilitation and effective response remain elusive goals because both are impeded by a lack of detailed knowledge about seismic hazards, an incomplete understanding of the complex behavior of structures and lifelines during extreme events, and societal impediments to launching a comprehensive loss reduction program. Furthermore, the high costs of conventional rehabilitation schemes are a serious disincentive, except perhaps to households, governmental entities, and organizations in the most active seismic zones.

Reducing the cost of rehabilitation, improving its reliability and removing barriers to implementation will substantially reduce future earthquake losses. Recent developments in advanced technologies offer great promise in this regard while at the same time offering a higher level of performance than is possible with conventional techniques. Furthermore, powerful new methodologies for quantifying expected losses make it possible to better characterize risks and to analyze the costs and benefits of alternative loss-reduction strategies, opening the door to meaningful incentives and the adoption of new advances in risk management. These same tools can be applied to strategic disaster planning and early damage assessment and thus improve the effectiveness of emergency response and crisis management.

Within this perspective, the Multidisciplinary Center for Earthquake Engineering Research (MCEER) has established a coordinated system-integrated research effort to answer the above needs. The mission of the Center is to discover,

[1] Director, Multidisciplinary Center for Earthquake Engineering Research, 100 Red Jacket Quadrangle, State University of New York at Buffalo, Buffalo, NY 14261. (Web: mceer.buffalo.edu).

[2] Deputy Director, Multidisciplinary Center for Earthquake Engineering Research, 100 Red Jacket Quadrangle, State University of New York at Buffalo, Buffalo, NY 14261.

[3] MCEER Research Committee Program Coordinator, Fred Champion Chair in Civil Engineering, University of Southern California, 3620 S. Vermont Ave. KAP 254, Los Angeles, CA 90089.

[4] MCEER Research Committee Program Coordinator, co-director of Disaster Research Center, University of Delaware, 77 E. Main St., Newark, DE 19711

nurture, develop, promote, help implement, and in some instances pilot test, innovative measures and advanced and emerging technologies to reduce losses in future earthquakes in a cost-effective manner.

Advanced technology research at MCEER includes innovative applications of:

- engineered systems and materials,
- scientific methodologies, and,
- concepts and analytical approaches

that have not traditionally been used in earthquake engineering and loss reduction problems, with an emphasis on applications which require a multidisciplinary effort.

This mission of the Center is predicated on the premise that the future of earthquake engineering lies in advanced and emerging technologies and associated innovative measures. These include, but are not limited to:

- site remediation technologies,
- structural control and simulation,
- high performance materials,
- condition assessment technologies, including technologies for estimating both potential and actual earthquake losses
- decision support systems.

However, the Center also recognizes that societal barriers to loss reduction and adoption of new technologies are real and substantive, and that they must be overcome before progress can be made. Thus, a significant effort is undertaken to address these impediments and discover rational workable incentives that accelerate the adoption of loss reduction programs and realize the potential that these exciting new technologies have to offer.

2. VISION AND RESEARCH PROGRAM

The ultimate vision of the Center is to help establish earthquake resilient communities. The Center progresses toward that goal through an interdisciplinary and coordinated research program, emphasizing fundamental and applied research combined with sustained and systematic education, outreach, and implementation efforts.

In this paper, only research activities are summarized.

The goals of the Center's activities in research are pursued through the following four major research thrusts:

2.1 Advancement of loss estimation methodologies for the quantification of building and lifeline performances in future earthquakes.

The first of these research thrusts is to develop the next generation of loss estimation methodologies, and to use them to quantify the threat to the built environment. These more efficient methodologies are key to the other two research thrusts involving the rehabilitation of critical facilities and response planning, crisis management and recovery. The development of real time remote sensing to rapidly assess earthquake damage, the study of socio-economic barriers against the mitigation of loss reduction measures, and the development of incentives for the implementation of new knowledge in loss reduction also support the objectives of this program.

2.2 Development of cost-effective, performance-based, rehabilitation technologies for critical facilities.

The second thrust is to identify, explore and develop advanced technologies for the rehabilitation of selected critical buildings and lifelines to meet or exceed the high level of performance expected of these facilities that, by definition, must remain operational following a major earthquake. The initial expense of these technologies may be high, but increased implementation based on sustained research efforts is expected to reduce future costs to the point where overall costs will be less than for conventional retrofitting. As in other Center programs, engineering and social science researchers involved in this program work together to identify impediments to rehabilitation and incentives for the adoption of new technologies.

2.3 Improvement of response and recovery through strategic planning and crisis management.

The third thrust focuses on two areas where emergency response and crisis management can be made more effective with the use of advanced technologies. These areas are pre-event strategic planning for immediate response and recovery using loss estimation methodologies, and crisis management involving response coordination, early damage assessment, and search and rescue with an emphasis on the use of advanced technologies.

2.4 User Networks in Facilities and Computation.

The fourth thrust requires MCEER investigators working on projects requiring networking to develop two User Networks, one for experimental facilities and computing environments and the other for computational and analytical resources. The ultimate objective is to make the networks accessible to individual researchers and practitioners sponsored by MCEER or by other research centers. The Facilities Network in Earthquake Engineering (FNEE) focuses on both computational and experimental facilities. It is to be established by linking and coordinating existing resources at member institutions and facilitating access by remote users. The Computational Network in Earthquake Engineering (CNEE) focuses on assembling a full range of analytical resources for the analysis, design, evaluation and testing of structural and lifeline systems including both existing and new software. Addition of this Network provides all MCEER's researchers with up to four levels of sophistication, ranging from basic back of the envelope estimates of critical structural response to high-end continuum approaches to compute time history response simulations.

Figure 1 attempts to illustrate, in a simplified manner, the close interaction that exists between these areas of research. It also shows that all activities lead to a comprehensive education mandate, that is particularly important in those regions of the United States when seismic awareness is generally low.

In the remainder of this paper, some of the advanced technologies that are considered within the MCEER/NSF research program are briefly described, to provide an overview of the type of technology applications being considered. Note that this research is conducted by 28 researchers in 13 affiliated institutions across the United States.

3. ADVANCED TECHNOLOGIES.

3.1 Performance Assessment of the Built Environment

The poor performance of the built environment during recent moderate-to-large earthquakes has been the principal cause for death and injuries and escalating social and economic losses. Thus, it is essential to develop reliable methodologies to assess the seismic performance of the built environment in terms of expected societal and economic loss resulting from a damaging earthquake. Estimated expected loss then becomes an important quantitative measure of the seismic performance of the built environment, providing the analytical basis for cost-effectiveness evaluation for the selection of optimal rehabilitation measures for the existing inventory. The loss estimation methodologies in this context requires information about three major ingredients: hazards, inventory and fragility. This Program generates and integrates the information on these ingredients in order to develop such methodologies by carrying out the following tasks.

Seismic Hazard and Ground Motion: Analytical models for ground shaking to be used for ENA (Eastern North America) earthquake events based on both engineering and seismological approaches are being developed and calibrated with recorded earthquakes in ENA. Current work includes development of response spectral amplitude and study of its sensitivity to magnitude and epicentral distance, and development of scattering function and models for near source ground motions. This is complemented by centrifuge model tests of

liquefaction and lateral spreading to investigate the nature of ground motion due to liquefaction. Seismological studies are also conducted in support of other tasks within MCEER's coordinated research effort, to assist investigators working on generating fragility information, particularly in terms of developing inelastic response spectra considering explicitly the soil behavior in the ground motion time histories and in introducing soil-structure interaction effects into fragility curve construction.

Advanced Technologies for Loss Estimation; Development of Damage Functions using Remote Sensing and Real-time Decision Support Systems: This research involves the review of advanced and emerging technologies with the objective of improving existing loss estimation methodologies. Technologies that are being investigated include: real-time earthquake monitoring systems, early warning systems, GPS technology, interferometric synthetic aperture radar (IFSAR) technology, optical satellite imaging, laser technology (Lidar) and aerial photography. Current work focuses on the development of building inventories for loss estimation using IFSAR and laser (LIDAR) technologies. Pilot studies and calibration are conducted using areas in the Los Angeles basin for the purpose of inventory development. This data permitted to develop "building height signatures" for these pilot areas. Building height signatures are cumulative plots of total building footprint area as a function of building height. These are created for standard grid cell sizes measuring a half a mile by half mile. The results show that depending upon the type of development (residential, commercial, industrial), building or construction density (square footage of ground floors), and distribution of building heights, a building height signature will have varying slopes and intercepts. In addition, for cells that contain a higher percentage of high-rise buildings, the curves will extend out to higher building heights. A comparison of building height signatures developed from the various methods (including the aggregation of data from the county assessor's files) will help to answer the question "can remote sensing methods be used to quantify the number and types of buildings in an urban environment, thereby enhancing or replacing conventional methods of building inventory development that are often costly and sometimes inaccurate. It is expected that the most suitable technologies identified by this research will be mature enough to be utilized in the inventory development and damage assessment studies conducted by other MCEER investigators.

Loss Estimation Methodologies: This research focuses on reliability analysis of a spatially extended system (LA County expressway network). Preliminary assessments are made on the basis of empirically developed fragility curves of bridges. To date, some examples have been used to demonstrate loss reduction using structures based-isolated and not base-isolated. Current work is focusing on the direct cost of damage sustained by individual bridges, buildings and lifeline systems. Selected existing loss estimation methodologies are being reviewed, and a benchmark dataset on losses in recent disasters is being developed. Research is also underway on methodological refinements to analyze the loss reduction potential of advanced technologies and strategies for pre-event rehabilitation and post-event response. In parallel, indirect loss estimates methods rely on the computable General Equilibrium analysis, and considers how influencing various economic factors that appear in the analysis can further reduce economic losses. These various approaches must then be integrated to develop a loss estimation methodologies, involving both direct and indirect, implementable for demonstration projects.

Inventory for LADWP Water Delivery System: Data collection and inventory identification must be accomplished in a digital format that permits consideration of advanced technologies for loss estimates. Hence, to date, the entire 100 km of trunk lines and 11,000 km of distribution pipelines were digitized and incorporated in a GIS model together with topographical, surficial soil and Northridge strong motion and ground water data. On-going work includes information gathering and incorporation into GIS system of the information needed to assess the interactive features of seismic performance of LADWP's water and electric power system. The result will be used for evaluation of loss reduction by system

rehabilitation by advanced technologies in the LADWP demonstration project.

Seismic Reliability Analysis and Retrofit Method for LADWP's Power System: Seismic data collected on the LADWP's power system permitted to improve an original systems analysis computer code (from the power engineering point of view). Work is underway to use a newly acquired flow analysis computer code from EPRI together with the improved systems analysis method, and Monte Carlo simulation assessments of the degradation of system performance under different levels of earthquake intensity, to examine the enhancement of system performance due to rehabilitation of key system components by means of advanced technologies.

Inventory Development for NY Hospitals: Following a workshop held in New York City to define the post-disaster needs of hospital owners/administrators, critical subsystem components, and desired seismic performance criteria, hospitals inventory data is being collected. This work is to support the demonstration project within MCEER's research plan. Further work is also underway to development a consistent hospital performance criteria by involving engineering practitioners and hospital administrators. Analytical models for seismic performance of hospital systems (e.g., fire protection system) is also being developed along with a computer code to identify critical components in these systems.

Development of Fragility Information: Studies here investigate the consequence of various levels of analytical sophistication on the reliability of fragility curves. Work is also underway to develop robust fragility curves for structures, nonstructural components and equipment, to be used by other MCEER researchers. The levels of analysis considered are consistent with (1) design compatible method, (2) response spectrum-based method, (3) analytical method utilizing such computer codes as ABAQUS and DIANA and (4) analytical method with the aid of high-performance computational platform. The results derived from these methods will be compared with one another and calibrated with empirically as well as experimentally obtained fragility curves. These methods will be integrated to form a coherent numerical and analytical procedure for fragility curve development that can be used for demonstration projects. In this context, the resulting coherent procedure will also be used to develop the fragility curves for rehabilitated structures, components and equipment.

Calibration of Fragility Information: This task relies on results from experimental studies to provide calibration of fragility analyses, more specifically shaking table tests at the University of Nevada Reno, and SUNY Buffalo, on pipeline joints and structural frames respectively

Much future work is foreseen on loss estimation methodologies, on identifying what constitute acceptable losses in various contexts, and integrating this multidisciplinary research through a demonstration project using the LADWP's power system, NYC's hospitals, LADWP's water system and Memphis lifeline systems.

3.2 Development of cost-effective, performance-based, rehabilitation technologies for critical facilities

The objective of this research trust is to identify, explore and develop advanced technologies for the rehabilitation of selected critical buildings and lifelines to meet or exceed the high level of performance expected of these facilities. The initial expense of these technologies may be high, but increased implementation based on sustained research efforts is expected to reduce future costs to the point where overall costs will be less than for conventional retrofitting. As part of this research program, engineering and social science researchers work together to identify impediments to rehabilitation and incentives for the adoption of new technologies.

Engineering research focuses on advanced technologies that can be effectively used for seismic retrofit in geotechnical, structural, and lifeline engineering. A schematic of these three separate major sub-objectives is presented in Figure 2.

The geotechnical engineering studies focus on site and foundation remediation technologies to mitigate soil liquefaction. Analytical and experimental centrifuge research investigates how shallow soil around pile caps can be either replaced by frangible materials, or stabilized by the injection of reactive materials. In the short term, this research investigates the adequacy of various materials for those tasks, including expanded polystyrene, light weight fills, crushable materials, as well as various chemical and bacteriological reactives toward the states objectives, and analytical models are developed in support of future experimental work.

The lifeline engineering studies investigate how advanced materials can be used to retrofit the capacity of welded slip joints on critical water trunk lines, and how critical substation power system components can be retrofitted to remain functional immediately following major earthquakes. Demonstration projects with the Los Angeles Water and Power division are imbedded within these two tasks. To date, development of analytical models and testing of non-reinforced specimens has been accomplished, with testing of retrofitted specimens to follow shortly.

The structural engineering part of this program is two-fold. A first task investigates how emerging advanced materials can be used in new seismic retrofit concepts, while a second tasks focuses on new approaches to provide seismic retrofit to critical buildings, i.e. facilities that require to be fully operational following earthquakes. Both tasks focus on hospital buildings at this time, although concepts that can find broad acceptance for other types of critical facilities are also investigated as appropriate. Currently, scissors-jack energy dissipation assembly and various types of advanced engineered composite frame infills are considered for structural retrofits. Non-structural retrofit schemes being considered include tether systems and isolating equipment supports, and reliability analyses are to be conducted and integrated with fragility analyses. Demonstration projects secure participation by the potential beneficiary of this research, and provide the test-beds where all related efforts converge, and where the true multidisciplinary aspects of this research emerges. In the medium term, selected hospitals will provide actual critical facilities against which adequacy, economy, and acceptability of the proposed concepts will be gauged. Such demonstration projects will further tighten the interactions between researchers working in the areas of advanced materials, advanced retrofit strategies, cost-benefit studies, and social sciences.

3.3 Intelligent Response and Optimal Recovery

Pre-earthquake mitigation strategies seek to reduce earthquake losses by implementing measures that prevent or reduce losses. Mitigation strategies include land-use regulations, seismic construction and retrofit codes, and improved engineering practices. Effective mitigation will result in the avoidance of many losses that could result from future earthquakes. However, since current knowledge about earthquakes and their effects on the built environment is incomplete, since major impediments exist that block the adoption of potentially effective mitigation strategies, and since comprehensive loss-avoidance is not economically feasible, earthquakes continue to produce damage and disruption on a very large scale. Additionally, although mitigation measures do provide considerable protection, one of the key features of earthquake disasters (in contrast with "routine" emergencies) is that they produce unanticipated impacts that overwhelm the coping capacities of affected social units. For these reasons, there is a continuing need for robust disaster response and recovery strategies.

Response activities encompass actions taken during and immediately after disaster impact that are designed to protect life and property and control secondary earthquake impacts (e.g., earthquake-induced fires and hazardous materials spills). Response activities must address the need to deal with both agent-generated demands (i.e., problems created by the disaster agent itself, such as injuries and physical damage) and response-generated challenges (i.e., the need for rapid situation assessment and for information on which to base decisions). Examples of response activities include rapid damage detection, search

and rescue, emergency medical care, emergency restoration of essential services, firefighting, emergency communications, and crisis decision making. The federal government, all states, and virtually all communities in the US have plans for responding to major disasters, including earthquakes, although both the quality of these planning efforts and the demonstrated capacity to respond to major disasters varies considerably nationwide.

Recovery activities consist of actions taken to return to (or, ideally, exceed) pre-earthquake levels of activity and productivity. These actions include restoring, repairing, and reconstructing lifelines and buildings, undertaking measures to overcome earthquake-induced economic downturns, and providing financial assistance to compensate for losses. The recovery period is also typically the time in which decisions are made about adopting new mitigation measures, with the long-term objective of increasing the earthquake resistance of the built environment. If undertaken properly, recovery strategies can contain indirect and induced earthquake losses, shorten the recovery period for affected social units, and avoid future losses through improvements in mitigation.

In the US, recognition has grown that it is highly desirable to plan for recovery before an earthquake occurs, and some communities (e.g., the City of Los Angeles) have begun to move in this direction. However, at present, earthquake response planning is much more extensive and more thoroughly institutionalized than recovery planning.

In that perspective, MCEER's Response and Recovery Research Program aims to conduct research on new technologies and technology applications that offer the promise of improving earthquake response and recovery decision making. To accomplish this goal, MCEER investigators will focus on two areas in which recent technological developments appear to have considerable potential for application in response and recovery contexts: remote-sensing, which can be used for rapid post-earthquake damage assessment; and advanced information (IT) and data-management technologies and decision-support systems (DSS).

These technologies are, of course, not truly "new." Remote-sensing technologies, for example, are widely used in defense applications. What MCEER's research seeks to determine are the feasibility and effectiveness of applying these technologies in new ways to address earthquake response- and recovery-related problems. MCEER's research plan is designed to address questions like these: Can remote-sensing technologies produce the kinds of data and information that would enable disaster responders to detect areas of major damage in a more timely and effective manner than they can using currently-available techniques? Is it feasible to use remote-sensing technologies in real-time or near-real time to improve response decision making? Do the agencies and organizations that are charged with responding to earthquakes have the capacity to use new information technologies to manage earthquake disasters, and if not, what would they need in order to be able to do so? How can knowledge about the design and use of decision support systems be used to help agencies improve the quality of their response and recovery decisions? What data needs and user needs are associated with the development of such systems? In what ways can information technologies enhance the ability of governmental units, agencies, and organizations to implement response and recovery plans?

This research is being carried out by investigators with backgrounds in engineering, sociology, public administration, and decision analysis. The studies that are currently being undertaken focus on enhancing post-earthquake response decision making through the use of new technologies.

As part of current research, field work is being conducted in six communities (New York, Memphis, Los Angeles, and one smaller communities in each of those three states) to collect baseline information on information and data management technologies that are currently being used by disaster response agencies and to assess the capacity of these agencies to use more advanced IT and DSS.

Within another project, research is conducted to develop earthquake response decision support systems that take advantage of new advances in computer software and decision analysis and that are tailored to users' needs. This research places a particular emphasis on the uncertainties inherent in crisis decision making and on the value of real-time information in the post-impact crisis response period.

Finally, a last project investigates the feasibility of using synthetic aperture radar (SAR) remote-sensing technologies to rapidly detect earthquake damage by comparing pre- and post-earthquake images of elements in the built environment. If this method proves capable of providing valid damage information, the next step will be to explore the extent to which such information can be used in real-time earthquake response decision making.

4. CONCLUSIONS

This paper has brushed a quick sketch of some of the advanced technologies investigated by the Multidisciplinary Center for Earthquake Engineering Research to reduce losses in future earthquakes in a cost-effective manner. This work is still in the early phases of an ambitious 10-year research agenda that includes fundamental research, technological integration and system development research, and multidisciplinary demonstration projects intended to bring together the various components required to achieve the stated objectives. While much of this research focuses on critical facilities, it is expected that the benefits from this research will prove transferable to other types of engineered work and facilities, thus leveraging the initial benefits.

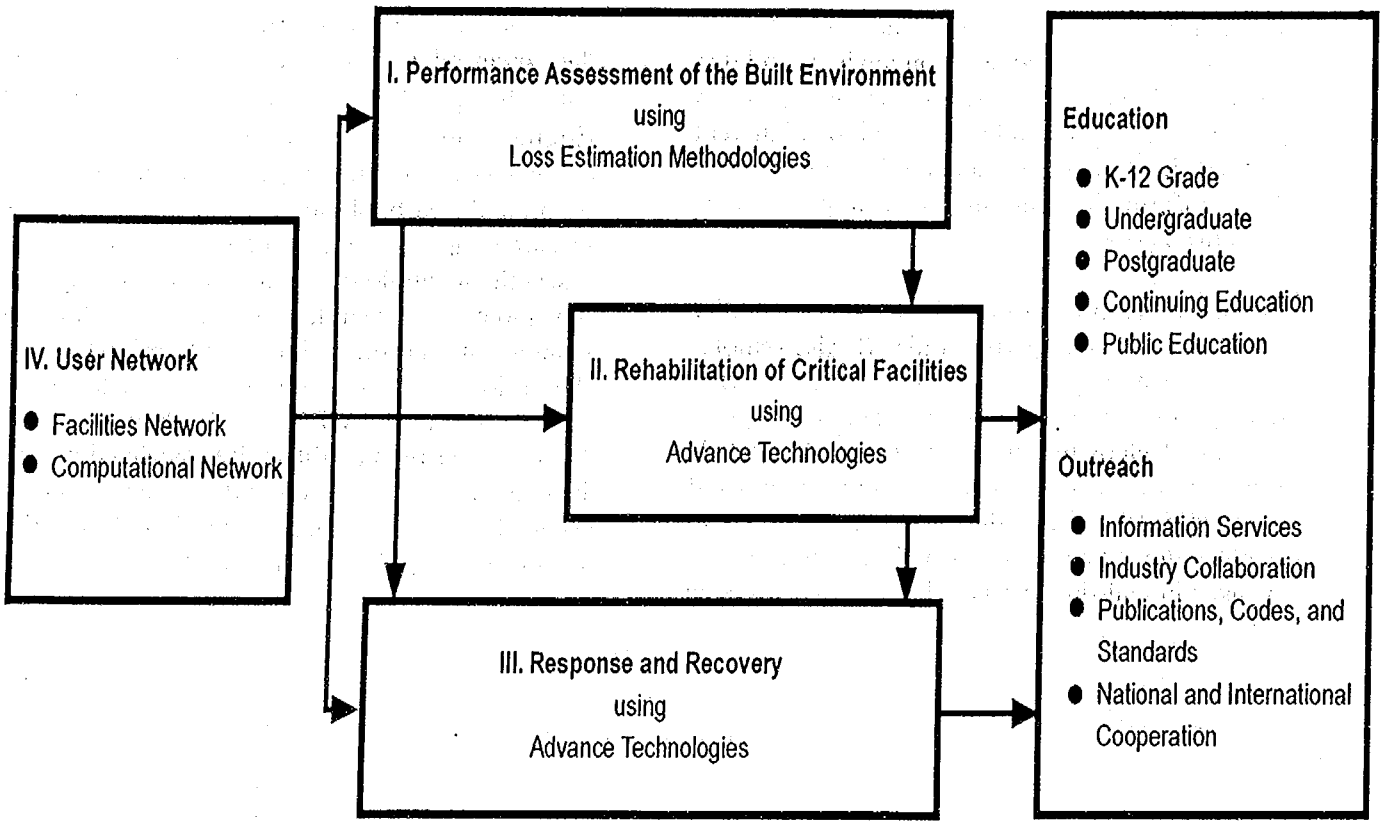


Figure 1. Interaction between various major research trusts

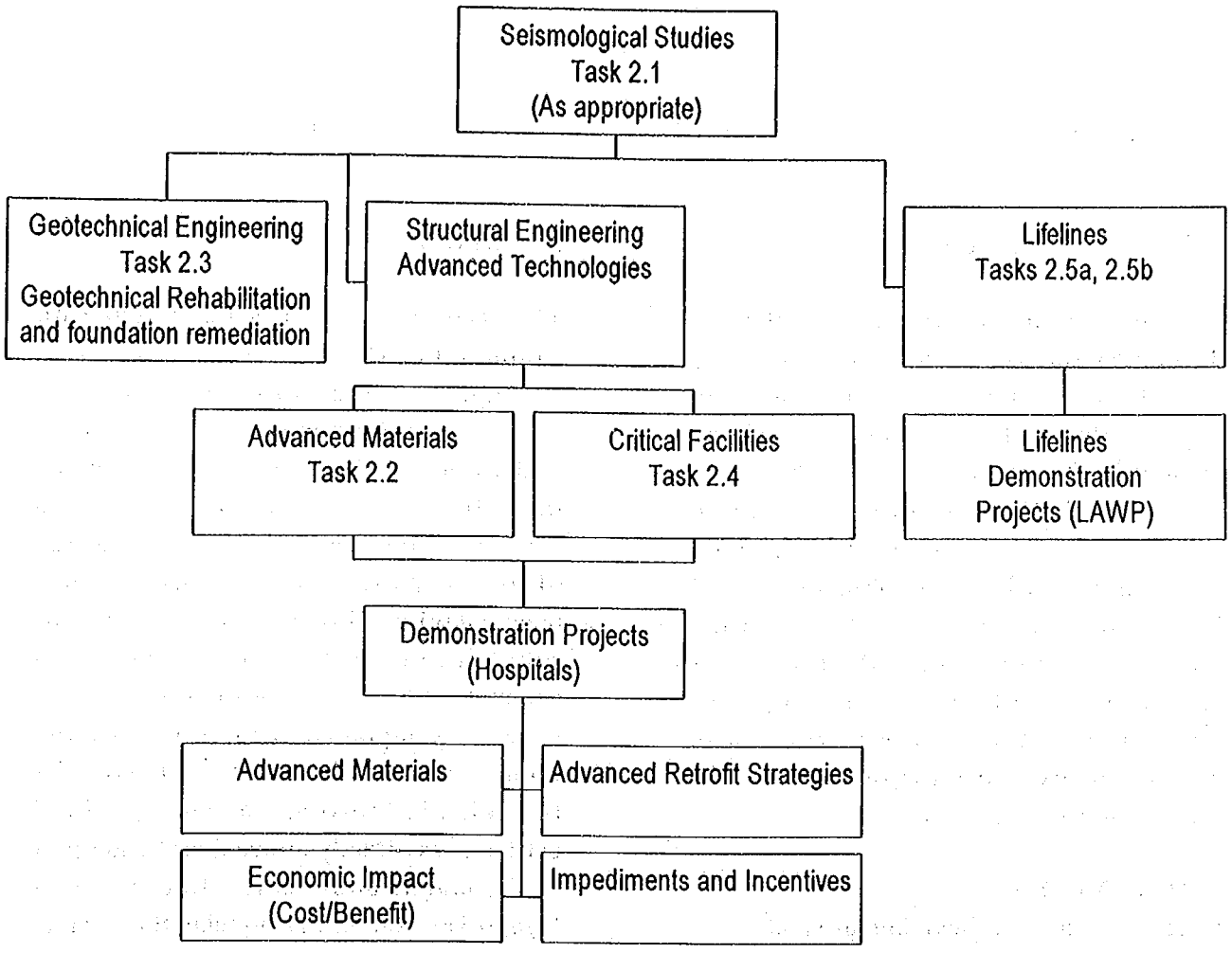


Figure 2. Schematic Structure of Research within Program 2.

A STUDY ON THE BEHAVIOR OF A SEISMIC ISOLATION DEVICE USING FULL-SCALE DYNAMIC PUSH-OVER EXPERIMENTAL EQUIPMENT

by

Takashi SATOU[1], Hiroshi MITAMURA[2], Akio HAYASHI[3], Toshihiko BESSYO[4]

ABSTRACT

Seismic isolation bearings of steel were developed for use in cold regions. They were designed to use the friction between polytetrafluoroethylene and steel and the geometric shape without using rubber. From the histeresis curves, seismic isolation bearing of steel that uses very large values of friction yield histeresis reduction, and to reduce natural free vibrations of a structure. It also has an effect of reducing such an impact inertia force that was generated by the equipment used in our experiment.

KEY WOARDS

: Seismic isolation bearings of steel
Full-scale
Dynamic push-over experimental equipment
Histeresis reduction

1. FULL-SCALE DYNAMIC PUSH-OVER EXPERIMENTAL EQUIPMENT

We have developed a full-scale dynamic push-over experimental equipment that can generate inertia forces reaching the ultimate limit, using an almost full-scale model of a bridge as a model structure.

1.1 Objective and idea

The Hyogo-ken Nanbu Earthquake on January 17, 1995, caused the greatest damage to various structures, since the Great Kanto Earthquake in 1923. Many bridges sustained serious damage, including the collapse of piers and girders. This experience let to a great change in design of highway bridges, and provision has been established that seismic motions of great intensity has to be taken into account, although the probability of such severe earthquakes occurring while the bridges are in service is little. To consider the seismic motions caused by inland earthquakes directly above their hypocenter in the magnitude 7 class, like the 1995 Hyogo-ken Nanbu Earthquake, the seismic motion of L2 type II was set up. Such an earthquake motion is extremely rare but has a great impact on structures. The motions of this type have an impact

1) Engineer,Structures Section,Structures Division, Civil Engineering Research Institute,Hokkaido Development Bureau, 1-3 Hiragishi, Toyohira-ku, Sapporo, 062-8602, Japan
2) Research Engineer, ditto
3) DE, Pacific Consultants Co.
4) Engineer, Muroran Plant The Japan Steel Works,LTD.

marked by short duration and a small number of cycles. Figure-1 shows the response spectrum, together with the seismic motions of the previous L2 type I.

To ensure the safety of bridges, the precision and validity of design calculations must always be verified. To guarantee the validity of design calculations, experiments are required in which an almost full-scale model of a planned structure and equipment that can faithfully reproduce seismic motions from design conditions are necessary. A conventional shaking table requires a sizable power unit and a control device to cause a sudden inertia force to act on full-scale model structures, and separately developed devices are needed to provide the needs of different designers.

Furthermore, the free vibration components of the behavior of a structure subject to seismic motions with an impact marked by a short duration and a small number of cycles are not so large, as typically shown by push-over analysis or the energy conservation law. From these viewpoints, we propose full-scale dynamic push-over experimental equipment.

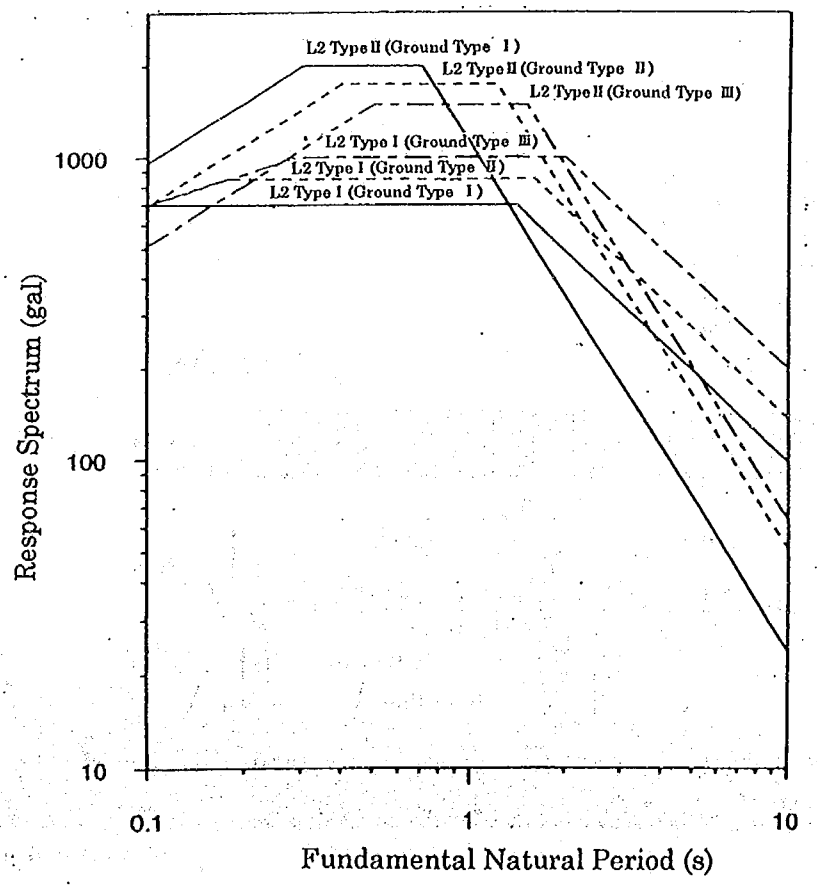


Figure-1 Response Spectrum

1.2 Construction and operation principle

Our proposed equipment operates in the following way: an almost full-scale model of a planned bridge is placed on a pallet. The pallet is raised by air bearings and accelerated. Then the pallet collides against an abutment test wall. The model structure and the pallet generate a great acceleration in the process of making a sudden stop. After this, free vibration, that is, the characteristic vibration of the model structure, occurs. Because making the first acceleration as moderate as possible is needed, equipment consisting of cables and a weight is used (Figure-2). The section where the collision takes place was provided with a shock absorber of expanded plastics and a rubber plate. The vibration was adjusted by changing the acceleration distance and the thickness of the shock absorber.

Equipment of this kind can reproduce the behavior of a structure subjected to seismic motions with a very noticeable shaking. But it is not useful for the behavior of a structure subjected to seismic motions with a long duration of vibration. However, it is considered to be effective in studying, at limited expense, the effects of impact motions characterized by short duration and a small number of cycles. Figure-3 shows the full-scale dynamic push-over experimental equipment.

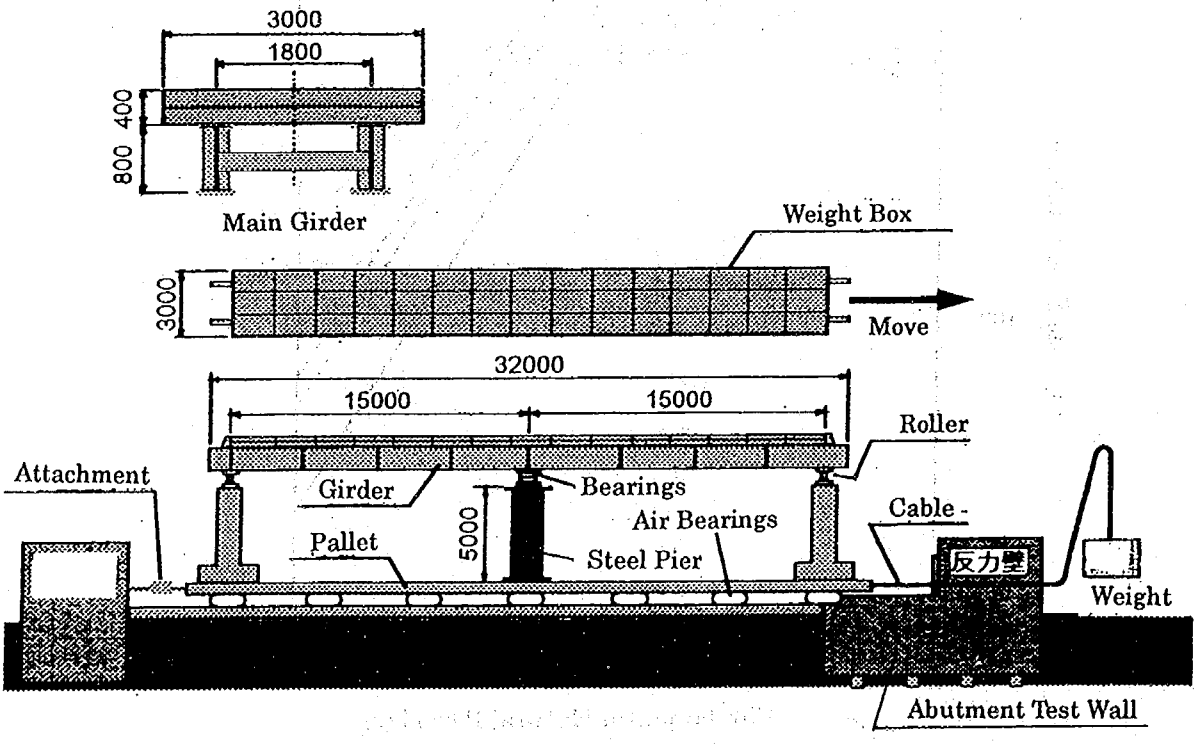


Figure-2 Whole of Experimental Equipment

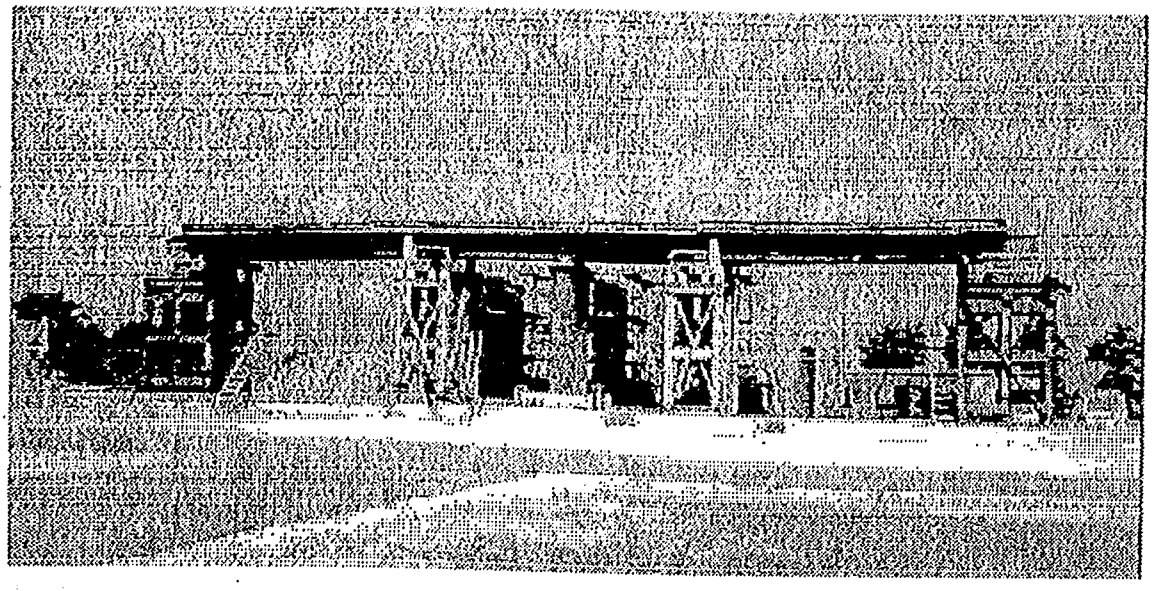


Figure-3 Whole View Picture of Experimental Equipment

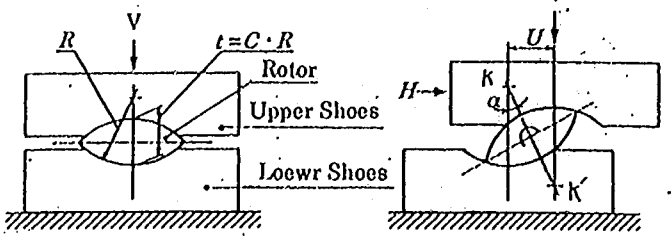
2. SEISMIC ISOLATION BEARINGS OF STEEL

2.1 Purpose and details of development

Seismic isolation bearings of steel were developed for use in cold regions. They were designed to use the friction between polytetrafluoroethylene and steel and the geometric shape without using rubber.

Rubber materials harden under cold temperatures. Consequently, seismic isolation devices that have been designed based on characteristics at ordinary temperature can not show the initial performance under cold conditions. This point may be factored into the design of seismic isolation devices, but considerable constraint will be put on the seismic isolation design when the severe motions described in section1.2 are in the design conditions.

Therefore, isolation devices whose restoring force characteristics do not vary with changes in temperature should be developed for use in cold regions. We propose seismic isolation bearings of steel as isolation devices that can fulfil this purpose. Figure-4 shows the shape of this device, which uses the friction between polytetrafluoroethylene and steel and the geometric form. That is, this device makes the same movement as the structure formed by linking Points K and K' (Figure-4), and flexibility of behavior and good energy absorption performance can be attained by properly selecting the diameter of the rotating part of the rotor in the center of the device. Furthermore, because the rotor in the center of the device behaves counter to the relative displacements of the upper and the lower shoes, the sliding plane provides a double. As a result, a frictional force representing a friction coefficient twice as large as the normal friction coefficient can be attained. Thus the histeresis curves of the seismic isolation device were modeled as a bilinear model that was very effective in absorbing energy (equations (1) to (5), Figure-5).



(a) Situation of Neutrally (b) Situation of Action

Figure-4

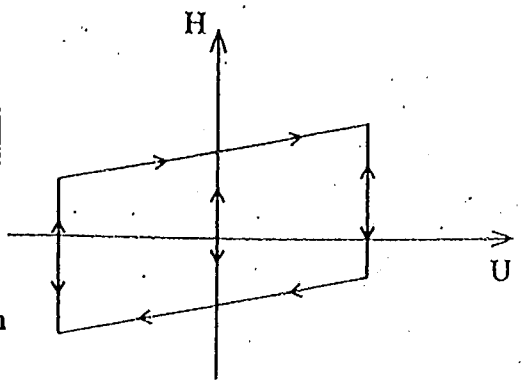


Figure-5

$$H = V \cdot \tan(\alpha + \rho) \quad \text{Eq (1)}$$

$$U = R \cdot (2\text{-}C_B) \cdot \sin(\alpha) \quad \text{Eq (2)}$$

$$\alpha = \sin^{-1}\{u_B / R(2\text{-}C_B)\} \quad \text{Eq (3)}$$

$$\sin\rho = 2 \cdot \mu / \{(2\text{-}C_B) \cdot \sqrt{(1+\mu^2)}\} \quad \text{Eq (4)}$$

$$C_B = t / R \quad \text{Eq (5)}$$

(H : Horizontal Load, V : Vertical Load, U : Horizontal Displasement, ρ : Coefficient by Eq (4), C_B: Coefficient by Eq (5), α : Turn Angle of Rotor, R : Radius of Rotor, t : Thickness of Rotor, u_B : Effective Displacement)

2.2 Verification of the device characteristics

To examine the histeresis characteristics of the steel isolation bearing proposed in this paper, we made an experiment on vibrations by the sine wave, using a simple shaking table into which a seismic isolation device was incorporated. We verified Equations that assumes the histeresis characteristics described in section "2.1". In addition, to further assess the characteristics of steel seismic isolation bearings, simulation by the finite element method (FEM) analysis was made.

Figure-6 compares the histeresis curves obtained from the experiment with those of Equations and the results of the FEM analysis. The histeresis curves of Equations and the FEM results were computed using a friction coefficient of 0.25, because of the low pressure of the bearing surface. The histeresis curves given by Equations agreed well with the experimental results, which proved the validity of the equations. At the same time, the FEM analysis showed a good reproduction of the experimental results.

2.3 Verification using a vibrating table

This experiment was made to cause a random sudden inertia force to act on a model structure on the shaking table. The model consisted of a mass corresponding to the superstructure and isolation bearings of steel. Actual seismic motions are so complicated and diverse

that fully simulating only using simple, continuing harmonic waveforms or waves of 1/2 cycle to one cycle with a great amplitude is impossible. Therefore, we found that understanding changes in input amplitude and cycle, and the aspects of transient vibrations that the structure responds to such changes, is necessary. The test was performed to reproduce the behavior of a model structure when receiving a sudden inertia force by using nonlinear dynamic analysis and the equivalent linear method and to obtain the constants used for theoretical equations.

1) Experimental method

Figure-7 shows a model structure and a shaking table. The table is placed on a linearway that is movable in a horizontal direction. An activator is provided by a lever to vibrate at a leverage of 1:3. Figure-8-21 show the results from the experiment and those of the simulation by the analysis, respectively.

By modeling from the theoretical equations and the dynamic analysis, the displacement behavior of the seismic isolation device was simulated almost accurately. From these results, the following were made clear.

(a) The friction coefficient "u" of polytetrafluoroethylene used for the theoretical equations of isolation bearings of steel was 0.1.

(b) In the nonlinear dynamic analysis, a good approximation was attained by allowing for the viscosity coefficients "c" in the following two cases to reflect the velocity dependency of the friction coefficient:

1) where the sliding surface of pure polytetrafluoroethylene,
   $c = 35$ kgf · s/cm
2) where the filler was included,
   $c = 5$ kgf · s/cm

This agrees with the tendency in past reports[11] that the latter case has a smaller velocity dependency than the former.

(c) The value of displacement response obtained by the equivalent linear method, which is commonly used as a design calculation method for seismic isolation bridges, is somewhat larger than the value obtained by the nonlinear dynamic analysis. Therefore this method gives a safer value than the actual value.

(d) The damping performance of the seismic isolation device, which has an almost rectangular histeresis curve, such as a steel seismic isolation bearing, was found to be higher than that evaluated by the equivalent linear assumption.

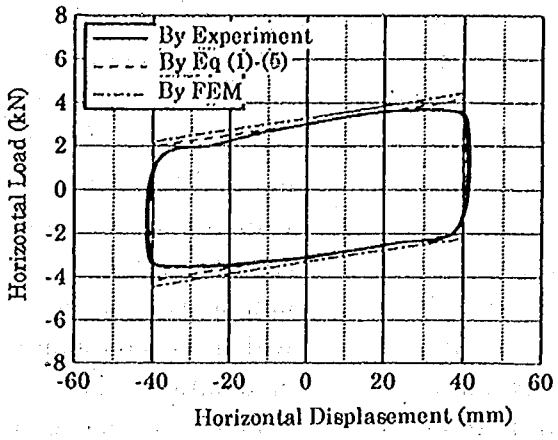


Figure-6 Histeresis Curve

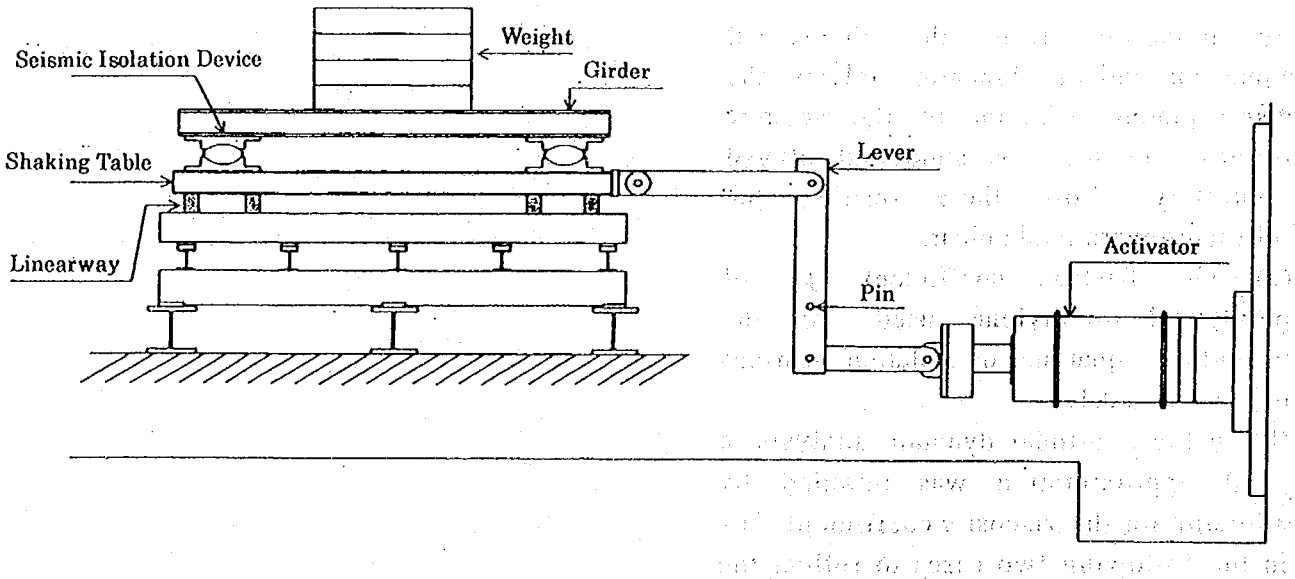


Figure-7 Model Structure and A Shaking Table

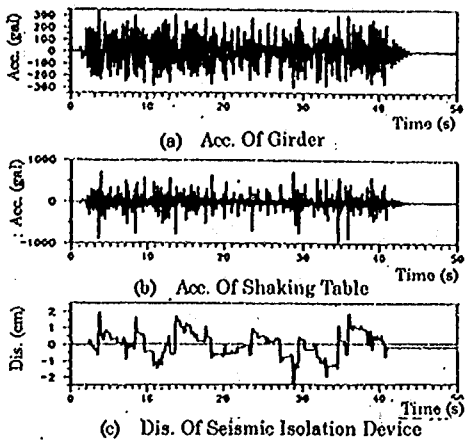


Figure-8 Experiment Value (Case A)
Input : Pink-Noise

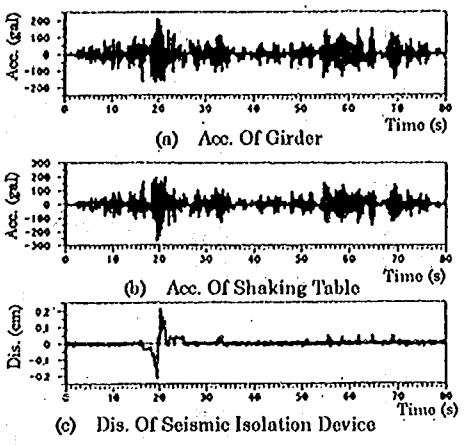


Figure-9 Experiment Value (Case A)
Input : Simulated Earthquake

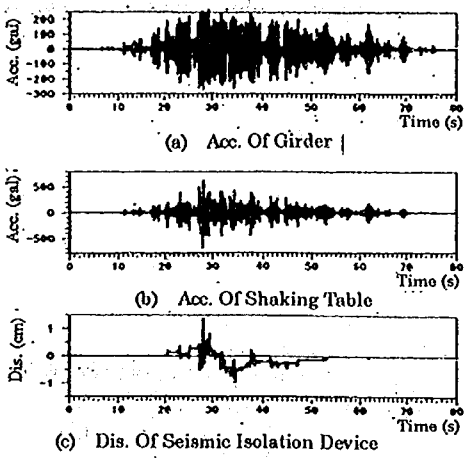


Figure-10 Experiment Value (Case A)
Input : Onnetou-Oohashi

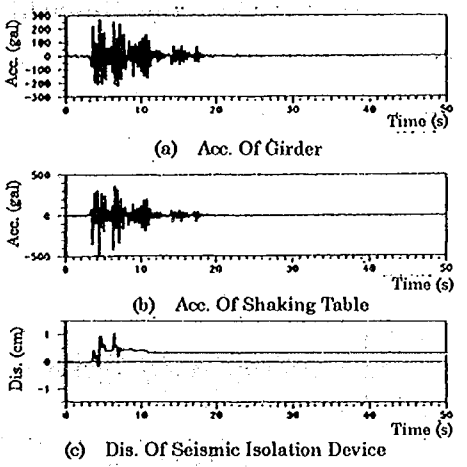


Figure-11 Experiment Value (Case A)
Input : Kobe Marine Observatory

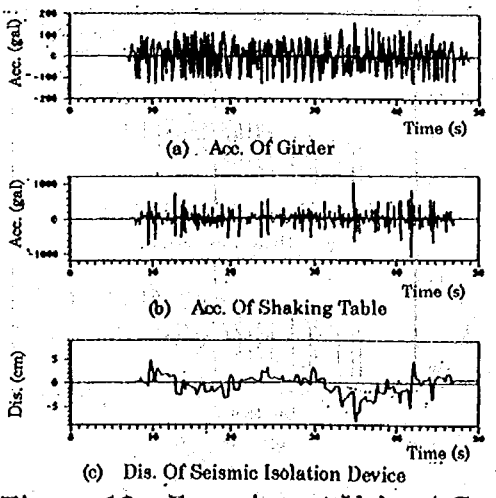


Figure-12 Experiment Value (Case B)
Input : Pink-Noise

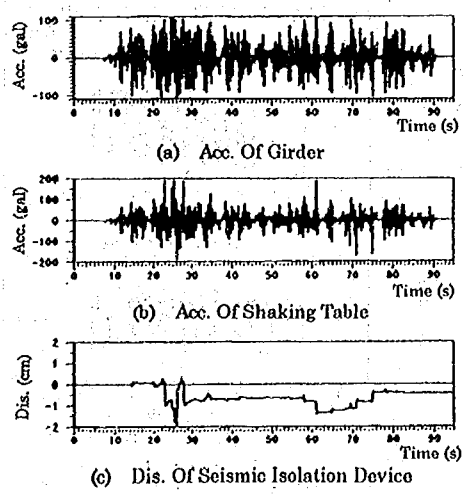


Figure-13 Experiment Value (Case B)
Input : Simulated Earthquake

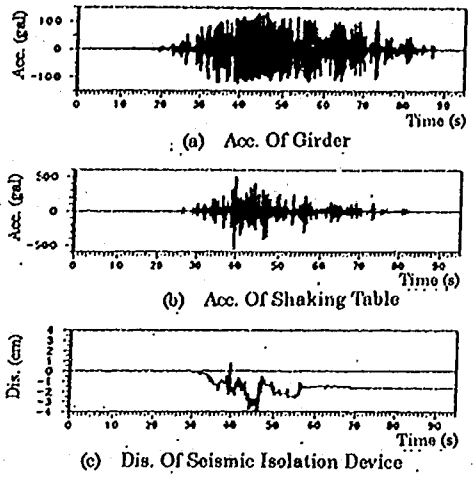


Figure-14 Experiment Value (Case B)
Input : Onnetou-Oohashi

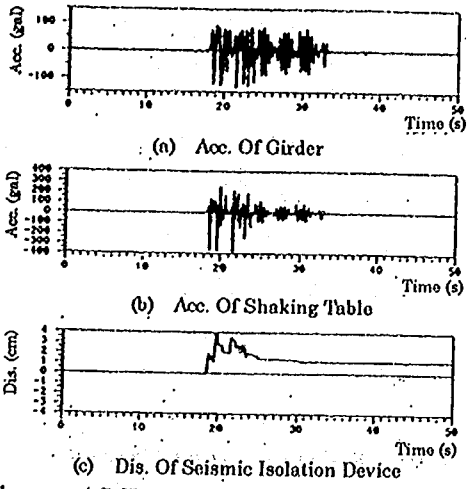


Figure-15 Experiment Value (Case B)
Input : Kobe Marine Observatory

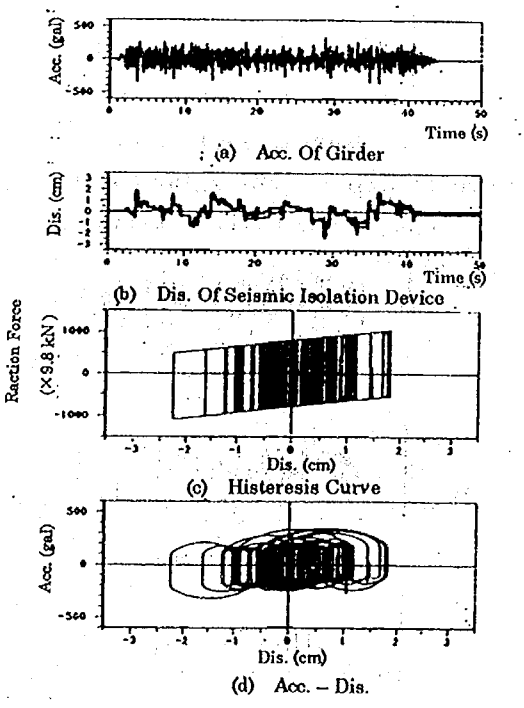


Figure-16 Nonlinear Dynamic Analysis
(Case A)

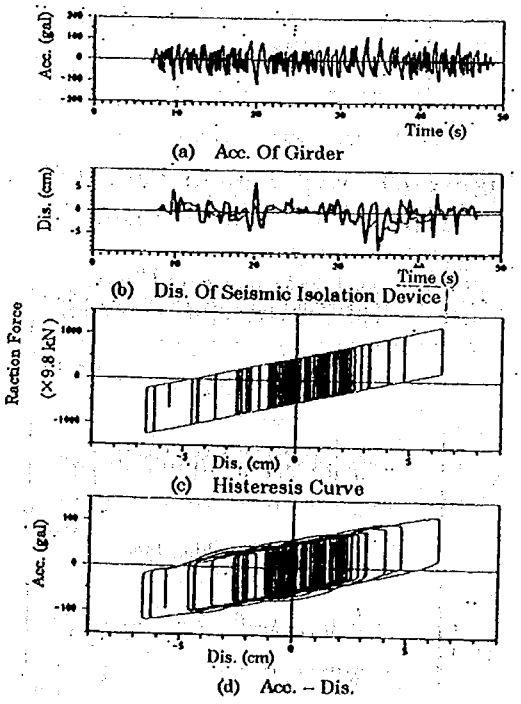


Figure-17 Nonlinear Dynamic Analysis
(Case B)

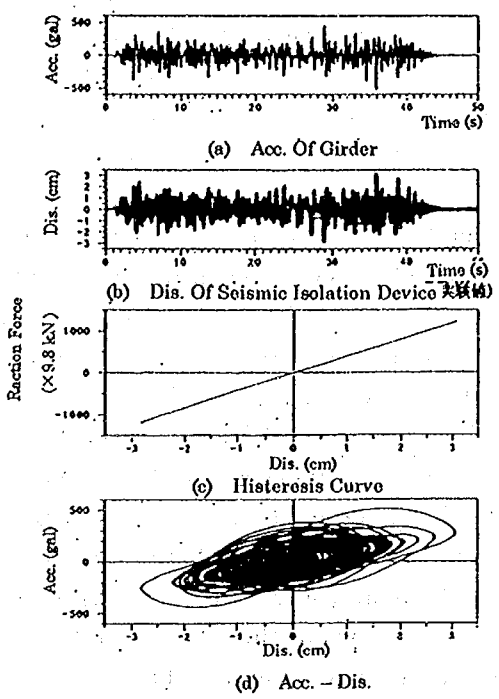


Figure-18 Equivalent Liner Method (Case A)

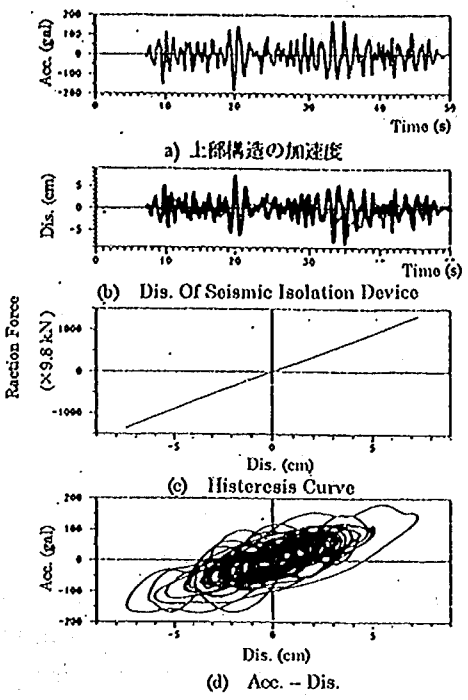


Figure-19 Equivalent Liner Method (Case B)

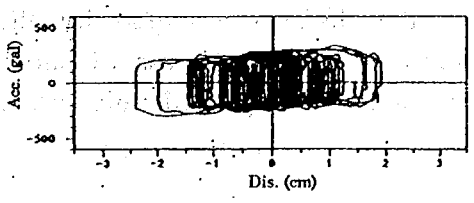


Figure-20 Histeresis Curve By Experiment (Case A)

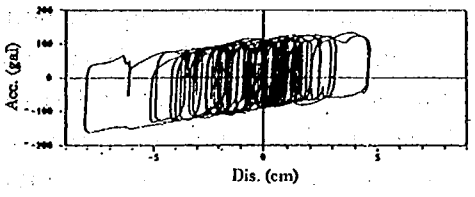


Figure-21 Histeresis Curve By Experiment (Case B)

3. EXPERIMENT USING AN ALMOST FULL-SCALE MODEL BRIDGE

3.1 An experiment using steel bridge piers for substructure

To confirm the performance level of seismic isolation bearings of steel required for a real bridge we made a dynamic loading test using a full-scale two-span continuous girder and steel piers. Seismic isolation bearings and pin bearings were used to investigate and compare their response behavior.

3.1.1 Experimental method

The configuration of the experimental equipment was a superstructure, two abutments, two bearings, two pier models, a substructure (pallet) , an air bearing, an abutment test wall and foundation (Figure-22). The movable part of the equipment of total weight 3340 kN was made collide against the abutment test wall. The Superstructure was a two-span continuous girder bridge (span: 15.0m×2, interval of main girder: 1.8m, H-steel 2 main girders). The ends of the main girders of the superstructure were supported on the abutments by two rollers that moved the girders. The two steel piers supported the superstructure by a bearing in the middle. Because the weight of the superstructure was 1025 kN, and because the effective span was uniform, the dead load on a middle supports was 5/8 of the total, or 640 kN.

The steel pier with a circular cross section (Figure-23) was used for the substructure. To save on costs, ready-made steel pipes (STK 400) were used for the columns of pier, while SM 400 were provided for all steel plate members other than the columns because of their weldability. The yield strength of the steel pipes used was 259 MPa. The sectional size of pier was determined so that the pier base could yield at a response acceleration of about 1 G.

We experimented with the following two bearings: 1) steel seismic isolation bearings, and 2) pin bearings. The steel seismic isolation bearing had a curvature radius of the rotating plate (R) = 30 cm and a thickness (t) = 18 cm (Figure-24). PTFE having a diameter of 3 cm were concealed as contact members in the upper and lower shoes of the seismic isolation bearing (30 each). The friction coefficient between the PTFE and the rotating plate was about 0.11, and the histeresis characteristics of a seismic isolation bearing are given by Equations (1) - (5) and are represented by the curve in Figure-25.

In the experiment, the substructure to which the pier was fixed was caused to run by dropping a 98-kN weight and to collide against the abutment test wall. At this time, input acceleration provided for the substructure was adjusted by changing the distance traveled by the substructure and the thickness of shock absorbing material (expanded polystyrene form).

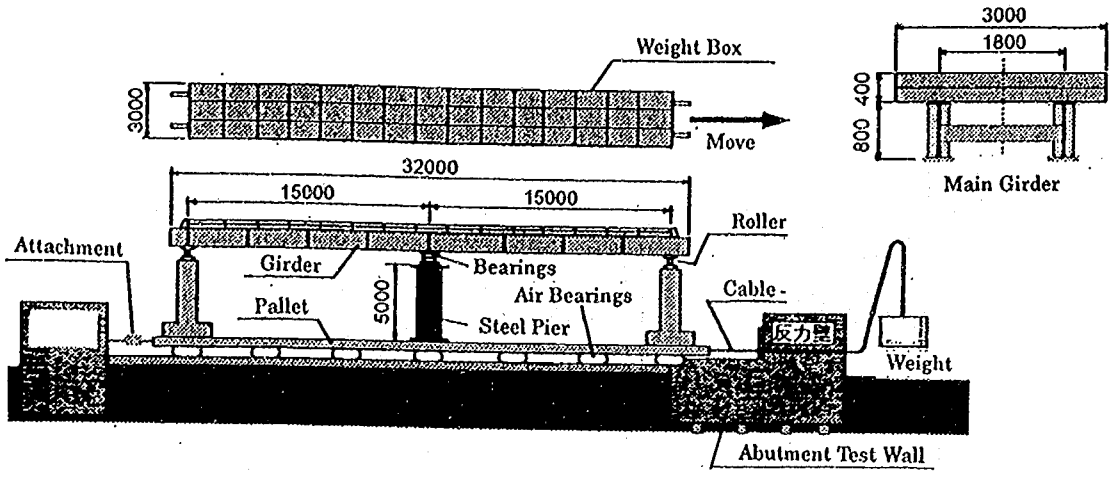


Figure-22 Experiment Equipment

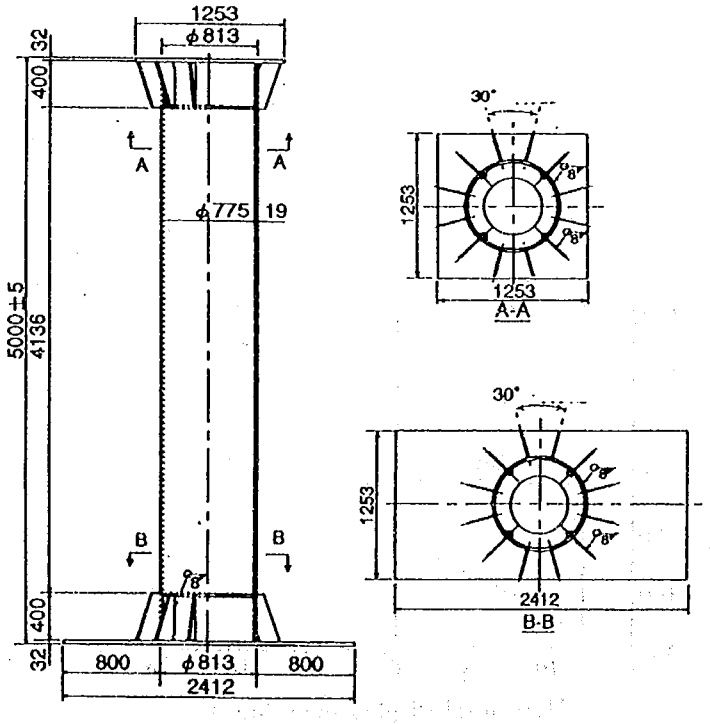


Figure-23 The Steel Pier

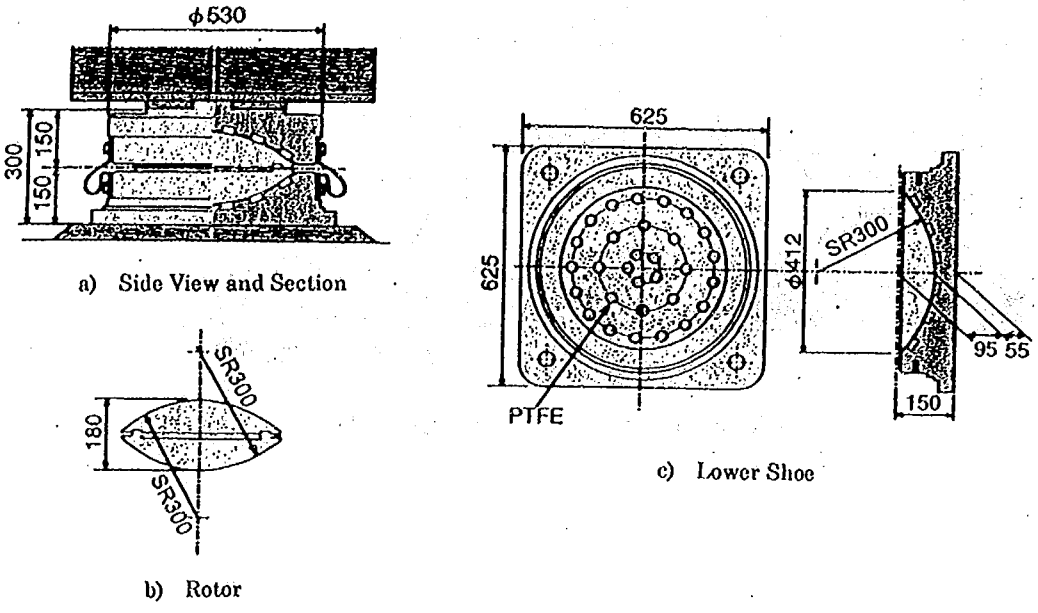


Figure-24 Seismic Isolation Bearings of Steel

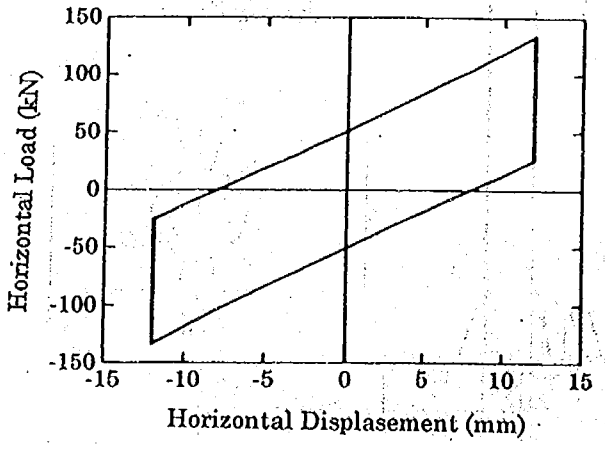
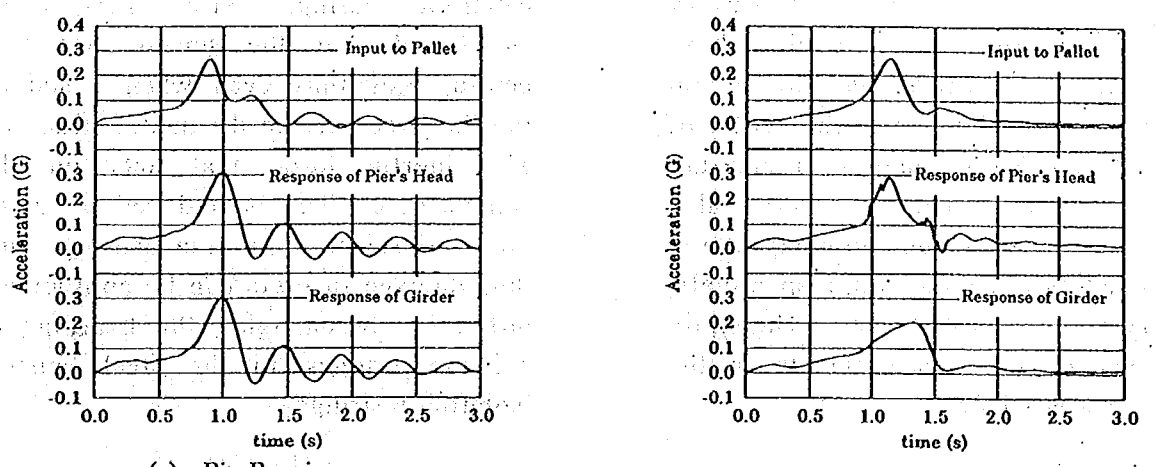


Figure-25 Histeresis Curve

3.1.2 Experimental results

Figure-26 shows an example of the input and the response acceleration wave forms that compares the steel seismic isolation bearings and pin bearings. When pin bearings were used, the wave forms of the response accelerations of the upper ends of the pier and the superstructure were almost the same, and the maximum value increased by about 10%, compared with that of the input acceleration. In addition, free vibration with the natural frequency of the system occurred after the collision. However, when the steel seismic isolation bearing was used, the response acceleration of the superstructure greatly decreased compared with that of input acceleration. Moreover, the vibration after the collision was reduced.

Figure-27 shows the relationship between the maximum input acceleration and the amplification factor under all conditions in the experiment. Here, the amplification factor was defined as the ratio of the maximum response acceleration of the superstructure to the maximum input acceleration. With the steel seismic isolation bearings, the response amplification was always a value of less than 1.0, a decrease of about 30 %, compared with the pin bearings.



(a) Pin Bearing (b) Steel Seismic Isolate Bearing

Figure-26 Acceleration Wave Forms

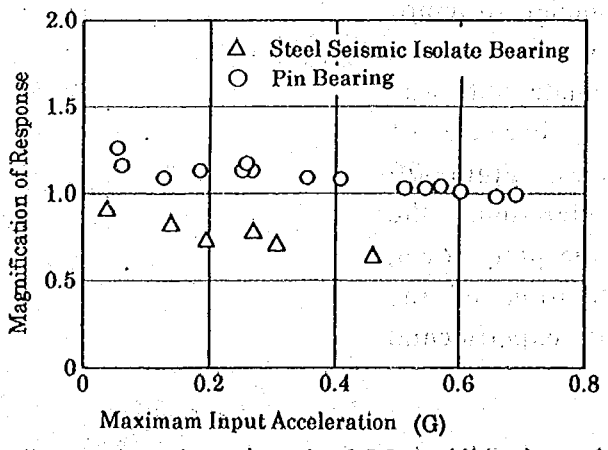


Figure-27 Input Acceleration And Magnification of Response

3.2 Experiment using substructure of reinforced concrete.

3.2.1 Model structure and measurements

The model structure was the wall type pier model (Figure-28) designed from earthquake-resistant design criteria. The wall had a thickness of 80 cm, a width of 250 cm and a height of 400 cm. The *dan-otoshi* was, or the reinforcement ratio of the pier changed, at a height of 150cm from the wall base.

The accelerations and strain of reinforcing bars were measured: accelerometers measuring the horizontal direction were installed on the side of the wall at every 50cm from the base, while those measuring the vertical and horizontal directions were attached to the center of the girders. Strain gauges to measure the main reinforcement were also attached on tension side and compression side of two reinforcing bars, respectively, at every 50cm from the base. The strain frequency of the measurements in the sampling was 1 kHz.

3.2.2 Experimental results

In this experiment, the model structure showed elastic behavior because a loading test up to the ultimate state was unable to be performed, because of experimental circumstances. Figure-29 shows the input acceleration, the response acceleration of the pier crown, and the response acceleration of the superstructure under this experimental condition.

The response acceleration of the pier crown reached the maximum acceleration having a response value of about 2G almost at the same time as the maximum input acceleration, while the superstructure reached the maximum response 0.3 sec. later than the peak input acceleration. This maximum response showed a small value of 0.4G. In an experiment using pin bearings with the model structure of the same design, when the response accelerations of the pier crown and the superstructure were about 1.3G, flexural and shear failure were observed at the *dan-otoshi* where the reinforcement ratio of the pier changed. However, in our experiment, no damage was found in the model structure using the seismic isolation bearing. From these facts, we found that the seismic isolation bearing functions even when a sudden inertia force acts on the model structure. The inertia force that acts on the superstructure can be reduced by using the steel seismic isolation bearings, and thus damage to piers can be appreciably mitigated by changing the bearings of existing bridges to the steel seismic isolation bearings.

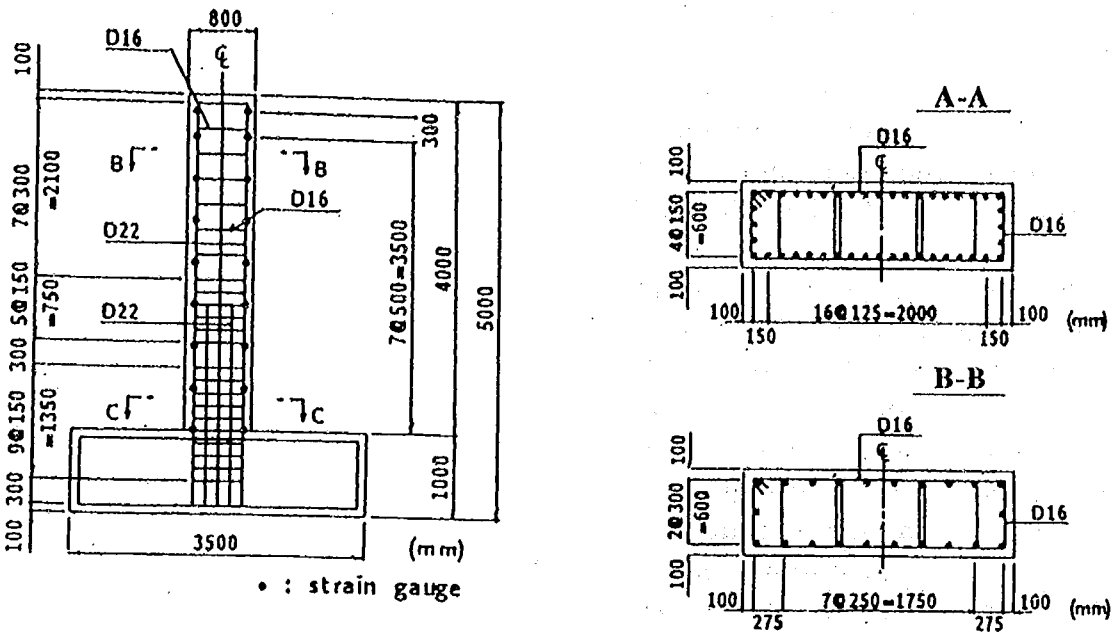


Figure-28 Model Structure

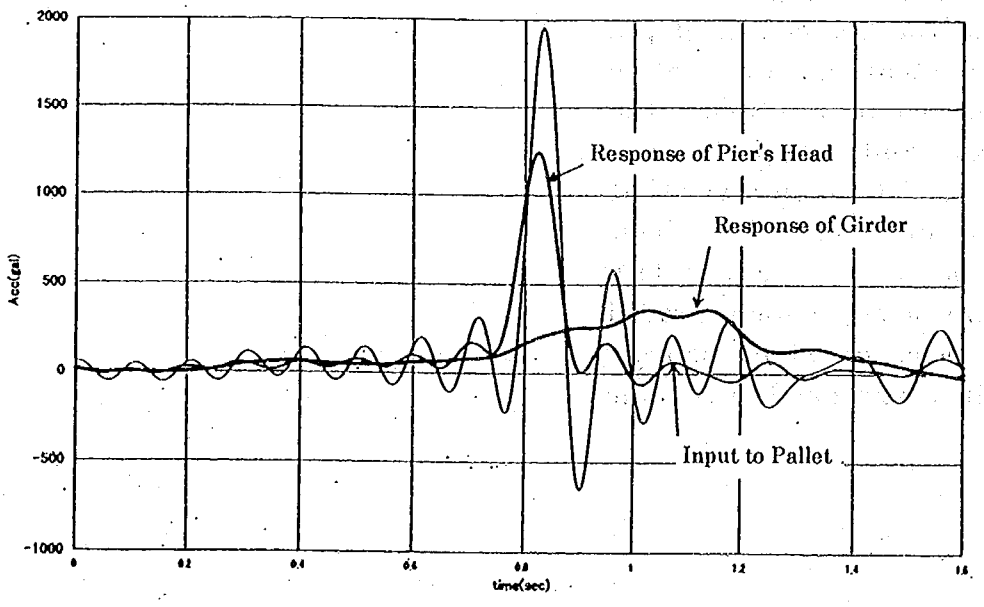


Figure-29 Acceleration Wave Forms

4. CONCLUSIONS

The experimental equipment of the air cushion made it possible to produce an acceleration of approximately 1.0G with almost full-scale model structures. Success in generating such a strong inertia force by a relatively low-cost equipment has provided the designers with opportunities to verify their design.

From the histeresis curves, seismic isolation equipment that uses very large values of friction yield histeresis reduction, and to reduce natural free vibrations of a structure. It also has an effect of reducing such an impact inertia force that was generated by the equipment used in our experiment. Thus it greatly contributes to not only the efforts to improve the effect of seismic isolation design, but also to its use in cold regions.

In the experiment using the steel pier columns, the responses of pin bearings and steel seismic isolate bearings were compared using the pin bearings and steel seismic isolate bearings. The result was that the response decreased by about 30 % when the steel seismic isolate bearings were used, which proved the effectiveness of steel seismic isolate bearings against the seismic impact.

INVESTIGATIONS OF ACTIVE FAULTS FOR DAM CONSTRUCTION - THE PRESENT STATE AT THE MINISTRY OF CONSTRUCTION -

by

Yasuhiko Wakizaka[1)]

ABSTRACT

The displacement of ground by an earthquake due to an active fault is difficult to handle in the design process. Therefore, the Ministry of Construction constructs dams after first checking that there are no active faults near the dam site. To avoid active faults, various investigations are systematically performed. First, the literature is researched for a radius up to 50 km from the dam site to understand the regional characteristics of active faults and to identify any active faults near the site. Next, photographs are interpreted for a radius up to 10 km to investigate the distribution and properties of active faults and to confirm whether active faults described in the literature are present or not. Identified active faults are classified based on the quality and quantity of their tectonic fault topography, and the results of the literature research and photograph interpretation are compared. If the literature research or photograph interpretation finds any active fault within 3 km of the dam site, then geological surveys for the fault are carried out.

KEY WORDS: active fault, dam construction, geological survey, photo-interpretation

1. INTRODUCTION

Dams must be completely safe and stable because of their immense impact in case of collapse. Therefore, during the design and construction of dams, detailed geological surveys are conducted on the stability of the slopes around reservoirs, as well as the mechanical properties and imperviousness of the basement rocks. Of all the natural disasters, earthquakes and volcanic eruptions are inevitable in Japan since the Japanese Archipelago lies on boundary between plates, and many earthquakes in inland areas are caused by active faults. The impacts of active faults upon dams are classified by types of earthquake motion and ground displacement. Although earthquake-resistant design against motion is performed, the problem of ground displacement cannot be addressed by the design process, so areas near active faults that could threaten dams are avoided when choosing dam sites at present. Accordingly, various quantitative and qualitative investigations on active faults are conducted equivalent to those on the mechanical properties and imperviousness of basement rocks and the slope stability around reservoirs.

2. OBJECTIVES OF ACTIVE FAULT INVESTIGATIONS FOR DAM CONSTRUCTION

The objectives of active fault investigations conducted prior to dam construction, focusing on ground displacement, include the following:

a) To confirm whether or not lineaments and faults, both of which are considered to be active faults, are indeed active faults.

b) To locate active faults with sufficient precision such that they can be avoided when building structures.

c) To identify the length of motion of an active fault by one earthquake and hence estimate the magnitude of earthquake that the fault could cause

d) To identify the activity history of active faults

1) Geology Division, Environment Department, Public Works Research Institute, Ministry of Construction, Tsukuba-shi, Ibaraki-ken, 305-0804, Japan

to predict future earthquake occurrence.

Active fault investigations for dam construction must cover all of the above, and so include literature research, geomorphological surveys, and geological surveys. Fig. 1 shows the flow chart of investigations.

3. LITERATURE RESEARCH

(1) Investigations of active faults

a) Purpose of investigations

The purpose of literature research on active faults is i) to understand the properties (distribution, direction, degree of activities, direction of displacement, etc.) of active faults over a wide area near a dam site for use as a reference in successive investigations, and ii) to confirm the existence of active faults near a dam site by researching the literature on past investigations.

b) Area of investigations

The area that needs to be investigated is around 50 km in radius from the dam site for purpose i) (in which case the properties of active faults distributed over a wide area can be identified as shown in Fig. 2), as well as around 10 km in radius from the dam site for purpose ii) (the width of an active fault system perpendicular to the line of the fault is almost always less than 10 km as shown in Fig. 3).

c) Contents of investigations

The book titled "Active Faults in Japan -Sheet Maps and Inventories[1]" is a helpful reference, which lists the distribution and properties of active faults throughout Japan. This reference is sufficient for purpose i). For purpose ii), research should be conducted on the references listed in "Active Faults in Japan -Sheet Maps and Inventories[1]", as well as on new references not yet listed.

d) Compilation of investigation results

Electronic copies of location maps and descriptions in the literature[1] are sufficient for purpose i). When compiling investigation results for purpose ii), the locations of active faults stated in the literature (hereafter referred to as reference fault(s)) should be marked on a topographical map on a scale of around 1:25,000, and the properties should be listed in a table. The locations of faults relative to the dam site should also be determined (the shortest distance between the dam site and the reference faults, and whether or not the reference faults are headed toward the dam site).

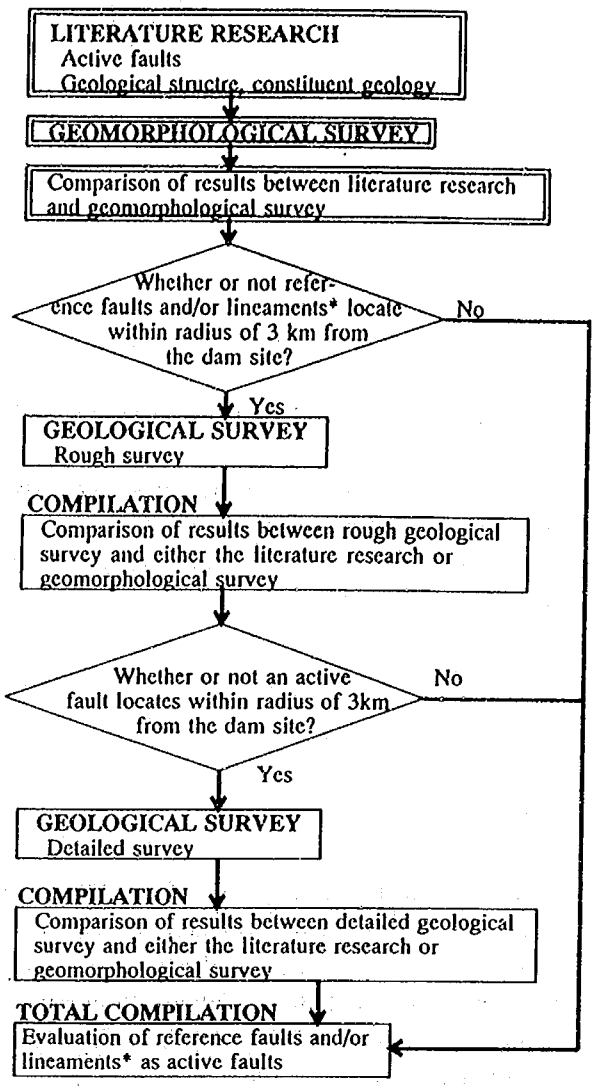


Fig. 1 Flow chart of active fault investigations. Lineaments* means lineaments which are accompanied by a tectonic fault topography.

(2) Investigations of the geological structure and constituent geology

a) Purpose of investigations

When researching the literature, the geological structure and constituent geology around the dam

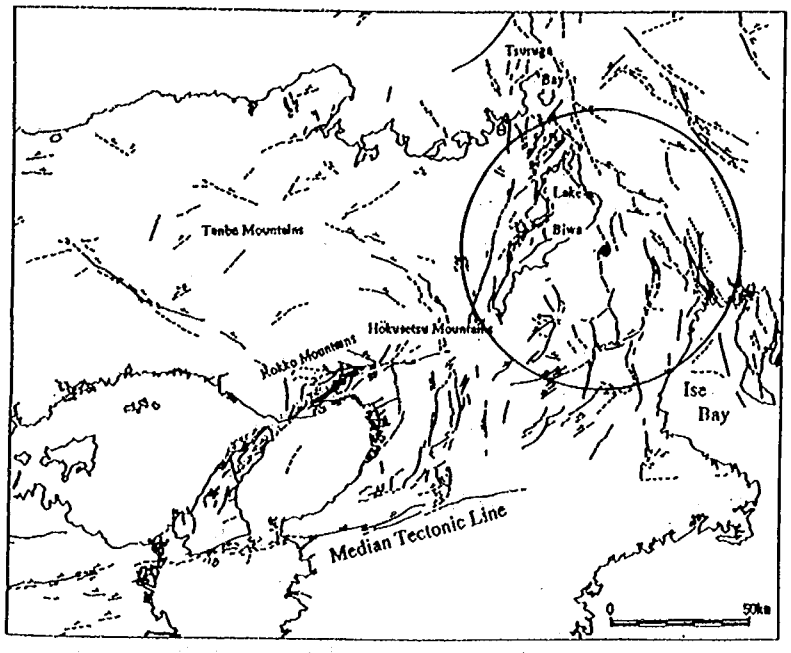


Fig. 2 Area (the circle in this figure) needed to identify the wide-area properties of active faults.

site should be investigated, in addition to direct information on active faults. This is for use in geological examinations of the origin of reference faults and lineaments accompanying a tectonic fault topography identified by geomorphological survey, such as how the locations of the reference faults and lineaments are related to the locations of dead faults and geological boundaries (particularly the boundary between geologies with different resistance to erosion).

b) Area of investigations

To be compatible with the literature researches of active faults, investigations of the geological structure and constituent geology should cover an area of radius of around 50 km from the dam site for a broad review of the relationship between faults and geological features, and a radius of around 10 km when the relationship is examined in detail.

c) Contents of investigations

When conducting investigations, existing geological maps on a scale of 1:200,000 to 1:50,000 shall be used.

d) Compilation of investigation results

Electronic copies of existing geological maps are sufficient. For detailed analysis, however, the data obtained should be marked on a topographical map on a scale of around 1:25,000 if required.

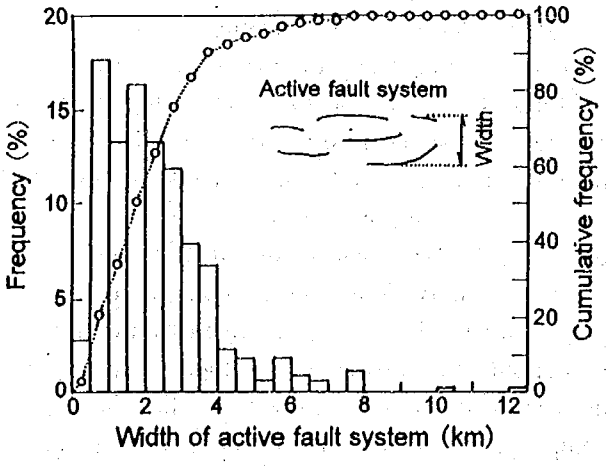


Fig. 3 Frequency distribution of width of fault system.

4. GEOMORPHOLOGICAL SURVEY

(1) Methodology

a) Purpose of survey

The purpose of a geomorphological survey is to identify active faults near the dam site and to confirm the existence and properties of the reference faults, notwithstanding the data of past investigations

b) Area of survey

A geomorphological survey should cover an

area of radius of around 10 km from the dam site. However, if a lineament accompanying a tectonic fault topography heading toward the dam site is discovered further than 10 km from the dam site, or if such a lineament is discovered near the boundary of this area, the survey area should be expanded in the direction of such lineaments.

c) Contents of survey

When conducting a geomorphological survey, items such as the location, length, direction of displacement, and constituent topographies of active faults are investigated.

The geomorphological method is principally for discovering tectonic fault topographies, which were formed by active faults, by interpreting aerial photographs and topographical maps. Actual active faults consist of several tectonic fault topographies (which may include single or multiple types of topography). When conducting the interpretation, aerial photographs on a scale of 1:40,000 to 1:10,000 are used. Interpretation of aerial photographs should begin with small- rather than large-scale aerial photographs on a scale of 1:40,000, to make it easier to understand the continuity of active faults. Large-scale aerial photographs are used when there is a lineament accompanying a tectonic fault topography in the direction toward the dam site or near the dam site, or when the existence and displacement of reference faults cannot be determined from small-scale aerial photographs. When interpreting a lineament accompanying a tectonic fault topography heading toward the dam site, the area between the lineament and the site should be included in the scope of investigation.

The interpretation is generally conducted as follows.[2]

i) Extract lineaments, then

ii) Select lineaments accompanying a tectonic fault topography from all the lineaments.

There is another method[1] as follows:

i) Extract lineaments, then

ii) Identify active faults based on discrepancies between base topographies of displacement (continuous geomorphic surfaces or geomorphic lines that were formed in the same age).

The lineaments identified by these procedures can then be classified with certainty. When conducting such a classification, the publications "Active Faults in Japan -Sheet Maps and Inventories[1]", Kuwahara[2], and Japan Society of Civil Engineers[4] are used as references, of which the Ministry of Construction uses Kuwahara[2]. It must be noted that lineaments with and without a tectonic fault topography should be clearly kept separate, by focusing on tectonic fault topographies and considering the geomorphological origin of extracted lineaments and whether these lineaments would have been formed by an ordinary geomorphic agent. Interpretation of large-scale photographs is often a useful way of examining the geomorphological origin of lineaments. In the case of a dip-slip fault, on the other hand, a summit level map needs to be drawn up for identifying the systematic differences of topographical elevation.

If found, base topographies of fault displacement should also be interpreted, such as geomorphic surfaces (terrace surfaces, depositional surfaces of pyroclastic flow, alluvial fan surfaces, talus surfaces, alluvial surfaces, etc.) and geomorphic lines (former shorelines, terrace scarps, stream channels, ridge lines, etc.). If a lineament is assumed to be running through, geomorphic surfaces should particularly be compared carefully.

d) Compilation of survey results

When aerial photographs of 1:40,000 are used, the results of interpretations should be illustrated on a topographical map on a scale of around 1:25,000. The length of lineaments, certainty, the constituent topography of lineaments, articulation of lineaments, and tectonic fault topographies should be arranged in order in tables. The topographies that constitute lineaments should be shown on the topographical map (Fig. 4), and changing the types and colors of lines depending on the certainty. When large-scale aerial photographs are used, the data obtained by interpretation should be illustrated on a topographical map on a scale of around 1:10,000 per lineament accompanying a tectonic fault topography. A lineament that is either near the dam site or heading

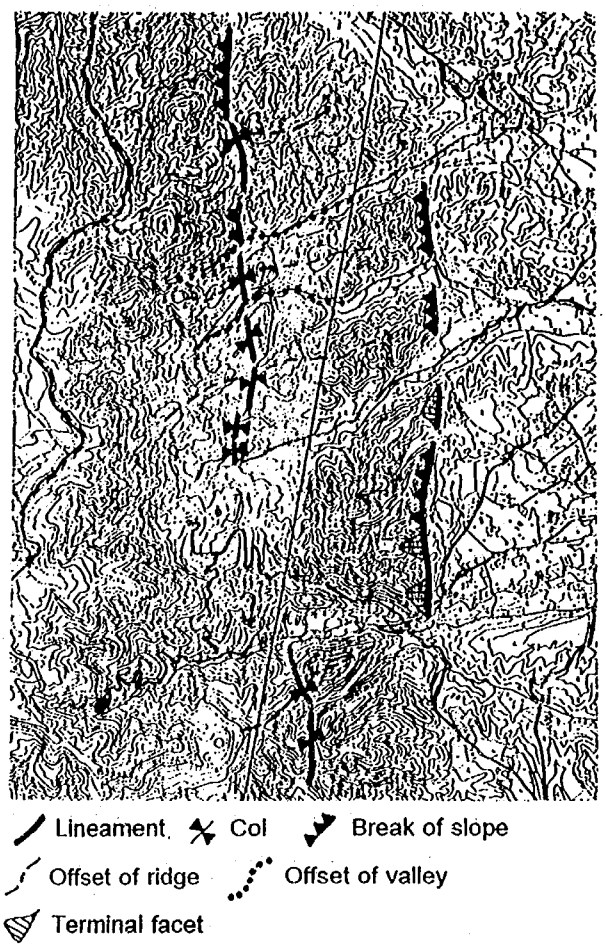


Fig. 4 Example of indicating the tectonic fault topographies along lineaments.

toward the dam site, the dam site should also be marked on the map for clarifying the relation between the dam and the lineament.

The base topographies of fault displacements should also be illustrated on the map, if found.

2) Problems of geomorphological surveys and their countermeasures

One problem with the geomorphological survey, or aerial photograph interpretation, is individual differences in recognizing active faults and judgment of certainty of lineaments[5]. Such differences are particularly noticeable when interpreting relatively low activity and low certainty faults in mountainous regions with no key topography for interpretation. These problems hinder the preliminary investigations for dam construction, especially since dams are usually built in mountainous regions.

Judgment differences among individuals arise because the criteria of certainty are not necessarily quantitative. It is considered that certainty can be judged more objectively by indicating the interpretation results along with the topography of faults as described above (Fig. 4).

Subjectivity in interpretations can be minimized by combining the extracted lineaments and surface landform classification that is commonly conducted. The Geology Division, PWRI, Ministry of Construction, is currently developing this method. With this method, lineaments that consist of cols in mountainous regions are extracted; the surface landform of the same area is classified; and then active faults are detected by comparing the both results[6]. Judgment objectivity can be improved by conducting interpretations based on these two different criteria. Nevertheless, since this method is still under development, it has not yet been confirmed as suitable for general-purpose use. The best method at present for reducing interpretation variations is for at least two persons to interpret aerial photographs of the same area separately, and then draw a conclusion by comparing the respective results.

5. GEOLOGICAL SURVEY

1) Methodology and purpose

There are two categories of geological survey of active faults: i) a rough geological survey for investigating both lineaments accompanying a tectonic fault topography, and reference faults; and ii) a detailed geological survey for investigating both lineaments accompanying a tectonic fault topography and reference faults near the basement of a dam body.

The purpose of the rough geological survey is to geologically confirm the existence of lineaments accompanying a tectonic fault topography and reference faults, and to identify whether or not they are active faults. The purpose of the detailed geological survey is to confirm the existence and precise locations of lineaments accompanying a tectonic fault topography and reference

faults, and to geologically identify the potential fault activity. Investigations of potential fault activity will be discussed in the next chapter.

2) Rough geological survey

a) Area of survey

As with the geomorphological survey, the objects of a rough geological survey is both lineaments accompanying a tectonic fault topography and reference faults within an area of radius of about 3 km from the dam site. If a lineament accompanying a tectonic fault topography and a reference fault are in two different locations but are considered to be identical, then both locations should be investigated.

b) Contents of survey

A rough geological survey includes surface exploration, which is basically the same as the conventional one. When deciding the route of surface exploration, however, the focus is on linear faults. Since, as will be described later, the location of a lineament that is identified by the geomorphological method does not necessarily coincide with the location of a geological fault (fault shear zone). So, the area of exploration needs to be expanded by a certain width on both sides of the lineament, and the route should cross the lineament perpendicularly.

Items to be checked and recorded are the geology of outcrops, the state of weathering and hydrothermal alteration, the features of faults if found (i.e., the existence of shear zones and fault gouges, the degree of shearing, the width per degree of shearing, the width of fault gouges, the structure of fault gouges, the dip and strike of fault surfaces, the existence of striations of fault surfaces, the dip and strike of striations, the amount of displacement, the direction of displacement, the geology of hanging walls and footwalls, the existence of cover beds, and the displacement of the cover bed), and the relation between fault outcrops and lineaments. Matsuda and Okada[7] proposed applying the rock mass classification, which is generally employed for dams, for classifying the degree of shearing of fault shear zones. Since cataclasite, mylonite, pseudotachylite, and some other fault rocks have recently been considered as shear zones that were formed deep underground (Sibson[8], for example), it is important to identify these also.

When conducting a surface exploration, topographies that could cause displacement such as tectonic fault topographies (particularly low fault-scarps that are difficult to pick out on aerial photographs) and terrace surfaces, should be observed, in addition to geological items.

c) Compilation of survey results

When conducting observations, the observation items stated above must be sketched and photographed, and the data written down on tabular cards for each outcrop. The observation data are then compiled into a route map, and tabulated for each fault. When compiling the results, it is important to clarify whether or not faults that coincide with the reference faults and the lineaments accompanying a tectonic fault topography were confirmed, and if so, whether they are active faults. In the stage of a rough geological survey, the fault is judged as active or inactive based on its relation with a Quaternary cover bed and its topography. Failure to confirm the existence of faults due to unfavorable outcrop conditions in the area around the target lineaments and reference faults should not be confused confirmation of no faults under favorable outcrop conditions.

3) Detailed geological survey

a) Target and area of survey

A detailed geological survey should cover the area surrounding lineaments accompanying a tectonic fault topography and reference faults found near the basement of a dam body. As with the rough geological survey, if a lineament accompanying a tectonic fault topography and a reference fault are in two different locations but are considered to be identical, then both locations should be investigated. When it is apparent that the lineaments accompanying a tectonic fault topography and the reference faults are not active ones based on the rough geological survey, no detailed geological survey is required.

b) Methodology

As with the rough geological survey, the first step of the detailed geological survey is to con-

duct a surface exploration, the contents of which are same as those of the rough geological survey. If surface exploration is not feasible because the outcrop conditions are not favorable, investigations should be conducted by other means such as trenching, adit investigations, drilling, investigations using the long Geo-slicer method, and geophysical explorations. The most appropriate method should be selected from the above, depending on the topographical and geological conditions in situ.

c) Trenching and adit investigations

Trenching is the most often used of the above methods for active fault investigations, and can achieve the purposes of the geological survey for investigating active faults most effectively. The details of trenching are described in Okada[9], and Okada and Matsuyama[10]. To determine potential fault activity, trenching is often conducted in locations where a fault is thought to pass through a Quaternary bed. To estimate potential fault activity, it is necessary to interpret fault displacements caused by past earthquakes, as described in Allen[11].

Adit investigations are similar to trenching.

d) Drilling

Drilling is conducted in the same manner as ordinary core drilling. The objectives of drilling for investigating active faults include: i) direct identification of faults by coring the faults themselves; and ii) indirect identification of faults by confirming the displacement between the hanging walls and footwalls of active faults. For i), core samples in good conditions should be taken, as with large-diameter drilling and drilling using a surface-active agent, regardless of whether the fault is in either a Quaternary bed or a basement rock. For ii), drilling should be conducted several sites on both the hanging wall and the footwall. When drawing a geological sectional map based on drilling data, the possibility of stratum displacement due to geological phenomena other than fault displacement must be considered.

e) Investigations using long Geo-slicer method

Recently, a fault investigation method other than trenching has been developed, called the long Geo-slicer method[12]. With this method, long iron sheet piles with a flat U-shaped cross section are driven into an unconsolidated bed; iron plate shutters are inserted to face these iron sheet piles; and then the piles and shutters are pulled out to take undisturbed samples of strata of a certain width. If the iron sheet piles are driven along the measurement line, continuous cross sections of strata can be observed. This method is advantageous in regard to the ease of securing land for conducting investigations compared with trenching, and the ease of bringing the strata samples back to the laboratory for detailed observations.

f) Geophysical exploration

All the methods described so far are for directly observing active faults. However, one problem is the difficulty of deciding where to conduct trenching and drilling because outcrops of active faults are seldom exposed and faults are sometimes covered with alluvium. In such cases, geophysical exploration is effective for identifying faults and approximate locations of the faults.

According to Takahashi et al.[13], the types of geophysical exploration for active fault investigations include the seismic reflection method, sonic prospecting, electric prospecting, electromagnetic prospecting, gravity prospecting, and radioactive prospecting. Of these, the seismic reflection method can locate faults if geological conditions are favorable, and confirm the accumulation of fault displacements based on the amount of displacements in strata that increases with strata age.

4) Problems of geological survey and their countermeasures

a) Problems of surface exploration

Since geological surveys for investigating active faults are mostly conducted based on geomorphological survey results, except for earthquake faults, the precision of the results must be considered when selecting the locations for the geological survey. Often, the location of a lineament that is estimated geomorphologically is several tens of meters away from the actual fault. This may partly be due to the precision of photograph interpretation; but such discrepancies are

geomorphologically significant, since there is a relation between the difference in elevation of geomorphic surfaces on both sides of a fault and the discrepancy of estimated and actual faults[14], as shown in Fig. 5. If the difference in elevation of geomorphic surfaces on both sides of a fault indicates a cumulative fault displacement, faults with a greater difference in elevation will be assumed to have been active for longer, provided their degree of activity is similar. Accordingly, Fig. 5 can be interpreted to mean that the distance between the estimated lineaments and actual faults increases with fault age. It is considered that the discrepancy in locations between lineaments and actual faults becomes greater with fault age, because older fault-scarps have had more chance of being recessed due to erosion or buried under talus deposits. Thus, when conducting a surface exploration, the discrepancy of locations between lineaments identified geomorphologically and actual faults should be considered.

The greatest problem with surface exploration is that fault outcrops seldom exist even when active faults definitely are present. The existence of a fault can be confirmed when a fault outcrop with features identical to geomor- phological features exists near a lineament (to judge the fault as active, there must be proof that it has displaced a Quaternary bed several times). However, the existence of a fault can be neither confirmed nor denied if no fault outcrop is dicovered. With surface exploration, the existence of an active fault can be denied only when no fault is recognized in continuous outcrops (cut slopes of roads and tunnels) within an area established by considering the discrepancy between a geomorpholo- gical location and an actual location. When there are generally few outcrops and no fault outcrops, then the investigation results should be compiled into columns, as with stratigraphy. This technique is used to measure the distances from the location where a lineament is assumed to pass through, to the respective outcrops; sort the outcrops by distance; and quantify them in figures and documents.

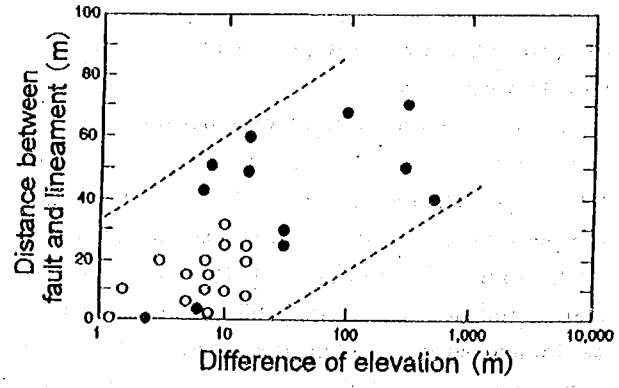


Fig. 5 Relationship between difference in elevation of geomorphic surfaces on both side of a lineament and distance between a lineament and a fault[14].

b) Problems with trenching, adit investigations, and drilling

As with surface exploration, the biggest problem with trenching, adit investigations, and drilling is that the location of a lineament does not necessarily coincide with that of an actual fault. Accordingly, before conducting these investigations, the precise location of a fault must be identified by conducting preliminary investigations such as preparatory drilling and geophysical explorations.

One problem with trenching is the difficulty of recognizing traces of past earthquakes remaining in Quaternary beds. There are usually more than one recognition criterion on trenched walls, so accurate classification of strata and comparison of the strata on both sides of a fault must be conducted to ensure that such traces are found.

When dealing with a reverse fault, it is necessary to start trenching over a wide area, and gradually narrow it down toward the target, due to discrepancies of locations between the reverse fault and the lineament. On the other hand, although it is comparatively easy to select a trenching area for a lateral fault. However, it is difficult to estimate the net displacement because there are not many criteria for estimating the displacement of lateral offset. These problems with trenching are common to adit investigations.

A problem with drilling is that the existence of a fault cannot be determined even based on a core sample that is taken by penetrating a fault, because a shear zone is unlikely to be formed in

young strata such as alluvium and diluvium. When the basement rock of alluvium and diluvium is shallow, drilling should be conducted by penetrating the fault in the basement rock. When the basement rock is deep underground, faults are detected based on the discrepancy of the sequence in the samples taken by drilling on both sides of the fault. Nevertheless, since the sequence is often disturbed due to buried valleys in alluvium and diluvium, trenching may be more suitable for investigating active faults in alluvial and diluvial areas because it can take samples of wide and continuous sections. If trenching is not feasible due to problems of securing land, investigations should be conducted by a combination of drilling and the seismic reflection method, as well as based on the long Geo-slicer method.

c) Problems with geophysical explorations

A problem with the seismic reflection method is that good results cannot be obtained unless a discontinuity, which acts as a reflection surface for earthquake waves. Electric prospecting, electromagnetic prospecting, and gravity prospecting can be used to resolve this problem, none of these methods has been proven reliable because they have rarely been used for active fault investigations. Shinagawa[15] recently conducted fault investigations in the Suwa basin using a type of electromagnetic prospecting method called the CSAMT method that can detect resistivity underground, and found a fault inside basement rock buried under alluvium. This method may be promising for prospecting for faults inside basement rocks.

To identify an active fault, the accumulation of fault displacements must be studied. Except for the seismic reflection method, the accumulation of fault displacements cannot be confirmed by geophysical exploration methods. Thus, geophysical exploration methods, except for the seismic reflection method, should be called fault investigation methods, rather than active fault investigation methods.

6. INVESTIGATION OF POTENTIAL ACTIVITY

1) Purpose of investigations

When a fault, which is thought to be active, is found near the basement of a dam body by detailed geological survey, its potential activity must be investigated.

2) Methodology

There are two methods for identifying the history of activities of an active fault: One is based on whether or not the stratum is cutted by a fault, while the other is to date the intrafault materials themselves.

a) Method based on cover beds

When either a natural or man-made fault outcrop is found and there is fault that has displaced a Quaternary bed, the time of activity can sometimes be identified. There are several strata whose sedimentation ages are known, and there are various displacement due to branching of faults, then the activities (called events) of the respective branched faults can sometimes be dated. In this case, the recurrence intervals of fault activity can be estimated. To specify the ages of strata, the ^{14}C age of carbonaceous matter and a distal tephra whose age is already known are often used. These are the most accurate methods at present for specifying the ages of active fault activity, provided sufficient information is available (the number of strata whose ages can be specified and the number of events).

b) Dating of intrafault materials

When dating intrafault materials, a Quaternary cover bed does not need to exist, since intrafault materials are investigated directly. Fault activities based on intrafault materials are dated by i) obtaining a relative date; ii) a direct method for obtaining the absolute date of fault activity; and iii) a method for obtaining indirectly the date of fault activity relative to the absolute date to be obtained[16].

Method i) includes a method to observe the surface conditions of quartz grains contained in intrafault materials[17), 18), 19)], which uses the change of surface conditions of quartz grains formed by breakage due to fault activity. The surfaces of quartz grains are eroded by the chemical action of groundwater. With this method, the absolute

date is not obtained directly but is estimated indirectly by comparing the surface conditions of target quartz grains with those of quartz grains of known date.

Method ii) includes electron spin resonance (ESR), thermoluminescence (TL), K-Ar, and fission track.

Method iii) focuses on mineral veins inside a fault, with which the date of fault activity is estimated based on whether or not mineral veins are cutted by a fault and whether or not a fault is cutted by mineral veins. Methods used for dating mineral veins are fission track, ESR, and TL.

3) Problems with investigating potential activity of faults

A problem common to the above-mentioned methods for investigating the potential activity of faults is that the results are not certain unless sufficient conditions.

The method based on cover beds is difficult to use the method in mountainous areas, because Quaternary cover beds often do not exist.

When dating intrafault materials, note that intrafault materials were not necessarily formed by fault movement at one time when using either method i) or ii). Also, when using method ii) the date of the target minerals must have been reset to zero due to fault movements. Fukuchi[20] points out some problems with ESR dating, such as i) ESR signal resetting by fault actions, ii) evaluation of annual dose, and iii) influence of hydrothermal solution on the total radiation dose. In regard to ESR signal resetting, he mentions that signals are completely reset at a depth about 620 to 670 m and a width of 2 to 3 mm from the fault surface based on a model due to frictional heat, and that signals are not reset completely at a depth of about 70 to 80 m underground or shallower based on the results of a ring shear test. On the other hand, Lin[21] conducted both ESR and TL dating of fault gouges sampled by varying the distance from the fault surface, and showed that ESR signals are more easily reset the shorter the distance to the fault surface is, since the intrafault materials are closer to the fault surface, the younger they are.

The problem with the method of observing the conditions of quartz grain surfaces is that the method may not be applicable nationwide due to variations of the physiochemical properties of groundwater.

7. COMPREHENSIVE COMPILATION OF INVESTIGATION RESULTS

1) Compilation

The existence of dangerous active faults for dam construction shall be clarified by compiling all investigation results.

a) Comparison of results between literature research and geomorphological survey

When assessing the relationship between reference faults and lineaments accompanying a tectonic fault topography found by the geomorphological survey, the following points are considered and the results shown in maps and tables.

i) Whether or not they correspond with each other, i.e., whether a lineament accompanying a tectonic fault topography corresponds to the reference fault, and vice versa.

ii) When they coincide, a) the location, b) length, c) certainty, and d) displacement must be identified.

iii) When they do not coincide, the case of when no lineament accompanying a tectonic fault topography corresponds to the reference fault should be clearly distinguished from the case of when no reference fault corresponds to the lineament accompanying a tectonic fault topography.

b) Comparison of results between rough geological survey and either the literature research or geomorphological survey

The results of the geological survey are compared with those of either the literature research or the geomorphological survey, regarding the reference faults and the lineaments accompanying a tectonic fault topography found by the rough geological survey in terms of the following:

i) Whether a geological fault exists that corresponds to the reference fault and the lineament accompanying a tectonic fault topography.

ii) When a corresponding fault exists, a) the location of fault outcrop, b) the basis of the corre-

spondence, and c) whether the fault is active must be clarified.

iii) When no corresponding fault exists, the origin of either the reference fault or the lineament accompanying a tectonic fault topography should be examined based on the results of the rough geological survey, the geological structures, and the geology obtained by the literature research.

iv) When the existence of a geological fault cannot be confirmed by the rough geological survey due to unfavorable outcrop conditions, it should be specified that the geological fault could not be confirmed due to unfavorable outcrop conditions.

c) Comparison of results between detailed geological survey and either the literature research or geomorphological survey

The results between the detailed geological survey and either the literature research or geomorphological survey should be compared in the same manner as the rough geological survey.

2) Evaluation of potential activity of faults

The criteria for judging whether a fault is active are as defined in the descriptions of active faults. In general, active faults are those that "have acted in the recent past, and are likely to act again in the future" (Tada[22] as an old reference). Recently, the concept of "past" differs depending on researchers; the Japan Association for Quaternary Research[23] considers the past as 730,000 years ago, while Matsuda[24] defines it to be hundreds of thousands to 1,000,000 years ago. What is important here is the phrase "faults that are likely to act again in the future." Since this cannot be predicted directly, the possibility of future activity is estimated based on previous repeated activity. Particularly, Yamasaki[25] emphasizes "activities that have occurred several times (cumulative displacement)," and states that it is wrong to determine a fault to be active if it has displaced a Quaternary bed only once.

Nevertheless, since it is not possible to check the history of fault activity other than partially by trenching for evaluating potential fault activity. A fault that is identified geologically and accompanies a tectonic fault topography, or a lineament accompanying a tectonic fault topography, often has to be judged as active. This is based on the idea that fault displacement remaining within a topography is proof of cumulative fault activity in the recent past, not a single activity. Thus, tectonic fault topographies must be analyzed carefully based on literature research, geomorphological surveys and geological surveys.

A lineament in a mountainous area that exists on both sides of an alluvial surface, such as a waste-filled valley, may sometimes be determined to have been inactive since at least the Würm glacial stage and thereafter if there is no tectonic fault topography such as a low fault-scarp on the alluvial surface. However, since the formation of a tectonic fault topography on an alluvial surface depends on the slip rate of the fault and the sedimentation rate of the alluvium, fault-scarps do not easily form on an alluvial surface when the degree of activity of the fault is low and the fault slip rate is smaller than the sedimentation rate of the alluvium. In addition, an alluvium surface is often modified artificially into paddy and upland fields. Therefore, active faults need to be analyzed carefully in the above case.

Fig. 6 shows the recurrence intervals of earthquakes in order of degree of fault activity, which were recently obtained by trenching. Despite some dispersions, there is a correlation between the degree of activity and the recurrence interval, with the recurrence interval becoming longer as the degree of fault activity decreases. If more such data can be gathered, it would facilitate judging whether a fault is likely to become active again, based on whether the date of last activity is sufficiently older than the recurrence interval

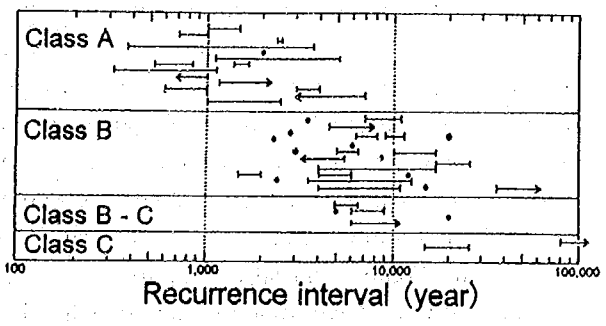


Fig.6 Recurrence intervals of active faults by degree of activity.

determined from the degree of activity of the fault.

3) Evaluation of length and continuity of an active fault

According to Matsuda[31], there is a relation between the length of an earthquake fault (L) and the magnitude of a corresponding earthquake (M) as follows:

$$\log L\,(\mathrm{km}) = 0.6M - 2.9 \qquad 1)$$

On the other hand, in general an earthquake with a magnitude of 6.5 or smaller does not form an earthquake fault[2]. When $M = 6.5$ is substituted into equation 1), L becomes 10 km. This means that a fault that is shorter than 10 km will not cause an earthquake that forms an earthquake fault. Thus, whether the length of active faults exceeds 10 km is important. Matsuda[32] recently proposed the following two equations for the relation between L and M based on the length of earthquake faults and magnitudes revised based on his recent reinvestigations and new data of earthquake faults:

$$M = 6.32 + 0.693 \log L\,(\mathrm{km}) \quad (8.0 \geqq M \geqq 6.8) \qquad 2)$$

$$M = 6.81 + 0.253 \log L\,(\mathrm{km}) \quad (7.3 \geqq M \geqq 6.8) \qquad 3)$$

These equations can be applied when $M \geqq 6.8$, since the minimum value of earthquake faults in inland areas in Japan was determined to be $L = 5$ km (or $M = 6.7$) based on the data of earthquake faults obtained thereafter. Accordingly, to determine the relation between the magnitudes of earthquakes that form earthquake faults and the length of faults, good quality and quantity of data are required in order to avoid vague discussions.

However, evaluation of the length of active faults involves problems of segmentation and grouping. The problem of segmentation is whether or not an extremely long fault, such as the Median Tectonic Line, acts as one body or in several segments. According to recent research, the Median Tectonic Line acts in several segments, and Okada[33] classifies it into eight segments and one inactive area. On the other hand, a close look at an active fault, particularly an earthquake fault, shows that the ground surface trace of a fault is divided into several segments that go side by side despite their simultaneous activities. Nakata et al.[10] divides the Nojima earthquake fault in the Hyogo-ken Nambu Earthquake of 1995 into five segments.

On the contrary, the problem of grouping is that several faults that are considered to be independent may cause an earthquake by acting as one body. In the case of the Hyogo-ken Nambu Earthquake of 1995, several active faults in the Rokko Fault System (including the Nojima fault) moved at the same time. Matsuda[35] mentions that several faults should be combined into one group, which is called a fault zone, with intervals of up to 5 km, for example.

As mentioned so far, when determining some active faults to be earthquake faults, it is hard to decide how to consider their lengths only by ground surface tracing. The length should therefore be determined based on seismological methods (such as the distribution of microearthquakes), morphological investigations of active faults deep underground, and confirmation of synchronism of the date of activities of the respective faults.

8. COUNTERMEASURES FOR GROUND DISPLACEMENTS BY ACTIVE FAULTS

Since no design method to counter ground displacements has yet been established, faults are avoided when constructing structures that would have a great impact if damaged, such as dams and atomic power plants. Although there are no clear criteria regarding the distance of such structures from a fault, in principle locations immediately above a fault where fault displacements occur must be avoided. The relation between the state of damage of the reservoir dam bodies in Awaji Island due to the Hyogo-ken Nambu Earthquake of 1995 and their distance from the Nojima fault gives a guideline as to the distance between the fault and the structure. According to Hiyoshi[36], all the reservoir dams that suffered huge cracks and leakage were located within 20 m of the Nojima fault. Since it is unlikely that fault displacement was the only cause of such

damage to the dam bodies, it should be sufficient not to build structures directly above a fault when considering only the impact of fault displacements. According to the Active Fault Act[37] of the State of California in the US, city and county governments shall not grant permission for developing areas within 500 feet (150 m) from major faults and 200 to 300 feet (60 to 90 m) from clear small faults, unless it is proven by preliminary geological surveys that the ground surface will not be displaced by future fault activity.

The problem here is how to determine faults that are likely to cause fault displacements. To ensure safety, fault shear zones should be considered as possible candidates. Ogata and Honsho[38] confirmed that the width of a fault shear zone is correlated with the length of faults in a granite area in the Chubu mountains, although this fault was not an active one. In addition, Matsuzaki et al.[14] confirmed a similar trend by investigating active faults (Fig. 7). Thus, since the length of a fault is considered to become longer as the width of the fault shear zone increases, structures should be built away from faults when the distribution of fault shear zones cannot be clearly identified.

9. CONCLUSIONS

Since the Hyogo-ken Nambu Earthquake of 1995, trenching and various other investigations have been conducted on active faults, and the location and history of activity of large-scale active faults and active faults located near major cities have been obtained. However, the state of active faults in mountainous areas where many dams are planned to be construct has not been clarified sufficiently, nor have effective methods been established for investigating and evaluating active faults in mountainous areas where little is known about the base topographies. Accordingly, since existing methods for investigating and analyzing active faults for dam constructions have not been fully established, further research is needed to establish such concepts by improving investigation methods and by accumulating knowledge on active faults.

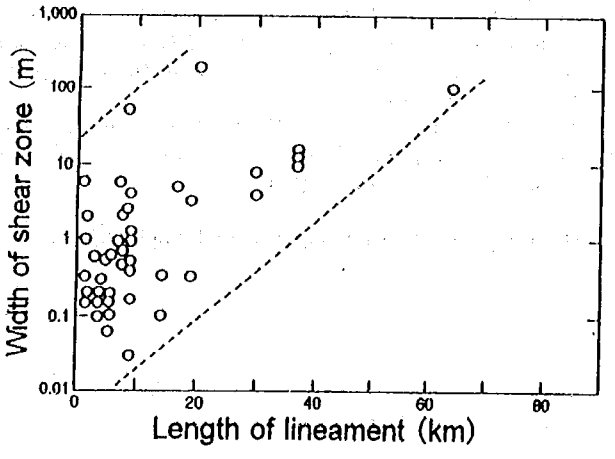


Fig. 7 Relationship between length of lineaments dirived from active faults and width of their shear zones[14].

ACKNOWLEDGMENT

I would like to thank Hisaya Harada for making Fig. 3.

REFERENCES

1) Research Group for Active Faults of Japan: *Active faults in Japan -sheet maps and inventories, Revised ed.* University of Tokyo Press, 437p. 1991. (JwE)

2) Yamasaki, H.: Judgment of certainty and photographic interpretation. In Ikeda, Y., Shimazaki, K. and Yamasaki, H., *What is a active fault?*, University of Tokyo Press, 74-84, 1996. (J)

3) Kuwahara, K.: Procedures of survey on Quaternary fault. *Civil Engineering Journal*, 29, 293-298. 1987. (J)

4) Japan Society of Civil Engineers, Committee on Nuclear Civil Engineering: Geological survey methods. *Investigation and testing methods of geology and ground, and evaluation methods of seismic stability of ground in an atomic power plant*, Part 2, 48p. 1985. (J)

5) Matsuda, T., Ota, Y., Okada, A., Shimizu, F. and Togo, M.: Aerial photo-interpretation of active faults -the individual difference and examples. *Bull. Earthquake Research Institute, Univ. Tokyo*, 52, 461-496, 1977. (JwE)

6) Kuroki, K. and Shinagawa, S.: Method for interpretation of photo-lineament consist of cols and geomorphic lines caused by active fault. *Civil Engineering Journal*, 40, 7, 62-67, 1998. (J)

7) Matsuda, T. and Okada, A.: Shearing degree of fault shear zones -tentative classification based on field observation. *MTL*, 2, 117-125, 1977. (J)

8) Sibson, R. H.: Fault rocks and fault mechanics. *Jour. Geological Society of London*, 133, 191-213, 1977

9) Okada, A.: Studies of active fault by trenching method. In Yonekura, N., Okada, A. and Moriyama, A., Eds. *Tectonic landforms*, 18-44, 1990. (J)

10) Okada, A. and Matsuyama, N.: *Trenching of active faults -investigate history of earthquake faults.* Fault Research Data Center, 28p. 1992. (J)
11)Allen, C. R.: Seismological and paleoseismological techniques of research in active tectonics, In *Studies in geophysics: Active Tectonics*, National Academy Press, 148-154, 1986
12)Haraguchi, T., Nakata, T., Shimazaki, K., Imaizumi, T., Kojima, K. and Ishimaru, K.: A new sampling method of unconsolidated sediments by long Geo-slicer, a pile-type soil sampler. *Jour. Japan Society of Engineering Geology*, **39**, 306-314, 1998. (JwE)
13)Takahashi, T., Mimoto, K. and Hayakawa, T.: Present state of applications of geophysical methods to characterization of active faults. *Jour. Japan Society of Engineering Geology*, **38**, 118-129, 1997. (J)
14)Matsuzaki, T., Kuroki, T., Shinagawa, S. and Wakizaka, Y.: Quantitative relationships beetween the geomorphological and geological features of active faults in East Japan. *Proceedings of the Annual Conference of the Japan Society of Engineering Geology*, 57-60, 1997. (J)
15)Shinagawa, S.: Investigation of buried faults in urban areas using electromagnetic exploration. *Civil Engineering Journal*, **41**, 2, 26-31, 1999. (J)
16)Tanaka, K.: Evaluation of activity of faults based on intrafault materials. *Proceedings of the Symposium*, Japan Society of Engineering Geology, 15-26, 1989. (J)
17)Kanaori, Y., Miyakoshi, K., Kakuta, T. and Satake, Y.: Surface texture of quartz grains from fault gouges. *Abiko Research Laboratory Report* No.**377011**, Central Research Institute of Electric Power Industry, 21p. 1978. (JwE)
18)Kanaori, Y., Miyakoshi, K., Kakuta, T. and Satake, Y.: Dating fault activity by surface textures of quartz grains from fault gouges (part I) -Classification and forming-process of surface textures-. *Jour. Japan Society of Engineering Geology*, **23**, 18-32, 1982. (JwE)
19)Kanaori, Y., Miyakoshi, K., Kakuta, T. and Satake, Y.: Dating fault activity by surface textures of quartz grains from fault gouges (part II) -Fracturing mode and movement age of fault. Jour. *Japan Society of Engineering Geology*, **23**, 65-75, 1982. (JwE)
20)Fukuchi, T.: ESR dating of active faults -Its controversial points and future prospect-. *Active Fault Research*, **7**, 13-21, 1989. (J)
21)Lin, A.: ESR and TL datings of active faults in the Iida area of the southern Ina valley. Active fault Research, **7**, 49-62, 1989. (J)
22) Tada, F.: Two kinds of active faults. *Geographical Review of Japan*, **3**, 983-990, 1927. (J)
23) Japan Association for Quaternary Research: *Quaternary Maps of Japan*. University of Tokyo Press, 119p. 1987. (J)
24) Matsuda, T.: Search active faults. In Shimazaki, K. and Matsuda, T., Eds. *Faults and Earthquakes*, University of Tokyo Press, 24-44, 1994. (J)
25) Yamasaki, H.: What is a active fault? In Ikeda, Y., Shimazaki, K. and Yamasaki, H., *What is a active fault?*, University of Tokyo Press, 35-71, 1996. (J)
26) Geological Survey of Japan: Interim report on active fault researches in the 1995 fiscal year. *Geological survey of Japan Interim Report*, **259**, 98p. 1996. (J)
27) Geological Survey of Japan: Interim report on active fault researches in the 1996 fiscal year. *Geological survey of Japan Interim Report*, **303**, 140p. 1997. (J)
28) Geological Survey of Japan: Interim report on active fault and paleocarthquake researches in the 1997 fiscal year. *Geological survey of Japan Interim Report*, **EQ/98/1**, 188p. 1998. (J)
29) Science and Technology Agency: *Proceedings of the meeting on earthquake research in the 1995 and 1996 fiscal years.* Science and Technology Agency, 241p. 1997. (J)
30) Science and Technology Agency: *Proceedings of the 2nd meeting on active fault research.* Science and Technology Agency, 344p. 1998. J)
31) Matsuda, T.: Magnitude and Recurrence interval of earthquakes from a fault. *Zisin, Jour. Seismological Society of Japan*, 2nd Ser. **28**, 269-283, 1975. (JwE)
32) Matsuda, T.: Present state of long-term prediction of earthquakes based on active fault data in Japan -An example for the Itoigawa-Shizuoka Tectonic Line active fault system-. *Zisin, Jour. Seismological Society of Japan*, 2nd Ser. **50**, 23-33. 1998. (JwE)
33) Okada, A.: Proposal of the segmentation on the Median Tectonic Line active fault system. *Mem. Geological Society of Japan*, **40**, 15-30, 1992. (JwE)
34) Nakata, T., Yomogida, K., Odaka, J., Sakamoto, T., Asahi, K. and Chida, N.: Surface fault ruptures associated with the 1995 Hyogoken-Nanbu Earthquake. *Jour. Geography*, **104**, 127-142, 1995. (JwE)
35) Matuda, T.: Seismic zoning map of Japanese Islamds, with maximum magnitude derived from active fault data. *Bull. Earthquake Research Institute, Univ. Tokyo*, **65**, 289-319, 1990. (JwE)
36) Hiyoshi, S.: The relationship between the damage on the reservoirs and the distance from the Nojima Fault in north Awaji Island. *Tsuchi-to- Kiso*, **43**, 11, 59-60, 1995. (J)
37)Hart, E. W.: Fault-rupture hazard zones in California; Aliquist-Priolo special studies zones act of 1972 with index to special studies zone maps (revised), *California Department of Conservation, Division of Mines and Geology Special Publication*, **42**, 31p. 1992.
38)Ogata, S. and Honsho, S.: Fault activity evaluation inthe case of electric power plants. *Jour. Japan Society of Engineering Geology*, **22**, 67-87. (JwE)

(J): in Japanese, (JwE): in Japanese with English abstract.

Present and Future Roles of Nonlinear Numerical Procedures in the Seismic Analysis of Concrete Dams

by

Robert L. Hall[1] and Enrique E. Matheu[2]

ABSTRACT

This purpose of this paper is to discuss the present and possible future roles of nonlinear numerical procedures in the seismic analysis of concrete dams. The application of nonlinear analysis procedures is pivotal for the rigorous seismic evaluation of these critical structures. The objective of these analysis procedures is to quantify accurately the extent of seismically induced damage. These type of approaches have the potential for determining the ultimate capacity of existing concrete dams by the appropriate modeling of nonlinear phenomena such as material behavior, interaction of monolith vertical joints, and behavior of horizontal lift joints. Some numerical procedures have been successfully developed to model the material nonlinear properties. Other procedures have been formulated to represent the dynamic behavior the joints. However, because of their inherent complexities and the difficulties involved in the determination of their parameters, nonlinear analyses may not be particularly suited for the design phase. On the other hand, linear analyses usually render a great amount of insight into the expected behavior of the system, but they can not predict accurately the extension of damage that may occur under moderate or strong ground motions. This situation opens an alternative avenue for the application of nonlinear models, in the form of the development of assessment tools based on nonlinear parametric studies, which can be used to obtain an estimate of the real performance of the system using the information provided by a linear elastic analysis.

KEYWORDS: Concrete dams; nonlinear response; tensile cracking; joint behavior; smeared crack model; scaled model experiments.

1. INTRODUCTION

A significant body of research has been devoted in the last thirty years to the study of the dynamic behavior of concrete dams under seismic excitations. Several extensive numerical studies have evaluated the influence of different interaction phenomena influencing the dynamic response. Many of these analyses were based on linear models and performed in the frequency domain. Although restricted by the linearity assumption, undoubtedly these types of studies still provide a great deal of information about the earthquake response that can be expected under more realistic conditions (NRC Panel, 1990). However, it is clear that severe ground motions could trigger different response mechanisms not predicted by the linear analysis. For example, dynamic stresses caused by strong earthquakes may create areas of localized damage, mostly associated with the low tensile strength of the mass concrete. In particular, seismically induced cracking is likely to occur along lift joints, which constitute inherent planes of weakness. Another nonlinear effects are related to the contraction joints between monoliths, which may move relative to each other during the seismic event, thus inducing the cyclic opening, closing and sliding motion of the joint. Additionally, the overall response of the system under severe excitations may be influenced by the spatial variation of the ground

[1] Supervisory Research Structural Engineer, Structural Mechanics Division, Structures Laboratory, U.S. Army Engineer Waterways Experiment Station, Vicksburg, MS 39180 (USA).
[2] Research Assistant Professor, Department of Engineering Science and Mechanics, Virginia Polytechnic Institute and State University, Blacksburg, VA 24060 (USA).

motion. In summary, the characteristics of the system when exposed to strong ground motions are such that the response will differ from that obtained under the assumption of linear behavior. The rigorous evaluation of the seismic response should take into account these features. However, the situation is complicated by the fact that any sophisticated constitutive model should be used in conjunction with a set of material parameters that can be experimentally determined with some appropriate confidence level.

It is widely accepted that the nonlinear behavior of concrete under compressive states it is not one of the most critical factors affecting the characteristics of the seismic response of dams (NRC Panel, 1990). On the other hand, the appropriate constitutive modeling of the material behavior under tensile conditions constitutes a substantial feature that undoubtedly needs to be incorporated into the analysis. Some of the most relevant efforts presented in the literature aiming to incorporate these nonlinear characteristics into the analysis are discussed next. This is not intended to be a state-of-the-art review, but just a description of only some of the relevant contributions in the field.

In a pioneering work, Pal (1986) studied the two-dimensional seismic response of the tallest non-overflow monolith of Koyna Dam (India), using a smeared crack approach to model tensile cracking. The smeared crack model is a finite-element modeling approach intended to capture the characteristics of the response under tensile conditions. This model monitors the stress/strain conditions at pre-specified points in the finite-element mesh. Crack initiation and propagation are defined in terms of some appropriate local criteria. After cracking, the local material properties are modified by introducing an orthotropic constitutive model whose orientation depends on the cracking plane. Mlakar (1987) studied the nonlinear response of three different gravity dam sections subjected to seismic ground motion. The dam sections, with different heights, were selected to be representative of the most common designs. A commercial, general-purpose finite element code was used, with a linear constitutive model in compression and tension, coupled with a smeared crack model. Approximate strain rate enhancements were used to define the material parameters, and particular consideration was given to the selection of the time history used for analysis. The hydrodynamic effects were approximated using Westergaard's assumption, which was implemented through lumped added masses distributed along the upstream face. The numerical simulations showed that the example sections cracked completely across the width, with most of the cracking phenomena initiating at the upstream edge of the base, and at the locations of abrupt slope change along the downstream face. The study demonstrated that the approximate representation of damage by means of additional damping in the corresponding linear model does not capture the characteristics of the nonlinear response. Mao and Taylor (1997) performed the same type of parametric study, but focusing on the response of medium-height gravity dams. They reported similar numerical behavior, with cracked areas usually concentrated near slope changes, which propagated almost instantaneously after initiation once the intensity of the excitation exceeded a critical value.

Vargas-Loli and Fenves (1989) carried out an extensive numerical study of the two-dimensional seismic response of Pine Flat Dam (USA) using a smeared crack model based on an equivalent tensile strength criterion. The tensile strength was defined as a function of the element size and the fracture energy of the material, but the computed values were considered too small and they were arbitrarily scaled up. The internal damping effects in the dam were modeled by damping proportional to the tangent stiffness matrix. The fluid domain was modeled using a mixed pressure-displacement formulation, which resulted in a symmetric matrix description for the coupled fluid-structure system. The reservoir model was truncated at a finite length with an appropriate boundary condition. Also, a partially absorbing boundary condition was used to model the bottom of the reservoir. Both empty and full reservoir conditions were examined, using ground motions scaled to various peak

acceleration values to investigate the influence of the excitation amplitude on the nonlinear response. This study showed that diffuse cracking patterns are likely to occur near stress concentration areas. In most cases, the ground excitation levels that induced crack initiation also generated severe damage by extensive crack propagation, forcing the structural system to reach its ultimate condition. In this context, the ultimate condition is defined as the system's condition immediately before loss of convergence in the numerical solution.

Another comprehensive study of the nonlinear seismic response of Pine Flat Dam was presented by El-Aidi and Hall (1989a, b). By defining a fictitious length normal to the two-dimensional dam section, they modeled the effects of the flexible foundation by using a frequency-independent approximation of a three-dimensional viscoelastic half-space. The hydrodynamic effects were incorporated by means of a displacement-based finite element model of the reservoir, truncated at a finite length. The irrotationality condition for the fluid domain was enforced through a penalty formulation, and a bilinear pressure-volumetric strain relationship was used to account for cavitation phenomena. Energy dissipation effects at the boundaries of the reservoir model were incorporated through an approximation based on the one-dimensional wave propagation problem normal to the corresponding interface. Following the approach commonly used for frequency-domain linear analyses (Hall and Chopra, 1982), the energy dissipation characteristics associated with a non-rigid reservoir bottom were defined in terms of a constant parameter, referred to as the reflection coefficient. The tensile behavior of the concrete was represented using the smeared crack approach. Crack propagation was governed by an element-dependent strength criterion applied to the elements ahead of the crack tip. The numerical simulation of the system response was performed in an interactive environment, where the propagation of cracks was ultimately controlled by the analyst, in an effort to avoid spurious cracking patterns. Global damping characteristics were modeled by a damping matrix proportional to the elastic stiffness matrix, with removal of the damping contributions corresponding to cracked elements. The numerical results showed that, in general, the occurrence of cracking in a dam is associated with a reduction of the dynamic pressures in the fluid domain, therefore decreasing the importance of cavitation phenomena.

The behavior of contraction and lift joints constitutes another important source of nonlinear effects. Lift joints could be introduced in the model as planes of weakness with low tensile strength (attributed to inter-lift bonding), whereas contraction joints should be in most cases treated directly as discontinuity planes. Ideally, the numerical models for both types of joints should account for the opening, closing and frictional sliding of the interfaces with the associated energy dissipation mechanisms. These planes of weakness could be introduced in the finite-element model by using the smeared crack approach with pre-defined crack orientations corresponding to the joints. Alternatively, the joints could be modeled explicitly using special elements. For example, the joint interfaces could be connected through a set of nonlinear spring elements acting in parallel. This arrangement introduces many additional degrees of freedom, because it requires a double-node discretization of the interface in which the spring ends connect the corresponding nodes of each surface defining the interface. In an attempt to partially circumvent this drawback, Hall and co-workers (Hall and Dowling, 1985; Dowling and Hall, 1989) developed a nonlinear element to model the two-dimensional opening and closing of joints for the analysis of arch dams. The advantage of this element is that it can be used straightforwardly with a single-element discretization of the dam, because it does not depend on additional degrees of freedom along the thickness direction. The joint behavior is represented by only two nonlinear torsional and translational springs. Equivalent stiffness parameters, as well as the offset of the translational spring are calibrated by numerically solving a representative problem in which the

joint is modeled by means of a multi-spring arrangement, which spans the width. The proposed element was used to simulate the seismic response of Pacoima Dam (USA). The analysis took into account the effects of the elastic foundation and the impounded reservoir, both modeled also by finite elements. The compressibility of the fluid was neglected, and a heuristic scheme was applied to incorporate the matrices corresponding to the foundation and fluid domains after condensation of the non-relevant degrees of freedom. The numerical results showed that significant separation of the contraction joints could be expected even under moderate levels of excitation. This would indicate the need to expand the analysis by including the possibility of relative sliding of the interfaces, which was not considered in the proposed joint element. Hall (1998) recently presented a study of the effects of cracks and contraction joints on the response of arch dams. The numerical model was based on the smeared crack approach. In this particular implementation of this versatile approach, the orientation of the cracking planes was pre-determined to simulate only the cracking induced by the cantilever stresses. As in previous works, the foundation was considered elastic and massless, and the fluid was assumed incompressible. Joint sliding effects were introduced in the formulation in the form of friction criteria limiting the magnitude of the corresponding shear stresses. The numerical results showed that the proposed formulation is able to capture the most important features of the nonlinear dynamic response with a reasonable computational cost.

2. LIMITATION OF PRESENT ROLES

As discussed in the previous section, several analytical procedures have been formulated to predict the two- and three-dimensional nonlinear seismic response of concrete dams. However, the structural response predictions obtained by means of these nonlinear analytical procedures are directly dependent on the availability and quality of the input parameters used to define the model representing the nonlinear behavior. While data is readily obtainable for simple material experiment or scaled model experiments, this is not the case with the full-scale data necessary for the proper validation of these complex procedures.

The response measurements needed to describe the actual seismic behavior of a concrete dam can be obtained from actual earthquake events, full-scale experiments, and scaled model experiments (Hall, 1988). There have been several cases of concrete dams suffering moderate or significant damage caused by seismic excitations. However, since no concrete dam has ever failed from earthquake ground motions, measurements of the dynamic response of a concrete dam beyond its ultimate capacity have not been recorded. A very well known case of damage to a concrete dam occurred in 11 December 1967 to the Koyna Dam (India). The damage to this structure consisted of significant cracking in the upper section of several monoliths, with cracks initiating near the points of abrupt slope change in the downstream face. The Sefid Rud (Iran) and the Hsinfengkiang (China) are concrete buttress dams that experienced cracking in the upper sections as a result of earthquake ground motions. The left thrust block and abutment of the Pacoima Dam (a concrete arch structure) experienced some damage during the 1994 Northridge earthquake. Since it is at best difficult to predict which dams are going to be subjected to earthquake ground motions, the effective placement of the instrumentation needed for interpretation of any observed seismic damage becomes practically impossible.

Forced vibration prototype experiments have been performed on many different concrete dams (Hall, 1988). These experiments have determined the dynamic properties of these complex structures and have identified the importance of interactions between the reservoir, foundation rock, and the concrete structure. The data from these experiments provides fundamental results, which can be used to validate linear elastic numerical procedures. However, forced vibration experiments do not reproduce the performance of these structures during an earthquake since the external

excitation is placed on the crest of the dam. The use of explosives to generate the excitation provides an alternative approach to determine the characteristics of the dynamic performance of a dam, as shown by Ghanaat and co-workers (1993) through a series of experimental tests performed on the Dongjiang Dam (China). The results of these experiments validated the fact that the high frequency ground motions generated by controlled explosions can be effectively used to excite the low frequency fundamental dynamic characteristics of the system. This type of experiments shows the advantage of simulating more closely a real earthquake event, since they excite the structure with hydrodynamic loads and with ground movements, thus providing important data for the study of the complex dam-foundation-reservoir interaction phenomena. It is clear that these experiments must be performed in extremely controlled conditions and they must be limited to exciting only the linear elastic response of the structure, avoiding the occurrence of damage.

The lack of measured data that describes the response characteristics under conditions of extreme damage, and the practical limitations of the approaches currently used for full-scale experiments have emphasized the importance of scaled model studies. This type of experiments provides a very effective framework for the study of the dynamic nonlinear performance of concrete dams. Nonlinear scaled model experiments must follow certain laws of similitude. In order to model the hydrodynamic loads on a dam neglecting the foundation effects, the ratio of the density of the model fluid to the density of the water in the reservoir must be identical to the ratio of the model concrete density to the prototype concrete density (Donlon, 1989). Since the density of most heavy fluids is no more than a factor of two greater than that of water, scaled model studies cannot accurately model all the influences of fluid-structure interaction. Even though exact similitude laws have not been followed, these experiments have provided useful data for investigating the nonlinear seismic response of concrete dams.

3. FUTURE ROLES

Currently, there are several sophisticated numerical models that can be used to represent the nonlinear response of concrete dams. The central issue is their calibration by using experimental results obtained at the appropriate scale. The focus of the calibration process should shift from representing accurately the response to a particular ground motion to reproduce accurately the average response characteristics when the system is subjected to an ensemble of ground motions. The final decision regarding the safety of the dam should not be based only on the accurate description of a particular crack, at a particular elevation, for a particular excitation. The uncertainties in the material input data and the underlying approximations in the numerical implementation do not seem to encourage an engineer's decision based only on the results of time-history nonlinear analyses without consideration of the influence that changes in the input parameters might have on the global response. It is clear that the results of even the most rigorous nonlinear numerical procedures need to be coupled with the appropriate engineering judgment.

The analyst should be provided not only with a reliable nonlinear numerical model of the dam-foundation-reservoir system, but also with an effective and rational tool for the proper interpretation of the corresponding results. In this framework, computationally efficient nonlinear models could be used in large-scale parametric studies, aiming to provide the engineer with enough information and facilitating a sound decision when the analyst is faced with a particular situation. Sensitivity analyses should provide an adequate framework to establish the importance and relative influence of the parameters used to describe the nonlinear behavior of the system. This is facilitated by the fact that extensive parametric studies are now feasible with a reasonable computational cost. In turn, this type of studies could be used to calibrate assessment tools based on linear analysis results. These assessment tools could use the results from linear analyses to

identify the severity of the average damage that could be expected for a particular situation. In principle, one could perform this by means of regression analyses, aiming to establish a relationship between the characteristics of the ground motion, the characteristics of the structure and the level of damage that can be expected. This relationship between the input excitation, the system characteristics and the resulting damage is expected to be highly nonlinear and it would depend on the response parameter(s) used to quantify the damage level. Perhaps, a more efficient and flexible approach is the use of neural networks and fuzzy systems to render an approximate quantification of the expected damage for a given set of input and system parameters. Cret and Katayama (1992) used a model for damage prediction of lifeline systems based on fuzzy logic. The proposed model generates a quick estimate of the severity of the earthquake-induced damage in terms of selected ground motion characteristics. Molas and Yamazaki (1995) proposed a damage-estimation system based on a neural-network model, which is used to correlate certain ground-motion indices with the damage suffered by building structures. The spectrum intensity and the peak ground acceleration, velocity, and displacement values were among the different indices used to describe the ground-motion characteristics. A representative nonlinear structural system was selected for training, and the damage suffered by the structure for a given ground motion was quantified in terms of the corresponding ductility factor. This work shows the applicability and potential usefulness of neural-network based systems for damage estimation. Once the system has been trained for an appropriate ensemble of ground motions, estimation of expected damage can be performed in a simple and quick way. The only computational burden lies on the training process, though in most cases it could be handled speedily by current computational resources.

4. CONCLUSIONS

The rigorous seismic evaluation of concrete dams requires an accurate quantification of the damage that can occur under earthquake excitations. Nonlinear analysis procedures can identify the ultimate capacity of existing concrete dams taking into account the most critical nonlinear phenomena controlling the response. However, the complexity of these procedures and the scarcity of appropriate calibration strategies frequently force the analyst to interpret the corresponding results using the best engineering judgment. The influence of the input parameters and ground excitation on the nonlinear dynamic response should be investigated by sensitivity studies that aim to identify the most critical conditions. The available nonlinear analysis schemes could be used to develop a rational assessment tool, which could provide a systematic estimation of the expected average damage based on the input ground motion characteristics and the material and geometric parameters defining the structural system. This would provide the analyst with a useful reference framework for the adequate interpretation of results.

5. ACKNOWLEDGEMENTS

This study was sponsored by the Civil Works Earthquake Engineering Research Program of the U.S. Army Engineer Waterways Experiment Station in Vicksburg, MS. We appreciate the cooperation of the authorities at the U.S. Army Engineer Waterways Experiment Station, which permitted us to prepare and present this paper. Permission to publish this paper was granted by the Chief of Engineers, U.S. Army Corps of Engineers.

6. REFERENCES

Cret, L., and Katayama, T., "On-Line Damage Estimation for Lifeline Systems during Earthquakes," Proceedings of the 10th World Conference on Earthquake Engineering, Vol. 9, pp. 5501-5504 (1992).

Donlon, W. P., "Experimental Investigation of the Nonlinear Seismic Response of Concrete Gravity Dams", Report No. EERL 89-01, California Institute of Technology, Pasadena, CA (1989).

Dowling, M. J., and Hall, J. F., "Nonlinear Seismic Analysis of Arch Dams," Journal of Engineering Mechanics, Vol. 115, No. 4, pp. 768-789 (1989).

El-Aidi, B., and Hall, J. F., "Nonlinear Earthquake Response of Concrete Gravity Dams – Part 1: Modeling," Earthquake Engineering and Structural Dynamics, Vol. 18, pp. 837-851 (1989a).

El-Aidi, B., and Hall, J. F., "Nonlinear Earthquake Response of Concrete Gravity Dams – Part 2: Behavior," Earthquake Engineering and Structural Dynamics, Vol. 18, pp. 853-865 (1989b).

Ghanaat Y., Chen H.-Q., Redpath, B.B., and Clough, R.W., "Experimental Study of Dongjiang Dam for Dam-Water-Foundation Interaction," Report submitted to the National Science Foundation under the US-PRC Protocol for Scientific and Technical Cooperation in Earthquake Studies; Report No. QS93-03, QUEST Structures, Emeryville, CA (1993).

Hall, J. F. and Chopra, A. K., "Two-Dimensional Dynamic Analysis of Concrete Gravity and Embankment Dams including Hydrodynamic Effects," Earthquake Engineering and Structural Dynamics, Vol. 10, pp. 305-332 (1982).

Hall, J. F. and Dowling, M. J., "Response of Jointed Arches to Earthquake Excitation," Earthquake Engineering and Structural Dynamics, Vol. 13, pp. 779-798 (1985).

Hall, J. F., "The dynamic and earthquake behavior of concrete dams: Review of experimental behavior and observational evidence", Soil Dynamic and Earthquake Engineering, Vol. 7 No. 2 (1988).

Hall, J. F., "Efficient Nonlinear Seismic Analysis of Arch Dams," Earthquake Engineering and Structural Dynamics, Vol. 27, pp. 1425-1444 (1998).

Mlakar, P., "Nonlinear Response of Concrete Gravity Dams to Strong Earthquake-Induced Ground Motion," Computers and Structures, Vol. 26, No. 1, pp. 165-173 (1987).

Mao, M., and Taylor, C. A., "Nonlinear Seismic Cracking Analysis of Medium-Height Concrete Gravity Dams," Computers and Structures, Vol. 64, No. 5, pp. 1197-1204 (1997).

Molas, G. L., and Yamazaki, F., "Neural Networks for Quick Damage Estimation," Earthquake Engineering and Structural Dynamics, Vol. 24, pp. 505-516 (1995).

Pal, N., "Seismic Cracking of Concrete Gravity Dams," Journal of the Structural Division (ASCE), Vol. 102, No. 9, pp. 1827-1844 (1976).

Panel on Earthquake Engineering for Concrete Dams, National Research Council, "Earthquake Engineering for concrete Dams: Design, Performance, and Research Needs," National Academy Press, Washington, DC (1990).

Vargas-Loli, L. M., and Fenves, G. L., "Effects of Concrete Cracking on the Earthquake Response of Gravity Dams," Earthquake Engineering and Structural Dynamics, Vol. 18, pp. 575-592 (1989).

Dynamic Response and Failure Mechanism of a Pile Foundation During Soil Liquefaction under Shaking Table Test Using a Large-scale Laminar Shear Box

by

Shuji TAMURA[1], Chikahiro MINOWA[2], Yasutsugu SUZUKI[3], Michio SUGIMOTO[4], Shunji FUJII[5] and Takaaki KAGAWA[6]

ABSTRACT

Shaking table tests using a large laminar shear box 6m deep were conducted to study the vibrational behavior and failure mechanism of reinforced concrete piles during soil liquefaction. It is shown that;(1) the damage to pile heads occurred not only by the lateral inertial force from the superstructure but also by the deformation of soils, just before surface layer liquefied;(2) the damage to the middle part of the piles was caused by the deformation of surface layer, immediately after the surface layer liquefied. These test results suggest that the responses of the pile-structure system can be significantly influenced by the conditions right before and immediately after soil liquefaction.

KEY WORDS: Liquefaction
Pile
Failure mechanism
Shaking table test

1. INTRODUCTION

During the 1995 Hyogoken-Nambu earthquake, extensive soil liquefaction occurred on the reclaimed land areas of Kobe and caused heavy damage to pile foundations. Attempts have been made to study the dynamic response of soil-pile-structure systems by model tests (Tokimatsu et al.,1991) and centrifuge tests (Miyamoto et al.,1992, Sato et al.,1995). However, knowledge of the failure mechanism of pile foundations during soil liquefaction is limited. The objectives of this study is to clarify the dynamic behavior and failure mechanism of piles during soil liquefaction by large-scale shaking table tests.

2. MODEL PREPARATION

The large-scale shaking table tests were performed at NIED (National Research Institute for Earth Science and Disaster Prevention) in Tsukuba, Japan. The size of shaking table is 15m by 15m and the capacity is 500 tons. The large-scale laminar shear box with the dimensions of 6 m in height, 3.5 m in width and 12 m in length (shaking direction) was mounted on the shaking table. A soil-piles-structure system was modeled in the laminar shear box as shown in Fig. 1. Four reinforced concrete piles with a diameter of 15 cm and a length of 6 meters were installed in saturated sand. The test sand was collected

1) Researcher, National Research Institute for Earth Science and Disaster Prevention, Tsukuba-shi, Ibaraki-ken, 305-0006, Japan
2) Cooperative Research Officer, ditto
3) Senior Research Engineer, Kajima Technical Research Institute
4) Chief Research Engineer, Takenaka Research & Development Institute
5) Chief of Earthquake Sect., Taisei Corporation, Technology Research Center
6) Professor, Wayne State University

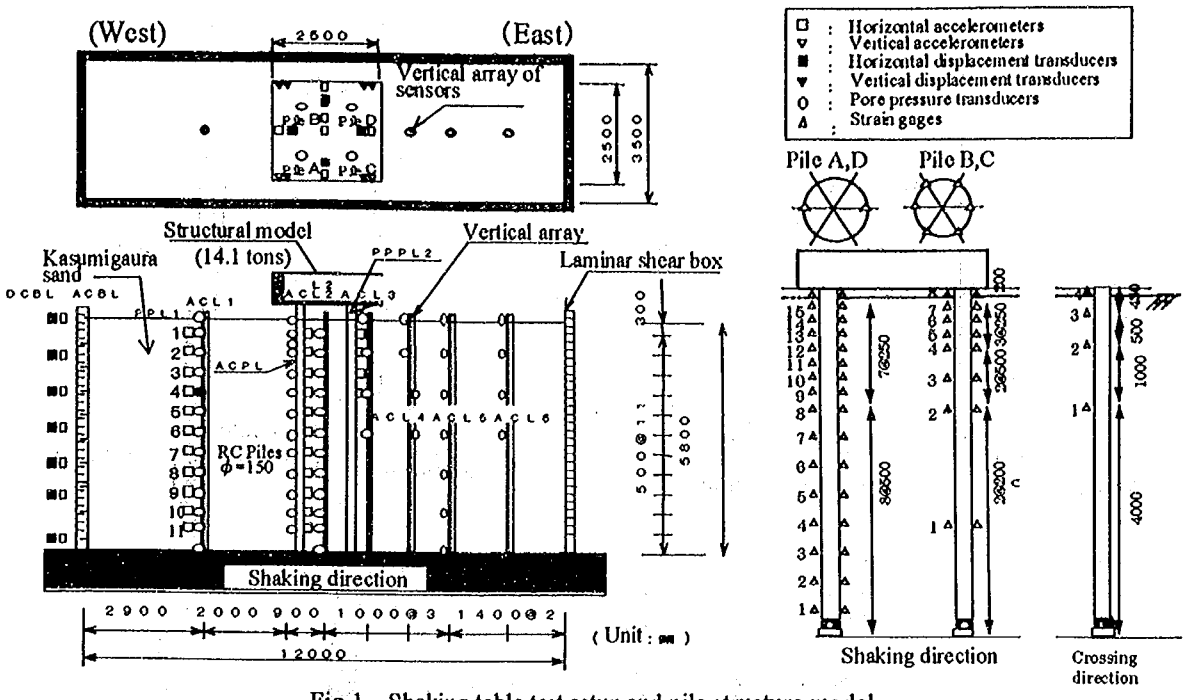


Fig.1 Shaking table test setup and pile-structure model

Table 1 Test cases

Test case	Input waves	A_{max}(cm/s^2)
Case 1	RINKAI92	10
Case 2	RINKAI92	30
Case 3	RINKAI92	60
Case 4*	RINKAI92	310
Case 5	RINKAI92	30

*: Full scale strong motion

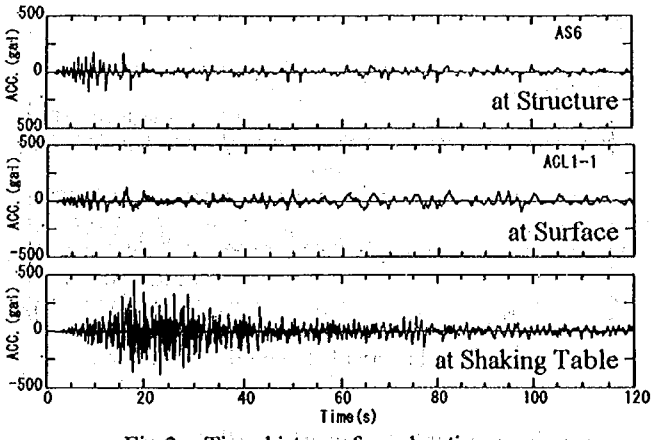


Fig.2 Time history of accelerations

from Hokota near the Lake Kasumigaura (D_{50}=0.275, U_c=2.64). A relative density was about 60 percent and the water level was ground surface. The structural model was a stack of steel plates with a total weight of 14.1 tons. Piles heads were rigidly linked with the structural model, while their tips were pined to the laminar shear box. Accelerations, excess pore-water pressures, displacements of the structural model and bending moments of the piles were recorded during the tests.

Input motion was RINKAI92, which a synthesized ground motion expected in the Tokyo bay area for seismic design of buildings. The amplitudes of the motion were scaled as shown table 1. The shaking tests were performed from Case 1 to Case 5. Case 4 is the shaking event using a full scale strong motion. This paper presents in details Case 4, the result of a full scale strong motion. The details of Case 1-5 has been described by Suzuki et al.(1998)

3. TEST RESULTS AND DISCUSSION

Fig. 2 shows the recorded structural acceleration, ground surface acceleration and shaking table acceleration time histories during the test. Fig. 3

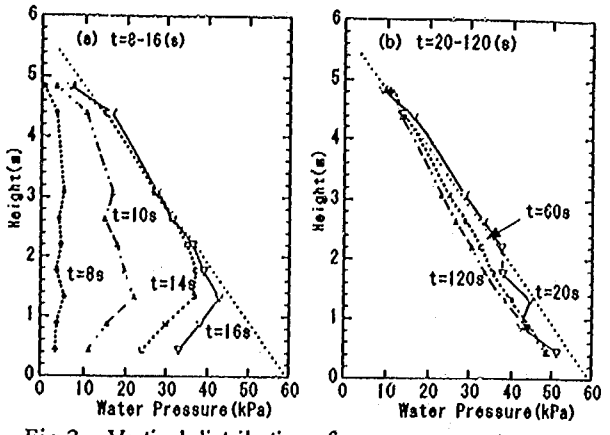


Fig.3 Vertical distribution of excess pore water pressure

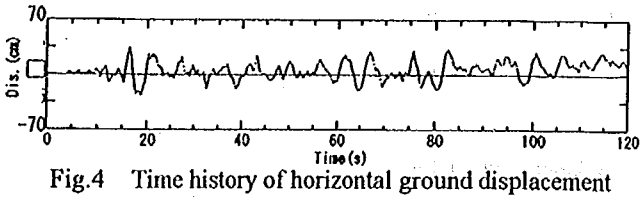


Fig.4 Time history of horizontal ground displacement

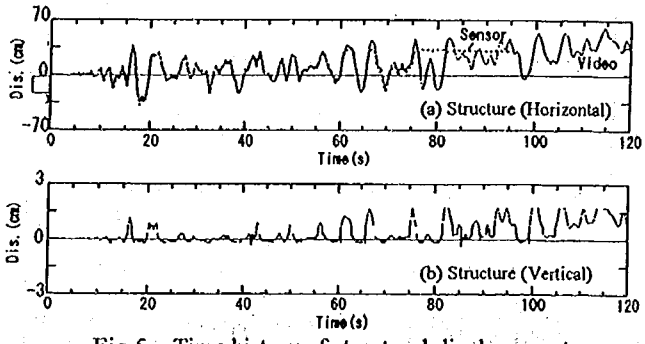


Fig.5 Time history of structural displacement

shows the vertical distribution of the excess pore water pressure. The upper part of the soil was liquefied at 16 seconds, although the lower part did not completely liquefy. The lower part was liquefied at 20 seconds. The soil liquefied at early stage of the shaking. The response accelerations were significantly smaller than the input motion due to the soil liquefaction. The peak acceleration of the ground surface was 120 gals, which was a quarters of the base acceleration. The amplitude of acceleration at the structural model reached 170 gals at 9.6 seconds, just before liquefaction.

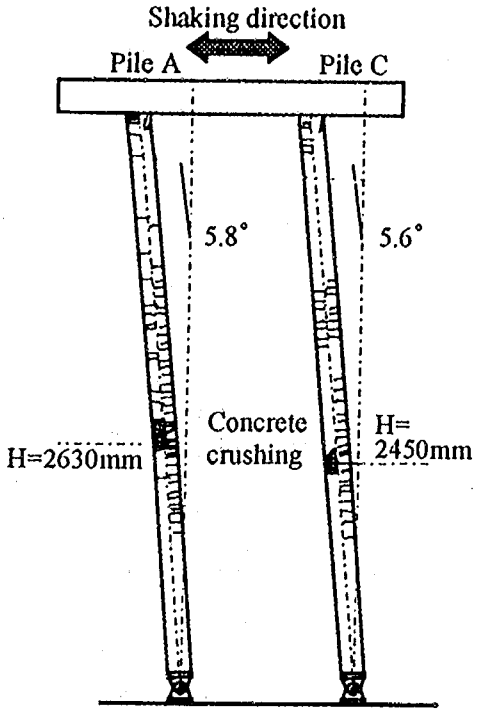
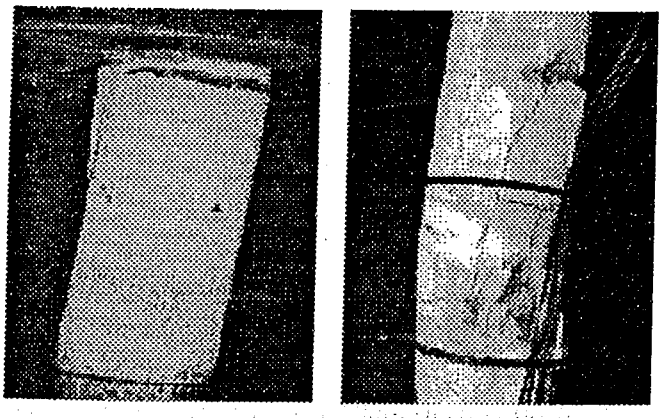


Fig.6 Cracks and deformation of damaged piles



(a) Damage of pile head

(b) Concrete crushing in the middle part of pile

Photo.1 Damage of Piles after shaking test

Fig. 4 and 5 shows the ground displacement and structural displacements time histories. At 16 seconds after the start of shaking, a large displacement of the ground surface occurred. At the same times, the structural model suddenly moved 36 cm and settled 1.1 cm. This result suggests that the pile foundations was heavily damaged at 16 seconds by the soil deformation. After 16 seconds, the displacements of the structural model increased steadily. Finally the

residual horizontal displacement reached 50 cm.

Fig. 6 shows the elevation of the piles after the tests. Some cracks occurred in the upper half of the piles, and the separation of the cover concrete was observed at the pile heads. It tilted by about 6 degrees. Concrete was crushed in the middle part of the piles. Photo 1 shows the damage of piles.

Fig. 7 shows the time history of the pile curvature. The curvature of the pile head increased steadily. The reinforcement yield at 12 seconds, just after the structural model acceleration reached its maximum. On the other hand, in the case of the middle part of the piles, the curvature increased rapidly at 16 seconds. The peak of curvature corresponded with the time when the structural model moved and settled. This suggest the concrete crushing occurred at 16 second.

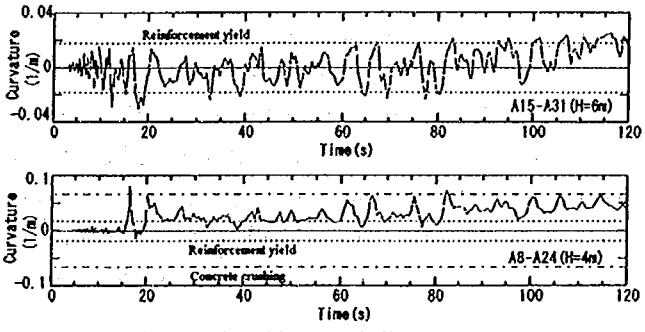


Fig.7 Time history of pile curvature

Fig. 8 presents the vertical distribution of the pile curvature. At 9.6 seconds, when the accelerations of the structural model reached the maximum level, large bending occurred at only the pile heads. This indicated that the curvature of the piles was caused by the inertial forces transmitted from the building to the foundation. At 12.4 seconds, when the reinforcement of the pile head yielded, the curvature of the piles occurred not only at the pile heads but also at the lower part of the piles. This result cannot be explained by the inertial force of the building. At 16.4 seconds, when the concrete was crushed, very large curvature appeared in the middle part of the piles. While, the curvature of the pile head was small. This suggested that the damage to the middle part of the piles was caused by the soil deformation.

Fig. 9 shows the vertical distribution of relative displacement and the pore water pressure ratio. The displacements were calculated by double-integrating the accelerations in the vertical array. At 9.6 seconds, when the acceleration of the structural model reached its maximum, the pore water pressure ratios and the soil displacement were small. At 12.4 seconds, when the reinforcements of the pile head yielded, the pore

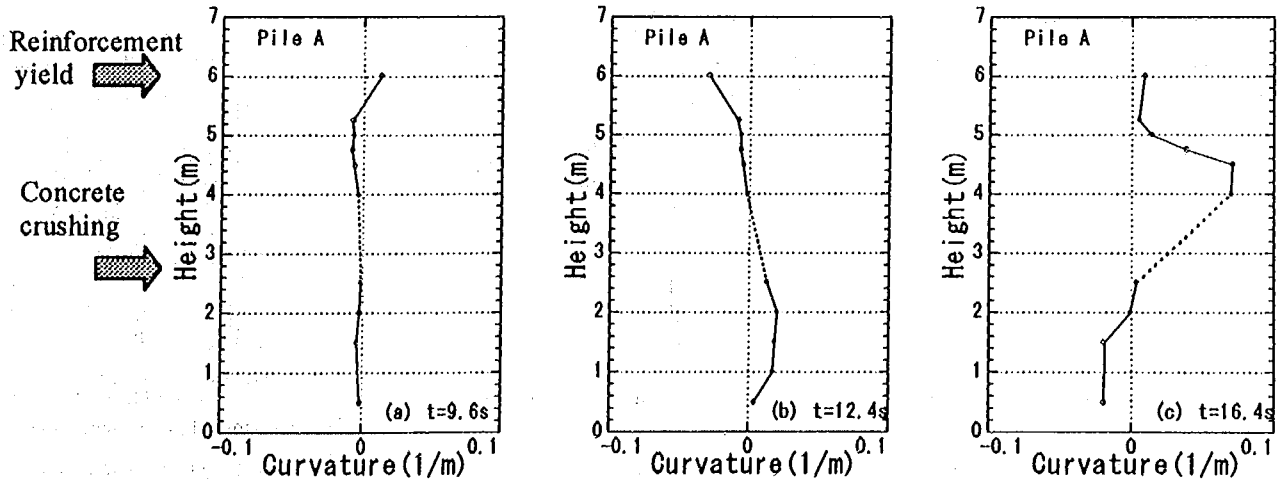


Fig.8 Vertical distribution of pile curvature

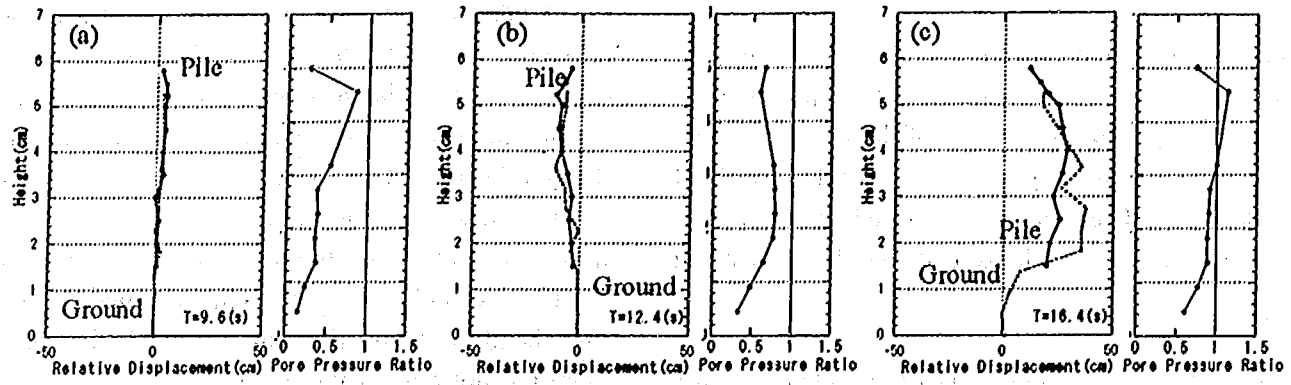


Fig.9 Vertical distribution of relative displacement and pore water pressure ratio

water pressure ratios reached 0.8 at the upper part of the sand layer and the displacements of the soil and pile was larger than the case of 9.6 seconds. The acceleration of the structural model was smaller than the case of 9.6 seconds. It is considered that pile heads were moved by the deformation of the soils. With a fixed pile head condition, bending can be caused by the displacements of the pile head. Therefore the damage to the pile heads occurred not only by the lateral inertial force of the structure but also by the deformation of surface layer. At 16.4 seconds, when the concrete was crushed, the pore water pressure ratios reach 1 at the upper part of the sand layer. On the other hand, the lower part did not completely liquefy. Thus, the relative displacement between the pile and the soil was large in the middle part of piles. Judging from the above, concrete crushing was caused by the soil deformation.

Fig. 10 shows schematic figures showing mechanism of pile foundation damages. Failure mechanism fell into three categories. First state when 0-10 seconds, the excess pore water ratios reach 0.5. The inertial force is large. While the deformation of the soils is extremely small. Some cracks occur at pile heads by the inertial forces of the building. Second state when 10-14 seconds, soil liquefaction is progressing. The excess pore water ratios reach 0.8. The inertial force is large and the deformation of the soils is

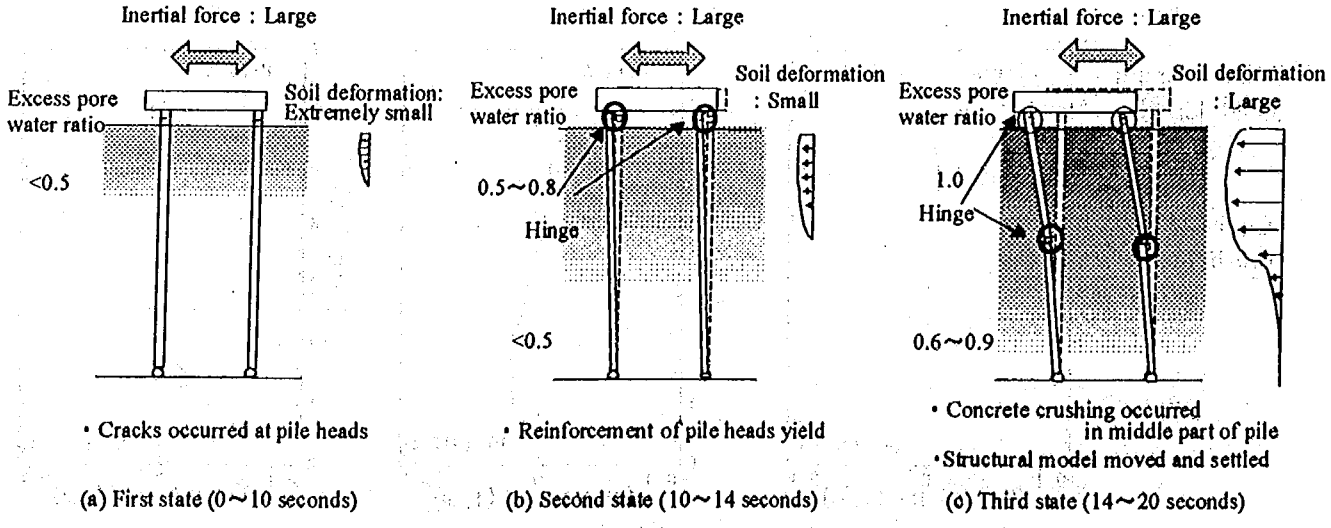


Fig.10 Schematic figures showing mechanism of pile foundation damages

small. The reinforcements of the pile heads yielded. The damage is caused not only by the inertial force of the superstructure and but also by the deformation of surface layer. Third state when 14-20 seconds, the upper part of the soil is liquefied, although the lower part do not completely liquefy. The process of liquefaction cause large relative displacement between the pile and the soils. Therefore concrete is crushed in the middle part of the piles, as a result the structural model move and settle suddenly.

4. CONCLUSION

Failure mechanism of pile foundations during soil liquefaction have been investigated based on large-scale shaking table tests. The following conclusion are drawn;

(1)The damage to the pile heads occurred not only by the lateral force from the superstructure but also by the deformation of the surface layer, just before surface layer liquefied.
(2)The damage to the middle part of the piles was caused by the deformation of surface layer, immediately after the surface layer liquefied.

These test results suggest that the failure of the piles were controlled strongly by the process of liquefaction of the sand layer.

REFERENCES

Miyamoto, Y., Miura, K., R. F. Scott, B. Hushmand: Pile Foundation Response in Liquefiable Soil Deposit during Strong Earthquakes, Journal of Struct. Constr. Engng. AIJ, No.439, pp.49-63, 1992.

Sato, M., Shamoto, Y. and Zhang, J. -M.: Soil-Pile-Structure during liquefaction on centrifuge. Proc., 3rd Inter. Conf. on Rec. Adv. in Geot. Earthq. Engrg & Soil Dyn., 1, pp.135-142, 1995.

Suzuki, Y., Yahata, K., Minowa, C., Sugimoto, M. and Funahara, K.: Dynamic Response of Pile Foundation and Liquefied Soil under Shaking Table Test Using Large Scale Laminar Box. Proc., 10th Earthq. Eng. Symposium, Vol. 2, pp.1389-1394, 1998. (in Japanese)

Tokimatsu, K. and Nomura, S: Effect of Ground Deformation on Pile Stresses during Soil Liquefaction, Journal of Struct. Constr. Engng. AIJ, No,426, Aug., 1991. (in Japanese)

Equivalent-Linear Ground-Response Calculations with Frequency-Dependent Damping

by

William B. Joyner[1]

ABSTRACT

Equivalent-linear procedures are widely used for calculating the response of soils to earthquake ground motion. They are not the only methods for this purpose; fully nonlinear calculation methods are available, as well as methods relying on empirical analysis of existing strong-motion data. At high levels of input motion, equivalent-linear ground-response calculations for sites in the Imperial Valley of California predict much greater depletion of high-frequencies in the Fourier amplitude spectrum than found for observed data or for calculations performed using fully nonlinear computer codes. Such behavior should be expected if, as suggested many years ago by Dobry, the motion produced by a small cyclic load superimposed on a large load suffers less damping than the motion produced by the large load. Strictly speaking, of course, the effects of two different loads can not be superimposed if the response is nonlinear. The approximate validity of superposition must be assumed, however, if equivalent-linear procedures are to be used at all. Since the spectrum of strain amplitude (which is similar in shape to the spectrum of particle velocity) decreases above the corner frequency of the earthquake approximately as the reciprocal of frequency, the strain-dependent damping used for equivalent-linear calculations should decrease with frequency above the corner frequency, rather than be constant over frequency as in the conventional equivalent-linear procedure. As recently proposed by Sugito, equivalent-linear procedures may be improved by allowing frequency-dependent properties at high strain. I show comparisons of response spectra of motions resulting from fully nonlinear calculations and equivalent-linear calculations using the conventional procedure and a modified procedure in which the damping at high frequency decreases as the reciprocal of frequency. The results of the modified equivalent-linear procedure agrees better with the results of the fully nonlinear calculations than the results of the conventional equivalent-linear procedure, for a site with zero low-strain damping. For a modest amount of low-strain damping, however, the differences between the response spectra for the conventional and modified equivalent-linear results is small, suggesting that conventional equivalent-linear procedures are adequate for many engineering purposes.

KEYWORDS: engineering seismology; equivalent-linear; nonlinear; soil response; strong motion

1. INTRODUCTION

Equivalent-linear methods are widely used in soil-response calculations. In the conventional application, response is calculated as if the soil material were linear, but the shear modulus and damping are chosen to correspond with the strain in each soil layer, determined by iterative calculation. Curves of shear modulus and damping as a function of strain are obtained from laboratory measurements.

For sites where strong-motion records were obtained in the 1979 Imperial Valley, California, earthquake, Durward et al. (1996) found that

[1] U.S. Geological Survey, 345 Middlefield Road, Menlo Park, CA 94025 USA

conventional equivalent-linear calculations of ground response predict much greater depletion of high frequencies in the Fourier amplitude spectrum than found for observed data or for calculations by fully nonlinear methods. Consideration of the physics of the process leads to the conclusion that damping and perhaps modulus should be frequency-dependent, as has been suggested by Sugito (1995). Many years ago Dobry *et al.* (1971) showed that, for the standard hysteretic soil model, the motion produced by a small-amplitude cyclic load superimposed on a large load suffers less damping than the motion produced by the large load. This point is illustrated in Figure 1. Strictly speaking, the effects of the two different loads can not be superimposed if the response is nonlinear, but the approximate validity of superposition must be assumed if the equivalent-linear method is to be used at all. The spectrum of strain amplitude is similar to the spectrum of particle velocity, which decreases above the corner frequency of the earthquake approximately as the reciprocal of frequency. The spectrum of strain amplitude will therefore decrease with frequency above the corner frequency, and the strain-dependent damping used for equivalent-linear calculations should decrease with frequency above the corner frequency, rather than be constant over frequency as in the conventional equivalent-linear calculations.

Sugito (1995) has recently suggested that frequency-dependent modulus and damping be used in equivalent-linear calculations. He obtained a much better fit to Fourier amplitude spectral ratios from a downhole array in Japan using an equivalent-linear method with frequency-dependent modulus and damping than by the conventional equivalent-linear method. In this paper I compare soil response calculated by the conventional equivalent-linear procedure and by an equivalent-linear procedure featuring frequency-dependent damping with response calculated by a fully nonlinear procedure

It is not my intention to promote the use of equivalent linear methods for determining site response. The alternatives, fully nonlinear methods and empirical analysis of strong-motion data from seismically active areas, may be preferable, particularly the latter. In view of the popularity of equivalent-linear methods, however, I thought it useful to explore ways of improving them.

2. EQUIVALENT-LINEAR GROUND-RESPONSE CALCULATIONS WITH FREQUENCY-DEPENDENT DAMPING

In this section I compare nonlinear calculations using the method of Joyner and Chen (1975), which assumes a hysteretic soil model obeying the Masing rules (Ishihara, 1996), with the conventional equivalent-linear method that assumes modulus and damping independent of frequency and with a modified equivalent-linear method featuring frequency-dependent damping. For the modified method, in each soil layer, damping is independent of frequency below the predominant frequency f_0 defined in terms of the number of zero crossings. The value of f_0 (Newland, 1975) is given by

$$f_0 = \frac{1}{2\pi}\left(m_2 / m_0\right)^{\frac{1}{2}},$$

where

$$m_k = \frac{1}{\pi}\int_0^\infty \omega^\kappa \mid E(f) \mid^2 d\omega,$$

$E(f)$ is the Fourier spectrum of strain, and $\omega = 2\pi f$. The damping for frequencies below f_0 is taken from the curve of damping versus strain. Above f_0 the damping is reduced by the factor (f_0/f). The soil profile is taken from the Gilroy #2 station, which recorded the Loma Prieta, California, earthquake. The shear velocities in the soil are given in Table 1, and the shear velocity in the underlying rock is 2.0 km/sec (Joyner *et al.*, 1981). The soil density is 2.0 gm/cm^3 and the rock density is 2.6 gm/cm^3. Below an overconsolidated zone 5m thick, the dynamic soil strength τ_{max} is given by

$$\tau_{\max} = C_s P_{ve},$$

where the strength coefficient C_s is equal to 1.0 and P_{ve} is the vertical effective stress. Above 5 m the preconsolidation vertical effective stress is assumed equal to the vertical effective stress at 5 m, and τ_{max} is given by

$$\tau_{max} = C_s P_{ve} (OCR)^T,$$

where C_s is equal to 1.0, OCR is the overconsolidation ratio in terms of vertical effective stress, and T is equal to 0.75 (Ladd and Edgers (1972). The soil is presumed saturated below 20 m. No degradation is permitted and no pore-water diffusion.

The curves of modulus reduction and damping versus strain for both the conventional and modified equivalent linear methods are chosen to fit exactly the modulus and damping of the model used in the nonlinear calculations. By that choice we see how well the equivalent-linear methods represent the Masing-type hysteretic soil model, which is the most widely accepted model for the dynamic behavior of soils. The frequency-dependence of damping in the modified equivalent-linear method is chosen in an attempt to improve agreement with the nonlinear model. For both the conventional and modified equivalent-linear calculations, the peak strain in each layer is multiplied by the magnitude-dependent reduction factor recommended by Idriss and Sun (1992) before being used to determine modulus and damping.

The input motion considered is the north component recorded in the 1989 Loma Prieta, California, earthquake at Gilroy #1, a rock site 2 km from Gilroy #2. The peak acceleration is 0.44 g. The results are shown in Figure 2, where the pseudoacceleration response obtained by the nonlinear method is shown by the line, the response obtained by the conventional equivalent-linear method is shown by the plus signs, and the response obtained by the modified equivalent linear method is shown by the octagons. For periods between about 0.07 and 0.2 second the response obtained by the conventional equivalent-linear method is significantly less than the response obtained by the nonlinear method. The modified equivalent-linear method agrees much better with the nonlinear method, particularly for periods between 0.08 and 0.2 sec.

Both the conventional and modified equivalent-linear calculations illustrated in Figure 2 were made assuming that the damping goes to zero at zero strain. Measurements of soil-damping *in situ* (Gibbs *et al.*, 1994, Gibbs, written comm., 1998) give values of low-strain damping that are typically greater than 2 percent. Figure 3 shows the results of repeating the equivalent-linear calculations of Figure 2 with a low-strain damping of 2 percent. The nonlinear calculations are not repeated because the computer program used does not allow nonzero damping at low strain. The difference between conventional and modified equivalent-linear calculations is much less in Figure 3, and suggests that conventional equivalent-linear calculations may be adequate for many engineering purposes. The comparison in Figure 3 is based on response spectra. Larger differences would probably be seen in Fourier spectra. The results of Durward *et al.* (1996) and Sugito (1995) indicating that conventional equivalent-linear calculations underestimate high-frequency response were obtained by comparing Fourier spectra. Response spectra, however, are a better measure of engineering significance.

3. REFERENCES

1. Dobry, R., R. V. Whitman, and J. M. Roesset (1971). Soil properties and the one-dimensional theory of earthquake amplification, Research Report R71-18, School of Engineering, Massachusetts Institute of Technology, Cambridge, Massachusetts.

2. Durward, J. A., D. M. Boore, and W. B. Joyner (1996). The amplitude dependence of high-frequency spectral decay: Constraint on soil nonlinearity, Proc. International Workshop on Site Response Subjected to Strong Earthquake Motions, Yokosuka, Japan, January 16-17, 1996, vol. 2, p. 82-103.

3. Gibbs, J. F., D. M. Boore, W. B. Joyner, and T. E. Fumal (1994). The attenuation of seismic shear waves in Quaternary alluvium in Santa Clara Valley, California, *Bull. Seism. Soc. Am.* vol. 84, p. 76-90.

4. Idriss, I. M. and J. I. Sun (1992). User's manual for SHAKE91: A computer program for conducting equivalent linear seismic response analyses of horizontally layered soil deposits, Center for Geotechnical Modeling, Department of Civil Engineering, University of California, Davis, California.

5. Ishihara, K. (1996). *Soil Behaviour in Earthquake Geotechnics,* Clarendon Press, Oxford, 350 p.

6. Joyner, W. B. and A. T. F. Chen (1975). Calculation of nonlinear ground response in earthquakes, *Bull. Seism. Soc. Am.*, vol. 65, p. 1315-1336.

7. Joyner, W. B., R. E. Warrick, and T. E. Fumal (1981). The effect of Quaternary alluvium on strong ground motion in the Coyote Lake, California, earthquake of 1979, *Bull. Seism. Soc. Am.*, vol. 71, p. 1333-1349.

8. Ladd, C. C. and L. Edgers (1972), Consolidated-undrained direct-simple shear tests on saturated clays, Research Report R72-82, Department of Civil Engineering, Massachusetts Institute of Technology, Cambridge, Massachusetts.

9. Newland, D. E. (1975). *An Introduction to Random Vibrations and Spectral Analysis,* Longman, London, 285 p.

10. Sugito, M. (1995). Frequency-dependent equivalent strain for equi-linearized technique, in *Earthquake Geotechnical Engineering,* Ishihara (ed.), Balkema, Rotterdam, p. 655-660.

Table 1. Shear-Wave Velocity Profile at the Gilroy #2 Station (Joyner *et al.*, 1981)

Thickness (m)	Shear-Wave Velocity (m/sec)
2.5	160
5.0	274
12.5	400
20.0	320
60.0	630
20.0	440
60.0	650

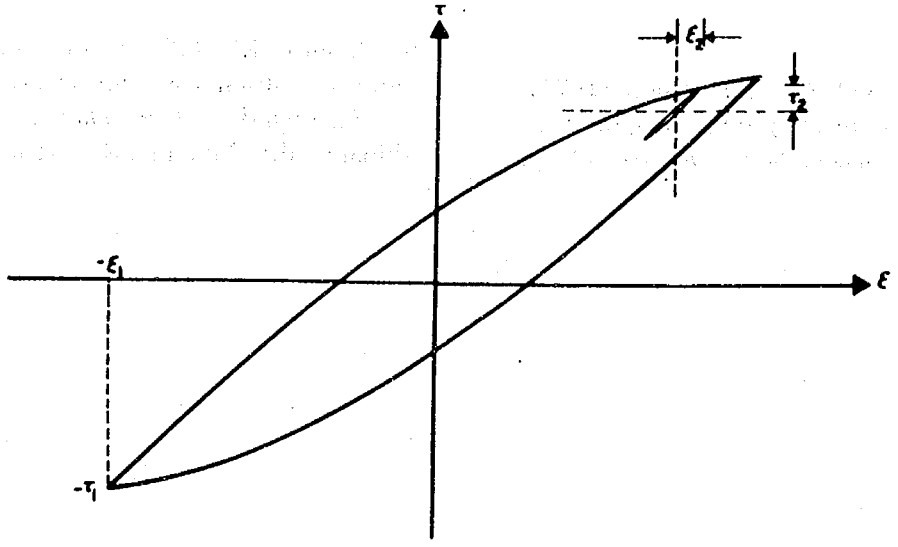


Figure 1.Idealized plot of stress (τ) versus strain (ε) for a soil sample showing the superposition of two sinusoidal loads. The energy dissipated in each loop is proportional to the area of the loop. (Dobry *et al.*, 1971)

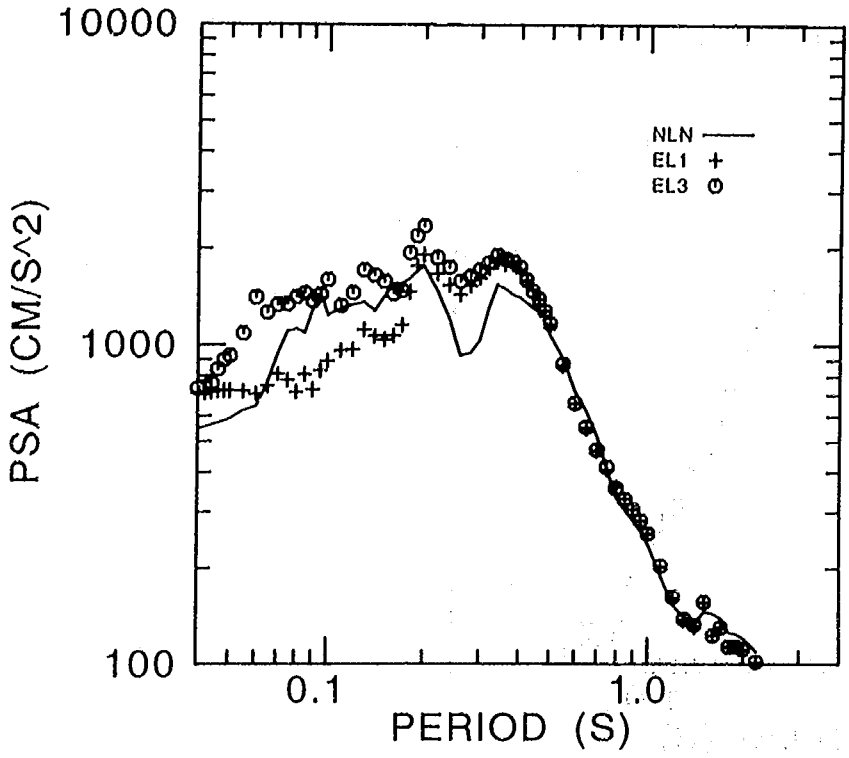


Figure 2. Pseudoacceleration response spectra (5 percent damping) for Gilroy station #2 computed by the nonlinear method (NLN), the conventional equivalent-linear method (EL1), and the modified equivalent-linear method described in the text (EL3). The input motion is the north component recorded in the 1989 Loma Prieta, California, earthquake at Gilroy station #1, a rock site 2 km from Gilroy # 2.

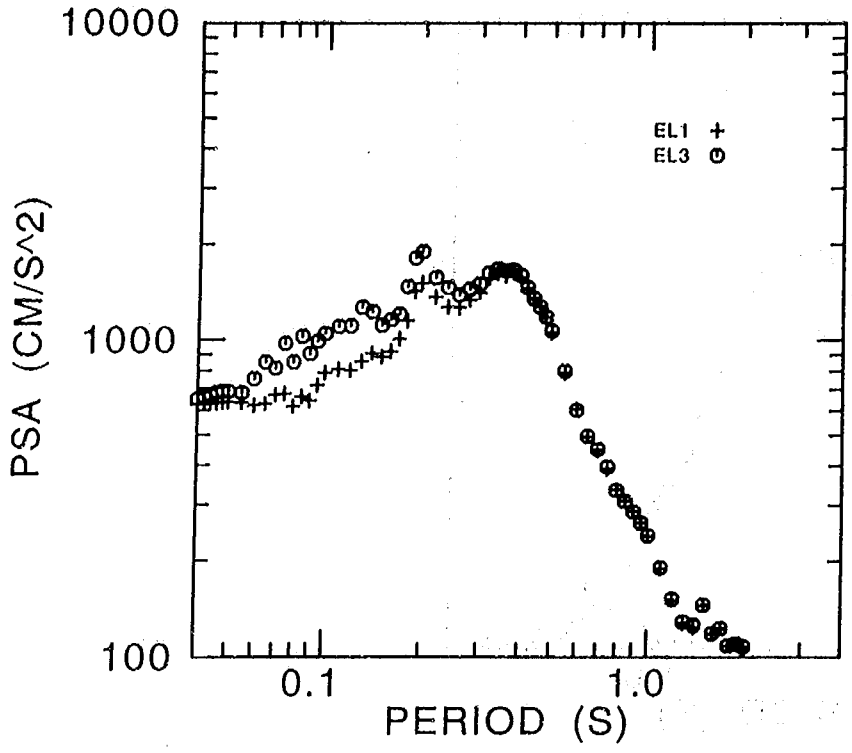


Figure 3. Pseudoacceleration response spectra from Figure 2 recomputed by the conventional equivalent-linear method (EL1) and the modified equivalent-linear method (EL3), assuming 2 percent low-strain damping.

DEVELOPMENT OF SMART STRUCTURE SYSTEM

by

Shunsuke OTANI[1], Hisahiro Hiraishi[2], Mitumasa MIDORIKAWA[3], and Masaomi TESHIGAWARA[4]

ABSTRACT

Building Research Institute, Ministry of Construction (BRI) has started the research and development of " Smart Structure Systems " cooperated with National Science Foundation, U.S.A. in 1998. Smart Structure Systems are defined as the systems that can appropriately respond the change of external disturbance and can reduce the safety margin for the safety design, improve the serviceability, and make the building life long. The research and development of (1) Concept and performance evaluation method of smart structure system, (2) Sensing of structure performance, and (3) Development and evaluation of structural elements using smart materials will be conducted.

KEY WORDS: Smart structure system, Health monitoring, Shape memory alloys, E/M rheological fluids, Induced Strain Actuators, Engineered cementitious composites

1. INTRODUCTION

Structure Systems in the past had chosen and constructed materials and framing system in order to achieve the intended function toward an expected loads and forces. It was undoubted that the existing system could not give full play to its ability to cope with an unexpected loads and forces. And a large safety factor at the safety design stage was needed to avoid the risk. Strengthening and a removal of existing buildings, which had problems in their safety, was also required. It was confirmed by the damage of HYOGO ken Nambu Earthquake. Here, Smart Structure Systems is defined as a structural system with a certain-level autonomy such as sensors, actuators and processors, which can appropriately respond the change of external disturbance and can reduce the safety margin for the safety design, improve the serviceability, and make the building life long.

2. TARGET ISSUES AND RESEARCH ORGANAIZATION

The research and development are conducted focusing on the following issues.

(1) Concept and performance evaluation method of smart structure system. In this research issue, Auto-adaptive system and high-performance system be developed are proposed, and performance evaluation method will be proposed.

---

1) Prof., Department of Architecture
Graduate School of Engineering
The University of Tokyo
7-3-1 Hongo, Bunkyo-ku, Tokyo 113-8656, JAPAN

2) Director, Dept. of Structural Engineering, Building Research Institute, Ministry of Construction, Tsukuba-shi, Ibaraki 305-0802, JAPAN

3) Director, IISEE, ditto

4) Head, Structure Div., Dept., of Structural Eng., ditto

(2) Sensing of structure performance. In this issue,damage detection technology using sensors utilizing smart materials, such as optical fiber, carbon fiber, shape memory alloy, PZT as well as existing sensors, and system identification method are proposed. And,

(3) Development and evaluation of structural elements using smart materials. In this issue, devices utilizing the auto-adaptive material such as shape memory alloy, PZT, magneto-, electro-rheological (MR, ER), high-performance material such as high tensile and ductility concrete, self-repairing material etc. are proposed and performance evaluation method will be proposed.

To conduct the target issues, three sub-committees; System chaired by Prof. A.Wada, Tokyo Institute of Technology, Sensor chaired by Prof. Y.Kitagawa Hiroshima Univ., Effector chaired by Prof. T.Fujita, corresponding to each R/D issues, and one technical coordinating committee (chaired by Prof. S.Otani Tokyo Univ.) are organized. Research organization is illustrated in Fig.1. Building Contractors Association, Housing and Urban Development Cooperation, Building Center of Japan and many materials and sensors makers collaborate the R/D project.

3. ACTIVITIES OF EACH SUB-COMMITTEE

(3-1) Sub-Committee on smart structures system concept

(1) Research Purpose

The objective of this sub-committee is to establish the basic concept and strategies for the development of smart structure system. The followings are the main topics which are discussed in this sub-committee:

1. Definition and categorization of smart structure system
2. Summary of the required performance of smart materials or devices to realize the smart structural system
3. Performance verification of proposed smart structure system concept by computer simulations and experiments
4. Establishment of guideline for the performance evaluation of smart structural system

(2) Research Plan

This sub-committee consists of the following three research working groups:

1. Auto-Adaptive Structural System WG

The objective of this WG is to develop a smart structural system with auto-adoptive features to external disturbance. The research plans are enumerated as follows:

① Propose smart structure system concept with auto-adoptive features

② Examine smart materials or devices to achieve target performance of structure system

③ Verify the proposed structure system concept by computer simulations and experimental tests

④ Establish performance evaluation guideline for the structure system with auto-adoptive features

2. High Performance Structural System WG

The objective of this WG is to develop a high-performance structural system with damage control features or robustness under external disturbance. The research plans are enumerated as follows:

① Propose high-performance structure system concept with damage control features or robustness under external loads

② Examine damage control devices to achieve target performance of structural system

③ Verify the proposed structure system concept by computer simulations and experimental tests

④ Establish performance evaluation guideline for the structure system with damage control features or robustness under external disturbance

3. Smart Seismic Rehabilitation System WG

The objective of this WG is to develop a smart structure system concept for seismic rehabilitation of existing buildings. The research plans are enumerated as follows:

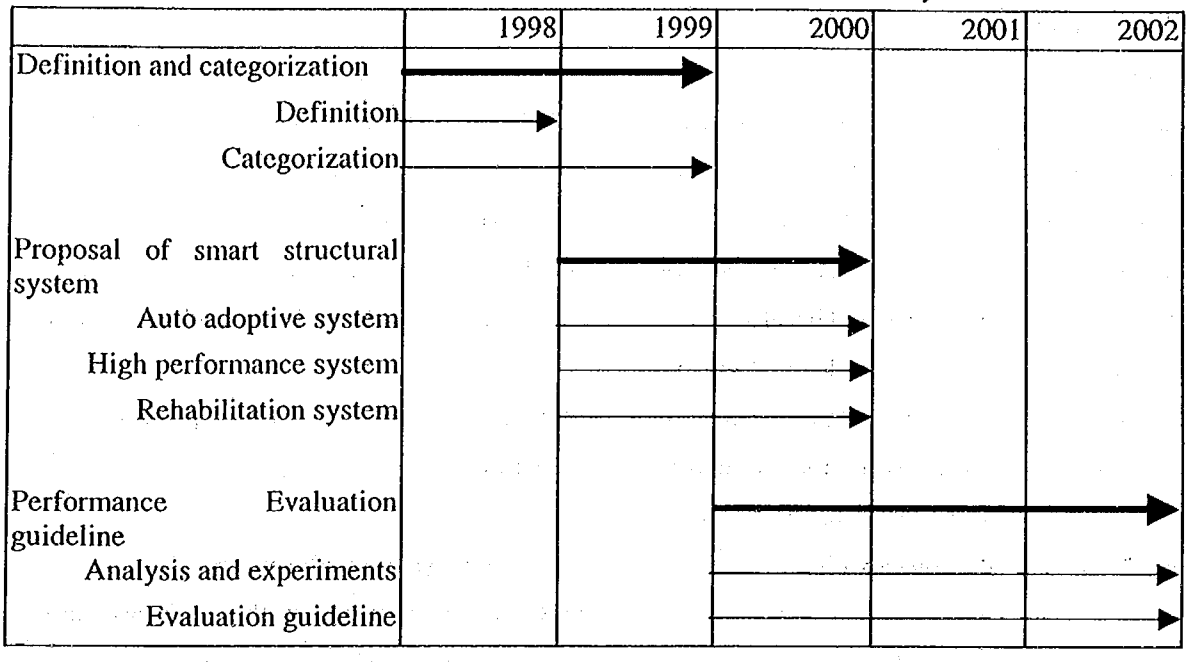
①Survey of seismic performance of existing buildings

②Propose smart structure system concept for seismic rehabilitation of existing buildings

③Verify the proposed structure system concept by computer simulations and experimental tests

④Establish usage guideline for the structure system for seismic rehabilitation of existing buildings

Research Schedule of Sub-Committee on smart structures system



(3-2) Sub-committee of sensing & monitoring

(1) Research Purpose

Sensing & monitoring technology and damage identification methods are treated in this sub-committee. The followings are the main targets of research and development which are discussed in this sub-committee:

1. Structural health monitoring system
2. Structural performance evaluation system
3. Information system with sensors

(2) Research Plan

1. Structural health monitoring system

In this system, the identification methods for detecting structural damages such as yielding, cracks, etc. with some sensors are developed. At first, the technologies for clarifying

whether there are damages or not are developed. Finally these for clarifying the kind and the degree of damage are developed. The followings are main technology and method used for the development.

① Damage identification methods using microtremor & actuator data

② Detection of damage using ultrasonic technique, optical fiber and so on.

2. Structural performance evaluation system

With this system, structural performance such as safety and serviceability can be predicted. Structural serviceability performance can be easily evaluated using minute displacement and vibration properties. However, it is difficult to evaluate structural safety performance without destruct. Therefore, it is important for this research and development issues to make the clear relation between information which are given nondestructive inspection and safety performance such as strength and deformation capacity.

3. Information system with sensors

In this system, the methods for selecting necessary information from enormous information and technology for on-line transaction with sensors are developed. Here the objective of this system is not only a building but also area. As the result, it is possible to make damage map in a moment, for example, and it leads to making change the infrastructures from physical to intelligent.

(3) Research Schedule

The followings are research schedule each R/D system.

Structural health monitoring system

1998 Feasibility study of damage identification

1999 Detection whether there is damage or not

2000 Detection of the part of damage

2001 Detection of the kind of damage

2002 Detection of the degree of damage

Structural performance evaluation system

1998-1999 Arrangement about relation structural Safety to structural performance

2000 Examination analytically

2001 Verification through the implementation example

2002 Final report about Safety performance evaluation

Information system with sensors

1998 Examination about the necessity and the way of using of network

1999-2000 Examination about the necessary technique and the building of a network

2001 Verification through the implementation example

2002 Proposal of a network system

(3-3) Sub-Committee of Effectors

(1) Research Purpose

The main goal of this Sub-Committee is to develop smart structural members which have:

1. embedded smart function(s) such as processors, sensors and/or actuators
2. improved performance (strength, ductility, usability, cost etc.)

(2) Research Schedule

This cooperative research will be held for five years from 1998 to 2002 (Japan side, Fiscal Year). Table 1 shows a typical schedule of development for example. Former three years will be spent to develop smart structural members and the rest two years we plan to perform in-situ, large scale experiment for smart structures with most possible smart materials.

Table 1 Research Schedule

FY	Research Items
1998	- Basic research for material properties and applications
1999 - 2000	- Element Test - Development of constitutive model - Analytical study
2001 - 2002	- Assemblage test - Utilization guidelines

(3) RESEARCH THEMES

Four working groups have been organized to discuss about both practical applications (short term) and future visions (long term) of structural elements with smart materials.

1. Shape Memory Alloys WG
2. Engineered Cementitious Composites WG
3. Electrorheological/Magnetorheological Fluids WG
4. Induced Strain Actuators WG

Possibly we may set additional WGs for other smart materials if their properties were worth to be applied to the building structures.

(3-3-1) Shape Memory Alloys WG

(1) Purpose:

Shape Memory Alloy(SMA) shows three different characteristics depending on the temperature; shape memory effect, pseudo elasticity and these transitional characteristic. The objectives of this study are to utilize SMA for the smart structural members in order to realize the smart structural system in buildings. Some smart devices will be developed for these purposes, and the guidelines on SMA for structural design will also be discussed.

(2) Research items and schedule

The research items are planned and scheduled as follows:

1. Survey on current application of SMA to building structures (in 1998)
2. Survey on mechanical properties of SMA for usage of building structural members (in 1998-1999)
3. Development of smart structural members using SMA

3.1) development of SMA devices(in 1999-2000)

3.2) evaluation method of performance of devices(in 2000-2001)

4) Design guidelines for usage of SMA for structural designers

4.1) chapter 1 ; description on mechanical properties of SMA(in 1999)

4.2) chapter 2 ; some application of SMA to structural members(in 2002)

(3-3-2) Engineered Cementitious Composites WG

(1) Purpose

Engineered Cementitious Composites (ECC) is chopped fiber reinforced mortar/concrete microstructurally designed using micro-mechanical principles. ECC exhibits strain-hardening with superior strain capacity, shear ductility, and extreme damage tolerant mechanical behavior.

The purpose of this research is to develop high performance cementitious structural elements as energy dissipation devices and damage tolerant elements utilizing Engineered Cementitious Composites (ECC) to achieve a smart damage tolerant structural system. A Concrete-encased steel column without reinforcing bar, which is a new type steel-concrete composite using high performance bonding agent and ECC, will also be developed as an example of application of ECC. Applications to both new structures and in retrofitting of existing R/C structures to withstand future earthquakes are considered.

(2) Benefits

ECC devices and ECC elements are expected to decrease the response and damage of building structures under external disturbances to realize a high level of building performance requirements. Those requirements are not only structural safety but also reparability, serviceability, and durability of buildings after external disturbances.

Stiffness, strength and ductility of the ECC devices can be controlled easily by it's dimensions and types of ECC materials used. Since the ECC device will be able to dissipate the input energy by external disturbances even in the small deflection state of the buildings, response and damage of building will be decreased. Then the column members can hold the vertical load without any damage by the expected horizontal deflection.

The damage tolerant elements can be achieved by the extreme damage tolerant mechanical behavior of ECC. Since crack width of ECC elements can be easily controlled less than 0.3 mm even in the large deformation state, high level of reparability, serviceability and durability can be added to the buildings.

(3) Research Items

1. Development and clarification of properties of ECC materials
2. Development of ECC devices by experimental and analytical

investigations

3. Development of damage tolerant elements
4. Design guideline for smart structural system with ECC devices and elements
5. Development of concrete-encased steel column elements without reinforcing bar

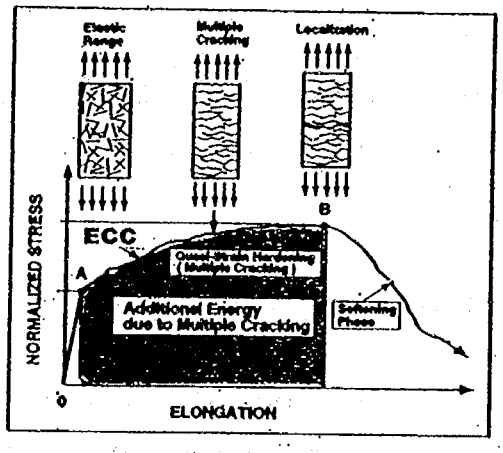


Fig.1 Uniaxial tensile stress-strain relationship of ECC

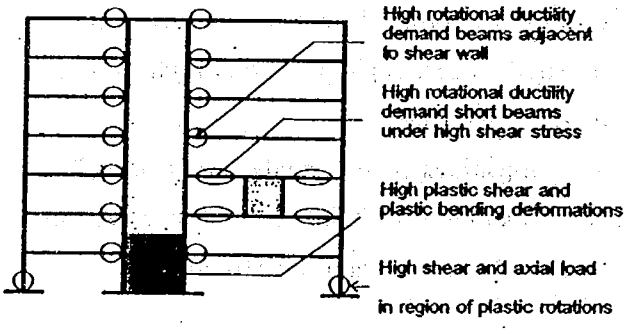


Fig. 2 Typical examples of selective use of ECC elements in seismic resistant structures

3.3 Electro/Magneto Rheological Fluids WG

(1) Purpose:

ER/MR fluids have essential characteristics that change from free-flowing, linear viscous fluid, to a semisolid with a controllable yield strength in milliseconds when exposed to an electric and magnetic field. These fluids are variable contenders for development controllable devices.

The purpose of this issue, is to develop an adaptive structure that controls its stiffness and damping characteristic to behave adaptively against earthquake or wind forces and obtain safety and function by using ER/MR devices with lesser energy (Figures 3-5). For the purpose, ER/MR devices and control algorithms are developed and their validity are discussed by analytical study and shaking table test.

(2) Research Items

1. Clarification of characteristics of ER/MR fluids
   - Viscous characteristic and achievable yield stress
   - Transition time and electric and magnetic intensity to become semisolid
   - Influence of outside, for example, temperature, etc.
2. Development of ER/MR devices
   - Damping coefficient obtained by the device
   - Capacity to fix the structural member, for example braces
3. Development of control algorithm
   - Adaptive control of the structure to obtain the safety and function against earthquake and wind forces
   - Saving energy

- Sensing system

4. Analytical study and shaking table test
   - Verification of the validity of the algorithm and devices

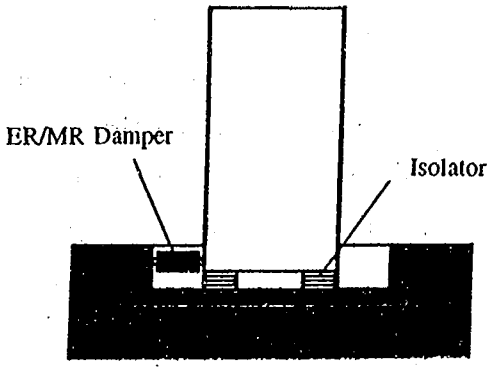


Fig. 3 Base Isolated System Controlled by Variable Damper

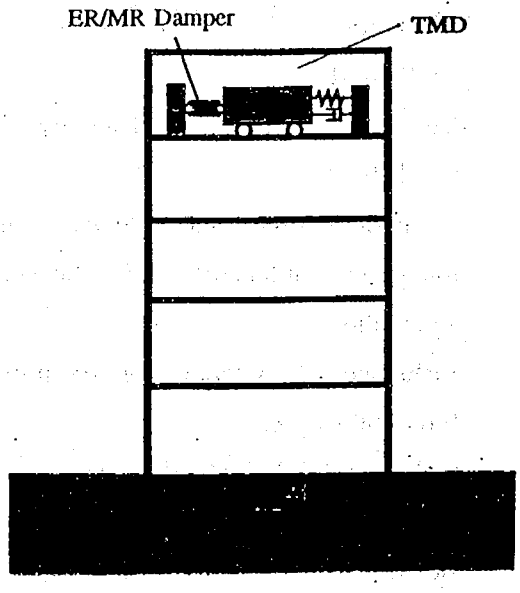


Fig. 4 Tuned Mass Damping System Controlled by Variable Damper

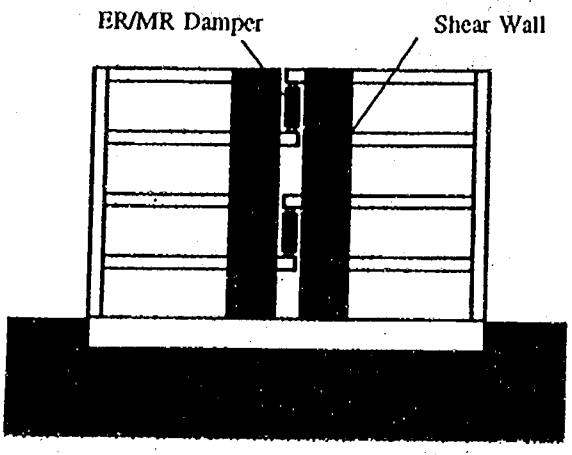


Fig.5 Semi-Active System Controlling Stiffness

(3-4) Induced Strain Actuators WG

(1) Purpose

Induced Strain Actuators (ISA) can change their own shapes according to external electric/magnetic fields, and vice versa. Recently these materials have been widely used for the small/precision machines because of some advantages from viewpoint of small sizes, rapid reaction, high power, high accuracy etc.

The objectives in this study are to develop smart members for building and to realize the smart, comfortable and safe structures.

(2) Research Items

(a) controlling members

ISA materials are very suitable for structural control. In addition, polymer based ISA films or distributed ISA devices can control vibration mode of plane members. We try to integrate ISA materials into normal structural members such as columns, beams, walls etc.

to realize smart structural systems. See Figs. 6-8.

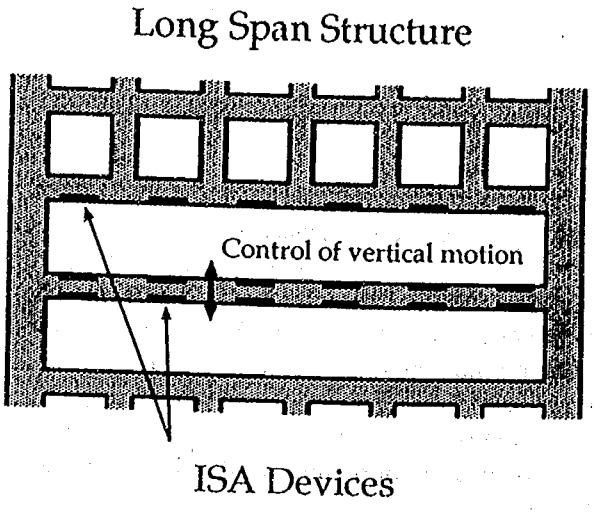


Fig. 6 Long Span Structure

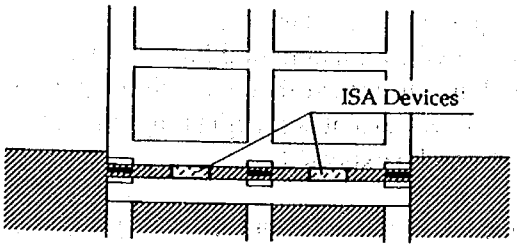


Fig. 7 Axial Force and Friction Control (for Base Isolator. Including trigger application)

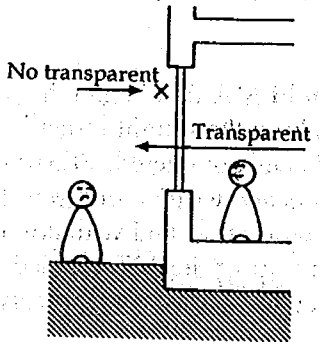


Fig. 8 Active Sound Transparency

(b) Sensing members

ISA materials can act as sensors because they cause change of electric or magnetic fields under deformation. Wireless application is also discussed.

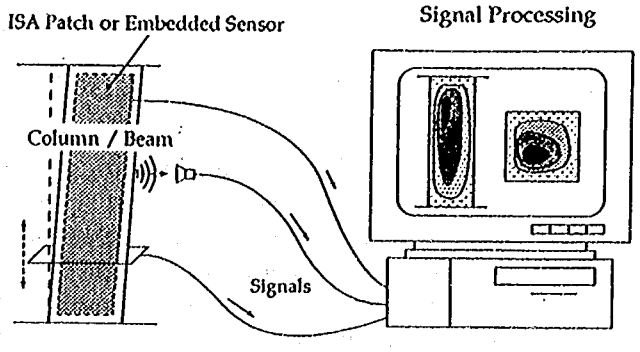


Fig. 9 Sensing with or without Cabling

4.CONCLUSIONS

This development research aims to apply the new technology like new materials and new structural systems, to develop smart structure systems which makes the performance of buildings advanced, to reduce the expense of construction and maintenance and eventually to ensure the future sustainability without trouble. Building Research Institute, Ministry of Construction (BRI) and National Science Foundation, U.S.A. has started the research and development of " Smart Structure Systems " in 1998. Feasibility study of smart structure system be developed are introduced.

DEVELOPMENT OF THE FEMA-273 DOCUMENT – GUIDELINES FOR THE SEISMIC REHABILITATION OF BUILDINGS

A. Gerald Brady
Applied Technology Council
Redwood City, California

INTRODUCTION

The nation's inventory of existing buildings continues to grow. In those areas where codes, up until a so-called "benchmark" year, did not contain significant seismic considerations, many of these buildings run a risk of life-threatening damage should an earthquake provide potentially damaging ground motion. The downtown, older sections of every city and town in the nation contain buildings which fit this category. Every earthquake reinforces society's conviction that something must be done to reduce the hazard posed by these unsafe buildings. Even in areas deemed at present to have low seismicity, there exists a sampling of possible earthquakes, maybe rare, that can cause, in decreasing order of severity: collapse, or loss of life without collapse, or damage warranting building entry to be unsafe, or damage that halts a building's functioning. The earthquake hazard is real even if it is unclear.

The National Earthquake Hazard Reduction Program (NEHRP) was funded by the U.S. Congress to take the required steps towards a national reduction of the earthquake hazard. This paper describes some of the steps taken towards the reduction of the earthquake hazard posed by existing buildings, rather than the implementation of codes governing the design of new buildings. It is clear that the nation's concern should be focused on rehabilitating existing buildings to whatever extent is practical, because more lives are at risk and more interruption to society and its economy can be expected.

The Federal Emergency Management Agency (FEMA), the lead agency for the NEHRP program, embarked on a comprehensive project in coordination with the other NEHRP agencies (at the time, the U.S. Geological Survey (USGS), the National Institute of Standards and Technology (NIST) and the National Science Foundation (NSF)). The agencies did what each does best: the USGS with information on strong ground motion, NIST with technical oversight, and NSF with funded engineering research. The Applied Technology Council (ATC) was the program manager for a number of the projects that produced reports listed and described briefly in the following section.

Borrowing from the FEMA Foreword to FEMA-273: Since 1984, when FEMA first began the program to address the risk posed by seismically unsafe buildings, FEMA-273 has been the sought target. Preparatory steps were needed, and by 1990 the technical platform had been completed. FEMA-273 required the varied talents of over 100 consultants: engineers, researchers and writers, orchestrated by BSSC, ATC, and ASCE. Hundreds more donated knowledge and time on review, and with comments, criticisms and suggestions. The balloting process of BSSC over the last year of the effort added further improvement. No-one who worked on this project, whether volunteer, consultant, or staff, received monetary compensation commensurate with effort.

PREPARATORY STEPS TOWARDS FEMA-273, GUIDELINES FOR REHABILITATION

The concepts at work in the planning for the NEHRP program can be seen in the titles of the following reports. The reports in this list are technical reports leading towards rehabilitation. All are accompanied by supporting documentation whose reporting is not listed.

Rapid visual screening for potential seismic hazards. (FEMA-154 report, developed by ATC in the ATC-21 project, 1988.) A method for the rapid identification of buildings that would probably be

hazardous in the event of an earthquake. This screening is conducted without gaining access. A city-wide application allows a local building department to determine the risk to its inventory.

NEHRP handbook for the seismic evaluation of existing buildings. (FEMA-178 report developed by ATC in the ATC-14 project (for NSF) and ATC-22 project (for FEMA); 1989, 1992.) A method for detailed evaluation of buildings, identifying structural flaws causing damage and collapse in the past and possibly again. FEMA-178 has been revised by ASCE to be an ASCE prestandard FEMA-310, 1998. FEMA-178 evaluates a building for a design earthquake comparable to one recurring in 500 years. FEMA-310 evaluates, in addition, for a bigger earthquake recurring in 2500 years.

NEHRP handbook of techniques for seismic rehabilitation of existing buildings. (FEMA-172 report, 1989, 1992.) These are useful techniques, although some are now dated due to the effectiveness of recent research results.

Seismic rehabilitation of buildings, Phase 1: issues identification and resolution. (FEMA-237 report, developed by ATC in the ATC-28 project, including a workshop for the resolution of the issues, 1992.) The guidance in this report shaped the development of the Guidelines.

NEHRP guidelines for the seismic rehabilitation of buildings. (FEMA-273 report, developed by ATC in the ATC-33 project, 1997.)

DEVELOPMENT OF FEMA-273

In 1991, the National Institute of Building Sciences (NIBS) entered a cooperative agreement with FEMA for a comprehensive seven-year program leading to the development of technically sound, nationally applicable guidelines for the seismic rehabilitation of buildings. Under the agreement, the Building Seismic Safety Council (BSSC) was program manager, and both the American Society of Civil Engineers (ASCE) and ATC were subcontractors. The program was to include the development of a consensus, that is, a unanimous consensus, among all the consultants working on the technical content, and to develop acceptance among all the potential users in the design engineering profession. The Guidelines were expected to be used as the primary resource in rehabilitation by engineers, academicians, code organizations, and building officials.

BSSC, as the program manager for FEMA, appointed the advisory panel, conducted the consensus review of the final draft from ATC, and developed an implementation plan that would ensure universal acceptance.

ASCE captured the research results to date (the project was not going to fund research to fill gaps in existing research results), and conducted the user workshops at the quarter points of the project.

ATC had responsibility for managing the technical content of the Guidelines, produced draft Guidelines at the quarter points of the work, responded to the consensus review comments, and developed examples of the Guidelines use. Sixty consultants were involved in the technical production.

THE APPLIED TECHNOLOGY COUNCIL – A SIDEBAR

The Applied Technology Council is a nonprofit, tax-exempt corporation established in 1971 through the efforts of the Structural Engineers Association of California. ATC's mission is to assist structural design engineers (in specialty fields such as earthquake, flood, soils, and wind) to keep abreast of technical developments and to use them effectively. To this end, ATC also identifies and encourages needed

research and develops consensus opinions on natural hazard structural engineering issues in a non-proprietary format. ATC thereby fulfills a unique role in funded information transfer.

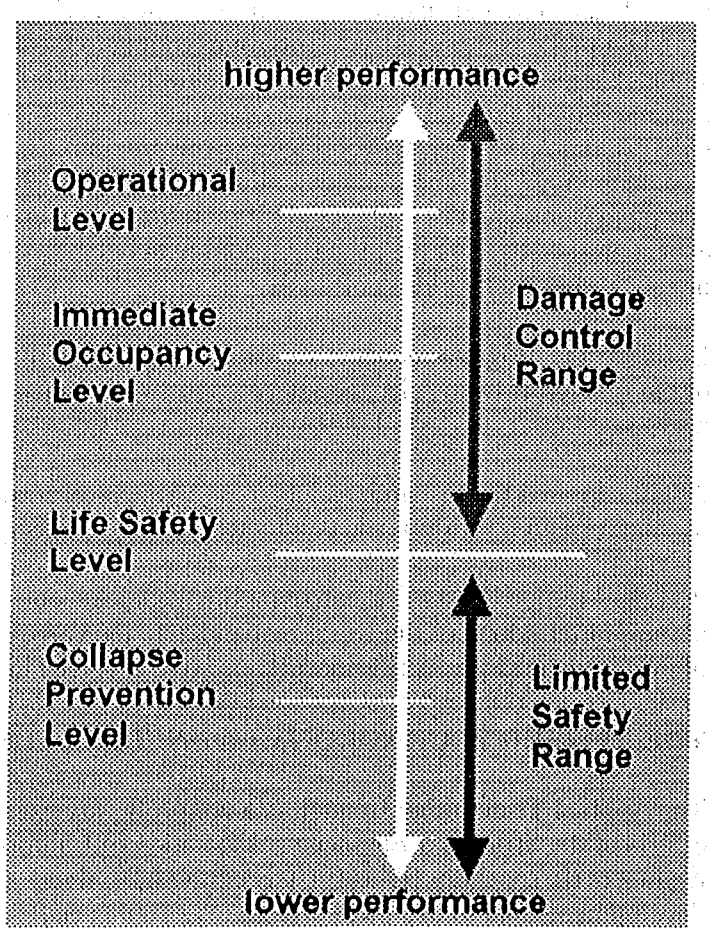
ATC is guided by a Board of fourteen directors. The Board consists of representatives appointed by structural engineers associations in the western United States and by ASCE, and four at-large representatives concerned with the practice of structural and multi-hazard engineering. Projects and administration are managed by a full-time Executive Director and support staff. ATC calls upon a wide range of highly qualified professionals as consultants on specific projects, thus incorporating the experience of many individuals from academia, research and professional practice, not available from any single organization.

ATC manages projects which benefit, and thereby fosters the advancement of, the structural engineering profession in all hazard reduction efforts, and which need a consensus of engineering opinion presented by a neutral source. Funding for projects is obtained primarily from government agencies.

IDENTIFICATION OF THE ISSUES

Issues were identified in FEMA-237 which reported on the first phase. Recommendations from FEMA-237 with a recognizable influence on FEMA-273, included:

- Provide a performance-based design approach;
- Address buildings and nonstructural components elements, but not other structures;
- Be nationally applicable (i.e., address an engineered building anywhere in the nation);
- Be written for design professionals (engineers, architects, and building regulatory personnel);
- Provide requirements that reflect the existence of different seismic zones;
- Include different performance goals, but specify minimum requirements for life safety;
- Include simple measures for simple, regular buildings not exceeding a specified size.



FEMA-273 SIGNIFICANT CONTENT

The use of three phrases needs some oversimplified clarification. The performance level of a building is directly related to how far along the yield plateau each seismic element, component, and joint of the building reaches; if it is not far, Operational Level may be attained; if it almost reaches rapid strength loss, Collapse Prevention Level may be attained. Earthquake ground shaking is greatly simplified to mean the design ground acceleration peak level, or the spectral acceleration response, and not a time-history (except in special applications). The recurrence interval for a specific earthquake

ground motion (as clarified above) is statistically recoverable from the probability that this level can be exceeded in the next 50 years; a low probability, 2%, implies a rare, large earthquake with a recurrence interval of (approximately) 2500 years. With these clarifications at hand, the document contains several new features that depart significantly from previous seismic codes:.

- Criteria and methods for achieving various performance levels at various expected earthquake ground shaking levels, defined regionally in terms of recurrence intervals. The combination of these parameters (performance level and expected level of ground shaking) enable the user to seek one of the following rehabilitation objectives:

a) Basic Safety Objective: Life Safety for ground shaking recurring in 500 years and Collapse Prevention for ground shaking generally recurring in 2500 years.

b) Limited Objectives: Rehabilitation objectives less stringent than the Basic Safety Objective, such as performance levels less than Life Safety (for example, Limited Safety) for ground shaking recurring in 500 years, or Life Safety for less ground shaking, recurring, for example, in 100 years.

c) Enhanced Objectives: Rehabilitation objectives that call for a higher level of performance than the Basic Safety Objective, such as Immediate Occupancy, or Damage Control, for ground shaking recurring in 500 years, or Life Safety for higher ground shaking, recurring, for example, in 1000 years and Collapse Prevention for higher ground shaking, recurring, for example, in 5000 years.

- A Simplified Rehabilitation Method, applicable primarily to small regular buildings in areas of low and moderate seismicity. This method is appropriate only for Limited Safety objectives.
- A Systematic Rehabilitation Method — complete procedures for considering all components and seismic elements necessary to reach a specified performance level for any building. These procedures address rehabilitation strategies, analysis procedures and their selection, and material acceptance criteria.
- New methods of analysis, including (a) a new Linear Static Procedure based on estimating maximum structural displacements, and (b) a new Nonlinear Static Procedure — a Pushover Analysis — that will better account for structural behavior caused by progressive yielding of structural components.
- Detailed procedures for determining acceptability of existing components as well as designing new ones in the four major material groups: wood, concrete, steel, and masonry. These depart from current standard design procedures for new buildings, which generally, and correctly, consider all parts of the structure to have similar characteristics.
- Procedures for incorporating emerging technologies in the rehabilitation design, including seismic isolation and supplemental damping.
- Criteria for seismic rehabilitation of nonstructural components, coupled with various performance objectives and emphasizing those components important for the Basic Safety Objective. Both prescriptive and analysis procedures are included.

TRAINING SEMINAR SERIES

Currently ATC and BSSC are sponsoring training seminars on FEMA-273 in cities throughout the nation. To date, seminars have been held in Los Angeles, New York, Portland, Salt Lake City, San Diego, and Seattle. Up to 13 additional cities will be added over the next several months.

The seminar program has been developed for practicing structural and civil engineers, architects, seismic engineering educators and students, building regulatory personnel, and other technical design professionals. The two-day seminars include 12 hours of presentations on the following topics: Issues, Overview, Simplified Rehabilitation, Systematic Rehabilitation, Structural Dynamics, Computer Modeling and Analysis, Foundations, Nonstructural Components, Steel, Masonry, Concrete, Wood.

Each seminar includes presentations by individuals specially selected because of their technical expertise and their ability to convey technical information effectively to large audiences. The seminars are being co-sponsored by local structural engineers associations and local chapters of ASCE.

POPULATION-BASED SURVEY ON INDIRECT HEALTH EFFECTS AFTER THE 1995 GREAT HANSHIN-AWAJI EARTHQUAKE

By

Keiko OGAWA[1], Ichirou TSUJI[1], Shigeru HISAMICHI[1], Keishi SHIONO[2]

ABSTRACT

A population-based survey was conducted to estimate the structural damage and non-structural damage in terms of inconvenience of daily life (IDL). The questions regarding indirect health effects were included to compare IDL according to their occurrence. IDL was high in Nada and Higashi-Nada districts of Kobe City and Ashiya City, and low in Itami City. IDL is an indicator to measure living conditions of the affected population in not only impact phase but also early recovery stage. Further analysis is required to define the meaning of IDL to decrease overall indirect health effects.

KEY WORDS : Inconvenience of daily life
(Daily living disruption)
Indirect health effects

1. INTRODUCTION

We presented regional variation of acute myocardial infarction (AMI) mortality among the affected populations[1] to show the magnitude of indirect health effects (any kind of health effects, not caused by seismic force) after the 1995 Great Hanshin-Awaji Earthquake. Nada and Higashi-Nada district suffered from large indirect health effects in terms of duration and magnitude of increased AMI mortality. Increased cardiac mortality had continued for a few months after the 1995 Great Hanshin-Awaji Earthquake[1],[2]. The period was much longer than those previously observed in USA[3],[4], Austraria[5], Greece[6],[7]. These results have made us recognize the need to analyze living conditions of the affected people to explain regional variation of indirect health effects.

There are very few studies to measure life conditions after an earthquake and compare among the regions. To estimate overall impact on the affected population, we conducted population-based survey regarding living conditions in several regions; Nada and Higashi-Nada district of Kobe City, Ashiya, Nishinomiya, Itami City and the Hokudan area of Awaji Island.

In addition to several questions regarding indirect health effects, inconvenience of daily life activities from post-earthquake suspension of utility services was measured, and their regional variation was analyzed.

1)Department of Public Health, Tohoku University School of Medicine, Sendai, Japan
2) Nagaoka College of Technology, Nagaoka, Japan

2. METHODS

We conducted simple random sampling between two and three years after the 1995 Great Hanshin-Awaji earthquake to select households and send self-administered questionnaires in Nada and Higashi-Nada district of Kobe City, Ashiya, Nishinomiya, Itami City and the Hokudan area of Awaji Island. The household selection was based on the voters registries at that time.

The questionnaires mainly consist of two parts. The one is about structural and non-structural damage including inconvenience of daily life activities from post-earthquake suspension of utility services[8],[9]. The other part is about indirect health effects.

We numerically evaluated difficulties people experienced in daily life at home due to water, power and gas suspension. We measured the extent of inconvenience in terms of a numerical score named the difficulty index, DI.

The difficulty index was defined as:

$$DI = \Sigma \{(\text{Degree of Difficulties})_i \times (\text{Duration of Difficulties})_i\}$$

Degree of Difficulties is a numerical score between 0 and 10 and shows the extent to which a daily life activity is restricted compared with that before the earthquake; 10 for total restriction and 0 for no restriction. Duration of Difficulties is in the number of days during which an activity was restricted due to lifeline disruption. The difficulty index is summed up regarding the following five life activities;

1) cooking
2) toilet use
3) washbasin use
4) taking a bath
5) washing clothes.

In addition, the following questions to indicate the occurrence of indirect health effects were included in the questionnaires:

1) Did you visit a doctor (excluding visits due to injuries) within six months after the earthquake?
2) Were you sick in bed and did you stay at home within six months after the earthquake?
3) Were you been hospitalized (excluding hospitalization due to injuries) within six months after the earthquake?
4) Did you suffer from any chronic diseases before the earthquake?
5) Did you discontinue your treatment or medication after the earthquake?

The questionnaire included age and sex of respondents.

Statistical analysis to compare IDL among groups were performed using the SAS variance component procedure PROC ANOVA.

3. RESULT

Table 1 shows completion proportions of the questionnaires in the six regions. They ranged from 31.9 to 38.6 percents.

Table 2 shows 95% confidence interval (CI) for a population mean of inconvenience of daily life (IDL) and a population proportion of completely destroyed houses (total damage rate). IDL was high in Nada (CI:

977-1295) and Higashi-Nada (CI: 1019-1229) and Ashiya (CI: 904-1154). Proportions of completely destroyed houses were high in Nada (CI: 25.2-33.1), Higashi-Nada (19.8-27.2), and Hokudan (CI: 16.2-32.4), followed by Ashiya (CI: 14.6-24.6) and Nishinomiya (CI: 13.6-17.9). In Hokudan, a proportion of completely destroyed houses was high, but IDL was low (CI: 247-485) in comparison with other regions.

Table 3 shows means and standard deviation (SD) of IDL according to the level of structural damage of the houses. IDL was high among the most damaged group and low among the least damaged group in Nada, Higashi-Nada, Nishinomiya and Hokudan. On the other hand, this finding was not observed in Ashiya and Itami. The difference in IDL among the regions was statistically significant ($P<0.001$) at all the levels of structural damage.

Table 4 shows 95% confidence interval for a population proportion regarding the occurrence of indirect health effects within 6 months after the earthquake. Itami City, which was less damaged, had lower proportions that people visited a doctor more than once or were sick in bed and stayed at home. There was no difference between regions regarding proportions that people had suffered chronic diseases before the earthquake. Proportions that affected people with chronic diseases could continue their medication as usual was lowest in Nada (39.6%) followed by Higashi-Nada (41.1%), Hokudan (57.7%), Ashiya (58.0%) and Nishinomiya (63.4%). The proportion was highest (86.9%) in Itami.

Table 5 shows analysis of variance of inconvenience of daily life (IDL) according to the occurrence of indirect health effects within 6 months after the earthquake. The group who suffered indirect health effects had higher IDL than the other. The difference between them was statistically significant ($P<0.01$ and $P<0.001$).

4. DISCUSSION

We conducted population-based survey regarding the structural damage and non-structural damage in terms of inconvenience of daily life (IDL). IDL was high in Nada and Higashi-Nada and low in Itami. It suggests IDL was high in a group with severe structural damage. On the other hand, Hokudan had relatively lower IDL even with severe structural damage. Considering the proportions regarding health episodes in the questionnaires, Nada and Higashi-Nada and Hokudan had suffered more indirect health effects. The group with more indirect health effects had higher IDL.

Our previous analysis [1] with respects to acute myocardial infarction (AMI) mortality following the 1995 Great Hanshin-Awaji Earthquake showed increased mortality in several regions such as Nada and Higashi-Nada district. The results of the questionnaires in this study agree with those findings. Prolonged duration of increased AMI mortality suggests that some factors in not only impact phase but also early recovery stage may be related with the occurrence of indirect health effects. Inconvenience of daily life due to lifeline disruption is an indicator to represent life

conditions after the earthquake. More detailed analysis will be required to show the relationship between IDL and indirect health effects. We should also estimate quantitatively the impact of disruption of their medication or treatment to chronic diseases. It may lead to increase of health effects.

This population-based survey was conducted under limited conditions (2 or 3 years after the earthquake). It resulted in relatively low completion proportion. Ecological study is very useful to develop the hypothesis about the etiology of some health effects. Population-based study is essential for this purpose even though high population movement after the earthquake makes it difficult.

REFERENCES

1. Keiko Ogawa et al. Comparison between the affected populations of indirect health effects after the 1995 Great Hanshin-Awaji Earthquake. Proceedings of The Joint Meeting of United States-Japan Panel on Wind and Seismic Effects. May12-15,1998, Gaithersburg
2. Kario K, Ohashi T. Increased coronary heart disease mortality after the Hanshin-Awaji Earthquake among the older community on Awaji Island. J Am Geriatr Soc 1997; 45: 610-613
3. Kloner R.A. et al. Population-based analysis of the effect of the Northridge Earthquake on cardiac death in Los Angeles County, California. Am J Coll Cardiol 1997; 30 (5): 1174-80
4. Leor J. et al. Sudden cardiac death triggered by an earthquake. N. Engl. J. Med. 1996; 34: 413-9
5. Dobson AJ, Alexander HM, Malcolm JA, Steele PL, Miles TA. Heart attacks and the Newcastle earthquake. Med J Aust 1991; 155: 757-761
6. Trichopoulos D, Katsouyanni K, Zavitsanos X, Tzounou A, Dalla-Vorgia P. Psychological stress and fatal heart attack: the Athens earthquake natural experiment. Lancet 1983; I: 441-444
7. Katsouyanni K, Kogevinas M, Trichopoulos D. Earthquake-related stress and cardiac mortality. Int J Epidemiol 1986; 15: 326-330
8. Shiono K. Inconvenience in resident's daily living activities from post-earthquake suspension of utility services. Comprehensive Urban Studies 1989; 38: 149-167.
9. Shiono K. ,Shumuta Y. Inconvenience in resident's daily living activities from post-earthquake suspension of utility services, part 2. Procedure for estimation. Comprehensive Urban Studies 1991 ;41: 37-46.

Table 1 Completion proportions to the questionnaires in the six regions

Region	Total number of households	Total number of mail surveys	Number of responders	Completion proportions (%)
Nada District, Kobe City	54,800	1,530	507	33.1
Higashi-Nada District, Kobe City	73,600	1,299	502	38.6
Ashiya City	33,400	705	240	34.0
Nishinomiya City	160,300	3,262	1,105	33.9
Itami City	68,200	1,380	456	33.0
Hokudan area	2,600	335	107	31.9

Table 2 95% confidence interval (CI) for a population mean of inconvenience of daily life and a population proportion of completely destroyed houses

Region	95% CI for a population mean of inconvenience of daily life	95 % CI for a population proportion of completely destroyed houses (%)
Nada District, Kobe City	977-1295	25.2-33.1
Higashi-Nada District, Kobe City	1019-1229	19.8-27.2
Ashiya City	904-1154	14.6-24.6
Nishinomiya City	741-843	13.6-17.9
Itami City	131-199	1.2-4.1
Hokudan area	247-485	16.2-32.4

Table 3 Means and standard deviation (SD) of inconvenience of daily life according to the level of structured damage of the houses

Region	Level of structural damage			
	Level 1	Level 2	Level 3	Level 4
Nada District,Kobe City	2429±2818 (N=51)	1044±717 (N=95)	905±560 (N=102)	576±342 (N=55)
Higashi-Nada District, Kobe City	1508±1387 (N=45)	1274±1000 (N=103)	931±597 (N=144)	715±434 (N=18)
Ashiya City	756±532 (N=12)	1176±831 (N=47)	1031±716 (N=63)	714±416 (N=17)
Nishinomiya City	1338±1212 (N=81)	926±718 (N=157)	724±534 (N=366)	517±442 (N=146)
Itami City	138±113 (N=7)	257±411 (N=80)	133±211 (N=135)	119±203 (N=54)
Hokudan area	706±706 (N=11)	320±360 (N=30)	278±314 (N=11)	108±78 (N=4)

Level 1; The house was completely destroyed.

Level 2; The house was partially destroyed.

Level 3; The house was slightly damaged (structural damage was less than that of level 2).

Level 4; The house was not damaged.

Table 4 95% confidence interval for a population proportion regarding the occurrence of indirect health effects within 6 months after the earthquake

Indirect health effects within 6 months after the earthquake (excluding those due to injuries)	95% confidence interval for a population proportion (%)					
	Nada	Higashi-Nada	Ashiya	Nishinomiya	Itami	Hokudan
1) Visiting a doctor more than once	42.4-51.3 (N=230)	45.1-54.0 (N=239)	35.7-48.5 (N=96)	34.3-40.1 (N=393)	19.5-27.4 (N=104)	36.9-56.9 (N=45)
2) Being sick in bed and stay at home	20.0-27.7 (N=113)	23.8-31.8 (N=133)	17.5-28.5 (N=52)	21.1-26.2 (N=247)	10.3-16.8 (N=57)	14.2-31.4 (N=21)
3) Being hospitalized	3.6-7.8 (N=27)	2.6-6.2 (N=21)	4.7-11.9 (N=19)	3.9-6.6 (N=55)	2.1-5.8 (N=17)	2.9-14.5 (N=8)
4) Suffering chronic disease before the earthquake	29.5-38.1 (N=157)	24.1-32.3 (N=131)	24.8-36.7 (N=71)	25.9-31.4 (N=293)	25.8-34.7 (N=123)	20.3-40.0 (N=26)

Table 5 Analysis of variance of inconvenience of daily life according to the occurrence of indirect health effects within 6 months after the earthquake

Indirect health effects within 6 months after the earthquake (excluding those due to injuries)		Mean ± SD	P-value
1) Visiting a doctor more than once	Yes	1046±1182 (N=677)	
	No	683±684 (N=1137)	P<0.001
2) Being sick in bed and stay at home	Yes	1069±995 (N=384)	
	No	744±752 (N=1403)	P<0.001
3) Being hospitalized	Yes	1148±1197 (N=78)	
	No	806±903 (N=1714)	P<0.01

Revisiting the public health consequences of natural disasters through an epidemiologic perspective

by
Josephine Malilay[1]

ABSTRACT

A synopsis of recent epidemiologic activities in disaster settings is presented for 1999, the fifth year of the involvement of the Centers for Disease Control and Prevention (CDC) in the United States - Japan Natural Resources Panel on Wind and Seismic Effects. The objectives are to: 1) describe the mission of disaster epidemiology at CDC in the context of emergency management; 2) outline different methods and field activities conducted by CDC; and 3) provide a framework for public health and epidemiology in the emergency management of natural disasters, particularly wind and seismic events. A conceptual framework using the goals of epidemiology in disaster settings and the phases of the emergency management cycle has been developed to address the public health consequences of natural disasters. For each selected goal and phase, epidemiologic assessments or studies may be conducted to answer questions posed by public health officials and emergency managers. The framework may provide a basis for direction for collaborative work between the U.S. and Japanese-equivalent public health sectors for UJNR activities.

KEYWORDS: public health, natural disasters, epidemiology

1. INTRODUCTION

Since 1995, the Centers for Disease Control and Prevention (CDC) has been a member of the United States - Japan Natural Resources (UJNR) Wind and Seismic Panel. The objectives of this participation are to stimulate an awareness of public health perspectives in addressing wind and seismic events, and to address public health issues in multi disciplinary studies that concern human health and safety. At the 27th Joint Panel Meeting in 1995, CDC presented an overview of epidemiology in disaster settings (1); in 1996, a study on the risks of deaths in wind and seismic events as related to structural collapse (2); in 1997, rapid needs assessment following Hurricane Marilyn in the US Virgin Islands (3); and in 1998, a description of the American Red Cross - CDC Health Impact Surveillance System for Natural Disasters (4). These presentations have provided a representative cross-section of the various activities conducted by CDC in disaster settings.

At the UJNR 29th Joint Meeting in 1997, the US-Japan Panel on Wind and Seismic Effects recognized that the public health sector could provide a significant perspective on multi disciplinary planning needed for mitigation of and recovery following natural disasters. In line with this recognition, the US-side proposed to develop a public health component that

[1] National Center for Environmental Health, Centers for Disease Control and Prevention, Atlanta, Georgia USA

would address health-related issues as they apply to wind and seismic hazards. The goals for including this component were to reduce the human impact of disaster and to improve the quality of human life. To achieve these goals, the Panel suggested two areas of investigation: 1) Field assessments. These assessments, performed by both the engineering and public health sectors, may be improved by developing and testing scientifically and statistically valid methodologies for rapidly gathering information after natural disasters. 2) Human outcome studies. The risks for outcomes -- such as deaths, diseases, injuries, disabilities, and behavioral reactions -- may be described by demographic, health, behavioral, meteorological, geological, environmental, and engineering data to obtain an understanding of how and why people are affected by natural disasters. Development of these topics under the direction of the UJNR would coalesce the engineering and public health sectors to further these goals.

For 1999, the fifth year of CDC involvement, we present a synopsis of recent activities as they pertain to the role of CDC in public health and the disaster cycle (also called emergency management cycle). The objectives of this synopsis are to: 1) describe the mission of disaster epidemiology at CDC in the context of emergency management; 2) outline different methods and field activities conducted by the National Center for Environmental Health (NCEH) at CDC; and 3) provide a framework for public health and epidemiology in the emergency management of natural disasters, particularly wind and seismic events. We hope that the objectives of this synopsis may assist in establishing a foundation for collaborative ties with Japanese counterparts whose work involves public health and with potential U.S. and Japanese collaborators in multi disciplinary fields.

2. EPIDEMIOLOGY IN DISASTER SETTINGS

Epidemiology is the study of the causes and determinants of health-related events in human populations (5). Methods from this discipline can be used to compare fatalities with survivors to learn how and where they differed, to identify risk groups of persons, time, and place by exposure, with the aim of preventing the occurrence of death, injury, or illness. The mission of disaster epidemiology therefore is to promote health and quality of life by service, research, and dissemination of information in preparing for, responding to, and recovering from a disaster event. The goals of this mission include: 1) to provide *service* to communities and organizations, e.g., initiate or conduct surveillance and needs assessment during preparedness, response, and recovery; 2) to conduct *research*, e.g., conduct studies on health effects from specific disaster events, conduct prevention effectiveness studies, refine surveillance and other methodologies; and 3) to *disseminate the knowledge base* to the community at large, state/local/foreign health departments, other Federal agencies, professional interest groups, academic institutions, and international organizations.

3. THE DISASTER CYCLE

The public health response to disaster

events, including wind and seismic events, addresses activities that occur before, during, and after the events, or "preimpact," "impact," and "postimpact." Epidemiologic methods which provide the basis for the response likewise are applied in each of the phases. The temporal sequences of these phases, lasting anywhere from seconds to months or years, have been translated for practical purposes into the "disaster cycle," also known as the emergency management cycle (6,7). The cycle consists of 5 phases: 1) non-disaster phase, in which hazard prevention and disaster preparedness measures are taken; 2) predisaster, or warning phase, which involves forecasting and early warning, evacuation of vulnerable populations; 3) impact phase, in which death, injuries, and destruction may occur; 4) emergency or relief phase, in which relief and assistance are provided to casualties, e.g., search and rescue, first aid; and 5) recovery or reconstruction phase, in which normal services are restored and damaged buildings and facilities reconstructed. Although the phases may overlap, each has a specific purpose and provides a basis for the next. In public health, these phases are often abbreviated into 3: preparedness, response, and recovery.

4. THE MATRIX

To illustrate the role of disaster epidemiology before, during, and after a disaster event, we present a matrix that outlines appropriate activities pertaining to application and service, research, and dissemination of knowledge, as shown on the horizontal axis, during preparedness, response, and recovery, indicated on the vertical axis (Figure 1). Each cell of the matrix presents epidemiologic activities that may be conducted as they apply to a particular goal of the mission of disaster epidemiology during a specific phase.

The main epidemiologic activities are described as follows:

1. Surveillance

Surveillance is the ongoing and systematic collection, analysis, and interpretation of health data used for planning, implementing, and evaluating public health interventions and programs. Surveillance data are used both to determine the need for public health action and to assess the effectiveness of programs (8). Commonly used surveillance systems in the post-disaster setting include those for disease, injury, and death. Examples are drawn from responses to Hurricanes Marilyn and Opal in the U.S. Virgin Islands and the southeastern United States in 1995, respectively (9); a severe ice storm in Maine in 1998 (10); and the American Red Cross-CDC Health Impact Surveillance System for Natural Disasters (4).

2. Rapid needs assessment

Rapid needs assessment refers to a collection of techniques -- epidemiologic, statistical, anthropological -- designed to provide quickly and at low cost, accurate population-based information about an affected community's needs after a disaster in a simple format to decision-makers (11). Examples include recent responses to a severe ice storm in Maine in 1998 (10); Hurricane Georges in the Dominican Republic in 1998 (12); and Hurricane Mitch in Honduras, Nicaragua, El Salvador, and

Guatemala in 1999 (13).

3. Descriptive and analytic studies

Both descriptive and analytic epidemiologic studies may be designed and conducted to determine risk factors that predispose the disaster-affected to a particular health condition or to evaluate the effectiveness of an intervention program. For example, a study of risk factors contributing to carbon monoxide (CO) poisoning after a major ice storm identified generators as a major CO source and generator location as the strongest risk factor (14). In another example, an evaluation of the health status of displaced communities in camps with and without water and sanitation services after an earthquake in Bolivia demonstrated that the presence of running water and latrines and the treatment of household water were each independently associated with a lower incidence of illness (15). Analyses of the costs, cost-benefits, and cost-effectiveness of interventions may also be performed.

5. CONCLUSIONS AND RECOMMENDATIONS

A conceptual framework using the goals of epidemiology in disaster settings and the phases of the emergency management cycle has been developed to address the public health consequences of natural disasters. For each selected goal and phase, epidemiologic assessments or studies may be conducted to answer questions posed by public health officials and emergency managers.

As such, the framework may provide a basis for direction for collaborative work between the U.S. and Japanese-equivalent public health sectors for UJNR activities. An initial step is to identify a public health-equivalent counterpart from the government sector and to list agencies having a potential interest in natural disaster reduction and health-related impacts for each selected goal and phase of the matrix. Finally, it is hoped that the matrix may stimulate ideas of comparable systems or frameworks in Japan for a joint public health collaborative effort for the UJNR Panel on Wind and Seismic Effects.

6. REFERENCES

1. Malilay J, Noji E. Epidemiologic methods for assessing wind- and seismic-related health effects in disaster response. In: Nakaoka T. Wind and seismic effects. Proceedings of the 27th Joint Meeting of the U.S.-Japan Cooperative Program in Natural Resources Panel on Wind and Seismic Effects; 1995 May 16-19; Tsukuba, Japan. Technical Memorandum of the Public Works Research Institute No. 3387, May 1995.

2. Malilay J, Wasley A, Fiedler L. Descriptive epidemiology of wind-related mortality. In: Raufaste NJ, editor. Wind and seismic effects. Proceedings of the 28th Joint Meeting of the U.S.-Japan Cooperative Program in Natural Resources Panel on Wind and Seismic Effects; 1996 May 14-17; Gaithersburg, MD. Washington, DC: National Institute

of Standards and Technology Special Publication 904, August 1996.

3. Selanikio JD, Malilay J, Flanders WD. Rapid needs assessment and loss estimation from natural hazards: lessons learned from Hurricane Marilyn, U.S. Virgin Islands. In: Okahara M, editor. Wind and seismic effects. Proceedings of the 29th Joint Meeting of the U.S.-Japan Cooperative Program in Natural Resources Panel on Wind and Seismic Effects; 1997 May 13-16; Tsukuba, Japan. Technical Memorandum of the Public Works Research Institute No. 3524, ISSN 0386-5878.

4. Paz-Argandoña E, Malilay J. The American Red Cross - Centers for Disease Control and Prevention Health Impact Surveillance System for Natural Disasters. In: Raufaste NJ, editor. Wind and seismic effects. Proceedings of the 30th Joint Meeting of the U.S.-Japan Cooperative Program in Natural Resources Panel on Wind and Seismic Effects; 1998 May 12-15; Gaithersburg, MD. Washington, DC: National Institute of Standards and Technology Special Publication 931, August 1998.

5. Lilienfeld AM, Lilienfeld DE. Foundations of epidemiology, 2nd ed. New York: Oxford University Press, 1980.

6. Noji EK. The nature of disaster: general characteristics and public health effects. In: Noji, EK, ed. The public health consequences of disasters. New York: Oxford University Press, 1997.

7. Drabek TE, Hoetmer GJ, editors. Emergency management: principles and practice for local government. Washington, DC: International City Management Association, 1991.

8. Thacker SB, Berkelman RL. Public health surveillance in the United States. Epidemiologic reviews 1988;10:164-190.

9. Centers for Disease Control and Prevention. Surveillance for injuries and illnesses and rapid health-needs assessment following Hurricanes Marilyn and Opal, September-October 1995. Morbidity and Mortality Weekly Report 1996;45:81-85.

10. Centers for Disease Control and Prevention. Community needs assessment and morbidity surveillance following an ice storm -- Maine, January 1998. Morbidity and Mortality Weekly Report 1998;47:351-354.

11. Anker M. Epidemiologic and statistical methods for rapid health assessment: introduction. World health statistics quarterly 1991;44:94-97.

12. Centers for Disease Control and Prevention. Needs assessment following Hurricane Georges -- Dominican Republic, 1998. Morbidity and Mortality Weekly Report 1999;48:93-95.

13. Jacobson J, Batts-Osborne D, Malilay J. Post-hurricane needs assessments in Central America, February 1999 [abstract for latebreaker]. Presented at 48th Epidemic Intelligence Service (EIS) Conference, April 19-23,1999. Atlanta, Georgia: CDC.

14. Daley WR, Smith A, Paz E, Malilay J, McGeehin M. An outbreak of carbon monoxide poisoning after a major ice storm, Maine, 1998 [abstract]. Presented at the 48th Epidemic Intelligence Service (EIS) Conference, April 19-23,1999. Atlanta, Georgia: CDC.

15. Jacobson J, Aguilar P, Paz E, Malilay J. Water, sanitation, and illness in camps after an earthquake in Aiquile, Bolivia [abstract]. Poster presentation at the 48th Epidemic Intelligence Service (EIS) Conference, April 19-23,1999. Atlanta, Georgia: CDC.

Figure 1. Conceptual matrix for epidemiology in disaster settings and emergency management

	Preparedness	Response	Recovery
Application and Service	■ Surveillance - degree of preparedness e.g., health outcome: prevalence of use	■ Surveillance e.g., health outcome: burden of disease, injury, and death ■ Rapid needs assessment (RNA)	■ Surveillance e.g., burden, type and circumstances of disease, injury, and death ■ Rapid needs assessment (RNA)
Research	■ Cost-effectiveness studies of prevention interventions e.g., sirens, weather radios, other watch and warning systems health outcome: -# lives saved ■ Comparison studies of warning systems (e.g., heat indices) ■ Descriptive studies of disasters (e.g., tsunamis, landslides and avalanches) ■Studies updating information on previously-described disasters (e.g., lightning) ■Theoretical perspectives on emergency management	■ Development of RNA methods ■ Refinement and evaluation of RNA methods ■ Comparison of RNA methods across disasters (intra- and interdisaster) ■ Development of training techniques for RNA (e.g., better training of volunteers) ■Descriptive and analytic studies of impact-related effects (e.g., wind-related injuries)	Specific disaster types: ■ Floods - respiratory outcomes related to mold/mildew, effectiveness of remediation techniques - health outcomes associated with flood-affected well water - effects of technological disasters initiated by flooding ■ Earthquakes -coccidioidomycosis -injury and hospital length of stay -stress-induced myocardial infarction ■ Hurricanes -Dengue fever disaster responders

Dissemination	Preparedness information: ■ Development of curricula - state/local health departments/Ministry of Health - public community - professional interest groups - academia ■ Development of training materials - outlines - literature - case studies - slides	Transmit methods to state/local health departments - on site - World Wide Web sites - other forms e.g., special workshops	Training sessions Consultations Presentations

Theme 3

Storm Surge and Tsunamis

OUTLINE AND PERFORMANCE OF NEW TSUNAMI FORECAST SERVICE IN THE JAPAN METEOROLOGICAL AGENCY

by
Yasuo SEKITA[1], Hidee TATEHATA[1], Tsuneaki ANAMI[1] and Takashi KADOWAKI[2]

ABSTRACT

The Japan Meteorological Agency (JMA) started a new tsunami forecast service on 1 April, 1999. In the new service, the JMA issues calculated tsunami heights in a specific number using tsunami numerical simulation. The ratio between calculated tsunami heights and observed ones correlates with a configuration of the coast at an observation point and the source area. With this correlation, we can improve the accuracy of tsunami height forecasts.

KEY WORDS: Tsunami Forecast
Numerical Simulation
Tsunami Height
Accuracy of Forecast

1. INTRODUCTION

Japan is one of the most seismically active areas in the world, and has frequently suffered from the tsunami disasters caused by earthquakes. In order to mitigate the tsunami disasters, the Japan Meteorological Agency (JMA) has issued tsunami forecasts since 1952.

The JMA started a new tsunami forecast service using tsunami numerical simulation on 1 April, 1999. In the new service, estimated tsunami heights are available in a specific number, while only rough scale were available in the previous service. Main features of the new service are following:

- Using numerical simulation,
- Estimated tsunami height being available in a specific number,
- Subdivision of the previous 18 tsunami forecast regions into 66.

This paper is intended to show the outline and the performance of the new tsunami forecast service.

2. OUTLINE OF THE NEW TSUNAMI FORECAST SERVICE

2.1 Application of numerical simulation to tsunami forecast

Over the past few decades a considerable number of studies have been made on the method of tsunami numerical simulation. It has been very difficult, however, to apply it to tsunami forecast, which ought to be issued within a few minutes after the occurrence of an earthquake. The reason is that numerical simulation is very time-consuming. Even if you begin the simulation just after the occurrence of an earthquake, it cannot be completed before tsunami arrival.

The JMA has made it possible to apply tsunami numerical simulation to tsunami forecast by a new scheme (Tatehata, 1998a). Heights and arrival times of tsunamis have already been computed by

1) Seismological and Volcanological Department, Japan Meteorological Agency, 1-3-4 Otemachi, Chiyoda-ku, Tokyo 100-8122, Japan
2) Osaka District Meteorological Observatory, 4-1-76 Otemae, Chuo-ku, Osaka 540-0008, Japan

numerical simulation for a large number of earthquakes, of which fault planes with various magnitudes and depths were located as Fig.1, and a database set have been made of the computed results. When a large earthquake occurs, appropriate tsunami heights and tsunami arrival times are searched from the database immediately, and the tsunami forecast is issued.

Just after an earthquake occurs, its hypocenter and magnitude are only information that can be obtained about it. We need, however, a fault plane model of an earthquake for tsunami numerical simulation. Hence, a fault plane is set up from the hypocenter and magnitude of an earthquake using the following assumptions (hereafter, referred to as "Model-V"):

- The length (L), width (W) and slip (D) of a fault model are related to the magnitude (M) of an earthquake as follows.
  $\log L = 0.5M - 1.9$
  $\log W = 0.5M - 2.2$
  $\log D = 0.5M - 3.2$
- The dip (δ) and slip (λ) angles of a fault plane, which are uniform everywhere, are as follows.
  $\delta = 45°$
  $\lambda = 90°$ (reverse fault)
- The strike of a fault is parallel to the trenches (or the coastline).
- A hypocenter is located at the center of a fault plane.

The JMA has done computer simulations for about 100,000 fault plane models set up in the way mentioned above. With a view to obtaining the average tsunami height along a 20 or 30km-long coastline, tsunami heights at the shore were calculated by Green's formula, as shown in Fig.2 (Tatehata, 1998b).

2.2 Forecast of tsunami height

Three types of tsunami bulletins were issued in the previous service (Table 1). As shown in Table 1, "Major Tsunami", for example, one of tsunami forecast bulletins, implied only that the height of tsunami was expected to be more than 3 meters in the worst places and did not show the height quantitatively. Consequently, it was not sufficient information for disaster prevention organizations to decide adequate measures for tsunami disaster mitigation.

The new tsunami forecast service provides the expected tsunami height for each tsunami forecast region in a specific number such as "3m", "4m" or "6m", in addition to the categorized bulletins "Major Tsunami", "Tsunami" or "Tsunami Attention" (Table 2). Using the new forecast, they can decide the detailed countermeasure for tsunami disasters.

2.3 Subdivision of tsunami forecast regions

The JMA had divided the entire Japan coast into 18 tsunami forecast regions, the average length of which was several hundred kilometers (Fig. 3a). Hence, sometimes only part of a tsunami forecast region was struck by tsunami when a tsunami warning was issued for the entire tsunami forecast region. In consequence, disaster prevention organizations often had to take excessive countermeasures.

With a view to fitting tsunami forecasts to real tsunami phenomena and making names and sections of the forecast regions understood easily by residents, the JMA has subdivided the previous 18 tsunami forecast regions into 66 regions, roughly each prefecture corresponding to one of the regions, in the new tsunami forecast service (Fig 3b). With this subdivision, tsunami forecasts are expected to fit tsunami phenomena much better than the previous forecast.

3. PERFORMANCE OF THE NEW TSUNAMI FORECAST SERVICE

Performance of the new tsunami forecast service was investigated by comparing calculated tsunami heights and observed ones with the following tests.

3.1 Correlation with configurations of coastlines

From the feature of a configuration, the entire Japan coast was divided into six categories, island, cape, rias coast, large bay (over several ten kilometers size), small bay (under several ten kilometers size) and other configuration. On each of the categories, the geometric mean and variance of the ratio between calculated tsunami heights and observed ones are shown in Table 3 using observation data of 27 earthquakes which occurred near Japan Islands from 1896 to 1996. The list of earthquakes used in this test is presented in Appendix 1.

In order to reduce the influence due to the situation that the fault planes used for the calculation of tsunami heights were different from the actual fault planes, reliable fault models estimated from seismic wave data and/or other observed data (hereafter, referred to as "Model-R") were used for tsunami height calculation instead of Model-V in this test.

Table 3 indicates that observed data tends to be higher than calculated ones in "island" area, while smaller in "small bay" area.

3.2 Correlation with earthquake source areas

Using the same earthquakes data as listed in Appendix 1, the geometric mean and variance of the ratio between calculated tsunami heights from Model-R and those from Model-V about earthquakes occurring in each source area are presented in Table 4. Earthquakes in the Nansei-Shoto area or the Japan Sea tend to cause larger tsunamis than those expected from Model-V, while earthquakes in the Pacific except the Nansei-Shoto area tend to cause smaller ones.

3.3 Influences of the relative location of a hypocenter to the earthquake fault and the error of the strike of the fault

Although hypocenters are assumed to be located at the center of the fault planes in Model-V, it is possible for an actual earthquake hypocenter to be located anywhere on the fault plane. If an actual hypocenter is located at the edge of the fault plane, a tsunami height at each observation point differs from a calculated value using Model-V even though the whole tsunami size is the same.

In Model-V, the strike of a fault plane is assumed to be parallel to the trench (or the coastline). As a result, a tsunami height at each observation point differs from a calculated one too, if an actual strike is different from that of Model-V. Figure 4 shows the distribution of the difference between the strike of an actual fault and that of Model-V. Since the differences of 83% earthquakes of all are within 25 degrees, it seems reasonable to suppose the error of the assumed strike to be 25 degrees.

The numerical experiments were done to estimate the influence of these assumptions. The location of a hypocenter was fixed and the relative position of the fault plane was moved as shown in Fig. 5. At the same time, the strike of the fault plane was shifted to -25, 0 and 25 degrees relative to that of Model-V. Tsunami heights at each observation point calculated from these 18 trial fault models were compared to those of Model-V for earthquakes with various locations and magnitudes. Fig. 6 shows the geometric variance of the ratio between tsunami heights of those trial models and those of Model-V versus the epicentral

distance to an observation point for each magnitude. The variance is small for an observation point far from an epicenter, while large for a point near to the epicenter and increases with the magnitude. Figure 7 shows, on the other hand, the variance of the ratio between the maximum value of tsunami heights for each trial model and that of Model-V. The variance is approximately constant, 1.2, for all the magnitude.

These results can be explained by the following consideration. At a point far from the epicenter, the variation of the tsunami height between each trial model and Model-V is small, since the effect of the change of the fault plane location is relatively small. It grows relatively larger with an observation point getting near to the epicenter. It also grows larger with the magnitude of an earthquake, because the size of the fault plane grows larger in keeping with the magnitude.

On the other hand, the whole tsunami size of each trial model is nearly as large as that of Model-V. For this reason, the maximum tsunami height of each trial model is not so different from that of Model-V, although a tsunami height at each point is quite different.

4. CONCLUSION

It depends on its accuracy whether the new tsunami forecast service is effective to mitigate tsunami disaster. The accuracy can be improved by correcting the calculated tsunami heights using the result of performance tests mentioned above. We intend to improve the accuracy of the forecast further by investigation of appropriate correction and making the computational method better.

5. References

Tatehata, H. (1998). The new tsunami warning system of the Japan Meteorological Agency, *Science of Tsunami Hazards*, **16**, 39-50.

Tatehata, H. (1998b). Application of tsunami numerical simulation to tsunami forecast (in Japanese), *Gekkan Kaiyo*, **extra 16**, 23-30.

Affordable Tsunami Mitigation

by

Michael E. Blackford

ABSTRACT

Thirty-five years have passed since tsunamis caused loss of life at distances of more than one thousand kilometers from the tsunamis' source areas. During that time the primary cause of the fatalities and the destruction is due to the locally generated tsunami. Japan has a highly developed program to mitigate the effects of local tsunamis. The United States, following the very great Alaska earthquake of 1964, has developed local or regional tsunami warning systems for Alaska, the Pacific coast States, and British Columbia of Canada, as well as for Hawaii. Tsunami mitigation involves three aspects: assessment, emergency management (warning and evacuation), and education. Tsunami assessment addresses past tsunami occurrence, both historical and paleotsunamis. It also involves tsunami inundation modeling and the definition of tsunami hazard zones. Tsunami emergency management involves a system of rapid earthquake characterization and communication of that information to appropriate emergency management authorities that, in turn, undertake appropriate evacuation procedures. Tsunami education involves a system of ongoing programs that reinforce tsunami awareness. These may consist of annual awareness programs centered on the date of some significant tsunami event. They may also take the form permanent signs or structures indicating tsunami evacuation routes or havens of safety. Japan and the United States should adapt their successful methods of tsunami mitigation and make them affordable to all nations in need of tsunami mitigation systems.

KEYWORDS

affordable; assessment; education; emergency management; mitigation; tsunami

1. INTRODUCTION

Thirty-five years have passed since tsunamis caused loss of life at distances of more than one thousand kilometers from the tsunamis' source areas. Damage in this far field was also minimal. Nevertheless, the number of people killed by tsunamis during this interval of time is in the thousands. The primary cause of the fatalities and the destruction is due to the locally generated tsunami.

Local tsunamis, or even regional tsunamis, are difficult natural hazards to deal with from an emergency management viewpoint. Cyclonic storms- hurricanes, typhoons, or cyclones- that build up to destructive force and follow relatively predictable paths over periods of days, give emergency managers time to prepare for their possible passage through the managers' areas of responsibility. Earthquakes' destructive ground shaking is usually over in a matter of minutes. The emergency managers' tasks are primarily focussed on search and rescue of victims and recovery of lifelines. Automatic systems that can detect the onset of the quake can shutdown critical facilities and thus mitigate some of the effects of earthquakes, but this is typically a small portion of all the destruction. Near source tsunamis, however, often allow you minutes or even several tens of minutes after the earthquake before they deliver their destructive force. This gives emergency managers a tantalizingly brief period of time to take some action to reduce the effect. In addition, measures may be implemented prior to the seismic event that can dramatically mitigate the potential tsunami destruction.

Japan and the United States are perhaps the

International Tsunami Information Center, NOAA/National Weather Service Pacific Region, Honolulu, Hawaii 96813

leaders among nations in the area of tsunami mitigation. Japan, with its dense population concentrated on its coastlines, is relentlessly attacked by tsunamis arising from nearby sources that wreak havoc on this population. It is no wonder that it has developed some of the world's best tsunami counter measures, an excellent local warning system, and an ongoing educational program that keeps its population aware of how to respond to earthquakes that have the potential to generate deadly tsunamis. The tsunami threat in the United States has been mainly from the distant tsunami. In response to this threat it established a warning system that in fifty years has not allowed a single destructive tsunami from a distant source to reach an American coast without giving emergency managers some amount of time to undertake evacuation measures. The very great earthquake in Alaska in 1964 and the major earthquakes in Hawaii in 1975 and California in 1992 focussed the attention of the United States on the local and regional tsunami threat as well. A regional warning system was established in Alaska, with responsibility for the western U.S. States and British Columbia in Canada. A regional system for Hawaii was also incorporated into the Pacific Tsunami Warning Center. Although these Regional Warning Centers have yet to be tested by a truly destructive local tsunami since their establishment, they continue to put much money and effort into their systems to be ready to respond to the local tsunami when it does occur.

This paper will look at some of the measures undertaken in Japan and the United States in an effort to see which measures may be suitable for countries with very small budgets for tsunami mitigation. Tsunami mitigation can be divided into three aspects. The first aspect is essentially an assessment of the hazard and the risk. Some easily affordable actions may be taken upon completion of such an assessment. The second aspect is the establishment of a warning system. The key to a warning system is communications. With the explosion in the types and methods of communications going on today, ways are evolving that can allow even the most financially strapped nation to have some degree of a local tsunami warning system. The third aspect of tsunami mitigation is education. Raising public awareness of the threat of tsunamis and providing them with instruction on what to do when one is bearing down upon them is perhaps the most affordable of all the aspects of tsunami mitigation.

2. TSUNAMI ASSESSMENT

The Tsunami Inundation Modeling Exchange (TIME) program, originally developed by Noburo Shuto when he was at the Tohoku University, is a fine example of tsunami hazard assessment procedure that can be implemented at relatively low costs to the users. TIME is a modeling procedure that enables the user to make estimates of the expected tsunami runup that may occur on a coastline, given the bathymetry and topography in the vicinity of the coastline. The procedure provides emergency managers and planners with basic information necessary to develop evacuation and zoning plans for their coastlines that are vulnerable to tsunami inundation. TIME software has been distributed to many tsunami-prone countries and training has been given to scientists on how to use the software to determine reasonable inundation models. The procedure is currently being applied to many coastal population centers in Central and South America, in particular, and at a number of other sites in the Pacific basin.

In the United States there has been a growing awareness in recent years of the magnitude of the potential threat of a local tsunami along the northern California, Oregon, and Washington coastlines where the Juan de Fuca tectonic plate is being subducted beneath the North American plate. Paleotsunami studies revealed repeated episodes of extensive tsunami inundation in a number of areas along this coastline. A major earthquake that spawned a small local tsunami near the southern end of this subduction zone in the early 1990's brought about an inundation modeling effort by the U.S. NOAA's Pacific Marine Environmental Laboratory. This effort produced tsunami inundation hazard maps for the communities of Crescent City and Eureka in northern California. The project has since developed into multimillion dollar program that not only involves tsunami hazard assessment, but also improving timely tsunami detection and

warning, and raising public awareness of the tsunami hazard through a variety of educational projects.

3. TIMELY TSUNAMI DETECTION AND WARNING

To provide timely warnings for local or regional tsunamis the key elements involved are a rapid characterization of the causative earthquake and communication of that information quickly to emergency managers at any time. Systems developed by the Japan Meteorological Agency (JMA) and the United States Pacific Tsunami Warning Center (PTWC) are exemplary. They automatically determine the location and size of earthquakes in reasonably sized areas of responsibility within minutes of their occurrence and pass that information on to the public directly or through emergency management systems in about five minutes or less.

Both of these systems are, however, expensive to operate and budget planners continually need to be reminded of the savings in human lives that are made through their existence. What sort of a system can be developed for a country or state with limited financial resources? How can one incorporate elements of the JMA and PTWC systems into a less expensive tsunami warning system?

Both systems recognize that it is impossible to successfully warn the public before all tsunamis strike a coastline. Therefore they encourage and support an educational effort to make the public aware of what actions can be taken to avoid becoming victims of a tsunami. The systems believe that persons who are within about ten minute's travel-time of a tsunami need to act on their own. A warning issued within five minutes of the causative earthquake becomes effective when a population is informed that the earthquake they may, or may not, have just felt has the potential to generate a destructive tsunami. The warning answers the question running through the minds of the public, "Was that earthquake severe enough for me to get to high ground or away from the coast?"

The systems of the JMA and PTWC use networks of relatively closely spaced seismic stations to determine the exact location of the starting point of an earthquake. They use the level of excitation of the seismic instruments of these stations to determine a size for the earthquake. They base their decision on the type of information to disseminate regarding the earthquake on this information. How can this be done at a lowered cost? One way is to make multiple use of seismic data. If some funded institution is operating a network of seismic stations for research or some other purpose, it may be possible to simply tap that data and feed it to a relatively low cost automated earthquake-processing system. The warning system would not have to maintain seismic stations and the research institution would have additional justification to seek funding for operating its seismic network.

What if there is no seismic network available in area of responsibility of a warning system? It may be possible to use data from a single three-component seismic station to obtain an earthquake location satisfactory for warning purposes. If the seismic system has a relatively broad response band and high dynamic range, it may also provide adequate information on the earthquake's size. France's Laboratorie d'Geophysique has developed in recent years a single station detection system, TREMORS, which fulfills the requirements for a tsunami warning system. While TREMORS may become saturated for the largest of earthquakes, it can yield sufficient information to make a decision on whether or not to issue a tsunami warning. Although the complete TREMORS package including the seismometers may be somewhat expensive, the system without the seismometers is affordable. The PTWC worked with the French to modify TREMORS so that it would except data from broadband stations deployed around the world by the IRIS consortium. Thus the possibilities of using TREMORS affordably has increased many fold.

4. TSUNAMI HAZARD EDUCATION

Raising the awareness of the public to the threat of tsunamis is perhaps the most affordable

element in a tsunami warning system. The Tsunami Warning System in the Pacific (ITSU) has developed educational materials for all levels of a school curriculum. Many innovative educational techniques that may be adapted for other countries are coming out the United States' National Tsunami Mitigation Program.

Perhaps the most important element of any tsunami awareness program is that it be ongoing. If a region has been struck by a particularly devastating tsunami, a period of time around the anniversary of that event can be used as a time of renewed effort to make the public aware of the tsunami hazard. In addition, signs delimiting tsunami danger areas, tsunami evacuation routes, and tsunami safety areas act as constant reminders to the public of the tsunami hazard potential.

An ongoing public education program can lead to an acceptance of perhaps the most important tsunami mitigation activity, namely, hazard zoning. Unfortunately in most instances hazard zoning comes about through repeated events of devastation. The goal in tsunami zonation should be to reduce exposure time to tsunamis. The ultimate zonation is to free inundation areas of any permanent occupancy by persons or facilities. This is often impossible because certain facilities such as harbors are needed for commercial and recreational activities. Permanent residency could be reduced through a program of resettlement. All such efforts may need to be accomplished gradually in order to be affordable.

In situations where there is no alternative but to live and work by the sea some readily accessible haven of safety is needed. The situation in Papua New Guinea that was the site of the devastating tsunami in July 1998 may be considered as an example. The affected areas had the sea on one side and a barrier to escape, in this case a lagoon, inland. Affordable safety havens for these situations could be artificial mounds rising to heights above projected tsunami on land depths. Perhaps a bit more expensive would be tsunami resistant structures that could be temporarily sealed during the passage of tsunami waves. These could vary from simple block structures to more elaborate, monument-like structures. Perhaps an old ship, rather than being converted into scrap metal, could even be used if the beaching operation and subsequent maintenance costs were not excessive. The basic principle would be to have a readily accessible haven available to those who have no choice but to live next to the sea. These havens would also act as a constant reminder of the tsunami threat as well.

5. CONCLUSIONS

Japan and the United States have demonstrated that they are the world's leaders in the area of tsunami mitigation. These countries have developed and implemented many impressive measures of tsunami mitigation that span the tsunami assessment, emergency management, and education spectrum. Many of these measures, however, are quite expensive and may not be affordable in countries lacking the financial resources that can be budgeted for tsunami mitigation. Japan and the United States should continue to demonstrate their leadership by seeking ways to make their successful tsunami mitigation programs affordable to all nations that need them.

6. REFERENCES

Yoshiaki Kawata, Boyd C. Benson, Jose C. Borrero, Hugh L. Davies, Willem P. de Lange, Fumihiko Imamura, Horst Letz, Jonathon Noll, and Costas E. Synolakis, "Tsunami in Papua New Guinea Was as Intense as First Thought" EOS, Transactions, American Geophysical Society, vol. 80, no.9 (March 2, 1999)

NOAA Pacific Marine Environmental Laboratory, "Tsunami Hazard Mitigation, A Report to the Senate Appropriations Committee" (March 31, 1995)

LARGE-SCALE EXPERIMENT ON DYNAMIC RESPONSE OF SAND BED AROUND A CYLINDER DUE TO TSUNAMI

by

Fuminori KATO[1], Shinji SATO[2] and Harry YEH[3]

ABSTRACT

The scour process around a vertical cylinder due to tsunami runup was investigated experimentally using the large-scale tsunami facility at Public Works Research Institute. Scouring around a cylinder during tsunami runup was optically observed with the multiple CCD cameras that were installed inside of the cylinder. All the other necessary information, e.g. water depth, flow velocity and pore pressure, were obtained by the conventional electronic sensors. In addition, we measured the topography changes before and after the tsunami runup. The temporal variations of the scour process were clarified. The correlations between scouring, wave height, water volume of runup and liquefaction were also discussed.

KEY WORDS: Liquefaction
Runup
Scouring
Tsunami

1. INTRODUCTION

It is well known that a tsunami attack causes substantial erosion and scour on the shore. For example, the 1960 Chilean tsunami scoured out the port entrance by more than 10 m at Kesen-numa Port in Japan. Several tsunami surveys, from the 1992 Nicaragua tsunami to the 1998 Papua New Guinea tsunami, also discovered substantial tsunami scouring effects around structures and trees. In fact, scouring is sometimes the primary cause of structure damage and destruction. There are a variety of structures exist in coastal zones, such as straight-line structures like revetments and cylindrical shape structures like oil tanks.

It is likely that the scouring around on-shore structures caused by tsunami runup is different from the present understanding of sediment transport and bridge-pier-type scour processes in river and coastal environments. Flows associated with tsunami runup are far from being steady or uniform, and the scouring takes place over a short duration, often less than fifteen minutes. It is also important to comprehend the onshore conditions during tsunami runup, where soils (sediments) are initially not fully saturated and suddenly become wet on the surface while the majority of pore spaces are still filled with air. This complex and important problem must first be approached experimentally to understand the physics and mechanisms of scour phenomena associated with tsunami runup. Because of the importance of the scale effects expected in sediment motion, the laboratory experiments must be performed in a sufficiently large experimental facility.

The previous investigation of tsunami scouring processes is limited. Uda et al. (1987) found that scouring near a revetment due to tsunamis is governed by topography behind a revetment. As for scouring in front of a revetment, Nishimura and Horikawa (1979) and Noguchi et al. (1997) identified some correlation between scour depth and water depth in front of a revetment for tsunami drawdown processes.

---

1) Research Engineer, Coast Division, Public Works Research Institute, Asahi 1, Tsukuba-shi, Ibaraki-ken, 305-0804, Japan
2) Former Head, ditto
3) Professor, Department of Civil and Environmental Engineering, University of Washington, Box 352700, Seattle, Washington 98195-2700, U.S.A.

2. EXPERIMENT CONDITION

A series of experiments was performed in a 135 m long, 2 m wide, 5 m deep sediment tank at Public Works Research Institute, Tsukuba, Japan. To generate a wide variety of long waves, the tank is equipped with a piston-type wave-maker driven by the large servo motor. The maximum stroke of the wave paddle is 2.4 m with the maximum speed of 1.11 m/s. It was tested and proven to generate a clean solitary wave of at least 40 cm high in a 3 m water depth. A beach of well-graded sediment (approximately D_{50} = 0.35 mm sand particles) was constructed with a uniform slope of 1/20. A model cylinder was placed upright on the beach. The cylinder is 50 cm in diameter, made of 1 cm thick Plexiglas, water tight at the bottom end, and connected above to an aluminum cylinder in order to assure its stiffness. Because of the transparent cylinder wall, the scour process can be recorded from the interior with three miniature CCD video cameras, which cover more than 180-degree view of the circumference from the upstream to the downstream sides. Wave gages, an electromagnetic flow meter and pore pressure transducers were placed as shown in Figure 1. In addition, before and after each experiment, topography surveys were conducted in the 4 m by 1 m region around the cylinder.

The experiments were performed for total 11 cases as listed in Table 1. Note that the last two cases in Table 1 are those for a plane beach without placing the cylinder. The nonlinearity of an incident solitary wave was parameterized by the ratio (a/h) of wave height a to offshore water depth h. Three different incident wave conditions were used in terms of the nonlinear parameter a/h = 0.13 (cases 1, 2 and 3), 0.09 (cases 4, 5, and 6), and 0.05 (cases 7, 8, and 9). Three different offshore water depths were used: 2.25 m for the case 1, 4 and 7: 2.45 m for the case 2, 5 and 8: 2.65 m for the case 3, 6 and 9. Since the location of the model cylinder is fixed throughout the experiments, the offshore water depth was varied with h = 2.25 m, 2.45 m and 2.65 m, which correspond with the cylinder location at 4 m onshore from the still shoreline, on the shoreline and at 4 m offshore, respectively.

In order to evaluate the effect of existence of the cylinder, the maximum runup heights were measured with and without the cylinder placement using the identical incident wave condition. Under the condition of 2.65 m offshore water depth, the maximum runup height of Case 6 (with the cylinder) is 2 cm lower than Case 10 (without the cylinder). With 2.45 m offshore water depth, the runup of Case 5 (with the cylinder) is 5 cm lower than Case 11 (without the cylinder). These results indicate that the presence of the cylinder reduces the tsunami runup height very slightly. Consequently the blockage of the runup motion by the cylinder is negligible and the tank width is considered wide enough to neglect the side-wall effects.

3. RESULT OF TOPOGRAPHY SURVEY BEFORE AND AFTER TSUNAMI

Before and after each experiment, topography survey was conducted in the area of 1 m wide from the center of the cylinder toward the tank wall, 2 m onshore and 2 m offshore from the center of the cylinder. The measurement interval of 20 cm was used before the experiment, and after the experiment, the finer interval of 5 cm was used within 50 cm from the cylinder, and 10 cm interval beyond 50 cm from the cylinder.

Figure 2 shows beach level changes along the offshore line from the center of the cylinder. The positive values indicate deposition and the negative values indicate scour. The beach level variations were normalized by the initial water depth offshore. The distance from the cylinder was normalized by the tank width. Only for Cases 2 and 5, apparent local scouring resulted in the offshore region from the cylinder.

Figure 3 shows beach level changes along the longshore line from the cylinder. Local scouring

occurred in most cases. The maximum scour depth of 10 cm was found in Case 3 at 10 cm away from the cylinder. The larger the wave height, the deeper the scour depth. Furthermore, for a given incident wave condition, the larger scouring depth appears to result when the cylinder was placed offshore. It is noted that, in the cases where the cylinder was on the shoreline, erosion occurred everywhere along the longshore line.

Figure 4 shows beach level changes along the onshore line from the cylinder. Local scouring was occurred in most cases. The maximum scour depth of 7.7 cm was measured for Case 2 at 5 cm inland from the cylinder. The larger the wave height, the larger the scouring depth. When the cylinder was placed on the shoreline (i.e. Case 2 and 5), resulting scouring was the most severe for a given incident wave condition. In Cases 2 and 5, the erosion was observed as far as 1 m off the cylinder.

Figure 5 shows the relation between incident wave height and scour area of the depth with more than 2 cm deep. The scour area was normalized by the area of the cylinder. The wave height was normalized by the initial water depth offshore. In comparison with the cases when the cylinder was placed inshore on the beach, the scour area was larger when the cylinder was placed on the shoreline or offshore. The scour area appears to be proportional to the wave height; the scour area is much more sensitive to the incident wave height when the cylinder is at the shoreline.

Figure 6 shows the relation between the incident wave height and the sediment volume change in the area near the cylinder. The area of the measurement is 1 m long in the cross-shore direction and 0.5 m wide in the along-shore direction with the one long edge bisecting the cylinder in the cross-shore direction. The volume was normalized by the cylinder area times the initial water depth offshore. The net volume change for the case with the cylinder being placed inshore is smaller than that the other cases; the changes are comparable for the cases of the cylinder on the shoreline and at the offshore location. The proportionality shown in Fig. 6 appears to be similar for all three cases with different locations of the cylinder.

4. SCOUR AROUND A CYLINDER ELUCIDATED BY VIDEO ANALYSIS

To clarify scouring mechanisms around the cylinder, sand response along the cylinder wall was observed with three miniature CCD video cameras installed inside of the cylinder. This can be accomplished due to its large size cylinder model (50 cm in diameter) that is made of a transparent (Plexiglas) cylinder wall.

The sand response at the cylinder wall for Case 3 is shown in Fig. 7. Camera 1 (left column), camera 2 (center column) and camera 3 (right column) cover the views from offshore to side, side direction, and from side to onshore, respectively; each covers more than 90 degrees of the view angle to ensure that obtained images overlap each other with sufficient margins. The images on the top of Fig. 7 represent the condition prior to the tsunami runup, the middle were those at the maximum inundation, and those on the bottom were after the tsunami drawdown. The scour depths of three points (offshore, side and onshore) around the cylinder were determined from these images.

Scour-depth variations at the point facing offshore are shown in Fig. 8. The depths are all normalized by the diameter of the cylinder. During the tsunami runup, scouring resulted in most cases, i.e. the sand-surface elevation decreased. During the drawdown, sand accumulation occurred in the cases with the large scour depth at the maximum inundation. This behavior is evident in the cases with the cylinder located onshore and on the shoreline; especially in case 4, its scour depth at the maximum inundation is five times as large as that just after tsunami drawdown. At the maximum inundation under the same incident wave condition, i.e. the same ratio of wave height to water depth (a/h), the scour depth was the greatest

when the cylinder was placed at the onshore location when a/h = 0.13 or 0.05. On the other hand, the maximum scour depth occurred for the cylinder on the shoreline if the incident wave is a/h = 0.09, i.e. Case 5. In Case 5, breaking of the incident wave occurred and plunged just in front of the cylinder. Perhaps, this is the reason why the maximum scour occurred when the cylinder at the shoreline.

Figure 9 shows scour-depth variations (normalized by the cylinder diameter) at the side point of the cylinder wall. During the tsunami runup, scouring occurred in all cases. During the tsunami drawdown, sand deposition occurred in Cases 1, 2, and 3 in which the scour depth at the maximum inundation was large; on the other hand, further scouring occurred in the other cases. Comparing Fig. 9 with Fig. 8, scouring during the runup process is greater at the side of the cylinder than that at the point facing offshore. For the cases with the same incident wave condition, a/h, the scour depth at the maximum inundation is the greatest when the cylinder is placed offshore for a/h = 0.13 and 0.05. (Note that the maximum scour depths at the offshore side of the cylinder resulted when the cylinder was placed inshore as discussed with Fig. 8.) On the other hand, with a/h = 0.09, the largest scour at the maximum inundation occurred when the cylinder was placed at the shoreline. Again, wave breaking near the shoreline must be the reason for the case of a/h = 0.09.

Figure 10 shows scour-depth variations at the point facing in the onshore direction (behind the cylinder). On the contrary to the offshore and the side points presented in Figs. 8 and 9, sands were deposited behind the cylinder in most cases during the tsunami runup. During the tsunami drawdown, severe scouring occurred in most cases. Scour depths after the tsunami drawdown were as large as that of the side point at the maximum inundation stage shown in Fig. 9. For a given incident wave condition, scour depths after the tsunami drawdown were the greatest in the cases where the cylinder was on the shoreline, and the least in the cases where the cylinder was placed at the onshore location.

5. RELATION BETWEEN SCOUR DEPTH AND WAVE HEIGHT AND RUNUP WATER VOLUME

Figure 11 shows correlation coefficients between wave height and scour depth: the wave heights are those measured with the wave gages at seven different points (see Fig. 1) and the scour depths are those at the three points around the cylinder during tsunami runup and tsunami drawdown. At ① in Case 2 and Case 5, and at ①, ②, ③ and ④ in Case 3, the maximum wave height was set at 60 cm for the purpose of calculation for correlation coefficients because the water levels there became higher than the wave gage range of 60 cm.

During the tsunami runup, the scour depths at the point at the cylinder facing offshore have direct correlation to the wave heights at H_2, little to H_3 and ①. The scour depth at the side point of the cylinder during tsunami runup had positive correlation to the wave height at all points.

Unlike during the tsunami runup, the scour depth at the point of the cylinder facing offshore had inverse correlation only to H_3 during the tsunami drawdown. The scour depth at the side point of the cylinder during tsunami drawdown have direct correlation to the wave height at all points, particularly offshore points.

The water volume, which passed the cross section at 3 m offshore from the cylinder during the runup and drawdown, was calculated with following:

$$V_{in} = \int hu\,dt \quad (u>0) \qquad (1)$$

$$V_{out} = -\int hu\,dt \quad (u<0) \qquad (2)$$

where V_{in} is the total water volume per unit width during the flow in the onshore direction, V_{out} is the total water volume per unit width during the flow in the offshore direction, h is the local water depth and u is the horizontal velocity. Table 2 shows the correlation coefficients between the water volume and the scour depth at each point. V_{in} had little correlation with the scour depth at the point of the

cylinder wall facing offshore during tsunami runup, but had obvious correlation to that at the side point of the cylinder wall during tsunami runup, and at the side point and the onshore point during tsunami drawdown. Relation between V_{in} and scour depth at the onshore point during tsunami drawdown is shown in Figure 12. It indicates that there is a possibility of scour depth prediction at the side point and the onshore point with water volume of tsunami runup.

6. RELATION BETWEEN PORE PRESSURE AND SCOUR PROCESS

Soil liquefaction in seabed is often caused by a time lag between the pore pressure variation in the soil and the water pressure variation on the bed. By following the expression used by Zen (1987), vertical effective stress σ'_v can be expressed as

$$\sigma'_v = \sigma'_{v0} + (p_b - p_m) \qquad (3)$$

where σ'_{v0} is the initial vertical effective stress, p_b is the water pressure variation on the bed, p_m is the pore pressure variation. In this study, water pressure variations on the bed are approximated by the assumption of hydrostatic pressure.

Figures 13 and 14 show the temporal variations of water depth, pore pressure and vertical effective stress at 10 cm deep at ① shown in Figure 1, for Cases 2 and 3, respectively. Note that the water depth reached higher than 100 cm in Case 3 as shown in Fig. 14. Since the wave gage can measure only up to 100 cm, we simply set the depth at 100 cm during the period of overshoot. Since the duration of overshoot is short (less than 1 sec.), we feel that this error associated with the overshoot will not cause significant discrepancies in terms of the interpretations of our results. Compared between Figs. 13 and 14, the vertical effective stress is smaller in case 3 (the cylinder was at the offshore location) than in Case 2 (the cylinder was on the shoreline). As shown in Figure 8, however, the scour depth at the offshore side of the cylinder at the maximum inundation stage was less in Case 3 than in Case 2.

Figures 15 and 16 show temporal variations of water depth, pore pressure and vertical effective stress at 10 cm deep at ② and ③ (see Figure 1), for Cases 2 and 3, respectively. In comparison with ③, the water depth at ② was greater just after the tsunami arrival and lower after its quick decrease during the tsunami drawdown in both cases. The pore pressure at ② was as large as that at ③ during tsunami runup for Case 3, but during the drawdown, it was larger at ② than at ③ in both cases. At ②, the vertical effective stress was smaller throughout the tsunami runup and drawdown processes, and was zero in a longer period. These indicate that the decrease in vertical effective stress at the side of the cylinder was caused by the rapid water-depth decrease during the runup process and by water depth fall and delay of pore pressure fall in drawdown process.

7. CONCLUSION

The principal findings may be summarized as follows:

(1) Area and volume of scour are proportional to wave height. They are also dependent on the relative location of a cylinder to shoreline.

(2) The scour depth changed dynamically in runup and drawdown process. Instantaneous maximum scour depth reached five times as large as scour depth measured after the tsunami drawdown.

(3) In seabed near a cylinder, effective stress decreased notably during tsunami runup.

REFERENCES

Nishimura H., K. Horikawa (1979) : Scouring at the toe of a seawall due to tsunami drawdown, Proceedings of the 25th coastal engineering conference, pp. 210-214. (in Japanese)

Noguchi K., S. Sato and S. Tanaka (1997) : Large-scale experiments on wave overtopping and scouring at the toe of seawall, Proceedings of coastal engineering, vol. 44, pp. 296-300. (in Japanese)

Uda, T., A. Omata and Y. Yokoyama (1987) : Report of experiments on tsunami runup, Technical Memorandum of PWRI, No. 2486, 122 p. (in Japanese)
Zen, K., H. Yamazaki and A. Watanabe (1987) : Wave-induced liquefaction and densification in seabed, Report of the Port and Harbor Research Institute, vol. 26, No. 4, pp. 125-180. (in Japanese)

Table 1 Experiment condition

Case	WaterDepth(m)	WaveHeight(m)	a/h	RunupHeight(m)	
1	2.25	0.29	0.13	0.695	
2	2.45	0.32	0.13	0.755	
3	2.65	0.34	0.13	0.765	
4	2.25	0.20	0.09	0.580	
5	2.45	0.22	0.09	0.610	
6	2.65	0.24	0.09	0.650	
7	2.25	0.11	0.05	0.420	
8	2.45	0.12	0.05	0.435	
9	2.65	0.13	0.05	0.465	
10	2.65	0.24	0.09	0.670	no cylinder
11	2.45	0.22	0.09	0.660	no cylinder

Table 2 Correlation between water volume onshore and offshore, and scour depth

	offshore point		side point		onshore point	
	runup	drawdown	runup	drawdown	runup	drawdown
onshore water volume	0.16	0.01	0.54	0.23	0.24	0.81
offshore water volume	0.04	0.08	0.64	0.24	0.31	0.65

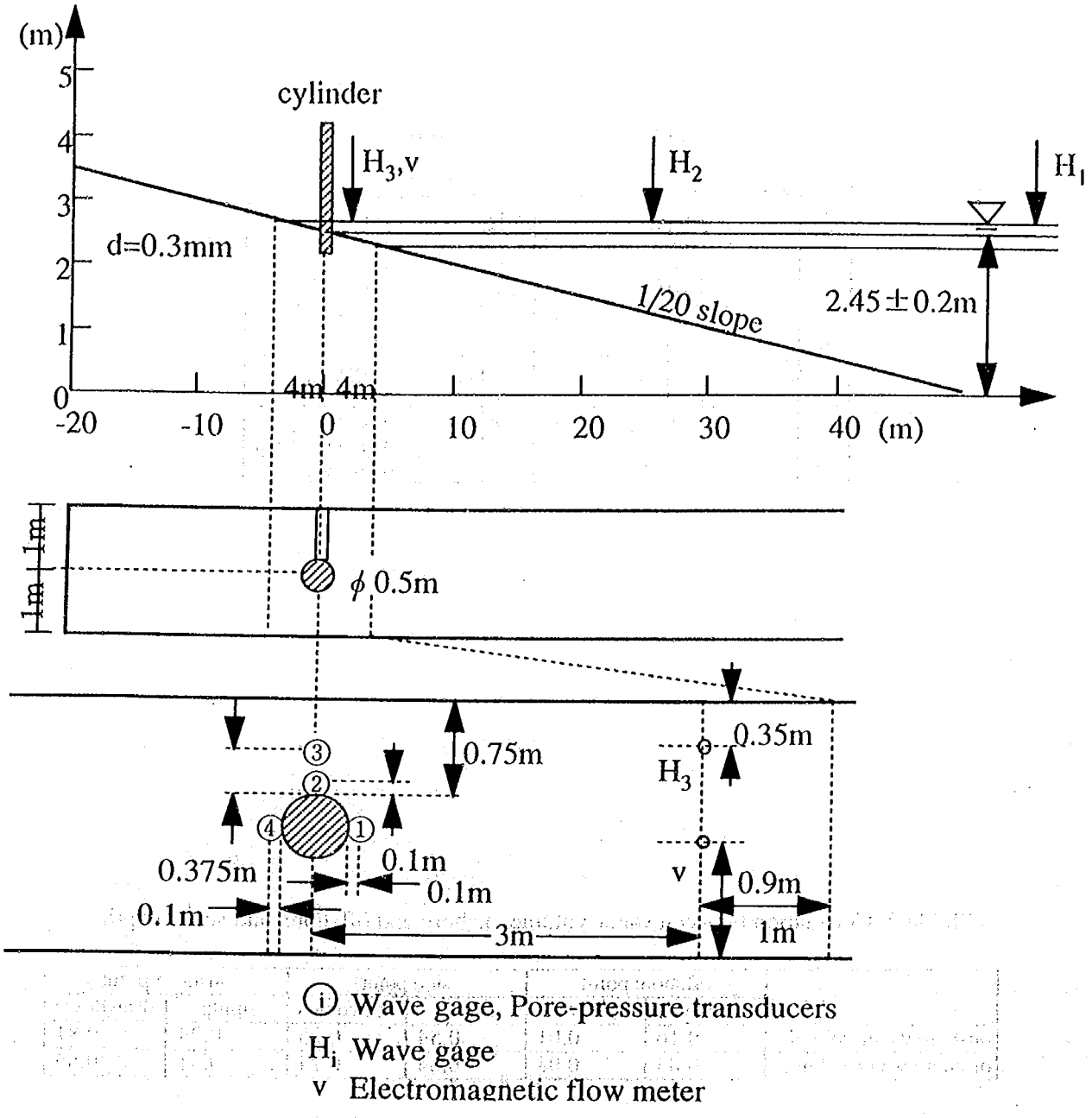


Figure 1 Experiment model

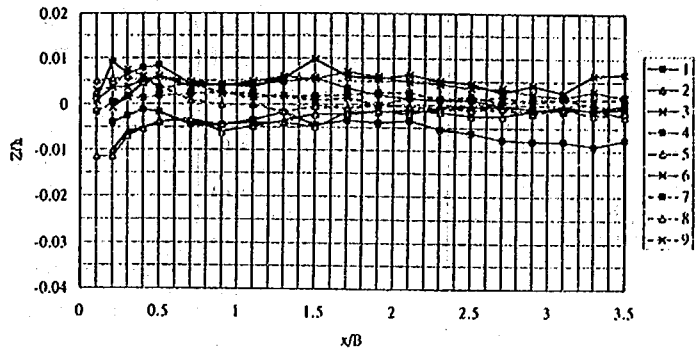


Figure 2 Seabed level variation on the offshore line from the cylinder

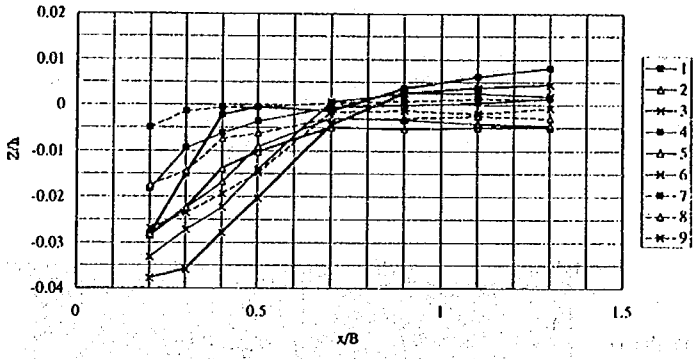


Figure 3 Seabed level variation on the longshore line from the cylinder

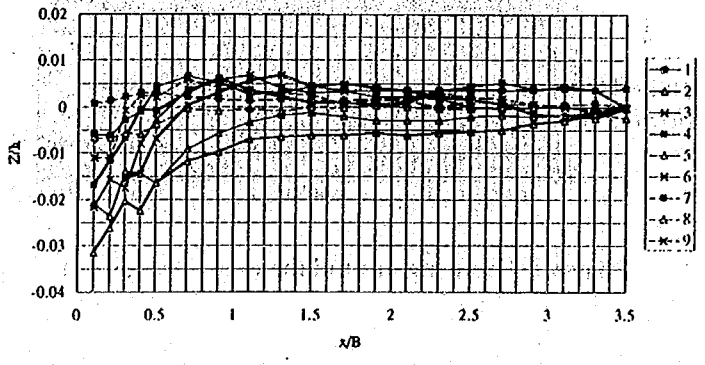


Figure 4 Seabed level variation on the onshore line from the cylinder

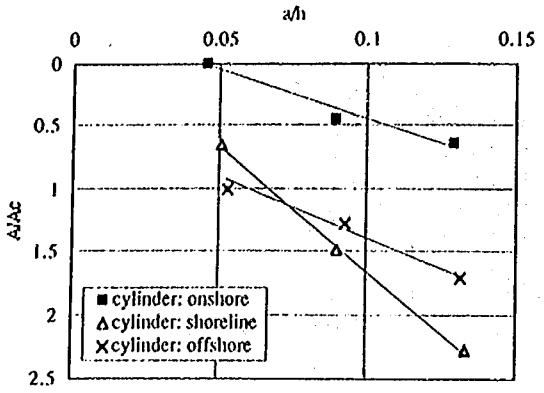


Figure 5 Wave height and scour area

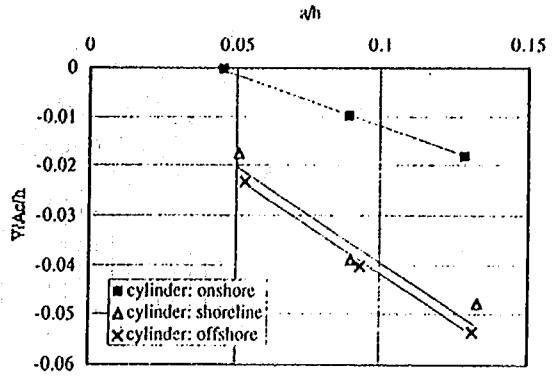


Figure 6 Wave height and scour volume

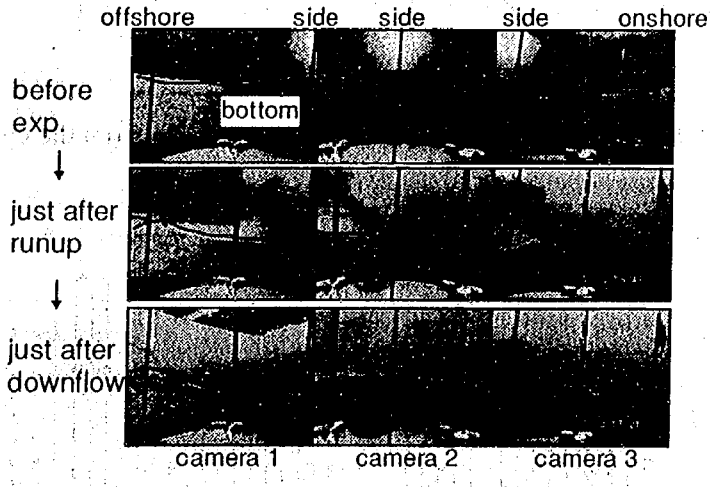


Figure 7 Scouring around the cylinder (case 3)

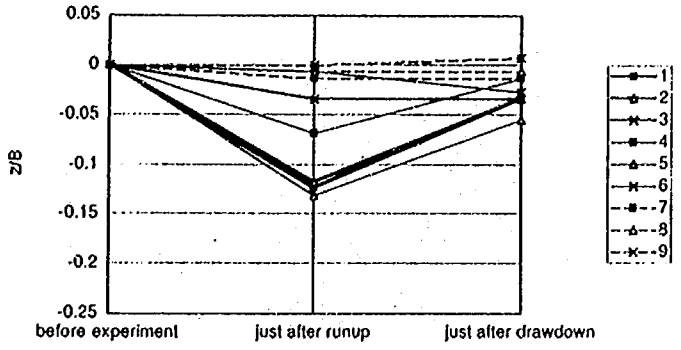


Figure 8 Scour depth at the offshore point

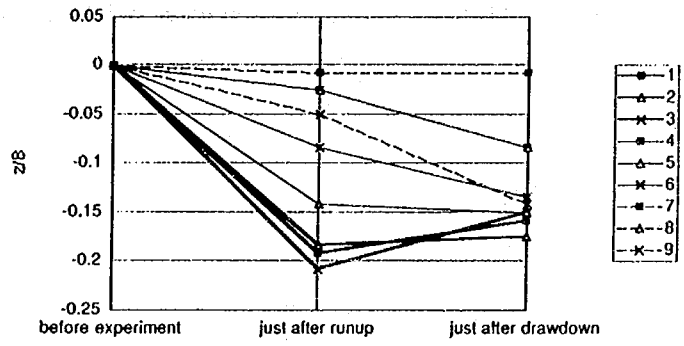


Figure 9 Scour depth at the side point

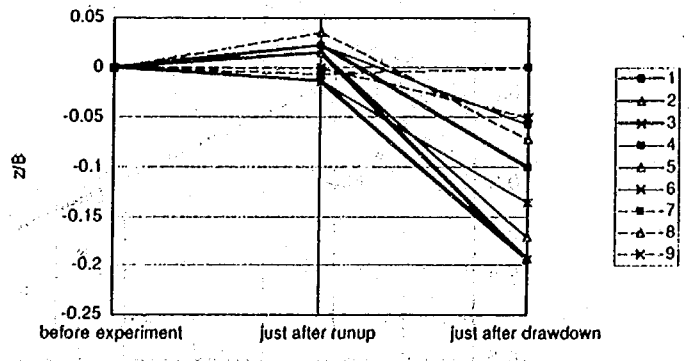


Figure 10 Scour depth at the onshore point

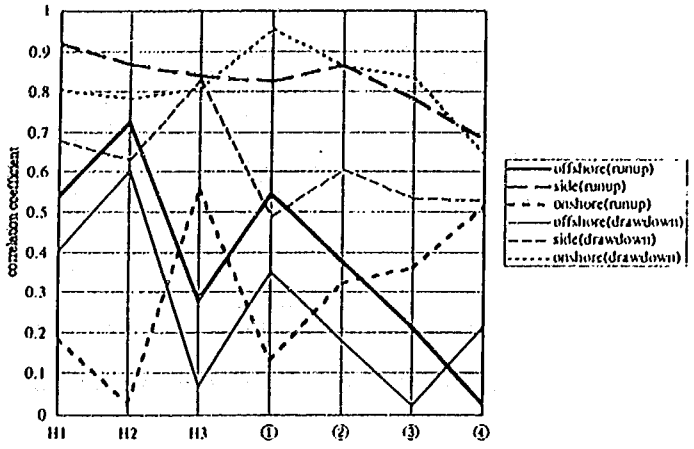


Figure 11 Correlation between wave height and scour depth

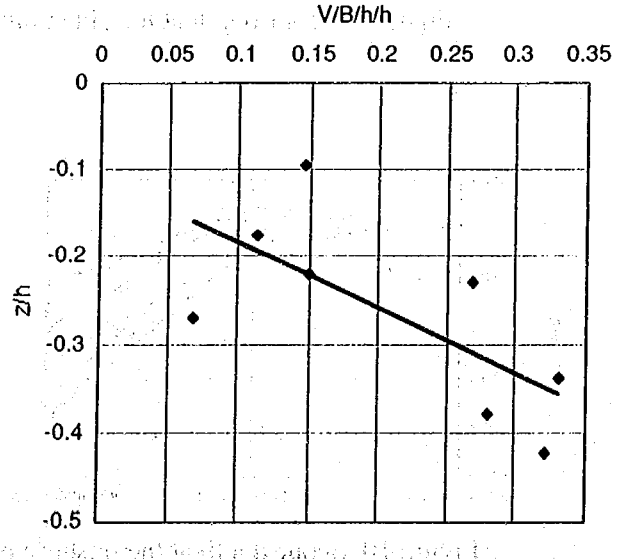


Figure 12 Onshore water volume and scour depth at the onshore point during tsunami drawdown

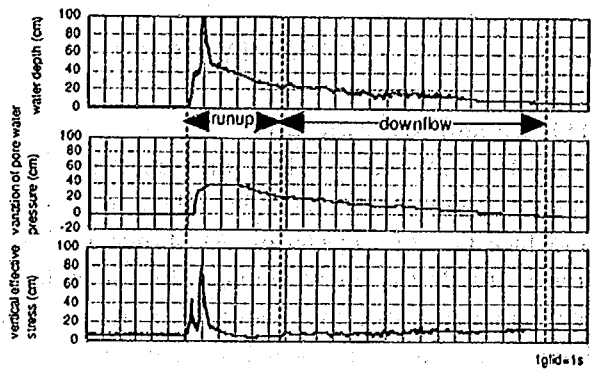


Figure 13 Water depth, pore pressure variation and vertical effective stress at the offshore point (case 2)

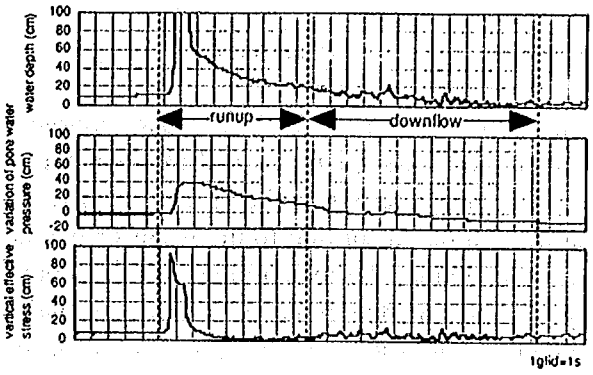


Figure 14 Water depth, pore pressure variation and vertical effective stress at the offshore point (case 3)

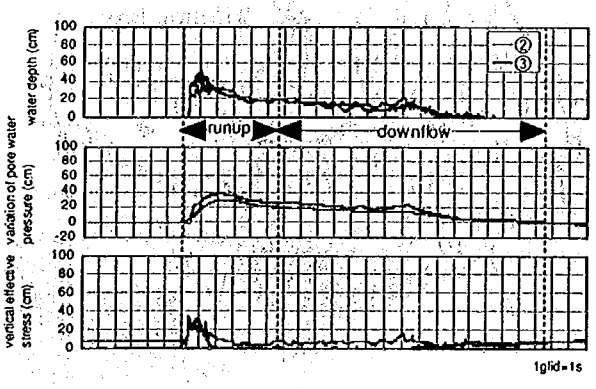


Figure 15 Water depth, pore pressure variation and vertical effective stress at the side point (case 2)

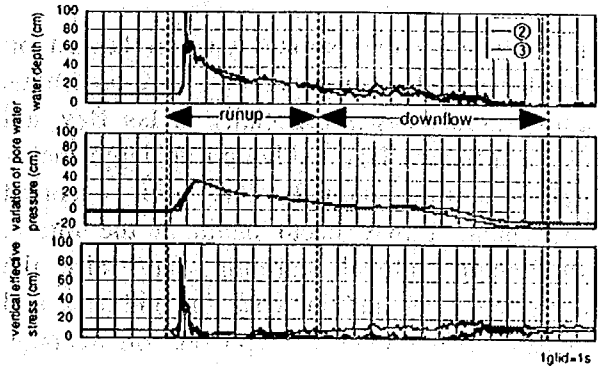


Figure 16 Water depth, pore pressure variation and vertical effective stress at the side point (case 3)

STORM SURGE IN ISE AND MIKAWA BAY CAUSED BY TYPHOON

by

Hiroyasu KAWAI[1)]

ABSTRACT

The typhoon No.15 in 1959 gave enormous storm surge disaster in Ise and Mikawa Bay in Japan. Such a strong typhoon may occur again in the future. According to the result of numerical simulation, the meteorological tide anomaly depends on the route of a typhoon, and is directly proportional to the progression speed, the pressure differential, and the radius. The mean sea level rising due to global warming may reduce the tide anomaly, but the sum of the tide anomaly and the mean sea level rising will become larger.

KEY WORDS: Isewan Typhoon
Mean Sea Level Rising
Meteorological Tide Anomaly

1. INTRODUCTION

In 1959, a terribly strong typhoon landed on the Honshu Island in Japan and gave enormous storm surge disaster especially in Ise Bay and also in Mikawa Bay. Although no large meteorological tide anomaly has been occurred since then, it may occur again in the future. Additionally, global warming may raise the mean sea level and increase the radiuses and pressure differentials of typhoons on average.

In this paper, the storm surge disaster caused by the Isewan Typhoon is introduced briefly, and the meteorological tide anomalies in the imaginary typhoons with various routes, progression speeds, pressure differentials, and radiuses are computed by a numerical model. The effect of the mean sea level rising on the tide anomaly is also discussed.

2. THE ISEWAN TYPHOON

(1) Ise and Mikawa Bay

Both Ise and Mikawa Bay are located at the central region of the Honshu Island in Japan, and face the Pacific Ocean. As shown in **Figure 1**, Ise Bay is approximately 20 km wide at the entrance from the Pacific Ocean, 60 km long to the inner end, and less than 40 m deep at the center. Mikawa Bay is approximately 10 km wide at the entrance from Ise Bay, 30 km long, and less than 20 m deep at the center.

Some sever typhoons go across the Honshu Island every year, and some of them cause large

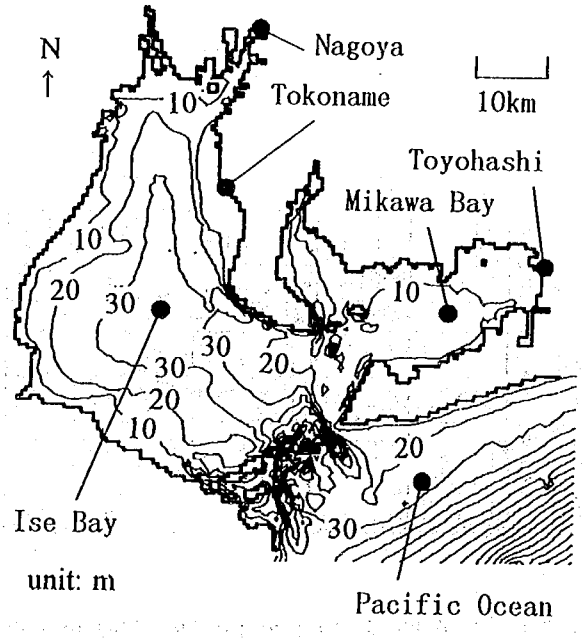


Figure 1 Topography of Ise and Mikawa Bay

1) Senior Research Engineer, Hydraulic Engineering Division, Port and Harbour Research Institute, Ministry of Transport; 3-1-1, Nagase, Yokosuka, 239-0826, Japan

meteorological tide anomaly in the inner parts of these bays. The water depth in these bays is enough shallow to cause conspicuous storm surge easily.

(2) Storm surge disaster by the Isewan Typhoon

The typhoon No.15 landed near Shionomisaki in the Honshu Island in Japan at about 6:20 p.m. on September 26, 1959. The minimum atmospheric pressure was 929.5 hPa.

The typhoon went toward the NNE, passed the west side of Ise Bay, and caused conspicuous storm surge in Ise and Mikawa Bay. At Nagoya, located at the inner end of Ise Bay, the wind speed began to increase in the afternoon, and reached a maximum between 8:00 p.m. and 10:00 p.m. The maximum instantaneous wind velocity was 50.2 m/s. The meteorological tide anomaly of 3.45 m was also recorded there at about 9:35 p.m. The tide anomaly has been the maximum record in Japan so far.

Some coastal dikes especially in Ise Bay and also in Mikawa Bay were collapsed, and subsequently the land areas at the backward were covered with sea water. The inundation increased the damage on humans, structures, and agriculture there. According to official reports, 4,697 people were killed, 401 missing, 38,921 wounded in the typhoon. The death toll has been worst in Japan since then until now. Additionally, approximately 7,600 boats and 834,000 residential building were damaged. The typhoon was named *Isewan Typhoon*, because most damages were focused on the coast of Ise Bay. *Wan* means *bay* in Japanese.

There are several accepted opinions on why the area in Ise Bay was deadly damaged. The first one is that the meteorological tide anomaly caused by the Isewan Typhoon was extremely large. **Figure 2** shows the tide anomalies which were measured in these 43 years (from 1952 to 1994) at the tide station in the Nagoya Port by the Meteorological Agency, Japan. Applying the occurrence probability of the tide anomalies to the type II extreme distribution function, the return period of the tide anomaly due to the Isewan Typhoon becomes approximately 120 years, and the extreme tide anomaly with a return period of 50 years becomes approximately 2.5 m.

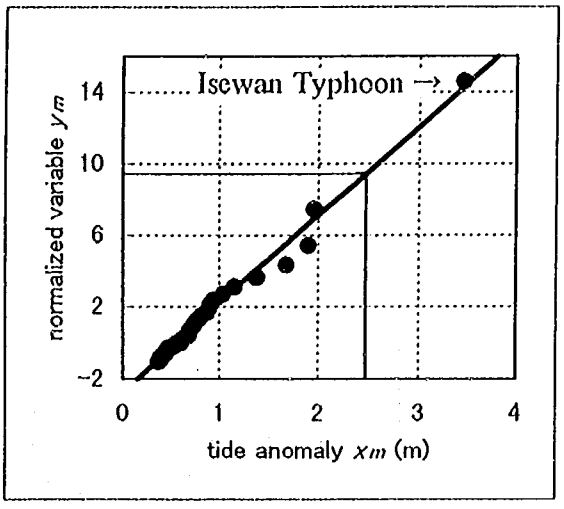


Figure 2 Occurrence distribution of extreme meteorological tide anomalies in Nagoya

The second is that the center of the Isewan Typhoon passed the west side of Ise Bay. In other words, the bay was within the dangerous semicircle of the typhoon. It will be confirmed later in the **chapter 4** by using a numerical model whether the route of the typhoon was worst for Nagoya or not.

The third is that the astronomical tidal level was higher than M.S.L. (mean sea level). The spring tidal range in autumn at Nagoya is approximately 2.3 m, but the tidal range on September 26, 1959 was less than 1.0 m and almost equal to the neap tidal range, as shown in **Figure 3**. When the meteorological tide anomaly became the maximum at around 9:35 p.m., the astronomical tidal level was only 0.2 m above the M.S.L. Assuming that the Isewan Typhoon attacked one week earlier, the high tide level was 1.1 m above the M.S.L. and the

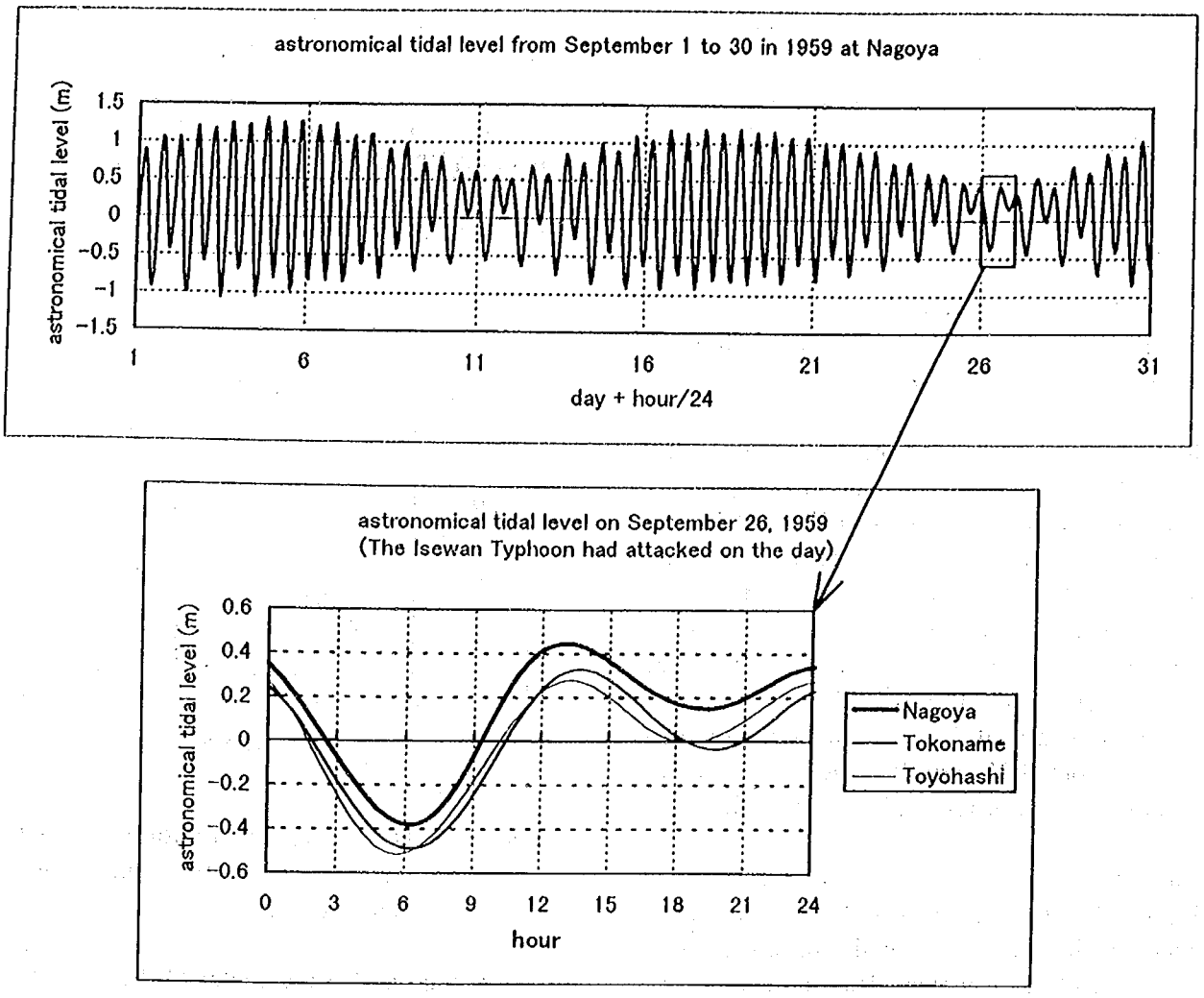


Figure 3 Profile of astronomical tidal level in September, 1959

disaster might become more enormous. The effect of tidal level on storm surge will be discussed later in the **chapter 4**.

The fourth is that much timber carried away from lumberyards in the Nagoya Port might destroy many residential building to kill many houses.

The fifth is that the Isewan Typhoon attacked at night. Electric power supply was shut down by violent winds and enormous floods, and subsequently it became hard to avoid destroyed or flooded houses and find a refuge without street lamps.

(3) Construction of storm surge breakwater

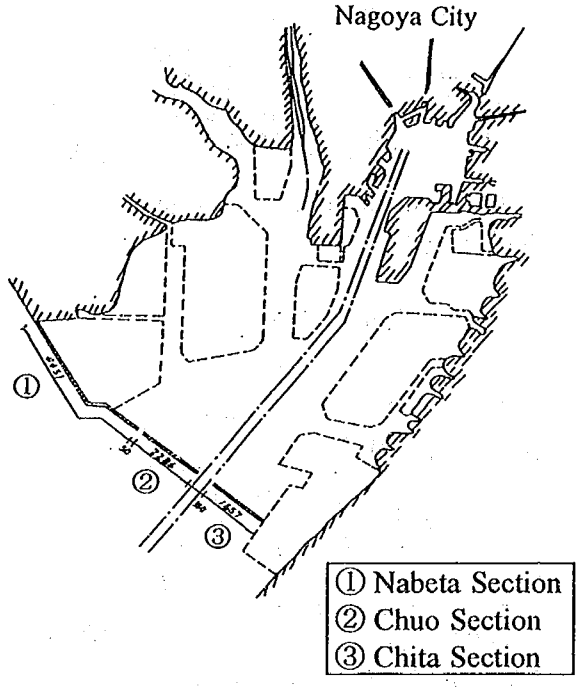
After the Isewan Typhoon had caused the disaster, a storm surge breakwater as shown in **Figure 4** was designed to mitigate the future disaster in the Nagoya Port. The breakwater consists of three sections, namely, the Nabeta Section, the Chuo Section, and the Chita Section. Their design length were 4.450, 2.285, and 1.515 km respectively. The design crest height was decided to be 4.50 m above the H.W.L. in autumn.

The following effects were expected.

(a) Reducing the peak of the meteorological tide anomaly by making the breakwater gap narrow.

(b) Preventing wind waves generated in Ise Bay from entering the Nagoya Port.

By the above two effects, it was expected that the design crest heights of quays and tide barriers at the backward of the storm surge breakwater could be low, and that the construction cost for port facilities also could be reduced totally.



(a) Layout of the storm surge breakwater

The construction of the breakwater had started in January, 1962 and finished in August, 1964. After that, the breakwater gaps had been expanded until 1968 for safe navigation. The lengths of the Nabeta Section, the Chuo Section, and the Chita Sections became 4.126, 2.136, and 1.331 km respectively. **Photo 1** shows the present condition of the breakwater. The breakwater has never damaged heavily until now, and is expected to keep its effects in the future.

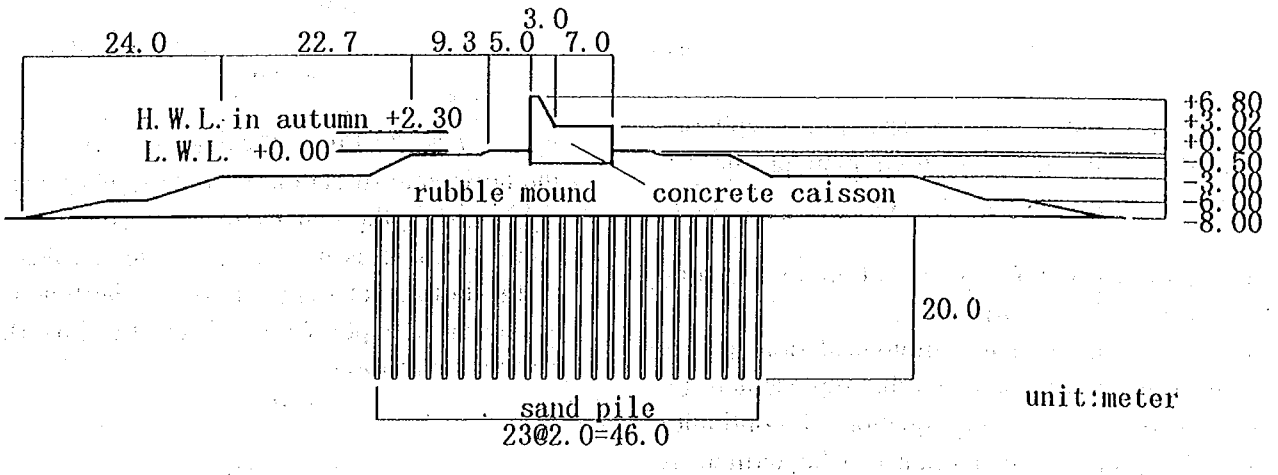
3. NUMERICAL MODEL FOR STORM SURGE

(1) Assumption for winds by typhoon

The distribution of the atmospheric pressure in a typhoon is given by the Myer's formula as follows.

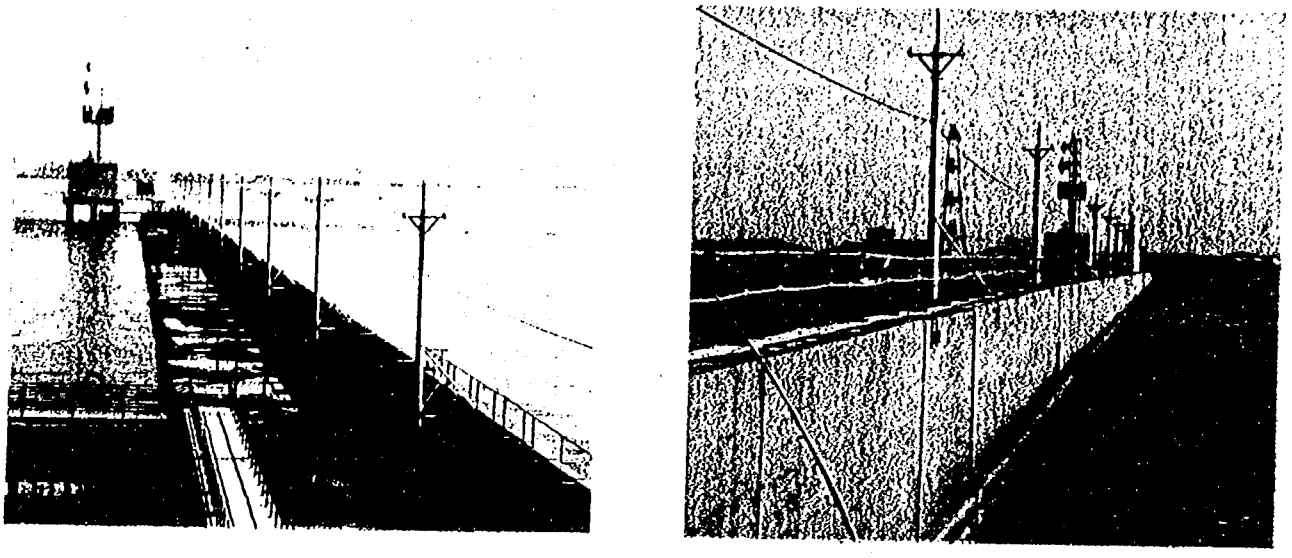
$$P=P_C+\Delta P\cdot\exp\left(-\frac{r_0}{r}\right) \qquad (1)$$

where, P is the atmospheric pressure at the point with a radial distance r from the center of a typhoon, P_c is the atmospheric pressure at the center of a typhoon, ΔP is the pressure differential, and r_0 is the influence radius of a typhoon. Assuming the distribution shown in the above equation, the gradient wind speed U_{gr} is given as follows.



(b) Cross-section of the Chuo Section

Figure 4 Storm surge breakwater at the entrance of the Nagoya Port



(a) Rear of the storm surge breakwater (b) Front of the storm surge breakwater

Photo 1 Present condition of the storm surge breakwater

$$U_{gr}=-\frac{rf}{2}+\sqrt{\left(\frac{rf}{2}\right)^2+\frac{\Delta P}{\rho_a}\frac{r_0}{r}\exp\left(-\frac{r_0}{r}\right)} \quad (2)$$

where, f is the Coriolis coefficient, ρ_a is the density of atmosphere. The wind speed is actually reduced by the friction along sea surface. The actual wind speed, namely marine wind speed, U_1 can be assumed as follows.

$$U_1=C_1U_{gr} \quad (3)$$

where, C_1 is the parameter assumed to be 0.66 in this paper.

The movement of a typhoon also generates the winds of which speed U_2 is given as follows.

$$U_2=\frac{U_1(r)}{U_1(r_0)}V \quad (4)$$

where, V is the progression speed of a typhoon. The directions of the wind component and the typhoon progression are identical.

(2) Assumption for propagation of meteorological tidal waves

The propagation of meteorological tidal waves caused by a typhoon can be represented by long wave theory. The equation of continuity and the equations of motion can be written as follows.

$$\frac{\partial \eta}{\partial t}+\frac{\partial M}{\partial x}+\frac{\partial N}{\partial y}=0 \quad (5)$$

$$\frac{\partial M}{\partial t}+\frac{\partial}{\partial x}\left(\frac{M^2}{D}\right)+\frac{\partial}{\partial y}\left(\frac{MN}{D}\right)$$
$$=+fN-gD\frac{\partial \eta}{\partial x}-\frac{D}{\rho_W}\frac{\partial p_0}{\partial x} \quad (6a)$$
$$+\frac{1}{\rho_W}(\tau_{sx}-\tau_{bx})+A_h\left(\frac{\partial^2 M}{\partial x^2}+\frac{\partial^2 M}{\partial y^2}\right)$$

$$\frac{\partial N}{\partial t}+\frac{\partial}{\partial x}\left(\frac{MN}{D}\right)+\frac{\partial}{\partial y}\left(\frac{N^2}{D}\right)$$
$$=-fM-gD\frac{\partial \eta}{\partial y}-\frac{D}{\rho_W}\frac{\partial p_0}{\partial y} \quad (6b)$$
$$+\frac{1}{\rho_W}(\tau_{sy}-\tau_{by})+A_h\left(\frac{\partial^2 N}{\partial x^2}+\frac{\partial^2 N}{\partial y^2}\right)$$

where, t is the time, x and y axes are taken in the horizontal direction, g is the gravity acceleration, ρ_W is the density of sea water, p_0 is the atmospheric pressure on the water surface, A_h is the horizontal eddy viscosity coefficient, D is the water depth, M and N are the flux flows defined as follows.

$$D=h+\eta \quad (7)$$

$$M=\int_{-h}^{\eta} u\,dz \quad (8a)$$

$$N=\int_{-h}^{\eta} v dz \qquad (8b)$$

where, z axis is taken in the vertical direction, and $z=-h$ at the sea bottom, $z=\eta$ at the water surface. u and v are the components of the velocities in the directions of the x and y axes respectively. Additionally, τ_{sx} and τ_{sy} are the tangential stress along the water surface, and τ_{bx} and τ_{by} are the tangential stress along the sea bottom in the directions of the x and y axes respectively shown as follows.

$$\tau_{sx}=\rho_a C_D W_x \sqrt{W_x^2+W_y^2} \qquad (9a)$$

$$\tau_{sy}=\rho_a C_D W_y \sqrt{W_x^2+W_y^2} \qquad (9b)$$

$$\tau_{bx}=\frac{\rho_w g n^2}{D^{7/3}} M \sqrt{M^2+N^2} \qquad (10a)$$

$$\tau_{by}=\frac{\rho_w g n^2}{D^{7/3}} N \sqrt{M^2+N^2} \qquad (10b)$$

where, C_D is the resistance coefficient along the sea surface, W_x and W_y are the wind velocities at 10 meters above the sea surface, n is the Manning's roughness parameter.

(3) Difference method and grid mesh

In this paper, the governmental equations are solved by a difference method with a stacked grid mesh for space successive steps and the leap-frog method for time successive steps.

The five regions shown in **Table 1** are combined with each other. The first region includes a part of the Pacific Ocean around the Japan Islands, and the fifth region includes Ise and Mikawa Bay. The meteorological tidal waves is reproduced during 24 hours, namely from 3:00 a.m. on September 26, 1959 to 3:00 a.m. on the next day. The time interval between successive steps is 0.5 s.

Table 1 Grid Mesh

region	number of grid points	space interval
I	58 × 56	32.4 km
II	78 × 44	16.2 km
III	63 × 49	5.4 km
IV	81 × 78	1.8 km
V	135 × 135	0.6 km

4. EFFECT OF VARIOUS FACTORS ON STORM SURGE

(1) Storm surge by Isewan Typhoon

Figures 5 and 6 show the profile of the atmospheric pressure, wind speed, wind direction, and meteorological tide anomaly, which are computed by the numerical model shown in the chapter 3. Nagoya and Tokoname are located in the inner part of Ise Bay, and Toyohashi in Mikawa Bay, as shown in Figure 1.

While the typhoon was approaching the Honshu Island, the wind direction was E and the wind speed was increasing to 20 m/s as shown in Figures 5(b) and 5(c). The meteorological tide anomaly along the west coast of Ise Bay became more than 0.5 m at 5:00 p.m. as shown in Figure 6(a).

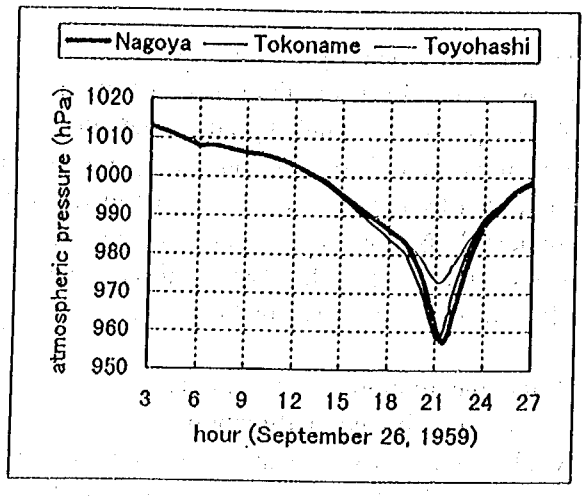
After the typhoon had landed on the Honshu Island at about 6:20 p.m., the wind direction changed into SE, the wind speed continued to increase, and the meteorological tide anomaly began to increase rapidly, as shown in Figure 5 (d). The meteorological tide anomaly especially along the northwest coast became large at 8:00 p.m. as shown in Figure 6(b). The wind direction changed quickly into SW, and the meteorological tide anomaly at the inner area of Ise and Mikawa Bay became more than 3 m at 10:00 p.m. as shown in Figure 6(c).

The atmospheric pressure reproduced by the numerical model reaches 957 hPa (958.5 hPa was recorded by the observation), the wind speed 37 m/s (37 m/s), and the tide anomaly 3.46 m (3.45 m) at Nagoya. The results of the numerical model and the observation get agree each other.

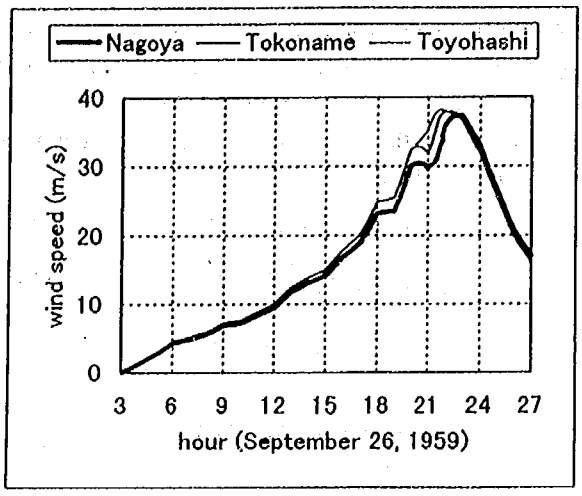
Figure 7 shows the distribution of the maxi-

mum meteorological tide anomaly at each place in Ise Bay and Mikawa Bay in the Isewan Typhoon. The maximum tide anomaly is larger than 1.5 m in all the area of Ise and Mikawa Bay, and larger than 3 m in the inner areas of these bays.

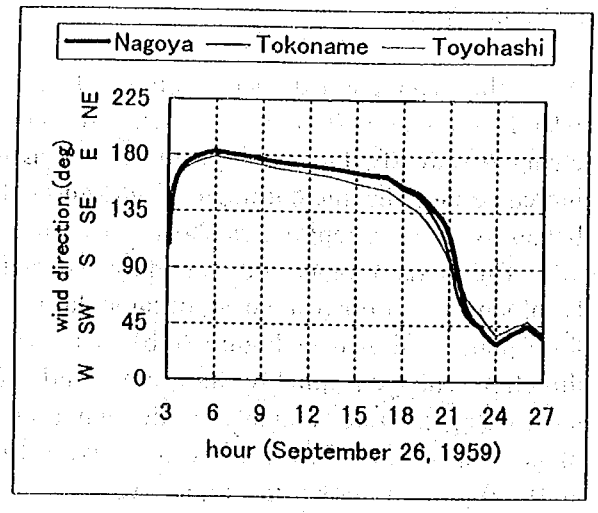
Immediately after the typhoon had passed, the meteorological tide anomaly became negative as shown in Figure 6 (d).



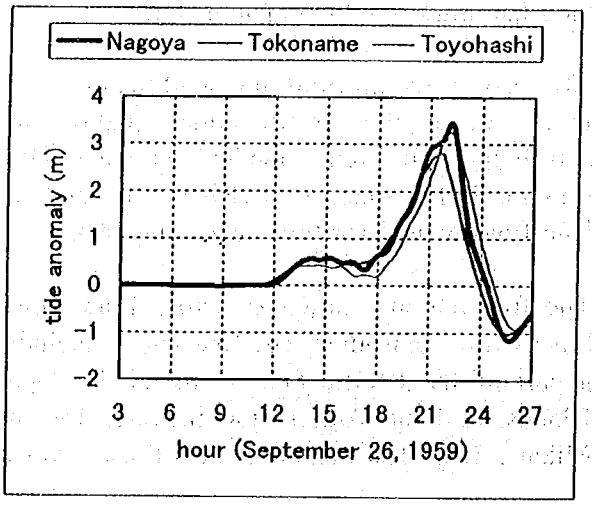
(a) Atmospheric pressure



(b) Wind speed

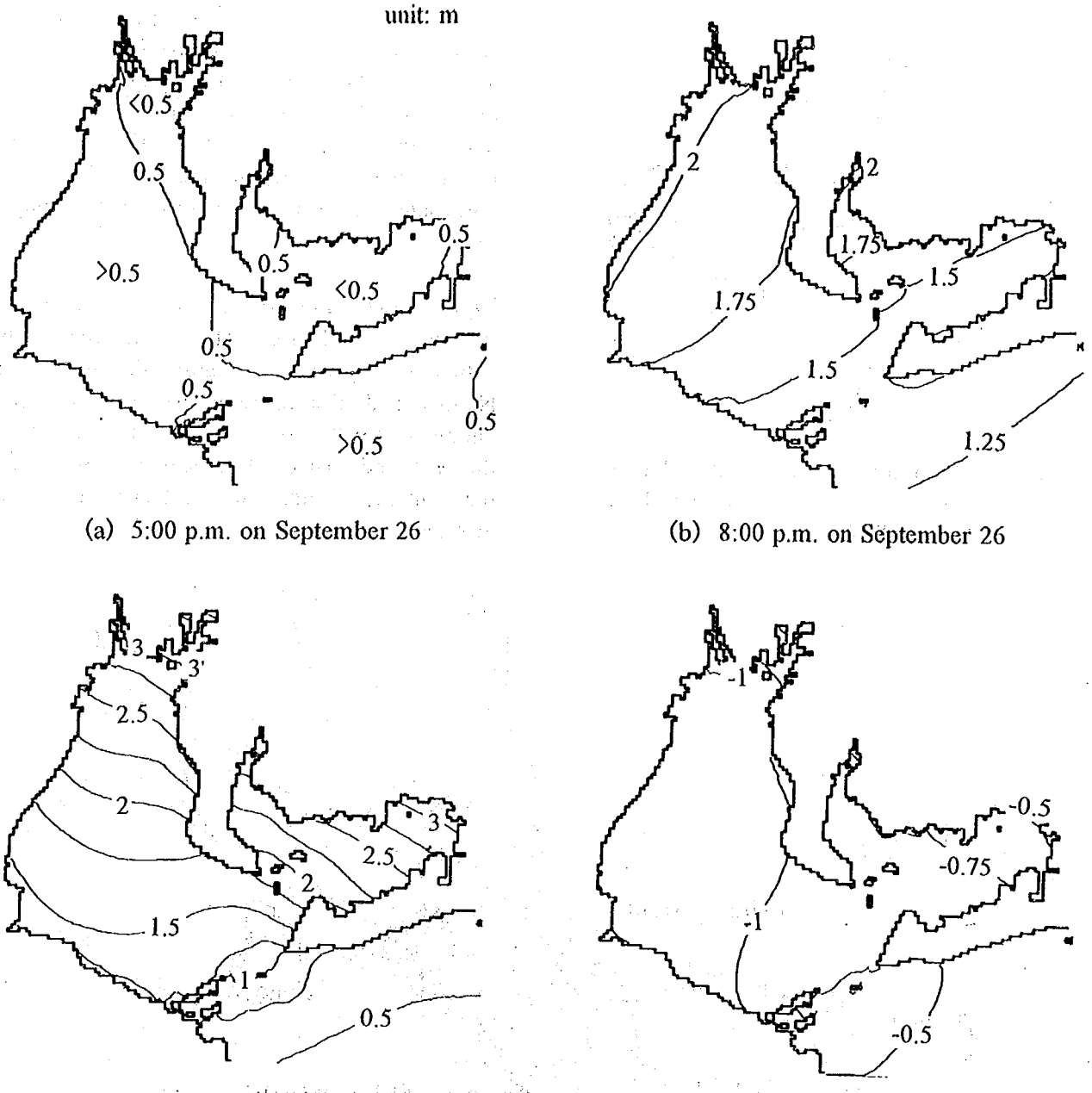


(c) Wind direction



(d) Meteorological tide anomaly

Figure 5 Profile of storm surge in the Isewan Typhoon



(a) 5:00 p.m. on September 26

(b) 8:00 p.m. on September 26

(c) 10:00 p.m. on September 26

(d) 1:00 a.m. on September 27

Figure 6 Meteorological tide anomaly in the Isewan Typhoon

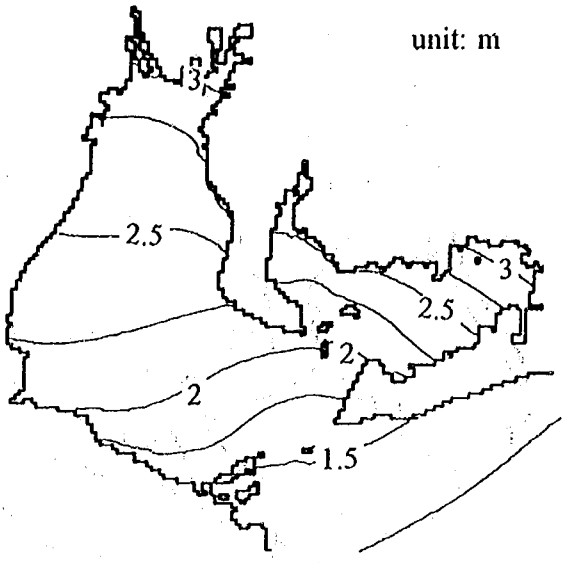


Figure 7 Distribution of Maximum Meteorological Tide Anomaly caused by the Isewan Typhoon

(2) Route of typhoon

According to an accepted opinion, the route of the Isewan Typhoon was most dangerous for the coast of Ise Bay. In this paper, the typical typhoon routes shown in **Figure 8** are assumed to estimate the effect of the typhoon route on the meteorological tide anomaly. All the imaginary routes W2, W1, and E1 to E4 are parallel to the actual route A, and the interval between one route and the next is 0.25 degree in longitude.

Figure 9 (a) shows the maximum meteorological tide anomaly for each typhoon route. The actual route gives the largest tide anomaly at Nagoya and Tokoname in Ise Bay. The tide anomalies for the routes W1 and E1, namely to the west and east by 0.25 degree from the actual route, are almost same as that for the actual route.

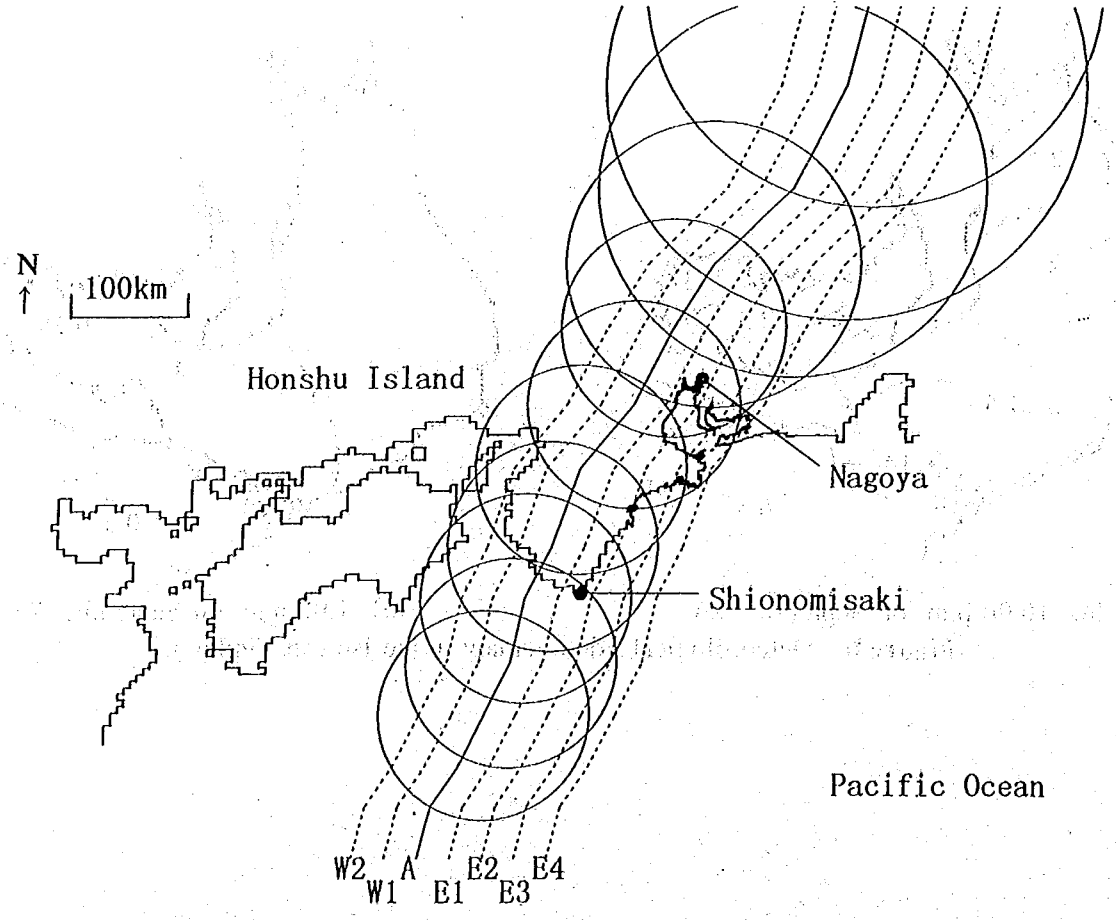


Figure 8 Typhoon routes simulated in this paper

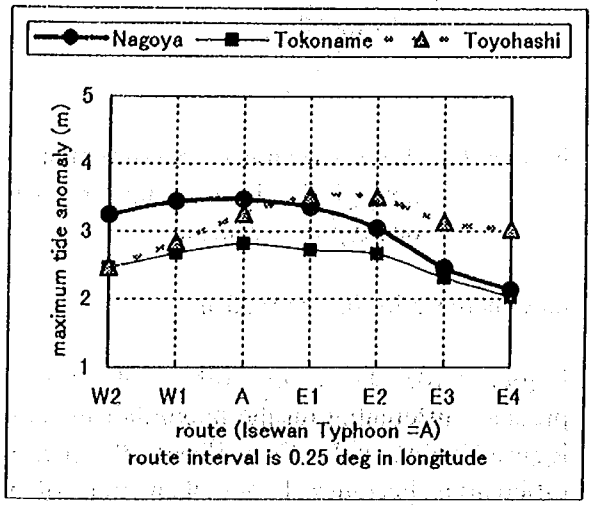
On the other hand, the routes E1 and E2, namely to the east by 0.25 and 0.5 degree from the actual route respectively, become most dangerous at Toyohashi in Mikawa Bay. The route E2 is most similar to the actual route of the typhoon No.13 in 1953, which gave more enormous disaster in Mikawa Bay than the Isewan Typhoon.

Figure 10 shows the most dangerous typhoon route at each place in Ise and Mikawa Bay, and **Figure 11** the largest value of the maximum meteorological tide anomalies for various imaginary typhoon routes.

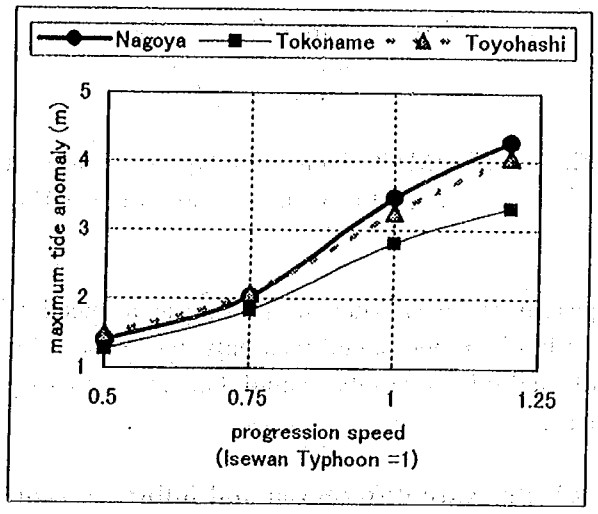
(3) Progression speed of typhoon

There are two components in winds caused by a typhoon. One is marine winds of which speed was shown in **equation (3)**, and the other is the effect of the movement of a typhoon shown in **equation (4)**.

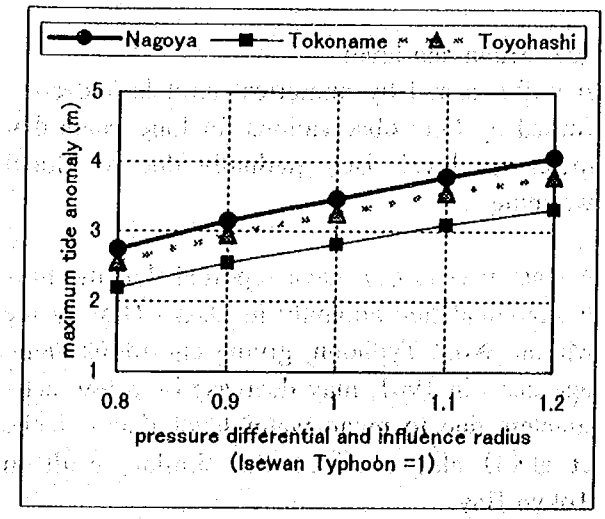
Figure 9 (b) shows the meteorological tide anomalies for various typhoon speeds. The tide anomaly is directly proportional to the progression speed of a typhoon. The Isewan Typhoon



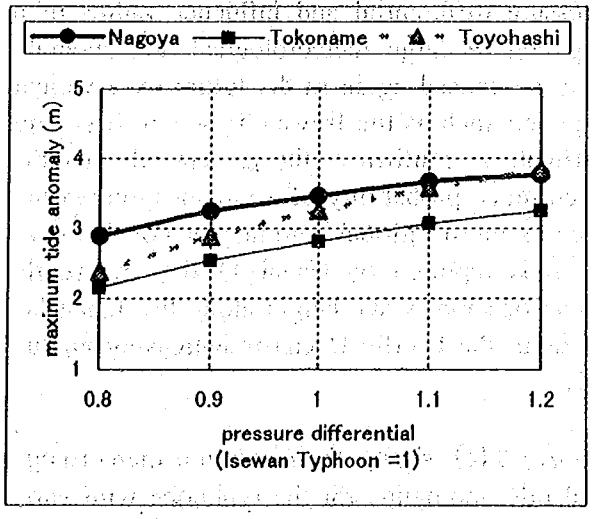
(a) Progression route of typhoon



(b) Progression speed of typhoon



(c) Pressure differential and radius of typhoon



(d) Influence radius of typhoon

Figure 9 Maximum meteorological tide anomalies in various typhoon conditions

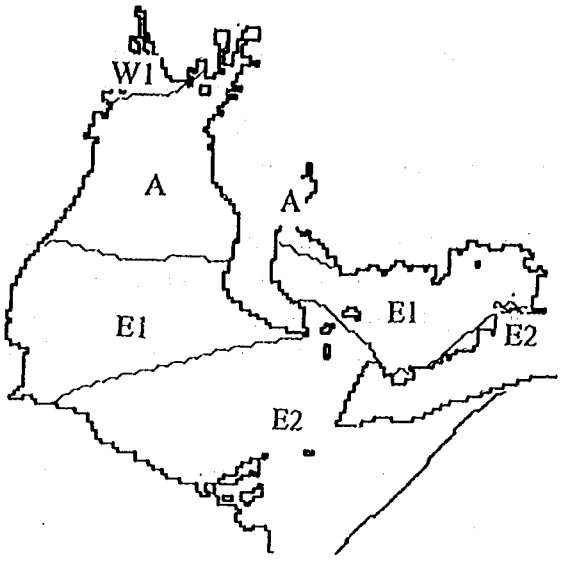


Figure 10 Most dangerous typhoon route at each place in Ise and Mikawa Bay

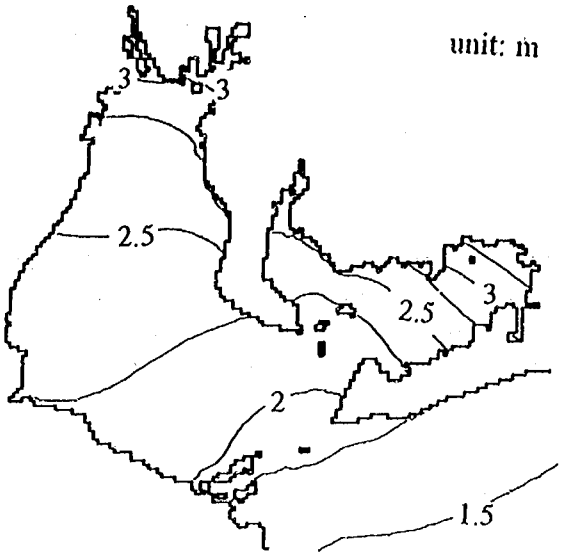


Figure 11 Largest value of maximum meteorological tide anomalies for various typhoon routes

passed the west side of Ise Bay at a speed of 70 km/h. If the speed was half, the peak value of the tide anomaly would become less than half.

(4) Pressure differential and influence radius of typhoon

The speed of marine winds depends on the pressure differential and influence radius of a typhoon. A large meteorological tide anomaly may be caused again in the future by a violent typhoon such as the Isewan Typhoon. It is very difficult to confirm at the present whether the occurrence probability of a violent typhoon increases due to global warming or not. However, it is reported by Nagai (1) that the yearly mean offshore wave height along the Japan Islands in the Pacific Ocean is increasing gradually.

Figure 9 (c) shows the maximum meteorological tide anomalies for the typhoons with various pressure differentials and influence radiuses. If both the pressure differential and the influence radius becomes larger than those of the Isewan Typhoon by 10%, the tide anomaly may increase by 0.2 ~ 0.35 m.

Figure 9 (d) shows the effect of only the pressure differential on the maximum meteorological tide anomaly. Even if only the pressure differential becomes larger than that of the Isewan Typhoon by 10%, the tide anomaly becomes larger by around 0.3 m.

(5) Mean sea level

It is forecasted by numerical models and confirmed by field observations for long years that mean sea level rises gradually due to global warming.

Nakatsuji et al. (2) have reported that the meteorological tide anomaly in Osaka Bay by the Muroto No.2 Typhoon, giving enormous damage there in 1961, may decrease by a few centimeters due to mean water level rising. Isobe et al. (3) also obtained the similar result in Tokyo Bay.

Figure 12 shows the maximum meteorological tide anomalies for various sea levels. The sea level becomes higher by 1 meter, the tide ano-

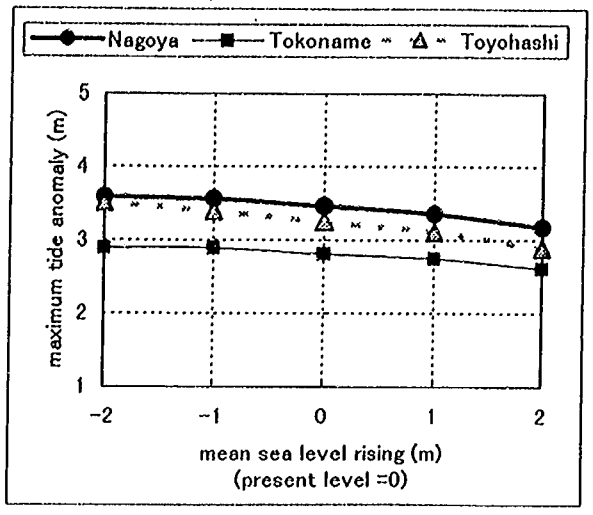


Figure 12 Maximum Meteorological Tide Anomaly for Various Sea Level

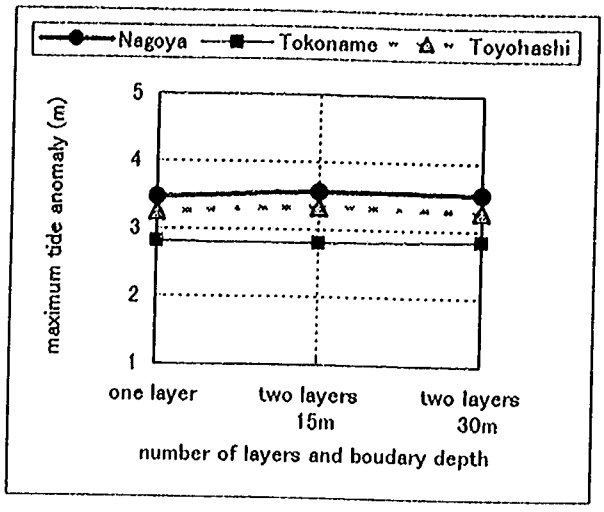


Figure 13 Comparison with the Meteorologicl Tide Anomaly by Two Layer Model

maly becomes smaller by only around 0.1 m. It means that the total tidal level becomes higher by 0.9 m under the mean sea level rising of 1.0 m.

(6) Number of layers in numerical model

The meteorological tide anomaly shown in the **paragraphs (1)** to **(5)** are obtained by one layer model. **Figure 13** shows the comparison with the tide anomaly by two layer model. The water depth at the boundary between the upper layer and the lower is assumed to be 15 and 30 m. The difference of the maximum meteorological tide amonalies among them is quite small, therefore one layer model has enough accuracy for the estimation of the meteorological tide anomaly in Ise and Mikawa Bay.

5. CONCLUSION

The meteorological tide anomaly depends on the route, progression speed, pressure differential, and influence radius of a typhoon. It is confirmed that the route of the Isewan Typhoon was most dangerous for the coast of Ise Bay. On the other hand, the mean sea level rising due to global warming in the future seems to give few effect on the meteorological tide anomaly.

We are in the 40th year after the enormous disaster caused by the Isewan Typhoon. Fortunately we have had no terrible typhoon since then. However it is possible to appear again. The mean sea level rising will reduce the crest heights of port facilities and coastal dikes. Therefore, it is necessary to recall the memory of the disaster, and confirm the safety degree of port facilities, coastal dikes, and residential areas at their backward.

REFERENCES

1. Nagai,T.: Study on Japanese coastal wave characteristics obtained from the NOWPHAS wave observation network, Technical Note of the Port and Harbour Research Institute, No.863, 113p., 1997.
2. Nakatsuji, K., K. Muraoka, H. Kurita, and N. Yamane: Numerical study of green house effects on storm surge in Osaka Bay, Japan, Proceeding of 1st Symposium on Earth En-

vironment, Japan Society of Civil Engineers, pp.209-215, 1993.
3. Isobe, M., H. Mishima, and J. Tsutsui: Prediction of flood due to storm surge under sea level rise in coastal area of Tokyo Bay, Proceeding of 2nd Symposium on Earh Environment, Japan Society of Civil Engineers, pp.168-173, 1994.

Theme 4
Seismic Information Systems

SEISMIC INFORMATION SYSTEM FOR NATIONAL LAND MANAGEMENT

by

SUGITA Hideki[1], NOZAKI Tomofumi[2]

ABSTRACT

This paper introduces the basic concept of National Land Management that is advocated by Ministry of Construction in Japan recently. By especially concentrating on the relation between the earthquake disaster prevention and the National Land Management concept, the function and the promising technologies of the seismic information system is explained. The technologies include the advanced ones such as the high-resolution image from the artificial satellites and GIS. Besides those hardware/ software technologies, the importance of the system architecture for data sharing is considered. Those topics for SIS are being organized as a manual by PWRI, whose structure is also explained.

KEY WORDS: Seismic Information System
Earthquake Disaster Prevention
Information Sharing

1. INTRODUCTION

To secure the energetic activities and to achieve the safety of the country, construction of civil infrastructures has been enforced in Japan. However, considering the recent circumstances such as change of natural environment and the experiences of severe natural disasters, only constructing facilities is not sufficient. To cope with those wide area problems or emergency situations, management for national land including observation and planning as well as construction is necessary. This concept is proposed as "National Land Management" (NLM) by Ministry of Construction (MOC).

As it concerns many advanced technologies, MOC has launched the new four-year project: "Development of Advanced Technologies for National Land Management" since fiscal year of 1999 as one of the Comprehensive Research Development Projects. One of its main sub projects is the risk management information system by utilizing the recent advanced technologies including the remote sensing from the artificial satellites and GIS.

However, there is not the completely united view or concept for NLM yet. Thus, first this paper shows one of the understandings of NLM from the viewpoint of earthquake disaster prevention. Second, it concentrates on the seismic information system (SIS) that realizes NLM-based earthquake disaster prevention, and lastly, state-of-the-art of the technologies which can be applied for SIS.

2. NATIONAL LAND MANAGEMENT AND EARTHQUAKE DISASTER PREVENTION

In this paper, NLM is defined as the combined tasks to cope with the missions to secure and improve the efficiency and the safety of the

1) Head, Earthquake Disaster Prevention Technology Division, Earthquake Disaster Prevention Research Center, Public Works Research Institute, Ministry of Construction, Tsukuba, Ibaraki 305-0804, Japan
2) Senior Research Engineer, ditto

people's life, where the various measures are utilized as well as the construction measures. General understanding of NLM is shown on Fig. 2.1.

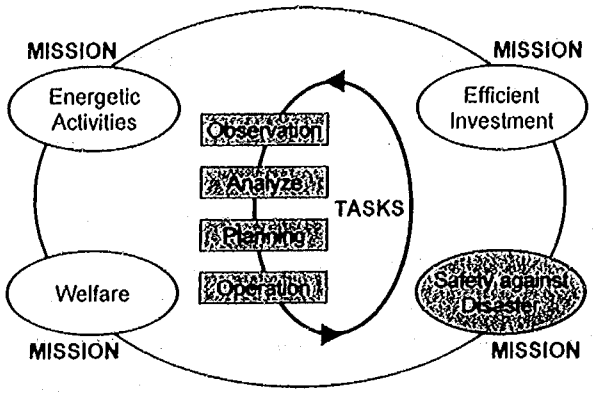


Fig. 2.1 General understanding of NLM

To cope with the missions, usually the four tasks are executed. Those tasks, observation, analyze, planning and operation are common to the activities of people and organization.

Disaster prevention is one of the important missions of NLM. There are two distinct management methods for the disaster prevention as shown on Fig. 2.2.

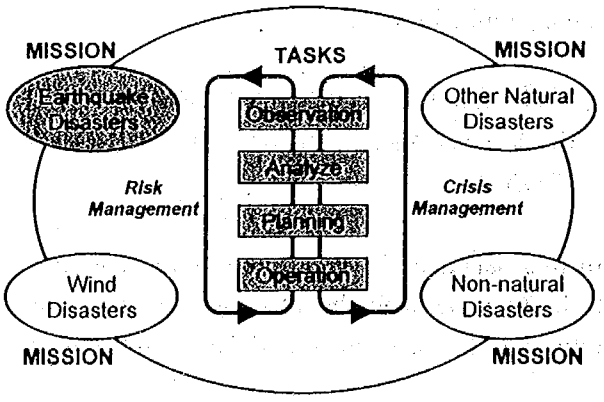


Fig. 2.2 Disaster prevention for NLM

One is the risk management where the risk means the expected loss or damage with uncertainty or chance of occurrence. Therefore, the risk management aims to minimize the expected risk based on the uncertain or probabilistic information before the disaster. The other is the crisis management where the crisis means the emergency situation after the occurrence of the disaster. Therefore the crisis management aim to localize and minimize the negative effects of the disaster once it occurs.

The earthquake disaster prevention is particular because of several characteristics: e.g., extremely small chance of occurrence and large amount of damage once it occurs, and demand for especially quick response immediately after the earthquake. In other words, the earthquake disaster prevention can be said that it deals with the very much specific aspect of NLM.

To cope with the difficulties of the earthquake disaster prevention, several methods are required to accomplish the four tasks of NLM.

- wide-area monitoring to acquire the overall information both before and after the earthquake
- data collection to acquire data at limited sites for detailed information of phenomena and state of facilities before/ after the earthquake
- analyze to aggregate, filter and overlay the data to extract the useful information for the planning and the response
- decision making support to provide information for choosing alternatives of planning and operation through more complicated execution than analyze

In reality, the methods above are executed by the personnel and the information system that organize the earthquake response system to cope with the earthquake disaster. The seismic information system (SIS) is expected to improve the speed/ efficiency of the earthquake resistant actions[1)2)](Fig. 2.3).

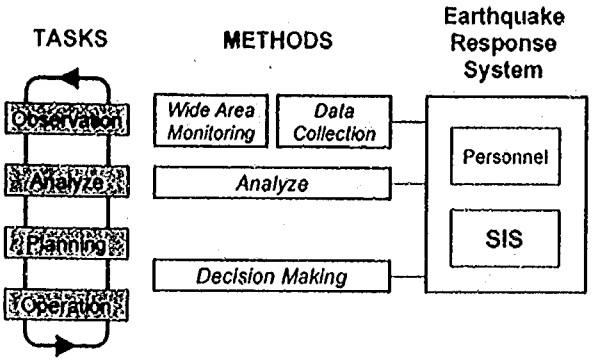


Fig. 2.3 Earthquake disaster prevention for NLM

The examples of the technologies regarding SIS are, the high resolution image data from artificial satellites, Global Positioning System (GPS) and Geographical Information System (GIS). Also, hi-performance personal computers (PCs) and network technologies are the key technologies. The state-of-the-art of those technologies are introduced in the sections from 3 to 6. Besides those element technologies, the system architecture especially concerning to data sharing is important to SIS, and is explained in section 7. From the viewpoint of the extensibility and efficient information sharing, Public Works Research Institute (PWRI) is preparing the draft construction manual of SIS, which is briefly introduced in section 8.

3. MONITORING TECHNOLOGY FOR WIDE AREA

Monitoring the state and the phenomena of the national land is the fundamental of NLM (Fig. 3.1), and it is also useful for SIS. Objectives of the wide area monitoring (WAM) are listed as follows.

- risk survey : detecting active fault, assessing landslide risks, monitoring crustal deformation, investigating risk factors such as accumulation of population and properties

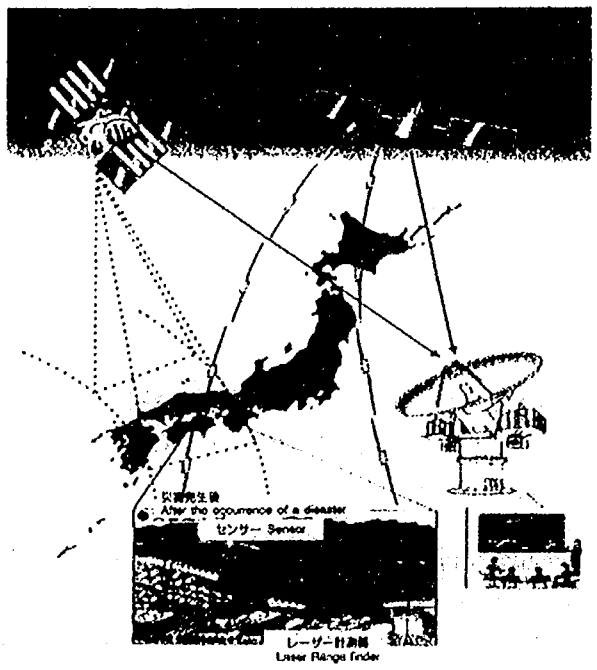


Fig. 3.1 Technologies for wide area monitoring and data collection

- event detection : detection of earthquake occurrence and direct/ indirect damage caused by earthquake
- damage state survey : surveying distribution of fire, facilities' damage and other disasters caused by earthquake

They are characterized by facts that the information comes from wide spread area and that it must be treated in extremely short time. Several advanced technologies can be applied to realize the objectives above.

(1) Artificial Satellites

As data from artificial satellites provides information of wide area from very high altitude, it fits to the wide area monitoring objective. Usually the data is provided as the images of surface that represents the surface topography or vegetation and the underground formation and so on. The satellite remote sensing is characterized by the orbit of the platform and the type of the sensor (Fig. 3.2).

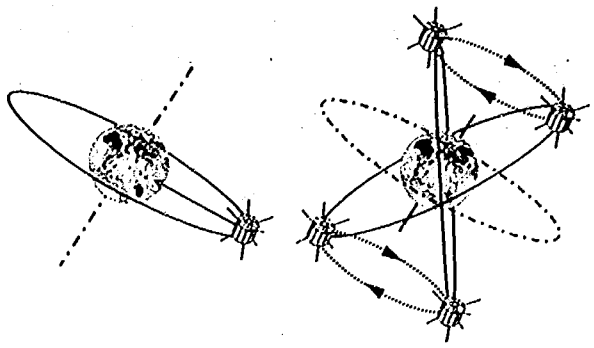


Fig. 3.2 Types of satellite orbits: geo-stationary orbit and sub-recurrent orbit

Because the height of the geostationary orbit is approximately 36,000 km, the resolution of the surface image cannot be much improved. For the monitoring satellites the sub-recurrent orbit with smaller height on which the satellite returns to the same position at several days interval is usually chosen.

The another characteristic is the types of the sensor equipped on the platform. The high-resolution images of the multi band sensors provide various kinds of information such as distribution of the temperature and the lineament as a clue to the active fault. The Synthetic Aperture Radar (SAR) can give the surface topography including the detailed shape of facilities.

The satellite data can be used following objectives.

- risk survey : detecting active fault by checking the lineament, surveying landslide risk based on the multi band images
- damage state survey : to detect and to survey the facilities' damage, liquefaction and landslides, fire and the secondary induced state such as traffic congestion.

Fig. 3.3 indicates the images of the same site

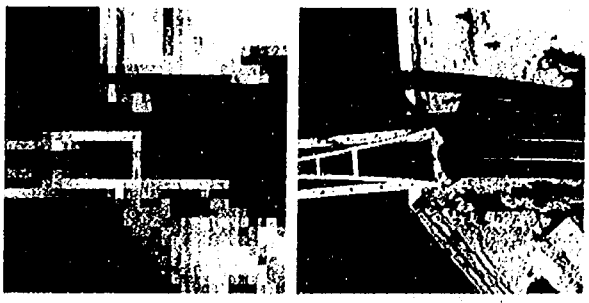


Fig. 3.3 Images: resolution 10m/ 1m

with different resolutions. Even the shape of large structure such as a bridge is hardly recognized for the resolution of 10m. On the other hand, from the high resolution image one can distinguish objects and phenomena as follows.

- structural damage in horizontal structural damage
- grand failure in horizontal direction such as ground flow and land slide
- signs of possible damages or failure in vertical direction

As the satellites with sub-recurrent orbit have their recurrent time, it may take several hours or days for them to take the image of the desired point. One must take the time for the image transaction, database control and the file transfer into account when he/she plans to use the satellite images to the emergency response.

(2) Sensors for Crisis Management

The rapid damage/ disaster detection is necessary for the efficient crisis management. Although installing sensors may cost more than WAM, it is still useful if one must detect the damage of the important facilities.

(a) GPS

Positioning a fixed point by GPS relative positioning is comparatively accurate (several centimeters for some products) than the point positioning, so one can monitor the displacement of the ground surface to detect the

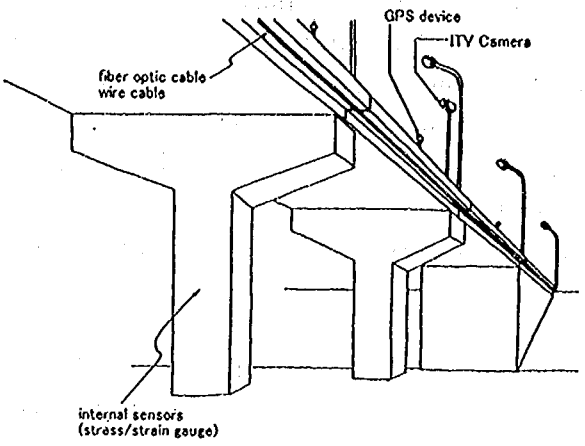


Fig. 3.4 Sensors for WAM

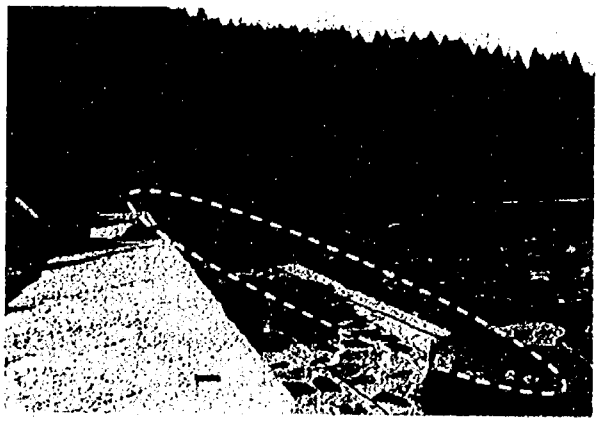


Fig. 3.5 Wire sensors installed at Sabo dam to detect debris flow (Erosion and Sediment Control Division, PWRI)

landslides and other earth disasters. Thus, GPS can be applied both for accurate risk monitoring before the earthquake and for the real-time detection of large deformation for the crisis management.

(b) Fiber optic cable

The fiber optic cable also can be used as the sensor to detect the unusual displacement/ deformation of the facilities. While GPS can monitor the positions of the dispersed points, the cable sensor can provide the location along the cable where the deformation exists.

(c) Accelerograph

(a) and (b) are the sensors to monitor the time dependent phenomena or to detect the unusual events. However, installing sensors to all the facilities will not be economically efficient. MOC has installed the accelerograph network with about 700 accelerographs so that the numerical data such as maximum accelerations are aggregated immediately after the earthquake and that they can help counter-earthquake response activities. The data cannot only be used for the reference, but also be used for other calculations such as the real-time damage estimation.

The image of the sensors installed at the bridge site is shown on Fig. 3.4. Such sensors are

Table 3.1 WAM technologies

	geostationary satellite	sub-recurrent satellite	GPS	fiber optic cable	accelerograph
risk assessment					
active fault	X	O	X	X	Δ
crustal movement	X	Δ	O	Δ	X
landslide risk	X	Δ	X	X	X
social state	O	O	X	X	X
crisis management					
earthquake ocurrance	X	X	X	X	O
facility damage	X	Δ	O	O	Δ

O : level of practical use
D : potentially practical with R/D
X : not level of practical use/ no relation

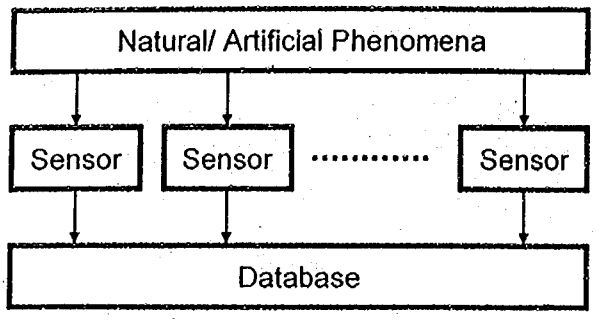


Fig. 3.6 WAM subsystems

already utilized for the response to other disasters including erosion and sediment control[2)3)]. Fig. 3.5 shows an example of the wire sensor installation to detect the debris flow.

The input of WAM system is various phenomena and they are transformed to the electromagnetic signals by the sensors, and stored to the database with certain format. The data are stored to the database system to be shared by the subsystems of SIS (Fig. 3.6). Also, efficiency of WAM technologies to the earthquake risk/crisis management is summarized on Table 3.1.

4. DATA COLLECTION TECHNOLOGY

While the data are required before or immediately after the earthquake with WAM, more detailed information of the facilities' damage is quite useful to manage the efficient counter-earthquake response. Also the information about the state of response activities is necessary once it starts.

The data sent from investigation teams may take various forms: e.g., text, photograph, image and numerical data. They are categorized to two groups: that is, the investigation information and the support information. Here, the system to collect these kinds of data is called the data collection (DAC) system.

The investigation information includes the damage data of facilities, and is directly used for the following earthquake response such as immediate restoration and rehabilitation. On the other hand, the supporting information is used to know the state of response activities, which includes the position of investigation teams and helicopters.

The technologies used for the data collection include the mobile terminal to input the text and numeric data, digital still camera, camcorder and the GPS device. Recent progress of the market of mobile gears may have installation of this type equipment easier (Fig. 4.1). As for the GPS, because the point positioning has more than several tenth meters, the relative positioning technologies that need the extra communication system will be appropriate (Fig. 4.2).

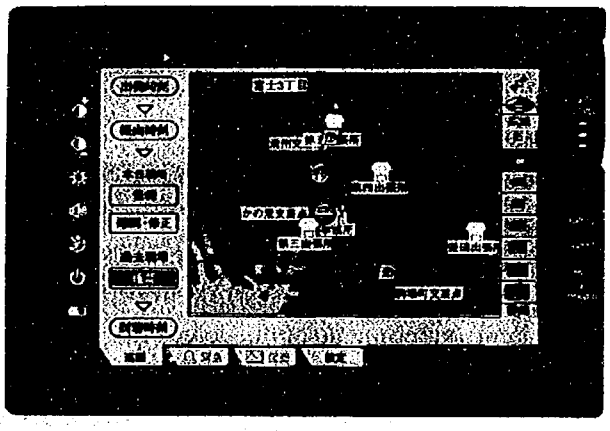


Fig. 4.1 Mobile terminal for investigation (Chubu Construction Bureau)

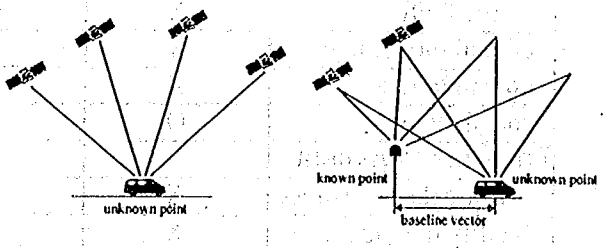


Fig. 4.2 GPS positioning: point positioning/ relative positioning

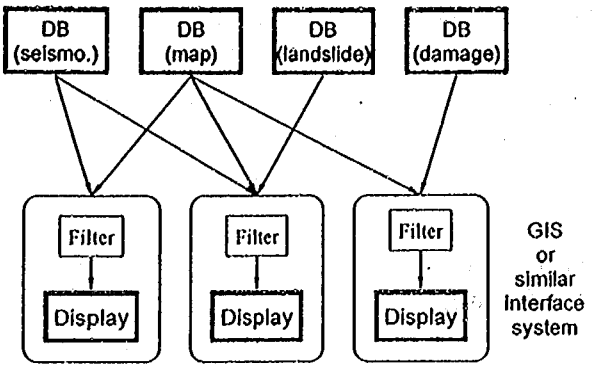


Fig. 4.3 DAN subsystems

The collected data are stored to the database just as same manner as the wide area monitoring (Fig. 4.3).

5. ANALYSING DISASTER CONDITION

As the data collected by DAC system are of the objects that have their own positions, attributes and the times of incidents, they are best to be treated on GIS system. With its ready-to-use functions such as route searching and buffering functions, GIS can be a good interface not only for the display but also for the analyzing equipment for investigation data and the investigation supporting.

The data that monitored, stored and collected are not very much useful until they are processed and combined together. Followings are the several examples of such data analyze.

- to analyze the image data: for example, survey active faults by emphasizing lineament with image filtering
- to clarify the seismic risk by overlaying the hazard data and the socioeconomic data to clarify the risk
- to check the emergency investigation activities by overlaying the damage map and the investigation teams' GPS data
- to search, sort and filter the facilities with specific keys such as types, routes and design conditions

Those data processing with general algorithms are defined as the data analyze (DAN) here, which can be realized with the stored data monitored or collected and with the general GIS or similar interface system. Here, such function that just displays the aggregated data on the CRT or other devices is included in this data analyze function. Fig. 5.1 shows the image of the data analyze (and display). Based on the databases of accelerograph observation, maps, landslide risk and facility damage, each terminal with filtering and displaying function can aggregate, filter, compose and display that each user wants to know.

6. DECISION MAKING SUPPORT

(1) Decision Making for Risk/Crisis Management

To support the decision making regarding the earthquake risk/ crisis management, more specific functions than simple data processing techniques are required[2]. Examples of such function, decision making support (DMS), are

- earthquake disaster loss estimation including

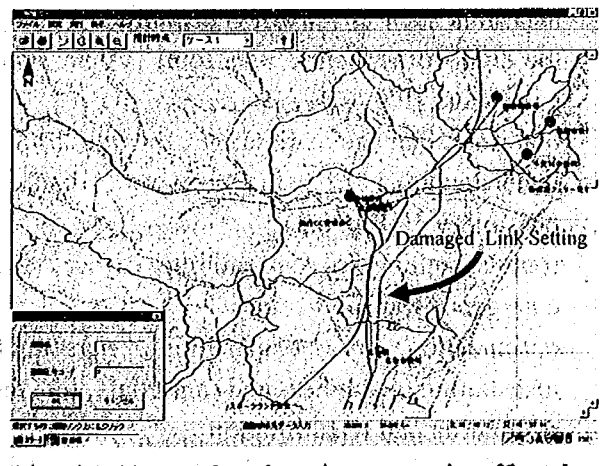


Fig. 6.1 Example of socioeconomic effect loss estimation system (PWRI)

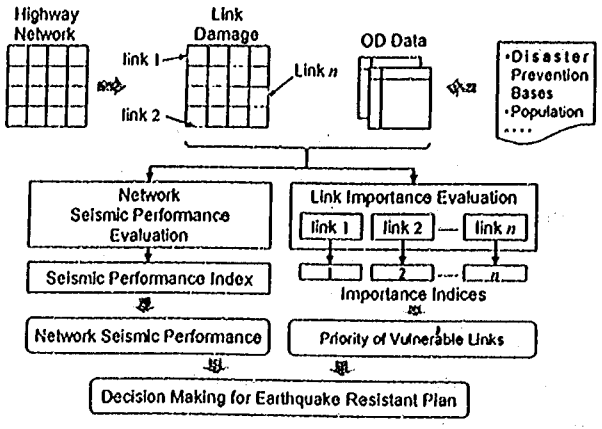


Fig. 6.2 Example of retrofit prioritizing

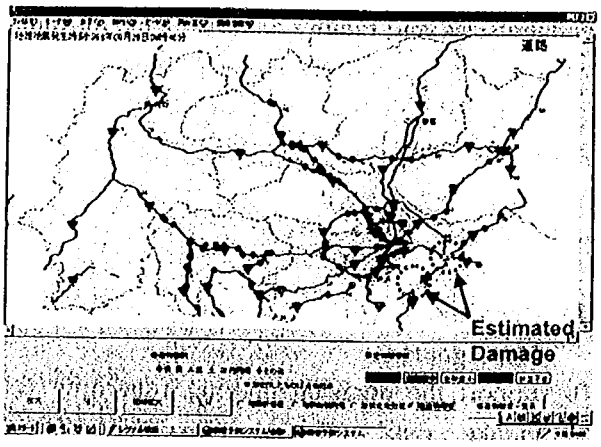


Fig. 6.3 Example of real-time damage estimation (PWRI)

direct/ indirect economic losses and other effects[4] (Fig. 6.1)

- prioritization for the earthquake resistant measures such as retrofit especially regarding the civil infrastructure as a total system such as network (Fig. 6.2)
- real-time damage estimation for the rough understanding of the severe damage possibility[5][6] (Fig. 6.3)
- route-searching for determining detours and emergency transport routes
- optimization of dispatching personnel, distributing machines and materials for the restoration and rehabilitation

The main bodies of those technologies are the execution modules with input data given by the databases. The calculated results are stored to the databases and referred and analyzed by each terminal. Each subsystem uses the input data, and stores its results to the database to be referred by DAN subsystems.

(2) Decision Making for Contingency Planning

Besides the application of SIS to the risk/ crisis management, examining if the SIS and the counter-earthquake system including it work correctly under contingent circumstances is important for the efficiency of SIS. First, as SIS in reality is operated by personnel, the counter-earthquake activity training is useful to know potential problems. In addition, examining the performance of the responding action by simulating various contingent state is important to compensate the limited chance of real training. Such simulation function is also included in SIS[2].

7. DATA SHARING AND EXTENSIBILITY

Even though there are many useful elemental technologies, the efficiency of the system varies depending on how it is organized. Followings are possible problems.

- if each subsystem is isolated, there are duplication of the data (*data duplication problem*)
- if SIS is developed as the single and huge system, maintenance of the data and the subsystems is complex (*maintenance problem*), and it is difficult to revise the subsystems when new technologies are obtained (*extensibility problem*).

One of the solutions to avoid those problems is to clarify the structures and the formats of the data dealt with in SIS so that each subsystem

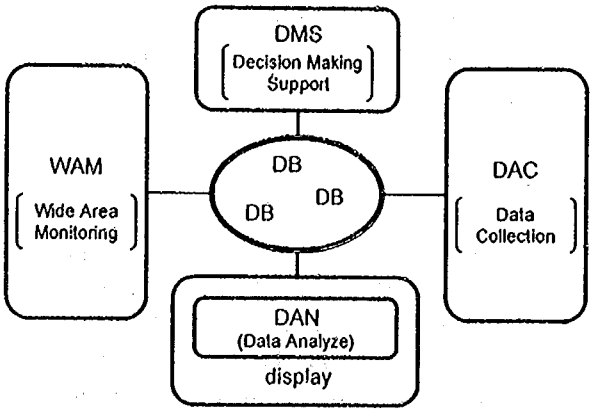


Fig. 7.1 Data sharing architecture

can understand how they are treated[2]. Once the data are shared in SIS, the former problems are solved and it acquires the important advantages.

- the system can increase its functions satisfying the new demand.
- the system can utilize the newest technologies at each time.

To obtain these advantages, first one must examine the activities and clarify the information dealt with in the system. Next, the structure of the information needs to be organized so that each subsystem can share the data (Fig. 7.1).

Recent movements in the information technology area coincide the concept proposed here. One is the 'unified modeling language' (UML) for the object oriented analyze and design. As it is for the programmers', the personnel of earthquake response system do not necessarily use it. However, it suggest that analyzing and designing the complex system needs to clarify the information structures and share them. The other example is 'extensible markup language' (XML) which is the unified method to share the data on the network regardless of the kind of hardware and software. This technology will be a candidate to develop an extensible, data-shared SIS.

8. MANUAL

As a guideline for the construction of efficient SISs, PWRI is developing the 'Construction Manual for Seismic Information System (draft)'. Instead that the conventional manuals of this kind usually focus on the elemental technologies, this manual also emphasizes the system architecture for extensible and data-shared system. The contents are shown below.

1. General
   - 1.1 Objective
   - 1.2 Structure of this Manual
   - 1.3 Terminology
2. Fundamental Philosophy of SIS Construction
3. Requirements of SIS in Terms of Counter-earthquake Activities
   - 3.1 Stages of Counter-earthquake Activities
   - 3.2 Information and Technologies for Counter-earthquake Activities
   - 3.3 Information and Technologies to Maintain Counter-earthquake System
4. Technologies of SIS
   - 4.1 Common Base Technologies
   - 4.2 Detection Technologies
   - 4.3 Communication Technologies
   - 4.4 Technologies for Display and Analysis
   - 4.5 Decision Making Support Technologies
5. Safety of SIS
   - 5.1 Reliability of SIS
   - 5.2 Security of SIS
6. Preliminary Design Example of SIS
   - 6.1 Target Determination
   - 6.2 Framework Design
   - 6.3 Design of Common Parts
   - 6.4 Design of Individual System
   - 6.5 Schedule to Improve SIS

9. CONCLUSIONS

(1) In this paper, first the concept of NLM is

reviewed, and the NLM for disaster prevention is carefully analyzed focusing on the tasks: i.e., observation, analyze, planning and operation. Then, focusing on the earthquake disaster prevention the methods to accomplish the tasks are examined.

(2) SIS is defined as the information/ communication systems that applies and supports earthquake disaster prevention related methods,

- wide area monitoring
- data collection
- analyze
- decision making

Also the state-of-the-art of its technological developments and their trends are examined. The points of technological developments of SIS are summarized as follows.

- Utilization of the data from satellites and GPS positioning for the wide area monitoring (WAM)
- Installation of fiber optic cables and GPS devices for the data collection (DAC)
- Application of GIS for the data analyze (DAN)
- Subsystem technologies including loss estimation, prioritization and optimization for the decision making support (DMS)
- Securing the data sharing and extensibility

(3) After the Hyogo-ken Nanbu earthquake, many public bodies and private sectors have developed the seismic information system. However, many of them are isolated in planning and development with each other. The SISs do not fully operate and support the earthquake response system until they and their subsystems are connected efficiently with each other. Thus, SISs need to be developed with common concept to share the information and to operate cooperatively.

REFERENCES

1)KAWASHIMA Kazuhiko, TOKIDA Kenichi, SUGITA Hideki, NAKAJIMA Tomoru and MATSUMOTO Hideo: Guidelines for Disaster Information Systems for Important Infra-structures, Proceedings of the 25th Joint Meeting of the U.S.-Japan Panel on Wind and Seismic Effects, UJNR, pp. 475-486, 1993.5

2)SUGITA Hideki, NOZAKI Tomofumi: Seismic Information System for Civil Infrastructures, Proceedings of the 30th Joint Meeting of the U.S.-Japan Panel on Wind and Seismic Effects, UJNR, pp. 306-318, 1998.5

3)YAMADA Takashi, MINSMI Noriyuki, MIZUNO Hideaki: Developing of Debris Flows Predictions and Detection Technology - Their Future Issues, Journal of the Japan Society of Erosion Control Engineering, Vol. 50, No. 5

4)NOZAKI Tomofumi, SUGITA Hideki: System To Assess Socio-economic Effect of Earthquake Disaster, Seventh U.S.-Japan Workshop on Earthquake Disaster Prevention for Lifeline Systems, 1997.11

5)ODAGIRI Shun-etsu, SUGITA Hideki, KANEKO Masahiro, NOZAKI Tomofumi and HAMADA Tadashi: Development of Real-time Information System for M.O.C, Proceedings of the 30th Joint Meeting of the U.S.-Japan Panel on Wind and Seismic Effects, UJNR, pp. 425-435, 1997.5

6)SUGITA Hideki, HAMADA Tadashi: Development of Real-time Earthquake Damage Estimation System for Road Facilities, Seventh U.S.-Japan Workshop on Earthquake Disaster Prevention for Lifeline Systems, 1997,11

Change Detection Using Geospatial Analysis

By

William E. Roper[1]

ABSTRACT

The ability to use remotely-sensed information that accurately characterizes the earth's surface can be a powerful capability during immediate response and longer term recovery from natural disasters. Four sensor systems are described and their ability to characterize terrain or bathymetry illustrates. Multi-Scan Sonar is a rapid, high-resolution sensor technology for underwater surveying. Through data processing developments, changes in bathymetry over time can be translated to volumetric changes at specific locations. Examples of LIDAR systems to measure ground surface conditions are presented. Results at a calibration test site in California are shown. The third sensor described is Interferometric Synthetic Aperture Radar (IFSAR). IFSAR has special characteristics applicable to rapid mapping of terrain features. Examples of data collection projects with IFSAR in the Sacramento Valley of California are presented. The fourth system described is SHOALS. SHOALS is a LIDAR-based, helicopter-mounted bathymetry and near-shore terrain measurement system. The application of this system to recovery efforts following Hurricane Opal in the western Florida panhandle are presented.

KEYWORDS: change detection; remote sensing; LIDAR; terrain characterization; IFSAR; multi-scan sensor; SHOALS; natural disaster recovery; bathymetry; rapid mapping.

1.0 INTRODUCTION

Over the last few years, a number of remote sensing systems have been developed and refined for specific applications ranging from environmental management to accurate mapping of floodplains. These evolving sensors and related data processing technology can have direct benefit to natural disaster response. Particularly if accurate rapid characterization of the terrain conditions is important as in an earthquake or landslide event. This paper describes four different systems that could be considered part of the remote sensing tool kit available to improve disaster response.

2.0 MULTIBEAM SONAR INTEGRATION METHODOLOGY

Multibeam sounding technology is a significant enhancement over single beam sounding in areas where 100% bottom coverage is necessary to determine detailed changes that may have occurred. In single beam sounding, a single sonar beam with a width from 3° to 8° is used to measure the depth. The area of bottom which is actually examined is very small and is dependent on the depth and the beam angle. Multibeam sounding allows the user to measure up to sixty depths along a narrow swath. The swath can cover from 90° to 120° beneath the hull of the survey vessel. These measurements are made up of 14 times per second, providing users with millions of soundings per day of survey. To provide 100% coverage, the spacing between survey lines is dependent upon the depth below the vessel and the width of the multibeam scan (Roper, 1999). Multibeam technology also provides an extremely valuable reconnaissance

[1] Director, U.S. Army Topographic Engineering Center
7701 Telegraph Road, Alexandria, VA 22315-3864
www.tec.army.mil

tool for performing real-time examinations of break walls, dikes, levees, bridges and other surfaces (Niles, A., 1997).

2.1 Enhancements in Multibeam Systems

The Topographic Engineering Center (TEC) began analyses of multibeam systems in 1989 with a test and evaluation of the Bathyscan system produced by Marconi, Ltd, of England. The Bathyscan was the first multibeam system developed for shallow water (under 100 feet) and featured some innovative beam forming and backscatter detection techniques (TEC Report 0008, 1992). However, the on-board data processor used late 1970's technology, which produced slow data logging and limited processing capabilities. Data editing was tedious. TEC recognized the need for more robust data processing and system calibration procedures, and 3-D graphic editing to enable effective analysis of tens or hundreds of thousands of data points (TEC Report 0012, 1992).

TEC performed a second test and analysis in 1992 of the German Atlas Fansweep system, installed and used by John E. Change and Associates (JECA), Inc., of Louisiana. The system performed well and demonstrated the ability to perform multibeam surveys to Corps Class I hydrographic survey accuracy standards. However, the JECA system used customized data collection and processing algorithms on a Unix data processor. During the tests, acoustics experts and system programmers were present to operate the system and make software modifications as needed. Although the system gave JECA impressive capability as a survey contractor, such expertise is not available on Corps vessels. Until the software was available on common processors, i.e., PC-based computers, multibeam technology did not appear to be feasible for Corps vessels nor a majority of contractor boats.

With such multibeam analyses experience, TEC participated with Coastal Oceanographics to develop standard procedures for multibeam operation, such as the patch test described in the following section. The timing of these developments was favorable, since PCs were becoming powerful enough to perform sophisticated processing yet retain an effective user interface (Training Course, 1996).

A multibeam file is loaded into the Coastal Oceanographics HYSWEEP program and then examined for trackline, heave-pitch-roll, gyro, tide and draft corrections included with the data. Sound velocity correction data can also be incorporated at this point to correct for "ray-bending" caused by variations in the speed of sound through the water column on sound waves which are not parallel to the bottom. Once these inputs are examined and verified, the user calculates a discrete X, Y, Z for each measurement (Training Notebook, 1995). The number of coordinates can be enormous, since nearly 1,000 depths per second are collected in the multbeam systems.

A three-dimensional editor is then used to examine the data and to eliminate questionable points. Users can manually edit the data, or use one of several automated filters available in the package. Figures 1 and 2 show examples of products using these systems at two Corps of Engineers projects. Once the data has been edited, users can save to either a binary X, Y, Z Beam Angle file or an ACSII XYZ file. These files can be reduced in the MAPPER program, which has gridding routines, or they can be read directly into he TIN MODEL program for surface generation and volume computations.

2.2 Channel Volume Determination from Multibeam Output

Triangulated Irregular Networks (TINs) are a relatively new method which can be used to calculate dredge volumes. In the TIN method, a terrain model is created through the triangulation of the three-dimensional spatial coordinates. The triangles in this model have no gap and do not overlap. TINs commonly use the Delaunay Principle, in which TIN is easily determined, is essentially unique, and avoids long, narrow triangles as much as possible. The Delaunay Principle requires that the circle circumscribed

around any triangle in the TIN contains no data points in its interior (TEC Report, 1993), as illustrated in Figure 3.

Through comparison of TIN models, volumes of material can be determined. In the case of scour or shoaling applications, a design model of a channel, consisting of planar surfaces for the floor and slide slopes, can be compared with the TIN representing the actual terrain. The TIN triangles are projected onto the design surface, resulting in volume elements for the area covered by the TIN. Volumes above the design surface would represent material to be dredged, while volumes below the surface represent areas where no dredging is needed or areas for dredge disposal. Similarly, two TIN surfaces, perhaps representing before- and after-dredge terrain, could show actual material that has been dredged or provide accurate information about dynamic surface changes (Training Notebook, 1995).

The TIN method, which can be computationally intensive, has become feasible with the availability of modern processors. TIN volume routines are now found in many site design and sophisticated survey software packages. TINs offer the user flexibility in the collection of survey data, since the data need not be aligned along pre-determined cross-section or profile patterns. A detailed analysis of the use of TINs in dredge volume applications was performed by TEC, and is presented in the following section.

TINs were being used at TEC in the 1980s for military applications involving terrain analyses. Much of the original software was for the terrain specific uses. TEC scientists, in coordination with mathematics experts from the National Institute of Standards and Technology (NIST), pioneered applications such as terrain visualization, line-of-sight determination, and flow analyses using TIN methods. From these applications, there was also potential to compute volume changes in civil applications.

2.3 Advances in TIN Volume Determination

The Surveying Division at TEC, therefore, began a detailed analysis in 1991 of the TIN volume technique which is documented in (U.S. Army, 1993) ETL 1110-2-348, The Use of TINs for Dredged Material Volumes. The analysis, in which NIST participated, included a mathematical examination of the method, comparison with the conventional average-end-area (AEA) technique, and the use of several test data sets. The test sets consisted of real and fabricated data representing navigation channel surveys. Among the more significant results, TEC and NIST concluded the follow:

1) TIN methods are at least as accurate as, and usually more accurate than the AEA technique. In straight, uniform channels with terrain above the design surface, results are essentially identical. In cases where the terrain extends above and below the design surface, the AEA technique overestimates the volume by as much as 50% or more, whereas the TIN accuracy is not affected.

2) The TIN method uses the survey data more effectively and efficiently. Unlike the AEA method, the data points need not be aligned in parallel cross-sections and can be utilized in any pattern. Multibeam or multi-transducer survey data, which produces virtually total bottom coverage, can be effectively used only with the TIN method. The technique can also utilize combined cross-sectional and longitudinal data, which are recommended for single-transducer systems to perform consistency checks (see ETL 1110-2-348). Complete utilization of the survey data without realignment or shifting to a required pattern results in more accurate volume results.

3) For the TIN method, verification of results by a manual method is not feasible. In cases of disputes with dredging contractors, Corps of Engineers districts have cited the need to reproduce computed volumes using hand computation or manual drafting methods. Such capability has always been an advantage of the AEA method. However, summing thousands, or even millions of TIN prismoidal volume elements is essentially impossible. Verification

of TIN volumes will only be possible when the technique has gained general acceptance by Corps offices and dredging contractors, and analysis of the utilized TIN algorithm and the user procedures will provide sufficient verification of results. TEC's demonstration and publication of TIN analysis results has helped achieve that acceptance.

4) At the time of TEC's analyses, there were no commercially available TIN software packages specifically designed for dredge volume applications. For example, none of the routines enabled computation of volumes on a station-by-station basis. More significantly, channel designs that did not consist of a simple, straight configuration could be tedious and difficult to create, and different users might obtain different results. As a result of the TEC/ Coastal Oceanographics Construction Productivity Advancement Research (CPAR) program, a software package that solves these problems is now available.

Prior to the detailed analyses, TEC and NIST began to develop a TIN software package specifically for dredge volumes. At the time, no commercial TIN routines for general civil use existed and the software, developed with Civil Works Research and Development funds, when completed, was planned for distribution to all Corps offices. However, TIN volume routines began to appear in site design software, such as Intergraph's InRoads application. Therefore, TEC abandoned plans to distribute the TEC/NIST program, and instead used the software for benchmark testing and the analyses described above.

The TEC/NIST routine, in FORTRAN language, was written primarily by the NIST mathematicians who are regarded as authorities in TIN and grid terrain modeling. The software uses a Delaunay triangulation scheme and computes volumes relative to design surface. The software also permits the use of break lines, which can be used to control triangulation so that prominent features, such as peaks or ridges, are not blunted in the model. The software has no graphical user interface, and uses six to eight input files to define the terrain, design surface and certain tolerances (Niles, 1997).

2.4 Product Development for Dredging Applications

Through a partnership with Coastal Oceanographics, the TIN modeling capability was enhanced. Coastal Oceanographics used algorithms in the TEC TIN software to create an improved routine in HYPACK. The TEC algorithms offered a robust TIN generation module, but had a weak interface. Coastal Oceanographic developed new graphical interfaces and adapted the TIN routines to read coordinate files from HYPACK. Coastal Oceanographics also re-coded much of the computation sections and modified the data structures for faster and more efficient run time.

Once development of the TIN routine was complete, Coastal Oceanographics developed terrain visualization pack algorithms and dredge volume capabilities (Coastal Oceanographics, May 1995). A contour algorithm using B-spline smoothing was integrated, along with the flexibility of user-defined color designations. The result is compatibility to generate plan-view plots showing user-defined contour intervals or 3-D perspective plots showing realistic terrain undulations, as in Figure 5. For volume calculations, Coastal Oceanographics developed a channel template routine that enables the user to specify angular vertices and/or side slopes. Using this procedures, channel designs, which can include any combination of turns, wideners, depths and side-slopes; can be easily entered with the completed layout displayed for review. An application in North Carolina is shown in Figure 6.

3.0 GROUND SURFACE CHARACTERIZATION WITH LIDAR

LIDAR-topographic-mapping systems have considerable promise for producing high-resolution digital elevation models (DEMs). Satellite communications and GPS navigation systems are critical parts of LIDAR mapping systems. TEC has acquired multiple LIDAR-

topographic-mapping data for the purpose of producing high-resolution DEMs. These will be evaluated and the results used to help develop criteria for future applications for floodplain mapping (Roper, June 1999).

However, processing of raw LIDAR data into useful and reliable DEMs is not yet mature. For example, unless exceptional effort is made to produce accurate LIDAR calibration, significant merging artifacts, and their associated errors, can occur. Another example is with merging artifacts that can presently be found in Houston Advanced Research Center (HARC) data.

Merging artifacts in LIDAR data are generally due to mis-calibration of the LIDAR sensor or residual GPS errors. Both kinds of errors can be described by mathematical models and corrected. Because data within overlap regions should match, the parameters of the mathematical models can be calculated. Subsequently, the data can be adjusted so that the errors are minimized. Least-squares estimation techniques have proven to be efficient, accurate, and reliable for this purpose,. The overall process is a least-squares model-based merging.

3.1 LIDAR Test Program in Lakewood, California

TEC is currently analyzing the LIDAR data sets from the FEMA-sponsored LIDAR collection in he Lakewood community, Los Angeles, California. This effort will undertake to develop appropriate mathematical models of merging errors. This LIDAR data set will be further developed to establish an automatic processing methodology, based on least-squares model-based merging, for adjusting the data to minimize merging errors. Sample collection images from Lakewood, California, are shown in Figures 7 and 8. There are clear differences in the sample images. Also, because of the high resolution, the data bases are time dependent,.

The LIDAR collection plan for the Lakewood, California, area includes a number of collection actions and products (Jorgensen, 1998). These include:

- Multiple LIDAR collections
- Long cross-flights over the AR zone
- Small mosaic area
- LIDAR-derived DEM at 3-meter postings
- X, Y, Z data from each LIDAR return
- LIDAR used to improve vertical accuracy of products

3.2 LIDAR Application for Levee Survey and Floodplain Mapping

Airborne LIDAR systems are capable of precise platform-to-ground ranging that produce decimeter-level height accuracy and meter-level post spacing topographic information of the surface. Some systems are capable of return pulse waveform digitization which provide precise ground surface AND vegetation height and volume measurements. Laser altimeter measurements are acquired along profiles or swaths up to a few hundred meters wide using small aircraft. These swaths could replace channel cross-sections (currently obtained via costly ground-based surveys) required by flood backwater models, which are used to predict floodplain extent.

A portion of the Jet Propulsion Laboratory (JPL) LIDAR data collection effort was over the levee system of the Sacramento River near Sacramento, California. This levee survey route is shown in Figure 9. A segment of this data set in the Meling Orange Grove area of California is shown in Figure 10. In the oral presentation of this paper, a 3-D dynamic fly-thru of this LIDAR data is shown. The fly-thru illustrates the ability to virtually enter the representation of the terrain and better understand the ground attributes.

4.0 INTERFEROMETRIC SYNTHETIC APERTURE RADAR (IFSAR) BASED FEATURE CLASSIFICATION MAPPING

The state of the art in exploiting interferometric synthetic aperture radar (IFSAR) for terrain

information is advancing, and provides significant potential for use in floodplain mapping, and flood crisis support operations, as well as other situations. Unlike conventional SAR imagery, IFSAR data permits the generation of rectified synthetic aperture (SAR) images co-registered with an accurate terrain elevation file. This imagery can have an absolute geographic accuracy of 3 meters RMS or less. The rapidity with which IFSAR data can be collected and processed over wide areas, and the all-weather, day-night capability offers significant potential for providing direct support to crisis situations as well as enhancing the performance of spectrally based assistance (Roper, 1998). In addition, IFSAR terrain elevations can be employed to rectify hyperspectral and other imagery, allowing for the registration of radar and hyperspectral imagery in the ground plane thus providing an improved, rapid digital elevation model (DEM) product (Figure 11).

The Interferometric Synthetic Aperture Radar for Elevations (IFSARE) was a joint industry-government program between TEC, the National Aeronautics and Space Adminstration, JPL and the Environmental Research Institute of Michigan (ERIM). This research effort resulted in the fabrication of an interferometric radar system integrated with a GPS internal navigation system which was mounted on a Learjet 36A. The National Aeronautics and Space Administration joined with the Jet Propulsion Laboratory in California to develop the processing software and the ground-processing environment. This software and ground processing capability has now been transitioned to Intermap Technologies Company and is available for commercial applications (Roper, 1998).

This effort represents a convergence of technology development by a large number of investigators and a pressing need for low cost, fine resolution, highly accurate terrain elevations for a wide variety of applications. It is critically dependent on recently devised Global Positioning System (GPS) capabilities and the advent of high-speed data processing capabilities.

It is anticipated that significant IDSAR data collections will occur in the next few years. Ongoing activities within the Topographic Engineering Center are focused on quantifying the performance of IFSAR techniques. Additional work will also be underway for demonstrating the capability to merge radar and LIDAR data.

TEC has been actively involved with the development of a capability to create maps from IFSAR with a minimum of human intervention. Automated algorithms operate on the IFSAR data files to extract land use classification, DEM generation, and bald earth estimations. Hydrology, elevated structures, power lines, and road network data layers can also be automatically extracted. TEC continues to enhance these automated algorithms to assess floodplain soil roughness and extend structure identification capabilities. A series of map products will be produced with IFSAR-based technology for selected test areas.

4.1 Floodplain Mapping With IFSAR and LIDAR

The California Department of Conservation (CalDoC), Federal Emergency Management Agency (FEMA), and the Topographic Engineering Center (TEC) initiated a joint project to assess IFSAR and LIDAR for floodplain mapping for California in 1998. The project was funded by FEMA with TEC as the project manager and CalDoC providing user input. The planned project area is shown in Figure 12. The Star-3I X-band radar terrain mapping system, operated by Intermap, was used to acquire the IFSAR DEM data. The NASA Jet Propulsion Lab's multibeam laser altimetry system was used to collect the LIDAR data.

Coverage of the flood data set extends from north of Sacramento south to Fresno, following the Sacramento and San Joaquin Rivers. The project area covers about 17,000 square

kilometers (or 6,564 square miles). Data was initially collected during September 1997 in two flights, one each for a northern and southern area. Strong turbulence caused the southern mission to be aborted; it was reflown in July 1998. Intermap began processing data in early 1998 and was completed by February 1999. JPL LIDAR data processing was completed in late 1998.

4.2 The Star-3I System

Traditional SAR systems in the past only gave two-dimensional views of the Earth and included geometric distortions inherent in slant range SAR data. IFSAR was developed to provide an elevation component to SAR imagery. The additional information from interferometric techniques provides a three-dimensional view of the Earth and removes some of the geometric distortions.

Three files are generated from the IFSAR instrument; a magnitude file, correlation file, and an elevation file. The magnitude file is a backscatter image that provides information on the shape of features, as well as terrain texture. The correlation image provides information on surface or volume backscatter. The elevation data, or DEM, provide information on terrain elevation and height of features. A sample DEM of the San Joaquin Valley is at Figure 11.

The STAR-3I system consists of two X-band radar antennas mounted in a model 36A Learjet. Data collection from the twin antennas occurs simultaneously. The set of acquired data are "interfered" by a digital correlation process to extract terrain height data that are used to geometrically correct the radar image. STAR-3I uses post-processed Differential GPS (DGPS) data, together with on-board, laser-based inertial measurement data, to obtain highly accurate positioning control. Terrain height and positioning data are enhanced by calibration of the baseline (the distance between the two antennas). The accuracy of the positioning information and calibration is such that no in-scene control points are required. The only requirement is that a ground-based GPS receiver must be located within 200 kilometers of the data collection site so that DGPS processing can take place (Jordan, 1998).

The STAR-3I is typically flown at 12,000 meters and requires a 10-kilometer wide swath of 2.5-meters resolution on the ground. The system has been designed to collect DEMs at a rate of 100 square kilometers per minute with 3-meter accuracy. Improved DEM accuracy is achieved by reducing the aircraft altitude to 6,000 meters, which reduced the swath width to six kilometers. At this low aircraft height, ground resolution stays the same; however, the signal-to-noise ration is one-half that of the higher altitude, thereby improving precision in the vertical direction.

5.0 RAPID BATHYMETRY MEASUREMENTS USING SHOALS

The Scanning Hydrographic Operational Airborne LIDAR System (SHOALS) system provides the capability for high spatial density utilizing state-of-the-art LIDAR technology consisting of a scanning laser transmitter/receiver that produces 200 soundings per second. SHOALS operates from a helicopter and includes a separate ground based data processing system. It is a highly mobile system capable of rapidly covering large areas. This unique capability produces a more comprehensive measurement of inlets and the adjacent near short bathymetry. Output from SHOALS is an accurate X, Y, and Z (position/depth) from each laser (Lillycrop, Parson, etal, 1994) sounding that is easily formatted for most data analysis software tools such as Geographic Information Systems (GIS), volumetric computations, or other contouring and mapping systems.

The SHOALS hydrographic survey system was developed for the U.S. Army Corps of Engineers (USACE) through a cost-shared project with the Canadian Department of Science, Industry, and Technology. Built by Optech, Inc., of Toronto, SHOALS consists of an airborne laser transmitter/receiver capable of measuring 200 soundings per second. The system operates

from a Bell 212 helicopter, flying at an altitude of 200 – 1,000 m with a ground speed of 0 to 100 knots. The Bell 212 is provided by the National Oceanic and Atmospheric Administration (NOAA), Aircraft Operations Center, through a Memorandum of Agreement. The SHOALS systems also includes a ground-based data processing system for calculating accurate horizontal position and water depth. Data processing utilizes a state-of-the-art depth extraction algorithm developed by the NOAA National Ocean Service. The SHOALS system completed field tests in February 1994. John E. Chance and Associates operate and maintain the SHOALS system, providing survey services nationwide (Roper, 1996).

5.1 Operating Principle

SHOALS uses LIDAR technology with the reflective and transmissive properties of water and the sea floor to gather high-density survey data. When a light beam hits a column of water, part of the energy is reflected off the surface and the rest, unless absorbed by particles in he water, is transmitted through the column.

Using this principle, SHOALS fires a laser into the water, where a significant amount of energy from the infrared beam is reflected off the surface and detected by receivers in the helicopter. The blue-green laser penetrates the surface and reflects off the sea floor. A computer calculates the depth from the time interval between the two reflected energy readings (Figure 13).

As the beam travels through the water column and reflects off the ocean floor, scattering, absorption, and refraction all combine to limit the strength of the bottom, return as shown in Figure 14; and, therefore, the system's maximum detectable depth. This depth is a function of water clarity, generally about three times the Secchi depth.

A typical plot of these energy readings, or waveform as illustrated in Figure 15. This graph shows the reflection off the water surface—the left most peak—to be a very strong return, while the bottom return, or right most peak appears much weaker.

The performance specifications for the SHOALS system are shown in Table 1.

5.2 Application to Hurricane Opal Recovery

As an example of rapid bathymetry analysis during recovery from a natural disaster, SHOALS was mobilized to assess shoaling problems at East Pass following landfall of Hurricane Opal.

In mid-October 1995, Hurricane Opal made landfall along the western Florida panhandle. Cited as one of the worst storms to hit that part of Florida in the past decade, the area has suffered billions of dollars in damage. Opal resulted in significant bathymetric change along Florida's coastline causing hazardous shoal formations in federally maintained navigation channels as well as severe beach erosion. The U.S. Army Corps of Engineers was tasked with quickly and accurately assessing conditions after Hurricane Opal and opted to use the SHOALS system to map two critical areas, Panama City Beach and East Pass. The SHOALS system collects water depths remotely from an airborne platform using state-of-the-art LIDAR technology. Under typical operating conditions, the SHOALS system is capable of surveying at a rate of three square miles per hour (eight square kilometers per hour) with a spatial resolution of 13 feet square (four meters), therefore providing complete coverage in a short time.

5.2.1 Opal's Impact in East Pass Area

During the storm, a 14-ft surge pushed a tremendous amount of water through the inlet and across Santa Rosa Island into Choctawhatchee Bay. The elevated bay, augmented by fresh water runoff from the Choctawhatchee River basin, drained out to sea through East Pass. Considering the height of the surge, it is likely that there were tremendous currents in the inlet and between the jetties as the ebb jet escape out to the Gulf.

Most of the coastal damage from Opal was caused by storm surge rather than from wind. Three surge effects can be seen in an aerial photograph of East Pass taken just after landfall (Figure 16). First, a narrow over wash fan projects into East Pass near the west end of the highway bridge. This part of Santa Rosa Island was low and provided little resistance to over wash. Second, almost half of the west jetty was over washed, with sand being carried from Santa Rosa Island into the channel. Third, Norriego Point was breached just to the northwest of the condominiums. Mobile District engineers, who conducted a post-Opal reconnaissance, estimated that about 80 percent of the above-water portion of the point was removed (Robinson, L., November 1995).

5.2.2 SHOALS Survey at East Pass

On October 10, 1995, just one week after Opal, the SHOALS system was used to survey East Pass. The survey was completed in just over one hour covering about one square mile and recording nearly 200,000 individual depth readings (Morang, Irish, and Pope, 1996). The results of this survey are shown in Figure 17.

The SHOALS generated results were compared with project channel requirements to determine changed dredging requirements. There was also an evaluation of risk to project structure, particularly the jetties, as a result storm induced changes within the inlet system. This analysis included a comparison of the SHOALS data with a 1990 survey (Morang, Irish, and Pope, 1996). A graphic display of the differences is shown in Figure 18. This clearly shows a significant growth in the scour hole at the tip of the west jetty. If it continues to deepen, the stability of the jetty tip may be at risk. There was also an accumulation of sediment north of the spur jetty.

For this disaster response application, SHOALS proved to be a rapid, accurate survey tool for accessing post storm changes in bathymetry. This can assist in post storm recovery planning and better allocation of recovery assets, and lead to an improved understanding of sediment dynamics of inlet and coastal systems. The SHOALS system is moving toward full deployment for Corps of Engineers projects. For the last nine coastal inlet surveys conducted there was a savings of $300,000 over traditional methods and a better product produced. When fully deployed, savings in the range of over $3 million is expected annually at Corps of Engineers projects. Through cooperative project applications for NOAA, Navy, Coast Guard and others, the savings to Federal government could be significantly greater. Planned improvement will further expand SHOALS capability, accuracy, and timeliness.

5.0 CONCLUSIONS

The remote sensing systems presented have unique capabilities for the applications they were initially designed for,. As a result, each system may fill a different need for the emergency response manager. For underwater detection, and characterization of changes in low visibility water, the multibeam sonar system has application. In clear water for wide area, rapid assessment, the SHOALS system is a good choice. For small area, high-resolution terrain features and changes, the LIDAR system works well. Lastly, for rapid, wide area, elevation terrain characterization, IFSAR is a good choice. In each case, the capabilities represented provide new tools to the emergency manager for better disaster response, recovery, and preventative planning.

6.0 REFERENCES

Coastal Oceanographics, Inc.; Report on RTK OTF Hydrographic Survey Testing in Baltimore; Pat Sanders, May 1995

Jorgensen, Thomas, Airborne Platform Remote Sensing and Related Technology, Research Report, U.S. Army Topographic Engineering Center, December 1998

Lillycrop, W. J., Parson, L. E., Estep, L. L., Laroque, P. E., Guenther, G. C., Reed, M. D., and Truitt, C. L., "Field Test Results of the U.S.

Army Corps of Engineers Airborne LIDAR Hydrographic Survey System," in proceedings U.S. Army Corps of Engineers 1994 Training Symposium, Surveying and Mapping Remote Sensing/GIS, New Orleans, LA, pp SM:2A 1-5, 1994.

Morang, A., Irish, J. L., and Pope, J., "Hurricane Opal Morphodynamic Impacts on East Pass, Florida: Preliminary Findings," U.S. Army Engineer Waterways Experiment Station, Vicksburg, MS, 1996

Niles, A., and Sander, P., Advanced Hydrographic Surveying and Dredging System, CPAR-TD-96-2, 1997

Robinson, L., Unpublished Reconnaissance Report, USAE Mobile District, Mobile, AL, November 1995

Roper, William E., Assessment of Hurricane Opal Impact on East Pass, Florida, with Airborne LIDAR, U.S./Japan Workshop on Two Great Tsunamis, Hilo, Hawaii, April 14, 1996

Roper, William E., Geospatial Analysis Support to Natural Disasters, U.S.-Japan Wind and Seismic Panel, International Conference, Washington, D.C., May 1998

Roper, William E., Geospatial Technology Support to the Nation's Navigation System, Transportation Research Board, National Research Council, National Meeting, January 1999

Roper, William E., High Resolution Terrain Characterization with LIDAR and RADAR Sensors, to be presented at the Fourth International Airborne Remote Sensing Conference and Exhibition, Ottawa, Canada, June 1999

TEC Report 0008, Evaluation of the Bathyscan Sweep Survey System; Anthony Niles, May 1992

TEC Report 0012, An evaluation of the HI-MAP Survey System, July 1992

Topographic Engineering Center Internal Report, Pilot Implementation of TINs for Dredge Material Volume Payment, Robert Fischer, Anthony Niles, March 10, 1993

Training Course Notebook, Coastal Multibeam Hydrographic Surveys, Volumes I and II, sponsored by the U.S./Canada Hydrographic Commission, Coastal Multibeam Working Group, St. Andrews, New Brunswick, June 18-29, 1995

Training Course Notebook, USACE Coastal Multibeam Sonar Short Course, sponsored by the U.S. Army Corps of Engineers Topographic Engineering Center, Mobile, Alabama, March 18-20, 1996

U.S. Army Corps of Engineers Engineer Technical Letter 1110-8156, Policies, Guidance and Requirements for Geospatial Data and Systems, April 1996

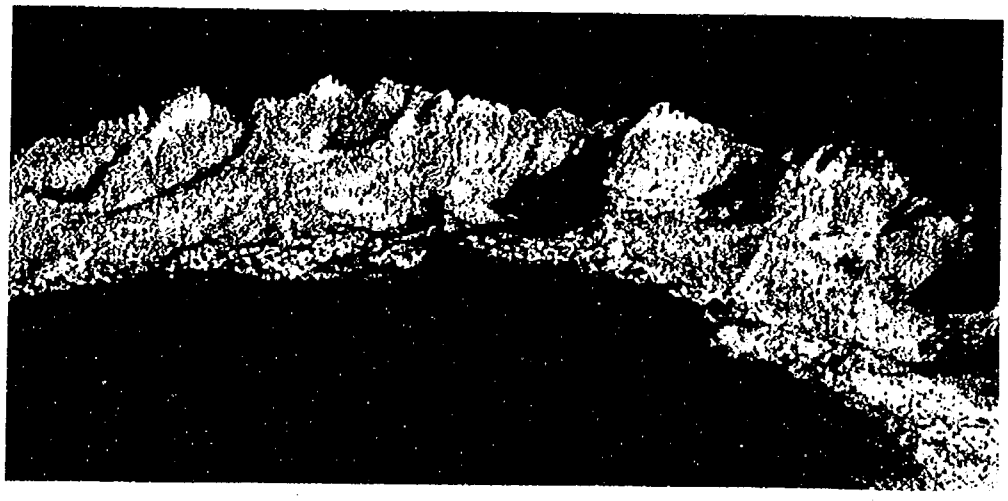


Figure 1: Bendway Weirs at Dogtooth Bend, Missouri

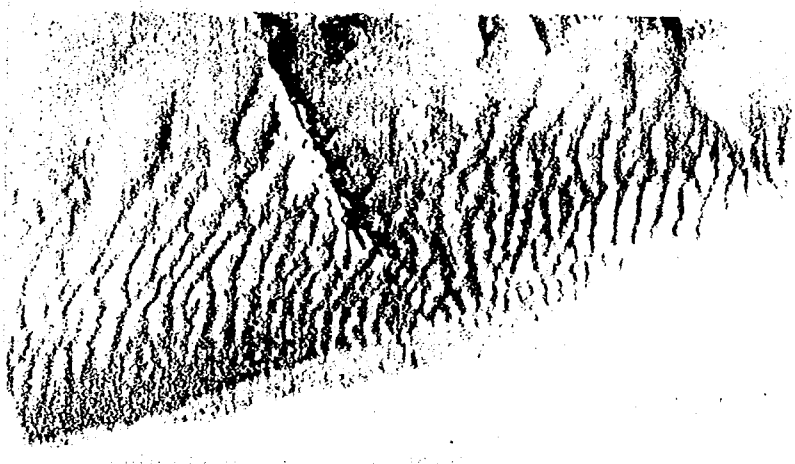


Figure 2: Sand Waves and Pipeline Crossings, Mississippi River

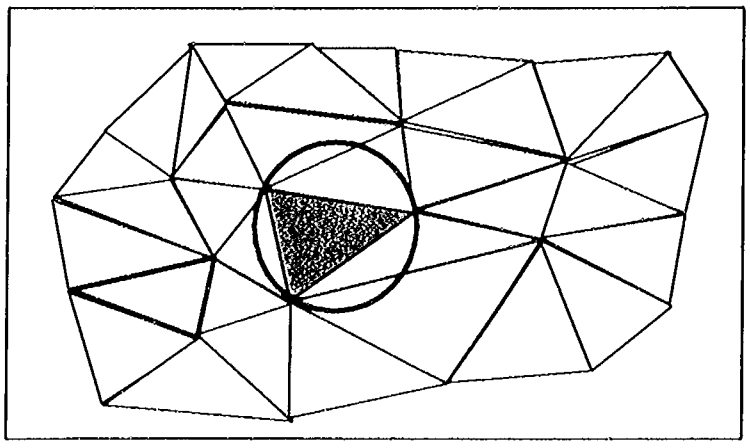


Figure 3: Delaunay TIN

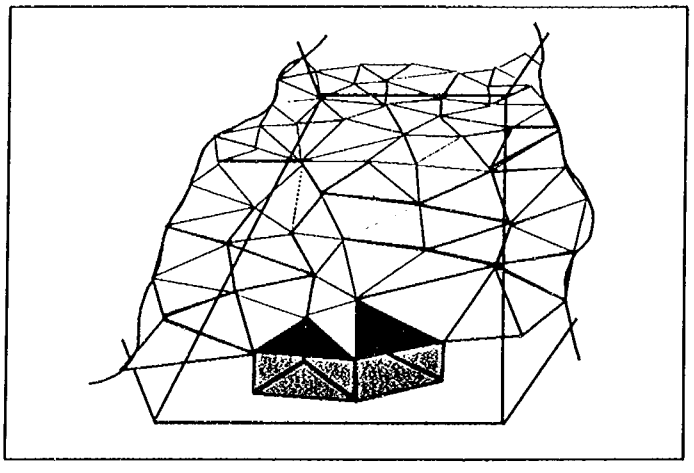


Figure 4: TIN Volume Determination

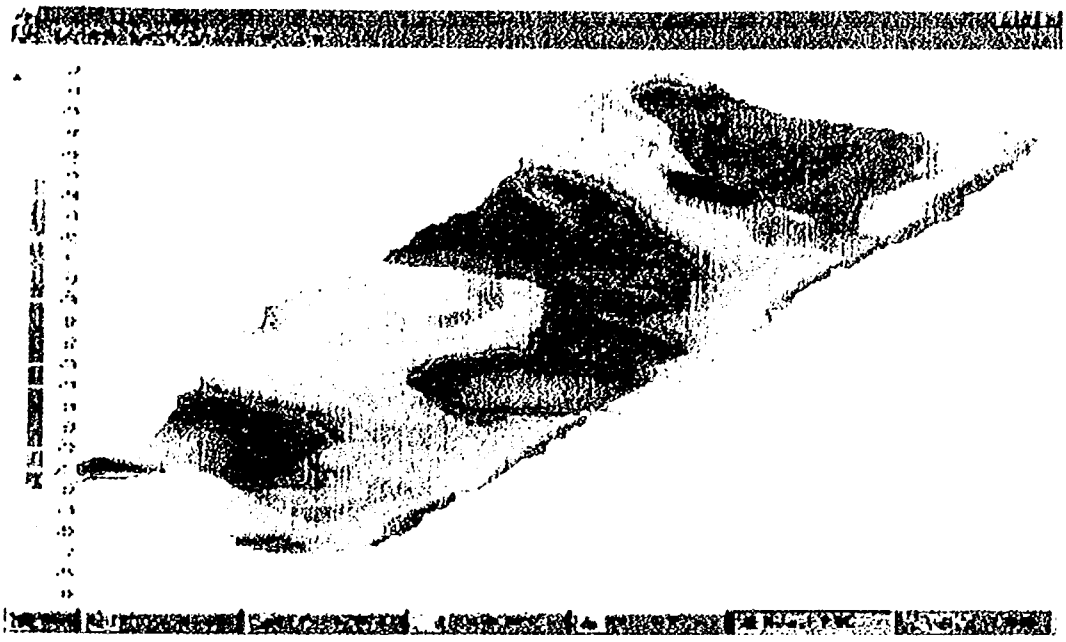


Figure 5: TIN Menu in HYPACK

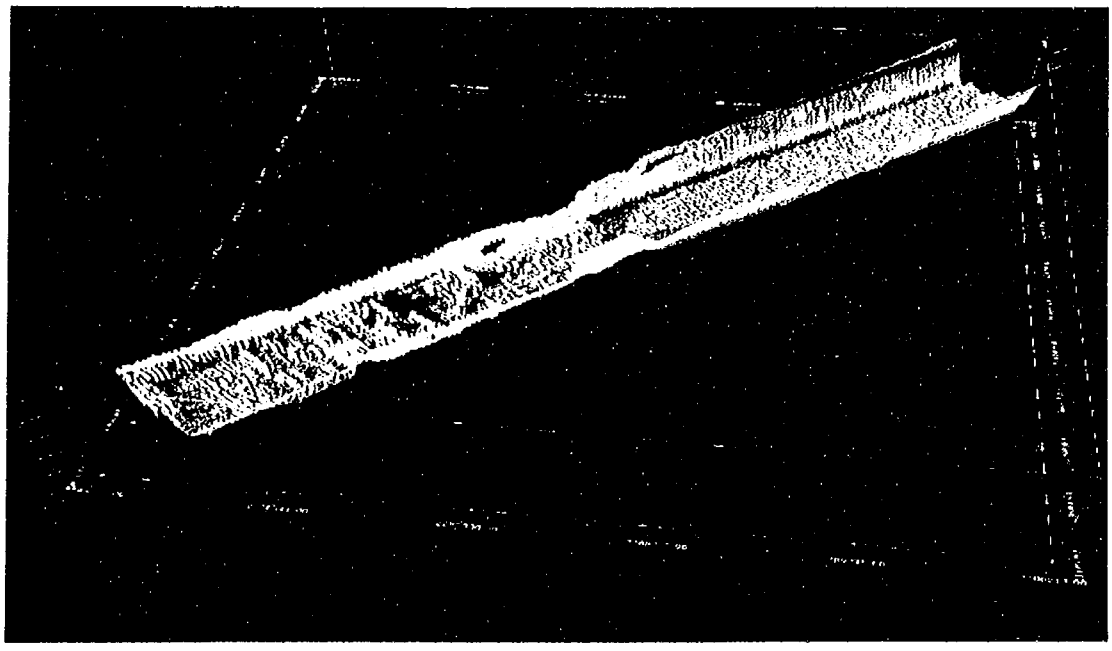


Figure 6: Wilmington Channel, Cape Fear River, NC

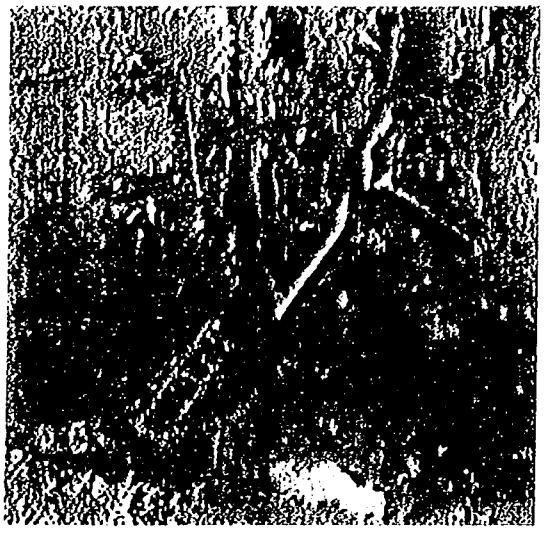


Figure 7: Lakewood, CA, Beginning of Circus Set Up

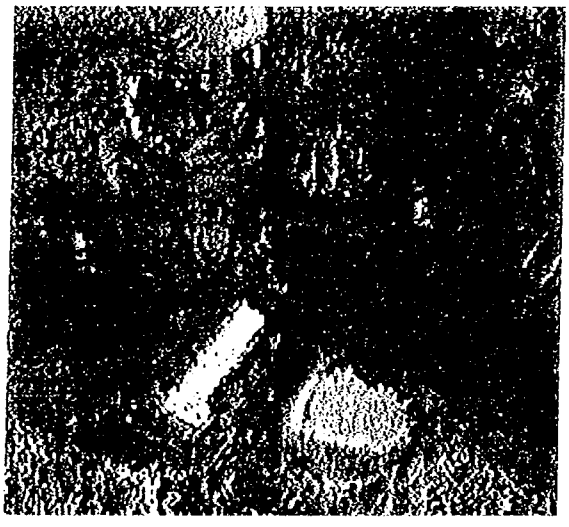


Figure 8: Lakewood, CA, with Tent & Other Attraction in Operation

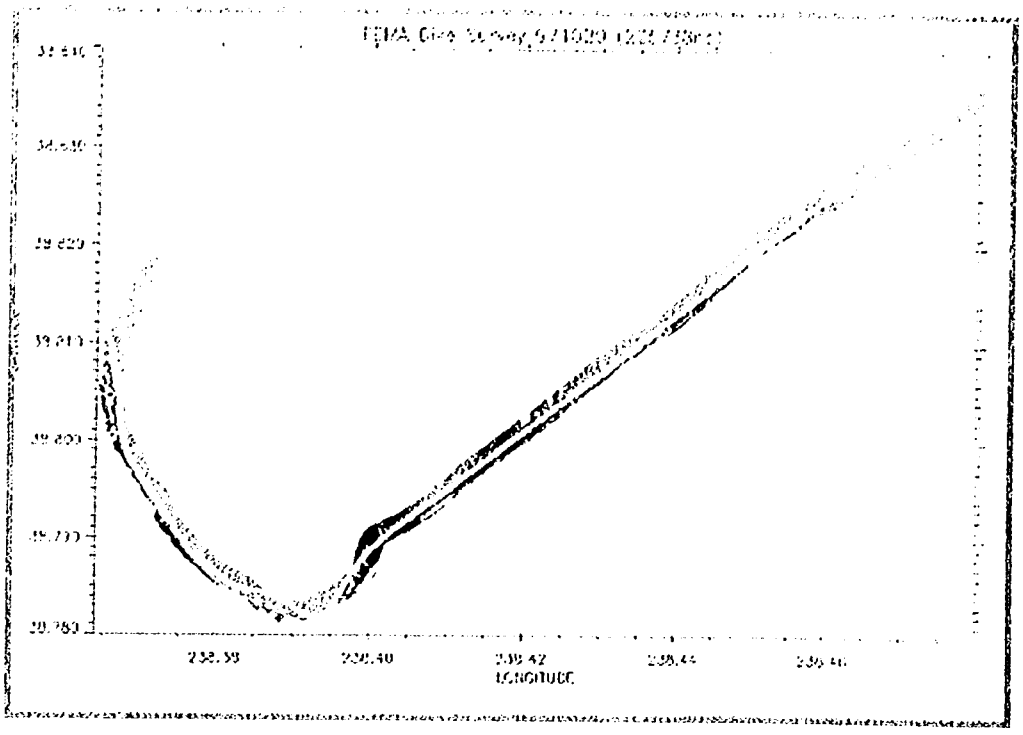


Figure 9: Portion of JPL LIDAR Collection Over Levees in the Sacramento Valley



Figure 10: DEM (Meling Orange Grove, CA)

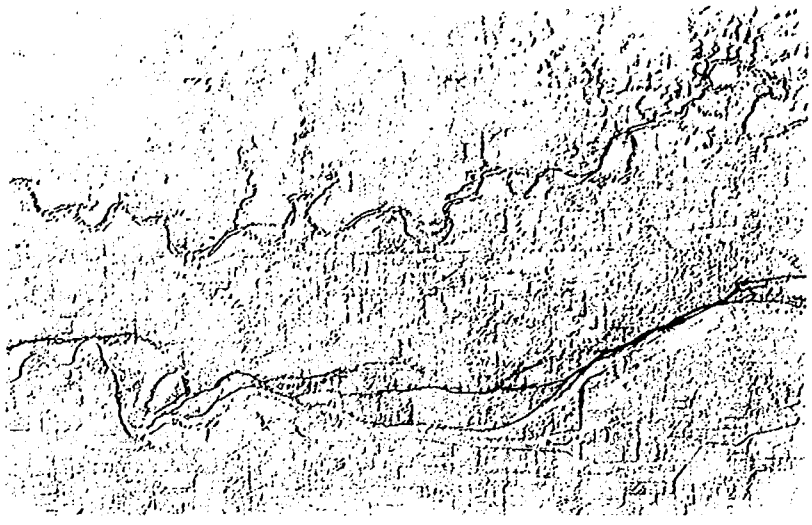


Figure 11: San Joaquin Valley IFSAR DEM

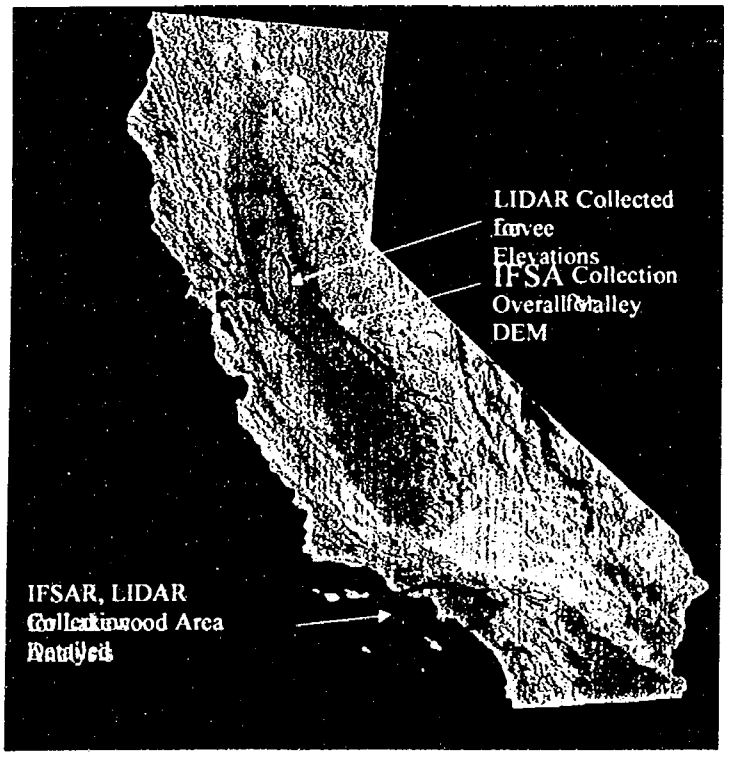


Figure 12: The California Test Areas

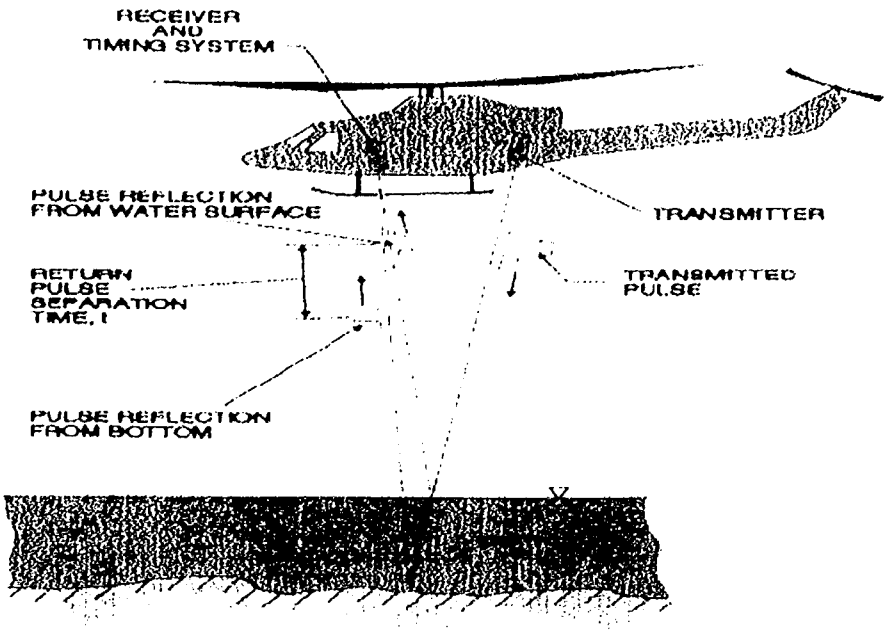


Figure 13: Overview of Operating Principles for SHOALS

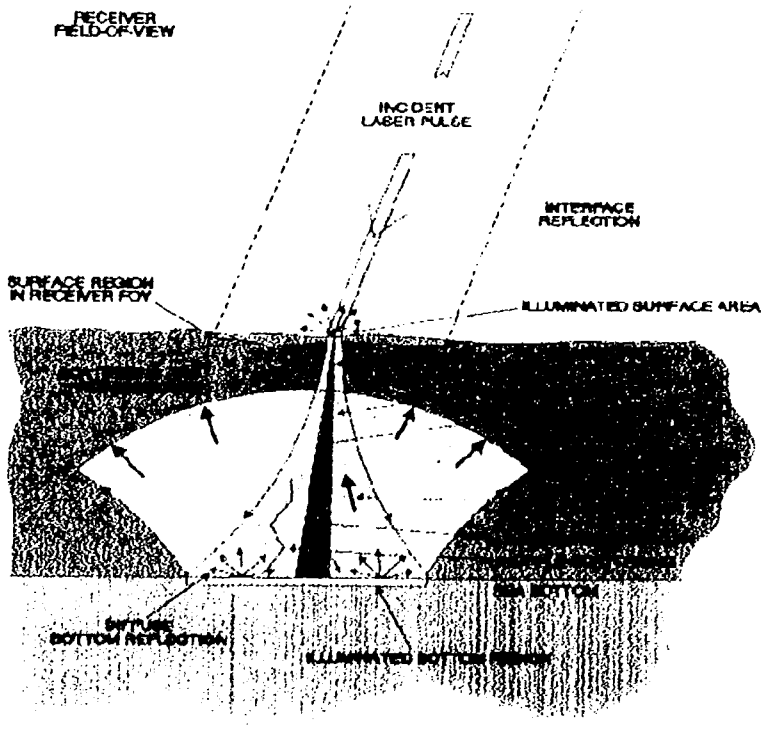


Figure 14: Water Surface and Bottom Reflection Relationships

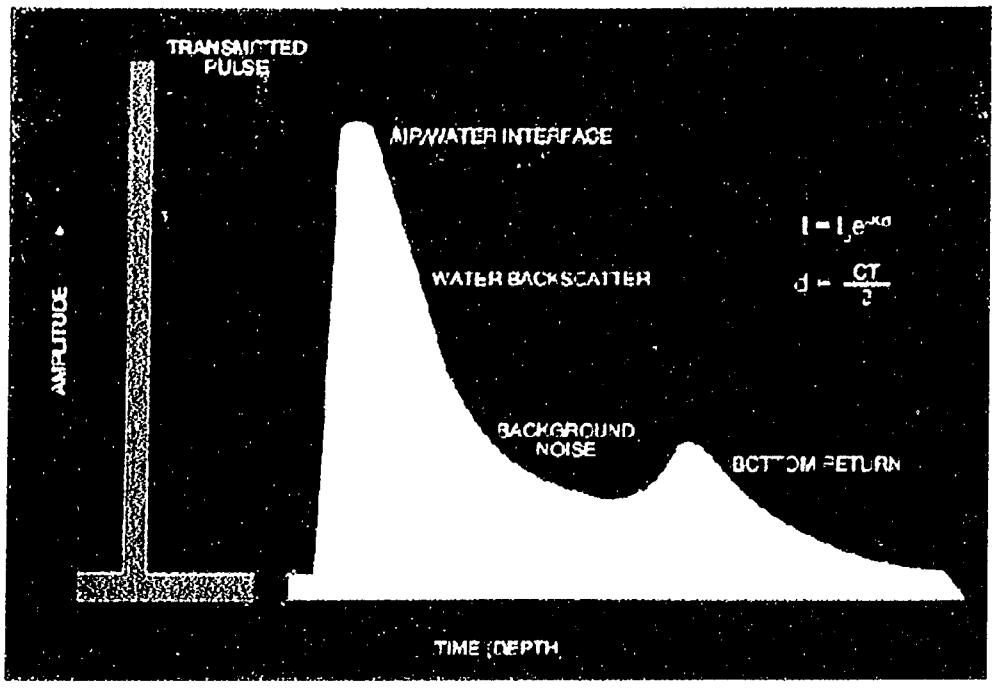


Figure 15: Typical Data Output Characteristics of SHOALS

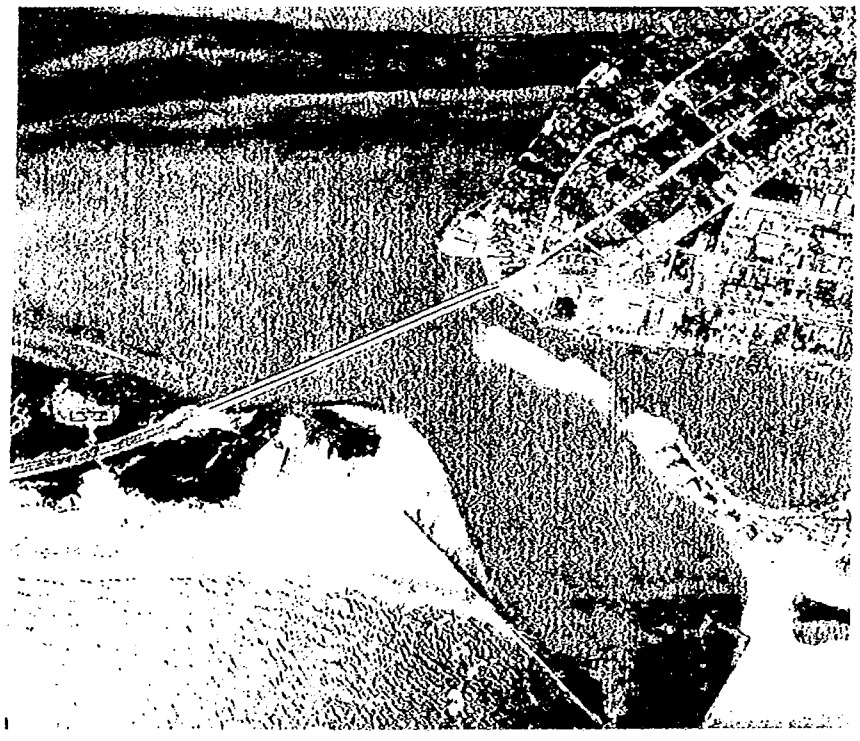


Figure 16: Aerial Photograph of East Pass After Hurricane Opal (north is to the top)

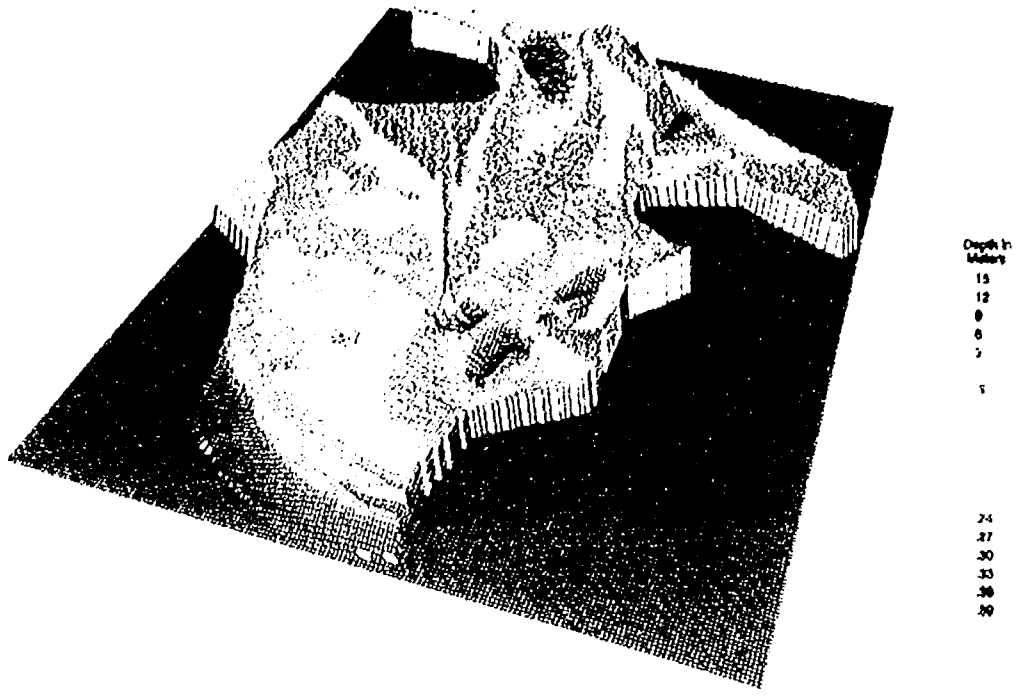


Figure 17: Elevation Plot of SHOALS Data at East Pass, Florida

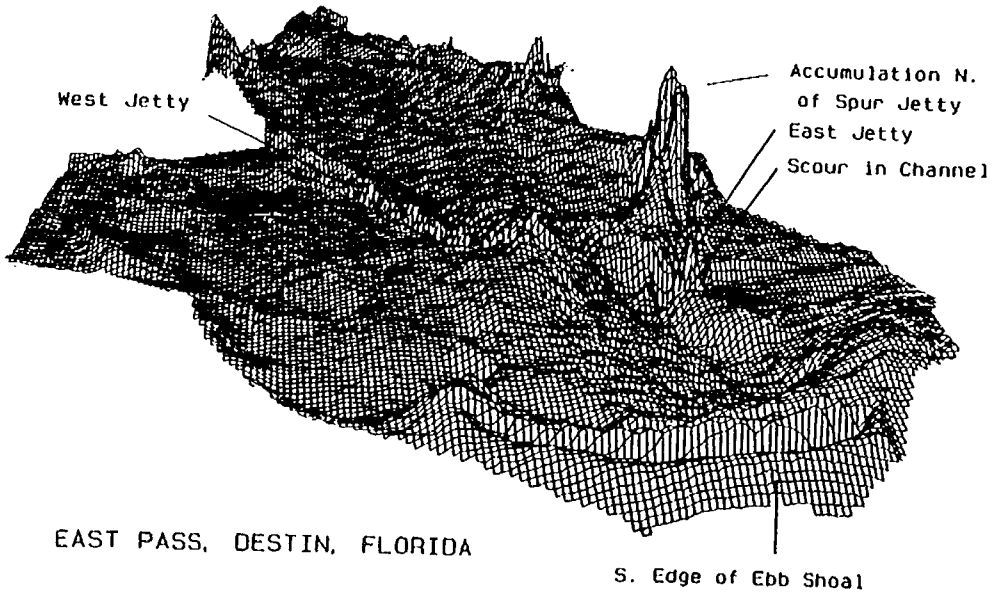


Figure 18: Sea Floor Elevation Changes Between 1990 and 1995 at East Pass

Vertical Accuracy	• +/- 15 cm
Horizontal Accuracy	• +/- 3 m
Depth Range	• maximum 60 m
Sounding Density	• 4 m x 4 m (variable)
Aircraft	• Bell 212 helicopter, Twin Otter fixed wing
Speed	• 20<v<120 knots
Altitude	• 200m<alt<800m
Data Processing	• 1:1

Table 1: Performance Specifications for the SHOALS System

Hurricane Mitch Recovery

By

William E. Roper[1]

ABSTRACT

The characteristics of Hurricane Mitch, the most destructive storm in the Atlantic Basin in the past 200 years, are described. A summary of Mitch's impact on Central America, including its path and impact on people, infrastructure and the environment are presented. Initial recovery efforts focused on saving people and opening transportation routes. That was followed by assessment of high-risk landslide areas and flood mitigation approaches. The planning approach including the use of geographic information system tools are summarized. Initial results and on-going recovery actions are reviewed.

KEYWORDS: Hurricane Mitch, flooding, flood mitigation, storm track, landslides, geographic information system, aerial photographs, mapping, remote sensing, image analysis

1.0 INTRODUCTION

In the Fall of 19978, the Caribbean Basin and surrounding Central American countries experienced the full fury of a rare level five hurricane: Mitch. From October 27 to November 1, 1998, the most destructive hurricane in the history of the Western Hemisphere hovered off the Honduran coast battering Honduras, Guatemala, Nicaragua, and El Salvador (Figure 1). Mitch's 180+ mph winds and torrential rainfall, varying from one to six feet of water in a 24-hour period, devastated major portion of these Central American countries. In the days following this natural disaster, a multi-national relief effort was launched and is still underway today. Initially, the focus was on locating and evacuating victims to safer areas and providing emergency relief supplies to them. The recovery effort soon expanded to assess the amount and type of infrastructure damage and to develop plans for restoration. In all phases, the application of remote sensing, image analysis, the global positioning system, and geographic information systems were used extensively.

2.0 HURRICANE MITCH STORM TRACK AND CHARACTERISTICS

Hurricane Mitch, the strongest October Hurricane ever recorded, formed in the southwest Caribbean sea from a tropical wave about 360 miles south of Kingston, Jamaica, late on October 21. The system initially moved slowly westward and intensified to a tropical storm (AcuWeather, 1999). Mitch then moved slowly northward. Its course changed to north-northwestward on the 23rd and 24th while gradually gaining strength. Early on October 24, Mitch became a hurricane. Later that day, as it turned towards the west, Mitch began to intensify rapidly. In about 24 hours, its central pressure dropped 52 MB to 924 MB by the afternoon of October 25. Further strengthening took place and the central pressure reached a minimum of 905 MB about 40 miles southeast of Swan Island on the afternoon of September 26. This pressure is the fourth lowest ever recorded in an Atlantic hurricane this century. It is tied with Hurricane Camille in 1969. This is

[1] Director, U.S. Army Topographic Engineering Center
7701 Telegraph Road, Alexandria, VA 22315-3864
www.tec.army.mil

also the lowest pressure ever observed in an October hurricane in the Atlantic Basin. At its peak, the maximum winds were estimated to be 180 mph, a strong Category 5 hurricane.

After passing over Swan Island, Mitch began to gradually weaken on September 27 while moving slowly west, then southwest toward the Bay Islands off the coast of Honduras. The center passed very near the Island of Guanaja wreaking havoc there. From mid-day on the 27th to early on the 29th, the minimum central pressure rose 59 MB. The center of the hurricane meandered near the north coast of Honduras from late on the 27th through the 28th before making landfall during the morning of the 29th about 70 miles east of LaCeiba with 100 MPH winds. Mitch moved southward over Honduras, weakening to a tropical storm early on the 30th. Mitch moved slowly over Honduras and Guatemala on September 30-31, gradually weakening to a depression. The storm generated torrential rains over portions of Honduras and Nicaragua where the associated floods were devastating. Some heavy rains also occurred in neighboring countries. Figure 2 shows rain bands associated with Mitch.

Although Mitch originally dissipated near the Guatemala/Southeast Mexico border Sunday afternoon, November 1. The remnants continued to produce locally heavy rainfall over portions of Central America and eastern Mexico for the next couple of days. On November 3, a low-level circulation became evident in the eastern Bay of Campeche and an Air Force Reserve reconnaissance aircraft investigating the system reported tropical storm-force winds and a 99 MB central pressure. Mitch had regenerated into a tropical storm on the afternoon of the 3rd while located about 55 miles west-southwest of Campeche, Mexico. Mitch weakened to a depression early on the 4th as it moved inland over the northwest Yucatan Peninsula. The center re-emerged over the south central Gulf of Mexico by mid-morning on the 4th regaining tropical storm strength. Mitch began to accelerate to the northeast as it became involved with a frontal zone moving through the aster Gulf of Mexico. Mitch made landfall on the morning of the 5th in southwest Florida near Naples with maximum sustained winds near 60 MPH. By mid-afternoon of the 5th, Mitch moved offshore of south Florida and became extratropical. Figure 3 shows the storm track of Hurricane Mitch.

3.0 IMPACTS ON CENTRAL AMERICA

Hurricane Mitch, which has been called the deadliest Atlantic storm since the eighteenth century, carved a week-long path of destruction through Honduras, Nicaragua, El Salvador, Guatemala and Belize. A quote from Daniel Alegria, a reporter for Orfam GB of Nicaragua: "Imagine your worst nightmare. Imagine waking up to something a hundred times worse." Latest reports of the human costs are staggering:

- More than 18,000 people are dead or missing.
- One million homes have been lost.
- More than three million people have lost their livelihoods.

Much of the transportation and communications infrastructure of Honduras and Nicaragua was devastated. In addition to the roads buried by landslides or washed away by floods, towers and bridges were destroyed (Figures 4, 5 6, and 7). Out of 94 known bridges in Honduras, 88 were either destroyed or damaged beyond use.

The crater of Honduran Volcano Casita became rain saturated from the monumental rainfall, causing the southern slopes to slide down the hillside as avalanches of mud, forty feet tall, at sixty miles per hour. Multiple devastating mudslides swept into nearby communities, killing 1900 people. Mudslides reached the town of Posoltega, almost ten miles away from the volcano (Figure 7). The landscape of the entire nation of Honduras has drastically changed—more soil, rock, and sediment was moved in these few days than in the last several hundred years (Collier, 1999).

Of special concern is the severe destruction of the public health infrastructure coupled with

severe flooding which has generated favorable conditions for widespread gastrointestinal and respiratory diseases and increased frequency of vector-borne diseases. Respiratory, diarrhea and skin diseases, along with eye infections can spread rapidly in large segments of the population left without homes, water, hygiene and sewage disposal. In southern Honduras, extensive flooding destroyed two pesticide factories containing over 400 barrels of pesticides and other industrial and agricultural chemicals. In Nicaragua, a large number of cases of respiratory infections, dengue, childhood diarrhea and leptopirosis were reported. Major health concerns continue to face the survivors of the flooding and mudslides.

4.0 GEOSPATIAL SUPPORT OF RECOVERY ACTIVITIES

4.1 Initial Emergency Response Efforts

U.S. military forces were some of the first international support units on the ground conducting recovery operations. As a result, a number of requirements for geospatial products were identified early in the operation (Operations Summary, January 1999).

In support of these requests maps, country studies, water areal appraisals and other available materials were collected and provided to the U.S. Army Corps of Engineers (USACE) Operations Center for use in immediate recovery operations, planning any additional deployments and future reconstruction efforts.

Separate requests for ground water resource data were received from support elements of the Second Mare Expeditionary Force and two Air Force Red Horse Squadrons (well drilling units) in Honduras. Maps and water areal appraisals were provided to two Marine Expeditionary Forces. Water detection data was also provided to the Air Force unit.

Initial analytical activities focused on assessing road and bridge damage in Honduras. Satellite imagery was reviewed and road and bridge assessment data were tabulated and served over the communication links. These data were keyed to a regional map, provided by the National Imagery and Mapping Agency (NIMA), to which a grid was added as an orientation aid for the user (Figure 9).

Photo maps of the Soto Cano Air Base and a slide area along the Chaluteca River in Tegucigalpa were also prepared and provided to the Army Corps of Engineers Operations Center.

The 30th Engineer Battalion, also in Honduras, requested specific Digital Topographic Data, and loan of high-capacity hard drives to process data. The Topographic Engineering Center imbedded current imagery data on the affected areas onto 14 CDs and provided them to the 30th Engineers. These CDs contained landsat and Spot imagery.

4.2 Joint Government and Private Sector Support

A cooperative effort of U.S. Government agencies and the private sector developed a Digital Atlas of Central America to assist in recovery efforts and planning for reconstruction. The geographic information sytem (GIS) based product provided a framework for displaying and organizing information in multiple layers useful to those responding to the disaster. Figure 10 is a sample product showing the path of Hurricane Mitch over a map with country boundaries and terrain elevation color coding (Digital Atlas, January 1999).

4.3 Geospatial Technology Applications

For the initial reconstruction phase, a number of geospatial products are needed to enhance planning and project execution (Heam, February, 1999). Some of these information products include:

4.3.1 Topographic Base Maps

Virtually all activities associated with the reconstruction effort required large-scale (high-resolution) base maps showing topography, drainage, and the location of roads, bridges, and

other infrastructure. This included 1:50,000 scale (I inch – 4000 feet) topographic maps in digital form – scanned and provided on CD-ROM with software to view and print the maps. In their simplest form, paper copies of these maps could be produced at data centers in Honduras and distributed to Honduran agencies, municipalities, and other agencies. The digital maps were also "georeferenced," so that when read by GIS software, precise geographic coordinates could be determined for any point on a map. Similarly, additional data or observations having geographic coordinates were added to the base map in a GIS. It is also important that hand-held Global Positioning System (GPS) units be available to allow USAID and Honduran agencies to readily determine location on the ground and be able to relate directly to map information.

4.2.2 Aerial Photography and Satellite Imagery

While base maps are essential to provide a geographic frame of reference, the information they contain is only as current as the date of the maps' publication. The best alternative to extensive observations on the ground is acquiring imagery of priority areas from satellites or aircraft. For large areas (e.g., agricultural areas), assessing the impact of floods and landslides was best done using medium-resolution satellite imagery. Landsat TM imagery provides 30 meter resolution and the ability to detect subtle differences in vegetation and ground cover. The highest-resolution and most convenient source of imagery for assessing dame to infrastructure was aerial photography. Aerial photographs allow rapid identification and assessment of damage infrastructure and can be used to prioritize and plan reconstruction activities. Photography acquired by the U.S. Air Force's Open Skies Program was available for most of the areas impacted by Mitch. The goal is to digitize and make available all existing photography for 123 municipal areas. Additional photography may be required for Tegucigalpa and other sites where there is either no coverage or where existing imagery is not acceptable due to cloud cover.

4.3.2 Geographic Information Systems (GIS)

GIS technologies allow base maps, imagery, data from landslide and flood risk assessments, water-quality data, site-reports, an other information to be integrated into comprehensive data bases that provide the same geographic frame of reference (Figure 11). For example, combining estimated floodplain boundaries with maps an aerial photography allows derivative maps to be quickly produced showing recommended no-build areas. Similarly, integration of base maps, satellite imagery, and ground-based observations in a GIS would allow rapid assessment of flood damage to agricultural areas. For this interim effort, a comprehensive GIS of Tegucigalpa at 1:10,000 scale, will be developed and technical assistance will also be required for the Honduran agencies.

4.3.3 Assessment of Landslide Hazards

Mitch-related landslides and flooding in Honduras were intricately interrelated, and the two processes interacted with each other in numerous places (Figure 12). Many of the landslides that caused loss of life and property were caused by stream-bank erosion and, conversely, major flooding was also triggered by landslide damming of rivers. Agricultural lands, population centers, transpiration corridors, and engineered structures such as dams and ports have been severely impacted by landslides and fluvial processes. USACE is assisting USAID and Honduran authorities with mapping and topographic analysis and evaluation of landslides affecting critical populated areas, facilities, transportation corridors, and engineered structures to assist authorities in the assessment of mitigation options.

5.0 RECONSTRUCTION IN THE AREA OF TEGUCIGALPA, HONDURAS

One of the large urban areas hardest hit by Hurricane Mitch in Honduras was the city of Tegucigalpa. The creation of a natural dam by

massive sediment deposits from the flooded Rio Choluteca Rier within the city limits is of particular concern with the fast approaching rainy season. Also a major landslide during Mitch has left a large area of unstable ground immediately above the city. Figure 13 is an airborne image of the landslide area, and Figure 14 is a GIS layered data base illustrating the area of unstable earth (Digital Atlas, 1999).

Because of the vulnerability of the city of Tegucigalpa to additional flooding and landslides during the upcoming rainy season and the limited time available to put protection measures in place; the majority of the effort in developing this action plans was placed on the short-term phase. The long-tern solutions to the flooding and landslides are conceptual at this time and will require substantial data gathering and engineering analysis to determine the most cost-effective solutions.

5.1 Short Term Phase

The short-term solutions are divided into five areas: 1. Restrict the use of the floodplain and landslides areas; 2. Clear and excavate the Rio Choluteca channel at the El Berrinche site; 3. Stabilize the El Berrinche an El Reparto landslides; 4. Repair broken sewer collection system near the river; and 5. Initiate topographic surveys and subsurface exploration of the slides and river channel (Duffy, April, 1999).

5.1.1 Restriction of Land Use

Government of Honduras/City of Tegucigalpa should condemn the properties on the landslide and in the floodplain, and should relocate the residents to an approved reconstruction site. Strict land use plans must be developed, implemented, and enforced by the city. To implement this action, relocation sites must be identified; water, electrical and sewerage infrastructure must be developed at the relocation sites, and the relocated property owners must be compensated for their losses of property due to condemnation.

This is the simplest, most direct action that can be taken to reduce the potential for loss of life and property resulting from flooding or landslides. However, politically it may be the most difficult to implement. The government institutions in Honduras and the City of Tegucigalpa must demonstrate the will to develop and implement this action. The City and Government of Honduras should clearly announce there would be no indemnification of losses in the future for those who build in these no-build areas. The costs associated with this action reflect the cost to acquire the relocation site, develop the site access, water and sewer systems. Also included in the cost is the compensation to the property owners for the loss of their property on the landslide or in the floodplain.

5.1.2. Clearing and Excavating the Rio Choluteca Channel

Excavate the Rio Choluteca channel to restore as much channel capacity as possible prior to the onset of the rainy season. The primary focus of this effort will be the El Berrinche landslide site since this is a choke point for the Rio Choluteca. The channel capacity will be increased by removing landslide material and by removing structures along the street parallel to the river. Excavated material will be disposed of in an area outside of the floodplain. Some of the building materials resulting from the demolition of the gymnasium and other structures will be used to protect the toe of the landslide from erosion during the upcoming rains (Preliminary Action Plan, February, 1999).

It is believed that some excavation can be performed at the toe of the El Barrinche slide prior to conducting a geotechnical investigation without undue risk of causing further movement of the slide. However, due to the scarcity of survey data, the initial excavation amounts cannot be accurately determined. Therefore, the initial excavation will be directed in the field, with a series of slopes and berms approximately twenty feet in height.

5.1.2 Stabilize the Landslide Sites

The El Berrinche and El Reparto landslides will be re-graded to seal open cracks, improve drainage and reinforce the toe of the slope. A waterproof membrane will be installed near the tope of the slide to prevent rain from entering the slide mass.

Stabilizing the landslide can best be accomplished by preventing water from entering the landmass during the rainy season. This will prevent the landslide mass from becoming saturated and unstable. Preventing water from entering the landslide can be accomplished by grading the upper portion of the slide to allow rain falling on the slide to flow on the surface and down to the river without penetrating the land mass. Installing a waterproof membrane, similar to that used to line landfills and ponds, near the top edge of the slide can further enhance this. If this is done, steps must be taken to prevent the membrane from being removed (stolen) and restrictions must be enforced to prevent human activities on the membrane and sloped areas.

5.1.3 Repair Sewers

Repair the major breaks in the sewage collection system along the Rio Choluteca near the El Berrinche site.

Raw sewage is draining into the river channel from the sewer collection system. Many breaks were experienced during the flood and landslide creating a highly unsanitary situation after the storm. The work will involve repairing as many of the breaks as possible during the time prior to the rainy season to reduce the amount of sewage entering the river near the city. The repair work will concentrate on the main collection system located near the river.

5.1.4 Initiate Surveys and Subsurface Explorations

Develop topographic and subsurface information for use by the engineers to develop long-term solutions to the flooding and landslide problems. Acquire the topographic survey, prepare risk-zone maps, install river-monitoring system and establish control point to monitor slide movements. The most important information needed for an engineering analysis of the flooding and landslide problems is topographic and subsurface data. Without this information, very little engineering can be accomplished with any assurance that the solutions are viable. It is recommended to initiate these actions as part of the short-term actions since the data is critical to any follow-on engineering activities.

5.2 Long Term Phase

5.2.1 Data Collection and Analysis and Recommendations

A detailed analysis is used to address the long-term solutions to the flooding and landslides associated with the Rio Choluteca in the vicinity of Tegucigalpa. This will require comprehensive data collection and analysis of the water resource problems, subsurface conditions an infrastructure needs including the following:

A. Hydrologic and hydraulic investigation
B. Determine proper flow relief for bridges
C. Landslide recovery
D. Sedimentation analyses to estimate production of sediment and movement of sediment in the floodplain
E. Develop mapping to delineate the 100-year floodplain
F. Analysis of alternative solutions to flooding problems including levees, channel modification, stream bank stabilization, multi-reservoirs, and other options.

It is estimated to take three years to complete these actions. Once these investigations are complete, design and construction of the most effective and efficient measures can begin.

5.2.2 Tegucigalpa Sewer System

A study is required to determine the cost of providing a sanitary sewer system to serve the

City of Tegucigalpa. The study would involve sending a two-man team to Tegucigalpa for a period of 30 days to gather information. Topographic maps and existing sewer system plans would be reviewed. The service area and potential locations of the treatment plant should be addressed on this initial site visit. After making the site visit, the report should be prepared. The report should provide a plan showing the preliminary layout of the sewage collection system, pumping station locations, and location/alternate locations for the treatment plant. The report would address alternate treatment plant processes and the reason for selecting a particular process. The report would be coordinated with city officials and three design review meetings would be held at Teguigalpa. It is estimated that the report would take 12 months to prepare.

6.0 CONCLUSIONS

Hurricane Mitch was a natural disaster of epic proportion to Central America. The recovery and reconstruction efforts have also been of a magnitude not encountered before in that region. For the first time in a major disaster, extensive application of geospatial technology was used to assist in all phases of the recovery. A digital atlas and Geographic Information System was created for the impacted area to form a framework to integrate new data and information over time in a systematic manner. Satellite, aircraft, and ground information sources were used to collect data and information to support the recovery activities. A variety of products were successfully generated tailored to user needs in the field and higher level decisionmakers in the recovery effort.

7.0 REFERENCES

Atlantic Hurricane Summaries, 1998, AccuWeather Service, April, 1999

Collier, Vincent, Hurricane Mitch Summary Report, U.S. Army Topographic Engineering Center, March, 1999

Diffy, Michael E., Plan for Short-term Landslide and Flood Mitigation Measures in Central America, Headquarters, U.S. Army Corps of Engineers, April 1, 1999

Digital Atlas of Central American, Version 1.0, Center for Integration of Natural Disaster Information, U.S. Geological Survey, January, 1999

Heam, Paul, Short-term Plan for the Mitigation of Risk from Flooding and Landslides, U.S. Geological Survey, February 10, 1999

Hurricane Mitch Flood Assessments, Dartmouth College, Hanover, New Hampshire, November, 1998

Operations Summary, Interagency Support to Hurricane Mitch Reconstruction, U.S. Army Corps of Engineers, January 25, 1999

Preliminary Action Plan for the City of Tegucigalpa in the Aftermath of Hurricane Mitch, U.S. Army Corps of Engineers, February 10, 1999

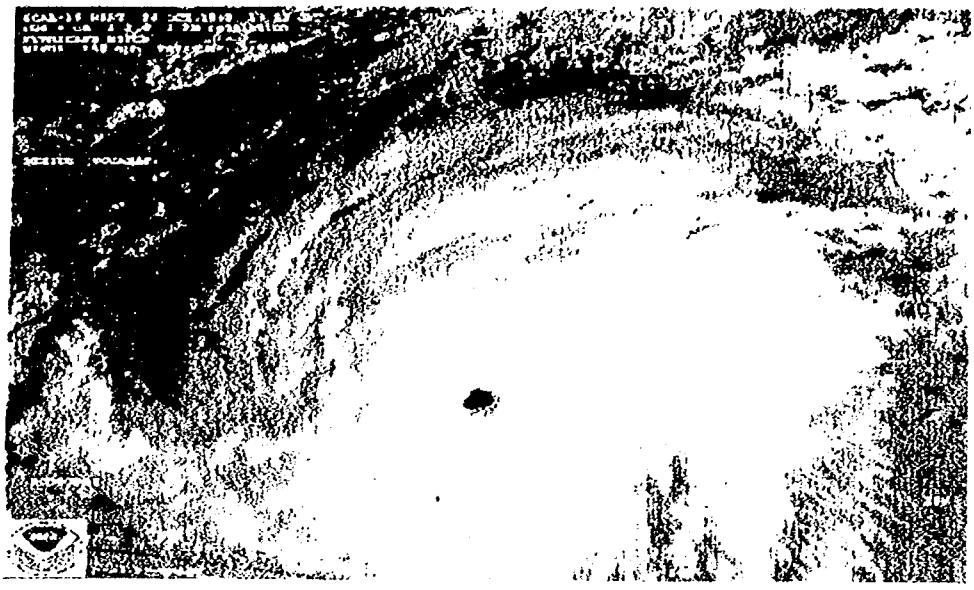


Figure 1: Visual Image of Hurricane Mitch
October , 1999

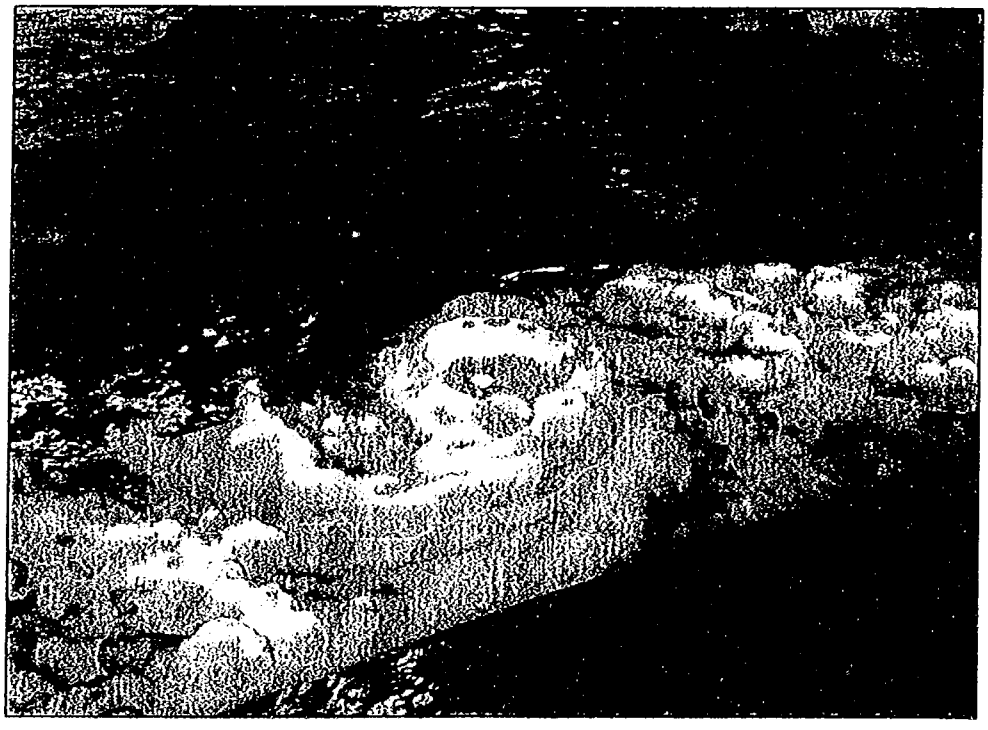


Figure 2: NASA Rain Density Model of Hurricane Mitch

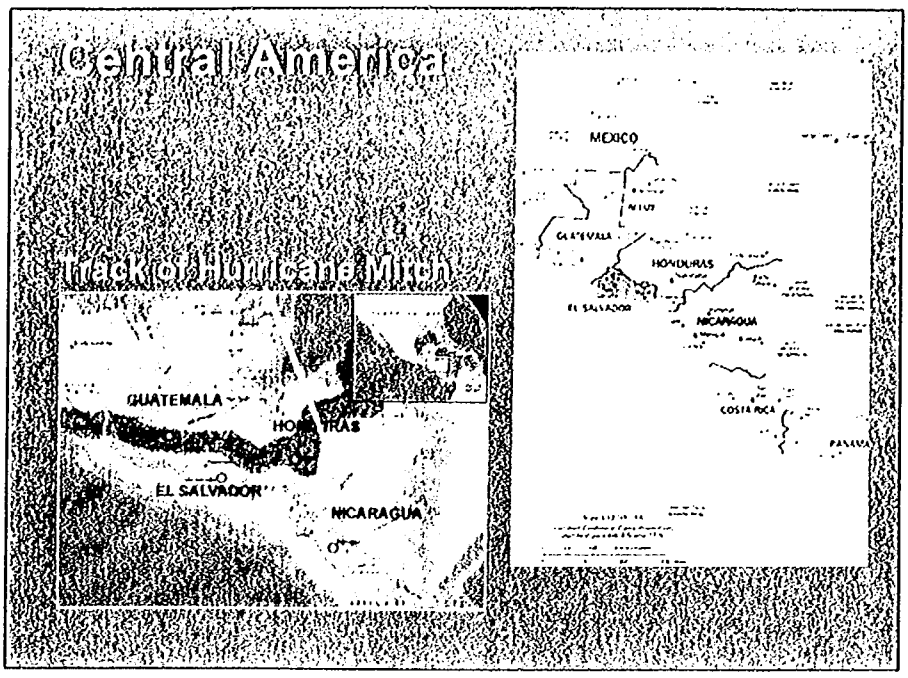


Figure 3: Storm Track of Hurricane Mitch

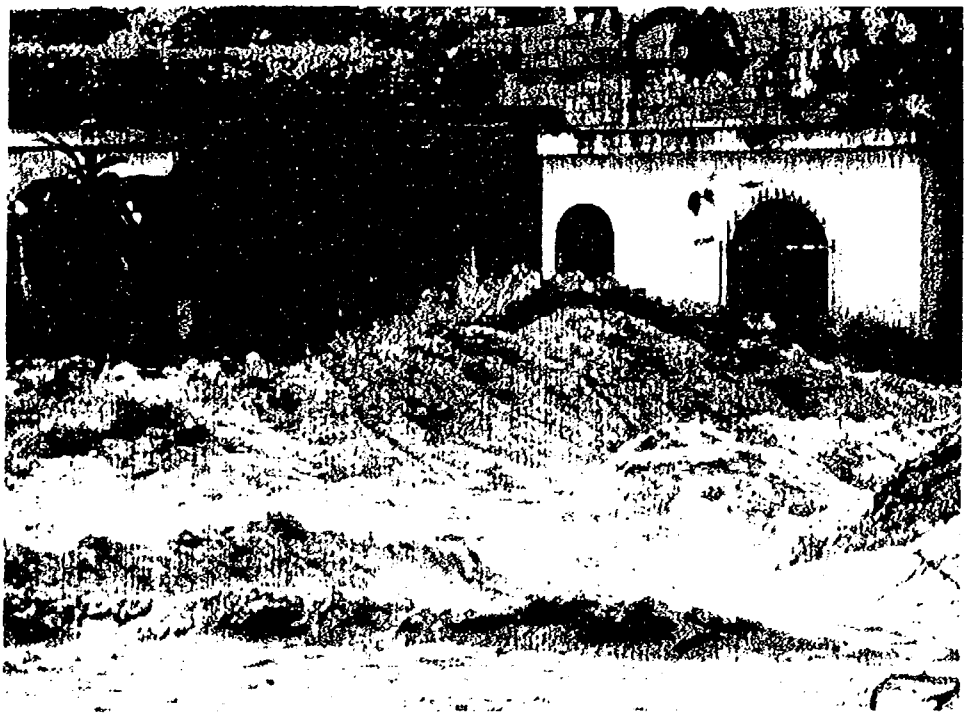


Figure 4: Flooding Along the Matagua River in Gualan County, Guatemala October 31, 1998



Figure 5: Flood Damaged Bridge and Road in Honduras

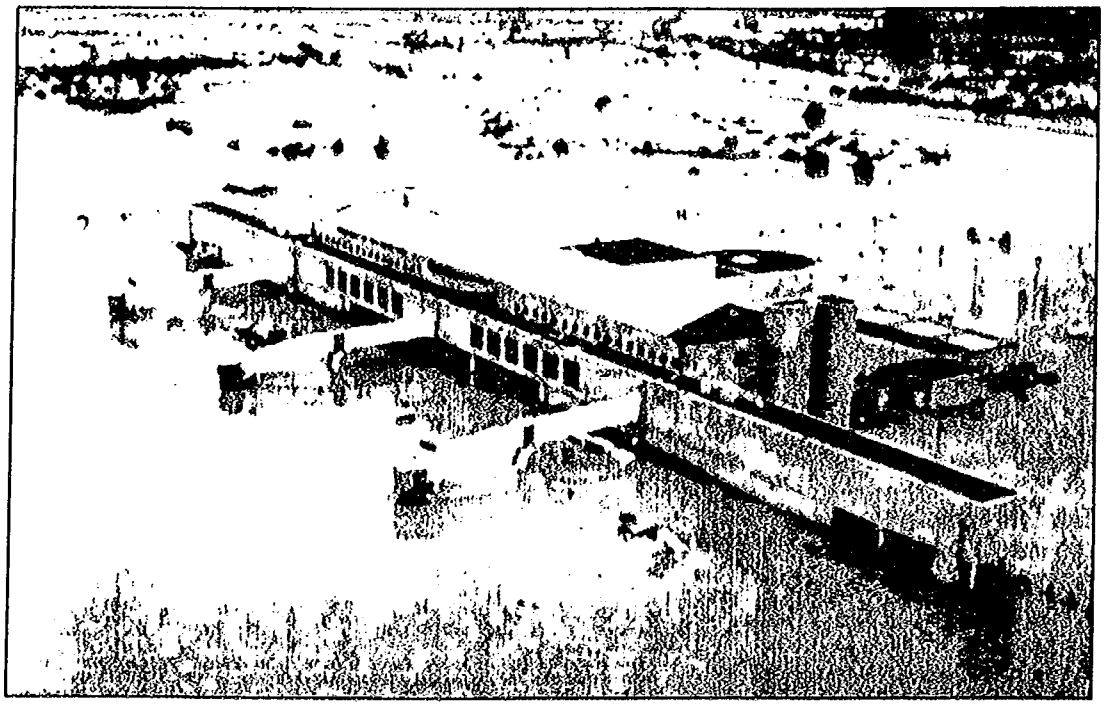


Figure 6: Flooded San Pedro Sula Airport, Honduras

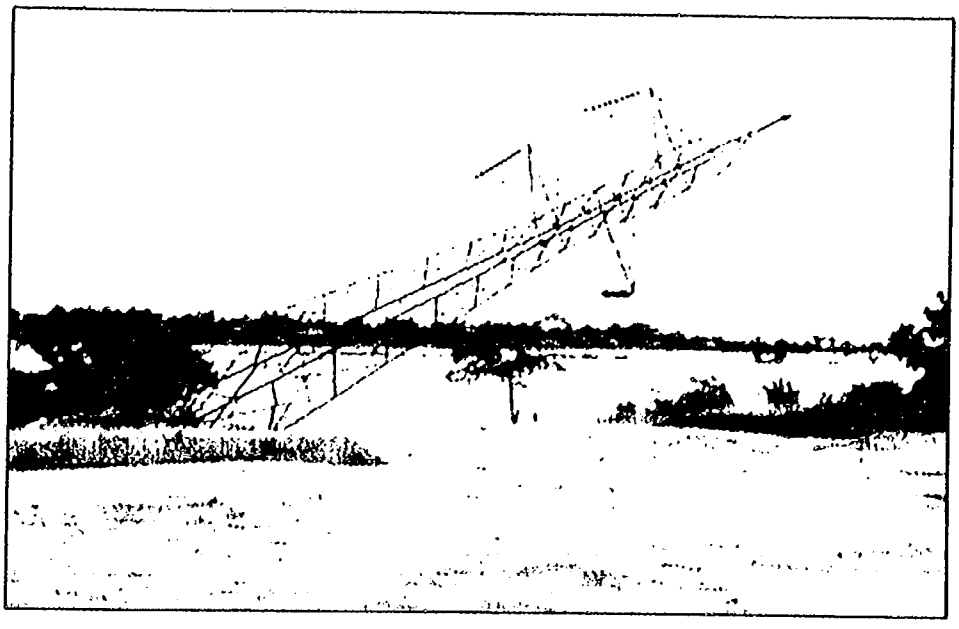


Figure 7: Damaged High Voltage Transmission Line on the Choluteca River

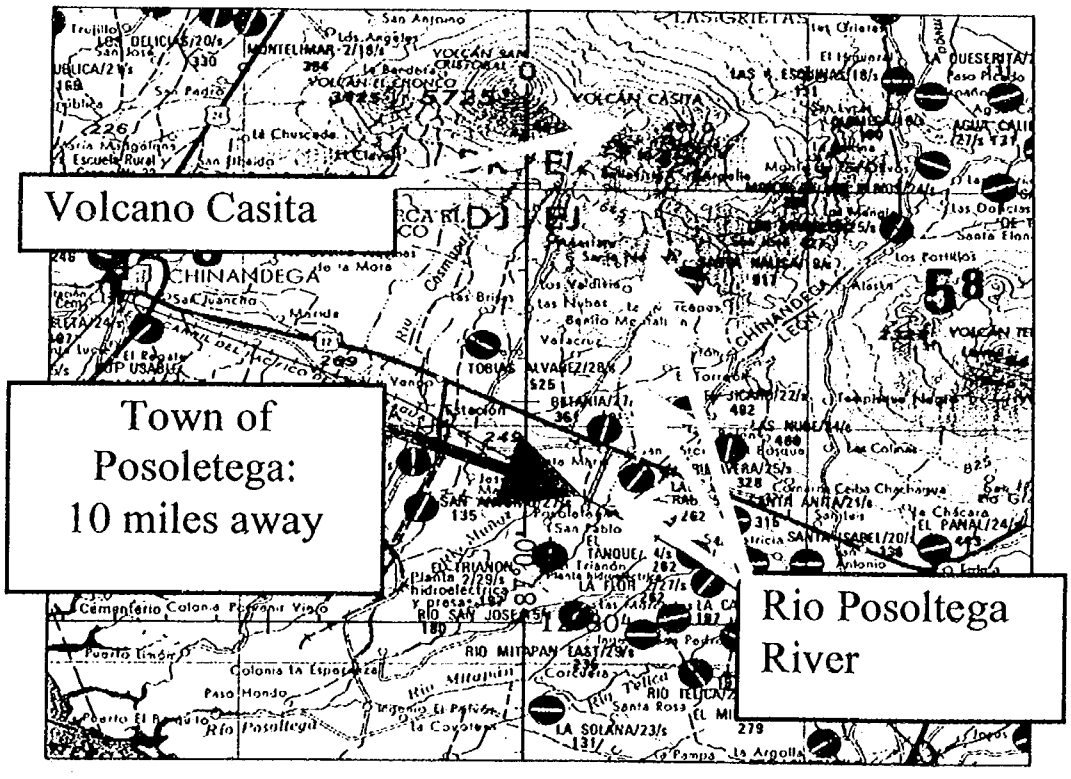


Figure 8: Map Showing Location of Landslide to Posoletega

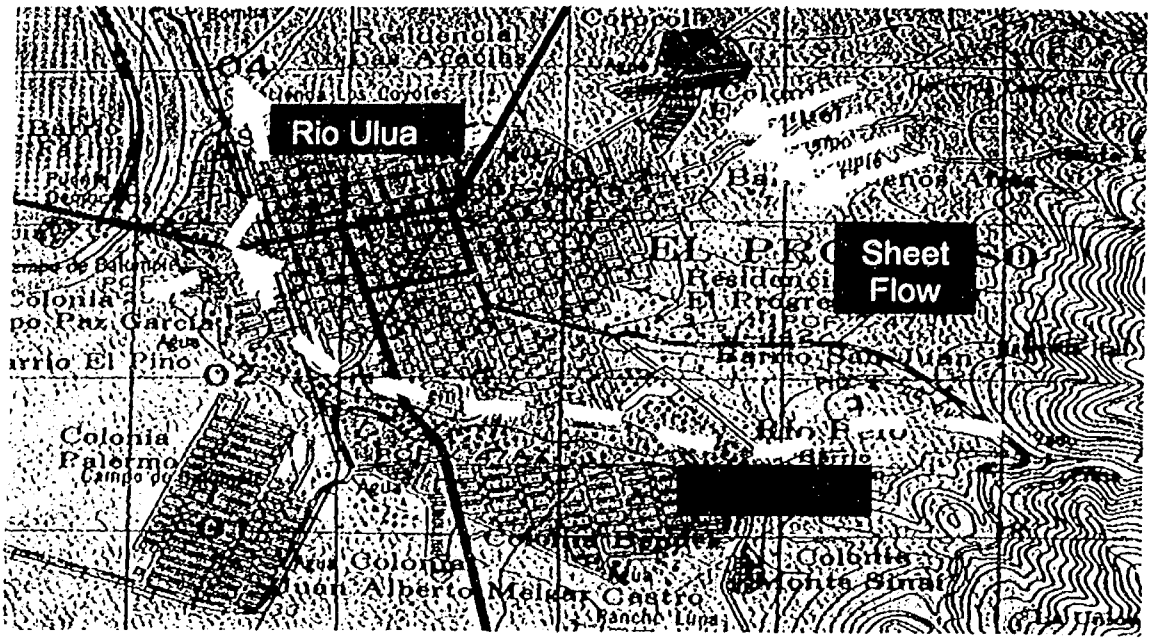


Figure 9: Road and Bridge Assessment Map

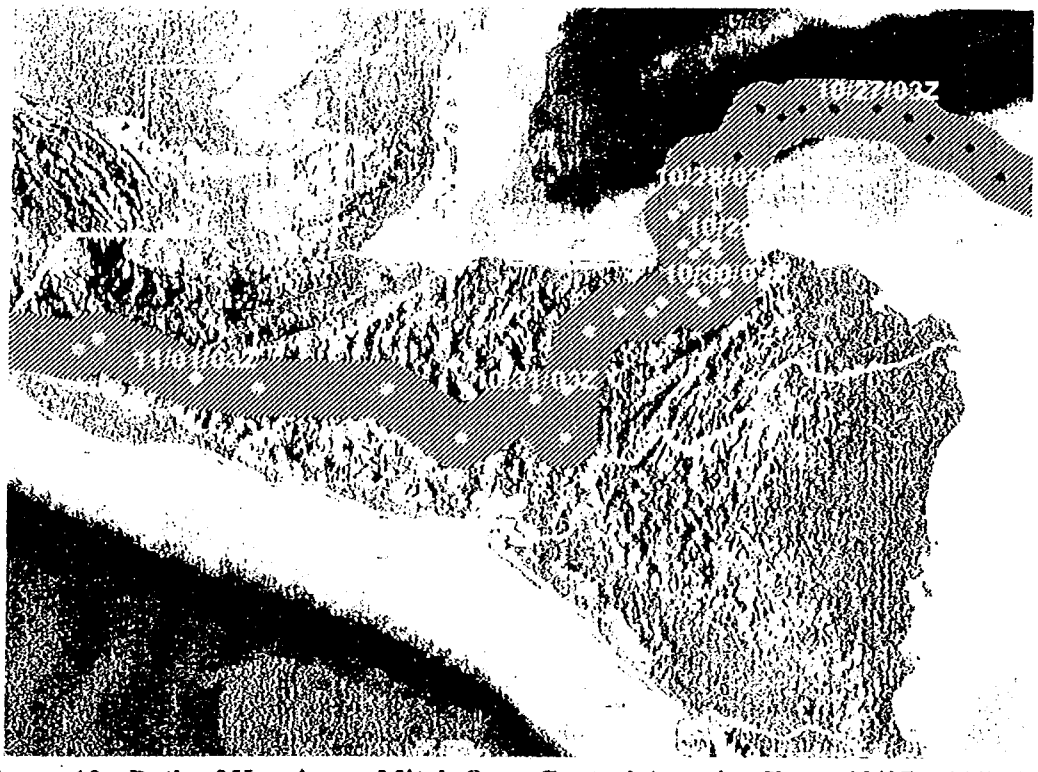


Figure 10: Path of Hurricane Mitch Over Central America From 10/27 – 11/01/98

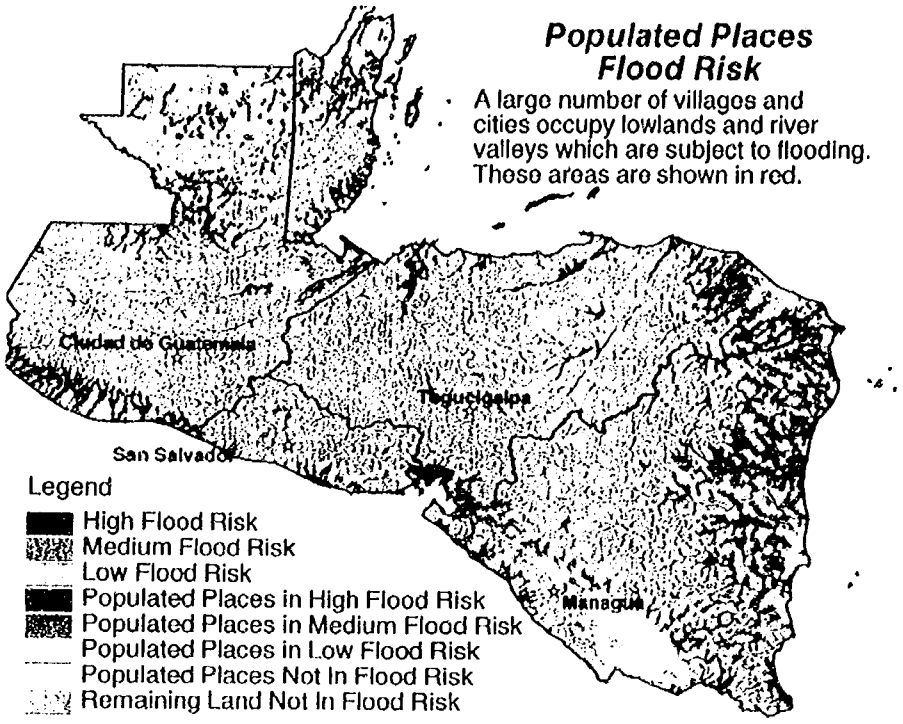


Figure 11: GIS Composite Product Showing Flood Risk in Populated Areas (Digital Atlas, January, 1999)



Figure 12: Landslide Damage to Bridge in Honduras



Figure 13: Image of El Berrinche Landslides in Tegucigalpa



Figure 14: GIS Overlay Showing Location of Landslide Areas

EARLY ESTIMATION SYSTEM FOR EARTHQUAKE DISASTERS

by

Takaharu Kiriyama[1] and Kazuo Okayama[2]

ABSTRACT

Out of the lessons learned from the Hanshin - Awaji Earthquake, the National Land Agency is developing a Disaster Information System (DIS) that can categorize and analyze information on earthquake disasters using a Geographic Information System (GIS). As one of the subsystems of this DIS is Early Estimation System (EES), which estimates the amount of damage immediately following an earthquake, in a short period of time. One such subsystem has been running since 1996. This paper gives an overview of the EES and explains how estimates are made.

Keywords: Damage Estimation,
Early Estimation
Estimate Method
Operation Record

1. OVERVIEW OF THE DISASTER INFORMATION SYSTEM

The Hanshin - Awaji Earthquake of January 17, 1995, taught us the importance of prompt emergency actions taken by disaster prevention organizations after an earthquake and especially the importance of finding out the state of damage suffered at as early a point as possible.

Based on the Hanshin - Awaji Earthquake experience, the National Land Agency started developing a Disaster Information System (DIS) that can categorize and analyze information on earthquake disasters using a Geographic Information System (GIS), with the objective of providing support to governments in making an initial response and taking emergency actions in the event of an earthquake. Subsystems of the DIS include an Early Estimation System (EES) which quickly provides a rough estimate of the scale of damage immediately after an earthquake has occurred, and an Emergency Measures Support System (EMS) that displays disaster and damage information on a digital map to support authorities in planning emergency actions.

The National Land Agency began development on the DIS in 1995 and the EES has been in operation since 1996. As for the EMS, development is currently underway for a scheduled start of partial operation in 1999.

2. OVERVIEW OF THE EARLY ESTIMATION SYSTEM

In a short amount of time after an earthquake, when information is scarce and limited, the EES gives a rough estimate of the scale of damage. EES aims at providing authorities with the information needed to make swift, correct decisions on establishment of a disaster countermeasure headquarters, emergency actions to be taken, etc.

A flowchart of how estimates are made with the EES is shown in Fig. 1. The system starts up automatically when the Meteorological Agency reports an earthquake of seismic intensity 4 or

1) Deputy Director, Earthquake Disaster Countermeasures Division, Disaster Prevention Bureau, National Land Agency, 1-2-2 Kasumigaseki, Chiyoda-ku, Tokyo 100-8972
2) Director, ditto

higher on-line. In the next 30 minutes, it estimates seismic intensity distribution with meshes (approx. 1 square kilo meter) and estimates structural damage (number of collapsed buildings) within each cell and the number of casualties (deaths, injured, etc.) likely to arise as a result. From this information, the scale of damage is roughly understood. The information is transmitted to agencies concerned and used towards helping governments study initial responses.

Since started operation in April 1996, EES has been used for 103 earthquakes of seismic intensity 4 or higher up until March 1999. This includes 4 earthquakes of seismic intensity 5+ and 2 earthquakes of seismic intensity 6- (M6.2 recorded on May 13, 1997 in the Satsuma area of Kagoshima Pref. and M6.1 recorded on September 3, 1998 in the northern part of inland Iwate Pref.).

3. EES ESTIMATE METHOD

Having been through many large-scale earthquakes, Japan has extensive records on past earthquakes and damage caused by them, enabling us to draw a relationship between the size of earthquake and damage, for each different area of the country. Using this know-how and analytical techniques developed in recent years, the EES estimates a seismic intensity distribution and estimates structural damage and potential casualties to arise as a result. Estimate method for each item is explained as follows.

(1) Seismic Intensity Distribution

The seismic intensity distribution is estimated from information gathered around the country after an earthquake occurs and transmitted on-line by the Meteorological Agency. It is estimated per mesh (approx. 1 square kilometer).

The process to estimate the seismic intensity distribution is shown in Fig. 2.

1) Area to be estimated is determined.
Data from all areas measuring a seismic intensity 3 or higher are sampled, and the area formed by these points and the surrounding area within an approximate 40 km radius is taken as the target area for estimate. To keep the estimate procedure as short as possible, area estimated is limited to the range in which damage can occur.

2) Seismic intensity is converted into velocity.
The seismic intensity measured in each measuring point is converted to velocity, as the velocity can be obtained on the surface and is basically constant when constructing a distribution of the earthquake motion. Though the relationship between seismic intensity and velocity has yet to be established, a conversion formula was created from data on the five most recent earthquakes including the Earthquake in south area of Hyogo Pref.

3) Velocity on the bedrock is estimated.
Using the surface velocity obtained at the measuring points and the surface amplitude, the velocity on the bedrock is estimated. By estimating the earthquake motion on the bedrock, it is possible to estimate a distribution of earthquake motion that is not affected by the type of surface. The surface amplitude was obtained for 13 types of terrain, using the Midorikawa-Matsuoka equation.[1] The terrain types of each measuring points were taken from digital national land data.

4) Distribution of bedrock velocity is estimated.
From the bedrock velocity obtained at each measuring point, contours (of velocity) are created and a mesh topographical distribution of the bedrock speed is estimated.

5) Velocity on surface is estimated.
The surface velocity is estimated per mesh using the bedrock velocity in the opposite way of step 3).

6) Velocity is converted into seismic intensity.
The seismic intensity is estimated per mesh using the surface velocity in the opposite way of step 2).

As described above, a topographical seismic intensity distribution is estimated per mesh, from the seismic intensity measured at each measuring point.

(2) Structural Damage

Structural damage is estimated as the number of collapsed buildings based on the estimated seismic intensity distribution (unit = mesh). Though an estimate is made for every mesh, results are tabulated and expressed for each municipality. An estimate is made separately for wood buildings and non-wood buildings.

The process to estimate structural damage is shown in Fig. 3.

1) Number of buildings is estimated.
The number of wood and non-wood buildings in each municipality is taken from the fixed asset ledger of the Ministry of Home Affairs. Age-wise, the buildings are divided into new and old as described later on. Then, the number of wood and non-wood buildings in each mesh is estimated based on the population ratio for each mesh.

2) Number of collapsed wood buildings is estimated.
For each mesh, the number of collapsed wood buildings is estimated by multiplying the collapse factor by the number of wood buildings. The collapse factor is determined based on 4 conditions - the previously estimated seismic intensity, predominant period, building age and area.

From the past experience we know that, if two wood buildings are subjected to the same seismic force, a building built on soft ground will suffer more damage than a building built on hard ground. Therefore, 2 categories have been set for predominant period based on ground hardness. Building age is categorized into new and old, using the 1960 revisions to the Building Standards Law as a dividing line. Area is categorized into Hokkaido, cold regions (Tohoku, Hokushinetsu and San-in) and ordinary areas, in consideration of the fact that buildings in snowy places are more rigid than in other places.

3) Data is tabulated for each municipality.
The number of collapsed wood buildings estimated in each mesh is tabulated on each municipality.

4) Number of non-wood collapsed buildings is estimated.
For every mesh, the number of collapsed non-wood buildings is estimated by multiplying the collapse factor by the number of non-wood buildings. The collapse factor is determined based on 2 conditions - the previously estimated seismic intensity and building age. Building age is categorized into new and old, using the 1981 revisions to the Building Standards Law as a dividing line.

5) Data is tabulated for each municipality.
The number of collapsed non-wood buildings estimated in each mesh is tabulated for each municipality.

(3) Casualties Resulted from Collapsed Buildings

The potential casualties are estimated as the number of deaths per municipality, based on the number of collapsed buildings in the respective municipality. The death toll estimated here is based entirely on the number of collapsed buildings and does not account for deaths from traffic accidents, fire and other causes. These factors have been left out of the estimate because there are too many undefined elements.

The process to estimate the number of deaths due to building collapse is given in Fig. 4.

1) Population is estimated.
Population is estimated by the time of day and behavior, from the daytime and nighttime populations for each municipality and data derived from surveys on people's move. Here, the time of day is divided into 24 hours, whereas behavior is categorized as staying at home, staying indoors somewhere else than at home and moving. Because sufficient data on people's move is not available, the difference in behavior patterns between different areas is not taken into account.

2) Number of persons staying in wood homes is estimated.
The number of persons staying in wood homes when the earthquake hit is estimated by multiplying the percentage of wood homes for the respective prefecture by the number of persons categorized as staying at home at the time of the earthquake occurrence. The percentage of wood homes is obtained from housing statistics.

3) Number of deaths resulted from wood home collapse is estimated.

The number of deaths resulted from wood home collapse is estimated by multiplying the death factor for wood homes by the number of persons staying at wood homes when the earthquake hit. The death factor for wood homes was determined in association with the number of collapsed wood buildings, that was taken from data on five comparatively recent earthquakes in which 300 or more persons died.

4) Number of persons in non-wood buildings is estimated.
The number of persons in non-wood buildings is estimated by subtracting the number of persons in wood homes from the number of persons categorized as being at home when the earthquake hit, and adding that to the number of persons categorized as being indoors somewhere else than at home.

5) Number of deaths resulted from non-wood building collapse is estimated.
The number of deaths resulted from non-wood building collapse is estimated by multiplying the death factor for non-wood buildings by the number of persons in non-wood buildings. The death factor for non-wood buildings was set in association with the number of collapsed non-wood buildings, which was taken from data on the Hanshin - Awaji Earthquake and other earthquakes.

6) Total death toll
The death toll is calculated for each municipality, by adding the total number of deaths resulted from wood building collapse and non-wood building collapse.

Although the explanation is omitted herein, the EES can estimate the number of heavily injured persons and critically injured persons for each municipality using the number of deaths.

4. EES OPERATION RECORD

As was mentioned earlier, the EES has been used on 103 occasions so far and it has been confirmed fairly adequate in estimating seismic intensity distribution (See Fig. 5). Its ability to estimate damage has yet to be verified because - fortunately - large-scale earthquakes, which can cause severe damage, have not occurred since the start of EES operation. In any case, however, in regard to the two seismic intensity 6- earthquakes that were recorded, results were close enough to indicate the scales, though they can be considered slightly overestimated as shown in Table 1.

As the system is used more and more, we plan to review the estimate methods as needed and improve the system performance.

5. ADDITIONAL TSUNAMI ESTIMATE CAPABILITIES

Japan is surrounded by ocean on all sides and has suffered from much damage caused by tsunami that accompanied earthquakes. Thus, protection against tsunami is a serious issue in coastal areas. However, before taking any sort of countermeasures, it is necessary to make a tsunami hazard map that indicates potential flood areas in the event of tsunami. Here, it would also be necessary to presume the type of tsunami that could occur in each specific area and the damage it could cause.

In setting the presumed tsunami, past experience with tsunami has been used. However, this yields an issue that past experience alone is not always enough to prepare for infrequent tsunami. Therefore, the National Land Agency teamed up with the Meteorological Agency and Fire-Defense Agency to compile techniques for making tsunami hazard maps into a "Tsunami Disaster Forecast Manual." These techniques utilize earthquake fault models and tsunami behavior simulations made possible from recent research findings and new computer technology.

Currently, the National Land Agency is using this Tsunami Disaster Forecast Manual to create tsunami hazard maps (See Fig. 6) for all coastal areas in Japan and to build a database of the map, with the ultimate goal of forecasting the potential damage of tsunami. The Meteorological Agency will announce a new tsunami forecast system in 1999, and National Land Agency will give the EES additional capabilities to make an early damage assessment under flooding caused by tsunami. The system will make it possible to know the state of flooding soon after a tsunami occurs, by searching the database for the tsunami hazard map that contains the area and wave height incorporated in the tsunami forecast.

With the EES capable of estimating tsunami, we expect that the system will be utilized by governments to rationalize their initial response to tsunami occurrence.

Reference

1) Masahiro Matsuoka & Saburo Midorikawa, Wide-Area Seismic Intensity Distribution Prediction Using Digital National Land Data, Structural Systems Papers for The Japan Architects Association, No. 447, pg. 51 - 56, 1994.

Table 1 Comparison of EES estimate against actual results

	Satsuma, Kagoshima Pref.		Northern Iwate Pref.	
	Number of collapsed buildings	Number of deaths	Number of collapsed buildings	Number of deaths
Estimate	Approx. 800	Less than 100 (15)	Less than 100 (11)	0
Actual results	77 (Completely or partially destroyed)	0	0	0

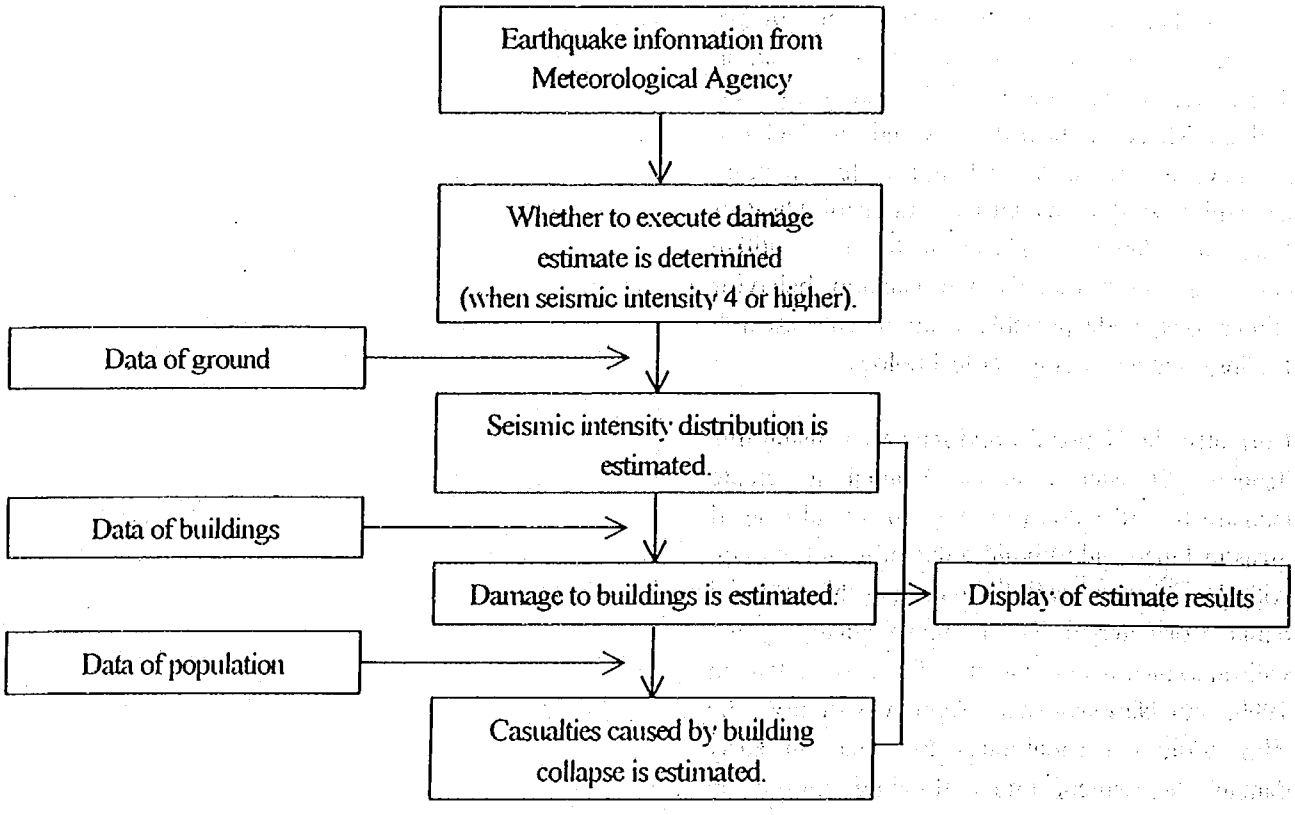


Fig. 1 Flow chart for earthquake damage estimate

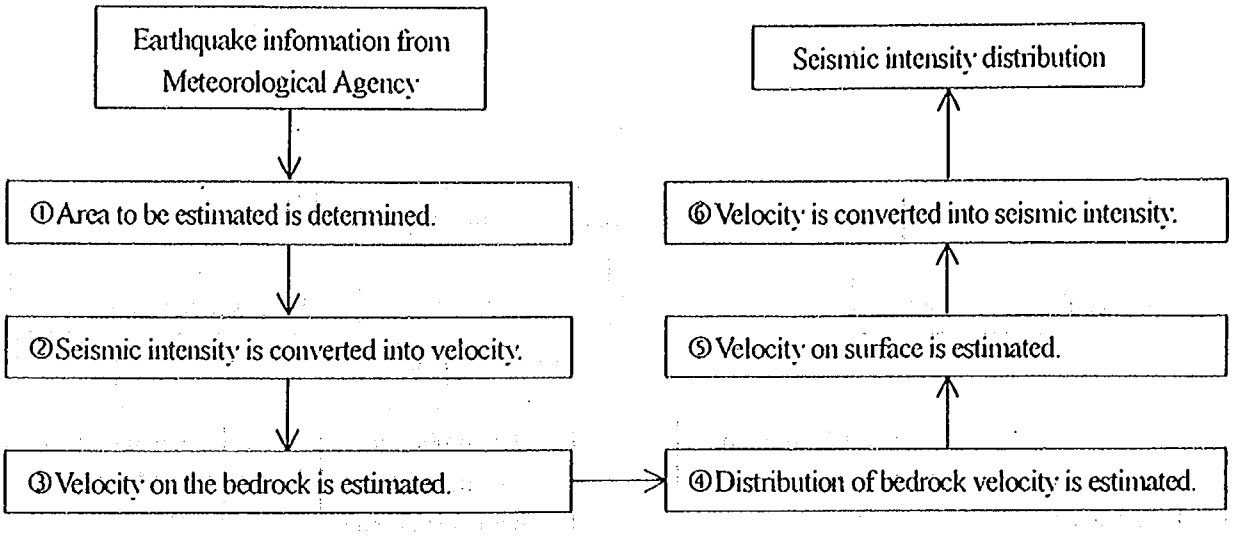


Fig. 2 Process for estimating seismic intensity distribution

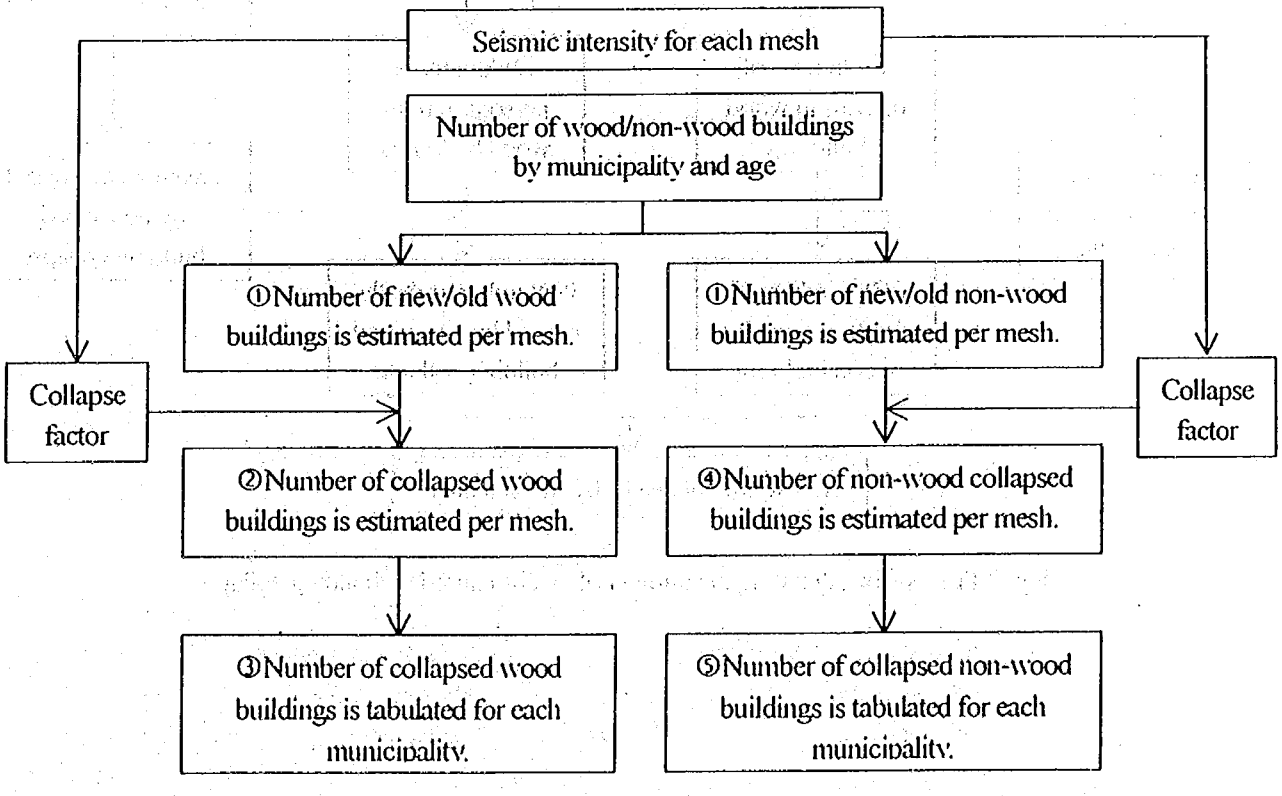


Fig. 3 Process for estimating structural damage

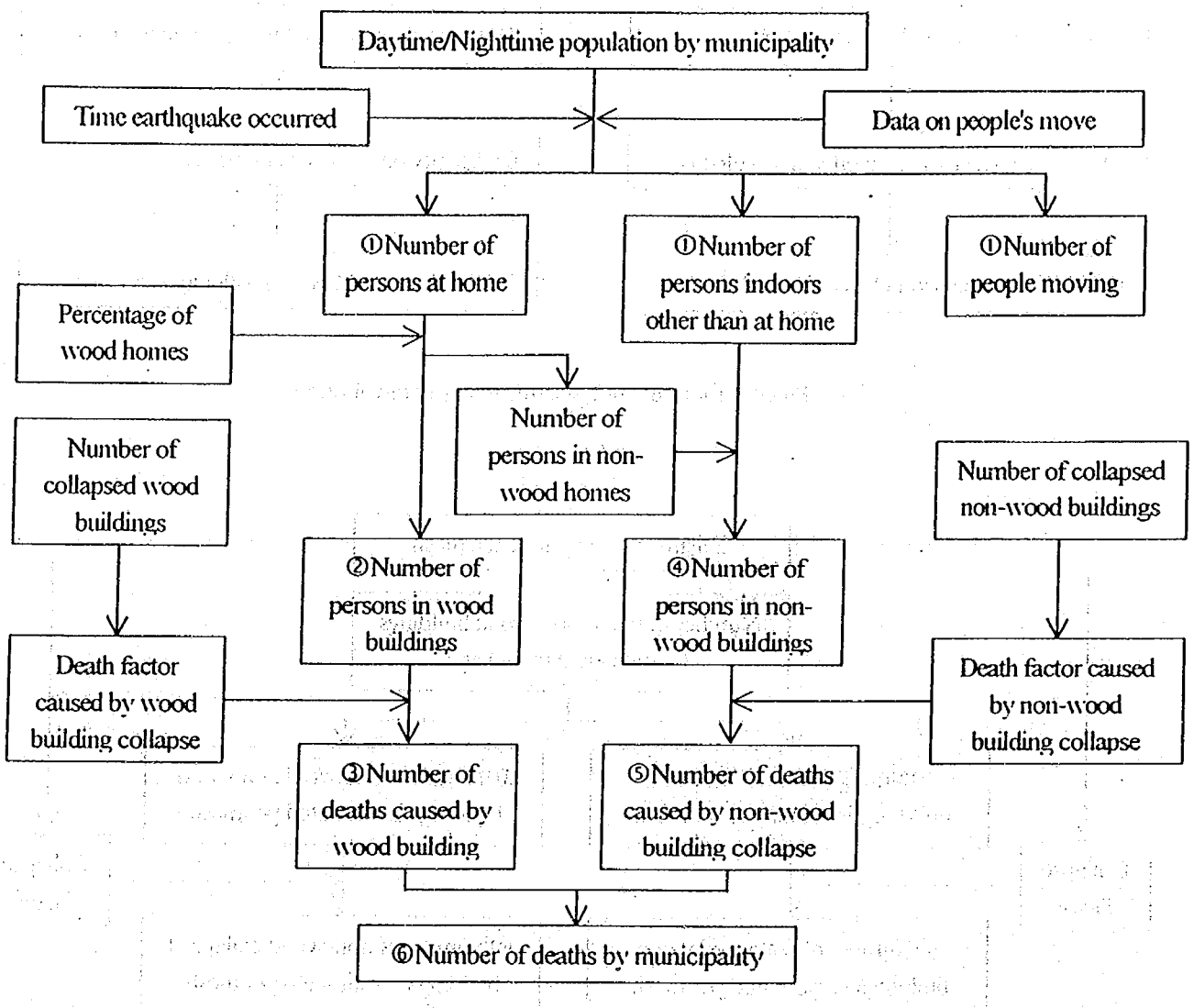


Fig. 4 Process for estimating the number of deaths caused by building collapse

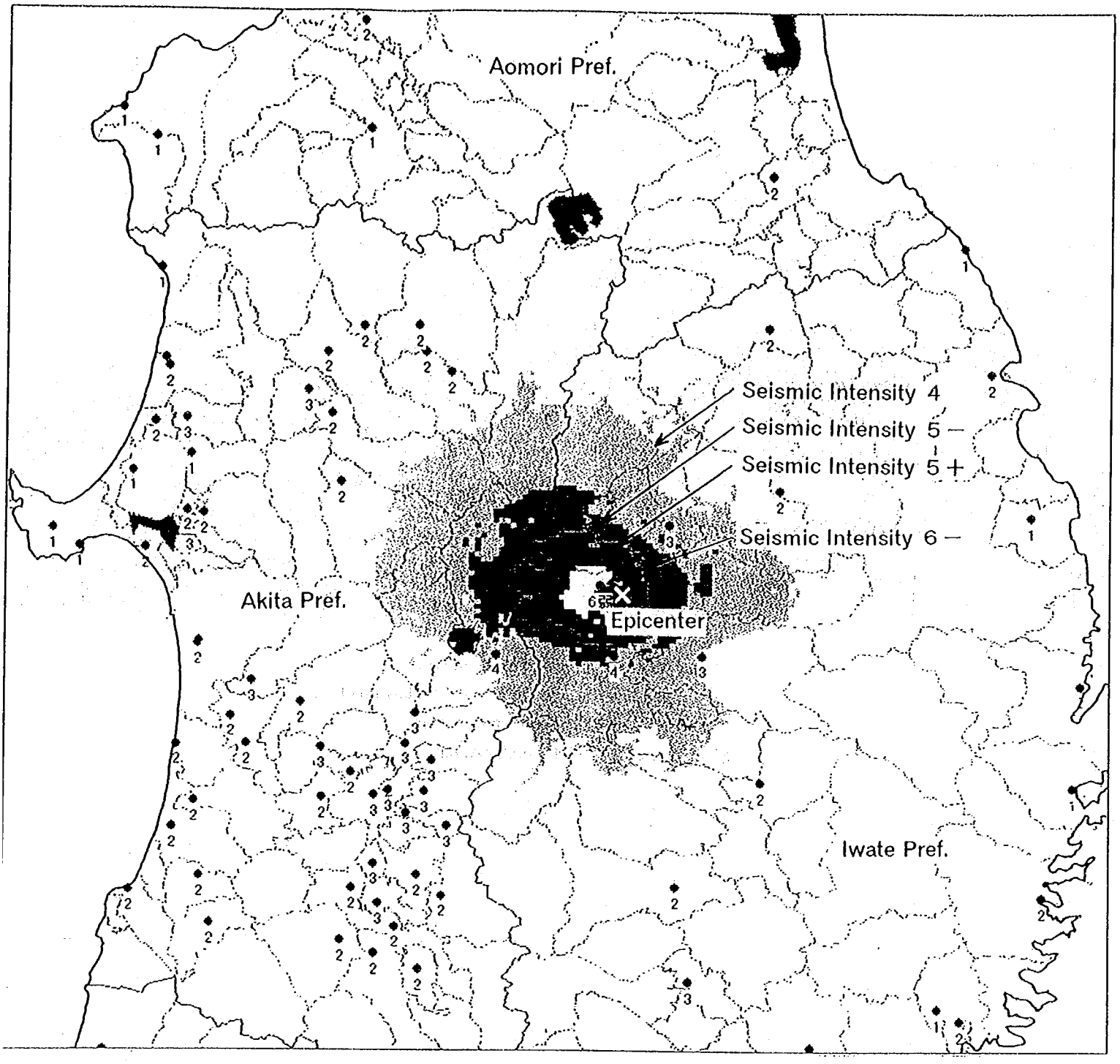


Fig. 5 Seismic intensity distribution
(Earthquake in the northern part of inland Iwate Pref.)
● measuring point
seismic intensity

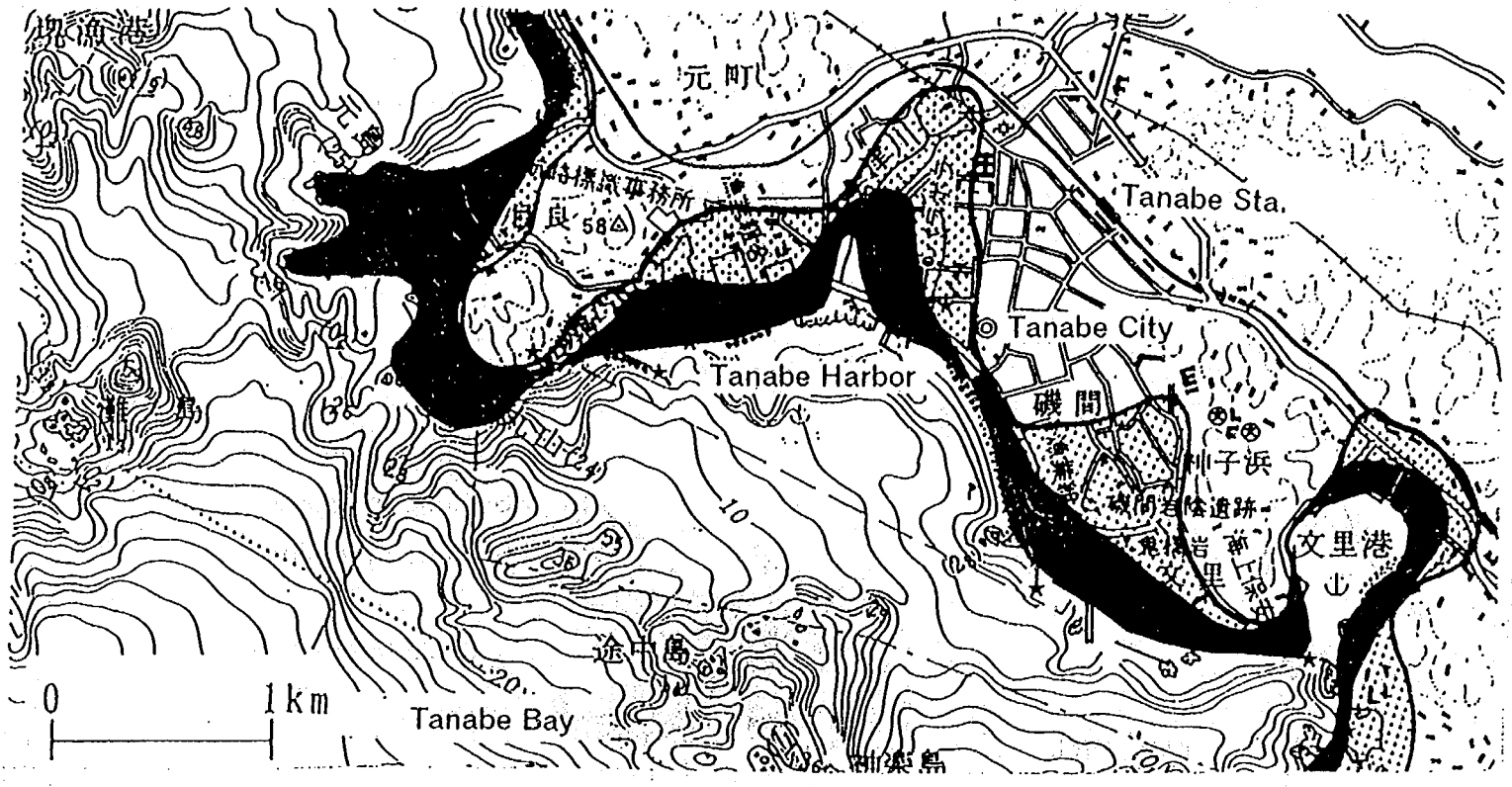


Fig. 6 Tsunami hazard map (example)
(Assume 4 meter tsunami hit the coast of Tanabe, Wakayama Pref.)
Dark area: 2 meter or more under water
Shaded area: 0 - 2 meter under water

Theme 5

Summary of Joint Cooperative Research Programs

30-YEAR ACCOMPLISHMENTS AND FUTURE CHALLENGES OF THE PANEL ON WIND AND SEISMIC EFFECTS

by

Yasutake Inoue[1] and Michio Okahara[2]

ABSTRACT

The Panel on Wind and Seismic Effects, which is one of the 18 Panels under the U.S. - Japan Cooperative Program in Natural Resources, was created in 1967 in order to promote technical cooperation between the U.S. and Japan for mitigating natural disasters caused by extreme wind, earthquakes, storm surge and tsunamis. Since the First Joint Panel Meeting held in Tokyo in 1969, Joint Panel Meetings have been held alternatively in Japan and U.S. every year, and the Panel celebrated its 30th Joint Meeting in 1998.

This paper prepared by the Japan-side Panel looks back on accomplishments of the Panel in the past 30 years and sets forth the future prospects.

KEY WORDS:
Wind Engineering, Earthquake Engineering, Storm Surge, Tsunami, Joint Cooperative Research Program

INTRODUCTION

The establishment of the U.S. - Japan Cooperative Program in Natural Resources (UJNR) was proposed by the United States at the First Plenary Meeting of the Third U.S. - Japan Joint Bilateral Committee on Trade and Economic Affairs held in Tokyo on January 27, 1964. In the same year UJNR was formed as a body unaffiliated to the U.S. - Japan Science Committee and the U.S. - Japan Joint Bilateral Committee on Trade and Economic Affairs.

The Panel on Wind and Seismic Effects, that is one of the 18 specialized Panels of UJNR, was proposed as a new cooperative activity at the Third UJNR Plenary Meeting held in Tokyo in 1967. The primary objective of this program was to exchange research results and views concerning the development of wind and seismic design methods, in view of the fact that both the U.S. and Japan suffer from earthquakes, high winds, storm surge and tsunamis. The range of Panel's activities has yearly expanded, and it includes exchanging results of research related to revision of design criteria and developing comprehensive measures and research fields to mitigate loss of lives and properties from natural disasters such as extreme winds and earthquakes. Since the First Joint Meeting of the Panel in Tokyo in 1969, Joint Meetings have been held every year alternately in Japan and U.S., and the Thirtieth Joint Panel Meeting was held in May, 1998.

The Panel has been jointly established in each country. The Public Works Research Institute provides the Japan-side chairman, and Japan-side Panel has about fifty members representing seven national research organizations and the ministries and agencies with which each of those organizations are affiliated. The National Institute of Standards and Technology provides the U.S.-side chairman, and the U.S.-side Panel consists of about fifty representatives of various research organizations. 11 Task Committees have also been formed to promote the Panel activities effectively by exchanging research information and holding workshops.

MAJOR ACTIVITIES OF THE PANEL

1) Since the First Joint Meeting of the Panel in Tokyo in 1969, Joint Panel Meetings have been held every year alternately in the U.S. and

[1] Director-General, Public Works Research Institute, Ministry of Construction, 1 Asahi, Tsukuba-shi, Ibaraki-ken 305-0804 Japan
[2] Director, Structure and Bridge Department, ditto

Japan.

2) At the Seventh Joint Panel Meeting held in 1975, to strengthen the Panel's activities it was decided to establish six Task Committees designated as Task Committee A to F, which cover strong motion instrumentation arrays, large-scale testing programs and so on. After that new Task Committees have been established, and 11 Task Committees; Task Committee A to K are presently active. The latest Task Committee, which deals with seismic information systems, was approved at the Thirtieth Joint Panel Meeting in 1998.

3) Since 1977, the Panel has exchanged researchers and conducted U.S. - Japan Joint Cooperative Research Programs, and the Task Committees have held workshops and technical coordinating committee meetings.

4) At the Tenth Joint Panel Meeting (1978), the Panel decided to expand activities to include the issues of storm surge and tsunamis, and the Panel membership was expanded. Since then lively activities have been conducted in this field.

5) The importance of earthquake prediction was recognized and the Panel conducted researches in this field. This research was taken over by the new Panel on Earthquake Prediction Technology in 1978. This Panel was reorganized as the Panel on Earthquake Research in 1996.

6) In 1979, the Public Works Research Institute, the Building Research Institute, the Geographical Survey Institute and the Meteorological Research Institute moved to Tsukuba Science City. On this occasion, new large-scale experimental facilities were installed and these facilities have been used effectively for the U.S. - Japan Joint Cooperative Research Programs.

7) In 1987, a charter clarifying the Panel's activity policies was enacted.

8) In 1991, an International Symposium on Disaster Prevention was held in Gifu City as part of the International Decade for Natural Disaster Reduction (IDNDR). A list of papers presented at the Joint Panel Meetings and workshops during the previous 23 years was published and distributed to various locations including those in developing nations.

9) In 1993, the Panel celebrated its 25th anniversary by holding a One-day Symposium on the IDNDR jointly with the Section of IDNDR, Ministry of Construction.

10) In December 1993, the Japan-side Panel published the first issue of the Wind and Seismic Effects Panel Newsletter. Five issues of the newsletter have been published alternately by the U.S. and the Japan sides. In 1996, the Panel opened its web site on the Internet to further disseminate the results of activities.

11) Since 1996, the Panel has been cooperating in various ways to reduce natural disasters in conjunction with the U.S. - Japan Common Agenda for Cooperation in Global Perspective (Common Agenda).

ACCOMPLISHMENTS OF THE PANEL

1) At the Joint Panel Meetings and Task Committee workshops, more than 1,800 research papers and reports have been presented. They have been published and distributed as proceedings, and have been used to improve wind and seismic technologies.

2) More than 250 U.S. and Japanese researchers have been exchanged to participate in the U.S.-Japan Joint Cooperative Research Programs, earthquake damage surveys and other activities in the counterpart country.

3) The U.S. - Japan Joint Cooperative Research Programs have been conducted on the 10 themes. These programs have facilitated exchange of technical information and personnel, including young researchers and design engineers, and contribute to further advancement of technology.

4) Since strong motion records are precious data for research on earthquake engineering, exchange system of strong motion records were developed between the U.S. and Japan. The National Research Institute for Earth Science and Disaster Prevention has recently opened the K-NET strong motion records. High wind, tsunami records and sea bottom topographical data have also been exchanged.

5) To disseminate technologies developed in Japan, Manual for Repair Methods of Civil Engineering Structures Damaged by Earthquakes, Base-isolation Systems for Buildings and Handbook on Liquefaction Remediation were translated into English.

U.S.-Japan Joint Cooperative Research Programs

Research Theme	Period
Research Program on Reinforced Concrete Structures	1979-1987
Research Program on Steel Structures	1981-1987
Lifeline Facilities	1982-1989
In-situ Testing Methods for Liquefaction	1983-1989
Research Program on Masonry Structures	1984-1988
Research Program on Precast Seismic Structural Systems	1989-1992
Seismic Improvement Technology using Hybrid Control Systems	1990-1994
Research Program on Composite and Hybrid Structures	1993 to present
Countermeasures against Soil Liquefaction	1994 to present
Research Program on Smart Structural Systems	1998 to present

6) Following disasters caused by strong hurricanes (Hurricane Hugo, Hurricane Andrew, etc.) and earthquakes (Loma Prieta Earthquake, Hokkaido Nansei-oki Earthquake, Northridge Earthquake, Hyogo-ken Nanbu Earthquake, etc.), either joint surveys or surveys assisted by experts from the counterpart country have been carried out. Causes of the disaster have been analyzed, and valuable information has been exchanged regarding restoration technology.
7) In regard to cooperation with developing countries, information was exchanged. Especially both U.S. and Japanese Panels investigated damage due to the Mexico and Chili Earthquakes and offered technical assistance. Results of cooperation were reported at the Joint Panel Meeting. In conjunction with IDNDR, the Panel held a symposium and a conference, published and distributed a list of its papers as a way to increase people's awareness of natural disasters and to provide technical support.
8) By providing expertise to the U.S. - Japan Earthquake Policy Symposia and reviewing proposals for the Earthquake Disaster Mitigation Partnership under the auspices of the Common Agenda, the Panel has been contributing to reduce natural disasters.
9) In order to disseminate the results of Panel activities, the Panel publishes newsletter and has constructed a web site.

FUTURE PLANS

Promotion of Exchanges

1) Personnel and technical information exchanges, which are fundamental activities of the Panel, should be enthusiastically continued.
2) Joint Cooperative Research Programs are effective ways to achieve great results and are to be aggressively conducted.

Establishing New Research Themes

Since UJNR is a cooperative science and technology program led by governmental research organizations of the U.S. and of Japan, the Panel should seek research themes for which government has responsibility of implementation. As Europe leads the trend to the disappearance of borders and new alliances get together, it is imperative that the U.S. and Japan consider the international role they should play in the fields of wind and earthquake engineering. Considering the above facts, the followings are examples of research themes that the Panel undertakes:

1) Application of new technologies not considered in the past wind and earthquake engineering research.
An example is the use of information technologies to perform national land management against natural disasters. In order to reduce disaster risks and effects by creating more efficient and systematic national land use, advanced information technologies such as GIS, GPS, remote sensing technology and other data communication technology are to be developed.

2) Comprehensive research subjects that are

related to several Task Committees
The development of performance-based design methodology is an example. Looking ahead to the cost reduction of public works projects and the spread of VE systems, the performance-based design technology should be established. It will also contribute to increase design freedom and reflect the creativity and innovative skills of designers to the greatest possible degree.

3) Subjects involving policy elements among international communities
Dealing with the ISO is one example. Most of technical committees of ISO have been composed of European countries, however acquisitions by governments and the private sectors will be based on ISO technical standards in the future. From this point of view, the Panel should technically contribute to ISO, e.g., proposing technical standards that are internationally compatible.

Reinforcing the Role of the Panel

Task Committees have been established to solve individual problems and hold actively workshops. To perform further smooth and effective activities of Task Committees, the Panel should make efforts to better communication and liaison among Task Committees.

Contribution to International Activities

1) The Panel will cooperate more closely with the High-Level U.S. - Japan Earthquake Policy Cooperation Forum (High Level Forum) established as a product of the U.S. - Japan Earthquake Policy Symposia and the Earthquake Disaster Mitigation Partnership in order to contribute to the achievement of the Common Agenda in the field of natural disaster reduction.
2) The Panel will disseminate technologies developed in both U.S. and Japan more widely. Recognizing that there are many developing countries that suffer from natural disasters, the Panel will transfer technologies such as technical standards, disaster planning techniques, and so on that are beneficial to those countries.

Active Information Dissemination

In addition to the publication and distribution of proceedings of Joint Panel Meetings and workshops, the Panel will accelerate and increase information dissemination activities through the use of the Internet and so forth.

ACCOMPLISHMENTS AND FUTURE PLANS OF TASK COMMITTEES

Task Committee A: Strong Motion Data and Applications

(1) Background

The Task Committee A was established by uniting the former Task Committee A (Strong Motion Instrumentation Arrays and Data) and former Task Committee E (Ground Motion and Seismic Design Forces) at the Twenty-fifth Joint Panel Meeting (1993). Task Committee A was established to perform two tasks: 1) To coordinate and promote activities intended to allow concerned researchers and technicians to effectively use strong motion records; 2) To carry out technology development and information exchanges related to the evaluation of the destructive force of earthquake motion.

The following five items represent the range of activities of Task Committee A:
1. Study of problems related to the installation of strong motion seismographs, etc.
2. Strong motion observations, processing of the records, and analysis of the records.
3. Clarification of the engineering characteristics of earthquake motion.
4. Application of seismic resistant design.
5. Earthquake danger zonation.

This Task Committee has continued to be extremely active since its establishment in 1993.

(2) Accomplishments

An international workshop concerning strong motion record data was held in Menlo Park in California in the U.S. in December 1993. At this event, strong motion observations from all parts

of the world were compared and a global scale comparative study of maximum accelerations and response spectra was carried out. The proceedings, which have already been published, include 36 papers from the U.S., Japan, New Zealand, France, and Chili. One product of this workshop was the creation of a fresh international awareness of differences in the attenuation equations of ground motions used in Japan, the U.S., and in Europe. Since then, various research projects have been undertaken to explain these differences.

Following this workshop, a series of large earthquakes occurred: the Northridge Earthquake of 1994 and the Hyogo-ken Nanbu Earthquake of 1995. The data provided by these earthquakes has substantially influenced research on strong motion records and their use, and in particular, research on earthquake motion near epicenters and ground seismic response. This has accelerated related research and prompted proposals from both Japan and the U.S. for new design earthquake motions. And since 1995, related activities of the ISO (unified international standardization organization) including international earthquake danger zonation have achieved remarkable progress, and plans call for the announcement of a series of new proposals in 1998.

As part of this trend, an international workshop on ground response to earthquakes was held in Yokosuka on January 16 and 17, 1996. More than 50 first-class internationally recognized experts in this field gathered to take part in extremely detailed discussions based on the strong motion records of the Northridge Earthquake and Hyogo-ken Nanbu Earthquake and the results of laboratory tests and numerical analyses. The discussions focused particularly on the nonlinear response of ground. The Port and Harbour Research Institute published the proceedings of this workshop in March 1996. This workshop resulted in the positioning of knowledge of the design use spectrum that accounts for the nonlinear amplification properties of the ground (U.S. NEHARP 1994, etc.), a technology not yet developed in Japan, as the common property of Japan and the U.S.

In the midst of rapid change in related standardization and research by various organizations such as the ISO mentioned above, Task Committee A has achieved the following successes:

1. The collection of the latest information regarding the UBC97 and NEHRP97 progressing in the U.S. and the most up-to-date information from the ISO/TC67 (international integrated standard preparation committee, marine structures); a body whose representative member is a member of the Japan-side Panel on Wind and Seismic Effects.
2. Proposal by the members of Task Committee A of U.S. - Japan cooperation in research on strong motion records as one of the achievements of the Earthquake Policy Symposium of the Common Agenda.
3. The K-net data provision method established by the members of Task Committee A, an ideal system for the rapid acquisition of data by concerned researchers, is a model that should serve as a reference for use by concerned organizations in the U.S. and Japan in the process of developing future strong motion observations. A CD-ROM (two disks) of K-net data has been provided to concerned organizations in both the U.S. and Japan.
4. Activity as a key member of the workshop on "nonlinear response of ground" (January 1998, sponsor; Seismic Engineering Center of the University of Southern California) of the Japan and the American Chairmen of Task Committee A and other members of the committee through their provision of the most up-to-date information and participation in debates.

It is clear from the tragic disasters caused by the Northridge Earthquake of 1994 and the Hyogo-ken Nanbu Earthquake of 1995 that reducing earthquake disasters is an urgent and important challenge for the Twenty-first Century. It has been pointed out that the weakness of the existing strong motion observation network in the U.S. is a serious obstacle to its efforts to reduce earthquake damage. The members of Task Committee A have undertaken the following activities in order to establish plans for a new strong motion observation system for

use in the Twenty-first Century:
1. Participation in the U.S. Committee for the Advancement of Strong Motion Programs (CASMP) by the members of the American side of Task Committee A.
2. Participation in the international workshop, "Vision 2005: Strong Motion Observation Promotion Action Plan for the Reduction of Earthquake Disasters in Urban Regions" (April 1997, Monterey in California).
3. Establishment of the Consortium of Organizations for Strong Motion Observational Systems (COSMOS).
4. Enactment of strong motion seismograph installation planning for buildings owned or occupied by offices of the federal government of the U.S. and approval of the plan by the CASMP and the Interagency Committee on Seismic Safety in Construction (ICSSC).

(3) Future Plans

The followings are activities Task Committee A plans to conduct in the future:
1. Up-to-date strong motion observation and data distribution systems such as K-net have been provided in Japan, but technology in this area has to be introduced in the U.S. Specific plans to achieve this goal include U.S. - Japan workshops for participants involved in strong motion observations.
2. The quantity of data regarding large earthquakes, particularly data obtained near epicenters that is extremely important in the design of structures, is limited and must be shared through international cooperation. Joint research intended to overcome this problem will continue. Specifically, it is necessary to prepare data bases linked to the internet such as the Rosrine Project (a data base of strong motion records, ground survey data, and laboratory experimental data related to the 1994 Northridge Earthquake) that has been completed in the U.S., and to establish systems for the cooperation of concerned organizations by providing access to related web sites here in Japan. Committee type activities to accomplish these goals are planned.

(Susumu Iai)

Task Committee B: Testing and Evaluation Procedures for Building Systems

(1) Background

At the Sixth Joint Panel Meeting in 1974, the following resolutions were adopted.
[Resolution 3]
Increased effort should be made in the near future to encourage joint research programs, especially in the area of mutual utilization of research facilities and the exchange of researchers.

In response to this resolution, the Task Committee on Large Scale Experiment Program was established at the Eighth Joint Panel Meeting in 1976. Then at the Tenth Joint Panel Meeting (1978), the Panel again indicated its strong support of the program by adopting the following resolution.
[Resolution 3]
The Panel on Wind and Seismic Effects recognizes the importance of the U.S.-Japan Cooperative Program on Large Scale Testing and it urges early implementation of the program under the auspices of this Panel.

Under the auspices of this Panel, the Task Committee has supported the implementation of U.S.-Japan Joint Research on building structural systems. At the Twenty-fifth Joint Panel Meeting (1993), the name of the Task Committee was changed to the Task Committee on Testing and Evaluation Procedures for Building Systems.

(2) Accomplishments

The activities of this Task Committee are carrying out U.S.-Japan Joint Research Program on building systems with under the auspices of the Panel. The following is an outline of the joint research it has conducted up till now.

1) Research Program on Reinforced Concrete Structures
Research on reinforced concrete structures was selected as the first theme for U.S.-Japan Joint Research Program. On August 10, 1979, the

Science and Technology Agency, the Ministry of Construction and the U.S. National Science Foundation (the Parties) signed the "Implementing Arrangement of the U.S.-Japan Joint Earthquake Engineering Research Program Utilizing Large-scale Testing Facilities". The Task Committee reviewed the program and recommended the endorsement to the chairmen of the Panel. The Panel chairmen endorsed the program to the Parties in July 1980.

The testing of a 7-story reinforced concrete building was started at the Building Research Institute in March 1981 and completed in November. Support tests conducted in Japan commenced in 1980 and were completed in 1982. Support tests performed in the U.S. started in 1981 and were completed in 1983.

2) Research Program on Steel Structures
On May 18, 1981, the Ministry of Construction and the U.S. National Science Foundation (the Parties) signed the "Implementing Arrangement of the U.S.-Japan Joint Earthquake Engineering Research Program Utilizing Large-scale Testing Facilities with Steel Structures". The chairmen of the Panel gave their endorsement to the Parties on May 22, 1981.

Full-size steel building testing began in 1983. All full-size testing and support tests in both countries were completed in 1986.

3) Research Program on Masonry Structures
In December 1984, the Ministry of Construction and the U.S. National Science Foundation signed the "Implementing Arrangement of the U.S.-Japan Joint Earthquake Engineering Research Program including Large-scale Testing on Masonry Structures". The chairmen of the Panel gave their endorsement during the Seventeenth Joint Panel Meeting.

Testing of 5-story masonry building began in November 1987 and completed in January 1988. Support tests in Japan commenced in 1985 and completed in 1987. In the U.S., the research was performed during 1985 to 1993.

4) Research Program on Precast Seismic Structural Systems (PRESSS)
Researchers from the U.S. proposed precast structural systems as the fourth theme, and after considering the proposal, the Japan side agreed. In October 1987, the U.S. National Bureau of Standards (now the National Institute of Standards and Technology) began to conduct a multi-year research project on the earthquake behavior of precast concrete structures. This research project was closely related to the U.S.-Japan Joint Research Program.

Testing research in Japan started in 1989 and completed in March 1992. The first stage research in the U.S. began in 1989 and ended in 1991. The second stage research extended from 1991 to 1994. The third stage research has been in progress since 1995.

5) Research Program on Composite Structure and Hybrid Structure Systems (CHS)
Researchers from the U.S. and Japan agreed on composite structures and hybrid structures as the fifth theme and the Japan planning group began its activities in May 1991.

Research in Japan began in 1993 and concluded in 1998. The Japan Structural Consultant Association performed practical research on the application of the research results. Research in the U.S. began in 1995 included more than 16 research projects.

6) Research Program on Smart Structural Systems (Auto-Adoptive Media)
The Joint Technical Subcommittee on "Research Revolution" met in Ann Arbor in February 1996 and the Joint Technical Subcommittee on "Concrete Filled Steel Pipe" met in Chicago in April 1996 to select the sixth theme for joint research. Based on their findings, the Smart Structural Systems were selected. Research in this field commenced in Japan in 1998. Work is now underway to complete plans for the research to be carried out in the U.S.

(3) Future Plans

U.S.-Japan joint research program on building structural systems including large-scale testing

is conducted divided into six themes. For the reasons related to differences in budget measures and research theme selection methods in the two countries, the research by the two sides has not been closely coordinated as was originally planned. But, the U.S.-Japan Joint Technical Coordinating Committees have functioned effectively to contribute to the success of the joint research.

In Japan, research on the fifth theme, composite structure and hybrid structure systems, has been completed and work to make use of the results has begun. Research has begun on the sixth theme, smart structural systems. In the U.S., research is continuing on two themes: the fourth theme, precast structural systems and the fifth theme, composite structure and hybrid structure systems. Studies are in progress in preparation for the beginning of research on the sixth theme, smart structural systems.

This Task Committee is striving to develop methods of disseminating the results of its joint research widely in countries in high seismic regions in order to contribute to the International Decade of Natural Disaster Reduction (IDNDR). And to maximize the use of its research data, it is planning to hold a Joint Workshop on Test Procedure, Documentation, Retrieval of Test Data, and Experimental Facilities.

A study is scheduled to plan the future U.S.-Japan joint research program performed at three Earthquake Engineering Research Centers established by the U.S. National Science Foundation. And, the future U.S.-Japan research program will consider using the 3-D Full Scale Earthquake Testing Facilities, which is constructed by the National Research Institute for Earth Science and Disaster Prevention, Science and Technology Agency. These plans include research on the destruction of structures that occurred during the Hyogo-ken Nanbu Earthquake and the Northridge Earthquake performed by carrying out dynamic evaluations of full-size model specimens.

(Keiichi Ohtani)

Task Committee C: Design, Evaluation, and Improvement of Structures

(1) Background

To promote measures and projects to improve the structural performance of new structures and to improve the wind and seismic resistance of existing structures, this Task Committee was organized by combining Task Committee C (Repair and Retrofit of Existing Structures) with Task Committee D (Evaluation of the Performance of Structures) in 1993.

The Task Committee C has been held six times since it was formed in 1993. The goals and range of its activities are listed below and it has concentrated on document exchanges and discussions related to research and technology in these areas conducted in Japan and the U.S.

1. Information exchange, preparation of research plans, and holding of workshops concerning new design methods, evaluation methods, and repair and retrofitting technologies.
2. Development of common systems concerning the screening and analysis of the wind and earthquake resistance of structures in Japan and the U.S.
3. Development of sensor technologies, measurement technologies, and expert systems to evaluate the condition of existing structures.
4. Performance evaluation of masonry structures, and precast concrete structures, and compound/hybrid structures, and provision of documentation to be used for the post-disaster performance evaluation.
5. Study of new materials and methods to be used for the repair and retrofitting of existing structures and to construct new structures.
6. Coordination between Japan and the U.S. in order to minimize the duplication of research projects and maximize the benefits obtained.

(2) Accomplishments

1) Repair and retrofitting of existing structures

1. A one and a half day workshop was held at the NIST in May 1990. With 12 participants from Japan and 12 from the U.S. in attendance for a total of 24, a total of 19 papers were

presented: 13 by Japanese and 6 by American delegates.
2. Regarding repair and retrofitting, in the U.S., FEMA published the ATC21 Existing Building Earthquake Resistance Diagnosis Handbook and ATC22 Existing Building Earthquake Resistance Repair and Retrofitting Technology. In Japan, the Japan Disaster Prevention Association completed the first revision in the 13 years since its original publication of the Existing Reinforced Concrete Building Earthquake Resistance Repair and Retrofitting Design Guidelines in October 1990. Then in March 1991, it issued new Technical Guidelines for the Assessment of the Degree of Damage and Restoration of Damaged Buildings. These guidelines made extensive use of the achievements of this Task Committee.
3. Exchange, translation, etc. of reports of wind and earthquake damage and documents concerning repair and retrofitting work.

2) Performance Evaluations of Structures
1. Panel members of Japan and the U.S. conducted earthquake damage surveys at the 1995 Hyogo-ken Nanbu Earthquake and other earthquakes.
2. In cooperation with Task Committee G, Task Committee C held workshops on smart materials and structures at the Building Research Institute in Tsukuba in May 1993 and Washington University in Maryland in December 1995. Task Committee C decided to make a smart structural system (auto-adaptive media) as the Sixth Phase of U.S. - Japan Joint Earthquake Engineering Research Program.
3. It carried out U.S.-Japan Joint Earthquake Engineering Research Program on reinforced concrete, precast structures and hybrid / composite structures. The followings are the outline of this research.
[Precast Concrete Structures]
- This research project involved a series of studies including full-scale experiments on buildings of PCa construction that clarified the structural strength of PCa structures and yielded the following results needed to prepare design guidelines.
- The committee prepared a design method for PCa buildings and a PCa joint design manual.
- Experiments to test the seismic performance of the elements that make up vertical joints and horizontal joints of PCa structures were performed along with experiments to test the seismic performance of the plane structures made of PCa members to provide background data to prepare a joint design manual.
- New design guidelines covering PCa buildings up to 60 m in height were developed.
- The trial design and dynamic response analysis of frame structures and earthquake resistant wall
- frame structures were performed to provide background data to prepare design guidelines.
- A U.S. - Japan common database of PCa joint details was constructed.

[Hybrid/Composite Structures]
This research obtained the following results in order to clarify the performance of hybrid / composite structures and to establish a seismic design method.
- A database was constructed and trial design work, experiments, and analytical research concerning concrete filled steel tube (CFT) structures were performed, and CFT design guidelines were developed.
- A database was constructed, trial design work was performed concerning structures consisting of reinforced concrete columns and steel frame girders (RCS), research on the stress transmission mechanism of the column beam joints was carried out, and design guidelines for such structures were developed.
- Along with the trial design of structures with reinforced concrete seismic resistant walls as its core and steel frameworks around the core (HWS), experiments were conducted on 1/3 scale 12-story seismic resistant walls with connecting beams in order to develop design guidelines.
- In the area of new systems utilizing new materials, studies of fiber reinforced concrete and high performance concrete were carried out to clarify the basic properties of these materials and their properties as members. As part of this research, design guidelines were prepared for a method of retrofitting of reinforced concrete members using FRP sheets. These guidelines are already in use.
4. Documents and books concerning

performance evaluations have been exchanged and translated. And personnel have been exchanged to work on joint Japan and U.S. Earthquake Engineering Research Program.

(3) Future Plans

1) The consolidation of Task Committees C and G was approved at the Thirtieth Joint Panel Meeting in May 1998. The following items are the scope of the activities and future activity plans of the new Task Committee.
1. Exchanging information, preparing research plans, and holding workshops concerning new design methods, evaluation methods, and repair and retrofitting technologies
2. Research on new materials and methods for the repair and retrofitting of existing structures and for use in new structures
3. Development of highly reliable methods of evaluating the condition of both new and existing structures.
4. Coordination between Japan and the U.S. to minimize the duplication of research and maximize the benefits obtained.

2) As the Sixth Phase of U.S. - Japan Joint Earthquake Engineering Research Program, smart structural systems will be developed. This research will be conducted in order to aggressively apply new materials, new structures, and other new technologies in order to improve the performance of the structures. This is expected to reduce the cost of construction and maintenance work and to contribute to the future sustainability of structures. The followings are the items for development.
1. Creation of a smart structural systems concept and development of performance evaluation methods for smart structural systems.
2. Development of structural property detection technologies.
3. Development of structural members made of smart materials and research on methods of evaluating such structural members.
4. Development of design methods and performance evaluation methods for smart structural systems and smart buildings.

(Hisahiro Hiraishi)

Task Committee D: Earthquake Engineering for Dams

(1) Background

At the Twenty-fifth Joint Panel Meeting held in May 1993, establishment of the Task Committee on Dam Earthquake Resistant Engineering was approved in recognition of the importance of cooperative research on the problem of the earthquake resistance of dams. The Task Committee was formed to develop measures that will contribute to the mitigation of earthquake damage to dams by conducting research exchanges concerning methods of preventing or mitigating damage to dams during earthquakes in both the U.S. and in Japan.

Earthquake resistant design of dams in Japan is based on the seismic coefficient method. No dam designed based on the seismic coefficient method has ever suffered damage that effected its safety as a result of a large earthquake. Although many civil engineering structures were severely damaged by the Hyogo-ken Nanbu Earthquake of January 1995, not one dam suffered any damage that reduced its safety. The Dam Earthquake Resistance Evaluation and Study Committee established by the Ministry of Construction after the earthquake confirmed that dams designed based on the present seismic coefficient method have earthquake resistance adequate to protect them from earthquake motion in the Hyogo-ken Nanbu Earthquake class.

But it is necessary to conduct studies based on dynamic analysis methods that can reproduce behavior during earthquakes in order to perform evaluations to determine the degree of earthquake motion that a dam designed using the seismic coefficient method can withstand safely and whether or not it is possible to create the optimum design with reference to the earthquake resistant performance a dam should have. The dynamic analysis method is an effective way to evaluate the dynamic response of a dam to verify its deformation properties, but

at this time, it is only used as a method of verifying the earthquake resistance under various earthquake motions of a section designed using the seismic coefficient method.

About 400 dams under the jurisdiction of the Ministry of Construction are now being constructed in Japan, and the Public Works Research Institute of the Ministry of Construction, the Water Resources Development Public Corporation, universities, and so on, are carrying out research on dynamic analysis methods in order to design dams that are safe from the effects of earthquakes.

In the U.S. on the other hand, while dam construction continues, there are many completed dams, and concerned organizations are working to quickly develop methods of selecting existing dams that require seismic reinforcement work and rationally establish counter-measure priorities and counter-measure construction methods. Research on ways to use dynamic analysis methods to evaluate the earthquake resistance of existing dams is underway, mainly by the Army Corps of Engineers and the Bureau of Reclamation of the Department of the Interior.

This Task Committee has, therefore, established the following three areas for research exchanges conducted to establish the systematic use of dynamic analysis methods to evaluate the earthquake resistance of both new and existing dams.

1) Numerical analysis methods of performing earthquake resistant design of dams and discharge facilities
- Comparison of design methods used in Japan and the U.S.
- Development of design ground earthquake motion.
- Study of dynamic analysis methods (modeling, calculation programs, etc.).

2) Dynamic deformation strength properties of dam body construction materials and foundation ground materials
- Study of the strength and deformation properties during earthquakes of dam body construction materials (concrete, soil quality, rock material) and foundation ground materials.

3) Analysis of measured behavior of dams and discharge facilities during earthquakes
- Analysis of behavior of dams and discharge facilities damaged by earthquakes and clarification of damage mechanisms.
- Reflection of analysis of the actual behavior of dams during earthquakes in earthquake resistant design.

(2) Accomplishments

Within less than one year after the 1993 establishment of this Task Committee, the Northridge Earthquake of January 1994 struck, and this was followed about one year later by the Hyogo-ken Nanbu Earthquake of January 1995. Immediately after the Hyogo-ken Nanbu Earthquake, members of the U.S. section of the Task Committee visited Japan to conduct a damage survey of dams and reservoirs. In March of the same year, Director Matsumoto (director at the time) of the Dam Department of the Public Works Research Institute of the Ministry of Construction visited the U.S. to give members of the U.S. section of the Task Committee an early report on damage to dams and on the earthquake motion records. In these ways, the Task Committee has carried out rapid exchanges of information about earthquake damage to dams and strong motion records.

As part of research exchanges conducted by this Task Committee, a workshop was held in the U.S. in November 1996. Based on earthquake motion records obtained at dams near the hypocenter during the Hyogo-ken Nanbu Earthquake, the workshop participants studied the properties of earthquake motion and the evaluation of earthquake resistance properties of existing dams. Reports of results of these research projects and the latest research on the U.S. side were exchanged.

And as part of researcher exchange activities, two researchers from the Public Works Research Institute of the Ministry of Construction have been sent to the Berkeley campus of the University of California to study the dynamic analysis of concrete dams and fill dams.

(3) Future Plans

In response to the Hyogo-ken Nanbu Earthquake, it is now considered necessary to design dams and other important structures to guarantee they have earthquake resistant performance able to protect them from Level 1 and Level 2 earthquake ground motions. It is, therefore, necessary to conduct research that will permit the use of dynamic analysis methods as a practical dam earthquake resistance evaluation method. In Japan, it is one of the major subjects of on-going research that looks into damage to dams, analysis of the cracking of concrete dams or the large-scale slippage of fill dams that would be caused by a large-scale earthquake, for example, so that the exchange through this Task Committee of information with the U.S. where research in this field is advanced is an effective way to contribute to this research.

During the coming ten years, the Japan side of this Task Committee plans further research exchanges with the U.S. in order to establish the systematic application of dynamic analysis methods to the evaluation of earthquake resistant performance of new dams and existing dams.

(Hitoshi Yoshida)

Task Committee E: Design for Wind and Wind Hazard Mitigation

(1) Background

The establishment of this Task Committee was approved by the Twenty-eighth Joint Panel Meeting, but prior to its formation, activities similar to those of this new Task Committee had been conducted by two other committees: the Task Committee on High Wind and the Task Committee on Wind Characteristics and Structural Response. This report will, therefore, begin with an explanation of these committees.

The Task Committee on High Wind was established by the Eighth Joint Panel Meeting and its principal activities were the exchange of high wind data, the exchange of information concerning wind observation systems, the promotion of research on the effects of high winds on structures, the exchange of data regarding wind pressure and wind velocity distribution, and the establishment of boundary layer wind tunnel experiment methods.

In order to expand the range of its activities, the Twelfth Joint Panel Meeting changed its name to the Task Committee on Wind Characteristics and Structural Response. The principal activities of this renamed Task Committee were the exchange of recording formats and recording periods for meteorological data provided by national government meteorological organizations, summarization of the results of actual wind measurements, the exchange of strong wind data and wind pressure data, the establishment of boundary layer experimental methods, encouragement of the exchange of boundary layer wind observation documents, the promotion of the exchange of information concerning methods of measuring and of estimating the wind response of structures, and the revision of standards for wind data accounting for its future uses.

In line with these activity policies, the Task Committee exchanged information, exchanged strong wind records, and arranged the exchange of researchers, but in response to the shared concern in both Japan and the U.S. with advanced technology for the design and construction of structures able to withstand strong winds and seismic forces, the Twentieth Joint Panel Meeting proposed the unification of the Task Committee on Wind Characteristics and Structural Response and the Task Committee on Evaluation of Structural Performance to form the Task Committee on Evaluation of Structural Performance, and this Task Committee commenced its activities in this new form at the time of the Twenty-first Joint Panel Meeting. At the Twenty-fifth Joint Panel Meeting, the Task Committee on Evaluation of Structural Performance and the Task Committee on Repair and Retrofit of Existing Structures were united to form the Task Committee on Design, Evaluation and Improvement of

Structures.

As a result of the above integration, the share of the range of activities of this Task Committee accounted for by wind engineering and wind resistance engineering shrunk. On the other hand, the damage caused by Hurricane Andrew and Hurricane Iniki was a reminder of the importance of wind hazard mitigation. In light of these events, the Twenty-seventh Joint Panel Meeting recommended a study of the possibility of establishing the Task Committee on Design for Wind and Wind Hazard Mitigation, and the Twenty-eighth Joint Panel Meeting approved the formation of the Task Committee on Design for Wind and Wind Hazard Mitigation.

The following five items outline the range of the activities of the Task Committee on Design for Wind and Wind Hazard Mitigation.
1. Characteristics of strong winds, particularly strong winds in the boundary layer
2. Effects of wind (wind load and wind-induced response of structures)
3. Experimental and analytical methods of predicting strong wind and its effects
4. Damage and risk assessment
5. Assessment and mitigation of wind hazard

(2) Accomplishments

The First U.S. - Japan Workshop on Design for Wind and Wind Hazard Mitigation was held at the Hawaii Imin International Conference Center at the East-West Center at the University of Hawaii from October 7 to 9, 1997. 10 U.S. members and 7 Japanese members of the Task Committee participated in the workshop. The participants presented papers concerning the control and prediction of wind-induced response, effects of topography on the characteristics of strong wind, risk assessment of strong wind, and computational fluid dynamics. The participants also discussed possible themes for future collaborative research between U.S. and Japan and concluded by recommending the following themes.
1. Application of models and field measurements to determine wind speed-up and turbulence characteristics associated with topographic features
2. Development and testing of procedures for using comprehensive aerodynamic and / or structural characteristics data bases to calculate wind loading effects and structural performance
3. Numerical simulations and measurements
a. Development of realistic aerodynamic loads for structural control applications
b. Computational Fluid Dynamics-based quantification of wind loads
c. Full-scale measurements and information obtained by numerical simulation on flow structure in cyclones and thunderstorms
d. Measurement of forces induced by wind on components, assemblies and structural systems
4. Aerodynamic control
a. Tailoring aerodynamic modifications for performance control (flexible structures, envelope / roofing)
5. Performance Evaluations
a. Evaluation of existing buildings and structures for wind vulnerability to develop retrofitting schemes
b. Evaluation of the performance of controlled systems
6. Development of prediction methods for wind response of long-span bridges
7. Cooperative efforts in post-storm damage assessment following strong wind events, e.g., tropical cyclones

In line with this final conclusion, collaborative research between the U.S. (University of Washington) and Japan (Public Works Research Institute) on the "Development of Prediction Methods for Wind Response of Long-span Bridges" is now commencing.

(3) Future Plans

The Task Committee intends to contribute to the rationalization of design for wind, and to the wind hazard mitigation by conducting cooperative research concerning the above seven themes. Of these themes, those related to bridges are now the objects of cooperative U.S. - Japan research projects, but the committee plans to study the possibility of cooperative research on themes related to buildings and to strong wind characteristics.

The Second U.S. - Japan Workshop on Design for Wind and Wind Hazard Mitigation will be held at the Public Works Research Institute in May 1999, and the Task Committee intends to take this workshop as an opportunity to present and discuss the results of present cooperative research and to arrange new cooperative research projects.

(Hisashi Okada and Hiroshi Sato)

Task Committee F: Disaster Prevention Methods for Lifeline Systems

(1) Background

It was adopted at the Seventh Joint Panel Meeting in 1975 to establish Task Committee F on Disaster Prevention Methods for Lifeline Systems. The first meeting of Task Committee F was held on the occasion of the Eighth Joint Panel Meeting in 1976. The Task Committee Report of that time identified the scope of this Task Committee as:

1. Improvement of design and disaster prevention technology for lifeline facilities should be pursued.
2. Lifeline is here defined as important facilities to take emergency measures within 72 hours after disaster occurred, including bridges, embankments, tunnels, slopes, pedestrian bridges, pipelines, water pipes, telephone and power transmission lines, waterways and tidal gates, inland water for fire fighting and the minimum facilities of wharves. Excluded from the category of Task Committee F are buildings, relay facilities, power generation plants and buildings for waterworks.

In 1978, the Miyagi-ken Oki Earthquake severely damaged lifeline facilities, resulting in increased demands for research on the safety of lifeline systems. At the Eleventh Joint Panel Meeting in 1979, it was agreed to initiate coordination of U.S. - Japan joint cooperative research on the safety of lifeline system and its component. Later, U.S. - Japan joint cooperative research on reinforced concrete column structures and embedded pipelines was conducted during 1982-1989.

On the occasion of the Twenty-first Joint Panel Meeting in 1989, the objective of this Task Committee was rearranged as follows:
Lifeline systems such as gas, oil, water and sewage pipelines; and power, communication and transportation systems are crucial to the survival and health of community, and the earthquakes affecting such systems cause severe social and economic disruptions to communities and cause human suffering to residents. In view of those facts, Task Committee F focuses on improving 1) behavior of lifeline systems during earthquakes and 2) engineering and other seismic countermeasures such as damage estimation techniques and inspection procedures. Those two points have continued to be the principal objectives of the Task Committee since then.

Following the Loma Prieta Earthquake of 1989, researchers from both the U.S. and Japan surveyed damage to lifeline facilities in the San Francisco Bay Area and conducted research on seismic behavior of lifeline facilities, repair, retrofit and so forth. After the Northridge Earthquake of 1994, with the assistance of the U.S. side, a survey team from Japan visited the damaged area in Los Angeles, where they investigated water pipes and transformer substations that were extensively damaged by the earthquake. One year later, the U.S. and Japan formed a joint damage survey team to investigate the Hyogo-ken Nanbu Earthquake. The results of the joint survey have been reported at various technical conferences, workshops, etc.

Those in the field of lifeline earthquake engineering have long been conscious of the needs for risk assessment and crisis management in addition to structural measures, and Task Committee F has promoted research in both areas. The importance of research on the former area has especially been increased after the Northridge and Hyogo-ken Nanbu Earthquakes. At the Twenty-ninth Joint Panel Meeting in 1997, "Seismic Information Systems" was adopted as a Panel Theme, and members of this

Task Committee presented papers on the subject.

(2) Accomplishments

1) U.S. - Japan Joint Cooperative Research
Since earthquake damage to lifeline facilities is a serious problem for both countries, U.S. - Japan joint cooperative research was initiated in 1982 to study the dynamic response, strength and deformation properties of lifeline facilities. This joint research project dealt with reinforced concrete column structures and embedded pipelines. The former was undertaken jointly by the Public Works Research Institute and National Bureau of Standards, and the latter was carried out primarily by the Public Works Research Institute, Columbia University, Cornell University and the National Center for Earthquake Engineering Research.

In the joint cooperative research on reinforced concrete column structures, scale effects were studied by the U.S. side with static loading tests of large specimen with cross sections as large as 2 m and medium size specimen. The effects of loading velocity and loading hysteresis were studied on the Japan side using dynamic loading facilities. The results of both investigations were complied in the form of technical reports on the scale effects by the U.S. side and on the effects of loading velocity, number of loading cycles, loading time histories, two directional loading and oblique loading by the Japan side. Technical findings and information was exchanged at the Joint Panel Meetings and workshops.

In the joint cooperative research on embedded pipelines, cooperation was initiated from strong motion monitoring for seismic response of embedded pipelines during earthquakes. Monitoring was undertaken at the site where a pipe crosses a fault in the U.S. and at the site with irregularly layered ground in Japan. Recorded data were exchanged between two countries, and the results of study on dynamic response of embedded pipelines were presented at the Joint Panel Meetings and workshops.

2) Workshops
Task Committee F has held seven workshops since the First U.S. - Japan Workshop on Lifeline Earthquake Engineering, which was held at the Highway Research Center, Federal Highway Administration in McLean, VA, U.S.A. in 1984. While UJNR is a cooperative science and technology program led by governmental organs, the Task Committee workshops are the scene of lively discussions among experts from various fields. Since this Task Committee does not focus on a specific structure but covers a wide variety of facilities that can be classified as lifeline structures, it is extremely important that the workshop participants include representatives of universities, public utility enterprises and private sectors in addition to those from governmental agencies.

At the Sixth and Seventh Workshops that were held after the Northridge Hyogo-ken Nanbu Earthquakes, results of analysis and restoration of earthquake damage and technology development following those earthquakes were actively discussed.

(3) Future Plans

The features of lifeline facilities and earthquake damage to them are:
1. Lifeline facilities have two characters; they not only function as individual structures, they are also linked in complex ways to many other structures to function as part of network systems.
2. There is a vast existing stock of lifeline facilities, and retrofitting of this stock and the rapid restoration of their functions after a disaster are important.
3. Damage to lifeline facilities has intensive socio- economic indirect impacts on the society in addition to direct impacts. Damage to water supply and sewerage facilities may cause public health problems.

Considering the above facts, the following fields are proposed as candidate themes for research and development through joint cooperative research, workshops, and so on:
1. Evaluation of seismic performance of lifeline facilities and design methods.
2. Reliability evaluation of lifeline facilities as

network systems.
3. Seismic vulnerability inspection and retrofit techniques.
4. Post-earthquake (post-disaster) response.
5. Damage assessment and evaluation of socio-economic impacts of damage to lifeline facilities.
6. Relationship between damage to water supply and sewerage facilities, and public health.

(Masahiko Yasuda)

Task Committee G: Structural Control and Intelligent Material Systems

(1) Background

The Twenty-second Joint Panel Meeting held in 1990 recognized the need for U.S. - Japan joint research on passive, active, and hybrid control systems, and formed Task Committee G (Passive, Active, and Hybrid Control Systems). Then the Twenty-fifth Joint Panel Meeting held in 1993 renamed this Task Committee the Task Committee on Structural Control and Intelligent Material Systems in response to a growing need for research on the use of new materials including smart or intelligent materials.

The following are the goals and the range of activities of Task Committee G.
1. Develop research plans in control of equipment and structures and in high performance structural and material systems;
2. Implement control techniques for motion reduction and modification;
3. Implement use of advanced materials in actual design and construction of buildings and other infrastructure systems under seismic or wind environments;
4. Promote U.S. - Japan cooperation in structural control and intelligent material systems research;
5. Bring together governmental, academic, and industrial participants in joint pursuit of these efforts; and
6. Contribute to IDNDR by organizing joint research and other technical activities in structural and intelligent material systems research based on international cooperation.

Task Committee G works closely with other organizations to provide the leadership in this emerging research by facilitating the exchange of data and information through UJNR mechanisms. The scope of work includes:
1. Providing technical assistance, consultation and coordination of UJNR affiliated research organization in the initiation, development, and execute their programs in research areas.
2. Promoting joint government - university - industry collaborative efforts to facilitate technology transfer and practical implementation.
3. Sponsoring and conducting interdisciplinary workshops and meetings to identify key area of research and opportunities for cooperation, and to stimulate public awareness and interest in this field of research.
4. Developing promotional and demonstrative activities to stimulate public awareness and interest in this field of research.
5. Providing information useful for the establishment of performance standards, design and also retrofit / rehabilitation of existing structures.
6. Promoting research in intelligent material systems, sensors, actuators, optional control system design, and encourage laboratory and field experiments of prototype and full-scale structures.

(2) Accomplishments

The successful results of the activities of Task Committee G are broadly categorized as three cooperative research activities. These are: U.S. - Japan joint research programs concerning structural control, cooperative research on passive (base isolation) and active control (vibration control) design for bridges, and cooperative research on smart structural material systems. Outlines of each of these cooperative research fields follow.

1) U.S. - Japan joint research programs concerning structural control
U.S.-Japan joint research on structural control started in 1990. Both Japan and the U.S. established domestic committees on structural

control that held workshops in their respective countries and conducted cooperative research by holding international workshops. Members of the UJNR took part in both of these national committees. The principal areas of this joint research are; 1) sensors and monitoring, 2) structural control; and 3) intelligent structures.

In August 1994, the First International Conference on Structural Control was held in Pasadena, California in the U.S. followed by the Second International Conference on Structural Control held in June and July 1998. Researchers from many countries attended both these conferences.

2) Cooperative Research on Passive (Base Isolation) and Active (Vibration Control) Control Design of Bridges

Technical information concerning passive and active control design for bridges has been exchanged at a series of workshops. The first was held in September 1991 at the National Center for Earthquake Engineering Research (Buffalo, New York). The principal activity at this workshop was the exchange of technical information regarding the application of passive design to bridges, passive control systems, etc. The second in this series was held in December 1992 at the Public Works Research Institute (Tsukuba City), the third in Berkeley in the U.S. in January 1994, and the fourth in Osaka in December 1996. The collected papers presented at these four workshops have been published by the National Center for Earthquake Engineering Research and by the Public Works Research Institute. A total of approximately 120 technical papers have been exchanged through these workshops.

This cooperative research commenced during the period when passive design was first applied to bridges. The technical information exchanged through these workshops is contributing to the enactment of design standards for passive control bridges and to the construction of actual passive control bridges in both Japan and the U.S.

With the cooperation of Task Committee J, a joint research project concerning hybrid control of bridge structures was conducted by the Public Works Research Institute, the National Science Foundation, the Federal Highway Administration, the National Institute of Standards and Technology, the National Center for Earthquake Engineering Research and the University of California at Irvine. As part of this project, vibration experiments were conducted at the Public Works Research Institute and the National Center for Earthquake Engineering Research. U.S. - Japan cooperative research includes shaking table experiments performed at the Public Works Research Institute to verify the effectiveness of a sliding base isolation system developed by the National Center for Earthquake Engineering Research. Another example is the simulation and analysis by the University of California at Irvine of the results of shaking table experiments to test variable dampers developed by the Public Works Research Institute.

3) Cooperative Research on Smart Structural Material Systems

In the field of structural technology using smart high performance materials, a U.S.-Japan Workshop on Smart High Performance Materials was held at the Building Research Institute (Tsukuba City) in May 1993. At the Building Research Institute, research on structural control and on smart material systems with self diagnosis and self restoration functions commenced in April 1994, and at the Public Works Research Institute, research on smart earthquake resistant structures made of self diagnostic material and self restoration materials commenced in April 1995.

In November 1996, the U.S.-Japan Workshop on Smart Structural Technology (Application to Large Structures) was held at the University of Maryland in the U.S. At this workshop, discussions of the next stage of Japan U.S. joint research on smart structural material systems began, and joint U.S.-Japan research on smart structural material systems commenced in 1998.

(3) Future Plans

Because the above research results have satisfied initial goals and because it appears that the research duplicates that of other Task Committees, the Thirtieth Joint Panel Meeting held in May 1998 confirmed that Task Committees C and G will be unified and that future cooperative research will be conducted by the newly organized Task Committee C.

(Shigeki Unjoh)

Task Committee H: Soil Behavior and Stability During Earthquakes

(1) Background

The establishment of this Task Committee was approved at the Eighth Joint Panel Meeting held in May 1976. The objectives of the Task Committee are to enhance the availability of technology for predicting dynamic behavior of soils, foundations and earth structures, and analyzing dynamic soil-structure interaction to assure their safe performance during earthquakes.

Although earthquakes cause devastating damage, research works on this field have a relatively short history. Even prior to the establishment of this Task Committee, both the U.S. and Japan were greatly interested in the related issues , and since the First Joint Panel Meeting, the two countries have carried on a lively exchange of information including comparison of a seismic design standards for soil structures.

(2) Accomplishments

Achievements of the Task Committee are briefly summarized below, focusing on the last decade. Major activities of the Task Committee have been the exchange of information through presentation of papers and discussions at the Joint Panel Meetings, holding workshops, exchanging researchers, and conducting joint surveys at earthquake damaged sites.

1) Exchange of information
More than 130 papers on this field have been submitted to the 30 Joint Panel Meetings. In general, interest of researchers in the field of soil dynamics may be classified into following categories through observation of subjects of the papers:
1. Mechanical properties of soil under cyclic loading.
2. Liquefaction and its related problems.
3. Prediction of permanent deformation of soil structures due to earthquakes.
4. Countermeasures against liquefaction and retrofit techniques for mitigating damage of structures.

Through observations of subjects of the papers presented in the 30 Joint Panel Meetings, which have been more than 130 papers in this field, it can be found out that research on themes 1. and 2. prevailed until about the Twentieth Joint Panel Meeting, and major interest of researches seem to have shifted to themes 3. and 4. during the last decade with the progress in analytical methods and advances in understanding dynamic properties of soils.

In order to understand the achievements in this field during the past ten years the subjects of the documents that have been exchanged in the period was analyzed in detail and divided into several categories as follows.
1. Introduction of aseismic design standards for ground, foundations and soil structures.
2. Introduction of site investigation technique and new methods for liquefaction assessments.
3. Introduction of earthquake resistant calculation methods, dynamic behavior, and case histories of earthquake damage.
4. Introduction of countermeasure techniques against liquefaction-induced damage of structures.
5. Introduction of centrifuge modeling of soil dynamics.

These are mostly results of experience and research works nurtured in the U.S. or Japan from the different point of view of the two countries. The exchanged information was believed to be extremely effective to have deepened mutual understanding between the U.S. and Japan. The materials that have been exchanged are not only papers submitted at Joint

Panel Meetings but material and data that were prepared by committees of the Panel on Wind and Seismic Effects.

2) The Workshops

Since the first workshop on in-situ testing for liquefaction assessment was held in San Francisco in August 1985, five workshops have been held so far. The second to fourth workshop dealt with a main topic of liquefaction countermeasures while the fifth workshop took up centrifuge modeling of soil dynamics problems. In this way, the Task Committee has established a record of useful achievements through taking up appropriate topics in time and exchanged views more frequently than possible at the Joint Panel Meetings or international conferences.

3) Exchanges of Researchers

The Task Committee has promoted a better mutual understanding in the two nations through the exchange of researchers. Researchers from both countries were sent to visit the other country for periods ranging from a month to a year to conduct research.

4) Joint Surveys at Earthquake Disaster Sites

Relatively large earthquakes have struck both Japan and the U.S. during the last 30 years. In particular, during the last decade, we have experienced the Loma Prieta Earthquake of 1989, the Kushiro-oki Earthquake of 1933, the Northridge Earthquake, the Hokkaido Nansei-oki Earthquake, the Hokkaido Toho-oki Earthquake of 1994, and the Hyogo-ken Nanbu Earthquake of 1995. After each of these earthquakes, engineers and researchers from Japan and the U.S. carried out joint surveys as a part of UJNR activities. The result of these surveys have yielded numerous valuable lessons.

(3) Future Plans

The 1989 Loma Prieta Earthquake and the 1995 Hyogo-ken Nanbu Earthquake have triggered important changes in a framework of earthquake resistance technologies in the both countries. It was a shift towards consideration of large earthquake motion in earthquake resistance design and towards performance-based design methods. With regard to earth structures, this was accompanied by the appearance of a mountain of research and development challenges.

In the recent years, liquefaction countermeasures have been widely executed in Japan. Indeed, it is important to share the knowledge gained through this experience with the U.S. side. In the U.S., on the other hand, research works have been extensively conducted concerning a framework for performance design, and methodologies for the prediction of damage due to strong earthquake motion. Cooperation with the U.S. in this field is considered to be extremely beneficial for Japan.

From a view point of mutual benefits, following research topics which should be tackled by the Task Committee in the future can be drawn:

1. Development of methods of predicting instability and deformation of earth structures and slopes induced by a large-scale earthquake motion.
2. Development of retrofit procedures of existing earth structures and foundations to improve their seismic stability.
3. Rationalization of design methods for liquefaction prevention measures.
4. Development of unified in-situ testing methods for the assessment of liquefaction potential of ground including gravel and fine grain soils.
5. Development of performance-based seismic design methods for earth structures.
6. Improvement of techniques of dynamic centrifuge tests and shaking table tests.

Themes 1. through 4. are extremely necessary in practice in both countries. Outcome of research on these topics could directly contribute to the improvement of reliability and to cost reductions. As necessary, information should be exchanged so that the latest information about research and practical works related to these issues is transmitted between the two countries. Themes 5. and 6. are considered to be medium term challenges, therefore, workshops should be

held at appropriate times to discuss research results and future research plan.

(Osamu Matsuo)

Task Committee I: Storm Surges and Tsunami

(1) Background

The Task Committee I was formed at the Eleventh Joint Panel Meeting in 1979 to strengthen cooperation in the field of research on storm surges and tsunami. After its formation, this Task Committee debated its activity policy and decided that its role would be the promotion of information exchanges concerning a storm surge forecasting model and a meteorological model to be used with it. At a meeting of the Task Committee in 1981, it was pointed out that the U.S. emphasized storm surge forecasting in real-time and that Japan put first priority on the design and execution of coastal structures intended to provide protection from storm surge and tsunami. To share the latest research in both countries and set common goals to be attained in the future, the First Tsunami Workshop was held in Tsukuba in 1983, with four more such workshops held alternatively in Japan and the U.S.

The Task Committee's activity policy has been reviewed through a series of discussions at workshops and at Joint Panel Meetings and it has now been summarized in the following form.

1. Exchanging the results of research on occurrence, generation, propagation, and effects of storm surge and tsunami. Particularly, the exchange of information concerning deep ocean tsunami measurements.
2. Exchanging information concerning study, planning, warnings and technology problems of storm surge and tsunami mitigation activities.
3. Exchanging technology information concerning numerical models to predict tsunami arrival time and run up height, the improvement of observation instruments, and the use of satellites for detection and prior warning.
4. Stimulating research on tsunami and storm surge by holding workshops, etc.

(2) Accomplishments

In addition to exchanging technology information regarding storm surge and tsunami that has been collected in the U.S. and in Japan, Task Committee I has held one workshop every two years to share the latest research in the field of storm surge and tsunami research. The Second Tsunami Workshop was held in Honolulu in Hawaii on November 5 and 6, 1990 and the Third Tsunami Workshop was held in Osaka on August 27 and 28, 1993. At the Third Tsunami Workshop, the results of the latest survey of the tsunami produced by the Hokkaido Nansei-oki Earthquake that devastated the community of Okushiri Island on July 12, 1993 was presented and guidelines to govern future research on the characteristics of this tsunami were confirmed. Immediately following the Hokkaido Nansei-oki Earthquake tsunami, many survey teams including one from the UJNR conducted surveys of the trace of the tsunami runup on Okushiri Island, helping clarify the characteristics of the tsunami and accumulating data that could be used to verify a numerical model. Based on these surveys and on information exchanges, the Public Works Research Institute prepared a model reproducing the seabed close to Cape Aonae at a scale of 1/1,100 to clarify the tsunami propagation mechanism and the Port and Harbour Research Institute has performed a mound scouring experiment on the breakwater of Okushiri Harbor.

A workshop on wind and earthquake engineering of marine and coastal structures was held from January 17 to 19, 1995 in Berkeley in the U.S. At this workshop, which was sponsored jointly with Task Committee K, Task Committee I presented research on the development and the prediction of storm surge in addition to research on tsunami. On the first day of the workshop, the extremely destructive Hyogo-ken Nanbu Earthquake occurred in the Hanshin and Awaji region of Japan, serving as a sharp reminder of the importance of earthquake disaster protection including protection from tsunami.

The Fourth Tsunami Workshop was held at Hilo in Hawaii from April 1 to 3, 1996. This workshop was held to commemorate the 50th anniversary of the Aleutian Tsunami that struck Hilo on April 1, 1946 and the 100th anniversary of the Sanriku Tsunami that came ashore in the Sanriku Region in 1896. From July 9 to 11, 1998, the Fifth Tsunami Workshop was held in the City of Sapporo in Hokkaido. This workshop was held to commemorate the fifth anniversary of the Hokkaido Nansei-oki Earthquake Tsunami of 1993. During this workshop, the tsunami researchers visited Okushiri Island where they attended a reception to exchange views with people who had experienced the tsunami and observed the state of recovery work in the part of the island it had devastated.

Participants in the International Tsunami Commission of 1997 realized that it was necessary to provide and improve gridded bathymetry for numerical calculation of tsunami and to undertake the international sharing of information. Task Committee I agreed to support these activities. The Fifth Workshop held in 1998 pointed out the importance of using large water tanks for model experiments of tsunami and initiated the tasks of making a list of such facilities at research institutions in Japan, U.S. and Europe, and clarifying the roles of large scale experiments in tsunami research.

(3) Future Plans

The Task Committee I will continue to study storm surge and tsunami damage reduction measures through information exchanges between Japan and the U.S. It will energetically tackle the following challenges during the coming five or six years.

1. Because it is possible to forecast tsunami generated by tsunami earthquakes with high precision using deep ocean tsunami detection systems, actual prior warning systems must be incorporated in the future. A lively exchange of information is now in progress, but because progress has been achieved in research to develop laser-type tsunami detectors and to optimize the arrangement of tsunami detectors, it is now necessary to develop low cost detection systems and to share information. The study of the possibility of using artificial satellites for tsunami detection will begin.

2. To use numerical models to predict the development and propagation of storm surge or a tsunami, it is important to provide gridded bathymetry in the modeled field. In shallow sea close to shorelines in particular, the precision of the gridded bathymetry governs errors in the prediction of the height and arrival time of tsunami. It is, therefore, necessary that precise data be provided. As two countries that have made progress in providing such data, Japan and the U.S. must play leading roles in order to create a international common environment, and Task Committee I will take part in this task. A common environment for gridded bathymetry in deep ocean will be achieved in 2000, followed by its expansion to shallow sea.

3. Based on the gridded bathymetry that has been provided, a numerical calculation model for tsunami and storm surge will be developed and improved. It is important that a tsunami model improve the precision of estimations of the initial wave profile at tsunami source area and that it reproduces wave deformation in shallow sea. In storm surge model, a wind estimation method and modeling of the stress that acts on sea surface are important. Because recent years have seen progress in research to develop such models, Task Committee I will develop and improve a practical model while jointing gridded bathymetry.

4. Because storm surge and tsunami are infrequent natural phenomena, it is difficult to obtain sufficient on-the-spot data. Hydraulic experiments performed using large-scale tanks are, therefore, effective ways to clarify the behavior of wave in coastal zone. At the Public Works Research Institute, experiments using a large-scale water tank have been performed to study scouring of the ground around structures by tsunami and joint research will be performed in order that the two countries organize their shared research objectives. Preliminary

experiments using the Public Works Research Institute's large-scale tank began in 1998, and they will continue in 1999 in order to develop a model for predicting scouring of the ground around structures by tsunami. In 2000, research intended to provide proposals for scouring prevention measures will commence.

(Shinji Sato)

Task Committee J: Wind and Earthquake Engineering for Transportation Systems

(1) Background

The Thirteenth Joint Panel Meeting held at the Public Works Research Institute of Ministry of Construction in Tsukuba Science City from May 19 to 22, 1981 tackled this theme by agreeing to form the Task Committee on Wind and Earthquake Engineering for Transportation Systems to carry out joint research between the U.S. and Japan in this field. The initial activities of the Task Committee were considering the scale of the range of wind resistance and seismic technologies related to traffic facilities and limiting the research to earthquake engineering problems with plans to expand the scope of the research to include the effects of both wind and earthquakes on traffic facilities in the future.

The principal objectives of this Task Committee were defined as the conduct of joint research and the periodical exchange of information concerning themes of common concern to both nations. Since 1982, information exchanges at annual meetings of the Task Committee have been accompanied by workshops, joint research, and ongoing consultations regarding future committee plans. Its activities related to research on the wind and earthquake engineering for transportation systems primarily concerned the wind resistant and seismic design of highway bridge structures.

The Twenty-eighth Joint Panel Meeting held in 1996 approved the establishment of the Task Committee on Design for Wind and Wind Hazard Mitigation, that has conducted research on the characteristics of strong wind and the mitigation of the damage caused by strong winds. But with this Task Committee intimately involved in wind resistance technology for transportation systems, it is to continue its research in recognition of the particular importance of the wind resistance of highway bridges.

(2) Accomplishments

Every year, this Task Committee has presented many papers and engaged in an extensive exchange of information with the participation of many researchers and papers on this theme in the past decade. Another noteworthy activity has been a series of damage surveys by cooperating American and Japanese teams immediately following a series of earthquakes in U.S. and Japan; the Loma Prieta Earthquake of October 17, 1989, the Northridge Earthquake of January 17, 1994 and the Hyogo-ken Nanbu Earthquake of January 17, 1995. The Task Committee has engaged in an exchange of information on the latest earthquake engineering technology including the results of the above surveys and detailed information obtained later, contributing to the early recovery from these disasters and the advance of seismic technology in both nations.

A Task Committee meeting held in 1983 planned the U.S. - Japan Bridge Engineering Workshop. The first U.S. - Japan Bridge Engineering Workshop was held at the Public Works Research Institute of Ministry of Construction in Tsukuba Science City in February 1984. With the venue alternating between U.S. and Japan, these workshops have continued almost every year with the thirteenth held in 1997. In Japan, these workshops have been held at the Public Works Research Institute, and in U.S., in San Francisco, San Diego, Lake Tahoe, Chicago and Buffalo. Participants have included a total of 265 representatives of U.S. and 439 from Japan, with a total of 429 papers presented. The workshops have been occasions for a lively exchange of views focused on the presentation of papers regarding design, construction, maintenance and new element technologies including criteria, related to the

wind resistance and seismic problems of highway bridges.

In addition to the Bridge Engineering Workshops, the Task Committee responded to a series of large earthquakes including the Loma Prieta Earthquake of 1989, the Northridge Earthquake of 1994, and the Hyogo-ken Nanbu Earthquake of 1995 that struck in U.S. and Japan by organizing a series of workshops on the seismic retrofit of bridges; the Workshop on Seismic Retrofit of Bridges. Three were held; one in Tsukuba in December 1990, second in Berkeley in January 1994, and the third in Osaka in December 1996. And the Task Committee also organized four Workshops on Earthquake Protective Systems for Bridges; in Buffalo in September 1991, in Tsukuba in December 1991, in Berkeley in January 1994, and in Osaka in December 1996. These workshops were integrated with the Bridge Engineering Workshops beginning in 1998.

The Task Committee has organized many exchanges of researchers between the U.S. and Japan. During the past decade, it has arranged for a number of researchers from U.S. and Japan to work at a research institute in the other country to survey and research seismic technology of highway bridges. In 1989, Dr. Shigeki Unjoh, researcher of PWRI was sent to University of Southern California and Mr. Ray Zelinsky of CALTRANS worked at PWRI. In 1990, Dr. Keiichi Tamura, senior researcher of PWRI studied at Stanford University and Mr. Kinji Hasegawa, researcher of PWRI, conducted research at University of California, Berkeley. In 1991, Mr. Inoue spent five months studying bridge maintenance and management at the Turner-Fairbank Highway Research Center. Mr. Mohsen Sultan of CALTRANS spent one year at PWRI where he carried out comparative research on seismic design of bridges between U.S. and Japan. In 1994, Mr. Mark Yashinsky of CALTRANS spent five months at Earthquake Engineering Division of PWRI conducting comparative research on seismic design of bridges between U.S. and Japan. In the same year, Mr. Michael Britt of FHWA researched bridge design technology during one year period spent at PWRI and Honshu-Shikoku Bridge Authority. Then in 1995, Dr. Phillip Yen of FHWA came to Japan for 20 days to research seismic design methods. In 1998, Dr. Jun-ichi Hoshikuma, researcher of PWRI, spent a year at University of California, San Diego to study the seismic design of bridges.

(3) Future Plans

Joint research which began in 1983 with joint research on the seismic performance of bridge piers and columns, has continued improved seismic retrofit and strengthening procedures, seismic isolation, and hybrid control for highway bridges based on experimental, analytical, and field studies, the comparison of seismic design criteria for bridges in U.S. and Japan, seismic, aeroelastic, aerodynamic response of long span bridges, seismic response and control, system identification techniques, nondestructive evaluation of bridge structures, use and performance of structural materials including new materials, and performance of jointless bridges, and so on. The Task Committee plans to undertake an active program of cooperative research on maintenance and application of high performance steel to bridges.

As the Task Committee continues to exchange research information concerning wind resistant and seismic technologies for transportation systems, arrange for the exchange of researchers in this field, and organize related joint research as described above, it must take up many new themes, and through close cooperation between its members in U.S. and Japan, become even more active than in the past.

(Kazuhiro Nishikawa)

Task Committee K: Wind and Earthquake Engineering for Offshore and Coastal Facilities

(1) Background

The Task Committee K was proposed by the Port and Harbour Research Institute of the Ministry of Transport of Japan and by the

Minerals Management Service of the Department of the Interior of the U.S., and it has been in operation since its formation was approved at the Twenty-third Joint Panel Meeting (1991). Task Committee K was established to perform technical surveys and research to prevent wind and earthquakes from damaging offshore facilities. It plans, supports, and executes surveys and research projects in line with this objective and conducts activities that apply the results of these research projects to future design standards.

The following are the specific themes studied by Task Committee K.

1. Sponsoring and conducting workshops and meetings to identify key areas of research, opportunities for cooperation, and the exchange of knowledge.
2. Predicting strong ground motions for offshore and coastal sites including assessing the effects of basin geometry, linear, and nonlinear local geological effects using actual seafloor response measurements.
3. Determining the dynamic response and the interaction of structure/foundation/soil systems to seabed motions and/or extreme wind forces.
4. Assessing the dynamic response and behavior of various operational facilities mounted on offshore and coastal structures.
5. Developing assessment methodologies for earthquakes and other characteristics of potential seismic sources (e.g., faults) for offshore and coastal sites in regards to how these conditions relate to structural design criteria.
6. Promoting the implementation of new research results into current design and construction processes.
7. Developing research efforts to include laboratory and field programs to obtain data on the response of offshore and coastal facilities to extreme wind and seismic forces.
8. Creating performance standards, design specifications, guidelines, and code recommendations for applications to new construction as well as remedial action for exiting facilities.

(2) Accomplishments

1) Holding Workshops

Two Workshops on Wind and Earthquake Engineering for Offshore and Coastal Facilities have been held. The first workshop was held in May 1993 at the Training Center of the Port and Harbour Research Institute of the Ministry of Transport. The eight and 22 representatives participated in this workshop from the U.S. and Japan, respectively. Each side presented 8 papers for a total of 16 papers. The papers dealt with the wind resistant and earthquake resistant design of marine facilities, damage inflicted on marine structures by Hurricane Andrew, earthquake observations of seabed ground, and so on. It was the first workshop, and its primary purpose was the exchange of information regarding the present state of offshore and coastal facilities in Japan and the U.S. and seismic, wind hazard mitigation design code/guidelines.

The second workshop was held at the Berkeley Campus of the University of California in the U.S. on January 1995. It was held jointly with the Task Committee I. The approximately 60 representatives who took part in the workshop were presented with a total of 40 papers: 20 from Japan and 20 from the U.S. The workshop confirmed that the following technological issues would be taken up by future joint research projects.

1. Development of earthquake risk evaluations
2. Improvement of numerical tsunami simulation technology
3. Development of methods of evaluating the wind resistance and earthquake resistance of existing structures
4. Appropriate evaluation of past high water and tsunami damage data

Information of many kinds has been exchanged as a result of these two workshops. Information concerning strong motion records of the seabed ground in deep waters obtained by means of earthquake observations at oil drilling platforms in the U.S. has been applied to the study of the earthquake resistance of deep-water structures in Japan.

2) Mutual Assistance with Earthquake Damage

Surveys
An earthquake damage survey was carried out following the 1994 Northridge Earthquake with the cooperation of the U.S., and this included a survey of damage in the Port of Los Angeles: a survey related to the concerns of Task Committee K. Then following the Hyogo-ken Nanbu Earthquake of 1995, Japan assisted with a damage survey in the Port of Kobe conducted by an earthquake damage survey team from the U.S. The results of the damage surveys in the two countries are information of use in the earthquake resistant design of port facilities in both Japan and the U.S.

3) Support for U.S. - Japan Joint Research
Task Committee K assisted with joint research by Old Dominion University of the U.S. and the Port and Harbour Research in 1992. This joint research focused on pressure acting on retaining walls during earthquakes, and Professor Ishibashi of Old Dominion University conducted the research while visiting the Port and Harbour Research Institute. The results of the project are being applied to more rational earthquake resistant design of port facilities.

4) Exchanges of Researchers
The Port and Harbour Research accepted a doctoral candidate from the University of California at Berkeley as a summer trainee for one month in August 1997, and accepted another doctoral candidate from the same university for four months beginning in August 1998 to perform model vibration experiments using a under water shaking table.

Mr. Nozu research of the Port and Harbour Research Institute is conducting research on earthquake resistant technology for offshore and coastal facilities at California Institute of Technology for a year beginning in October 1998. This researcher exchange by Mr. Nozu is connected to an exchange involving Prof. W. Iwan of California Institute of Technology who attended the first workshop held in Japan.

5) Cooperation at International Conferences
Members of Task Committee K helped to organize and participated in the workshop, "Earthquake Criteria Workshop - Recent Development in Seismic Hazard and Risk Assessment for Port, Harbor, and Offshore Structures" held concurrently with the International Offshore Mechanics and Arctic Engineering (OMAE1997) Conference in Yokohama, Japan on April 17, 1997.

(3) Future Plans

1. The Third Workshop on the Seismic, Wind and Hazard Mitigation Technique for Offshore and Coastal Facilities will be held in Japan; a specific time for this workshop are now being studied.
2. The Task Committee plans to support the provision of information concerning Japan's port facility earthquake resistant design standards that have been revised since the Hanshin Awaji Earthquake Disaster to the "Pacific Earthquake Engineering Research (PEER) Program on Ports and Harbors" of the University of Southern California.
3. Japan will carry out earthquake observations of structures in deep water and the exchange of information and research cooperation regarding the results of earthquake observations in both Japan and the U.S. will continue so that more rational earthquake resistant design methods for deep water structures can be developed.
4. The Port and Harbour Research Institute has a large-scale three-dimensional underwater shaking table of a kind not available in the U.S.; the possibility of U.S.-Japan joint research involving the use this test device to study the dynamic interaction of marine structures and water is being studied.
5. U.S.-Japan joint research will be undertaken to study the applicability to of advanced technologies such as nuclear magnetic resonance imaging (NMRI) technology and micro electric mechanical systems (MEMS).

(Tatsuo Uwabe)

Task Committee on Seismic Information Systems

(1) Background

Based on the recent large earthquakes including the 1994 Northridge Earthquake and 1995 Hyogo-ken Nanbu Earthquake, both the U.S. and Japan strongly promote developing seismic information systems for the earthquake disaster reduction. On the other hand, the U.S. and Japan policy makers have exchanged information regarding the utilization of seismic information systems to disaster prevention measures at the U.S.- Japan Earthquake Policy Symposia (September 1996 in Washington, D.C. and September 1997 in Kobe) held under the Common Agenda framework. Participants recognized the importance of further discussions on the following subjects at the U.S.- Japan Earthquake Policy Cooperation Forum that is conducted as the next stage of the Earthquake Policy Symposium.

1. Development and utilization of real-time earthquake information systems
2. Development and utilization of earthquake damage estimation models
3. Post earthquake emergency response measures and restoration measures

In response to these conditions, seismic information systems were featured as a technical session theme at the Twenty-ninth and Thirtieth Joint Panel Meetings. And the Panel approved the establishment of a new Task Committee on Seismic Information Systems at the Thirtieth Joint Panel Meeting. Objectives and scopes of the new Task Committee are as follows:

1. Improve understanding of earthquake phenomena and their social effects through the utilization of seismic information systems, earthquake damage estimation methodologies and analysis models.
2. Technically assist the earthquake policy cooperation under the Common Agenda framework by facilitating the cooperative efforts between policy makers and researchers.
3. Review the principals, objectives, structures and methodologies of both sides seismic information systems, and facilitating the practical application to earthquake prevention measures.

(2) Future Plans

The emphases of the Task Committee activities will be placed on following specific subjects.

1) Research cooperation on earthquake monitoring and notification systems

Both U.S. and Japan have been developing and practically utilizing these systems, i.e., CUBE, REDI, the Japan Meteorological Agency system, the Ministry of Construction System and others. It will be effective for both countries to exchange information on the real-time collecting / analyzing / disseminating technologies of earthquake ground motion data, and procedures of activating the ground motion data to emergency activities.

2) Research cooperation on damage estimation systems and decision-making support systems

The U.S.-side has been conducting researches on the application of GIS / GPS / remote sensing technologies, and information processing / disseminating technologies through communication networks. Japan-side has been developing and practically utilizing the damage estimation technologies using the real-timely collected ground motion data. Comprehensive research on the utilization of artificial satellites and other urgent disaster monitoring / analyzing technologies have also been initiated for the appropriate national land management against natural disasters. It will be effective for both countries to exchange knowledge and experiences on these advanced technologies.

3) Research cooperation on earthquake damage estimation models

Although several models have been developing in both the U.S. and Japan, i.e., the FEMA model, the National Land Agency model, the Ministry of Construction model and others, the verification of estimation models is not necessarily enough at this time. To exchange existing earthquake damage data possessed by each country and to compare simulated damage situations between models will be effective to improve estimation models in both countries.

The Task Committee will facilitate to promote efficient research cooperation by planning / conducting workshops with attendees of policy makers and researchers from government and

other public bodies, planning / conducting cooperative research projects, and exchanging information and personnel. The workshop will serve as a forum to technically support cooperative activities of policy makers under the U.S. - Japan Earthquake Policy Cooperation Forum. Also, the Task Committee will make efforts to exchange information with related working frameworks; i.e., Task Committee A "Strong Motion Data and Applications" regarding the real-time collecting / analyzing / disseminating technologies of ground motion data, and the Joint Panel on Earthquake Research regarding the remote sensing / GIS / GPS technologies.

(Kazuo Okayama and Hideki Sugita)

CONCLUDING REMARKS

The activities of the Panel on Wind and Seismic Effects were summarized on the occasion of the Twentieth Joint Panel Meeting. Passing ten years since then, this paper, prepared by the Japan-side Panel to commemorate the 30th anniversary of the Panel, looks back on thirty years of accomplishments and sets forth future prospects. The authors expect this paper will be a starting point to discuss future course of the Panel with the U.S.-side.

U.S.-Japan Cooperative Earthquake Research Program on Composite and Hybrid Structures - U.S.-side Progress

by

Subhash C. Goel[1]

ABSTRACT

A five-year research program on Composite and Hybrid Structures as Phase 5 of the U.S.-Japan Cooperative Earthquake Research Program was recommended to be initiated in 1993 in both countries. The research work in Japan started in fiscal year 1993. However, fuller participation of researchers on both sides started in early summer 1995. The sponsorship of the program is by the National Science Foundation in the U.S. and by the Ministry of Construction along with a number of industry groups in Japan. This paper presents a brief status report of the program and research progress made to date on the U.S. side. Because of diverse and broad scope of the subject area, the research program is organized into the following four groups: Concrete Filled Tube Column Systems (CFT); Reinforced Concrete (RC) and Steel Reinforced Concrete (SRC) Column Systems (RCS); and RC/SRC Wall Systems (HWS); New Materials, Elements and Systems (RFI). A theme structure with well selected layout, geometry and design loads for the research is also presented, which provides a common focus for various systems to be studied, and also a common prototype structure from which the components and sub-assemblages are drawn.

Key Words:
Concrete Filled Steel Tube;
RC Column with Steel Girder;
RCS Core Wall with Exterior Steel Frame;
New Materials Elements and Systems.

1. INTRODUCTION

The U.S.-Japan Cooperative Earthquake Research Program began in 1979 under the auspices of the UJNR Panel on Wind and Seismic Effects. The overall objective of the total program is to improve seismic safety practices in both countries through cooperative studies to determine the relationship among full-scale tests, small-scale tests, component tests, and related analytical and design implication studies. First four phases of the program have been Reinforced Concrete (RC) Structures, Steel Structures, Masonry Structures, and Precast Concrete Structures. Research on Mixed Steel/RC Structures was identified as an important phase of the program as recommended in the planning group report.

It is widely recognized that innovative uses of two or more different materials in a structure leads to more efficient system for resisting seismic forces. During the past ten years the use of composite and hybrid structures has increased in the U.S. and Japan. In spite of some research and development work by Japanese construction companies, not enough is known at present regarding their seismic behavior or performance. Design procedures and codes for use in typical design offices are not well developed at present.

Considering the importance of developing design guidelines (a unified code development) for typical composite and hybrid structures that are used in current practice, and of developing new and innovative composite structural elements and hybrid systems using advanced new materials and/or devices, a five-year research program on Composite and Hybrid Structures was recommended as the fifth phase of the ongoing U.S.-Japan Cooperative Earthquake Research Program. The recommendations were based on a number of technical meetings of the U.S. and Japan Planning Groups and finally a Joint Planning Group Workshop held in Berkeley on September 10-12, 1992 (Ref. 1).

Because of diverse and broad scope of the subject area, the research program is organized into the following four groups: Concrete Filled Tube Column Systems (CFT); RC/Steel Reinforced Concrete Column Systems (RCS);

[1] Professor, Dept. of Civil and Environmental Engrg., University of Michigan, Ann Arbor, MI 48109-2125, USA

and RC/SRC Wall Systems (HWS); New Materials, Elements and Systems (RFI). A theme structure provides a common focus of the program to facilitate cross comparison between various system types identified and to derive structural elements and sub-assemblages for detailed studies.

2. PROGRAM MANAGEMENT, COORDINATION AND CURRENT STATUS

The research program is planned for a period of five years in both countries, and funding has been provided accordingly. Research work on the Japanese side started in the spring of 1993. However, fuller participation and coordination of research work on both sides started in early summer 1995 when the first group of U.S. research projects were awarded. Cooperation and coordination of work by all participants are most essential to successful completion of this program. Various committees have been formed for this purpose. A Joint Technical Sub-Committee (JTSC) in each of the four components of the research program provides technical advice and coordination. Each JTSC has a co-chairman from each side with membership including all researchers in that area. These groups meet as often as needed. All participants and institutions are also part of the bigger Joint Technical Coordinating Committee (JTCC) to review progress and discuss scientific and technical issues on a common basis. This committee meets once a year. The last (fifh) JTCC meeting was held in Tokyo, Japan, in October 1998. The sixth JTCC meeting is scheduled to be held in August 1999 soon after the award of the fifth year U.S. research projects which is expected in April-May 1999. A smaller group called Joint Steering Committee (JSC), which consists of key representatives from the JTCC, oversees the entire program and provides guidance on issues that are common to the four components of the program. The overall program has a technical coordinator and a co-chairman from each side.

In addition to sharing of technical information and ideas among researchers, exchange of personnel involved is strongly encouraged. This is happening more now as the research program has gotten into its advance stage. Active participation of practitioners and various industry representatives in planning, coordination and execution of the research work is also a strong feature of this program.

3. PROGRAM OBJECTIVES

Since the subject area of the Composite and Hybrid Structures is diverse and broad, the research program was organized into the following four groups: CFT Column Systems; RC/SRC Column Systems; and RC/SRC Wall Systems; New Materials, Elements and Systems. The first three groups aim at developing practical design guidelines (a unified code development) for typical composite and hybrid structures currently used. The last group aims at developing new and innovative composite structural elements and hybrid systems using advanced new materials and/or devices.

4. THEME STRUCTURE

The theme structure provides a common focus and a strong link between various components of the research program, facilitate cross comparisons between various systems to be studied, and also provides a common prototype structure from which the structural elements and sub-assemblages for detailed studies are drawn. The following criteria were used for selection of the theme structure:

- The building plan was selected so as to reflect the benefits that the hybrid structures provide over non-hybrid structures.
- The basic plan is common to various types of hybrid structures. The number of stories and the make-up and combination of structural components and details can be varied.
- Rules to determine dead load, live load and seismic forces to be used in design simulation are common in the U.S. and Japan Groups.

5. RESEARCH ON CFT SYSTEMS

A number of research projects were funded during the first two years. These projects focused on the behavior of CFT column-to-WF beam moment connections. The specimens are nearly full size and include circular and square tube sections for columns. The connection details include the use of diaphragms, shear studs, welds, and bolts. The main variables are the connection details to transfer beam forces into the column. The objectives are:

1) To determine the force transfer mechanism, examine the effects of various connection details on this mechanism, and on the connection strength, stiffness and ductility under cyclic loading.

2) Develop and evaluate practical and economical connection details for seismic resistance.

3) Formulate practical design guidelines.

Some testing work also includes study of beam-columns under combined axial force and bending. Analytical studies accompany the experimental work. The analytical models include complex finite element formulations in an effort to develop simpler empirical or mechanics based models for practical design work. Analytical work is also aiming at studying the bond and shrinkage effects, and confinement effects in CFT members subjected to different load conditions.

6. RESEARCH ON RCS SYSTEMS

RCS structures in the U.S. generally consist of columns made of light steel shapes encased in RC. The light steel shape provides ease of erection and connection to the steel beam. Currently, there are seven active projects in the U.S., that are related to RCS structures. The projects include preparation of database on connections, testing of exterior and interior beam-to-column connections with and without floor slab, composite frames with partially restrained connections, and use of high strength steel and concrete. The joint detail variables include: lateral ties, beam bearing plates, use of FRC in place of stirrups. Analytical studies focus on modeling the connection and frame behavior to address practical analysis and design issues.

7. RESEARCH ON HWS SYSTEMS

In one research project seismic behavior of steel/composite coupling beams and their connections to the RC shear wall have been studied experimentally and analytically. One-third scale specimens were tested which represented a portion of the wall and one half length of the coupling beam from a 20 story theme structure. The effect of concrete encasement of the steel beam and details of the connection in the embedded portion have been studied. Two more research projects were started in the second year which deal with studies of composite SRC shear walls with steel boundary elements, and steel frames with RC cast-in-place in-fill walls. During the current (fourth) year, seven research projects were added. Three projects deal with further studies of HWS through wall tests and modeling, effects of slab and system on coupling beams, and interaction of steel frames with in-fill shear walls. The other four projects deal with analytical and experimental studies of innovative composite shear walls, design and behavior of HWS, unbonded post-tensioned coupled walls, and HPFRC coupling beams for energy dissipation.

8. RESEARCH ON NEW MATERIALS, ELEMENTS AND SYSTEMS (RFI)

The research work in this group aims at developing and application of new and advanced materials in innovative composite structural elements and systems (Research For Innovation - RFI). Thus, the studies in this group are more of feasibility type than those in the previous three groups where the objectives are to develop detailed guidelines for practical design work.

Significant amount of research work has been devoted to advanced cementitious and plastic composite materials. Albeit, the available information needs to be expanded to application in seismic load conditions. In two projects under this program, work is in progress on developing innovative composite systems consisting of steel and fiber reinforced concrete (FRC). The structural elements are made of selective combinations of FRC and steel members. The combinations under study include: FRC-encased open web steel joists, and high performance FRC core encased in slurry infiltrated mat concrete (SIMCON) shells for reinforcement as well as stay-in-place form work. In another project application of fiber reinforced concrete in the joint regions of RCS systems is being studied. Work is also in progress on further development of Engineered Cementitious Composite (ECC) materials and their selective use in structural elements, such as columns with large ductility demands.

9. CONCLUDING REMARKS

A brief overview of the progress of U.S.-Japan Cooperative Earthquake Research Program on Composite and Hybrid Structures has been presented in this paper. This five-year

program started in 1993 in Japan and in 1995 in the U.S. The two year time lag is being taken as an opportunity to plan the future research work in a more careful and useful manner in order to derive the most benefit from the work that has already been completed on both sides. The overall coordination efforts, cooperation and exchange of information have been excellent. More active exchange of research personnel is currently occurring in this program. At least four or five researchers from each side have participated for short and long term durations.

More details on the current status and technical progress made in this program can be found in the minutes of the last (fifth) JTCC meeting (Ref. 2). A listing of the general recommendations from that meeting is given in the Appendix of this paper. A www site has also been established which contains updated information on the overall status of this program as well as summary of results and findings from individual research projects (www.eerc.berkeley.edu/usjchs).

REFERENCES

1. "Recommendation for U.S.-Japan Cooperative Research Program - Phase 5 Composite and Hybrid Structures," Report No. UMCEE 92-29, Department of Civil and Environmental Engineering, The University of Michigan, Ann Arbor, MI, 48109-2125, November 1992.

2. "Summary, Resolutions and Recommendations of the Fifth Joint Technical Coordinating Committee Meeting," Report No. UMCEE 98-43, Department of Civil and Environmental Engineering, The University of Michigan, Ann Arbor, MI, 48109-2125, December 1998.

APPENDIX

General Recommendations from the 5th JTCC meeting:

1. Exchange of researchers, and research data (e.g., via www) on both sides should be continued at an increased level.

2. Close cooperation and collaborative research effort on both sides should be continued till the end of the five year program of both countries.

3. Efforts to synthesize and interpret knowledge gained in the program, and to disseminate this knowledge and design/analysis methodologies to the design profession and industry should be accelerated.

4. Planning effort should be initiated to perform testing work on carefully selected full frames in possible cooperation with other research programs.

5. Material manufacturers, construction and other industrial organizations should continue to actively support the research program.

6. Each JTSC should meet as needed to achieve good coherence in the cooperative research work.

7. Each JTSC should continue development of performance criteria as related to design guidelines to be developed in each country.

8. Funding should be provided for joint coordinated publication of research work with practical implications.

9. The 6th JTCC meeting should be held in late summer of 1999 at a place to be hosted by the U.S. side.

U.S.-JAPAN COOPERATIVE EARTHQUAKE ENGINEERING RESEARCH PROGRAM ON COMPOSITE AND HYBRID STRUCTURES
- JAPANESE SIDE RESEARCH ACCOMPLISHMENTS -

by

Isao NISHIYAMA [1], Hiroyuki YAMANOUCHI [2] and Hisahiro HIRAISHI [3]

ABSTRACT

The U.S.-Japan Cooperative Earthquake Engineering Research on Composite and Hybrid Structures initiated from 1993 fiscal as a five-year research project. Many research results obtained in this project have been presented in many technical papers. This paper summarizes the general objectives and the results of this project and makes clear the position of each technical output.

KEY WORDS: Composite and Hybrid Structures; Concrete Filled Steel Tube Column System; RC Column and Steel Beam System; RC Core Wall with Exterior Steel Frame System; and New Materials, Elements and Systems.

1. INTRODUCTION

Recently, "composite and hybrid structures" which uses the different material in the right man for job is very generally told in the world of research and development. However, it is the actuality that it is very slow on the gait of the popularization in the business world. This is a result of basing on there being no design code recognized [1].

In the Building Research Institute - Ministry of Construction, the basic examination was carried out through the research on beam-column connection of the composite and hybrid structures which makes the beam to be steel structure and the column to be reinforced concrete construction from 1985 [2, 3]. Then, the U.S.-Japan Cooperative Earthquake Engineering Research on Composite and Hybrid Structures [4] was started by the five-year project from 1993. The research operation system is shown in Figure 1. Domestic cooperative research by the Building Research Institute, the Building Contractors Society, the Japan Structural Consultants Association, the Kozai Club, and the Building Center of Japan was organized with the research collaboration from the universities. Research adjustment with the U.S. side was carried out by the Technical Coordinating Committee and the Technical Sub-Committees, which synthetically adjusted the research content.

There is a purpose of the research for making clear how to evaluate the composite and hybrid structures in general, but not handling individual composite and hybrid structures. However, the concrete research goal is a pile in the length, even if it goes with that the composite and hybrid structures in which the limitless variation is possible is generally handled from the research beginning. Therefore, both Japan and

---

1) Head, Housing Construction Division, Production Engineering Dept., Building Research Institute (BRI). (Tachihara-1, Tsukuba, Ibaraki 305-0802, Japan)
2) Director, Codes and Evaluation Research Center, BRI
3) Director, Department of Structural Engineering, BRI

U.S. selected the any concrete structures in which the interest together had, and the research for these was advanced. If there is common part in the aseismic designing method of which each structure is proposed, they should be synthesized. By equipping 4 sub-committees of the structures using concrete filled steel tube column system, RC column and steel beam system, RC core wall with exterior steel frame system, and new materials, elements and systems, the research was advanced.

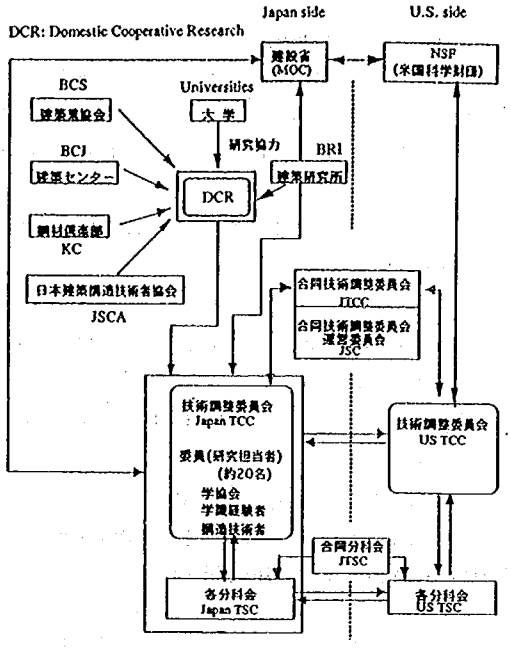


Figure 1. Research Operation System

In the U.S. side, 2 years will continue the research in future, since the start of the research was retarded a little, thus, the information exchange of research result between U.S. and Japan is continued. In this report, the outline of the technical result of every structural form of concretely selecting research result [5, 6, 7, 8, 9] in the Japan side is reported, because provisional settlement was carried out by 1997 fiscal, and it summarizes whole result of this study.

2. CLASSIFICATION OF COMPOSITE AND HYBRID STRUCTURES

It is possible to classify the composite and hybrid structures into three structural forms, as it is shown in Figure 2. Each classification is correspondent to one-dimensional, two-dimensional and three-dimensional composite and hybrid structures.

The first classification is the composite and hybrid member. Single member such as beam and column has been composed of the different material in this classification. It is considered that the SRC member is typical example of this classification. Both CFT member and fiber reinforced concrete member enter this category.

The second classification is the composite and hybrid frame. Even if the individual members such as beam and column are not special, by combining these becomes the composite and hybrid structure. RC column and steel beam system is in this category.

The third classification is the structure that different materials and members were combined three-dimensional. Typical example of this classification is the RC core wall with exterior steel frame system, and RC frame in the lower stories with steel frame in the upper stories is in this category.

Three structures of CFT, RCS and HWS selected in this study as concrete research objects are positioning of choosing for exemplification like as representative player of each classification of composite and hybrid structure forms. Therefore, it is considered that the research may be advanced by the process equal to this study, when other composite and hybrid structure of identical classification will be examined in future. On the structures of these three, the practical application had already been made in the part, and the research was advanced with the aim of the development of design guidelines, which had the generalization in mind.

In addition to 3 classification of the above, the RFI research positively making use of new materials, members and systems non-usable in the architectural field at present is being promoted parallel, because the variation of the composite and hybrid structures may be rapidly expanded. On this research, the research was advanced in the mid-and-long viewpoint with the aim of the storage of basic technical information.

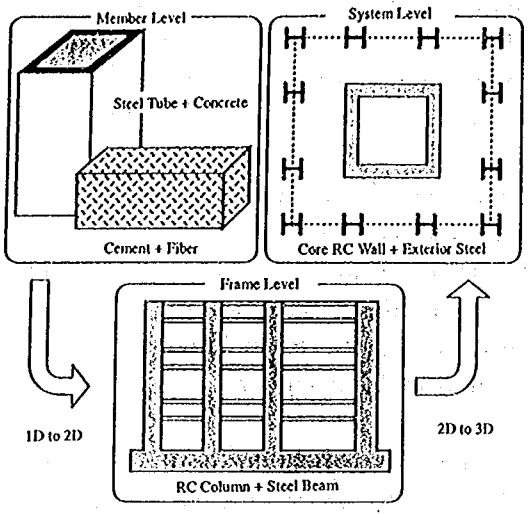


Figure 2. 3 Classification of Composite and Hybrid Structures

3. CONCRETE FILLED STEEL TUBE COLUMN SYSTEM

The CFT structure is handled at the SRC Standard of Architectural Institute of Japan [10] as a kind of SRC. However, it becomes the handling of the special structure on the Building Standard Law for the reason that the requirement of concrete cover thickness for steel tube is not satisfied. A quantitative grasp of improved strength and ductility by the synergetic action between concrete and steel tube, investigation of mixture of concrete and placement, and improvement in the fireproof performance by filling concrete was done by New Urban Housing Project. However, left examination subjects are as follows: the more exact examination of the synergetic action between filled concrete and steel tube, the applicability to larger diameter-thickness (width-thickness) ratio (152 for circular section and 74 for square section), the applicability to high strength materials (20 ~ 90MPa for concrete and 270~850MPa for steel tube), the effect of variation of axial force (between 0.3 of tensile yield force and 0.7 of compressive yield force), the effect of the direction of seismic force (45 and 22.5 degrees in loading direction), and the structural performance of beam-column connection. Then, the examination by experiment and analysis was carried out on these problems in this study. From the viewpoint of the design business, various plan and number of stories were designed, and the rational application method of the CFT system was also examined.

(A) Short column central compression experiment,
(B) Short column eccentricity compression experiment,
(C) Beam-column experiment,
(D) Beam-column connection experiment, and
(E) Examination by the trial design.

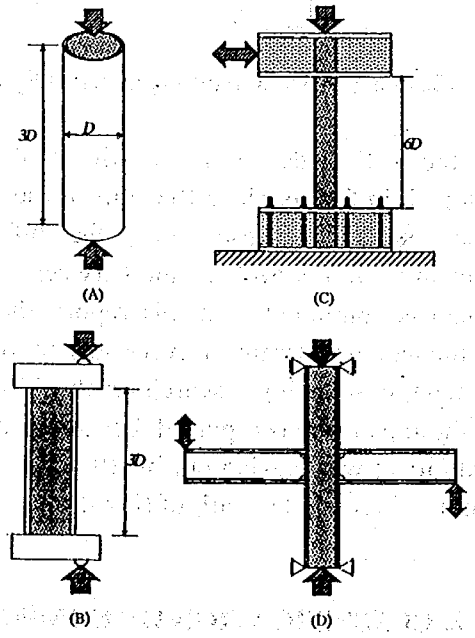


Figure 3. Experimental Method

Got conclusions are arranged as follows. More detailed explanation of the conclusions is written in the reference [6].

(1) There was a clear scale effect, when performance of structure was examined by the experiment on CFT column of larger cross section (450mm in outer width for square section and 323mm in outer diameter for circular section) than that of standard test specimen handled in past. Therefore, the strength formula considering synergistic effect must be corrected a little in the downward.

(2) As a result of the more detailed examination considering the scale effect got in (1), it was proven that the confinement effect for filled concrete could not be included.

(3) The stress-strain model of steel tube which receives circumferential stress and that of the concrete which receives the tri-axial restraint were proposed. The calculated bending moment-curvature relation of the cross section from the stress-strain model for steel tube and concrete agreed well with the experimental result.

(4) It was shown that to balance the material strength between steel tube and filled concrete was important. Especially in the case of using high strength concrete, the steel tube is relatively weak, the confinement by steel tube is not possible.

(5) It was possible to evaluate the elasto-plastic behavior of the column which receives the combined bending and shear by using stress-strain model proposed in (3), when the appropriate plastic hinge region was assumed. However, since the calculation is complicated, the restoring force characteristics were evaluated as empirical formula using post-yield rigidity and deformability from past experimental result from the practical view point, while the strength was calculated from proposed stress-strain model. This proposal is also fundamentally possible on the application to the high strength material.

(6) On the behavior of beam-column connection, systematic examination were not carried out. This study verified that the conventionally proposed strength formula can evaluate the strength safely and can be applied to high strength materials.

4. RC COLUMN AND STEEL BEAM SYSTEM

In the RCS system, the flow of the force between steel beam and RC column was a problem to be dealing with. It was Tominaga et. al. [11] who gave the practical solution for this problem first, in which the method for restricting the connection by the similar approach to the CFT system was proposed. As this system is quite rational to buildings which has long beam span with small number of stories like the shopping center, many construction companies originally proposed beam-column connection reinforcement method and the performance verification experiment is carried out. These are achieved over 20 types of connection details, even if they are classified very roughly. Like this, as the knowledge on the RCS system is accumulated to some extent, to arrange and generalize past technical information was made to be the goal in this study.

To begin with, past test data was collected, and the database was constructed. In the meantime, the details of mainly existing beam-column connection was classified into the through column type and through beam type. The additional experiment was carried out on each of the insufficient part. Studies on the exterior column to beam connection, the effect of floor slab, the column top to beam connection, the 3 dimensional column to beam connection under 2

directional seismic force, and the frame behavior were newly carried out, which were generally not required in the structure examination in the past. FEM analysis was also carried out thanks to the rapid advance on the elasto-plastic finite element method and the feasibility of 3 dimensional beam-column connection by advance of the capacity of the computer. It becomes the following, when research item is enumerated.

(A) Construction of the database and the examination of strength formula.
(B) Examination on the stress transfer mechanism.
(C) Effects of various reinforcement methods of the through beam connections.
(D) Effects of various reinforcement methods of the through column connections.
(E) Strength evaluation of the exterior column to beam connection.
(F) Behavior of the 3 dimensional beam-column connection.
(G) Elasto-plastic behavior of the frame.
(H) Examination of the reliability of the elasto-plastic finite element analysis.
(I) Examination by the trial design.

The obtained conclusions are summarized as follows. It is well-informed in the reference [7].

(1) The database was constructed on past 436 test data. According to this database, evaluation accuracy of various existing strength calculation formulas (shear strength, bearing strength).
(2) Based on the database constructed in (1), the evaluation of the shear behavior of beam-column connection was proposed.
(3) From the experiments and analyses on the exterior column to beam connection and column top to beam connection, the shape factor of the beam-column connection showed being approximate to 3:2.4:1.4 relation.
(4) From 2 directional loading testing on the 3 dimensional beam-column connections, the phenomenon in which the restoring force characteristics of beam-column connection repeatedly deteriorated was observed. However, it was also proven that the contrary good performance in the viewpoint of the energy absorption was shown.
(5) Frame experiment of the 2 story with 2 spans was carried out, and the effect of the yielding in the panel-zone on the restoring force characteristics of the frame was examined. Through the analysis by the elasto-plastic finite element analysis, it was confirmed to be estimable in respect of the micro stress state and macroscopic deformation in and around the beam-column connection, which showed the applicability of finite element analysis method for future business application.
(6) Whether the design of beam-column connection was practically possible by the trial design was examined for the building of 6 and 12 stories.
(7) Transfer mechanism of bending moment and shear force from steel beam to RC column was newly proposed from the basic experiments.

5. RC CORE WAAL WITH EXTERIOR STEEL FRAME SYSTEM

HWS system is the structure in which the structural elements are clearly sharing the role to resist external / internal force, that is, the core RC wall is made to bear most of the seismic force, while the external steel frame bears only the vertical load. In the region where the earthquake does not become a problem like the east coast region in U.S., the structure of this type spreads as a generalized technology, however on the earthquake performance, there are many indefinite points. Then, the examination of the ideal way of earthquake-

resistant design of such structure was made to be a goal of this study.

It is possible to design the RC wall as a clear bending yield type. It is self-evident that the deformability of bending yield type wall is very large. However, Ds=0.4 was required even in the minimum in the current Building Standard Law. So, the main examination object was: how far demand strength is reduced actually, and how each element should be designed.

The first problem is the stress transmission in the junction. The steel beam fundamentally supports only the vertical load, and the steel beam end which connects the core RC wall and the exterior steel frame is made to be the pin connection. It is necessary to examine whether the beam end satisfies the actual pin condition.

The inertial force must be transmitted through the slab as shear, because most horizontal force is borne in RC wall of the center core. The shear force is transmitted to the exterior frame at the first floor level, when there is the underground stories, and in the underground, the reverse shear force seems to work. It is necessary to examine how to deal with these. This point is the second issue to be examined.

The third is how to deal with large axial force produced in the edge of the wall by large overturning moment. The placement of the much reinforcements is required in the wall in order to deal with this axial force, and after all, it becomes a reason of bringing about the non-ductile behavior in the earthquake resisting wall. It is also necessary to examine that the yielding of coupling beam which connects RC walls gives what kind of effect in the structural performance of the overall structure.

Then, lateral loading test (Photo 1) of 12 storied coupled shear wall was carried out by 1/3 scales in this study. Through this research, the detailed examination of the exchange of the shear force between two walls through the coupling beam was carried out. From the becomingness of the earthquake resisting wall to be 3 dimensional, L- and T-shape walls received the axial force fluctuation and the shear span ratio fluctuation. The examination of the behavior in receiving these effect was carried out.

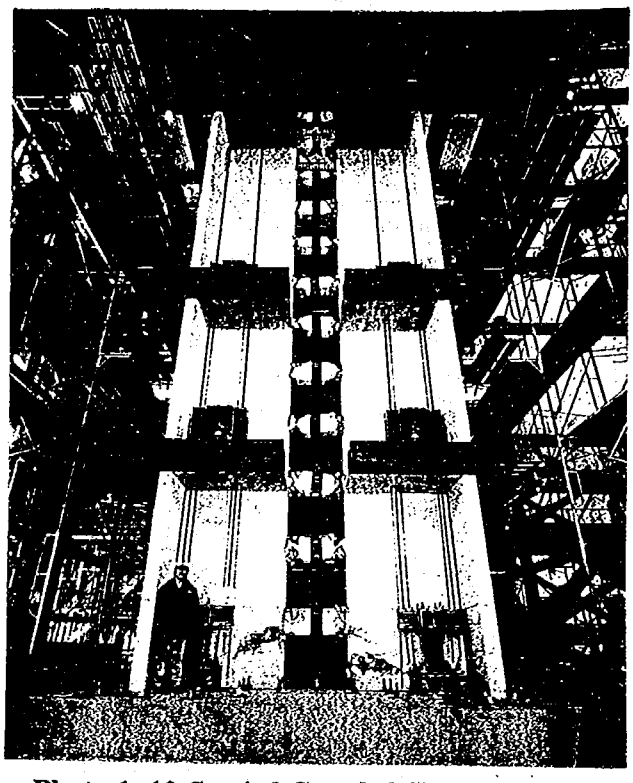


Photo 1. 12-Storied Coupled Shear Wall Test

The outline of the research result [8] on this structure is shown in the following.

(1) From experiment and analysis on the coupled shear wall of 12 story, it was shown that there was wedge action by the coupling beam, which produces concentration of the shear force in the compression. This will give basic information on the shear design of shear wall. This result did not contradict the study result in Canterbury University and Univ. of California, Berkeley carried out in the past.

(2) From the experiment of T- and L-shape walls, the effect of the fluctuation axial force, the effect of the bending moment gradient, the confinement effect at the edge of the wall under 2 directional seismic force were evaluated.
(3) The evaluation method of restoring force characteristics of the RC coupling beam reinforced diagonally was proposed from past research data.
(4) The recommended details on the joining method between steel beam and core RC wall was proposed.
(5) The 12 storied HWS building was designed, and it made clear the problems in carrying out the practical design. The seismic designing method which put the base on the equivalent linearlization method was proposed, here, the damping characteristics of shear wall and coupling beam were properly evaluated.

6. NEW MATERIALS, ELEMENTS AND SYSTEMS

Remarkably the variation of the structural system expands, if newly available materials are applied in the list of the building construction material. Therefore, in this study [9], the feasibility study on the usability of some selected materials from various fields was carried out. As the result, continuous fiber reinforced concrete and high-performance cement-based materials were made to be an examination object.

On continuous fiber reinforced concrete, the utilization to the plate elements, the application to strengthening of existing RC members, and the use for electrical facilities were examined. Since the need of application to strengthening of RC members after Hyogo-ken Nanbu Earthquake, the research rapidly developed unexpectedly. The practical research on the application to column with side wall and beam with spandrel wall was carried out.

In the meantime, on high-performance cement-based materials, realization of light-weight high strength and high ductility were aimed at.

In the light-weight high strength study, 30 MPa in strength with specific gravity of 1.2 and 60 MPa in strength with specific gravity of 1.6 were made to be a target to be developed.

These concrete materials were developed in this study, and the problems which brought about when applying the design technique of conventional RC member to the member made of these concrete materials were investigated.

On high ductility, improvement of tension and compression ductility further than the conventional concrete by mixing the short fiber into the cement was studied, which is expected to be used in the damage control portion of the structure. Types, aspect ratios, mix amount and water to binding material ratio of the short fiber were varied based on the approach of the fracture mechanics. It was confirmed that the strain hardening characteristics which is rich in ductility is obtained, and some structural tests were carried out. The examination from the practical design viewpoint was carried out on the relation between material ductility and the performance of the structural element.

Further research is in need in the RFI research field.

7. SUMMARY

By the revision of the Building Standard Law (June 12th, 1998), the seismic design by new verification method became possible together with the conventional prescribed design method. In the new verification method, the constraint by

the structural form is not received, if the structural performance is confirmed to satisfy the goal performance. Therefore, it will be possible to usefully use a technical knowledge on the structural performance of the composite and hybrid structures variously got in this study in the application of the new verification method.

The conventional prescribed design method is also reviewed with the revision of the Building Standard Law. Based on the technical storage by this study, CFT system and RCS system are under the examination of handling in the prescribed design method. HWS system is the most ideal structural system which may be examined by the new verification method. The result obtained in this study is utilized to develop the new verification method in detail. The mid-and-long term result is expected on the RFI system. However, the research progress is unexpectedly advanced on carbon fiber sheet wrapping method for RC member, which is under the process of developing design guidelines.

It is regret that the integrated seismic design method, which can cover composite and hybrid structures in general, could not be proposed in this study. However, the result is steadily being utilized for generalization. We consider that this study will give some incentive to those who plan to research and develop new composite and hybrid structural systems.

ACKNOWLEDGEMENTS

The authors would like to give their sincere thanks to members of Technical Coordinating Committee and Technical Sub-Committee for their suggestions and comments. Especially, Prof. Emeritus H. Aoyama (University of Tokyo), Prof. S. Morino (Mie University), Prof. H. Noguchi (Chiba University), Prof. A. Wada (Tokyo Institute of Technology) and Prof. A. Tanaka (Utsunomiya University) are acknowledged for serving as chairmen for Technical Coordinating Committee and each Sub-Committees.

REFERENCES

1) Building Center of Japan: Research Report on Composite and Hybrid Structural Technology, 1990.3, 1991.3, 1992.3.
2) I. Nishiyama, T. Hasegawa and H. Yamanouchi: Strength and Deformation Capacity of Reinforced Concrete Column to Steel Beam Joint Panels, Building Research Institute, Kenchiku Kenkyu Shiryo, No.71, Sep. 1990.
3) I. Nishiyama and N. Kamoshita: Beam-to-Column Panel Shear Strength of Hybrid Structure Composed of Reinforced Concrete Columns and Structural Steel Beams -Comparison of diagonal splitting tests and sub-assemblage tests-, J. Struct. Constr. Eng., AIJ, No.461, pp.153-160, July 1994.
4) U.S.-Japan Planning Groups Joint Planning Workshop: Recommendations for U.S.-Japan Cooperative Research Program - Phase 5 Composite and Hybrid Structures, UMCEE92-29, 1992.11.
5) H. Yamanouchi et al.: U.S.-Japan Cooperative Structural Research Project on Composite and Hybrid Structures, Pat 1: Overall Research Program, Proceedings of AIJ Annual Convention, Vol. II, Sep. 1994, pp.1521-1522.
6) A. Mukai et al.: U.S.-Japan Cooperative Structural Research Project on Composite and Hybrid Structures (CFT-1 to CFT-35), Proceedings of AIJ Annual Convention, Vol. II, Aug. 1995 - Sep. 1998.
7) H. Kuramoto et al.: U.S.-Japan Cooperative Structural Research Project on Composite and Hybrid Structures (RCS-1 to RCS-46),

Proceedings of AIJ Annual Convention, Vol. II, Aug. 1995 - Sep. 1998.
8) M. Teshigawara et al.: U.S.-Japan Cooperative Structural Research Project on Composite and Hybrid Structures (HWS-1 to HWS-26), Proceedings of AIJ Annual Convention, Vol. II, Aug. 1995 - Sep. 1998.
9) H. Fukuyama et al.: Experimental Study on Shear Capacity of Reinforced Concrete Column using Sheet Type Fiber, Part 1, Proceedings of AIJ Annual Convention, Vol. IV, Sep. 1996, pp.283-284; H. Fukuyama et al.: Study on Ductile Cement Composites for Structural Elements (Part 1), Proceedings of AIJ Annual Convention, Vol. IV, Sep. 1998, pp.931-932
10) Architectural Institute of Japan: Standard for Structural Calculation of Steel Reinforced Concrete Structures, 1987 revision.
11) H. Tominaga et al.: Strength and Ductility of Frames Composed of RC Columns and Steel Beams, Proceedings of AIJ Annual Convention, Vol. II, Aug. 1986, pp.1427-1434.

Manuscripts Authored for Panel Meeting But not Presented Orally

Perforated Shear Walls with Conventional and Innovative Base Restraint Connections

By

Jay Crandell, P.E.[1]
William Freeborne[2]
Shawn McKee[1]

ABSTRACT

Ideally, the residential construction industry wants to build stronger, safer buildings that can withstand hurricane and earthquake loads while at the same time using material and labor resources more efficiently. Shear walls are a primary lateral force resisting assembly in conventionally wood-framed construction. This paper reviews the current status of shear wall design using the perforated shear wall method. Past perforated shear wall research is discussed. The findings from this phase of research support the use of the perforated shear wall method for 2 ft. (0.61 m) narrow wall segments, 6 ft. (1.83 m) on center anchor bolt spacing, and nailed sole plate anchorage.

KEYWORDS: anchorage, design, energy dissipation, force-displacement, perforated shear wall method, stiffness, uplift

1. INTRODUCTION

Between one and two million new homes are built in the United States each year, predominantly with wood framing. For this reason, efficient utilization of our lumber supply is important. Ideally, the residential construction industry wants to build stronger, safer buildings that can withstand hurricane and earthquake loads while at the same time using material and labor resources more efficiently. In order to accomplish this goal, the actual performance of these structures must be better understood from an engineering standpoint.

Shear walls are a primary lateral force resisting assembly in conventionally wood-framed construction. Traditional shear wall design requires individual sheathed wall sections to be restrained against overturning. Design of exterior shear walls containing openings, for windows and doors, involves the use of multiple shear wall segments and is required to be fully sheathed and have overturning restraint supplied by mechanical anchors. The design capacity of shear walls is assumed to be equal to the sum of the capacities for each full height shear wall segment. Sheathing above and below openings is typically not considered to contribute to the overall performance of the wall.

The traditional method of design described above is significantly different than wall bracing methods used historically in conventional residential construction in the United States. It is also more expensive than conventional construction while providing greater strength. However, there are significant opportunities to optimize this design process so that both safety and economy are achieved through more accurate design approaches. This report is a continuation of an effort to develop, confirm, and enhance such an approach. The ultimate goal is to provide optimum value in both safety and economy for housing construction in all wind and seismic areas.

An alternate empirical-based approach to the design of shear walls with openings is the perforated shear wall method that appears in the *Standard Building Code* [1] and the *Wood*

[1] Structures and Materials Division, NAHB Research Center, Inc., Upper Marlboro, MD, USA, 20774
[2] Division of Affordable Housing Research and Technology, U.S. Department of Housing and Urban Development, Washington, DC, USA, 20464

Frame Construction Manual for One and Two Family Dwellings [2]. The perforated shear wall method consists of a series of simple empirical equations used for the design of shear walls containing openings. When designing for a given load, shear walls resulting from this method will generally have a reduced number of overturning restraints than a similar shear wall constructed with multiple traditional shear wall segments. The inferred performance will be achieved due to the accuracy of the method. Only when strength demands exceed the capabilities of the perforated shear wall method will the more traditional engineering approach be more cost effective and desirable.

2. BACKGROUND

Yasumura and Sugiyama conducted tests studying one-third scale monotonic racking tests of wood stud, plywood sheathed shear walls with openings [3][4]. The loads required to displace the wall at a shear deformation angle of 1/60, 1/75, 1/100, 1/150, and 1/300 were monitored. The shear deformation angle is defined as displacement of the top of the wall minus the bottom of the wall divided by the total height.

Sugiyama defined r, the sheathing area ratio, in order to classify walls based on the amount of openings a wall contains. This value is determined by the ratio of the area of openings to the area of the wall with full height sheathing to the total length of the wall. The sheathing area ratio, r, is defined as

$$r = \frac{1}{1 + \frac{A_o}{H\Sigma L_i}} \qquad \text{(Eq. 1)}$$

where:

A_o = total area of openings
H = height of the wall
L_i = length of the full height wall segment

Sugiyama and Matsumoto determined an empirical equation to relate shear capacity and sheathing area ratio, based on the scaled tests. According to Sugiyama and Matsumoto the following empirical equation is applicable for the apparent shear deformation angle of 1/100 radians and for ultimate capacity:

$$F = r/(3-2r) \qquad \text{(Eq. 2)}$$

This equation relates the ratio, F, of the shear load for a wall with openings to the shear load of a fully sheathed wall at a particular shear deformation angle.

A significant number of full scale monotonic and cyclic tests have provided verification of the perforated shear wall method [5] [6] [7] [8] [9]. The first verification studies included full-scale monotonic tests with 4 ft. (1.22 m) wall segments [5] [6] [7]. A series of tests investigated the use of corners as end restraints instead of mechanical hold-down devices [8]. An additional series of tests confirmed the performance of full scale tests with 2 ft. (0.61 m) wall segments, reduced base restraint, and the use of alternative framing practices that further optimize the perforated shear wall performance [9]. The use of an alternative empirical equation:

$$F = r/(2-r) \qquad \text{(Eq. 3)}$$

resulted in a more accurate prediction of capacity on average than did Eq. 2 [9]. The following study provides additional information about the performance of full scale tests with 2 ft. (0.61 m) wall segments and various conventional and innovative methods of providing base restraint.

3. EXPERIMENTAL PROGRAM

3.1 Wall Specimens

A total of 8 shear wall specimens were tested in this investigation (Table 1). Two hold-down anchors were used on specimens Wall 1 through Wall 7 applied to each end of the wall specimens. Wall 8 utilized an 18 gauge strap to attach each stud to the foundation using four 10d bright common nails on each side of the connection. In addition to the hold-downs, the

bottom plate of the specimens were anchored with either 5/8 in. (15.9 mm) diameter bolts 2 ft. (0.61 m) on center, 5/8 in. (15.9 mm) diameter bolts 6 ft. (1.83 m) on center, or 2 – 16d pneumatic nails (3 in. x 0.131 in. diameter) at 16 in. (0.41 m) on center.

Wall 1, Wall 2, and Wall 3 were fully sheathed and served as the control from which shear ratios were derived for walls with openings having variations in base restraint. Also, 1-5/8 in. (41.3 mm) diameter flat washers were used with the 5/8 in. (15.9 mm) diameter anchor bolts throughout the testing program. Previous tests utilized a 3 x 3 x 1/4 in. (76.2 x 76.2 x 6.4 mm) steel plate washer on each anchor bolt [5][6][7][8].

All specimens were constructed with Spruce-Pine-Fir Stud grade lumber. Studs were spaced 16 in. (406.4 mm) on center for Wall 1, Wall 2, Wall 3, Wall 4, Wall 5, and Wall 8. Stud spacing was increased to 24 in. (609.6 mm) on center for Wall 6 and Wall 7 to coincide with the investigation of 2 ft. (0.61 m) wall segments. Headers and window sills were constructed to span openings, and a king and jack stud were used on either side of openings. Exterior sheathing consisted of 7/16 in. (11.1 mm) OSB, oriented vertically. The OSB was attached using 8d pneumatic nails (2-3/8 in. long x 0.113 in. diameter) spaced 6 in. (152.4 mm) along the perimeter and 12 in. (304.8 mm) in the field of the panels. Interior sheathing consisted of 1/2 in. (12.7 mm) GWB, oriented vertically. The GWB was attached with #6 screws spaced 7 in. (177.8 mm) along the perimeter and 10 in. (254.0 mm) in the field. Both interior and exterior sheathing were cut in separate pieces to fit above and below the doors and windows. A summary of the wall materials and construction data can be found in Table 2 and Table 3.

3.2 Test Procedures

The shear walls were tested in a horizontal position according to ASTM E564 [13] using a monotonic loading. A hydraulic actuator, with a range of 12 in. (304.8 mm) and capacity of 115,000 lb. (511.5 kN), applied the load to the top right corner of each shear wall through a 4x4 structural steel tube at a rate of 0.3 in/min. A 1/2 in. (12.7 mm) thick steel plate was welded to the end of the tube to provide a uniform loading area for the actuator. A 50,000 lb. (222.4 kN) capacity load cell was attached to the end of the actuator to enable load recordings. The load cell was calibrated immediately prior to the tests using the NAHB Research Center's Universal Test Machine. Casters, which were attached to the tubing, and roller-plate assemblies were used to allow horizontal motion. The casters and the roller-plate assemblies were positioned parallel to the direction of loading.

Three linear variable differential transformers (LVDT) were used to measure the displacement of the specimens during the test. The LVDTs measured the horizontal displacement of the top of the wall, the horizontal displacement (or slip) of the bottom sole plate of the specimen, and the uplift of the end studs relative to the foundation. In addition, six "donut" shaped load cells were used to monitor the uplift forces in the sole plate anchor bolts. These load cells have a 1-5/8 in. (41.3 mm) outside diameter and were attached to the anchor bolts between the flat washer and the anchor bolt nut. A 1-5/8 in. (41.3 mm) flat washer was placed between the sole plate and the load cell. A hex-head bolt was then tightened directly onto the load cell. The hold-down anchor resisting uplift was tightened to a value of 500 lb. (222.4 N) and the remaining anchors were tightened to a value of 200 lb. (889.6 N). This was done to ensure consistency throughout the testing program. All readings were zeroed at the beginning of each test. Each load cell was calibrated immediately prior to the tests using the NAHB Research Center's Universal Test Machine.

All tests were one directional, displacing the top of the wall to a maximum of six inches over a twenty minute period. Data from the load cells and LVDTs were collected 2 times per second. Each of the seven wall configurations was tested once. Items of interest are ultimate load capacity, initial stiffness, energy dissipated, and uplift. Load-displacement curves were plotted for each of the wall specimens to better understand and compare the behavior of the walls during the test.

4. RESULTS

4.1 Force-Displacement Response

The response of the shear wall specimens to the loading history are shown in the force-displacement curves of Figures 1, 2, 3, 4, and 5. The initial stiffness was high, but the entire load-deflection behavior was essentially non-linear. The ultimate load, F_{max}, as well as the corresponding displacement, Δ_{Fmax}, was gathered directly from the data. Resistance at failure was determined as the capacity of the specimen immediately prior to a significant decrease in strength or when the load dropped to $0.8F_{max}$, whichever occurred first. These loads and displacements are presented in Table 4. Table 5 and Table 6 compare the predicted shear ratio to the actual shear ratio using Wall 2 and Wall 3, respectively.

Walls 1, 2, and 3 were fully sheathed with different sole plate anchorage and were used as the control specimens in this study. Each of these specimens had an ultimate capacity (F_{max}) of at least 20.8 kips (92.5 kN) with a mean F_{max} of 21.7 kips (96.5 kN) and a COV of 0.04. These consistent results indicate that the types of sole plate anchorage investigated do not significantly effect the ultimate capacity for the fully sheathed walls.

All specimens using 4 ft. (1.22m) and 2 ft. (0.61 m) wall segments performed in conservative agreement with the perforated shear wall predictions as shown in Figure 6. The type of sole plate anchorage used had a more noticeable effect on the specimens with openings. Walls 5 and 7 (nailed sole plate anchorage) provided 18% and 28% higher ultimate loads respectively to Walls 4 and 6 (anchor bolts 6ft. on center). These findings suggested that nailing the sole plate with 2-16d nails at 16 in. (0.41m) results in higher ultimate capacities than the anchor bolts 6 ft. (1.63 m) on center for specimens with openings. The use of straps on Wall 8 (with no hold-downs) increased the ultimate capacity of the specimen by 17% over Wall 5, which had no straps but used hold-downs at the ends only for overturning restraint. Additionally, the combination of straps with the nailed anchorage provided 38% higher capacity than a similar perforated wall using bolts at 6 ft. (1.63m) on center. However, it should be noted that all specimens (Walls 4, 5, 6, 7, and 8) reached ultimate capacities well above the predicted curve using the perforated shear wall method (see Figures 6, 7 and 8).

Predicted shear load ratios, F, were determined using Eq. 2 and are presented with the actual shear load ratios in Table 4, Table 5 and Table 6 using Wall 1, Wall 2 and Wall 3 as the reference in the calculation, respectively. The ratio of actual to predicted values is also presented in Table 4 through Table 6 where a ratio greater than 1.0 indicates a conservative prediction. Figures 6, 7, and 8 plot actual capacities and shear load ratios found from the testing. As shown in Figure 6, Eq. 2 conservatively estimates the capacity for all wall configurations in this investigation.

Due to the conservative predictions of Eq. 2, the following equation was used as an alternative to predict the shear load ratios [9]:

$$F = r/(2-r) \qquad \textbf{(Eq. 3)}$$

The additional predicted shear load ratios, F, were determined using Eq. 3 and are presented with the actual shear load ratios in Table 7 through Table 9 using Wall 1 through Wall 3 as the reference. The ratio of actual to predicted is also presented, where a ratio equal to 1.0 is an exact prediction and a greater ratio is a conservative prediction. Figure 9 plots actual capacities and shear load ratios found from the testing. As shown in Figure 9, Eq. 3 estimates the capacity for Walls 1 through 8 more accurately than that of Eq. 2. However, Eq. 3 slightly overpredicts the shear capacity of Wall 4, which had a 6 ft. (1.83m) on center anchor bolt spacing. Using the more similar Wall 3 as the reference for comparison produces a more accurate curve (see Figure 10 and Figure 11).

4.2 Initial Stiffness

The initial portion of the force-displacement curves were fit with a linear least-squares trend, the slope of which is taken as the initial stiffness. That portion of the curve for which the magnitude of the force did not exceed 40

percent of the peak load was used in the calculation. The initial stiffnesses are listed in Table 4.

In general, initial stiffness was proportional to the sheathing area ratio, hence as the sheathing area ratio decreased the initial stiffness also decreased as expected. Wall 1 experienced a larger initial stiffness than that of Walls 2 and 3. This indicates that the reduced sole plate anchorage allowed for a more flexible wall which can be advantageous in resisting seismic loads provided sufficient capacity is maintained. The nailed sole plate resulted in slightly larger initial stiffnesses than did the anchor bolts 6 ft. (1.83 m) on center. The strap reinforcement of Wall 8 significantly increased the initial stiffness.

4.3 Energy Dissipated

The toughness of a wall can be quantified by its ability to dissipate energy while deforming. Cumulative energy dissipation was obtained by calculating the area under each force-displacement curve up to $0.80F_{max}$ using Simpson's Method. These values are listed in Table 4.

The 2 ft. (0.61 m) narrow wall segments in Walls 6 and 7 did not adversely affect the energy dissipation capacity of the walls. Also, the performance of the nailed sole plate anchorage and the 6 ft. (1.83m) on center anchor bolt spacing were very similar for the specimens with openings. However, the nailed sole plate anchorage did have an adverse affect on the energy dissipation capacity of the fully sheathed specimen when compared to the 2ft. (0.61m) and 6ft. (1.83m) anchor bolt spacing. Thus, the fully sheathed wall would require greater nailing at the sole plate to transfer the total wall shear load more effectively so that the energy capacity of the fully sheathed wall is maximized. The addition of straps to Wall 8 provided some improvement in this area of performance as compared to Wall 5.

4.4 End Stud Uplift

Loading each wall resulted in uplift zones at the end of the walls due to end panel rotation, wall drift, and overall overturning forces. This condition is not dissimilar to the type or magnitude of restraint that may occur in actual conditions. The vertical displacement of the end stud was measured by an LVDT. The uplift displacement and load at the specimen's ultimate capacity is given in Table 4.

The maximum uplift load experienced at the hold-down remained relatively constant throughout this testing phase. The specimens with openings and 4 ft. (1.22 m) wall segments experienced the largest uplift loads while the specimens with 2 ft. (0.61 m) wall segments experienced slightly lower loads at the hold-downs. In every case, the hold-down load was well below the load that would be predicted theoretically by multiplying the unit shear capacity by the wall height (i.e. conventional overturning design analysis).

The vertical displacement of the end stud remained fairly constant for Wall 1, Wall 3, Wall 4, Wall 5 and Wall 8. Thus, increased anchor bolt spacing, using nails instead of bolts, and the alternative strap anchor approach had little effect on the uplift displacement at the end stud. The narrow wall segments, regardless of sole plate anchorage, developed 50% less displacement at the end stud in comparison to the fully sheathed and 4 ft. (1.22 m) wall segments.

4.5 Failure Modes

All walls tested had similar failure characteristics except for Wall 2. The initial loading was generally linear until the interior sheathing, GWB, began to pull through the screws. This failure resulted in a slight reduction in stiffness. As the load approached ultimate capacity, the OSB sheathing near the loaded end began to buckle, and bending of OSB and framing nails was observed elsewhere. Racking of full height OSB panels was observed, while the OSB above and below openings acted as a rigid body. After ultimate capacity, the nails tore through the edges of the OSB.

Wall 2 also was characterized by a generally linear initial loading. Failure of the specimen was not characterized by failure of the sheathing, but rather nail slippage (shear failure) at the sole plate to foundation was the mode of failure. This failure mode explains the lower energy dissipation levels in this specimen. However, the ultimate capacity was 93 percent of that for walls with anchor bolts 6 ft. (1.83 m) on center. The sole plate at the hold-down resisting the wall uplift experienced failure as shown in Photo 1. This failure mode may be prevented by the addition of sole plate nails in accordance with the total shear load on a wall line. The nailed sole plate connection in Wall 5, Wall 7, and Wall 8 did not fail because of the lower total shear load due to the perforations in the specimens.

Although the above failure mechanisms were consistent throughout the testing, some differences were observed which explain the results discussed above. Separation of the sole plate and foundation was more evident on walls using anchor bolts at 6 ft. (1.83 m) on center, such as Wall 3. Sensors on anchor bolts along the sole plate registered the largest loads for Wall 3. However, failure of the sheathing panel connection was the cause of ultimate failure of the specimen. Wall 5 also had slight nail withdrawal from the foundation, but this occurred after ultimate load had been realized. The alternative strap anchor method in Wall 8 experienced both tension and compression of the straps throughout the length of the specimen (See Photo 2). As expected, the first two straps experienced the greatest overturning load (See Photo 3).

Comparing Walls 5 and 7 (nailed sole plate) to Walls 4 and 6 (bolted anchors, 6 ft. (1.83 m) on center, nailed sole plates provided larger ultimate loads and initial stiffness over their bolted anchor counterparts. Once ultimate load was achieved, the two openings in Walls 4 and 5 were no longer square and the two end sheets of OSB had pulled through the nails causing a sudden decrease in load. However, the narrow wall segments in Walls 6 and 7 prevented the racking of the openings after ultimate load. This was evident from the tearing of the full height GWB along the top of the openings. The bottom of these intermediate sheets remained relatively stable while the rigid body motion of the sheathing above the openings caused tearing of the full height GWB at the top opening corners.

While the behavior of Walls 4 and 8 was very similar, the results were quite different. The alternative framing practices of Wall 8 (strap anchors) provided a 17 percent increase in ultimate capacity, a 16 percent increase in energy dissipated, and a 89 percent increase in initial stiffness even without hold-downs at the ends. The lack of hold-down restraints in Wall 8 is only evident in the vertical stud displacement at the end of the wall, which was very consistent with similar specimens with hold-down brackets instead of strapping (Wall 4 and Wall 5).

Increasing the anchor bolt spacing to 6 ft. (1.83 m) on center in Wall 3 or using the 2-16d nails as the sole plate anchorage in Wall 2 only resulted in a slight decrease in ultimate capacity. In general, the nailed anchor plates produced better results than the 6 ft. (1.83 m) on center bolt anchors.

This phase of testing gives additional promise to the use of the perforated shear wall method with reduced base restraint that is common to conventional framing practices. In addition, the use of straps in this study and truss plates in the previous study [9] provide an efficient enhancement to the perforated shear wall method while maintaining simplicity in construction detailing and assembly.

5. CONCLUSIONS

The perforated shear wall method was first developed by conducting tests on one-third scale monotonic racking tests of shear walls. Eq. 2 was developed to predict the shear load capacity for shear walls with openings [3][4]. The perforated shear wall method was confirmed to be a conservative design approach using full scale tests of 40 ft. (12.19 m) long shear walls with openings constructed with 4 ft. (1.22 m) wall segments [5]. Additional testing was conducted to determine the effect of overturning restraints. Again, it was concluded

that the perforated shear wall method results in conservative design values for shear walls [6]. The next phase of testing quantified the effects of corners on uplift restraint. The 2 ft. (0.61m) and 4 ft. (1.22 m) corner returns provided sufficient end restraint to allow 85 percent and 90 percent, respectively, of the fully-restrained wall's tested unit shear to be realized [8]. Each of the aforementioned phases of research refined the perforated shear wall method resulting in a more efficient and economical shear wall design. Subsequent testing provided additional refinement to the perforated shear wall method [9]. The research presented in this report further evaluated the effectiveness of reduced base restraint, alternative overturning restraints (i.e. redundant strapping), and narrow wall segments.

The data presented provides additional verification of the perforated shear wall method using reduced base restraint and 2 ft. (0.61 m) wall segments. The calculated shear capacity using the empirical equation developed by Sugiyama and Matsumoto (Eq. 2) conservatively estimates the capacity of all specimens tested. The use of the alternative empirical equation (Eq. 3) resulted in a more accurate prediction of ultimate capacity. This research produced similar results to a previous preliminary test with regard to increasing anchor bolt-spacing [9]. The use of 6 ft. (1.83 m) on center bolt anchors slightly decreases the ultimate capacity, initial stiffness, and energy dissipated. Similar reductions were seen with the use of nailed sole plate anchorage in comparison to 2 ft. (0.61 m) on center bolt anchors. However, in general, nailed anchors faired better than 6 ft. (1.83 m) on center bolt anchors. Despite these decreases, the empirical equation (Eq. 2) developed by Sugiyama and Matsumoto conservatively estimates the capacity with either increased anchor bolt spacing or sole plate nails, even when using a fully sheathed wall with anchor bolts 2 ft. (0.61 m) on center as the reference. The amount of shear resistance (base anchorage) needed at the sole plate can be reasonably determined using Eq. 2 or Eq. 3 with perforated shear walls. The alternative framing practice (straps and nails with no hold-downs) investigated in this report shows promise for high-wind and high-seismic applications.

The findings of this research support the use of the perforated shear wall method for 2 ft. (0.61 m) narrow wall segments, 6 ft. (1.83 m) on center anchor bolt spacing, and nailed sole plate anchorage. However, certain limits need to be placed on these conclusions such as the degree of sheathing nailing and the resulting unit shear value, as well as the amount of restraint provided by sheathing above and below openings. These results would not necessarily apply to the perforated shear walls with many large, full-height openings. In such cases, the segmented shear wall method may be more appropriate.

6. REFERENCES

[1] *Standard Building Code*, Southern Building Code Congress International, Inc., Birmingham, AL, 1994.

[2] *Wood Frame Construction Manual for One and Two Family Dwellings*, American Forest & Paper Association, American Wood Council, Washington, DC, 1995.

[3] Sugiyama, H. and Yasumura, M., *Shear Properties of Plywood Sheathed Wall Panels with Openings*, Trans. of A.I.J., No. 338, 1984.

[4] Sugiyama, H. and Matsumoto, T., *Empirical Equations for the Estimation of Racking Strength of a Plywood Sheathed Shear Wall with Openings*, Summary of Technical Papers Annual Meetings, Trans. of A.I.J., 1994.

[5] Dolan, J. and Johnson, A., *Cyclic and Monotonic Tests of Long Shear Walls with Openings*, Prepared for the American Forest & Paper Association by Virginia Polytechnic Institute and State University, 1996.

[6] Dolan, J. and Heine, C., *Monotonic Tests of Wood Frame Shear Walls with Various Openings and Base Restraint Configurations*, Prepared for the NAHB Research Center, Inc. by

Virginia Polytechnic Institute and State University, 1997.

[7] Dolan, J. and Heine, C., *Sequential Phased Displacement Cyclic Tests of Wood Frame Shear Walls with Various Openings and Base Restraint Configurations*, Prepared for the NAHB Research Center Inc. by Virginia Polytechnic Institute and State University, 1997.

[8] Dolan, J. and Heine, C., *Sequential Phased Displacement Tests of Wood Framed Shear Walls with Corners*, Prepared for the NAHB Research Center, Inc. by Virginia Polytechnic Institute and State University, 1997.

[9] *The Performance of Perforated Shear Walls with Narrow Wall Segments, Reduced Base Restraint, and Alternative Framing Methods*, Prepared for the U.S. Department of Housing and Urban Development and The National Association of Home Builders by the NAHB Research Center, Inc., Upper Marlboro, MD, 1998.

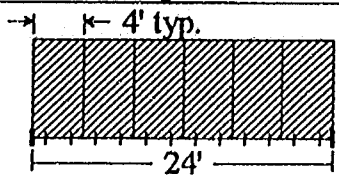
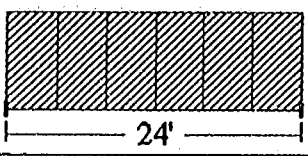
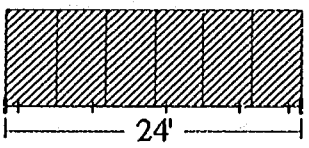
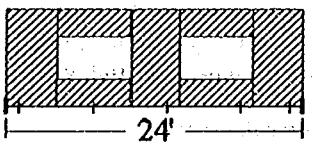
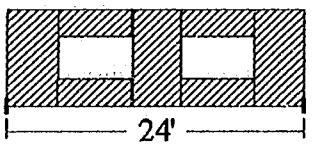
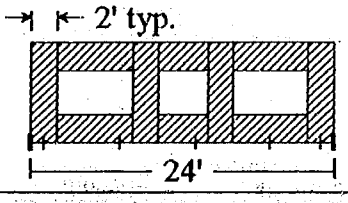
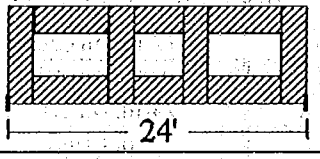
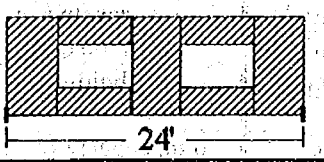
[10] Porter, M. L., *Sequential Phase Displacement Procedure for TCCMAR Testing*, Proceedings of the Third Meeting of the Joint Technical Coordinating Committee on Masonry Research, US-Japan Coordinated Earthquake Research Program, Tomamu, Japan, 1987.

[11] Karacabeyli, E. and Ceccotti, A., *Nailed Wood-Framed Shear Walls for Seismic Loads: Test Results and Design Considerations*, Proceedings of the Structural Engineers World Congress, San Francisco, CA, American Society of Civil Engineers, 1998.

[12] *The One and Two Family Dwelling Code*, The Council of American Building Officials (CABO), Falls Church, VA, 1995.

[13] ASTM E564-95, *Standard Method of Static Load Tests for Shear Resistance of Framed Walls for Buildings*, American Society for Testing and Materials (ASTM), West Conshohocken, PA, 1995.

Table 1
Shear Wall Configurations

Specimen	Wall Configuration	Openings	Headers	Sheathing Area Ratio (r)[1]	Sole Plate Anchorage	Hold-downs
Wall 1		None	None	1.0	5/8" dia. bolt @ 2' o.c.	Ends
Wall 2		None	None	1.0	2-16d nails @ 16" o.c.[3]	Ends
Wall 3		None	None	1.0	5/8" dia. bolt @ 6' o.c.	Ends
Wall 4		(2) - 6' x 4'	2 - 2x6	0.67	5/8" dia. bolt @ 6' o.c.	Ends
Wall 5		(2) - 6' x 4'	2 - 2x6	0.67	2-16d nails @ 16" o.c.[3]	Ends
Wall 6		(2) - 6'x 4' & (1) - 4' x 4'	2 - 2x6 & 2 - 2x4	0.50	5/8" dia. bolt @ 6' o.c.	Ends
Wall 7		(2) - 6'x 4' & (1) – 4' x 4'	2 - 2x6 & 2 - 2x4	0.50	2-16d nails @ 16" o.c.[3]	Ends
Wall 8		(2) - 6'x 4'	2 - 2x6	0.67	2-16d nails @ 16" o.c.[3]	None[2]

Notes: For SI: 1 ft. = 0.3048 m, 1 in. = 25.4 mm.

1. The sheathing area ratio (r) is calculated in accordance with Equation 1.
2. 18g straps used to connect each stud to the base with 4 – 10d bright common nails on each end of the strap
3. Nails were 16d pneumatic nails (3 in. long x 0.131 in. diameter)

Table 2
Wall Materials and Construction Data

Component	Construction and Materials
Framing Members	Stud, Spruce-Pine-Fir, 2x4.
Sheathing	
Exterior	7/16 in. OSB, 8d common nails with 6 in. spacing on panel edges and 12 in. spacing in panel field (sheets installed vertically).
Interior	1/2 in. Gypsum Wallboard, #6 screws with 7 in. spacing on panel edge and 10 in. spacing in panel field (sheets installed vertically, joints taped).
Headers	
4'-0" opening	2-2x4 with an intermediate layer of 7/16 in. OSB. One jack stud and one king stud at each end.
6'-0" opening	2-2x6 with an intermediate layer of 7/16 in. OSB. One jack stud and one king stud at each end.
Structural Base Connections (Bottom of Wall)	
Hold-down	Simpson HTT 22, nailed to end studs with 32-16d sinker nails, 5/8 in. diameter tie rod to connect to reaction beam at the wall ends only (not used in Wall 8).
Anchor Bolts	5/8 in. diameter tie rods with 1-5/8 in. diameter flat washer.
Loading Tube Connections (Top of Wall)	
No Openings	1/2 in. diameter bolts with 1-5/8 in. flat washer @ 2 ft. on center.

For SI: 1 ft. = 0.3048 m, 1 in. = 25.4 mm

Table 3
Fastening Schedule

Connection Description	Type of Connector	Spacing
Framing:		
Top Plate to Top Plate (face-nailed)	16d pneumatic[1]	12 in. on center
Top/Bottom Plate to Stud (end-nailed)	2-16d pneumatic[1]	per connection
Stud to Stud (face-nailed)	2-16d pneumatic[1]	24 in. on center
Stud to Header (toe-nailed)	2-16d pneumatic[1]	per stud
Stud to Sill (end-nailed)	2-16d pneumatic[1]	per stud
Header to Header (face nailed)	2-16d pneumatic[1]	16in. on center
Hold-down (face nailed)	32-16d sinker	per hold-down
Sheathing:		
OSB	8d pneumatic[2]	6 in. edge/12 in. field
GWB	#6 screws	7 in. edge/10 in. field

Notes: For SI: 1in. = 25.4 mm
1. 16d pneumatic nails were 3 in. long and 0.131 in. diameter.
2. 8d pneumatic nails were 2-3/8 in. long and 0.113 in. diameter.

Table 4
Force-Displacement Data from Testing

	1	2	3	4	5	6	7	8
Sole Plate Anchorage[a]	B–2ft	Nail	B–6ft	B–6ft	Nail	B–6ft	Nail	Strap
Sheathing Area Ratio	1.00	1.00	1.00	0.67	0.67	0.50	0.50	0.67
Predicted Shear Ratio[b]	1.00	1.00	1.00	0.40	0.40	0.25	0.25	0.40
Actual Shear Ratio	1.00	0.93	0.98	0.48	0.56	0.39	0.51	0.66
Actual/Predicted	1.00	0.93	0.98	1.18	1.40	1.58	2.02	1.64
F_{max} (kips)	22.5	20.8	22.0	10.7	12.7	8.8	11.3	14.8
Δ_{Fmax} (in.)[c]	1.842	1.466	2.117	2.305	2.327	1.790	2.382	2.160
$F_{failure}$ (kips)	18.0	16.6	17.6	8.6	11.5	7.1	9.1	11.8
$\Delta_{failure}$ (in.)	2.901	2.239	2.910	3.549	3.122	4.007	4.240	3.040
Initial Stiffness (kips/in)	54.7	36.0	35.1	10.8	16.8	10.7	11.9	20.4
Energy Dissipated (kips*in)	55.4	35.1	52.1	29.7	30.7	29.2	37.4	34.5
$F_{hold\text{-}down}$ (kips)[c]	3.7	4.6	4.1	5.9	5.6	4.0	4.5	NA
$F_{hold\text{-}down\text{-}max}$ (kips)	4.2	4.6	5.2	6.3	6.0	4.3	5.4	NA
$\Delta_{slippage}$ (in.)[c]	0.281	0.779	1.066	0.350	0.219	0.370	0.373	0.382
Δ_{uplift} (in.)[c]	0.440	0.136	0.376	0.468	0.455	0.240	0.234	0.487
Δ_{uplift} (in.)[d]	0.599	0.136	0.481	0.564	0.540	0.304	0.372	NA

Notes: For SI: 1 ft. = 0.3048 m, 1 in. = 25.4 mm, kip = 4.45kN.

a. Sole plate anchorage abbreviations: B-2ft = 5/8in. bolts 2ft. o.c. B-6ft = 5/8in. bolts 6ft. o.c. Nail = 2-16d nails 16in. o.c. Strap = 18g strap @ each stud

b. The predicted shear ratio is based on the empirical formula, F=r/(3-2r), developed by Sugiyama and Matsumoto for wood-framed shear walls. Wall 1 is the reference.

c. Measured at F_{max} (peak wall capacity)

d. Measured at $F_{hold\text{-}down\text{-}max}$

Table 5
Predicted Shear Load Ratios for
2-16d Nails at 16in. On Center Sole Plate Anchorage

	Wall Specimens			
	2	5	7	8
Sheathing Area Ratio	1.00	0.67	0.50	0.67
Predicted Shear Ratio	1.00	0.40	0.25	0.40
Actual Shear Ratio	1.00	0.61	0.55	0.71
Acual/Predicted	1.00	1.53	2.20	1.78

Note: The predicted shear ratio is based on the empirical formula, F=r/(3-2r), developed by Sugiyama and Matsumoto for wood-framed shear walls, Wall 2 is the reference.

Table 6
Predicted Shear Load Ratios for
5/8in. Diameter Bolts 6ft. On Center

	Wall Specimens		
	3	4	6
Sheathing Area Ratio	1.00	0.67	0.50
Predicted Shear Ratio	1.00	0.40	0.25
Actual Shear Ratio	1.00	0.49	0.40
Acual/Predicted	1.00	1.23	1.60

Note: The predicted shear ratio is based on the empirical formula, F=r/(3-2r), developed by Sugiyama and Matsumoto for wood-framed shear walls, Wall 3 is the reference.

Table 7
Predicted Shear Load Ratios, $F = r/(2-r)$, Wall 1 as Reference

	Wall Specimens					
	1	4	5	6	7	8
Sheathing Area Ratio	1.00	0.67	0.67	0.50	0.50	0.67
Predicted Shear Ratio	1.00	0.50	0.50	0.33	0.33	0.50
Actual Shear Ratio	1.00	0.48	0.56	0.39	0.51	0.66
Acual/Predicted	1.00	0.96	1.12	1.18	1.55	1.32

Note: The predicted shear ratio is based on the empirical formula, F=r/(2-r), using Wall 1 as the reference.

Table 8
Predicted Shear Load Ratios, $F = r/(2-r)$, Wall 2 as Reference

	Wall Specimens			
	2	5	7	8
Sheathing Area Ratio	1.00	0.67	0.50	0.67
Predicted Shear Ratio	1.00	0.50	0.33	0.50
Actual Shear Ratio	1.00	0.61	0.55	0.71
Acual/Predicted	1.00	1.22	1.67	1.42

Note: The predicted shear ratio is based on the empirical formula, F=r/(2-r), using Wall 1 as the reference.

Table 9
Predicted Shear Load Ratios, $F = r/(2-r)$, Wall 3 as Reference

	Wall Specimens		
	3	4	6
Sheathing Area Ratio	1.00	0.67	0.50
Predicted Shear Ratio	1.00	0.50	0.33
Actual Shear Ratio	1.00	0.49	0.40
Acual/Predicted	1.00	0.98	1.21

Note: The predicted shear ratio is based on the empirical formula, F=r/(2-r), using Wall 3 as the reference.

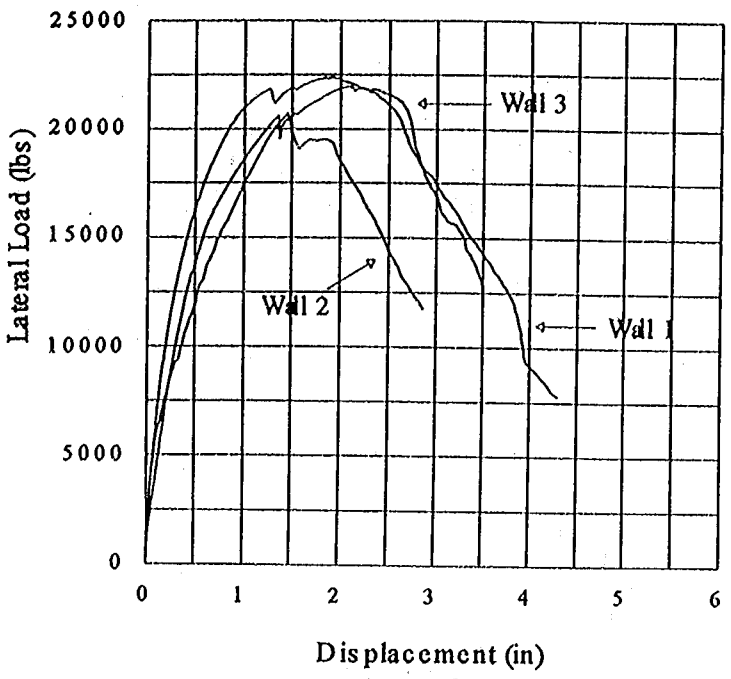


Figure 1[I]
Force-Displacement Response for Walls 1, 2, and 3 (r = 1.0)

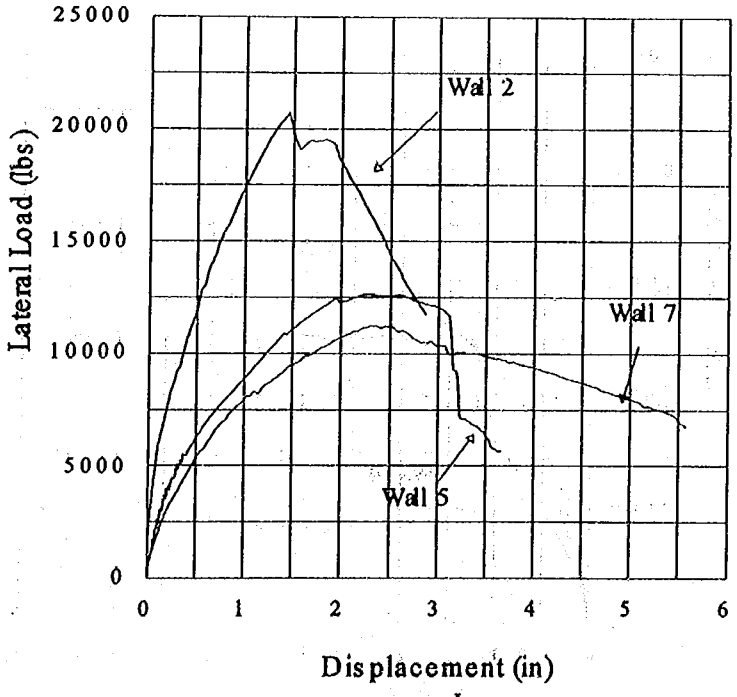


Figure 2[I]
Force-Displacement Response for Walls 2, 5 and 7
(Sole Plate Anchorage: 2 - 16d pneumatic nails @ 16in. o.c.)

[I] For SI: 1kip = 4.45kN, 1in = 25.4mm

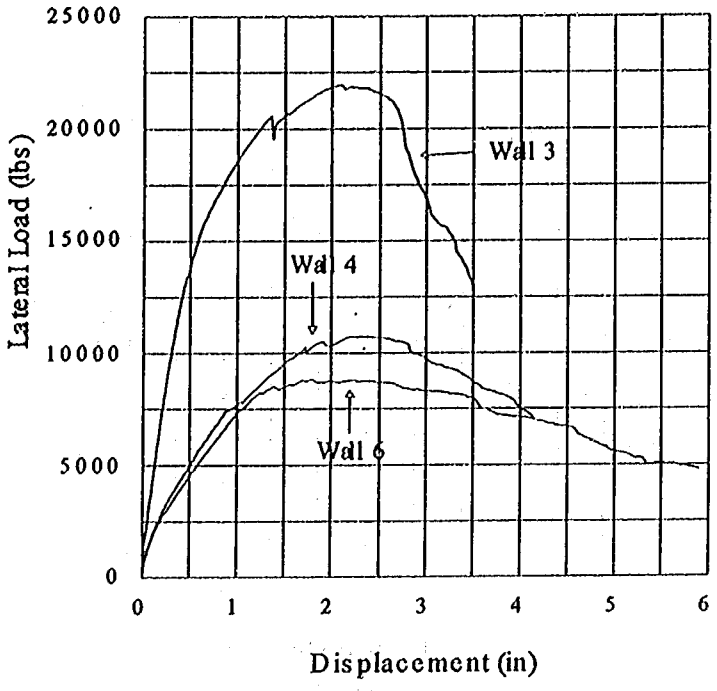


Figure 3[I]
Force-Displacement Response for Walls 3, 4 and 6
(Sole Plate Anchorage: 5/8in. diameter bolts 6ft. o.c.)

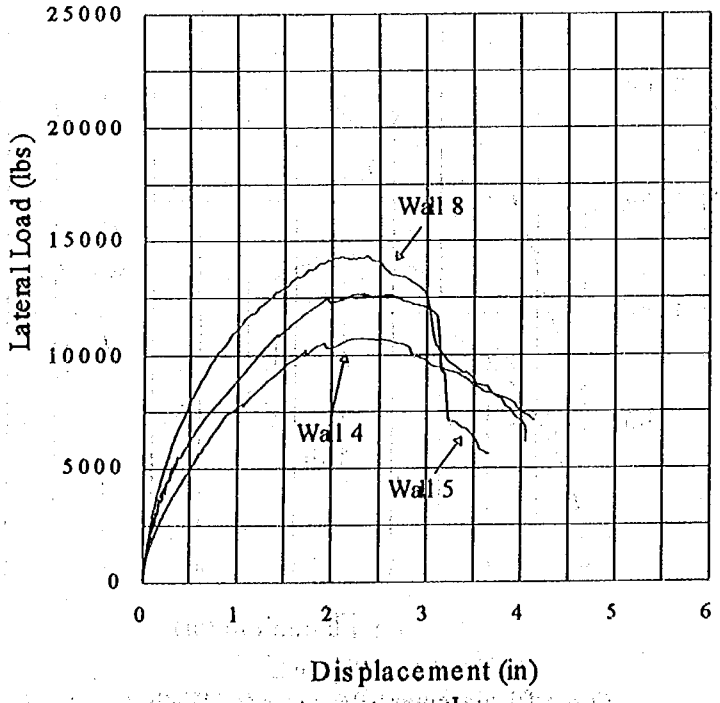


Figure 4[I]
Force-Displacement Response for Walls 4, 5 and 8 ($r^1 = 0.67$)

[I] For SI: 1kip = 4.45kN, 1in = 25.4mm

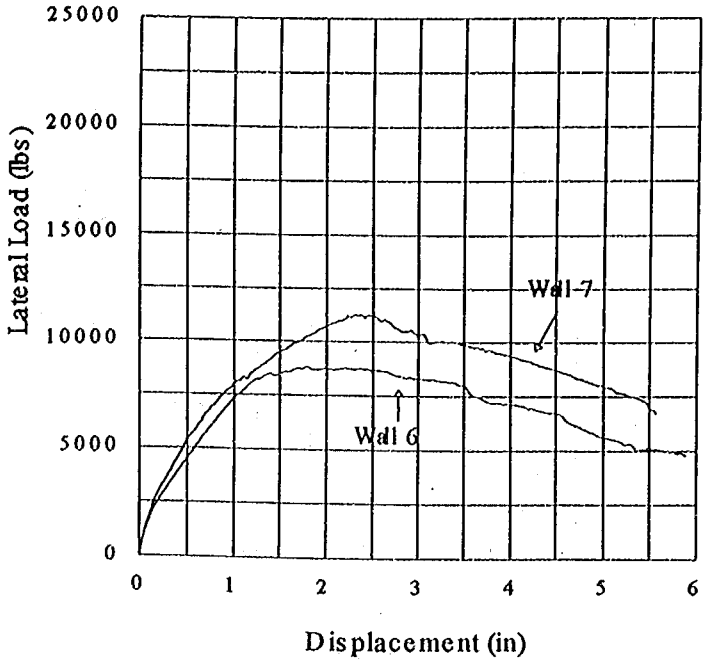


Figure 5[I]
Force-Displacement Response for Walls 6 and 7 (r = 0.50)

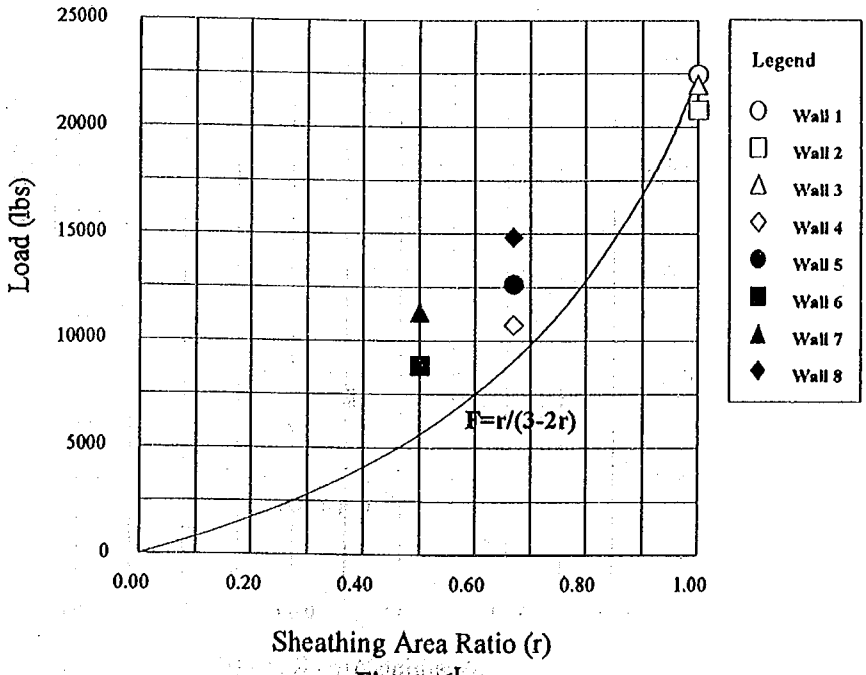


Figure 6[I]
Ultimate Capacity vs. Sheathing Area Ratio
Wall 1 as Reference

[I] For SI: 1kip = 4.45kN, 1in = 25.4mm

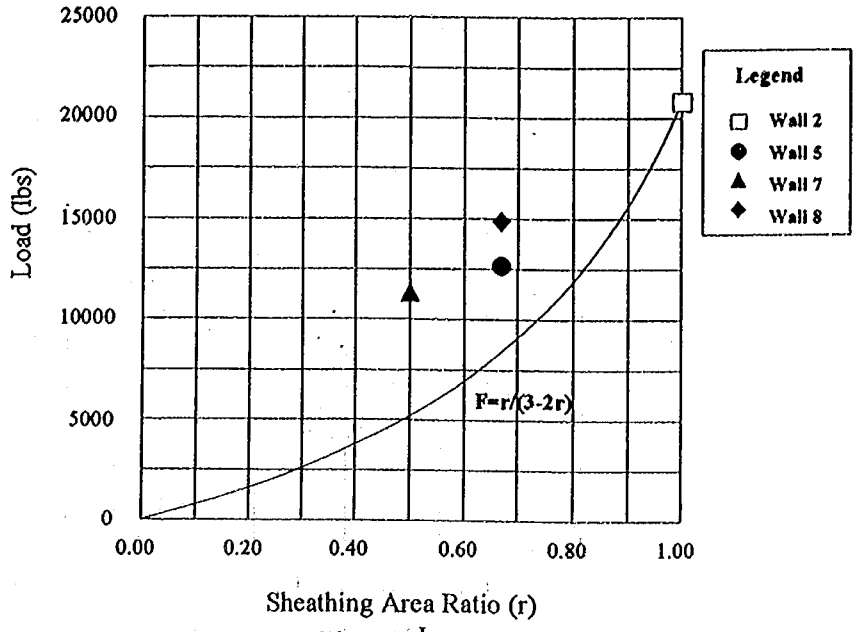


Figure 7[I]
Ultimate Capacity vs. Sheathing Area Ratio
Wall 2 as Reference

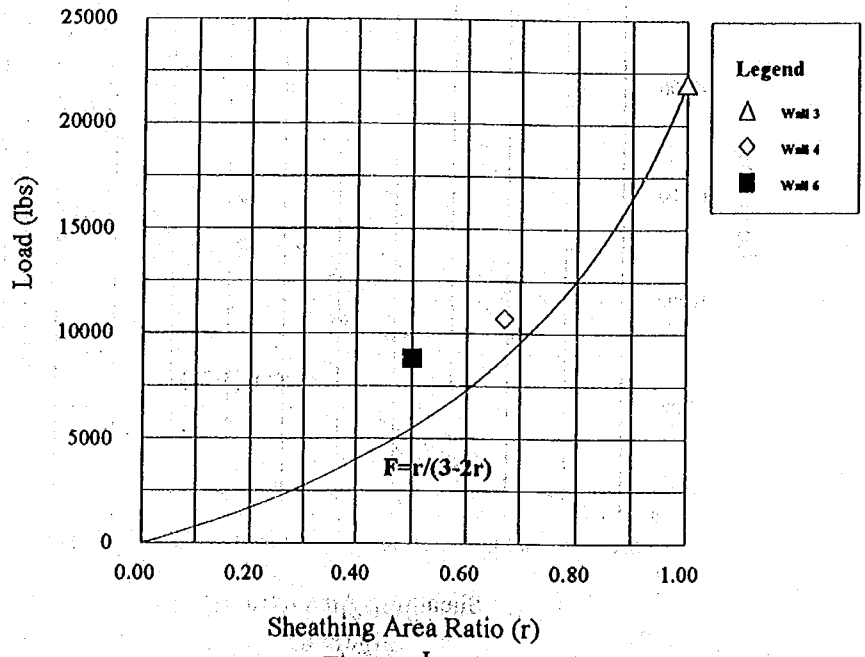


Figure 8[I]
Ultimate Capacity vs. Sheathing Area Ratio
Wall 3 as Reference

[I] For SI: 1kip = 4.45kN, 1in = 25.4mm

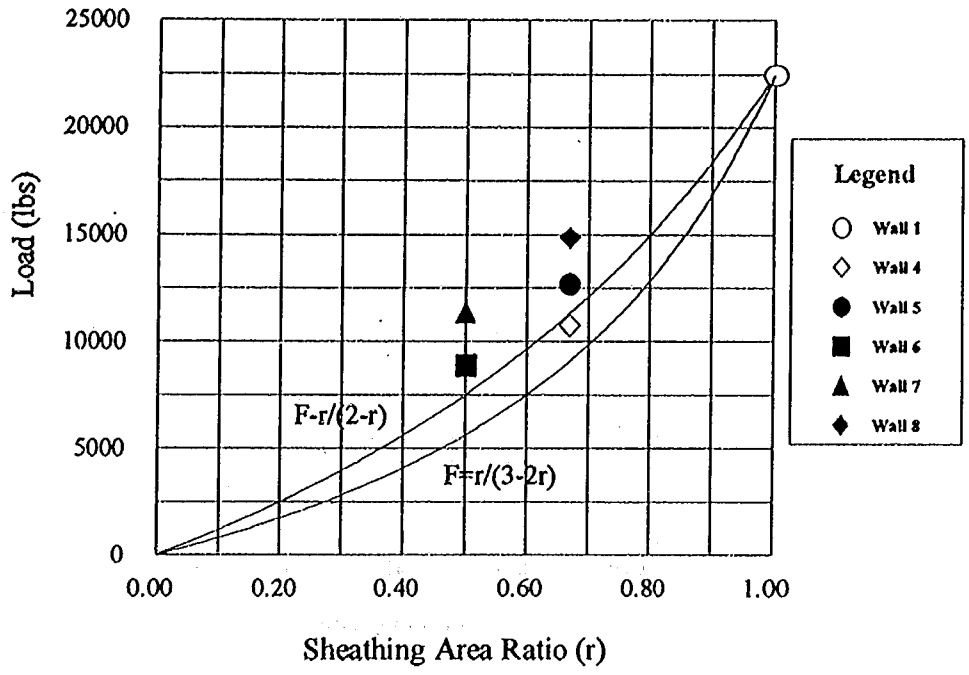


Figure 9[1]
Ultimate Capacity vs. Sheathing Area Ratio (Wall 1 as Reference)

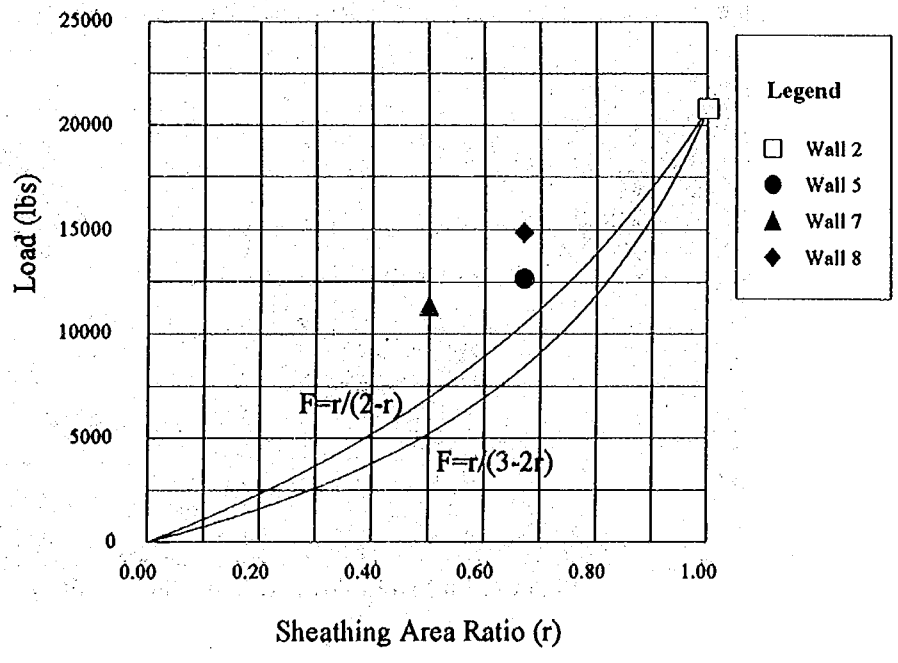


Figure 10[1]
Ultimate Capacity vs. Sheathing Area Ratio (Wall 2 as Reference)

[1] For SI: 1kip = 4.45kN, 1in = 25.4mm

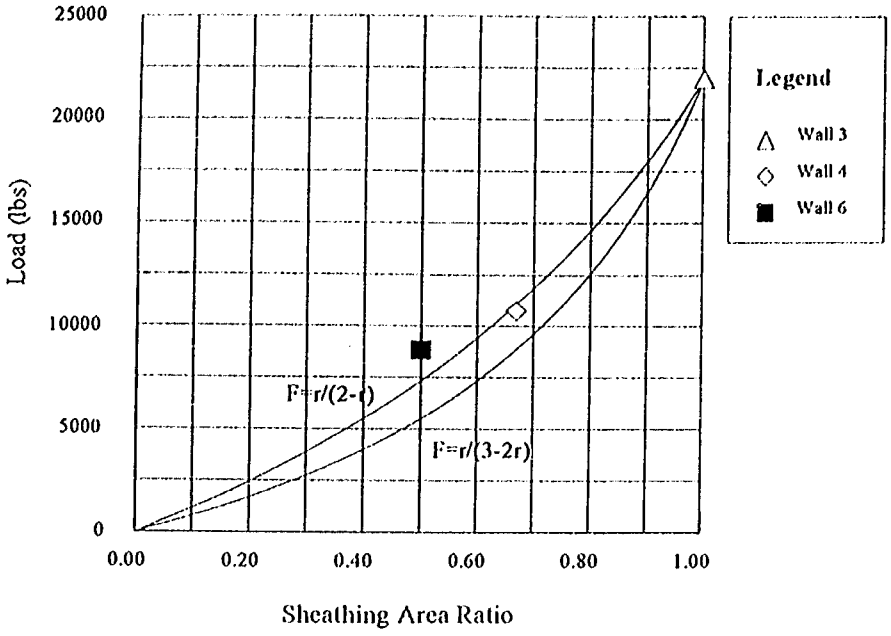


Figure 11[1]
Ultimate Capacity vs. Sheathing Area Ratio (Wall 3 as Reference)

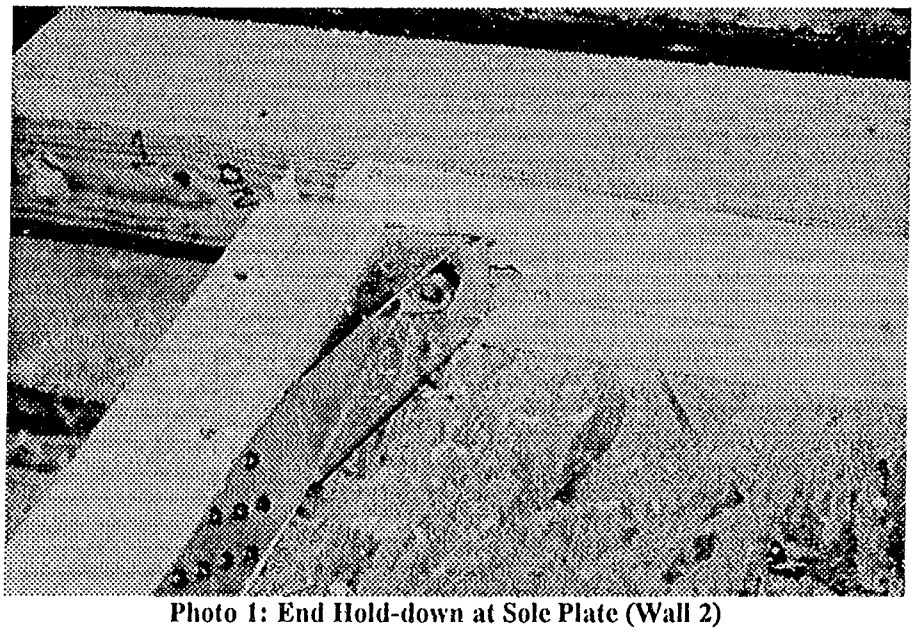


Photo 1: End Hold-down at Sole Plate (Wall 2)

[1] For SI: 1kip = 4.45kN, 1in = 25.4mm

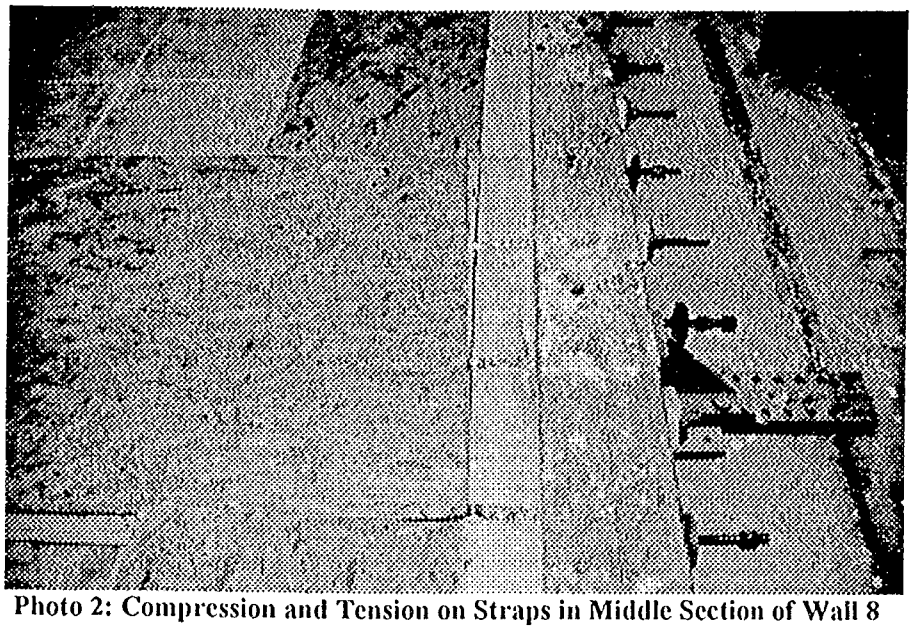


Photo 2: Compression and Tension on Straps in Middle Section of Wall 8

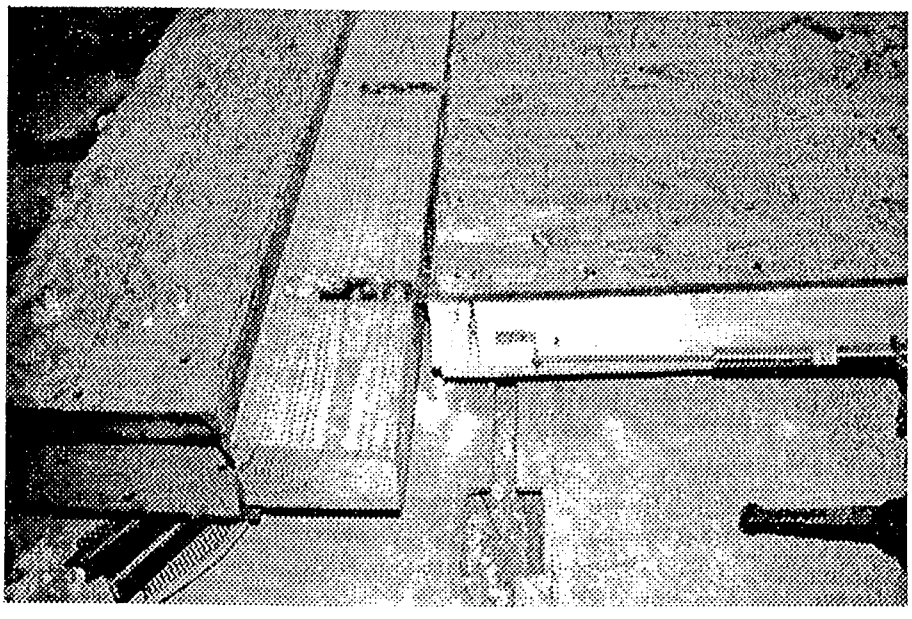


Photo 3: Load on First Two Straps of Wall 8

The New FHWA/MCEER Seismic Vulnerability Study of Highway Systems: Loss Estimation Methodology and the Seismic Design and Retrofitting of Long Span Bridges

by

Ian M. Friedland, P.E.[1]
W. Phillip Yen[2]
John D. O'Fallon[2]

ABSTRACT

In the fall of 1998, the Multidisciplinary Center for Earthquake Engineering Research was awarded a 6-year, $10.8 million contract by the Federal Highway Administration of the U.S. Department of Transportation to conduct a series of studies related to the seismic performance of the U.S. national highway system. The research being conducted under this contract is intended to provide improved tools for evaluating and assessing the societal impacts of earthquakes on highway systems and bridges, and to reduce the amount of damage that may occur to existing and future highway structures from a moderate-to-significant seismic event. The focus of this paper is on two aspects of this comprehensive program: (1) development of formal loss estimation methodologies for highway systems subject to damaging earthquakes, and (2) the development of a manual for the seismic design and retrofitting of long span bridges.

KEYWORDS: earthquake engineering; seismic vulnerability; loss estimation; seismic risk assessment; seismic design; seismic retrofitting

1. INTRODUCTION

Surface transportation is a critical component of the infrastructure that society relies on. Surface transportation systems act as key links within and between population centers and business sectors, and provide for the movement of people and goods throughout a region, nationally, and globally. This transportation network must continue to function during and after the occurrence of a natural disaster such as an earthquake so that the lifelines of our society can continue to function and emergency services can be provided to minimize the loss of life and economic distress.

Of all the components of the surface transportation system, bridges have been shown to be among the most vulnerable to earthquake damage. About 70 percent of the approximately 500,000 highway bridges in the U.S. were constructed prior to 1971, with little or no consideration given to seismic resistance. Recent earthquakes, such as the 1989 Loma Prieta, 1994 Northridge, and 1995 Kobe earthquakes, have demonstrated the need to find new and improved ways to design and construct bridges and highways which can withstand the force and displacement demands placed on them, and to cost-effectively retrofit existing seismically-vulnerable structures.

Recognizing the shortcomings evident in both existing highway bridges and current design specifications for new bridges, the Federal Highway Administration (FHWA) initiated a comprehensive seismic research program for

[1] Assistant Director for Transportation Research, Multidisciplinary Center for Earthquake Engineering Research, University at Buffalo, 102 Red Jacket Quadrangle, Buffalo, NY 14261-0025
[2] Research Structural Engineer, Federal Highway Administration, HNR-10, Turner-Fairbank Highway Research Center, 6300 Georgetown Pike, McLean, VA 22101

bridges and highways in 1992. That program was comprised of two contracts: Seismic Vulnerability of Existing Highway Construction, FHWA contract DTFH61-92-C-00106 (a six year study) and Seismic Vulnerability of New Highway Construction, FHWA contract DTFH61-92-C-00112 (a four year project). Both studies were initiated in cooperation with the Multidisciplinary Center for Earthquake Engineering Research (MCEER) [formerly the National Center for Earthquake Engineering Research]. Final products of these two studies will include a 3-volume seismic retrofitting manual for highway systems, and recommendations for improving future seismic bridge design specifications.

Despite these gains in knowledge, there is still some distance to go before seismic resistant highway systems are a reality. Some classes of bridges have yet to be studied in any systematic manner, such as long span bridges, and structures on or crossing difficult sites continue to be a problem. Some of these structures are very old and have piers constructed of unreinforced masonry and members assembled from non-ductile steels and cast iron. Many are located on unknown foundations or, if the foundations are known, they are usually massive underground lightly reinforced concrete structures, often constructed in weak soils. Their seismic resistance is difficult, if not impossible, to quantify given the current state of knowledge. This is a major concern because these structures are usually critically important to the region they serve. Any loss of access will have a major impact on emergency services following an earthquake and impede post-earthquake recovery. Society expects a higher level of performance from these structures than for more conventional highway structures. Yet little is known about their capacity for extreme loads, such as earthquake loads, and assurances of unrestricted access following an earthquake cannot be given at this time.

The high cost of retrofitting the nation's bridges is a major disincentive to owner agencies who are faced with extensive upgrade programs. A more intelligent way of prioritizing a bridge inventory, and selecting bridges to be retrofitted, is necessary to ensure that scarce resources are used in the most cost-effective manner. For this purpose, a seismic risk assessment procedure has been developed by MCEER under one of the earlier FHWA contracts. This procedure allows for the determination of traffic flow impacts due to bridge-related damage caused by various scenario earthquakes. To reach its full potential however, the methodology must be extended to assess the direct and indirect costs of this damage and include the effects of damage to other components of a highway system such as tunnels, slopes, pavements, and retaining structures. But in order for the bridge engineering community to have confidence in this refined loss estimation methodology, it must be calibrated against actual earthquake experience-data and validated by independent consultants against data sets from both large and small earthquakes. It is noted that such a tool, once developed, will not only be invaluable for bridge engineers, but will also allow emergency response personnel to plan ahead using earthquake scenarios, perform rapid damage assessments following an actual earthquake, and manage recovery in an optimal way.

To address these and other related needs, the Multidisciplinary Center for Earthquake Engineering Research (MCEER) was awarded a 6-year, $10.8 million contract in the fall of 1998 by the Federal Highway Administration (FHWA) of the U.S. Department of Transportation. This contract, which was authorized under the 1998 Transportation Efficiency Act for the 21st Century (TEA-21), is addressing research on the seismic vulnerability of the U.S. national highway system. This contract is intended to draw on and extend the work that has been conducted under the prior two FHWA research projects being conducted by MCEER.

2. SEISMIC VULNERABILITY OF THE HIGHWAY SYSTEM

The earlier FHWA contracts are primarily focussed on the seismic design and retrofitting of typical highway bridges found throughout the U.S. The TEA-21 contract focuses on several special issues considered as critical to the future of the Nation's highway transportation infra-

structure. The TEA-21 research addresses:

- Development of formal loss estimation methodologies for highway systems. This research is intended to draw on and extend the work being conducted by MCEER on the development of a seismic risk assessment methodology for highway systems.

- Development of a seismic design and retrofitting manual for long span bridges. The earlier FHWA-sponsored research is developing a series of seismic retrofitting manuals for application to typical highway bridges and highway structures (retaining structures, slopes, tunnels, culverts, and pavements). The new manual will address long span bridges which are typically critical lifeline structures, including long span trusses, suspension, and cable stayed bridges.

- Development or improvements for "smart" or "intelligent" earthquake protective systems, including bearings and dampers, specialty materials, and other passive and hybrid semi-active systems.

- Studies related to foundation design and soil behavior and response, including large pile group behavior, long period ground motions, and improvements in ground remediation technologies.

The project will also address a series of special studies, including the development of post-earthquake non-destructive assessment technologies for retrofitted bridge components, support for NCHRP Project 12-49 which is developing a new seismic design specification for highway bridges, and designing and implementing a seismic instrumentation system for the Cape Girardeau cable-stayed bridge, which is currently under construction across the Mississippi River between Missouri and Illinois and is within the New Madrid seismic hazard zone, to record seismic free field and structural response data.

Dr. George C. Lee, MCEER director, is the project principal investigator, and Mr. Ian M. Friedland, P.E., MCEER assistant director for transportation research, is the project manager.

This six-year research program will study the seismic vulnerability of highway systems and components, and will develop cost-effective methods of retrofitting system components and facilitate the implementation of these methods in the field. The program has a national focus and addresses structure types and issues not currently being addressed in other research programs or projects. The program includes a mix of analytical and experimental studies, and will result in a number of manuals, guides, and design and retrofitting recommendations for evaluating and improving the seismic vulnerability of highway systems and their components. Some of the new and improved knowledge and technologies may have applicability to other modes of transportation and opportunities for the transfer of this information to these other modes will be pursued.

The program is comprised of eight primary tasks, as follows:

Task A – Project Administration and Highway Seismic Research Council
Task B – Loss Estimation Methods for Highway Systems
Task C – Seismic Design and Retrofit Manual for Long Span Bridges
Task D – Earthquake Protective Systems
Task E – Foundation and Geotechnical Studies
Task F – Special Studies
Task G – Technology Exchange and Transfer
Task H – Reports

The objective and focus of the research being conducted under Tasks B and C are detailed in the following.

3. LOSS ESTIMATION METHODS FOR HIGHWAY SYSTEMS

Loss estimation methods have moved to the forefront as earthquake hazard reduction tools. As a result of technological advances in data collection and management, relational data analysis, and software development, loss estimation methodologies are now packaged in

user-friendly platforms and are capable of performing calculations in a matter of minutes. This is in contrast to studies a decade ago that were largely static (that are performed for single scenarios) and performed essentially on paper maps.

In addition to these advances in computer hardware and software, our understanding of the performance of a wide range of systems, including highways, has been improved considerably. Much of this advancement in the highway field has been as a result of the seismic risk assessment (SRA) methodology developments under the FHWA-sponsored MCEER Highway Project. Due in large part to the occurrence of several recent events, our ability to model in more depth and in more detail the impacts of large earthquakes has grown significantly.

Acknowledging that the assessment of socioeconomic impacts caused by the failure and disruption of transportation systems was essentially absent until roughly five years ago, the current state of knowledge in this area is ripe for continued rapid advancement. Researchers in the U.S., Japan, and New Zealand now consider the assessment of impacts beyond direct losses critical in justifying future seismic mitigation programs.

The role of loss estimation methods in the present study is three-fold. First, loss estimation methods will be used in the estimate of seismic vulnerability for existing transportation systems, in particular highway networks. Second, based on this analysis, loss estimation methods will be used to project future benefits, in terms of reduced losses, from the execution of retrofit programs. Like most policy-related studies, it is important to identify and understand fully the impact of suggested changes in policy: will this program result in long-term savings? does the implementation of the program have ancillary benefits that help to improve other factors beyond earthquakes? is there an optimal schedule for retrofitting that takes into consideration the age of the structure, the regional variation of seismicity, and ongoing maintenance programs? These are all questions that can be answered in part by loss estimation methods. Finally, loss estimation can be effectively applied in a post-earthquake environment.

When a major earthquake hits a metropolitan area, one of the first priorities for emergency response officials is to determine the extent of damage; that is, identify which areas have been hardest hit and will therefore require the most resources in order to restore service or minimize loss of life and economic hardship. By knowing this information, reconnaissance efforts and emergency repairs can be prioritized, thus eliminating the possibility of over-committing resources for relatively insignificant events. In addition, loss estimation methods can be used to help assess optimal recovery strategies. Is it better to repair a particular structure or just replace it? An analysis of future seismic hazards and risks could allow a comparison of the relative benefits associated with each strategy or action.

The research being conducted by MCEER is focused on the development and application of loss estimation methods for a broad range of purposes. The approach is structured to maximize the potential for achieving each of the above objectives. It must be understood, however, that in order to develop a tool that is implementable, considerable effort must be spent in designing the methodology, incorporating state-of-the-art models, calibrating and validating the methodology, and eventually testing the methodology using potential users.

The approach for integrating loss estimation methods into the current overall program is to build on what has been accomplished previously under the MCEER Highway Project, by enhancing that model and expanding the types of losses are that estimated (including indirect losses), incorporating new developments and data where appropriate, ensuring the usability of the methodology so that it is presented as a flexible and user-friendly software tool with ample documentation, and expanding the methodology to address other highway system components and other transportation systems, where appropriate.

The research for this task is comprised of three major components:

Task B1 – Loss Estimation Methodology Development, Additional Refinement of the Current Project SRA; System Calibration and Validation
Task B2 – Other Highway Components
Task B3 – Other Transportation Systems

Task B1 is comprised of five parts: (1) validation, calibration, and refinement of the current seismic risk assessment (SRA) methodology; (2) development of direct and indirect loss modules for incorporation into the SRA system; (3) calibration of the complete system and validation by independent testing; (4) completion of the system software and documentation; and (5) demonstration and workshops.

Under the earlier FHWA project, a major focus has been on bridge damage state modeling and traffic state analysis, with limited additional work in direct loss modeling and other highway system elements. While significant progress was made in that study, there are still important gaps in several areas. These include applicability of models outside of the demonstration city, i.e., Memphis, Tennessee; more accurate modeling of impaired traffic states; continued enhancements in network analysis uncertainties; and more rigorous treatment of site-specific assessments of certain seismic hazards (e.g., lateral spread damage is currently being evaluated under that project but may not be fully characterized). As part of Task B1-1, refinements in the current methodology will be made to address these and other limitations and provide needed enhancements.

In order to extend the current SRA methodology to incorporate a more rigorous assessment of direct and indirect economic losses, further model development will take place in Task B1-2. In this task, a comprehensive set of measures will be identified that will address direct and indirect losses. Some measures will focus on the impacts on the highway system itself, such as repair costs and debris removal; other measures will concentrate on the impacts to surrounding exposures (e.g., populations and businesses). To insure the credibility of these new models, calibration and validation studies of the complete integrated system, including the incorporation of other highway system components and transportation modes and discussed under Tasks B2 and B3, will be performed in Task B1-3 using data from a series of actual large and small earthquakes.

To expand the current SRA methodology to other highway components, damage models will be developed for retaining structures, slopes, tunnels, culverts, approach fills, and pavements under Task B2. These models will be incorporated into the current methodology, as they may have significant impact on the traffic flow analyses. Specific model development will include damage state fragility modeling, including uncertainty analysis, restoration modeling, and traffic flow impact modeling based on different levels and types of damage. The goal of this task is to improve the overall modeling of damage and impacts to highway networks by including all key components.

Finally, in order to adapt the methodology to other transportation systems, a series of studies under Task B3 that address freight and urban mass transit (UMT) rail systems may be conducted, if time and project funds permit. Past experience in the U.S. and Japan has shown that, in the presence of earthquake damage to highway systems, freight and UMT rail systems can greatly facilitate the return of workers to their jobs, and the transport of essential materials and goods into and out of the region. This, in turn, can effectively reduce overall economic losses due to earthquake damage, and can also enhance the region's emergency response and recovery operations. Accordingly, the objective of Task B3 is to integrate freight and UMT rail transportation systems models with the highway system models above. The end result of this integration will be a multi-modal land-transportation SRA methodology.

There is a tremendous opportunity to also facilitate cross-disciplinary research to improve particular loss estimation modules. For example, the work that will be completed on long span bridges under Task C (as described below)

will necessarily feed into the fragility and damage/loss modeling in this part of the program. By incorporating the results from this related research, we can be assured that the most logical set of parameters and data needed to represent or characterize the performance of long span bridges are incorporated in the overall SRA methodology. By the same token, the loss estimation methodology might also identify the relative importance of long span bridges with regard to overall system performance. This kind of information could be valuable in explaining the need for retrofitting such structures. In addition to the long span bridge task, the advanced bridge earthquake protective system task may provide important insights and information in the application of the methodology. By understanding what new measures might improve the specific performance of a particular bridge, we can identify more effective ways of improving the overall performance of the system. Similarly, we can use loss estimation tools to estimate the relative benefits associated with these new and advanced technologies. Relative benefits could be extended to include the larger system benefits associated with this implementation.

4. SEISMIC DESIGN AND RETROFIT MANUAL FOR LONG SPAN BRIDGES

In 1983, the FHWA published the *Seismic Retrofitting Guidelines for Highway Bridges*, the first attempt at providing nationally-applicable guidance on screening, evaluating, and retrofitting seismically vulnerable highway bridges. That report (and its 1995 update, *Seismic Retrofitting Manual for Highway Bridges*, which was developed under the FHWA-sponsored MCEER Highway Project) are intended to address the vast majority of typical short-to-medium span structures contained in the U.S. National Bridge Inventory. However, very limited information is available on a national basis concerning evaluating the seismic vulnerability or retrofitting of long span bridges. At the current time, long span bridges are evaluated on a case-by-case basis and are usually considered as "special studies." However, there are a number of similarities between the structural systems and components of many long span bridges, and the development of a manual with recommended guidance on their evaluation and retrofitting could provide some uniformity and technical assistance in their evaluations nationwide.

Some long span bridges are very old and have piers of unreinforced masonry, or members fabricated from non-ductile steels and cast iron. Some are located on unknown foundations or, if known, they are usually massive lightly reinforced concrete pedestals in weak soils. Their seismic resistance is difficult, if not impossible, to quantify given the current state of engineering knowledge. This is a major concern because these structures are usually critically important to the region they serve, and any loss of access will have a major impact on emergency services following an earthquake, with the potential to impede post-earthquake response and recovery. Society expects a higher level of performance from these structures than for the more conventional highway structures; yet little is known about their capacity to accommodate or resist extreme loads, such as those experienced during an earthquake, and assurances of unrestricted access following an earthquake cannot be given at this time. This part of the TEA-21 project will address this problem in a consistent and transparent manner, drawing on experience from recent earthquakes and the expertise of a team of skilled researchers and practitioners.

For the purpose of this project, long span bridges have been defined as those structures where the main span exceeds 120 m. In contrast with short-to-medium span bridges that are generally comprised of simply-supported or continuous girders, long span bridges are generally made up of an assemblage of elements in the form of trusses, arches, cables, or a combination thereof. Most long span bridges can be classified into the following superstructure types:

- Steel Trusses – through trusses, deck trusses; articulation defined as simple span, cantilever, continuous, gerber, or combination
- Steel and Concrete Arches – through arches, deck arches; articulation defined as full arch,

two or three hinged arch, or tied arch (single or multi-spans)

- Steel and Concrete Cable Stayed – single and double towers, single and multi-planes of cables; varied articulation

- Steel Suspension Spans – earth anchored, self anchored; typically three spans of articulation

The most prolific of all long span bridges in the U.S. is the truss-type of structure. Therefore it is planned to primarily, but not exclusively, focus on the truss-type of long span bridge in this research. In addition, most substructures for long-span bridges can be classified into the following types: spread footings, timber piles, concrete piles, steel piles, or caissons.

Long span bridges, especially those of the truss type, can be quite old. Therefore the nature, integrity, and seismic performance of the substructure and foundation systems are generally unknown.

For this project, a *Seismic Design and Retrofitting Manual for Long Span Bridges* will be developed. This manual will be complementary to but distinct from the 1995 *Seismic Retrofitting Manual* and the revision of that manual that is currently underway via the MCEER Highway Project. Some of the issues to be covered in the proposed long span manual are discussed in the following. A number of these issues were identified during a Long Span Bridge Workshop, which was conducted under the MCEER Highway Project in 1994.

4.1 Structural Issues

One of the distinctions between short span and long span bridges is in the definition of importance. Long span bridges generally cross waterways at locations where there is little, if any, redundancy in the highway network. The operational demands on such bridges are therefore considerably greater, and it is of paramount importance to ensure that a long span bridge remains open following a large earthquake. This dictates that long span bridges should behave in a "mostly elastic" fashion. This performance objective raises difficulty in determining the extent of permitted inelastic behavior of the main structural elements.

Retrofitting measures for such bridges are also challenging. Schemes that have been proposed to date are largely untested and therefore unproven. It is necessary to conduct experimental studies on critical subassemblages that are representative of typical long span bridge structures in order to gain an understanding of their expected performance and behavior under dynamic loading. Of particular importance are braced and unbraced sway frames, bearing-pedestal seating systems, and the strength and ductility of bridge piers and foundations. Retrofit measures for these critical elements and subassemblages are also considered to be important and will be addressed during the life of the project. However, prior to conducting research on retrofitting measures, a series of analytical studies will be performed to ascertain the most critical elements along with the need for retrofitting. This analytical phase of work will take place over the first two years of the project, whereas studies on retrofit measures will commence in the third year.

Experience in California has shown that many of their long span bridge piers and towers require some form of retrofitting. Although this experience is useful in identifying research needs, the extent of their applicability to national guidelines is unknown. For example, in low-to-moderate seismic zones, it may be neither expedient nor feasible to seismically retrofit a long span bridge that only has modest seismic demands imposed upon it. Some limited form of retrofitting (for example, bearings and seats) or the " do-nothing" option may be more economically justified. This option is rather attractive considering the exceedingly expensive retrofit measures that may be required if these bridges are retrofitted for long return period earthquakes. Research is therefore needed to in order to provide owners guidance on assessing the vulnerability of long span structures and the expected outcome if the "do-nothing" option is adopted.

4.2 Geotechnical and Foundation Issues

There are a number of important geotechnical and foundation considerations for long span bridges that must be addressed. These include the need for studies on improved evaluation of long-period ground motion characteristics in existing earthquake records, developing methods for estimating liquefaction-induced lateral spreading loads on caissons and pile supported piers, consideration of soil-foundation interaction from large pile groups and caissons, and characterization of the site response at soft soil sites.

Ground acceleration characteristics and related spectral accelerations have historically formed the basis for seismic design. However, in the case of long span bridges, natural periods of vibration may be in the range of 3 to 10 seconds. In this period range, the signal-to-noise ratio of recorded accelerograms require the use of high pass filters to eliminate the noise. Consequently, the accuracy of spectral ordinates in the 3 to 10 second range is questionable. As peak ground displacements occur in this range and spectral displacement ordinates provide essential design criteria, research is needed to clarify the nature and magnitude of displacement spectra and peak ground displacements associated with design earthquakes.

In the case of large caissons and pile-supported bridge piers where current retrofit analyses indicate the potential for liquefaction-induced lateral displacements, ground remediation options are often impractical, particularly where foundations are located in river channels. Consequently, the need to assess whether the load and displacement demands on the foundations are of concern becomes a critical need, as does the option of developing an economical structural retrofit, if required.

The typical input to a soil-structure interaction analysis relies on free field site response results. Recent sensitivity studies on soil-structure interaction indicate that the resultant overall bridge solution is very sensitive to the site response analysis results. For large pile groups and caisson foundations, excitation to the structure comes from input ground motions at various depths along the pile group and caisson length. In addition to the overall level of shaking, phase differences in depth-varying ground motions will introduce rotational excitation on the structure. The depth-varying input ground motion will introduce a tilting motion in addition to horizontal and translational motions in the structure. This effect can be very significant for cantilevered foundation systems; i.e., when the pile cap or cross-bracing is cantilevered a big distance above the mudline. Whereas available site response analyses have been verified to some degree by comparing surface motion to recordings, some of the subtleties in phase change with depth (i.e., the apparent propagation speed with depth) have not been verified resulting in drastic changes in shaking of the structure as implied by the tilting mode of the input to the structure. This aspect can be addressed by examining some of the available down-hole strong-motion recordings, e.g., at Port Island from the Kobe earthquake and the SMART-1 array. Also, some sensitivity studies can be conducted to compare the phase angle change between nonlinear and equivalent linear site response analyses and 2-D site response analyses, which inherently decompose 1-D shear waves at reflecting boundaries to compressional and shear waves. Some guidance on this issue can improve the level of confidence in the state-of-practice for soil-structure interaction analyses and in design practice.

Extremely large pile groups (involving hundreds of piles) are very common for long span bridges and group effects for such systems are believed to be extremely important. However, available pile group test data is limited to mostly 3 x 3 pile groups. The University of Florida had developed some data on a 4 x 4 pile group and these data have been used to compare with the elasticity pile group theory, which was found to be somewhat misleading as it over-predicts group effects. This lack of experimental data has left designers to make subjective judgements, usually by modifying p-y curves. Completely ignoring group effects can lead to very serious errors for very large pile groups, while relying on the elasticity approach has been found to be deficient even for small pile groups. Research in this area is needed and the advance of constitutive modeling and 3-D finite element

programs can tremendously improve our ability to account for group effects by analytical approaches.

5. CONCLUSIONS

The FHWA-sponsored research program recently initiated by MCEER will address a number of important aspects related to the seismic vulnerability of the national highway system. Two of four major research thrust areas, loss estimation methodologies for highway systems and seismic design and retrofitting of long span bridges, have been described in this paper. Other thrust areas, including advancing the state of practice with respect to the development of intelligent earthquake protective systems, and geotechnical studies on soils and foundation behavior, will be discussed in subsequent papers and presentations.

The results of this work are expected to have significant short- and long-term impacts on the performance and economics associated with earthquake impacts on highway systems, and it is expected that some of the advances made in this program will have direct application to other surface transportation modes. As the research is still in its initial stages, the first set of results and products will not be available for approximately 3 or more years.

Development of Test Guidelines for Passive Energy Dissipation Devices

By

Michael A. Riley[1] and Fahim Sadek[2]

ABSTRACT

Passive energy dissipation devices are effective for improving the dynamic response of structures by reducing their response to earthquake and wind excitations. Wide acceptance of these devices for structural applications depends on their performance being well documented, and on the availability of standards for their evaluation and testing. In response to this latter need, the Building and Fire Research Laboratory of the National Institute of Standards and Technology has initiated a research program to develop guidelines for testing supplemental damping devices.

The objective of the guidelines is to provide a standardized series of prototype and production tests for passive energy dissipation devices. The test guidelines are intended to be independent of both the device type and application. They are also meant to assist manufacturers, researchers, and practitioners in performing and interpreting the test results.

This paper provides an overview of the guidelines and describes their development.

KEYWORDS: passive dampers; passive energy dissipation; test guidelines; structural control; supplemental damping.

1 INTRODUCTION

Extensive research and initial implementations have shown that passive energy dissipation devices can significantly improve the dynamic response of structures (Hanson, et al., 1993; Soong and Constantinou, 1994; Sadek, et al., 1996; and Soong and Dargush, 1997). These devices, which are also known as passive control devices, supplemental dampers, or passive dampers, can reduce structural responses due to wind, earthquake, and other dynamic loads. Such devices can absorb part of the energy induced in the structure, minimizing the energy dissipation demand on the primary structural members, and thus reducing the inter-story drifts and nonstructural damage. In addition, they can be designed to provide additional stiffness to the structure and to be easily replaced if they are damaged.

Research and development have led to a variety of passive energy dissipation devices. They use a range of materials and mechanisms, which operate on principles such as sliding friction, yielding of metals, deformation of viscoelastic materials, and fluid flow through orifices.

These devices are now used in the design of new structures and the rehabilitation of existing ones in Canada, Japan, Mexico, New Zealand, Europe, and the United States. Nevertheless, most of these devices are still designed and manufactured on a per-project basis. Design and test standards are

[1] Research Structural Engineer, National Institute of Standards and Technology, 100 Bureau Dr., Stop 8611, Gaithersburg, MD 20899-8611

[2] Research Associate, Southern Methodist University, Dallas, TX 75275; on Assignment, National Institute of Standards and Technology, 100 Bureau Dr., Stop 8611, Gaithersburg, MD 20899-8611

necessary for their widespread use. Although some design and test guidelines already exist (NEHRP, 1997; Taylor and Constantinou, 1994), most are specific to certain types of structures or have limited applications.

In response to this lack of test standards, the Building and Fire Research Laboratory of the National Institute of Standards and Technology has initiated a program to develop guidelines for testing supplemental damping devices. A draft version of these guidelines, titled "Guidelines for Testing Passive Energy Dissipation Devices" (Riley, et al., 1999), has been completed and is being reviewed. The guidelines recommend *prototype* and *quality control* tests for passive energy dissipation devices. In addition, they describe a series of *basic property* tests, which may be used as the basis for evaluating future devices as they are developed.

2 ENERGY DISSIPATION DEVICE TYPES

Some common types of passive energy dissipation devices are described below. These devices are currently available, and have been used in structures or laboratory experiments. This list of devices is not complete, due to the large number of existing devices. Moreover, the industry is rapidly evolving and, therefore, it is anticipated that many additional devices will be developed in the future. The test guidelines described in this paper are applicable to many other types of devices; not just those included below.

For the purpose of the test guidelines, these devices can be categorized according to their mechanical behavior as rate dependent, rate independent, or others. The following is a brief description of the properties and types of devices in each category.

2.1 Rate Independent Devices

Devices with force-displacement response characteristics that are primarily a function of the displacement amplitude are classified as rate independent devices. The behavior of these devices is generally independent of the relative velocity or the frequency of motion. They include friction and metallic devices.

2.1.1 Friction Devices

Friction devices use the friction between sliding surfaces to dissipate energy. They generally exhibit rigid-plastic behavior and their force response can be modeled by simple Coulomb friction, so the force-displacement curves of the devices are rectangular loops. These devices can be characterized by their displacement amplitude and slip-load.

Friction devices can dissipate large amounts of energy even at low velocities, while their peak forces are bounded even at large velocities. Unfortunately, their effective stiffness can be large when motions are small and their non-linear response complicates structural designs.

A variety of mechanisms can be used to create the friction forces, including sliding or twisting between simple metal surfaces. Performance of the devices may be enhanced by using friction pads or wedges. One type of friction device combines friction pads with a spring mechanism, which gives the device a re-centering capability and slip forces that are proportional to the displacement. Friction devices are typically located in braces or at the intersection of cross braces.

2.1.2 Metallic Devices

Metallic yielding devices take advantage of the stable hysteretic force-displacement be-

havior of metals to absorb energy. These devices use flexural, shear, or extensional deformations in the metal's plastic range to provide the structure with increased stiffness and energy dissipation capacity. They typically exhibit hysteretic force-displacement behavior, which can be approximated as bilinear or trilinear.

These devices tend to be inexpensive to produce and their properties will remain stable over the long lives of buildings and bridges. Unfortunately, they often have a limited number of working cycles, which may require them to be replaced after large seismic events. Like friction devices, their non-linear response can complicate structural designs.

These devices can be installed in the bracing systems of building frames, or used between the structure and foundation of seismically isolated structures to increase the damping in the isolation system.

2.2 Rate Dependent Devices

Rate dependent devices have force-displacement response characteristics that are a function of either the relative velocity between the ends of the device or the frequency of the motion. The response of the devices in this category, however, may be a function of the relative displacement as well. These devices include solid viscoelastic, fluid viscoelastic, and viscous fluid devices.

2.2.1 Solid Viscoelastic Devices

Solid viscoelastic devices are constructed from constrained layers of acrylic polymers and designed such that they produce damping forces through shear deformations in the polymers. When deformed, the viscoelastic materials exhibit the combined features of an elastic solid and viscous liquid. The resulting response can be modeled using a Kelvin model, which consists of a spring and dashpot in parallel.

These devices have proven to be efficient and cost effective for reducing wind induced vibrations. Unfortunately, their effective stiffness and the damping forces are generally dependent on the excitation frequency and the operating temperature, including the temperature rise due to excitation. Because of this temperature dependence, these devices may not be useful in structures where the climate is not continuously controlled.

These devices are typically used in moment resisting frames, where they are installed in cross braces or in connections between floor trusses and columns.

2.2.2 Fluid Viscoelastic Devices

Fluid viscoelastic devices, such as viscous shear walls, operate by shearing viscoelastic fluids. Their behavior and response characteristics are similar to solid viscoelastic devices, except that the fluid viscoelastic dampers do not exhibit stiffness when static loads are applied. These devices can be modeled with Maxwell model, which consists of a spring and dashpot in series.

2.2.3 Fluid Viscous Devices

Fluid viscous devices are used extensively in a variety of structural and mechanical systems, to reduce responses to vibrations and shock. These devices operate on the principle of fluid flow through orifices. They tend to act as ideal viscous dampers, generating only damping forces, but they may exhibit some stiffness at high frequencies.

Fluid viscous devices can dissipate large amounts of energy, over a wide range of excitation frequencies. Their force response is proportional to velocity, so designing

Table 1. Test Categories

Type of Test	Test Category	Notes
Quality Control Tests	Material Properties	Tests of materials and components.
	Production Unit	Tests of completed devices.
Prototype Tests	System Properties	Determination of response properties.
	Applied Loads	Validation of response to realistic loads.
	Reserve Capacities	Validation of response to extreme loads.
Basic Property Tests	Basic Properties	Tests for device development only.

structures that use these devices is generally straightforward. The life span of these devices tends to be limited only by wear of their seals.

The devices are typically installed in the bracing systems of buildings or used in conjunction with the isolators in seismically isolated structures. They can be used effectively for buildings, bridges, and other structural systems.

2.3 Other Types of Dampers

Other energy dissipation devices have been developed that cannot be classified as either rate dependent or independent. One such device type is shape memory alloys, which undergo a reversible phase transformation and exhibit superelastic behavior when deformed.

3 OVERVIEW OF THE GUIDELINES

The guidelines include a series of test procedures and requirements for how the tests should be performed. The test procedures are grouped into five categories in two series, according to the nature and purpose of the tests. The test series are *quality control* tests and *prototype* tests. In addition, the guidelines describe a series of *basic property* test, which are not required, but are intended as guidance for how to test newly developed device types. The test types and categories are listed in Table 1.

All of the tests in these guidelines are presented in a standard format, which includes the procedure and any applicable performance criteria. Systems that fail to meet the performance criteria may not perform adequately in service.

3.1 Scope

The guidelines are intended to be comprehensive and to apply to all passive energy dissipators, all structural systems, and many types of dynamic loads. Therefore, the need to develop standards for a particular damper type or application is minimized. Although many of the proposed tests may be applicable to components of active, semi-active, or hybrid systems, these guidelines are not being developed for such devices.

The guidelines are not intended to recommend one energy dissipation system over another. They are intended only to validate that a particular device will perform properly in a given application; therefore, they are expected to encourage competition between various systems.

3.2 Test Requirements

The guidelines include a set of general requirements that apply to all prototype and quality control tests. All tests should be conducted in accordance with these requirements; however, certain requirements may be waived if they are deemed unnecessary for a particular device or design. When necessary, additional special requirements are presented with the individual test specifications.

The general requirements define the necessary facilities and reported information. The necessary test apparatus, instrumentation, and data acquisition are described. The data that should be recorded, analyzed, and reported are also defined.

The requirements also describe how to define the device classification and capacity. To properly test a device, the required force, amplitude, and stroke capacities of the device need to be known. The design response must also be defined, to allow comparison between the actual and required response of the device.

Finally, the devices need to be categorized according to how their response varies to external influences. The devices should be categorized according to whether or not their response depends on the excitation frequency, the loading rate, stroke position, or device temperature. The devices should also be categorized according to how their response degrades with continued use.

3.3 Test Series

As listed in Table 1, above, the guidelines contain three test series and six test categories. A graphical description of how the test series are related, and when each test series should be performed, is shown in Figure 1. The three test series - *quality control* tests, *prototype* tests, and *basic property* tests - are described in detail below.

3.3.1 Quality Control Tests

The quality control tests are intended to verify the as-built characteristics of the completed devices and should be performed on all units before installation. This test series includes two test categories, the *material property tests* and *production unit tests*.

The material property test category includes tests of the materials used in the device and tests of each unit's sub-components. These tests are conducted to monitor the quality and consistency of the manufacturing process. They should be performed during fabrication of the devices and should meet the appropriate test standards. The details of these tests are not described in the guidelines; instead, appropriate tests should be performed for each type of device, as necessary.

The production unit test category consists of four tests, which are intended to verify the as-built properties of the devices. In general, only one of the four tests will need to be performed on a particular device, although in some cases a second test will be needed. All four tests investigate the stiffness and energy dissipation properties of the devices.

The response of the devices during the production unit tests is considered acceptable if the properties fall within a defined range of acceptable values.

3.3.2 Prototype Tests

The prototype tests are intended to verify the design properties of a specific device. This test series includes three test categories, the *system property tests*, *applied load tests*, and *reserve capacity tests*. These tests

should be performed on two specimens for each design and unique application.

The system property test category consists of four tests. The first test in this category is designed to determine the response properties of the device. This test is identical to the first production unit test, and needs to be performed only if the first production unit test was not performed. The remaining three tests are designed to determine how the properties change with changes in the loading conditions. These tests need to be performed only on devices whose response is dependent on the loading frequency, stroke offsets, or device temperature.

The applied loads test category consists of three tests that are intended to validate the device's ability to withstand realistic loading. The first test verifies that the device can survive a lifetime of the expected loads. The second and third tests verify the device's ability to withstand seismic and wind loads. Only those tests that are applicable to a particular device and application need to be performed.

The reserve capacity test category consists of two tests that are intended to verify that the device can withstand loads that exceed the design values. The first test verifies that the device will perform properly when subjected to the maximum expected loading velocity. The second test verifies that the device has a reserve capacity for withstanding displacements and forces beyond the design values.

The device's response during the prototype

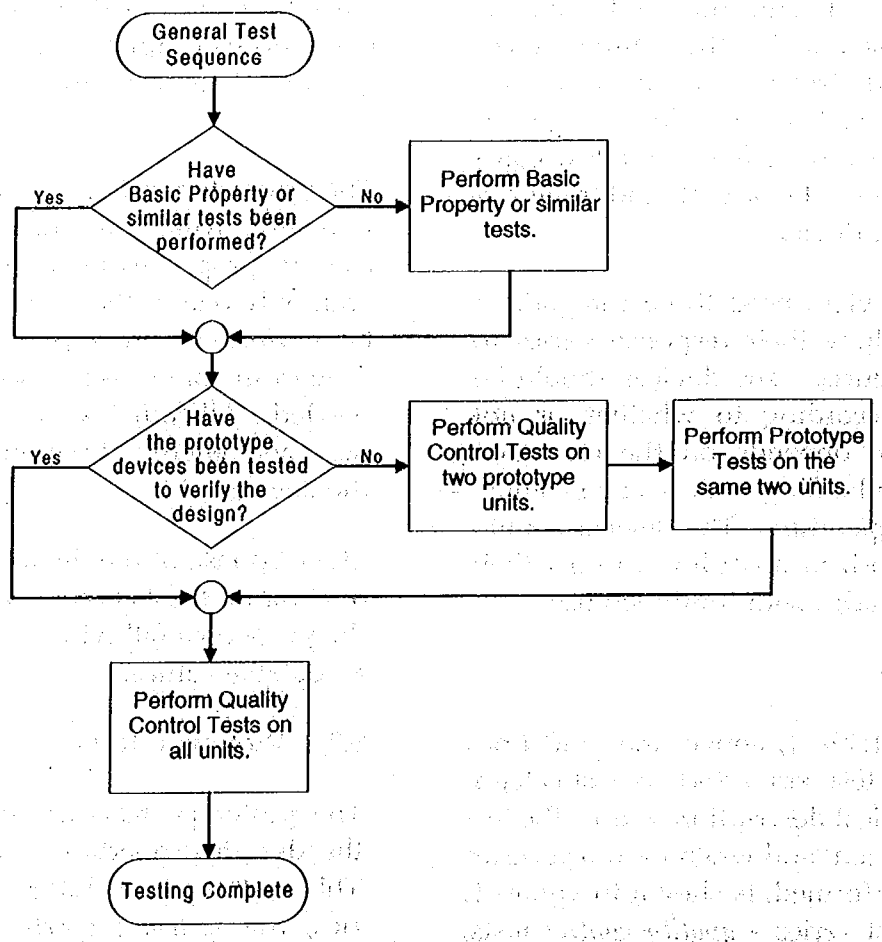


Figure 1. Test Sequence for Passive Energy Dissipation Devices.

tests is considered acceptable if the properties fall within a defined range of acceptable values or if the variation of the properties is accurately predicted by mathematical models of the device. In addition, the device should not be permanently damaged by the tests.

3.3.3 Basic Property Tests

The basic property tests are included in an appendix to the guidelines. These tests are not required, but may be used to determine the characteristics of new devices or existing ones that are substantially modified. These test guidelines provide only guidance on how to perform these types of tests. The basic property tests consist of three subcategories: preliminary characterization tests, device durability tests, and realistic load tests.

The preliminary characterization tests are intended to determine how the device will respond to a variety of loading conditions. These tests characterize the device properties and determine how the properties will vary with changes in loading frequency, load amplitude, temperature, and load history. These tests are intended to provide results that can be used to develop mathematical models of the device response.

The device durability tests are intended to determine the device's usable life and resistance to damage. These tests characterize how the device will respond to extended cycling, extreme loads, extreme temperatures, impact, and aging. The results of these tests can be used to develop practical guides for how long the devices will last and under what circumstances they will need to be replaced.

The realistic load tests are intended to verify that the devices and structure will perform properly when used as a complete system. These tests include realistic seismic, wind, and service loads. Preferably, these tests should be performed with the devices installed in realistic, scale-model structures.

There are no acceptance criteria for the basic property tests, since these tests are intended only to determine how the device will perform in various conditions. The tests are not intended to verify how a device will perform in a particular application.

4 DEVELOPMENT PROCEDURE

The proposed test guidelines are being developed with the assistance of an advisory committee, feedback from experts working in the area of passive energy dissipation, and a workshop to be sponsored by NIST before the guidelines are finalized. To develop confidence in the guidelines and to foster adoption of the proposed test procedures, the guidelines will be evaluated by conducting selected tests on typical supplemental damping devices. These tests will expose any inconsistencies, omissions of important data, or other unforeseen problems with the procedures, in addition to investigating the applicability of the test procedures.

Through this process, we expect to develop guidelines that will be valuable to the civil engineering community, and will facilitate the use of these devices.

5 SUMMARY

The development of these guidelines is intended to lead to more systematic evaluations of passive energy dissipation devices. Properly used, these guidelines will ensure the quality of the installed devices and should expedite the development of new systems, by allowing direct comparisons between devices. Since they will be independent of the application and applicable to all passive energy dissipation devices, these guidelines should assist in the design and

construction of structures with supplemental dampers and enhance the use of this promising technology.

6 REFERENCES

Hanson, R. D., Aiken, I. D., Nims, D. K., Richter, P. J., and Bachman, R. E., (1993), "State-of-the-Art and State-of-the-Practice in Seismic Energy Dissipation," *Proc., ATC-17-1 Seminar on Seismic Isolation, Passive Energy Dissipation, and Active Control,* Applied Technology Council, Redwood City, CA., Vol. 2, pp.449-471.

NEHRP Guidelines for the Seismic Rehabilitation of Buildings, (1997), FEMA-273, Building Seismic Safety Council, Washington, D.C.

Riley, M. A., Sadek, F., and Mohraz, B. (1999), "Guidelines for Testing Passive Energy Dissipation Devices," *Report NISTIR xxxx,* National Institute of Standards and Technology, Gaithersburg, MD. (*In progress*).

Sadek, F., Mohraz B., Taylor A. W., and Chung R. M., (1996), "Passive Energy Dissipation Devices for Seismic Applications," *Report NISTIR 5923,* National Institute of Standards and Technology, Gaithersburg, MD.

Soong, T. T., and Constantinou, M. C. (eds.), (1994), "*Passive and Active Structural Vibration Control in Civil Engineering,*" Springer-Verlag, Wien and New York.

Soong, T. T., and Dargush, G. F., (1997), "*Passive Energy Dissipation Systems in Structural Engineering,*" John Wiley and Sons, New York.

Taylor, D. P., and Constantinou, M. C., (1994) "*Test Methodology and Procedures for Fluid Viscous Dampers used in Structures to Dissipate Seismic Energy,*" Technical Report, Taylor Devices, Inc., Tonawanda, NY.

A Liquefaction Evaluation Procedure Based on Shear Wave Velocity

by

Ronald D. Andrus[1] and Kenneth H. Stokoe, II[2]

ABSTRACT

This paper outlines a procedure for evaluating liquefaction resistance of soils using shear wave velocity measurements. The procedure follows the general format of the Seed-Idriss simplified procedure based on SPT blow count. It was developed following suggestions from industry, researchers, and practitioners, and using case history data from 26 earthquakes and over 70 measurement sites in soils ranging from sand to sandy gravel with cobbles to profiles including silty clay layers. The procedure correctly predicts moderate to high liquefaction potential for over 95 % of the liquefaction case histories. A case study is provided to illustrate the application of the proposed procedure.

KEYWORDS: Building technology; earthquake engineering; *in situ* measurements; seismic testing; shear wave velocity; soil liquefaction.

1. INTRODUCTION

Evaluating the liquefaction resistance of soils is an important step in the engineering design of new structures and the retrofit of existing structures in earthquake-prone regions. The evaluation procedure widely used in the United States and throughout much of the world is termed the *simplified procedure*. This simplified procedure was originally developed by Seed and Idriss (1971) using blow counts from the Standard Penetration Test (SPT) correlated with a parameter representing the seismic loading on the soil, called the *cyclic stress ratio*.

Small-strain shear wave velocity, V_S, measurements provide a promising alternative, or supplement, to the penetration-based approach. The use of V_S as an index of liquefaction resistance is soundly based, since both V_S and liquefaction resistance are similarly influenced by void ratio, state of stress, stress history, and geologic age. Furthermore, the strong theoretical basis underlying stress wave propagation offers the opportunity for additional advances in the approach.

During the past two decades, several simplified procedures for evaluating liquefaction resistance based on V_S have been proposed (Dobry et al., 1981; Dobry et al., 1982; Seed et al., 1983; Bierschwale and Stokoe, 1984; de Alba et al., 1984; Hynes, 1988; Stokoe et al., 1988; Tokimatsu and Uchida, 1990; Tokimatsu et al., 1991; Robertson et al., 1992; Kayen et al., 1992; Andrus, 1994; Lodge, 1994; Rashidian, 1995; Kayabali, 1996; Andrus and Stokoe, 1997; Rollins et al., 1998; and Andrus et al., 1999). Some of these procedures follow the general format of the Seed-Idriss simplified procedure, where V_S is corrected to a reference overburden stress and correlated with the cyclic stress ratio. Nearly all were developed with limited or no field performance data. This paper outlines the procedure proposed by Andrus and Stokoe (1997), and updated by Andrus et al. (1999) using an expanded database.

The expanded database compiled by Andrus et al. (1999) consists of field performance data from 26 earthquakes and V_S measurements at

[1] Research Civil Engineer, National Institute of Standards and Technology, 100 Bureau Drive Stop 8611, Gaithersburg, Maryland 20899-8611.
[2] Professor, Department of Civil Engineering, ECJ 9.227, The University of Texas at Austin, Austin, Texas 78712

over 70 sites. Much of the new data are from the 1995 Hyogoken-Nanbu (Kobe), Japan earthquake (moment magnitude, M_w = 6.9).

2. LIQUEFACTION RESISTANCE FROM V_S

2.1 Cyclic Stress Ratio (*CSR*)

The cyclic stress ratio, τ_{av}/σ'_v, at a particular depth in a level soil deposit can be expressed as (Seed and Idriss, 1971):

$$\mathrm{CSR} = \frac{\tau_{av}}{\sigma'_v} = 0.65 \left(\frac{a_{max}}{g}\right)\left(\frac{\sigma_v}{\sigma'_v}\right) r_d \qquad (1)$$

where τ_{av} is the average equivalent uniform cyclic shear stress caused by the earthquake and is assumed to be 0.65 of the maximum induced stress, a_{max} is the peak horizontal ground surface acceleration, g is the acceleration of gravity, σ'_v is the initial effective vertical (overburden) stress at the depth in question, σ_v is the total overburden stress at the same depth, and r_d is a shear stress reduction coefficient to adjust for flexibility of the soil profile.

2.2 Stress-Corrected Shear Wave Velocity

Following the traditional procedures for correcting SPT blow count to account for overburden stress, one can correct V_S to a reference overburden stress by (Sykora, 1987; Robertson et al., 1992):

$$V_{S1} = V_S \left(\frac{P_a}{\sigma'_v}\right)^{0.25} \qquad (2)$$

where V_{S1} is the overburden stress-corrected shear wave velocity, P_a is a reference stress, 100 kPa or about atmospheric pressure, and σ'_v is initial effective overburden stress in kPa. In using Eq. (2), it is implicitly assumed that the initial effective horizontal stress, σ'_h, is a constant factor of the effective overburden stress. The factor, generally referred to as K'_o, is assumed to be approximately 0.5 at sites where liquefaction has occurred. Also, in applying Eq. (2), it is implicitly assumed that V_S is measured with both the directions of particle motion and wave propagation polarized along principal stress directions and one of these directions is vertical (Stokoe et al., 1985).

2.3 Cyclic Resistance Ratio (*CRR*)

The value of *CSR* separating liquefaction and non-liquefaction occurrences for a given V_{S1}, or corrected blow count, is called the *cyclic resistance ratio*.

Andrus and Stokoe (1997) proposed the following relationship between *CRR* and V_{S1}:

$$CRR = \left\{ a\left(\frac{V_{S1}}{100}\right)^2 + b\left(\frac{1}{V^*_{S1} - V_{S1}} - \frac{1}{V^*_{S1}}\right)\right\} MSF \qquad (3)$$

where V^*_{S1} is the limiting upper value of V_{S1} for liquefaction occurrence, a and b are curve fitting parameters, and *MSF* is the magnitude scaling factor. The first term of Eq. (3) is based on a modified relationship between V_{S1} and *CSR* for constant average cyclic shear strain suggested by R. Dobry (personal communication to R. D. Andrus, 1996; Andrus and Stokoe, 1997). The second term is a hyperbola with a small value at low values of V_{S1}, and a very large value as V_{S1} approaches V^*_{S1}.

The magnitude scaling factor, which accounts for the effect of earthquake magnitude on *CRR*, can be expressed by:

$$MSF = \left(\frac{M_w}{7.5}\right)^n \qquad (4)$$

where n is an exponent. The lower bound for the range of magnitude scaling factors recommended by the 1996 National Center for Earthquake Engineering Research (NCEER) Workshop on Evaluation of Liquefaction Resistance of Soils (Youd et al., 1997) is defined by Eq. (4) with n = -2.56 (Idriss, personal communication to T. L. Youd, 1995).

Figure 1 presents the case history data for magnitude 5.9 to 8.3 earthquakes adjusted using Eq. (4) with n = -2.56. Also presented in Fig. 1 are the proposed CRR-V_{S1} curves. The curves are defined by Eq. (3) with a = 0.022, b = 2.8, V_{S1}^* = 200 m/s for fines content $(FC) \geq 35$ %, V_{S1}^* = 208 m/s for FC = 20 %, and V_{S1}^* = 215 m/s for $FC \leq 5$ %. The case histories, and CRR-V_{S1} curves, are limited to relatively level ground sites with average depths less than 10 m, uncemented soils of Holocene age, ground water table depths between 0.5 m and 6 m, and V_S measurements made below the water table.

Of the 90 liquefaction case histories shown in Fig. 1, only two incorrectly lie in the no-liquefaction region. The two liquefaction cases that lie in the no-liquefaction region are for sites at Treasure Island, California. These sites are located along the perimeter of the island where liquefaction was marginal during the 1989 Loma Prieta earthquake (M_w = 7.0).

2.4 Factor of Safety

A common way to quantify the hazard for liquefaction is in terms of a factor of safety, FS. The FS against liquefaction can be defined by:

$$FS = \frac{CRR}{CSR} \qquad (5)$$

Liquefaction is predicted to occur when $FS \leq 1$, and liquefaction is predicted not to occur when $FS > 1$. The acceptable value of FS for a particular site will depend on several factors, including the acceptable level of risk for the project, the extent and accuracy of seismic measurements, the availability of other site information, and the conservatism in determining the design earthquake magnitude and the expected value of a_{max}.

3. CASE STUDY

Figure 2 presents the liquefaction evaluation for a crosshole test array at the Treasure Island Fire Station site and the 1989 Loma Prieta earthquake. Values of V_{S1} and CSR shown in Figs. 2(a) and 2(d), respectively, were calculated assuming soil densities of 1.76 Mg/m^3 above the water table and 1.92 Mg/m^3 below the water table. Based on a_{max} of 0.16 g and 0.11 g recorded in two horizontal directions at the fire station during the 1989 earthquake (Brady and Shakal, 1994), a geometric mean value of 0.13 g was used to calculate CSR.

Values of FS shown in Fig. 2(e) are less than 1 for the depths of 4 m to 9 m. Between the depths of 4 m and 7 m, the sand contains non-plastic fines and is considered liquefiable. Between the depths of 7 m and 9 m, the soil exhibits plastic characteristics and may be non-liquefiable by the so-called Chinese criteria. According to the Chinese criteria, non-liquefiable clayey soils have clay contents (particles smaller than 5 μm) ≥ 15 %, liquid limits ≥ 35 %, or moisture contents ≤ 90 % of the liquid limit (Seed and Idriss, 1982). Thus, the layer most likely to liquefy, or the critical layer, lies between the depths of 4 m and 7 m.

Although no sand boils or ground cracks occurred at the site during the 1989 earthquake, there is a sudden drop in the fire station strong ground motion recordings at about 15 seconds and small motion afterwards (Idriss, 1990). This behavior is unlike behavior observed in recordings at other seismograph stations located on soft-soil sites in the San Francisco Bay area. De Alba et al. (1994) attributed this behavior to liquefaction of an underlying sand. It is possible that the 4 m thick layer capping the site, predicted not to liquefy in Figs. 2(d) and 2(e), prevented the formation of sand boils at the ground surface (Ishihara, 1985).

4. CONCLUSIONS

Outlined in this paper is a procedure for evaluating liquefaction resistance through V_S measurements. The proposed procedure follows the general format of the Seed-Idriss simplified procedure based on SPT blow count. Liquefaction criteria based on V_S have been developed with case history data from soils ranging from sand to sandy gravel with cobbles

to profiles including silty clay layers. Caution should be exercised when applying the procedure to sites where conditions are different from the database. Additional well-documented case histories with all types of soil that have and have not liquefied during earthquakes are needed, particularly from denser soils (V_{S1} > 200 m/s) shaken by stronger ground motions (a_{max} > 0.4 g), to further validate the procedure.

5. ACKNOWLEDGMENTS

The authors gratefully acknowledge the review of this work by the participants of the 1996 NCEER and the 1998 Multidisciplinary Center for Earthquake Engineering Research (MCEER, formally NCEER) Workshops on Evaluation of Liquefaction Resistance of Soils. We thank Riley Chung for his support and encouragement, and Nicholas Carino and Alan Rauch for their reviews. Also, special thanks to Susumu Iai, Kohji Ichii, Osamu Matsuo, Susumu Yasuda, Mamoru Kanatani, Yukihisa Tanaka, Kohji Tokimatsu, K. Ishihara, and Takeji Kokusho for the information on Japanese liquefaction studies graciously shared with the first author.

6. REFERENCES

1. Andrus, R. D. (1994). "In Situ Characterization of Gravelly Soils That Liquefied in the 1983 Borah Peak Earthquake," *Ph.D. Dissertation*, The Univ. of Texas at Austin.

2. Andrus, R. D., and Stokoe, K. H., II (1997). "Liquefaction Resistance Based on Shear Wave Velocity," *NCEER Workshop on Evaluation of Liquefaction Resistance of Soils*, Technical Report NCEER-97-0022, T. L. Youd and I. M. Idriss, Eds., 4-5 Jan. 1996, Nat. Ctr. for Earthquake Engrg. Res., Buffalo, NY, pp. 89-128.

3. Andrus, R. D., Stokoe, K. H., II, and Chung, R. M. (1999). "Draft Guidelines for Evaluating Liquefaction Resistance Using Shear Wave Velocity Measurements and Simplified Procedures," *NISTIR 6277*, Nat. Institute of Standard and Technology, Gaithersburg, MD.

4. Bierschwale, J. G., and Stokoe, K. H., II (1984). "Analytical Evaluation of Liquefaction Potential of Sands Subjected to the 1981 Westmorland Earthquake," *Geotech. Engrg. Report GR-84-15*, The Univ. of Texas at Austin.

5. Brady, A. G., and Shakal, A. F. (1994). "Strong-Motion Recordings," *The Loma Prieta, Calif., Earthquake of Oct. 17, 1989--Strong Ground Motion*, U.S. Geological Survey Professional Paper 1551-A, R. D. Borcherdt, Ed., U.S. Gov. Printing Office, Washington, D.C., pp. A9-A38.

6. de Alba, P., Baldwin, K., Janoo, V., Roe, G., and Celikkol, B. (1984). "Elastic-Wave Velocities and Liquefaction Potential," *Geotech. Testing J.*, ASTM, Vol. 7, No. 2, pp. 77-87.

7. de Alba, P., Benoît, J., Pass, D. G., Carter, J. J., Youd, T. L., and Shakal, A. F. (1994). "Deep Instrumentation Array at the Treasure Island Naval Station," *The Loma Prieta, Calif., Earthquake of Oct. 17, 1989--Strong Ground Motion*, U.S. Geological Survey Professional Paper 1551-A, R. D. Borcherdt, Ed., U.S. Gov. Printing Office, Washington, D.C., pp. A155-A168.

8. de Alba, P., and Faris, J. R. (1996). "Workshop on Future Research Deep Instrumentation Array, Treasure Island NGES, July 27, 1996: Report to the Workshop Current State of Site Characterization and Instrumentation," Univ. of New Hampshire at Durham.

9. Dobry, R., Ladd, R. S., Yokel, F. Y., Chung, R. M., Powell, D. (1982). "Prediction of Pore Water Pressure Buildup and Liquefaction of Sands During Earthquakes by the Cyclic Strain Method," *NBS Building Science Series 138*, Nat. Bureau of Standards, Gaithersburg, MD.

10. Dobry, R., Stokoe, K. H., II, Ladd, R. S., and Youd, T. L. (1981). "Liquefaction Susceptibility from S-Wave Velocity," *Proc., In Situ Tests to Evaluate Liquefaction Susceptibility*, ASCE Nat. Convention, 27 Oct., St. Louis, MO.

11. Fuhriman, M. D. (1993). "Crosshole Seismic Tests at Two Northern California Sites Affected by the 1989 Loma Prieta Earthquake," *M.S. Thesis*, The Univ. of Texas at Austin.

12. Hynes, M. E. (1988). "Pore Pressure Generation Characteristics of Gravel Under Undrained Cyclic Loading," *Ph.D. Dissertation*, Univ. of Calif., Berkeley.

13. Idriss, I. M. (1990). "Response of Soft Soil Sites During Earthquakes," *H. Bolton Seed Memorial Symposium*, BiTech Publisher, Vancouver, B.C., Vol. 2, pp. 273-289.

14. Ishihara, K. (1985). "Stability of Natural Deposits During Earthquakes," *Proc., Eleventh Int. Conf. on Soil Mechanics and Found. Engrg.*, A. A. Balkema Publishers, Rotterdam, Netherlands, pp. 321-376.

15. Kayabali, K. (1996). "Soil Liquefaction Evaluation Using Shear Wave Velocity," *Engrg. Geology*, Elsevier Publisher, New York, NY, Vol. 44, No. 4, pp. 121-127.

16. Kayen, R. E., Mitchell, J. K., Seed, R. B., Lodge, A., Nishio, S., and Coutinho, R. (1992). "Evaluation of SPT-, CPT-, and Shear Wave-Based Methods for Liquefaction Potential Assessment Using Loma Prieta Data," *Proc., Fourth Japan-U.S. Workshop on Earthquake Resistant Design of Lifeline Facilities and Countermeasures for Soil Liquefaction*, Technical Report NCEER-92-0019, M. Hamada and T. D. O'Rourke, Eds., 27-29 May, Honolulu, Hawaii, Nat. Ctr. for Earthquake Engrg. Res., Buffalo, NY, Vol. 1, pp. 177-204.

17. Lodge, A. L. (1994). "Shear Wave Velocity Measurements for Subsurface Characterization," *Ph.D. Dissertation*, Univ. of Calif. at Berkeley.

18. Rashidian, M. (1995). "Undrained Shearing Behavior of Gravelly Sands and its Relation with Shear Wave Velocity," *Thesis*, Geotech. Engrg. Lab., Dept. of Civil Engrg., Univ. of Tokyo, Japan.

19. Robertson, P. K., Woeller, D. J., and Finn, W. D. L. (1992). "Seismic Cone Penetration Test for Evaluating Liquefaction Potential Under Cyclic Loading," *Canadian Geotech. J.*, Vol. 29, pp. 686-695.

20. Rollins, K. M., Diehl, N. B., and Weaver, T. J. (1998). "Implications of V_S-BPT $(N_1)_{60}$ Correlations for Liquefaction Assessment in Gravels," *Geotech. Earthquake Engrg. and Soil Dyn. III*, Geotech. Special Pub. No. 75, P. Dakoulas, M. Yegian, and B. Holtz, Eds., ASCE, Vol. I, pp. 506-517.

21. Seed, H. B., and Idriss, I. M. (1971). "Simplified Procedure for Evaluating Soil Liquefaction Potential," *J. of the Soil Mechanics and Found. Div.*, ASCE, Vol. 97, SM9, pp. 1249-1273.

22. Seed, H. B., and Idriss, I. M. (1982). *Ground Motions and Soil Liquefaction During Earthquakes*, Earthquake Engrg. Res. Institute, Berkeley, CA.

23. Seed, H. B., Idriss, I. M., and Arango, I. (1983). "Evaluation of Liquefaction Potential Using Field Performance Data," *J. of Geotech. Engrg.*, ASCE, Vol. 109, No. 3, pp. 458-482.

24. Stokoe, K. H., II, Lee, S. H. H., and Knox, D. P. (1985). "Shear Moduli Measurements Under True Triaxial Stresses," *Proc., Advances in the Art of Testing Soil Under Cyclic Conditions*, ASCE, pp. 166-185.

25. Stokoe, K. H., II, Roësset, J. M., Bierschwale, J. G., and Aouad, M. (1988). "Liquefaction Potential of Sands from Shear Wave Velocity," *Proc., Ninth World Conf. on Earthquake Engrg.*, Tokyo, Japan, Vol. III, pp. 213-218.

26. Sykora, D. W. (1987). "Creation of a Data Base of Seismic Shear Wave Velocities for Correlation Analysis," *Geotech. Lab. Misc. Paper GL-87-26*, U.S. Army Engineer Waterways Exp. Station, Vicksburg, MS.

27. Tokimatsu, K., Kuwayama, S., and Tamura, S. (1991). "Liquefaction Potential Evaluation Based on Rayleigh Wave Investigation and Its Comparison with Field Behavior," *Proc., Second Int. Conf. on Recent Advances in Geotech. Earthquake Engrg. and Soil Dyn.*, S. Prakash, Ed., 11-15 Mar., St. Louis, MO, Univ. of Missouri at Rolla, Vol. I, pp. 357-364.

28. Tokimatsu, K., and Uchida, A. (1990). "Correlation Between Liquefaction Resistance and Shear Wave Velocity," *Soils and Found.*, Japanese Society of Soil Mechanics and Found. Engrg., Vol. 30, No. 2, pp. 33-42.

29. Youd, T. L., Idriss, I. M., Andrus, R. D., Arango, I., Castro, G., Christian, J. T., Dobry, R., Finn, W. D. L., Harder, L. F., Jr., Hynes, M. E., Ishihara, K., Koester, J. P., Liao, S. S. C., Marcuson, W. F., III, Martin, G R., Mitchell, J. K., Moriwaki, Y., Power, M. S., Robertson, P. K., Seed, R. B., and Stokoe, K. H., II (1997). "Summary Report," *NCEER Workshop on Evaluation of Liquefaction Resistance of Soils*, Technical Report NCEER-97-0022, 4-5 Jan. 1996, Nat. Ctr. for Earthquake Engrg. Res., Buffalo, NY, pp. 1-40.

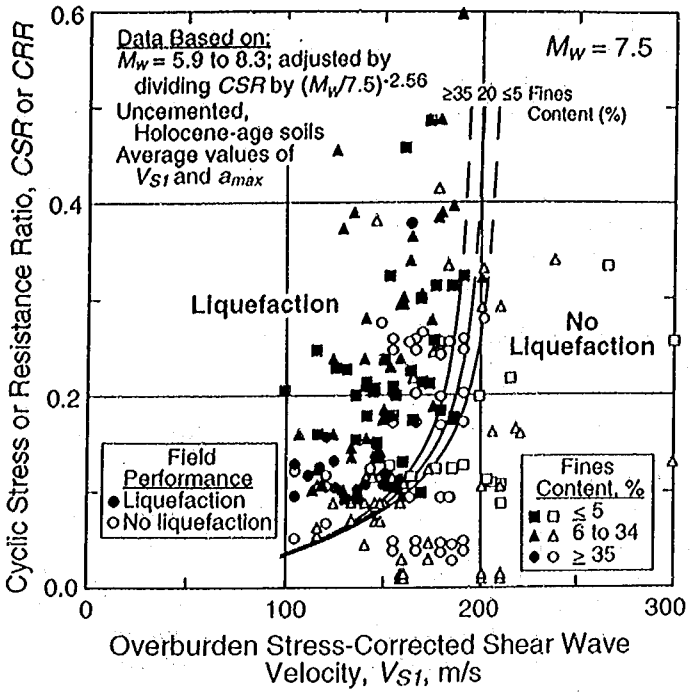


Fig. 1 - Curves Proposed by Andrus et al. (1999) for Calculation of CRR from V_S Measurements Along with Case History Data Based on Lower Bound Values of MSF for the Range Recommended by the 1996 NCEER Workshop (Youd et al., 1997) and Average r_d Values Developed by Seed and Idriss (1971).

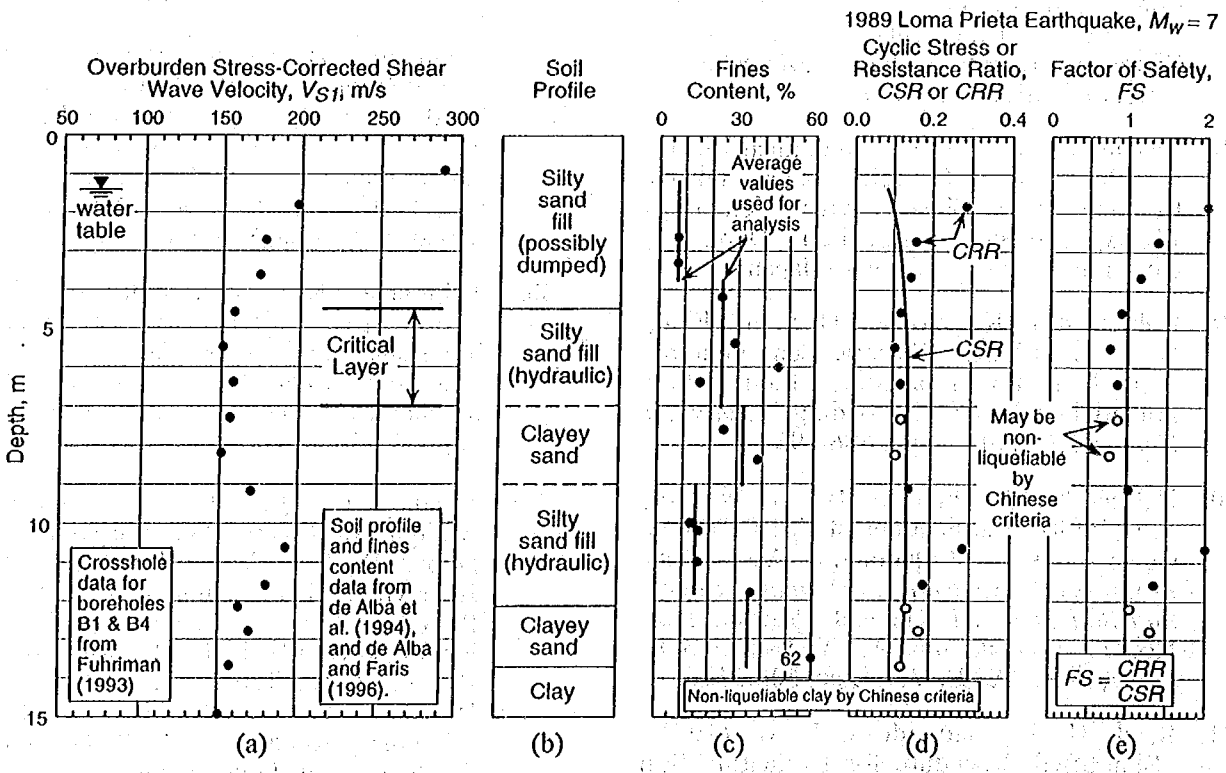


Fig. 2 - Application of the Recommended Procedure to the Treasure Island Fire Station Site, Crosshole Test Array B1-B4.

Influence of Confining Stress on Liquefaction Resistance

by

Mary Ellen Hynes[1] & Richard S. Olsen[2]

ABSTRACT

The confining stress factor K_σ is used in liquefaction evaluations to extend empirical charts for liquefaction resistance to confining stresses higher than the empirical field-performance database, approximately 1 atm (100 KPa). Estimates of K_σ from Harder (1988), Hynes (1988), Olsen (1984, 1994, 1996) indicated relatively large reductions in liquefaction resistance ratios with increasing confining stress. Laboratory work by Vaid and colleagues (1985, 1995) indicated higher values of K_σ. In this study, a database was developed to investigate the reasons for the broad scatter in K_σ. From our study we conclude that: 1) K_σ is strongly influenced by method of deposition, stress history, aging effects, and density; 2) reconstructed, pluviated specimens in the laboratory may represent recently deposited dredged materials or recently liquefied materials; however, 3) high quality undisturbed samples are needed to determine field-relevant values of K_σ. The MCEER International Liquefaction Committee (Youd & Idriss 1997) adopted the K_σ recommendations from this study.

KEYWORDS: Liquefaction, confining stress effects, gravels, stress focus, K sigma, earth dams, laboratory testing, stress history, pluviation.

1. BACKGROUND

Laboratory measurements typically indicate that for a given soil, consistency (relative density for sands and gravels) and stress history, there is a non-linear relationship between liquefaction resistance and confining stress (Seed & Idriss 1981; Seed 1983; Vaid et al. 1985; Hynes 1988; Harder 1988; Seed & Harder 1990; Pillai & Byrne 1994; Youd & Idriss 1997). Consequently, if cyclic strengths, either from laboratory measurements performed at a confining stress of 1 atm or estimated from correlations to in situ measurements such as Standard Penetration Tests (SPT), are linearly extrapolated to higher effective confining stress levels, the calculated liquefaction resistances may be too high. The effect of confining stress on liquefaction resistance is further complicated by soil compressibility and stress history.

The state-of-the-practice approach to account for the non-linear relationship between liquefaction resistance and vertical effective stress is to use published charts derived from existing laboratory data on similar materials or to determine a site specific relationship with a comprehensive laboratory testing program. Whichever approach is used, liquefaction resistance is conventionally represented as the Cyclic Resistance Ratio (CRR, the ratio of cyclic shear strength (τ_{cy}) divided by the vertical effective stress, (σ_v')). For a given soil at a given consistency and stress history, the CRR generally decreases with increasing vertical effective stress. This decrease is described by the factor K_σ which is defined as the ratio of CRR for a given σ_v' to the CRR at a vertical effective stress of 1 atm, CRR_1 (compared at the same relative density).

[1,2] Earthquake Engineering and Geophysics Divison, Geotechnical Laboratroy
U.S. Army Waterways Experment Station (WES)
3909 Halls Ferry Road, Vicksburg, MS 39180

The use of laboratory tests to establish CRR_l for a material has decreased over the last decade in favor of in situ test correlations because of the cost-effectiveness of in situ measurements, the robustness of the Seed SPT-liquefaction chart (Seed et al. 1985, Youd & Idriss 1998), and concerns over sample disturbance and other issues associated with laboratory test results. The CRR_l can be determined from in situ measurements such as the SPT, Cone Penetration Test (CPT), or shear wave velocity (V_s), or from laboratory measurements. The state-of-the-art for estimating CRR_l using the SPT is given by Seed et al. (1985); using the CPT is given by Stark et al. (1995), Olsen et al. (1996), or Robertson & Wride (in Youd & Idriss 1997); and using V_s is given by Andrus & Stokoe (in Youd & Idriss 1997).

The database for these CRR_l correlations consists of information from water-laid deposits of sands and silty sands, level to slightly sloping ground, under vertical effective stresses of less than 3 atm.

Consequently, laboratory tests have been used to provide a relative scale to adjust the CRR_l values from in situ tests to higher confining stress levels and non-level ground stress conditions. The purpose of this study was to review the current state of knowledge with respect to the influence of overburden stress on liquefaction resistance. An emerging concept will be presented, namely the Stress Focus theory (Olsen 1994), which provides an alternative framework for interpreting confining stress effects on in situ measurements such as penetration resistance, and soil properties such as liquefaction resistance.

2. HISTORICAL K_σ DATA AND CHARTS

2.1 *K_σ Data and Charts*

Cyclic laboratory tests provide a means of determining liquefaction resistance of a soil under various controlled conditions--density, confining stress, stress history, applied cyclic load or strain history, and drainage boundary conditions. The influence of confining stress can be evaluated by conducting cyclic laboratory tests for a soil, holding the other parameters constant, at several confining stress levels. In this section, historical cyclic laboratory test data for a variety of soils are examined to observe trends in K_σ from the historical database.

Early tests on sands and silty sands indicated considerable scatter in the values of K_σ. These data, summarized in Figure 1 and taken in part from Harder (1988), include Upper and Lower San Fernando Dams (Seed et al. 1973, Seed et al. 1989) and Fort Peck Dam (Marcuson & Krinitzsky 1976). Superimposed on Figure 1 is an early K_σ relationship suggested by Seed (1983). As more data became available, the K_σ chart was updated by Harder (1988), and again by Seed & Harder (1990).

Olsen (1984) generalized the data trends from the preliminary K_σ relationship by Seed (1983), together with project data at WES into the following expression: $K_\sigma=(\sigma'_v)^{f-1}$. This expression is plotted in Figure 1. Olsen (1984) reported that the stress exponent, f, ranged from 0.6 to 0.95 with 0.7 recommended for sands. This recommendation is similar to the updated Seed curves shown in Figure 1.

Gravel data from Oroville Dam (Banerjee et al. 1979) and WES project files (Ririe, Folsom and Success Dams) were added to the database; these data are from large-scale cyclic triaxial tests on moist-compacted specimens. Silt, silty sand and sandy silt data was added from a number of dam studies, notably Upper and Lower San Fernando, Fort Peck, Enid and Arcadia Dams.

Byrne & Harder (1991) selected K_σ values for clean sands from previous work to develop a recommendation for the clean sands and gravels present at Terzahgi Dam, Canada. Their data set included the work by Vaid et al. (1985) and Vaid & Thomas (1995) as well as clean sand data from Seed & Harder (1990). The resulting "clean sand" K_σ curve is shown in Figure 1.

2.2 *Stress focus plots of cyclic strength*

Trends in geotechnical data with confining stress are sometimes easier to see when the data are plotted in log-log plots. These log-log plots are termed stress focus plots from Olsen (1994). If data fit as a straight line on a log-log stress focus plot, then these data are well fitted by a simple exponential curve. Stress focus plots were used in this study as a framework for investigating confining stress effects on cyclic strength and CRR.

Stress focus theory (Olsen 1994) shows that curves for cyclic strength, penetration resistance, and other soil properties that are functions of confining stress and density tend to converge as confining stress increases. This point (or zone) of convergence is termed the stress focus, and is a function of soil type and mineralogy (Olsen 1994).

The slope of a line in a cyclic strength stress focus plot corresponds to the inverse of the exponent used by Olsen (1984) to describe K_σ: $K_\sigma=(\sigma'_v)^{f-1}$ (Figure 1). This is shown in the stress focus plot of cyclic strength in Figure 2, which shows generalized stress focus cyclic strength lines for a very loose to dense sand. As density increases, the cyclic strength at a confining stress of 1 atm, CRR_1, increases and the slope, f, decreases. The corresponding K_σ curves ($K_\sigma=(\sigma'_v)^{f-1}$) are shown in Figure 1. As density increases, the exponent f decreases and K_σ decreases, resulting in a more severe reduction to CRR.

2.3 *Observations from the K_σ Database*

The K_σ data were reviewed by soil type (sand, gravel and silt mixtures) and by method of deposition (laboratory pluviation, moist compaction and undisturbed samples of water-laid deposits). The data in Figure 1 are identified by method of deposition. We observed that K_σ is more strongly affected by stress-history, aging effects and density than by soil type. This was most clearly illustrated by the data from Fort Peck Dam. Marcuson & Krinitzsky (1974) report laboratory tests on undisturbed and wet-pluviated reconstructed specimens, as well as in situ blowcounts. The resulting cyclic strengths are plotted in Figure 3.

Figure 4 was used to estimate equivalent $N_{1,60}$ values (based on relative density) for the fine clean sands tested by Vaid et al. (1985) and Vaid & Thomas (1995). In situ $N_{1,60}$ values for the gravel data from WES were estimated from Becker blowcounts. Corresponding values of CRR_1 were estimated from the Seed et al. (1985) liquefaction chart. A comparison of the CRR_1 determined from laboratory tests with values determined from $N_{1,60}$ are shown in Figure 5 as a function of relative density.

Figure 5 indicates that cyclic strengths from laboratory pluviated specimens underestimate CRR_1 values by a factor of about 2 to 3; undisturbed specimens underestimate CRR_1 by about 10 to 20 percent; moist-tamped specimens overestimate CRR_1 at low relative density and underestimate at high relative density.

The pluviated specimens had low cyclic strength and high values of K_σ ($f > 0.9$). However, laboratory strengths from undisturbed specimens and CRR_1 values determined from blowcounts are approximately 2.5 times the strengths from the pluviated specimens. This indicates that the K_σ values from the pluviated specimens are unconservatively high.

3. CONCLUSIONS

We conclude from this study that method of deposition, aging, stress history and density strongly influence K_σ. These effects are emphasized at low confining stresses, such as 1 atm, and are de-emphasized as confining stresses increase, and ultimately converge at the stress focus. Within the stress range of interest for dams, typically less than 10 atm, K_σ is not strongly influenced by soil type. Specimens pluviated in the laboratory may represent recently deposited materials such as dredged and liquefied materials.

However, for water-laid foundation deposits typical for dams, high quality undisturbed specimens are necessary to determine field-relevant values of K_o.

4. RECOMMENDATIONS

For practical liquefaction evaluations, it is recommended that K_o be estimated as suggested by Olsen (1984): $K_o=(\sigma'_v)^{f-1}$. For relatively loose deposits the exponent f is about 0.8; f decreases to 0.7 for medium dense, and to 0.6 for dense or slightly overconsolidated deposits. For very dense or higher overconsolidation (stress history and aging effects), the exponent f may be less than 0.6. In their August 1998 meeting, the MCEER International Liquefaction Committee (Youd & Idriss 1997) adopted the K_o recommendations from this study.

5. ACKNOWLEDGMENT

This study was sponsored by the Civil Works Earthquake Engineering Research Program of the US Army Corps of Engineers, and the Panama Canal Commission. Permission was granted by the Chief of Engineers to publish this information.

6. REFERENCES

Andrus, R. D. & Stokoe, K. H. 1996 (in prog.). Guidelines for evaluation of liquefaction resistance using shear wave velocity, 1996 Salt Lake City Workshop on evaluation of liquefaction resistance, Youd & Idriss, editors, NCEER publication.

Banerjee, N. G., Seed, H. B., & Chan, C. K. 1979. Cyclic behavior of dense coarse-grained materials in relation to the seismic stability of dams, Report No. UCB/EERC-79/13, University of California, Berkeley, CA.

Bieganousky, W. A. & Marcuson, W. F. III. 1976. Liquefaction potential of dams and foundations, Report 1: Laboratory standard penetration tests on Reid-Bedford model and Ottawa sands, Research Report S-76-2, USAE Waterways Experiment Station, Vicksburg, MS.

Bieganousky, W. A. & Marcuson, W. F. III. 1977. Liquefaction potential of dams and foundations, Report 2: Laboratory standard penetration tests on Platte River sand and standard concrete sand, Research Report S-76-2, USAE Waterways Experiment Station, Vicksburg, MS.

Byrne, P. M. & Harder, L. F. 1991. Terzaghi Dam: Review of deficiency investigation, Report No. 3, prepared for BC Hydro, Vancouver, British Columbia.

Harder, L. F. 1988. Use of penetration tests to determine the cyclic loading resistance of gravelly soils during earthquake shaking, PhD Dissertation, University of California at Berkeley.

Hynes, M. E. 1988. Pore pressure characterization of gravels under undrained cyclic loading, PhD Dissertation, University of California at Berkeley.

Gibbs, H. J. & Holtz, W. G. 1957. Research on determining the density of sand by spoon penetration testing, Proceedings, Fourth international conference on soil mechanics and foundation engineering , vol. I, pp 35-39.

Marcuson, W. F. III & Krinitzsky, E. L. 1976. Dynamic analysis of Fort Peck dam, Technical Report S-76-1, USAE Waterways Experiment Station, Vicksburg, MS.

Olsen, R. S. 1984. Liquefaction analysis using the cone penetrometer test (CPT), Proceedings, Eighth world conference on earthquake engineering, July, San Francisco, CA.

Olsen, R. S. 1994. Normalization and prediction of geotechnical properties using the cone penetrometer test (CPT), PhD Dissertation, University of California at Berkeley.

Olsen, R. S., Koester, J. P., & Hynes, M. E. 1996.

Evaluation of liquefaction potential using the CPT, Proceedings, 28th Joint meeting of the US-Japan cooperative program in natural resources-panel on wind and seismic effects, US National Institute of Standards and Technology, Gaithersburg, MD, May 1996.

Olsen, R. S. 1996. The influence of confining stress on liquefaction resistance, Proceedings, First US-Japan workshop on advanced research on earthquake engineering for dams, USAE Waterways Experiment Station, Vicksburg, MS, November 1996.

Olsen, R. S. 1998. Cyclic liquefaction based on the cone penetrometer test, Proceedings, NCEER workshop on evaluation of liquefaction of soils, Youd, L. & Idriss, I. M., editors, Technical Report NCEER-97-0022, State University of New York at Buffalo, Buffalo, NY.

Pillai, V. S, & Byrne, P. M. 1994. Effect of overburden pressure on liquefaction resistance of sands, Canadian Geotechnical Journal, vol. 31.

Robertson, P. K. & Wride, C. E. 1997. Cyclic liquefaction and its evaluation based on the SPT and CPT, Youd, L. & Idriss, I. M., editors, Workshop on evaluation of liquefaction resistance of soils, Proceedings, Technical Report NCEER-97-0022, Salt Lake City, UT.

Seed, H. B., Lee, K. L., Idriss, I. M., & Makdisi, F. I. 1973. Analysis of the slides in the San Fernando dams during the earthquake of February 9, 1971, Report No. EERC-73-2, College of Engineering, University of California, Berkeley, CA.

Seed, H. B., Seed, R. B., Harder, L. F., & Jong, H. L. 1989. Re-evaluation of the Lower San Fernando dam - Report 2: examination of the post-earthquake slide of February 9, 1971, Contract Report GL-89-2, USAE Waterways Experiment Station, Vicksburg, MS.

Seed, H. B. & Idriss, I. M. 1981. Evaluation of liquefaction potential of sand deposits based on observations of performance in previous earthquakes, Proceedings, ASCE national fall convention, Session No. 24, St. Louis, MO.

Seed, H. B. 1983. Earthquake-resistant design of earth dams, Proceedings, Symposium on seismic design of embankments and caverns, May, ASCE pg 41-64.

Seed, R. B. & Harder, L. F. 1990. SPT-based analysis of cyclic pore pressure generation and undrained strength, Proceedings, H. B. Seed memorial symposium, May, Bitech Publishers, vol. 2, pg 351-376.

Stark, T. D., & Olson, S. M. 1995. Liquefaction resistance using SPT and field case histories, Journal of Geotechnical Engineering, ASCE, New York, NY, vol. 121(12), pp 856-868.

USAE District, Tulsa. 1982. Arcadia Lake, Deep Fork River, Suppl 1 to Design Memorandum No. 9, Embankment and spillway, Tulsa, OK.

USAE District, Vicksburg. 1988. The Sardis earthquake study, Suppl 1 to Design Memorandum No. 5 (1985), Vicksburg, MS.

Vaid, Y. P., Chern, J.C. & Tumi, H. 1985. Confining pressure, grain angularity, and liquefaction, Journal of Geotechnical Engineering, ASCE, October, vol. 111(10), pg 1229-1235.

Vaid, Y. P. & Thomas, J. 1995. Liquefaction and post liquefaction behavior of sand, Journal of Geotechnical Engineering, ASCE, February, vol. 121(2), pg 163-173.

Youd, L. & Idriss, I. M., editors. 1997. Workshop on Evaluation of liquefaction resistance of soils, Proceedings, Salt Lake City, Technical Report NCEER-97-0022, sponsored by FHWA, NSF and WES, published by NCEER, Buffalo, NY.

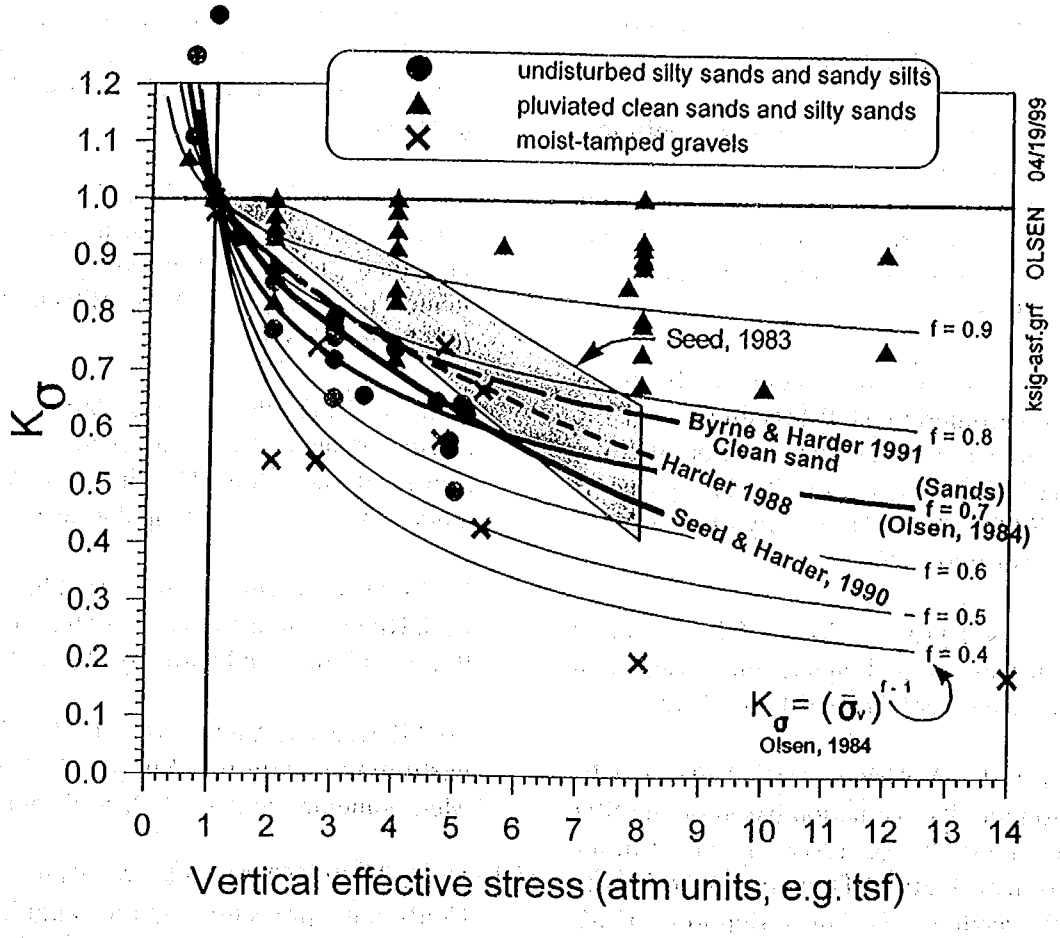


Figure 1 Laboratory data and K_σ relationships

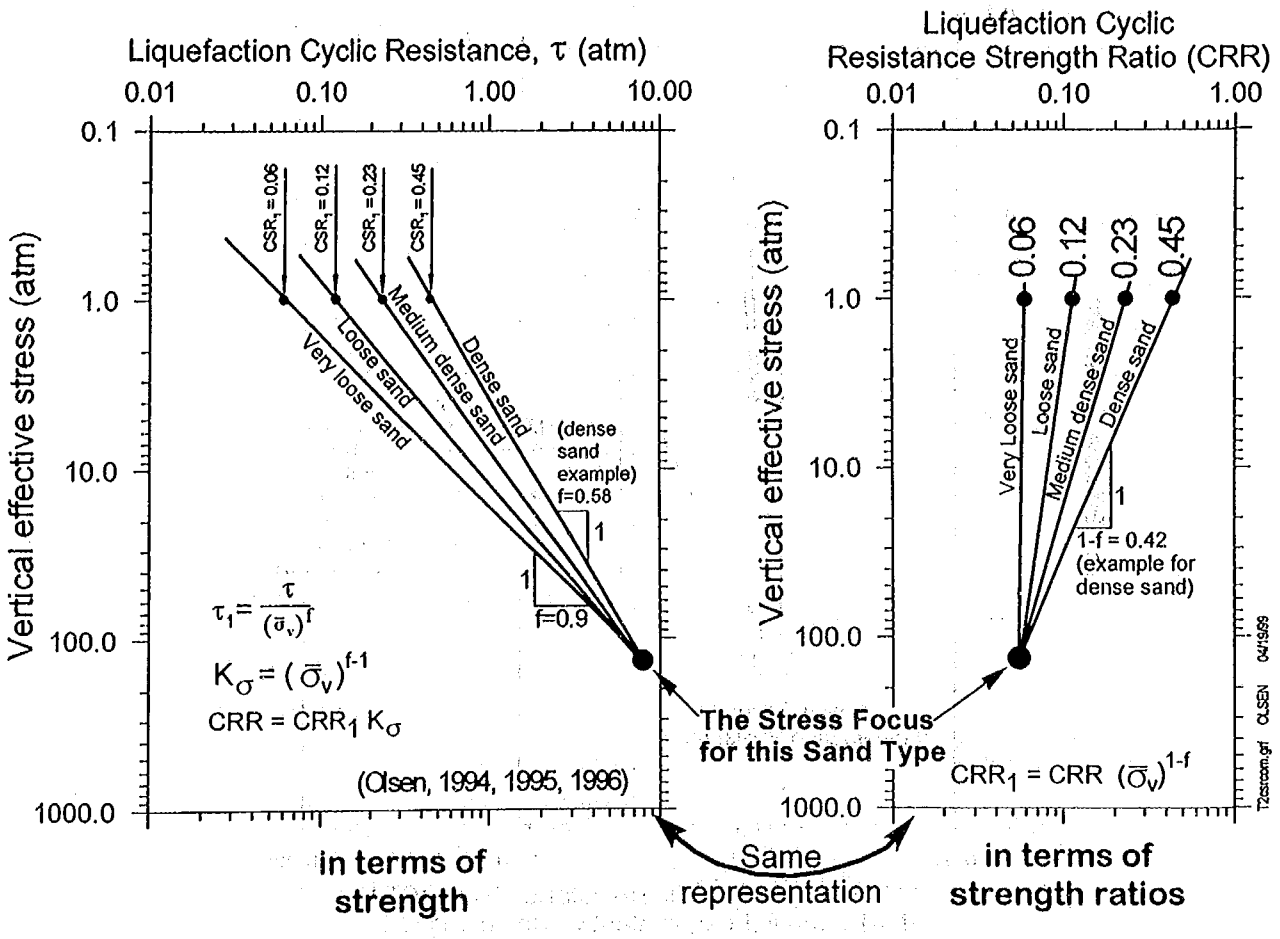


Figure 2 Generalized stress focus plots of cyclic shear strengths and stress ratios

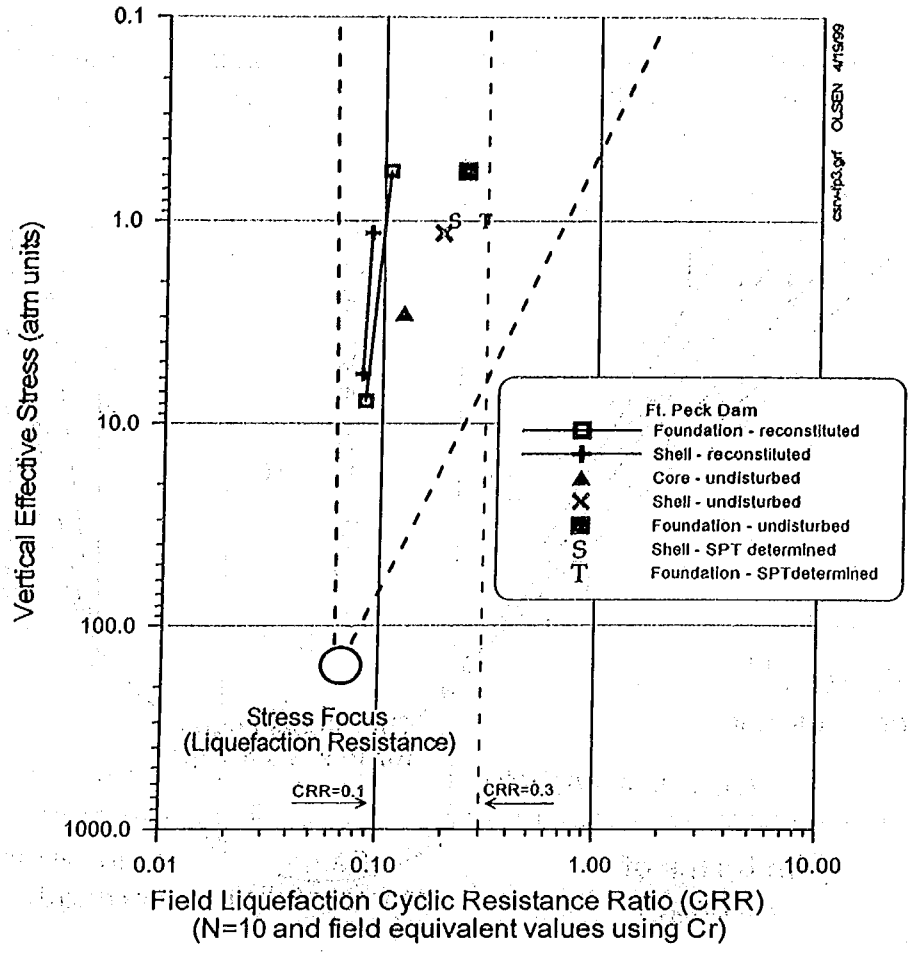


Figure 3 Stress focus plot of field and laboratory estimates of cyclic stress ratios for Fort Peck Dam

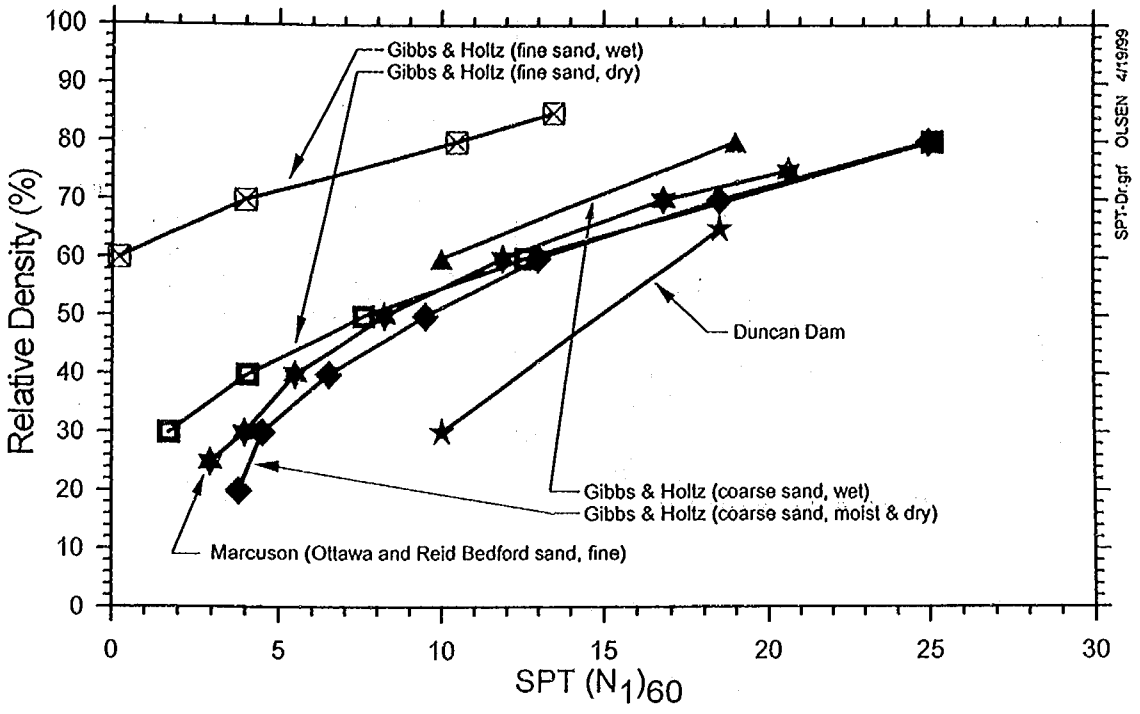


Figure 4 Relationship between relative density and $N_{1,60}$

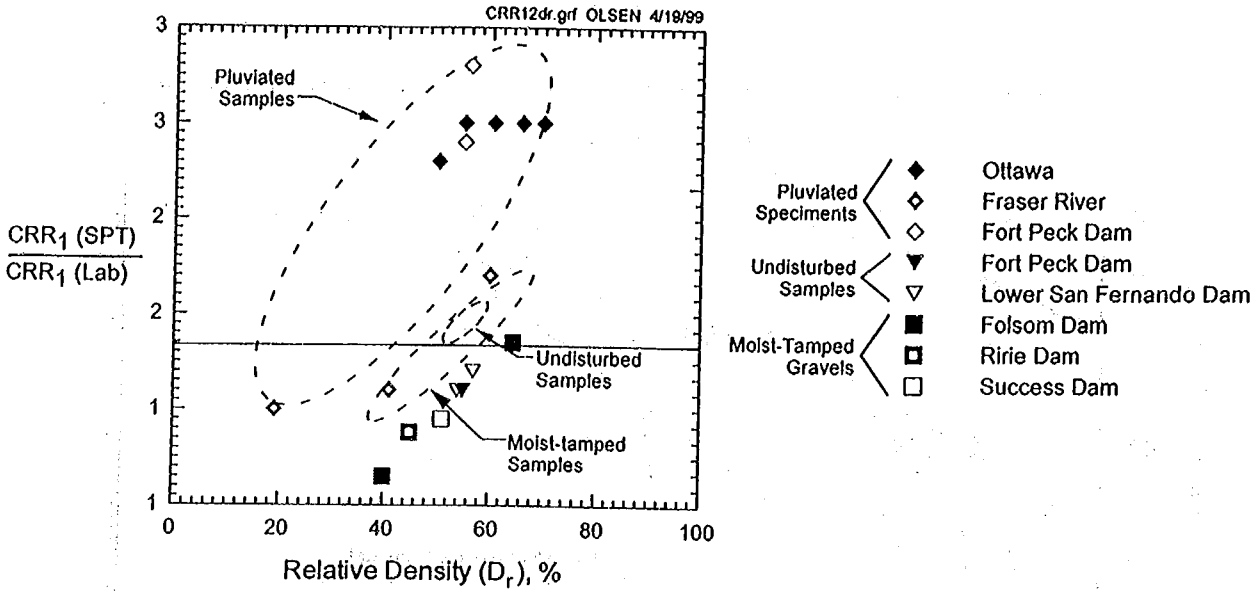


Figure 5 Comparison of CRR_1 from laboratory tests with CRR_1 from SPT blowcounts

State-of the-art of Stability Assessment of Underground Structures during Liquefaction

by

Osamu MATSUO[1] and Tetsuya SASAKI[2]

ABSTRACT

Soil liquefaction often induces damage to underground structures. The most typical mode of the liquefaction-induced damage is uplift displacement of the structures. The paper presents the state-of-the-arts of the problem. First, case records on damage to underground structures induced by soil liquefaction are briefly reviewed. Then, the stability assessment techniques that are used in practice and that was developed before/after the 1995 Hyogoken-Nanbu earthquake are introduced, and the research issues are summarized. In the last part of the paper, a recent research works is described to study the mechanism of the damage and to improve the currently used stability assessment techniques.

KEY WORDS: Liquefaction
Underground Structure
Uplift

1. INTRODUCTION

During past earthquakes, underground structures have suffered damages caused by liquefaction of surrounding soils, which include sewerage treatment ponds and pipes, petroleum storage tanks, etc. The most typical mode of the damage is uplift movement. In Japan, a stability assessment procedure for the uplift behavior was developed in 1986 (Japan Road Association, 1986) and the method has been used widely with slight modification. The method, however, is based on limit equilibrium and thus cannot evaluate the extent of damage or magnitude of uplift displacement.

Since the occurrence of the Hyogoken-Nanbu earthquake of 1995, a consensus has been developed that for any civil engineering structures the Level 2 earthquake, which is conceptually defined as the possible maximum earthquake, should be considered in the design, and that the design should be based on seismic performance. From this viewpoint, the stability assessment procedure mentioned above has limitations and requires to be elaborated.

In this paper, case records on damage to underground structures induced by soil liquefaction during past earthquakes are briefly reviewed. Then, the stability assessment techniques that are used in practice and that was developed before/after the 1995 Hyogoken-Nanbu earthquake are introduced and the research issues related to the methods are summarized. In the last part of the paper, a recent research works is presented to study the mechanism of the damage and to improve the currently used stability assessment techniques.

2. CASE HISTORIES

In Japan, several types of underground structure having relatively light unit weight were damaged by liquefaction of subsoils during past earthquakes. Case histories on the damaged underground structures in Japan are briefly summarized in Table 1. The observed modes of damage were uplift, settlement, and extrusion

1) Head, Soil Dynamics Division, Earthquake Disaster Prevention Research Center, Public Works Research Institute, Ministry of Construction, Tsukuba-shi, Ibaraki-ken, 305-0804, Japan
2) Research Engineer, ditto

and distortion at pipe joint, among which liquefaction-induced uplift is the most typical mode of damage to underground structures. Uplift distortion occurred to sewage treatment pipelines, ponds and petroleum tanks during the 1964 Niigata earthquake (PWRI 1965), the 1983 Nihonkai-Chubu earthquake (Taniguchi and Morishita 1985), the 1993 Kushiro-Oki earthquake (Koseki et al. 1997, Japanese Society of Soil Mechanics and Foundation Engineering 1994), the 1993 Hokkaido-Nansei--Oki earthquake (PWRI 1994), the 1994 Hokkaido-Toho-Oki earthquake (JGS 1998) and the 1994 Sanriku-Haruka-Oki earthquake (Koseki et al. 1998a). During the 1995 Hyogoken-Nanbu earthquake, the pile foundation of the Higashinada sewage treatment plant suffered serious damage caused by lateral flow of liquefied ground. In this section, case records on damage to underground structures induced by soil liquefaction are briefly reviewed.

(1) Damage to sewage treatment tanks during the 1964 Niigata earthquake

Fig.1 shows a typical damage to a sewage treatment tank during the 1964 Niigata earthquake. The tank located at Zoshobori, Niigata City, left of the Shinanogawa River, suffered severe uplift distortion induced by subsoil liquefaction and broke at the construction joint. The mechanism of the damage would have been as follows. The tank was subjected to a buoyant force of the liquefied soil. The left half segment had a maintenance house on it, thus the center of self weight was eccentric to the house side. Accordingly, the left half segment was pushed up unevenly, leading to opening of the construction joint. The similar damage was reported for the Koshinanogawa and Kawabatacho sewage pomp stations as well.

Sewer pipes were also suffered severe damage by this earthquake. A total length of the damaged pipes amounted to about 31 km, which were about 60 % in length of all the sewer pipes in Niigata City. Damage modes were uplift, settlement of underground structure cased by ground subsidence after liquefaction and extrusion and displacement of pipe at joints. The maximum uplift displacement in the damaged sites ranged from 10 cm to 2 m.

(2) Damage to underground fuel tank during the 1983 Nihonkai-Chubu earthquake

Eighty underground fuel tanks and two underground water tanks were suffered uplift damage during the 1983 Nihonkai-Chubu earthquake in Aomori prefecture and Akita prefecture. Most of the damaged sites were located in flood plain. Maximum uplift displacement of the damaged tanks was about 2 m, which is shown in Fig. 2 The ground surface of surrounding soil around the fuel tank subsided about 70 cm. Fig.3 shows grain size distributions of sand boils or backfill soils retrieved around the damaged sites. The range of potentially liquefiable distributions was also shown in Fig.3.

(3) Damage to sewer manholes during the 1993 Kushiro-Oki earthquake

During the 1993 Kushiro-Oki earthquake, damage to sewer pipes took place in Kushiro City, Kushiro Town, Shibecha Town. During the 1994 Hokkaido-Toho-Oki earthquake, that hit the same area, sewer pipes were damaged in Kushiro City, Kushiro Town, Shibetsu Town. In Kushiro City, sewer pipes of a total length of about 19 km were damaged by the two earthquakes, which corresponded to about 2 % of all the sewer pipes in length. In Shibetsu Town, those of 10 km were damaged by the Hokkaido-Toho-Oki earthquake, which corresponded to about 56 % of all the sewer pipes. Especially, during the 1993 Kushiro-Oki earthquake, several sewer manholes in Kushiro Town were ejected up to 1.5 m (see Fig.4).

In order to evaluate their failure mechanism, the level and boring surveys, cut-off investigation

were carried out on the sewer manholes in Kushiro Town, which ejected up during the 1993 Kushiro-Oki earthquake. Liquefaction resistance ratio F_L of backfill and original subsoil was evaluated by using the SPT N-values and other soil parameters. The location of the area surveyed is shown in Fig.5. Typical soil profile and uplift displacements are shown in Figs.6 and 7, respectively, which were estimated based on the results of an observation of the soil profile during the restoration work and the SPT N-values measured. Based on the results of the surveys and analyses of liquefaction resistance ratio F_L, backfill soil of the manholes was estimated to have liquefied extensively and to have moved laterally toward the bottom of the ejected manholes as shown in Fig.8 (a). In the original subsoil surrounding the manholes which were ejected by more than 50 cm, relatively clean sands with a fines content less than 15 % existed at the same depth as the bottom of the manhole, and impermeable peat and clay layers thicker than 1 m also existed adjacent to the saturated backfill soil. Based on liquefaction resistance ratio F_L, the sand layer in the original subsoil surrounding the manholes might have liquefied moderately and squeezed the backfill soil as shown in Fig.8 (b). The low permeability of peat and clay layer was considered to have affected the extent of liquefaction of backfill.

Based on the above results, liquefaction of the backfill soil was considered to be a major cause of the damage, while existence of peat and clay layer and/or a liquefiable sand layer in the original soil was considered to have affected the extent of the damage. Additional research is required to reveal the possible effect of the original subsoil on the local amplification of earthquake motion. The similar results were concluded by Koseki et al. (1998b) and Sasaki et al. (1999), who conducted statistical causal analyses on damaged/undamaged sewer pipes in Kushiro City during the 1993 Kushiro-Oki earthquake and the 1994 Hokkaido-Toho-Oki earthquake and those in Shibetsu Town during the 1994 Hokkaido-Toho-Oki earthquake, respectively.

(4) Behavior of common utility ducts during the 1995 Hyogoken-Nanbu earthquake

The 1995 Hyogoken-Nanbu earthquake caused severe damage to buried structures (PWRI 1996). These damages were mainly caused by the earthquake-induced ground displacements including lateral flow and settlement of ground, and by excessive inertia force during earthquake. During this earthquake, however, despite very strong ground motion, uplift damage to buried structures, especially to common utility ducts, in liquefied area was insignificant. Fig.9 shows the typical cross section of common utility ducts buried in liquefied area in Kobe City during the earthquake and soil profile based on boring survey result, which was conducted after the earthquake. The liquefaction resistance ratio F_L which were evaluated by using SPT-N-value and other soil parameter and in accordance with "Specifications for highway bridges (1997)" are also shown in Fig.9. The results indicate that liquefaction had occurred in the subsoil surrounding the common utility ducts. Actually, sand boils were observed around those sites after the earthquake (Hamada et al. 1995). These common utility ducts, however, suffered no uplift damage despite of liquefaction of the surrounding subsoil. The possible reason for the performance will be discussed later in 5.(3).

3. CURRENT PRACTICES AND ISSUES ON STABILITY EVALUATION DURING LIQUEFACTION

(1) Current practices on stability evaluation during liquefaction

The previous section has suggested that the major damage mode of underground structures due to liquefaction is uplift damage. In this section, the stability assessment techniques against uplift that are used in practice and that

was developed before/after the 1995 Hyogoken-Nanbu earthquake are introduced and the research issues related to the methods are summarized.

Table 2 summarizes the effects of liquefaction taken into account in the existing design manuals or guidelines which treat underground structure including common utility ducts, underground parking facilities, sewage facilities, water supply facilities or open-cut railway tunnels. The effects of liquefaction considered in the manuals are uplift, settlement, lateral spreading and increased earth pressure during earthquakes. The manuals for sewage facility, water supply facility and open-cut railway tunnels, which were revised after the 1995 Hyogoken-Nanbu earthquake, require consideration of high intensity (Level 2) ground motion according to importance of structures, and the effect of lateral spreading of surrounding subsoils. The effects of subsidence of surrounding subsoil are considered in the manuals for sewer pipes and open-cut railway tunnels. In the manual for sewer pipes, settlement of surrounding soil estimated according to thickness of liquefied layer is considered in designing flexible joints. For open-cut railway tunnels, settlement is required to be less than an allowable value. Lateral spreading displacements of the ground are considered in the manuals for sewer pipes and water supply pipes in designing flexible joints, and cross section of open-cut railway tunnels based on the response displacement method. For open-cut railway tunnels, increase of intermediate component of earth pressure during liquefaction is considered designing cross section of structures. If the tunnels are penetrated into non-liquefiable layer, then cyclic component of total earth pressure, which is formulated as the modified Westargaard's dynamic pressure, is considered in designing the cross section. All of the manuals, however, treat uplift.

Table 3 summarizes the methods of uplift stability techniques adopted in the manuals. Safety factor against uplift F_U specified in "Design manual for common utility ducts" (Japan Road Association 1986) is defined as shown in Fig.10, which is a ratio of the total weight to the total uplifting force acting on the underground structure, given by

$$F_U = \frac{W_S + W_B + Q_S + Q_B}{U_S + U_D} \quad (1)$$

where, W_S: weight of overburden soil, W_B: weight of structure, Q_S: shear resistance acting on side wall of overburden soil block, Q_B: frictional resistance acting on side wall of structure, U_S: buoyancy force due to hydrostatic pore pressure, U_D: buoyancy force due to excess pore pressure. Buoyancy force due to excess pore pressure U_d is given from the liquefaction resistance ratio F_L by using the empirical relationship as shown in Fig.11. Shear resistance is assumed to be dependent on the excess pore water pressure ratio, given by

$\tau_s = K_0 \sigma_{n0}' \tan \phi'$ $(Lu > 1.0)$

$= 0$ $(Lu <= 1.0)$

Frictional resistance acting on side wall of structure is given by

$\tau_s = K_0 \sigma_{n0}' \tan 2/3\, \phi'$ $(Lu > 1.0)$

$= 0$ $(Lu <= 1.0)$

The method has been used widely with slight modification for other manuals.

(2) Issues on the uplift stability evaluation method

During the 1995 Hyogoken-Nanbu earthquake, no common utility duct suffered uplift damage despite of liquefaction of the surrounding subsoil. The applicability of uplift stability method based on "Design manual for common utility ducts" is investigated on the case history of common utility ducts during the 1995 Hyogoken-Nanbu earthquake.

Common utility ducts, which were located in liquefied areas, were evaluated. According to the visual inspection conducted after the quake, the ducts were in alignment, suggesting that

virtually no uplift displacement had taken place. Safety factors against liquefaction of surrounding soil were evaluated based on "Specifications of highway bridges (1996)", in which a PGA of 0.6 was employed.

Fig.12 shows the results of calculated values of F_U in relation to the observed residual uplift displacement. This figure also shows the result for aforementioned case histories of damaged manhole in Kushiro City during the 1993 Kushiro-Oki earthquake (Koseki et al. 1997). Although these common utility ducts in Kobe City were suffered no insignificant uplift damage, the values of F_U was less than unity in all sites. The method evaluates the limit equilibrium of vertical force acting on underground structures and does not evaluate the extent of damage or magnitude of uplift displacement.

This method is still widely used for several manuals including sewage facilities, water supply facilities and cut-off railway tunnels, which were revised after the 1995 Hyogoken-Nanbu earthquake and consider level 2 design earthquake. It is, however, presumed that if aforementioned evaluation method of uplift stability such as that provided by "Design manual for common utility ducts (1986)" is employed for a very strong design earthquake like the Hyogoken-Nanbu earthquake, it may yield too conservative design. In manual for railway, although the relationship between F_L and R_U has been revised to consider strong design earthquake (see Fig.11), basis for this relationship are not explained.

To enable a more rational design of the buried structures, a more reasonable uplift stability design method for strong earthquake is required. In the following section, recent studies are presented that has been conducted in order to improve the evaluation method of uplift stability.

4. EXPERIMENTAL STUDIES

A series of dynamic centrifugal model tests was conducted in order to investigate the effects of several factors on the stability of the structures against uplift. The test results were compared with a conventional stability analysis (Japan Road Association (1986)) in order to verify applicability of this method.

(1) Test procedure

A series of dynamic centrifuge tests at a scale of 1/50 was conducted by using dynamic geotechnical centrifuges in the Public Works Research Institute, Japan (Koga et al. (1986) and Matsuo et al. (1998)).

Cross sections of the models used in the centrifugal tests are shown in Fig.13 and the test conditions are summarized in Table 4. In the tests, density of sand layer, amplitude and waveform of input acceleration and apparent unit weight of the buried structure were varied. The models were prepared in a rigid steel container with inner dimensions of 80 cm long, 20 cm wide, and 30 cm high. The model consists of sand layer with a thickness of 20 cm and acrylic box assuming underground structure with a base area of 10 cm by 19 cm and a height of 7.5 cm in model scale. The apparent unit weight of the model box was controlled at designated value, shown in Table 4.1, by putting lead shot inside.

Toyoura sand and Edosaki sand were used for the tests. Edosaki sand has a fines content of approximately 11%. A sand layer was prepared by pouring air-dried Toyoura sand through air in a rigid soil container for most cases, while in case 98-6 and case 98-8, Edosaki sand with a water content of approximately 21% was compacted to a designated relative density by tamping. To fulfill the requirement in the similarity law, the sand layer was saturated by silicon oil having a viscosity of 50 centi-stokes (50 times as viscous as water).

In the tests, after applying a centrifugal acceleration of 50 G a horizontal shaking was conducted. A sinusoidal wave of 20 cycles and 60 Hz was applied to the most of models, while in several cases, the earthquake motion of N-S component recorded at the Hachinohe-Harbor during the 1968 Tokachioki-Oki earthquake or N-S component recorded at the Kobe Maritime Observatory during the 1995 Hyogoken-Nanbu earthquake was applied.

During the tests, horizontal accelerations of the shaking table, sand layer and the model box, excess pore pressure in the sand layer and at the bottom of the model box, and uplift displacement of model box and settlement of ground surface, were measured. Locations of the measurements are shown in Fig.13. After the tests, the ground deformation was sketched.

(2) Results and discussions

a) Permanent deformation
Typical ground deformation that was sketched after the test in case 98-1 is presented in Fig.14. Sand layer beside model box settled and distorted toward the bottom of the model box, accompanying uplift displacement of model box and overlying soil. This deformation mode is very similar that given in Fig.8.

b) Time histories
Fig.15 plots the time histories of selected measurements during shaking for cases 97-4, 98-2 and 98-3. The following are seen from these data.

Uplift movement of the model box initiated after the surrounding sand layer had attained liquefaction. Uplift displacement proceeded at nearly constant rate during shaking in cases with sinusoidal input motion. After the shaking, it proceeded at a slow rate. In case 98-3 with earthquake shaking, uplift displacement developed significantly during the main shocks.

The excess pore pressure was reached on initial effective overburden pressure at first 2 or 3 cycles in all cases. In the case 98-2 with high sand density, the pore pressure exhibited spiky drops due to positive dilatancy. Although pore pressure after shaking maintained the value equal to that during shaking, uplift displacement rate decreased after shaking. Therefore, it is suggested that uplift displacement be affected by shaking intensity in addition to pore pressure.

c) Input acceleration vs. uplift displacement
Relationships between input acceleration and uplift displacement of the model box are shown in Figs.16. Fig.16 (a) plots the data for the cases with the ground water level of 0 mm and the apparent unit weight of the model box ρ_m of 0.8 in order to investigate influences of density of sand layer and input acceleration. Fig.16 (b) shows the effect of the apparent unit weight of the model box, and Fig.16 (c) shows the effect of the ground water level. The following can be seen from the data.

From Fig.16 (a), if the amplitudes of input acceleration are same, the amount of uplift displacements increases with the decrease of sand density. The amount of uplift displacement increases as the amplitude of input acceleration increases. Regarding the effect of input wave, if maximum amplitudes of input acceleration are equal, the amounts of uplift displacement in the cases with sinusoidal wave are larger than in cases with earthquake wave.

From Fig.16 (b), if both sand densities and magnitude of input acceleration are equal, the amounts of uplift displacement are almost same despite of different apparent unit weight of model. The effect of the apparent unit weight of model box is insignificant.

From Fig.16 (c), the amount of uplift displacement in case with ground water level of -6.5 cm is almost same as in case with that of 0 cm. However, the amount of uplift displacement in case with ground water level of -11.5 cm is

much smaller than in case with that of 0 cm.

5. STUDIES ON UPLIFT STABILITY EVALUATION DURING LIQUEFACTION

The results of aforementioned centrifugal model tests and the case records during the 1995 Hyogoken-Nanbu earthquake were analyzed with the conventional stability procedures (Japan Road Association (1986) and Koseki and Matsuo (1995)) in order to verify applicability of those method.

(1) Safety factor against uplift

Safety factor against uplift *Fu* based on "Design manual for common utility ducts" (Japan Road Association 1986) is defined as already shown in Fig. 7. For the centrifugal model tests, buoyancy force due to excess pore pressure *Ud* were calculated based on the recorded excess pore pressure during tests.

Relationship between minimum safety factor F_{Umin} against uplift during shaking and amount of residual uplift displacement of model box is shown in Fig.17. This figure also shows the aforementioned results of the case histories of the common utility ducts during the 1995 Hyogoken-Nanbu earthquake and the results for previous shaking table and centrifugal model tests by Koseki and Matsuo (1995). Fig.17 demonstrates that F_{Umin} was smaller than 1.0 when the model box suffered residual uplift. However, the amount of uplift displacement is not differentiated by F_{Umin} but depend on density of sand layer and amplitude of input acceleration.

(2) Safety factor against sliding

Koseki and Matsuo (1995) proposed the uplift stability evaluation method based on safety factor against sliding, in which uplift of underground structure was regarded as lateral movement of surrounding liquefiable soil toward the bottom of underground structure as shown in Fig.18. The safety factor against sliding is defined as the equilibrium of moments due to weight of soil block and structure and due to shear resistance acting on sliding surface, given by

$$F_s = \frac{M_{r1}+M_{r2}+M_{r3}+M_{r4}}{M_{d1}+M_{d2}-M_{d3}} \quad (1)$$

where, Mr1: resistant moment due to weight of overburden soil and structure, resistant moment due to shear resistance acting on sliding surface, Mr1-3: active moments due to weight of sliding soil blocks. Shear resistance is assumed to be dependent on the excess pore water pressure ratio, given by

$$\tau_f = (1 - R_U)\sigma_n' \cdot \tan\phi' \quad (2)$$

where, τ_f: resistant shear stress, R_U: excess pore water pressure ratio, σ_n': component of initial overburden effective pressure perpendicular to sliding surface.

Fig.19 shows the relationship between minimum safety factor against sliding F_{Smin} and residual uplift displacement for aforementioned centrifugal model test and case history during the 1995 Hyogoken-Nanbu earthquake. This figure also shows results for the previous shaking table and centrifugal model tests by Koseki and Matsuo (1995). From Fig.19 demonstrates that F_{Smin} was smaller than 1.5 when the model box suffered residual uplift. If values of F_{Smin} are relative large, uplift displacements are considered to relatively relate to the value of F_{Smin}. However, if F_{Smin} was smaller than 1.0, the amount of uplift was not clearly related to the value of F_{Smin} but depend on density of sand layer and amplitude of input acceleration. Especially, although the values of F_{Smin} were almost same, uplift displacement was increased when density of sand layer was higher and magnitude of input acceleration was larger. Consequently, the uplift stability evaluation methods based on safety factor against sliding can not considered the effect of density of sand layer and magnitude of input acceleration for uplift displacement.

As for the case histories, the values of F_{Smin} at all site were less than unity despite of no uplift damage. Consequently, the uplift stability evaluation method based on safety factor against sliding is considered to provide conservative result.

(3) Subject for the reasonable uplift stability evaluation method

These results demonstrates that the conventional uplift stability methods, which include safety factor against uplift *Fu* and safety factor against sliding *Fs*, can not estimate the residual uplift displacement

The major defect of the methods would be that for liquefied soil, shear resistance that calculated by Eq.(2) is regarded as completely zero. However, liquefied soils actually have some shear resistance due to so-called cyclic mobility. In addition, based on result of model tests, uplift displacement progressed during shaking and was related to the magnitude of input acceleration. These factors are not considered in these methods. This post-liquefaction shear resistance depends on the soil density and the degree of liquefaction. Therefore, it is required to reveal relationship between the shear resistance of liquefied soil and the effects of input acceleration and density of soil.

5. SUMMARY

Case histories of damage to underground structures caused by liquefaction were briefly reviewed. As a result, uplift damage was the most typical damage mode of underground structures.

The current practices of stability assessment for underground structures were briefly summarized, all of which are based on the safety factor approach. Back analyses of the model tests and the case histories of the common utility ducts during the 1995 Hyogoken-Nanbu earthquake demonstrated that the conventional uplift stability technique yield conservative results.

A series of dynamic centrifugal model tests was conducted in order to investigate the effects of several factors on the stability of the structures against uplift. The tests showed. Uplift displacement of the model box increased with duration of shaking and also after shaking. The rate of displacement decreased when shaking stopped. Residual uplift displacement of the model box increased as magnitude of input acceleration increased. The amounts of uplift displacements in the cases with sinusoidal wave are larger than in cases with earthquake wave. Residual uplift displacement of the model box decreased as the sand density increased.

Minimum safety factors against uplift F_{Umin} and against sliding F_{Smin} of model tests were smaller than 1.0 and 1.5 respectively when the model box suffered residual uplift. The amount of uplift displacement was not clearly related to the value of F_{Umin} and F_{Smin} but depended on density of sand layer and amplitude of input acceleration.

REFERENCES

Hamada, M., R. Isoyama and K. Wakamatsu 1995. The 1995 Hyogoken-Nanbu (Kobe) Earthquake, Liquefaction, Ground Displacement and Soil Condition in Hanshin Area, Association for development of earthquake prediction.

Japan Road Association 1986. Design manual for Common Utility Ducts. pp.58-71 (in Japanese).

Japan Road Association 1997. Specification for Highway Bridges V Seismic Design, (in Japanese).

Japanese Society of Soil Mechanics and Foundation Engineering 1994. Research Report of Damage Caused by the 1993 Kushiro-Oki Earthquake and the Noto-

Hanto-Oki Earthquake, 289-303 (in Japanese).

Koga, Y., E.Taniguchi, J.Koseki and T.Morishita 1988. The newly introduced geotechnical dynamic centrifuge, Civil Engineering Journal, Vol. 30, No. 5 (in Japanese)

Koseki, J. and O. Matsuo 1995. Simplified method to evaluate uplift stability of common utility ducts during earthquakes, Proc of 30 th Japan National Conf. on Soil Mechanics and Foundation Engineering, pp.1049-1052 (in Japanese).

Koseki, J., O. Matsuo, Y. Ninomiya and Y. Yoshida 1997. Uplift of sewer manholes during the 1993 Kushiro-oki earthquake, Soils and Foundations, Vol.37, No.1, 109-121.

Koseki, J., O. Matsuo and S. Tanaka 1998a. Uplift of sewer pipes caused by earthquake-induced liquefaction of surrounding soil, Soils and Foundations, Vol. 38, No.3, 75-87.

Koseki, J., Matsuo, O., Sasaki, T., Saito, K. and Yamashita, M., 1998b. Effect of peat layer on damage to sewer pipes during earthquakes," *Proc. of Int. Symp. on Problematic Soils, Sendai, Balkema*,Vol.1, 109-113.

Matsuo, O., T. Tsutsumi, K. Kondo and S. Tamoto 1998. The dynamic geotechnical centrifuge at PWRI, Proc. Int. Conf. Centrifuge 98, Tokyo. Balkema: 25-30.

Public Works Research Institute 1965, Report of Niigata Earthquake, Report of the Public Works Research Institute Ministry of Construction, Vol.125 (in Japanese).

Public Works Research Institute 1994. Report on the Disaster Caused by the Hokkaido Nansei-Oki Earthquake of 1993, Report of The Public Works Research Institute Ministry of Construction, Vol.194 (in Japanese).

Public Works Research Institute 1996. Report on the Disaster Caused by the 1995 Hyogoken Nanbu Earthquake, Report of PWRI, Vol. 196.

Sasaki, T., J. Koseki, O. Matsuo, K. Saito and M. Yamashita 1999 Analyses of damage to sewer pipes in Shibetsu Townduring the 1994 Hokkaido-Toho-Oki earthquake, 5th U.S. Conf. on Life line Earthquake Engineering (submitted).

Taniguchi, E. and Morishita, Y. 1985, Damage of uplift of underground structure during 1983 Nihonkai-chubu Earthquake, Technical Memorandum of PWRI, No. 2235.

Table1 Case histories of earthquake induced damage to underground structures in Japan

Earthquake	Damaged underground structure	References
Niigata (1964), M=7.5	Sewage treatment tank, sewer manhole and pipe (*Niigata City*)	PWRI(1965)
Nihonkai-Chubu (1983), M=7.7	Fuel tank, Water tank, sewer pipes (*Noshiro City*)	Morishita and Taniguchi (1985)
Kushiro-Oki (1993), M=7.8	Sewer manhole (*Kushiro Town*), sewer pipe (*Kushiro Town, Kushiro City and Shibetya Town*)	Koseki et al. (1997a), JSSMFE (1994)
Hokkaido-Nansei-Oki (1993), M=7.8	Fuel tank (*Esashi Town*), sewer manhole (*Oshamanbe Town and Kamiiso Town*)	PWRI(1994)
Hokkaido-Toho-Oki (1994), M=8.1	Sewer manhole (*Shibetsu Town*),sewer pipe (*Kushiro City*)	JGS (1998)
Sanriku-Haruka-Oki (1994), M=7.5	Sewer pipe (*Towada City*)	Koseki et al.(1998a)
Hyogoken-Nanbu (1995), M=7.2	Water tank (*Nishinomiya City*), Sewage treatment facility (*Kobe City*)	PWRI(1996)

Table2 Effects of liquefaction considered the existing design manuals

Titles	Year published and organization	Object structure	Design ground motion		Effects of liquefaction taken into account							
					Uplift		Post-earthquake subsidence		Lateral spread		Seismic earth pressure	
			L1	L2	Effects of liquefaction	Check items	Effects of liquefaction	Check items	Effects of liquefaction	Check items	Effects of liquefaction	Check items
Design manual for common utility ducts.	1986 Japan Road Association	Common utility ducts	○	–	Excess pore water pressures and reduction of	Uplift stability	–	–	–	–	–	–
Design and execution manual for underground parking lots	1992 Japan Road Association	Underground parking facilities	○	–	Excess pore water pressure	Uplift stability	–	–	–	–	–	–
Guidlines of aseismic measures for sewage facilities	1997 Japan Sewage Association	Sewage pipes	○	○	– *	– *	Subsidence of surrounding ground	Design of flexible joint	Lateral spread displacements	Design of flexible joint	–	–
		Sewage treatment facilities	○	○	Excess pore water pressures and reduction of	Uplift stability	–	–	Lateral spread forece	Design of pile	–	–
Guidlines of earthquake resistant methods for water supply facilities	1997 Japan Waterworks association	Water supply facilities	○	○	Excess pore water pressures and reduction of shear	Uplift stability	–	–	Lateral spread displacements	Design of flexible joint	–	–
Design standards for railway structures, Seismic design	1998 Railway Technical Research Institute	Open-cut railway tunnels	○	○	Pore water pressure and reduction of shear resistance	Uplift stability	Subsidence of surrounding ground	allowable settlement	Lateral spread displacements	Design of cross section of structure	Intermediate and cyclic component of seismic earth pressure	Design of cross section of structure

*using non liquefiable backfill soil

L1: Ground motion highly probable to occur during service period
L2: Ground motion with high intensity, though less probable to occur during the service period

Table3 Uplift stability methods in each design manual

Titles	Established year and organ	Object structures	Formula	Excess pre water pressure	Shear resistance	Safety factor	Design lateral forece coefficient	Notes
Design manual for common utility ducts.	1986 Japan Road Association	Common utility ducts	$F_s = \frac{W_s + W_B + Q_s + Q_B}{U_s + U_D}$	$L_u = \begin{cases} F_L^{-4} & (F_L \geq 1) \\ 1 & (F_L < 1) \end{cases}$	considered	1.1	0.15	
Design and execution manual for parking	1992 Japan Road Association	Undergro und parking facilities	$F_s = \frac{W_s + W_B}{U_s + U_D}$	$L_u = \begin{cases} F_L^{-4} & (F_L \geq 1) \\ 1 & (F_L < 1) \end{cases}$	–	1.0	0.15	provide soil inprovemen t for bottom of
Guidline of aseismic measure for sewage facilities	1997 Japan Sewage Association	Sewage facilities	・Sewer pipes –* ・Sewage treatment facilities $F_s = \frac{W_s(1-K_v)+W_f+P_r}{V_c \cdot \gamma_c + V_l \cdot \gamma_l}$	–	considered	1.2		*using non-liquefiable backfill soil
Guidline of earthquake resistant method for water supply	1997 Japan Waterworks association	Water supply facilities	$F_s = \frac{W_s + Q_s}{V_l \cdot \gamma_l}$	–	considered	1.0	0.16 ~ 0.8	
Design standerd for railway structure, seismic design	1998 Railway Technical Research Institute	Cut and cover tunnel	$F_s = \frac{W_s + W_B + Q_s + Q_B}{U_s + U_D}$	$L_u = \begin{cases} 0.4 - 1.3 F_L & (F_L \geq 0.5) \\ 1 & (F_L < 0.5) \end{cases}$	considered	according to importance	acceleration resposse spectrum for Level 1 and Level 2	unnecessary to examin if temporary sheet piples were leaved

F_S: Safety factor against uplift, W_S: Weight of overburden soil, W_B: Weight of structure, Q_S: Shear resistance acting on side wall of overburden soil block, Q_B: Frictional resistance acting on side wall of structure, U_S: Buoyancy force due to hydrostatic pore pressure, U_D: Buoyancy force due to excess pore pressure, P_r: Pulling resistance of a pile, V_c: Volume of structure, V_s: Volume of part of structure below ground water level except liquefied layer, V_l: Volume of part of structure in liquefied layer, γ_w: Unit weight of water, γ_l: Unit weight of liquefied soil, L_U: Excess pore water pressure ratio, Δu: Excess pore water pressure, F_L: Liquefction resistance ratio, K_v: Design vertical force coefficient

Table 4 Test conditions

Case	centrifugal Acc.(G)	unit weigh of model	ground material	relative density Dr(%) [D(%)]	preparation method	ground water level (cm)	shaking condition wave type	(G)
97-1	50	1.3	Toyoura sand	20	air pluviated	0	sinusoidal	5.6
97-2	50	1.3	Toyoura sand	71	air pluviated	0	sinusoidal	16.0
97-3	50	0.8	Toyoura sand	49	air pluviated	0	sinusoidal	8.9
97-4	50	0.8	Toyoura sand	71	air pluviated	0	sinusoidal	14.5
97-5	50	0.8	Toyoura sand	28	air pluviated	0	sinusoidal	6.8
97-6	50	0.8	Toyoura sand	28	air pluviated	0	sinusoidal	15.7
97-7	50	0.8	Toyoura sand	54	air pluviated	0	sinusoidal	14.4
97-8	50	0.8	Toyoura sand	47	air pluviated	0	Hachinohe wave	19.6
97-9	50	0.8	Toyoura sand	47	air pluviated	-6	sinusoidal	10.0
97-10	50	0.8	Toyoura sand	67	air pluviated	-6	sinusoidal	14.9
98-1	50	0.8	Toyoura sand	52	air pluviated	0	sinusoidal	16.0
98-2	50	0.8	Toyoura sand	84	air pluviated	0	sinusoidal	40.0
98-3	50	0.8	Toyoura sand	53	air pluviated	-11.5	sinusoidal	16.0
98-4	50	0.8	Toyoura sand	83	air pluviated	0	Kobe wave	40.0
98-5	50	0.8	Toyoura sand	54	air pluviated	0	Kobe wave	40.0
98-6	50	0.8	Edosaki sand	14 [75]	wet tamping	0	sinusoidal	15.0
98-7	50	1.6	Toyoura sand	52	air pluviated	0	sinusoidal	15.0
98-8	50	0.8	Edosaki sand	57 [85]	wet tamping	0	sinusoidal	15.0
98-9	50	0.8	Toyoura sand	93	air pluviated	0	Kobe wave	40.0
98-10	50	0.4	Toyoura sand	51	air pluviated	0	sinusoidal	15.0

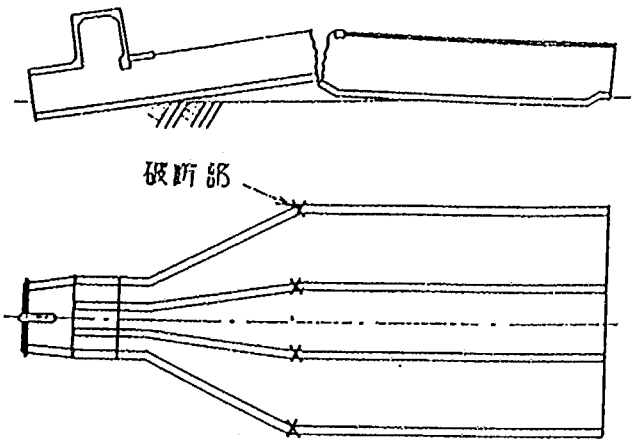


Fig.1 Schematic uplifted sewage treatment tank during the 1964 Niigata earthquake (the Zoshobori sewage pomp station)



Fig.2 Uplifted fuel tank during the 1986 Nihonkai-Chubu earthquake

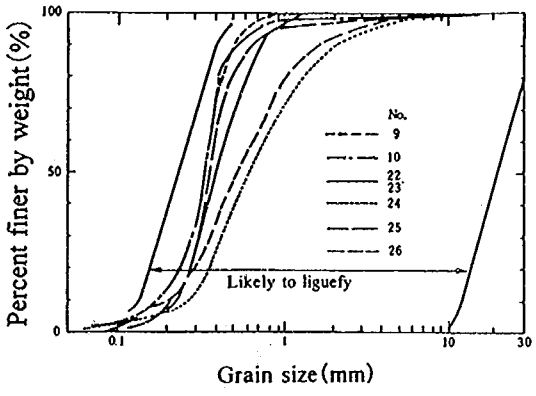


Fig.3 Grain size distribution of sand boil and backfill soil

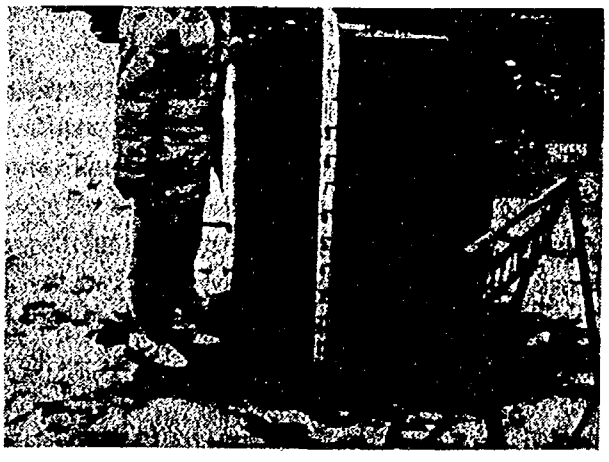


Fig.4 Uplifted sewage manhole during the 1993 Kushiro-Oki earthquake

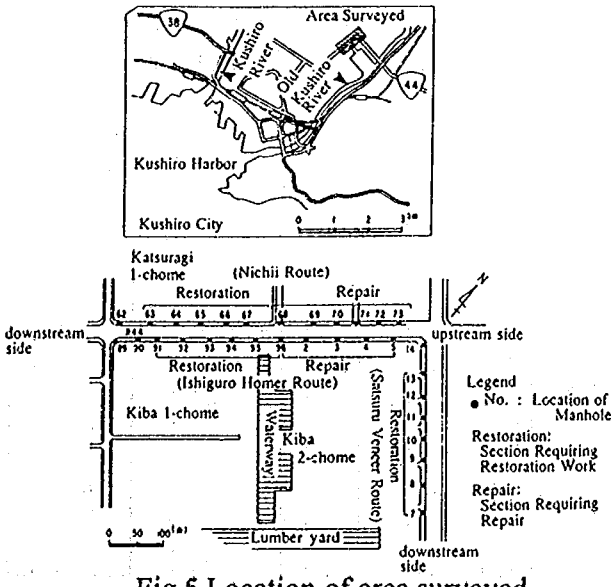


Fig.5 Location of area surveyed

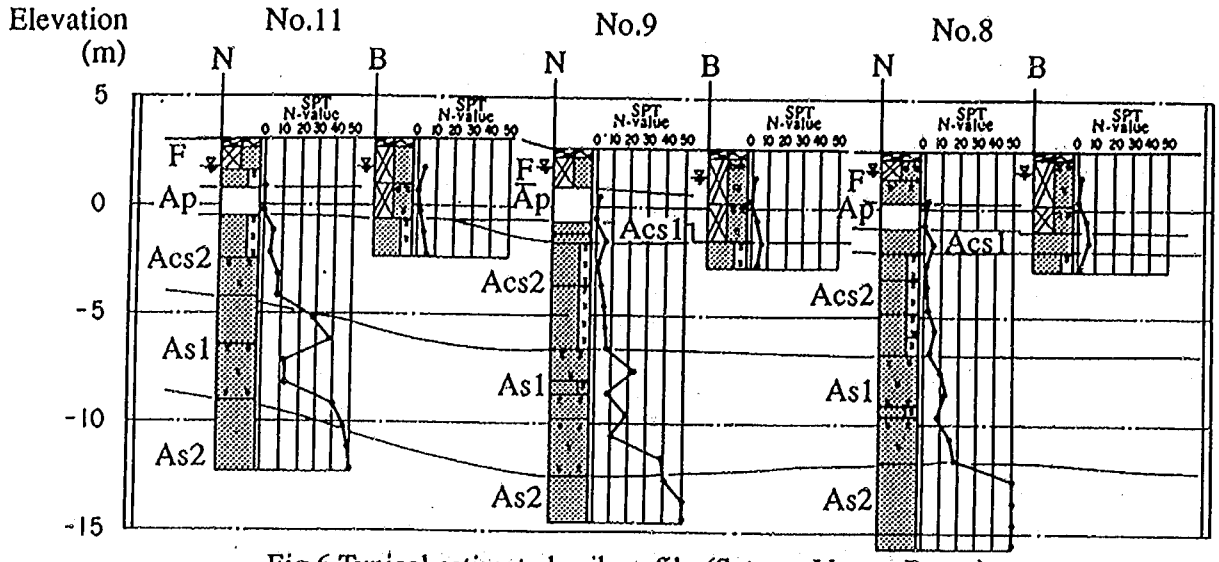


Fig.6 Typical estimated soil profile (Satsuru Veneer Route)

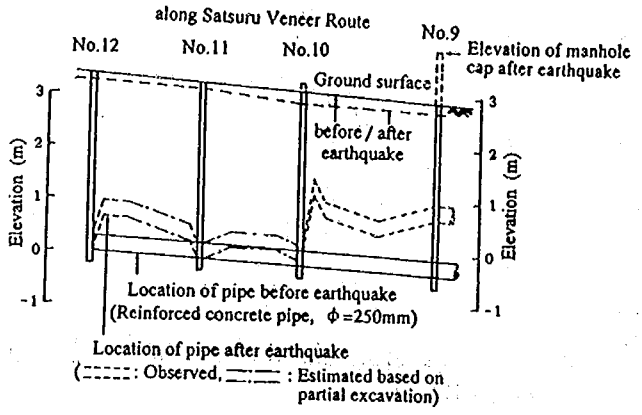


Fig.7 Vertical displacement of sewer pipes along Satsuru Veneer Route

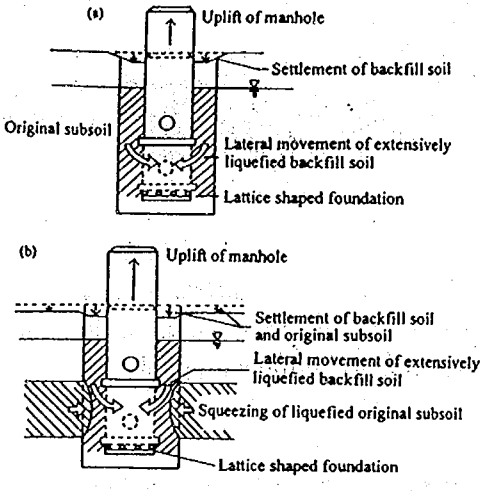


Fig.8 Schematic mechanism of manhole uplift

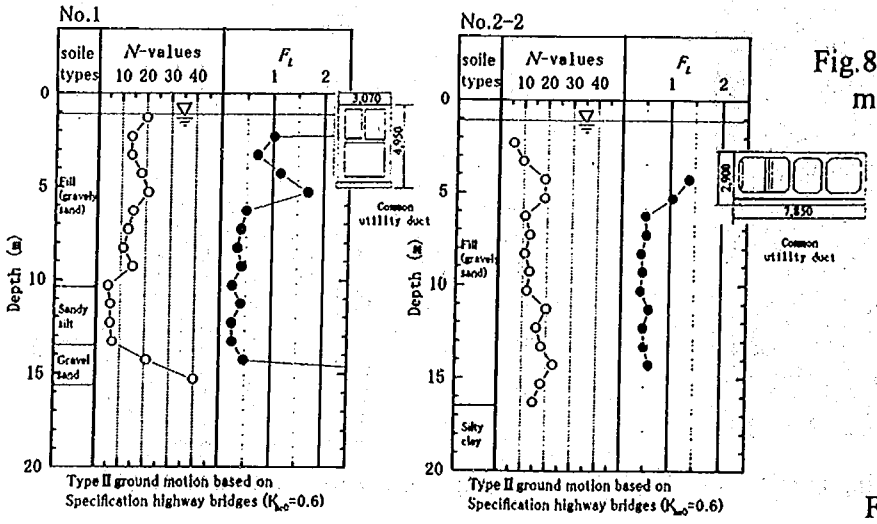


Fig.9 Typical soil profiles

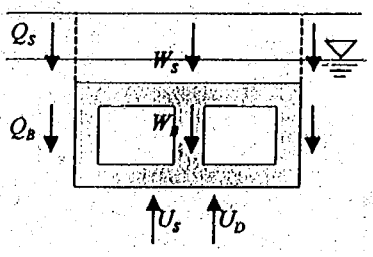


Fig 10 Definition of safety factor against uplift F_U

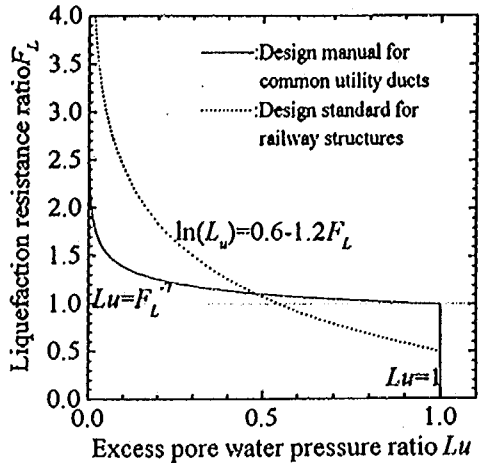


Fig.11 Relationship between Excess pore water pressure ratio R_U and liquefaction resistance ratio F_L

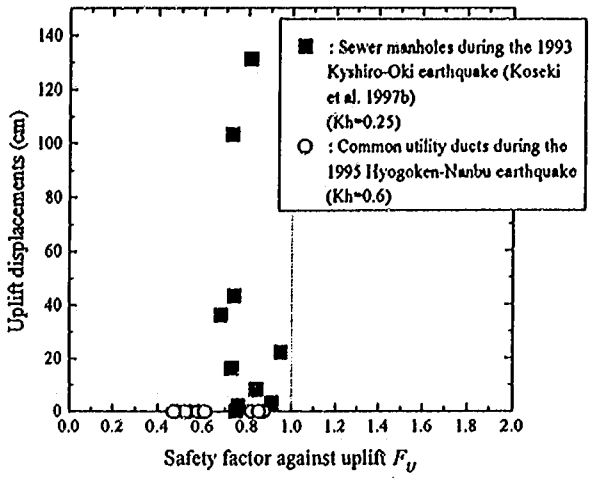


Fig.12 Relationship between uplift displacement and safety factor against uplift F_U

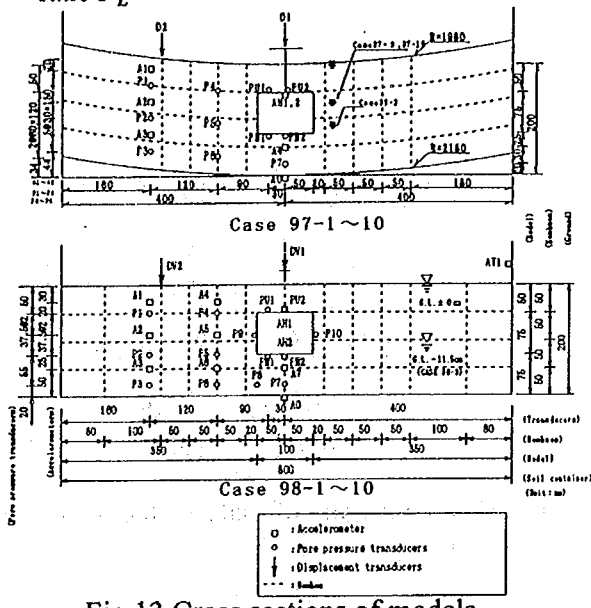


Fig.13 Cross sections of models

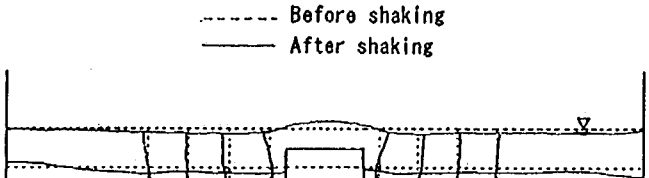
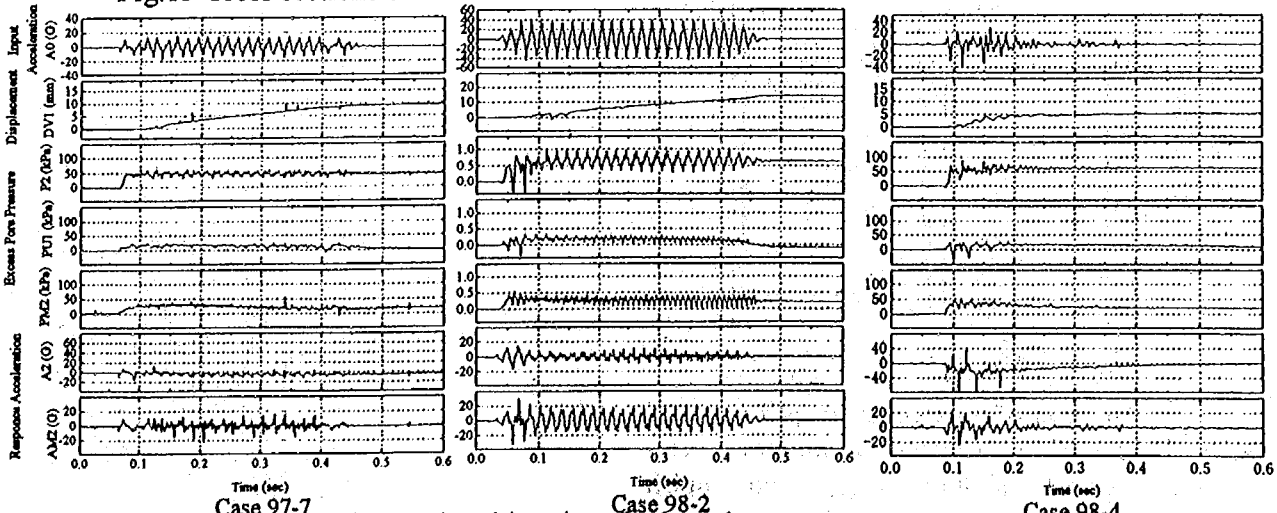
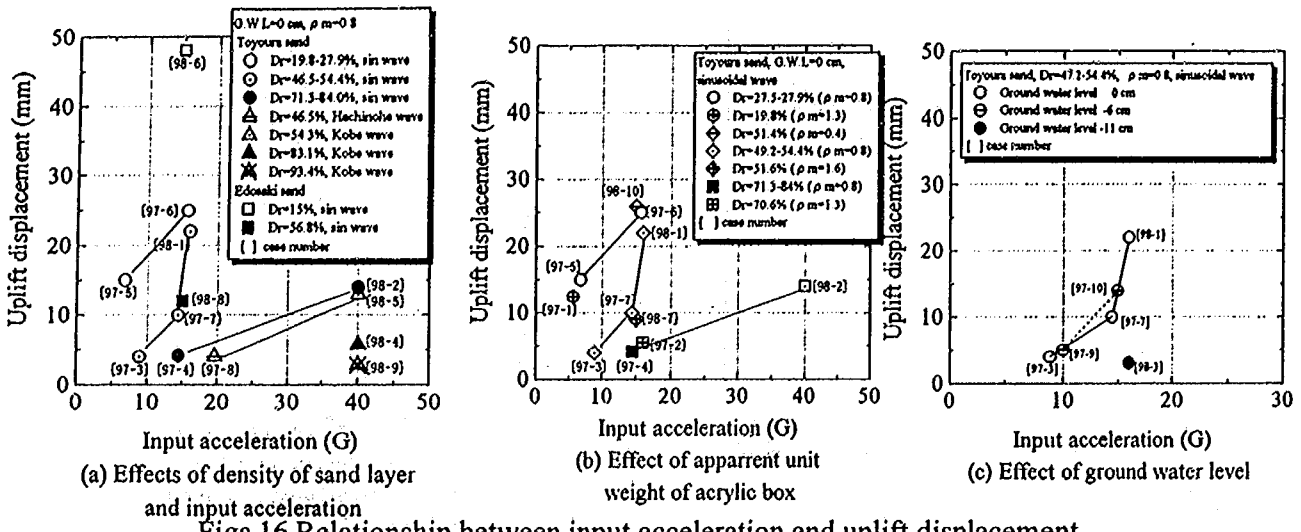


Fig.14 Observed deformation of sand layer after shaking (case 98-1)



Case 97-7 Case 98-2 Case 98-4

Fig.15 Time histories of selected measurements



(a) Effects of density of sand layer and input acceleration

(b) Effect of apparrent unit weight of acrylic box

(c) Effect of ground water level

Figs.16 Relationship between input acceleration and uplift displacement

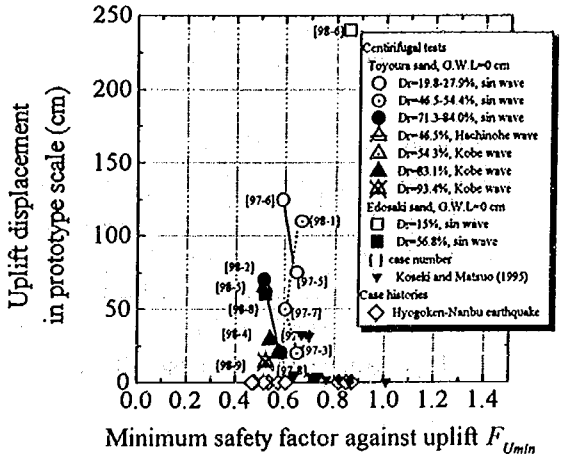


Fig.17 Relationship between minimum safety factor against uplift F_{Umin} and uplift displacement

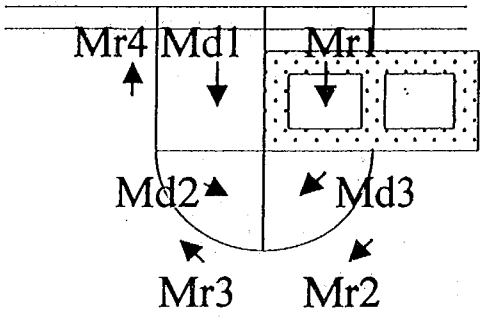


Fig.18 Definition of safety factor against sliding F_S

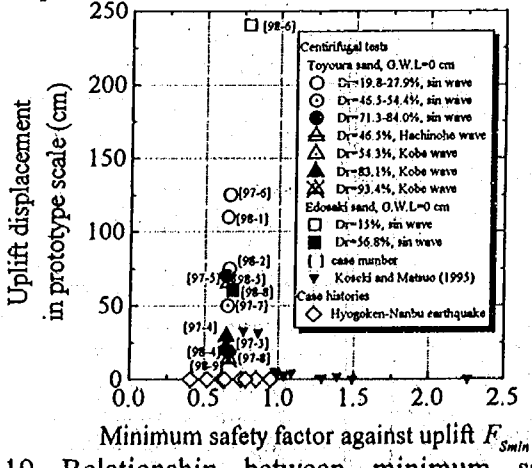


Fig.19 Relationship between minimum safety factor against sliding F_{Smin} and uplift displacement

DEVELOPMENT OF SEISMIC PERFORMANCE EVALUATION PROCEDURES IN BUILDING CODE OF JAPAN

By

HIRAISHI Hisahiro[1], MIDORIKAWA Mitsumasa[2], OKAWA Izuru[3], IIBA Masanori[4], TESHIGAWARA Masaomi[5], and ISODA Hiroshi[6]

ABSTRACT

The building code of Japan will be changed from current prescriptive into performance-based type by 2000.

This paper presents the evaluation procedure of structural seismic performance against major earthquake motions in the performance-based building code of Japan under development at the Building Research Institute (BRI). The basic concept of BRI proposal for seismic design spectra for major earthquake motions is 1) basic design spectra defined at the engineering bedrock, and 2) evaluation of site response from geotechnical data of surface soil layers. The principle of evaluation procedures is that the predicted response values should not exceed the estimated limit values. In case of major earthquakes, the maximum response values of strength and displacement of a structure should be smaller than the ultimate capacity for strength and displacement. The proposed evaluation procedure applies the equivalent single-degree-of-freedom (ESDOF) system and the response spectrum method, while the current procedures are based on the estimation of the ultimate capacity for lateral loads.

The proposed evaluation procedure makes it realistic and simple to predict maximum structural response in case of major earthquakes as well as to confirm whether the predicted response values are smaller than the limit ones.

***KEYWORDS**: building code of Japan, evaluation procedure, seismic performance, major earthquake motions, equivalent linearization, equivalent single-degree-of-freedom system, response spectrum method, site response, soil-structure interaction*

1. INTRODUCTION

On February in 1996 it was officially announced by the Ministry of Construction authorities that the Building Standard Law of Japan should be revised on the basis of performance principles. In the Building Council report[1] of March 24, 1997, entitled "For a New Building Administration Framework, which could cope with the economic & social changes and their prospects in the 21st century", it was clearly stated that in order to compile a highly flexible New Building Standard Law, the current provisions must be revised into those based on performance. That served as a basis for the compilation of "Guidelines for the Performance-based Building Code".

Unlike the in-current-use conventional building code, the performance-based building code prescribes clearly the type and the level of the required performance for a given building structure. In other words, for the precisely

1) Director, Dept. of Structural Engineering, Building Research Institute, Ministry of Construction, 1 Tachihara, Tsukuba, Ibaraki, 305-0802 Japan.
2) Director, International Institute of Seismology and Earthquake Engineering, BRI, MOC.
3) Head, Construction Techniques Div., BRI, MOC.
4) Head, Structural Dynamics Div., BRI, MOC.
5) Head, Structure Div., BRI, MOC.
6) Senior Research Engineer, Structure Div., BRI, MOC.

determined response of the structure subjected to assumed loads and forces, it prescribes the evaluation procedures to be used for the estimation of structure's conformity with the required structural safety.

However, even in the case of the performance-based provisions, the prescription of a minimum required level is necessary, being the same as in the current building code provisions. In this sense, the performance-based code is different form the performance-based design, which has been a current topic among structural engineers. The latter deals with a design procedure, which is based on a clearly defined target performance for the structure considered, normally being prescribed higher than the minimum required performance level. Basically, the performance-based design is the structural design on the basis of consultation between the structural engineer and the owner of the building.

This paper presents the evaluation procedure of structural seismic performance against major earthquake motions in the performance-based building code of Japan under development at the Building Research Institute (BRI)[2), 3), 4)].

The basic concept of BRI proposal for seismic design spectra for major earthquake motions is 1) basic design spectra defined at the engineering bedrock, and 2) evaluation of site response from geotechnical data of surface soil layers.

The principle of evaluation procedures is that the predicted response values should not exceed the estimated limit values. In case of major earthquakes, the maximum response values of strength and displacement of a structure should be smaller than the ultimate capacity for strength and displacement. The proposed evaluation procedure applies the equivalent single-degree-of-freedom (ESDOF) system and the response spectrum method, while the current procedures are based on the estimation of the ultimate capacity for lateral loads.

It should be noticed here that presented in this paper is just the state-of-the-art and up-to-now level of development of the performance-based structural provisions at BRI in Japan. It should not be considered as a fully completed version, ready to be presented for the final official approval.

2. CONCEPTUAL FRAMEWORK OF PERFORMANCE-BASED STRUCTURAL CODE

The conceptual framework of performance-based structural code proposed by BRI is shown in Fig. 1. Following the principles of structural safety, the evaluation procedures to be used for the estimation of structure's conformity with the required performance level are roughly classified as:

a. Proposed route
b. Conventional route
c. Small building route, and
d. Others

The proposed route represents a new evaluation procedure to be used instead of the current one, which is based on the calculation of allowable stress and estimation of ultimate capacity for lateral load. It considers the effects of major earthquakes as well as other forces and loads. The other effects, which are not considered in the structural calculations, such as construction quality, durability, quality of construction materials, and nonstructural elements, are covered by structural specifications. In essence, by using this procedure it is possible to evaluate and verify the structural performance possessed by a designed structure, regardless of the design method used. It is just an evaluation procedure that verifies whether or not the prescribed performance objectives are met.

The second route represents the conventional evaluation procedure now in use, adopted as the standard structural calculation method. It can be supplemented with additional provisions in addition to those of the first route described above. However, if the principles of performance-based provisions are to be followed, it should be noticed that the obviously unnecessary parts to be considered by structural calculations are eliminated. To this extent, this route can be considered as a kind of deemed-to-satisfy evaluation procedure.

The third route applies to small buildings. This route does not require structural calculations and is considered to be deemed-to-satisfy provisions. It prescribes only

conventional-based structural specifications.

In the fourth route are included all other alternative evaluation procedures and deemed-to-satisfy provisions, such as those developed and certified by private institutions as well as those requiring expert judgments.

The types of loads and forces considered in the newly proposed evaluation procedure remain almost the same with those currently in use. However, for the case of seismic effects only, new earthquake motion provisions are prepared to replace the current earthquake force provisions.

In a definite proposal, the earthquake motion response spectra at the engineering bedrock, assumed to be the stratum having shear wave velocity in the range of several hundreds m/s, is considered as the basic design spectra. On the basis of this conception for the earthquake input motion, it is possible that earthquake effects be not only accounted rationally through the incorporation of influence of local soil conditions on ground motion characteristics at the free surface but also conveniently incorporated in the newly developed design procedures of seismically isolated and response controlled structures. Furthermore, it is anticipated that the future proposals expected for the evaluation and design procedures are suitably implemented.

3. REQUIRED SEISMIC PERFORMANCE LEVEL FOR BUILDING STRUCTURES

An outline of requirements for building structures and earthquake motion levels is shown in Table 1. In the vertical column on the left hand side of the table are shown the requirements for building structures, while in the rest of the table are shown the earthquake motions to be considered and their corresponding levels for each of the requirements assigned for building structures.

As it is shown in Table 1, requirements for building structures are classified in two categories, which are explained below.

3.1 Life Safety

The essential purpose of this requirement is the safety of life. It should be expected that under the action of earthquake motions taken into consideration, the building should not experience any story collapse.

3.2 Damage Limitation

The aim of this requirement is damage limitation. Under this provision, it is required first that after the action of earthquake motions taken into consideration, no structural damage which could threaten the structural safety of the building will take place. In other words, the structural safety performance required by Section 3.1 should be preserved. Furthermore, it is required that no other kind of damage causing in the building structure a situation which does not comply with other requirements of the Building Standard Law concerning fire safety should be experienced.

3.3 Maximum Earthquake Motion Level

This level of earthquake motions corresponds to the category of requirements in Section 3.1 for building structures and is assumed to produce the maximum possible effects on the structural safety of a building to be constructed at a given site. The maximum possible earthquake motion level is determined on the basis of historical earthquake data, recorded strong ground motions in the past, seismic and geologic tectonic structures, active faults, and others. This earthquake motion level corresponds nearly to that of highest earthquake forces used in the current seismic design practice, representing the horizontal earthquake forces induced in the building structures in case of major seismic events.

3.4 Once-in-a-Lifetime Event Level

This level of earthquake motions corresponds to the category of requirements in Section 3.2 for building structures and is assumed to be experienced more than once during the lifetime of the building. A return period interval of 30-50 years is supposed to cover these events. This level of earthquake motion corresponds nearly to the middle level earthquake forces used in the current seismic design practice, representing the horizontal earthquake forces induced in the building structures in case of moderate earthquakes.

4. EVALUATION PROCEDURES FOR A REQUIRED PERFORMANCE LEVEL

Various response and limit values are considered for use in proposed evaluation procedures, in accordance with each of the requirements prescribed for building structures. A representative example of this arrangement is shown in Table 2. The principle of evaluation procedures is that the predicted response values due to the action of earthquake motions on building structures should not exceed the estimated limit values. Fundamentals of proposed evaluation procedures corresponding to each level of earthquake motions are described below.

4.1 Evaluation Procedures Corresponding to Maximum Earthquake Motion Level

The maximum response values of the building structure subjected to earthquake motions should be smaller than the limit values. In defining strength and displacement limits for earthquake motions, it may be necessary to consider the effects of repeating cycles in the plastic region of the response as well.

4.2 Evaluation Procedures Corresponding to Once-in-a-lifetime Event Level

For this level of earthquake motions, it is required to be confirmed whether the internal forces and displacements taking place at each structural element satisfy the condition of being smaller than the limit strengths and displacements. The limit strengths and displacements mentioned here imply that the whole structure behaves generally within the elastic range.

5. PROPOSED EVALUATION PROCEDURE FOR THE CASE OF MAJOR EARTHQUAKES

Hereafter the focus is put on the proposed evaluation procedure for the case of major earthquakes.

The variety of linearization techniques has already been studied (for example, Ref. 5). Several applications have also been presented in the publicetions[6)-9)].

In the analytical methods to be used for predicting the structural response in the newly proposed evaluation procedure for the case of earthquake excitations, it is expected to apply the ESDOF system and the response spectrum method using the linearization technique.

5.1 General Flow of Proposed Evaluation Procedure

A flow chart of this procedure is illustrated in Fig. 2. There are indeed various analytical methods for predicting the response of structures subjected to earthquake excitations. The one that is shown here is based on the ESDOF system and the response spectrum method.

According to this procedure the steps to be followed are:

I. Confirm the scope of application of the evaluation procedure and the mechanical characteristics of materials and/or members to be used.

II. Determine the response spectra to be used in the evaluation procedure.

i) For a given basic design spectrum at the engineering bedrock level, draw up the free-field site-dependent acceleration (Sa) and displacement response spectra (Sd), for different damping levels.

ii) In the estimation of free-field site-dependent acceleration and displacement response (step i) above), consider the strain-dependent soil deposit characteristics.

iii) In case of need, present graphically the relation of Sa-Sd, for different damping levels.

III. Determine the hysteretic characteristic, equivalent stiffness and equivalent damping ratio of the structure.

i) Model the structure as a simplified ESDOF system and establish its force-displacement relationship (see Fig. 2a).

ii) Determine the limit strength and displacement of the structure corresponding to the ESDOF system mentioned above.

iii) The soil-structure interaction effects should basically be considered.

iv) In case of need, determine the equivalent stiffness in accordance with the limit values.

v) Determine the equivalent damping ratio on the basis of viscous damping ratio, hysteretic dissipation energy and elastic strain energy of the

structure (see Fig. 2b).
vi) In case that the torsional vibration effects are predominant in the structure, these effects should be considered when establishing the force-displacement relationship of the ESDOF system.
IV. Examine the safety of the structure.

In this final step, it is verified whether the response values predicted on the basis of the response spectra determined according to the step II satisfy the condition of being smaller than the limit values estimated on the basis of step III (see Fig. 2c).

In order to determine the limit strength and displacement of the structure, a specific displaced mode is necessary to be assumed in advance for its inelastic response (see Fig. 2a). Basically, any predominant or possible to be experienced displaced mode of the structure subjected to earthquake motions can be applied. The predominant or possible to be experienced displaced mode implies any of the failure modes observed during the major earthquakes such as beam failure mode, story failure mode or any other definite failure mode.

5.2 Basic Response Spectrum at Engineering Bedrock

In the BRI proposal, the evaluation earthquake load is specified with earthquake ground motion not with seismic force. The earthquake ground motion is basically given at the exposed (outcrop) engineering bedrock. The evaluation earthquake motion is represented with the acceleration response spectrum in the following formula.

$$S_a = ZGS_0 \quad (1)$$

where,

S_a: acceleration response spectrum for evaluation,

Z: seismic zoning factor,

G: soil amplification factor, and

S_0: basic acceleration response spectrum at engineering bedrock.

The engineering bedrock is defined as a layer with more than 400 m/s in shear wave velocity.

The basic concept in estimating the evaluation earthquake motions is expressed in the followings.

The basic acceleration response spectra to be given at the engineering bedrock shall be consistent with the design seismic shear force given in the current Building Standard Law of Japan.

In this case, the consistency is maintained so that the newly defined evaluation spectrum preserves the equivalent seismic effects in the seismic forces specified for buildings constructed on the soil condition with soil profile of Type-2, which contains the majority of the ordinary buildings in Japan.

The basic response spectrum shown in Fig. 3 is to be given within specific ranges of period. The shorter period range is determined with uniform acceleration amplitude and the longer period range is determined with the uniform velocity amplitude. Each level of spectra is understood simply related with the peak ground acceleration (PGA), and the peak ground velocity (PGV) at the engineering bedrock expected at the site.

The relationship between the base shear coefficient and the acceleration response spectrum is given with the earthquake response of the uniform shear beam model. It is reported that in this model the base shear force shall be multiplied by 1.23 for uniform acceleration spectrum, and shall be multiplied by 1.1 for uniform velocity spectrum[10]. In addition to this simplified relationship, we assumed the soil amplification factors 1.5 for acceleration dominated period range, and 2.0 for velocity dominated period range. These factors of 1.5 and 2.0 are based on the nonlinear response computations using simplified models of surface soil layers. With these assumptions, the basic acceleration response spectrum is derived as shown in Fig. 3.

The seismic zoning factor represents the relative difference in the expected earthquake intensity values for specified periods. The earthquake intensity values are represented with peak ground acceleration (PGA) and peak ground velocity (PGV). Based on the earthquake source catalogue during the recent 500 years larger than the magnitude of 5.0, and the empirical attenuation equations which are consistent with the near source records during recent major earthquakes such as the 1995 Hyogoken-nambu earthquake, we computed the expected amplitudes

in acceleration and velocity for 500 and 50 years for every 0.05 degree in longitude and latitude point. Here, we considered the source area for larger earthquakes whose fault model is available. And we also included the influence of active faults. The major active faults in Japan are being investigated for its possible return period and probabilities for causing earthquakes in near future. Based on these computation results, we drew the hazard maps for the representative values as shown in Fig. 4. Our proposal on the seismic zoning factors will be based on these results.

5.3 Acceleration Response Spectrum at Ground Surface

To evaluate the acceleration response spectrum at ground surface, the amplification of surface soil deposits on the engineering bedrock is estimated. An evaluation method by using the equivalent linearization technique considering soil properties of nonlinearity is explained below.

(1) Evaluation procedure

The acceleration response spectrum at the ground surface is obtained as follows.

a) Transformation of response spectrum defined at outcropped engineering bedrock

The earthquake motion defined at the outcropped engineering bedrock is given as the acceleration response spectrum with 5% damping ratio; $S_{ao}(T, \zeta=0.05)$. The acceleration response spectrum with arbitrary damping ratios; $S_{ao}(T, \zeta)$ is calculated based on $S_{ao}(T, \zeta=0.05)$. $S_{ao}(T, \zeta=0)$, a velocity response spectrum; S_v, and a Fourier spectrum of acceleration; $F_{ao}(T)$ have the approximate relation as follows.

$$F_{ao}(T) \fallingdotseq S_v(T, \zeta=0) \fallingdotseq (T/2\pi) S_{ao}(T, \zeta=0) \quad (2)$$

b) Eigen value analysis of soil profile

With subdividing the soil profile, a shear model of n degrees of freedom is formed, as shown in Fig. 5. The shear springs; K_i, damping coefficients; c_i and masses; m_i at discrete points, and a spring at the bottom of the surface soil layers are defined as follows.

$$K_i=G_i/d_i \qquad c_i=h_i G_i T_i/(\pi d_i) \quad (3)$$

$$m_i=0.5(\rho_i d_i+\rho_{i-1} d_{i-1}) \quad (4)$$

$$K_b=8 G_b B/(2-\nu_b) \quad (5)$$

Where G_i, ρ_i, d_i and h_i are shear modulus, mass density, layer height, and damping ratio at the i-th layer from the surface. G_b and υ_b are shear modulus and Poisson's ratio at the engineering bedrock, and B = 0.564m. T_1 is the fundamental natural period of the surface ground. Through the eigen value analysis, the natural period, the vibration mode; U_i (normalized by the value at the surface) and the modal damping ratio; ζ_1 are obtained.

c) Equivalent shear wave velocity and impedance

The surface soil layers is replaced to an uniform stratum with an equivalent shear wave velocity; V_{se} and an equivalent mass density; ρ_e and an equivalent damping ratio; ζ_1, which are calculated from properties in each layer.

$$V_{se}=\frac{1}{H}\sum_{i=1}^{n-1} V_{si} d_i \quad (6)$$

$$\rho_e=\frac{1}{H}\sum_{i=1}^{n-1} \rho_i d_i \quad (7)$$

where, $V_{si}=\sqrt{(G_i/\rho_i)}$ and H is the total thickness of the surface soil layers. The impedance of a wave motion; α between the equivalent uniform surface ground and the engineering bedrock is expressed as follows.

$$\alpha=(\rho_e V_{se})/(\rho_b V_{sb}) \quad (8)$$

where, V_{sb}: shear wave velocity, and

ρ_b: mass density.

d) Amplification of surface ground

The amplification, in frequency domain, of the uniform surface ground to the outcropped engineering bedrock is obtained by using the one-dimensional wave propagation. The transfer function of the surface ground and the engineering bedrock to the outcropped one are expressed as follows.

1) surface/outcropped engineering bedrock;

$G_s(T, \zeta_1, \alpha)$

2) engineering bedrock /outcropped;

$G_b(T, \zeta_1, \alpha)$

e) Response acceleration and displacement at ground surface at fundamental natural period T_1

The response acceleration of the ground surface; $A_s(T_i)$ and of the engineering bedrock; $A_b(T_1)$, and their response displacements; $D_s(T_1)$ and $D_b(T_1)$ are obtained as the product of the Fourier amplitude of the outcropped engineering bedrock; $F_{ao}(T_1)$ and the amplification factor of the surface ground.

$$A_s(T_1)=(1/T_1) G_s(T_1, \zeta_1, \alpha) F_{ao}(T_1) \quad (9)$$

$$A_b(T_1)=(1/T_1) G_b(T_1, \zeta_1, \alpha) F_{ao}(T_1) \quad (10)$$

$$D_s(T_1)=(T_1/2\pi)^2 A_s(T_1) \quad (11)$$

$$D_b(T_1)=(T_1/2\pi)^2 A_b(T_1) \quad (12)$$

f) Nonlinearity of surface ground

The relative displacement; u_i of the i-th mass points to that of the engineering bedrock is estimated by the following equation.

$$u_i=\{D_s(T_1)-D_b(T_1)\} \quad (13)$$

An effective strain; γ_{ei} is

$$\gamma_{ei}=0.65(u_i-u_{i+1})/d_i \quad (14)$$

An equivalent shear modulus; G_{ei} and an equivalent damping ratio; h_{ei} are calculated through the G-γ, h-γ relationships of soil properties.

g) Convergence judgement

Setting new values of soil properties (G_{ei}, h_{ei}), the evaluation is repeated from item b). The evaluation will be repeated until the natural period of the surface ground is converged.

h) Acceleration response spectrum at ground surface and engineering bedrock.

The acceleration response spectra at the ground surface and the engineering bedrock are evaluated as follows.

$$S_{as}(T, \zeta=0) \fallingdotseq F_{ao}(T)\, G_s(T, \zeta_1, \alpha)/(T/2\pi) \quad (15)$$

$$S_{ab}(T, \zeta=0) \fallingdotseq F_{ao}(T)\, G_b(T, \zeta_1, \alpha)/(T/2\pi) \quad (16)$$

i) Modification of acceleration response spectrum at ground surface

To estimate the acceleration response spectrum conservatively at the ground surface, the spectrum is modified as follows.

1) Connect the two peak points, by a straight line, of the acceleration response spectrum corresponding to the first and second modes of the surface ground, in order to avoid an excessive dip between those peaks.

2) Equalize the acceleration of the spectrum at the ground surface with that at the outcropped engineering bedrock in the very short period range.

(2) Examples of evaluation

a) Soil properties of surface soil layers

Figure 6 shows shear wave velocities (V_s) in several soil deposits, which are evaluated. These velocities are measured by the PS logging method. The soil layer with more than 400m/s of Vs is selected as the engineering bedrock. The model proposed by Ohsaki et al.[11] is used as the nonlinear characteristics of the surface ground. The mass density of the soil is around 1.6 to 2.0.

b) Acceleration response spectrum at ground surface

The amplification factors (transfer function) of the ground surface to the outcropped engineering bedrock are shown in Fig. 7. The figures include the results from three analytical methods in the following.

1) Transfer functions in case of multi-layers with V_s by the linear analysis (indicated with "LINEAR").

2) Ratios of acceleration response spectrum at the ground surface to that at the outcropped engineering bedrock, which are calculated through the program Shake (indicated with "SHAKE").

3) Transfer functions obtained through the proposed method (indicated with "METHOD")

The predominant periods of the surface ground subjected to severe earthquake motions are longer by 1.3 to 2.0 times than those to moderate earthquake motions because of nonlinear behavior of soils. The proposed method gives the shorter periods than those by Shake in Sites 3 and 4. The amplification factors in Sites 3 and 4 by the proposed one are a little less than those by Shake.

Figure 8 shows the acceleration response spectra at the surface, which are obtained by the proposed method and the Shake program. A seismic base shear force of buildings for medium soil deposits in the Building Standard Law, which is modified to the value for one degree of freedom is also included. The response spectra by the proposed method have a good agreement with those by the Shake program.

5.4 Hysteretic Characteristics and Equivalent Damping Ratio of Structure

A multi-story building structure is reduced to an ESDOF system as shown in Fig. 9. The reduction to ESDOF system is based on the result of a push-over static analysis by applying horizontal forces at each floor level. The force-displacement relationship of SDOF system is assumed that its force corresponds to the base shear (Q_B), and its displacement ($_1\Delta$) corresponds to the displacement at the height (h_e) where the natural modal participation function is equal to 1.0 ($\beta_1\{u\}_1=1.0$).

The equivalent damping ratio is defined by the viscous damping ratio, hysteretic dissipation energy, elastic strain energy of structure, and radiation effects of ground. Here,

the effects of soil-structure interaction are considered. As for the structure, the equivalent damping factor of SDOF system, h_{eq}, is given by the following equation (see Fig. 10).

$$h_{eq} = \frac{1}{4\pi}\left(\frac{\Delta W}{W}\right) \quad (17)$$

where,

ΔW: dissipation energy of SDOF system, and

W: potential energy in SDOF system ($= Q_B \cdot {}_1\Delta/2$)

Here, the dissipation energy of stationary hysteretic loop at the assumed maximum response of the structure can be calculated by the cyclic loop of the structure using the application of push-over static analysis, or based on the total of damping ratio of all members and joints to be considered.

5.5 Prediction of maximum response

The response spectrum method using equivalent linearization technique is applied as typical procedure for predicting the maximum earthquake response. In this method, as shown in Fig. 2(c), the intersection of the force-displacement curve of SDOF system and the required seismic performance spectrum is the maximum response point. In the Sa-Sd spectrum, the acceleration response is divided by the gravity acceleration, g. In general, the maximum response calculated by the equivalent damping h_{eq} obtained from Equation (17) is too small, because Equation (17) is theoretically valid in case of stationary vibration. In case of nonstationary vibration caused by earthquakes, h_{eq} based on the assumed response has to be reduced appropriately for predicting the maximum response. Through the examination under recorded and synthesized earthquake motions, and some hysteresis curves that consist of bi-linear or tri-linear skeleton curves such as normal bi-linear and Takeda models, the factor for reducing h_{eq} is examined. Figure 12 illustrates an example of the results on bi-linear skeleton curve shown in Fig. 11. Hysteresis curves are normal bi-linear, degrading bi-linear and slip bi-linear. The input earthquake motions are four that are a synthesized earthquake motion examined by the Building Center of Japan and three recorded earthquake motions; 1995 Kobe NS, 1968 Hachinohe EW and 1940 El Centro NS. In this analysis, there are some analytical parameters that are the natural period, yield stiffness and yield strength. The damping ratio of 2% except for the hysteretic energy dissipation is included. The equivalent damping ratio estimated is reduced to 70 percent of h_{eq}. As a result of comparison of the responses between the time history analysis and the equivalent linearization method, they have a good agreement on the whole, though the deviation becomes large at the range of large ductility.

6. CONCLUDING REMARKS

In this paper, presented is the state of the art of the performance-based building code in Japan, currently under development at BRI. In essence, performance-based provisions intend to provide as clearly as possible answers to the frequently raised questions: for what purpose, towards what objective, and for what conditions. The greatest advantage of this new approach lies on the fact that it focuses primarily on the achievement of the prescribed objectives, regardless of the methodology used.

The evaluation procedure presented in this paper is in essence a blend of ESDOF modeling of building structures with the site-dependent response spectrum concept, which makes possible the prediction of maximum structural response in case of major earthquakes without using time history analyses.

The proposed evaluation procedure also make it realistic and simple to predict the maximum structural response in case of major earthquakes as well as to confirm whether the predicted response values are smaller than the limit ones.

In the proposed evaluation procedure, the limit value referred to is the maximum value. Nevertheless, besides maximum values any other measures can be used, for example energy. In this case, both the response and limit values should be expressed in terms of energy.

ACKNOWLEDGMENT

This manuscript was stimulated by the authors' participation as members of the "Task Committee to Draft Performance-based Building Provisions" established at BRI, where they have shared their opinions with other members. They

would like to express their gratitude towards all of them.

REFERENCES

1) BCR: *For a New Building Administration Framework, which could cope with the economic & social changes and their prospects in the 21st century*, Building Council Report, March, 1997 (in Japanese).
2) BRI: *Towards performance-based standards*, BRI-H9 Autumn Seminar Notes, Building Research Institute, Ministry of Construction, November, 1997 (in Japanese).
3) Hiraishi, H., Midorikawa, M., Teshigawara, M., and Gojo, W.: *Development of Performance-Based Building Code in Japan -Framework of Seismic and Structural Provisions-*, Proc. of the 30th Joint Meeting of the U.S.-Japan Cooperative Program in Natural Resources Panel on Wind and Seismic Effects, Gaithersburg, Maryland, pp. 260-271, August, 1998.
4) Hiraishi, H., et al.: *Seismic Evaluation of Buildings by Acceleration Spectrum at Engineering Bedrock (Part 1-Part 13)*, Structures II, Summaries of Technical Papers of Annual Meeting, Architectural Institute of Japan, September, 1999 (in Japanese, to be published).
5) Shibata, A., and Sozen, M. A.: *Substitute Structure Method for Seismic Design in R/C*, Journal of the Structural Div., ASCE, Vol. 102, No. ST1, pp. 1-18, January, 1976.
6) Freeman, S. A.: *Prediction of Response of Concrete Buildings to Severe Earthquake Motion*, Douglas McHenry International Symposium on Concrete and Concrete Structures, SP-55, American Concrete Institute, Detroit, Michigan, pp. 589-605, 1978.
7) AIJ: *Seismic Loading - Strong Motion Prediction and Building Response*, Architectural Institute of Japan, 1992 (in Japanese).
8) AIJ: *Recommendation for the Design of Base Isolated Buildings*, Architectural Institute of Japan, September, 1989 (in Japanese).
9) ATC-40: *Seismic Evaluation and Retrofit of Concrete Buildings*, Report No. SSC 96-01, Applied Technology Council, November, 1996.
10) Ishiyama, Y.: *Base Shear Coefficient Obtained by Response Spectrum Method*, Structures II, Summaries of Technical Papers of Annual Meeting, Architectural Institute of Japan, pp. 621-622, October, 1987 (in Japanese).
11) Ohsaki, Y., et al.: *Stress-strain Model of Soils for Seismic Analysis*, 5th Japanese Earthquake Engineering Symposium, pp.679-704, 1978 (in Japanese).

Table 1 Requirements for Building Structures and Earthquake Motion Levels

Requirement	Earthquake
(a) Life Safety (to prevent failure of stories in structural frames)	Maximum Earthquake to be considered (earthq. records, seismic and geologic tectonic structures, active faults, etc.)
(b) Damage Limitation (to prevent damage to structural frames, members, interior and exterior finishing materials in order to avoid the conditions not satisfying the requirement (a) and others)	Once-in-a-lifetime Event (return period: 30-50 years)

Note: The deterioration of materials during the lifetime of a structure should be considered.

Table 2 Representative Illustration of Proposed Evaluation Procedures

Requirement		Earthquake
a) Life Safety	Level	Maximum Earthquake
	Response Value	Maximum Internal Force/Displacement
	Limit Value	Limit Strength/Displacement*1
b) Damage Limitation	Level	Once-in-a-lifetime Event (Return period 30 - 50 years)
	Response Value	Internal Force/Displacement taking place at each structural element
	Limit Value	Limit Strength/Displacement*2

*1 - Repeating cycles effect at plastic region of response to be taken into account.
*2 - The whole building structure behaves roughly within elastic range.
Notes :
1) The limit values corresponding to Maximum Event Level are determined based on the condition that equilibrium of forces and displacement compatibility in the structural system are guaranteed.
2) Displacement and acceleration related limit values, determined on the basis of the requirements for architectural, mechanical and electrical elements permanently attached to building structures, are thought to be considered in certain cases.

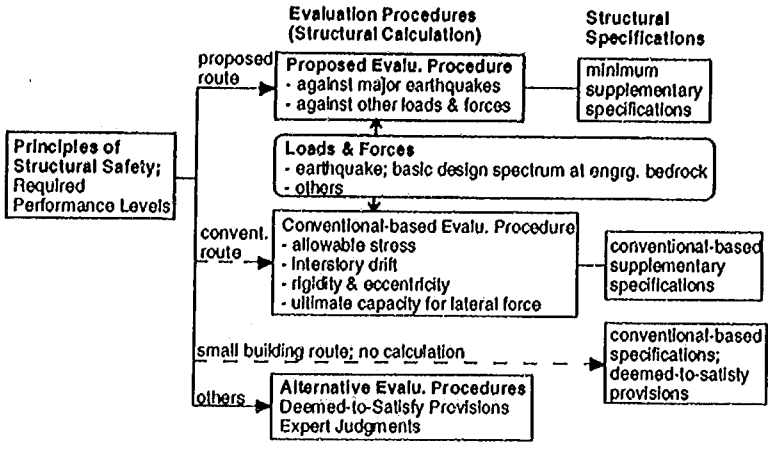
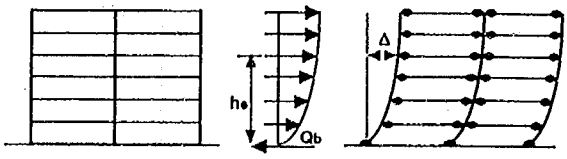
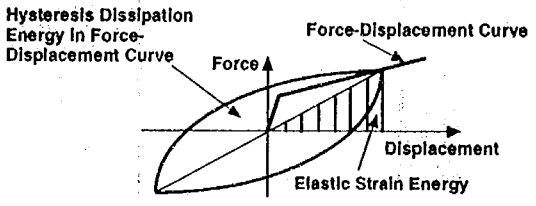


Fig. 1 Conceptual Framework of Proposed Performance-Based Structural Provisions

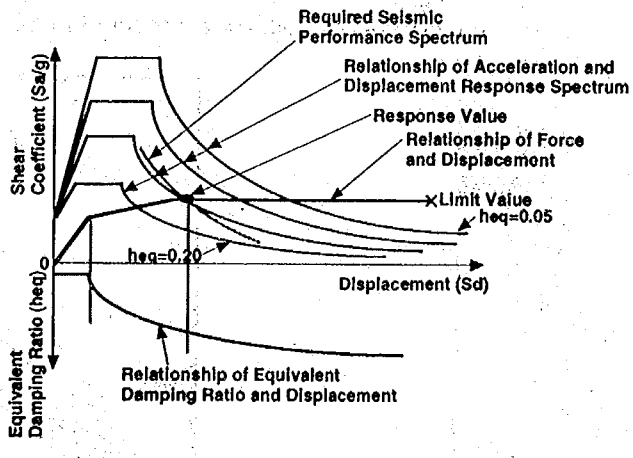


he : equivalent height
Δ : horizontal displacement at equivalent height
Qb : base shear force

(a) Structure Model and Inelastic Response



(b) Energy for Equivalent Damping Ratio



(c) Comparison of Expected Response Values and Estimated Limit Values

Fig. 2 Illustration of Proposed Evaluation Procedure for Major Seismic Events

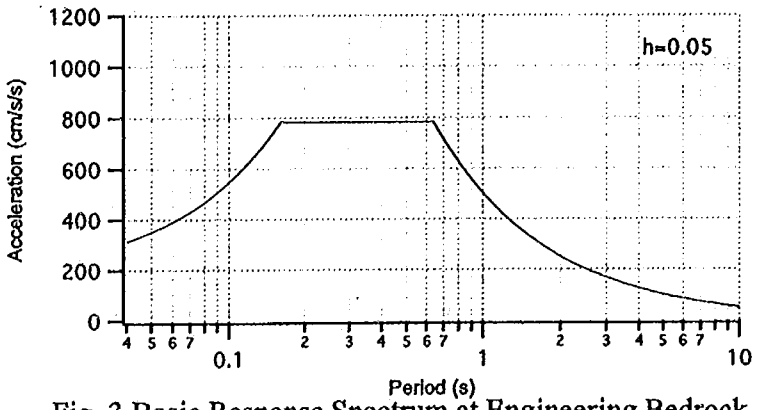


Fig. 3 Basic Response Spectrum at Engineering Bedrock

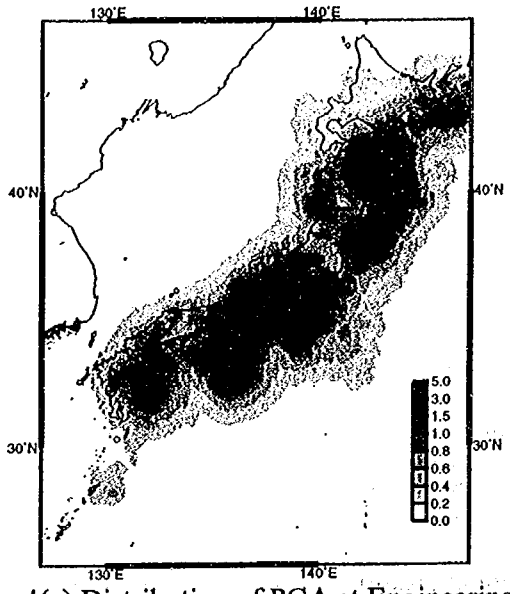


Fig. 4(a) Distribution of PGA at Engineering Bedrock expected in 50 years (normalized with 0.064g)

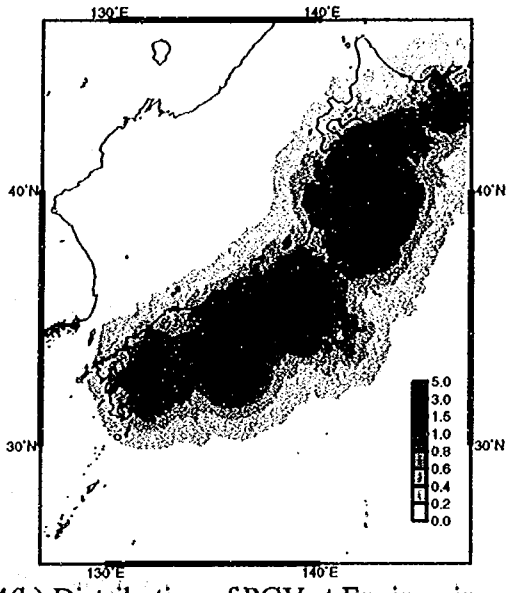


Fig. 4(b) Distribution of PGV at Engineering Bedrock expected in 50 years (normalized with 8 cm/s)

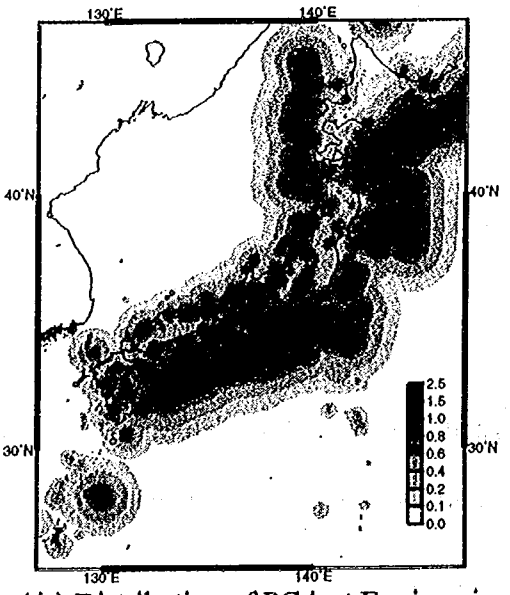


Fig. 4(c) Distribution of PGA at Engineering Bedrock expected in 500 years (normalized with 0.32g)

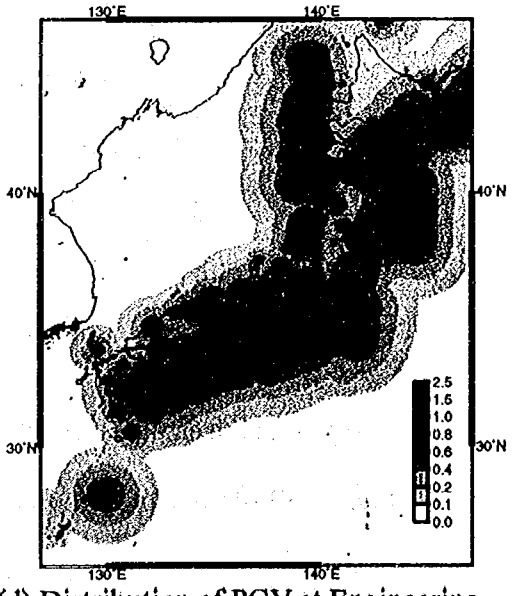


Fig. 4(d) Distribution of PGV at Engineering Bedrock expected in 500 years (normalized with 40 cm/s)

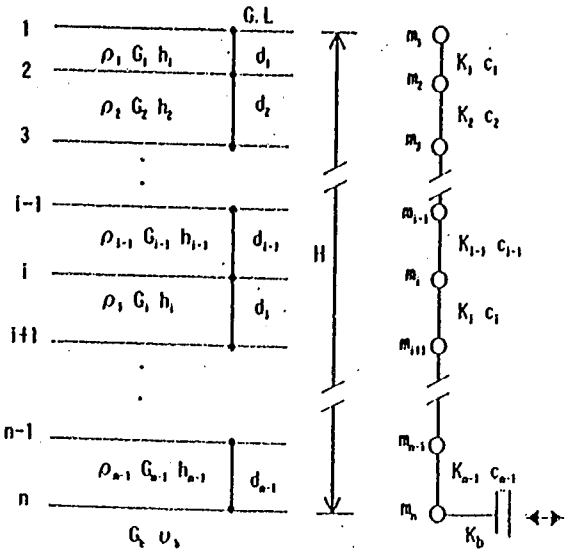


Fig. 5 Analytical Model of Surface Soil Layers

Fig. 6 Shear Wave Velocity Distribution at Several Sites

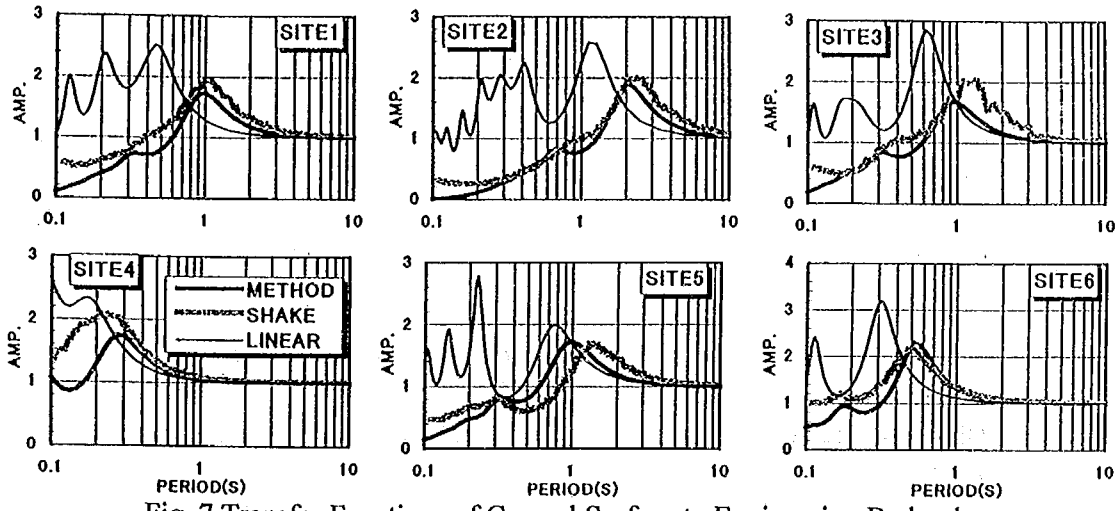


Fig. 7 Transfer Functions of Ground Surface to Engineering Bedrock

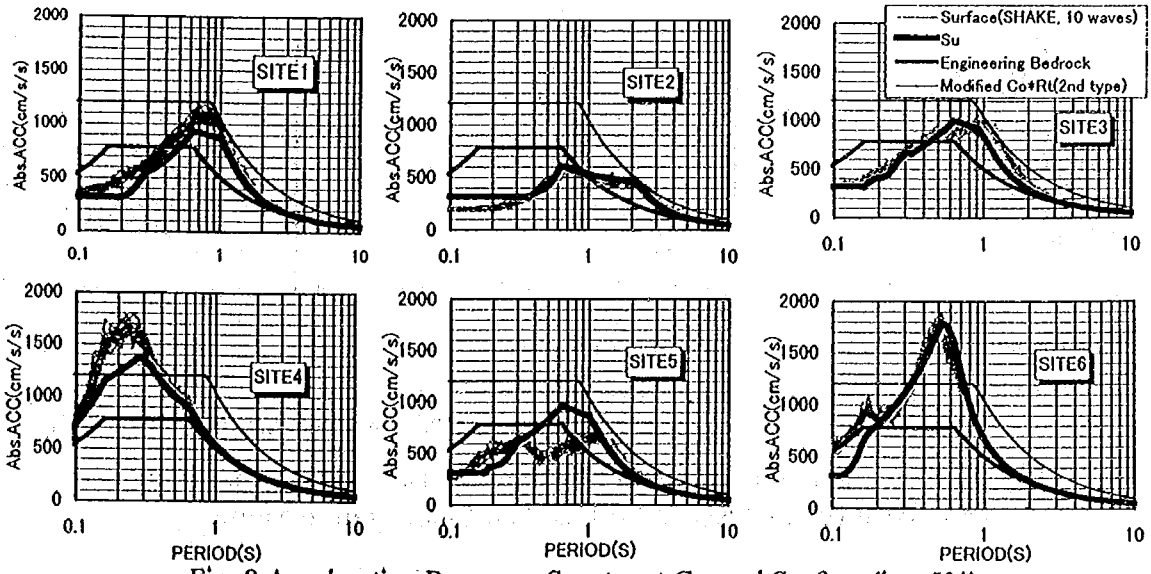


Fig. 8 Acceleration Response Spectra at Ground Surface (h = 5%)

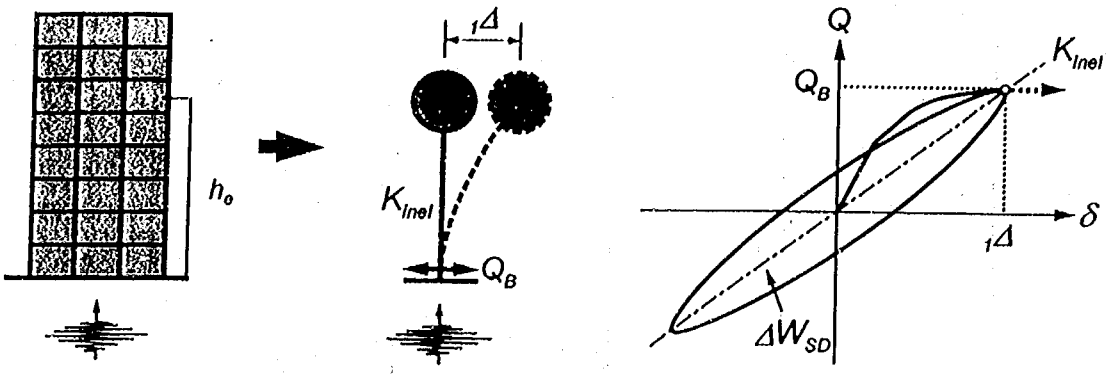


Fig. 9 Reduction to Single-Degree-of-Freedom System

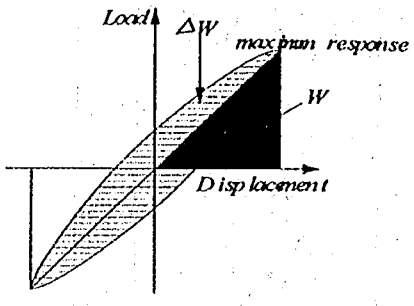


Fig. 10 Hysteretic Dissipation Energy and Potential Energy

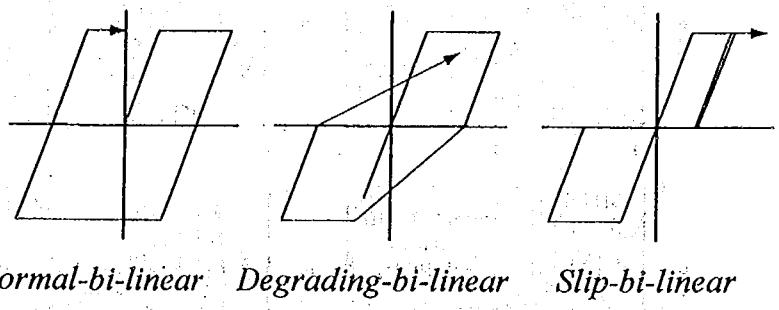


Fig. 11 Analytical Hysteresis Models

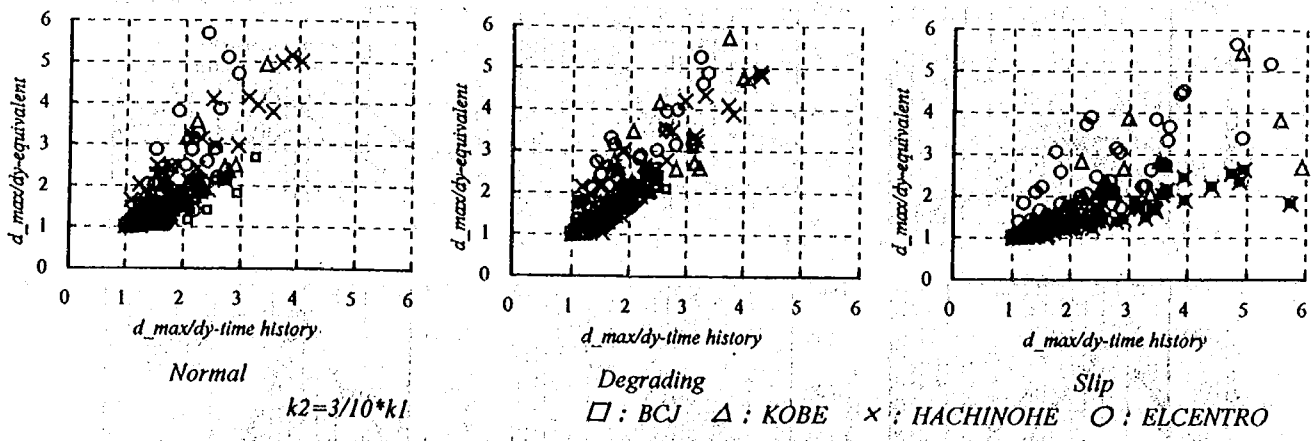


Fig. 12 Comparison of Maximum Response Displacements between Time History Analysis and Equivalent Linearization Method

Seismic Performance of an Existing RC Frame Retrofitted by Preacast Prestressed Concrete Shear Walls

by

Mizuo INUKAI[1], Takashi KAMINOSONO[2]

ABSTRACT

This paper describes the seismic performance of a new retrofit method. This new retrofit method is using precast prestressed concrete shear walls on outer frames of an 5 storeys existing reinforced concrete building.

In order to develop this new retrofit method, two types of specimens were carried out. One type is a part of a pressure joint between the shear wall and the existing column or beam, and another is a frame part which is lower 2 storeys of this 5 storeys building.

Key Words: Finishing Mortar
Hyougoken Nanbu Earthquake
New retrofit method
Precast Prestressed Concrete Shear Wall

1. PURPOSE

Since the 1995 Hyougoken Nanbu Earthquake, the retrofits for the old buildings are done but there are few researches about the retrofit method which the resident people can use it continuously during this retrofit.

Therefore, it is needed to develop the retrofit method using a precast reinforced concrete shear wall on the surface of existing reinforced concrete frame structure without taking out the mortar in finishing(Fig.1 and Fig.2).

So, this paper describes the experiments about this retrofit method and these seismic performance. The experiments include the element part which means a part of the shear wall and the existing column or beam(Fig.3, Photo 1 and Table 1), and the frame part which means a 2 storeys shear wall retrofitting the existing frame(Fig. 5, Fig.6, Photo2, Table2 and Table3).

2. OUTCOMES

The element specimens are parts of a shear wall connecting with a column or a beam by prestress bars. The parameter of these specimens is to include the finishing mortar or not between the shear wall and the column or the beam. These specimens make clear the friction property between the shear wall and the column or the beam.

The frame specimen is a 2 storeys precast prestressed concrete shear wall connecting with 2 storeys reinforced concrete frame structure by prestress bars. This specimen is supposed to be a lower part of the 5 storeys old building which is constructed before the building code was modified. And this building's seismicity is appropriately a half of new buildings.

3. CONCLUSIONS

It is possible to use the retrofit method which includes the finishing mortar because the element specimens have the sufficient property to transfer the shear strength between the shear wall and the column or the beam(Fig 4).

And it is made clear that the precast prestressed concrete shear wall is available for the retrofitting the old buildings because the frame specimen has the sufficient performance to increase the seismicity of the old buildings(Fig 7 and Fig 8).

---

1) Senior Research Engineer, Structural Division, Department of Structural Engineering, Building Research Institute, Ministry of Construction, Tsukuba-shi, Ibaraki-ken, 305-0802, Japan)

2) Associate Director for International Codes and Standards, Codes and Evaluation Research Center, ditto.

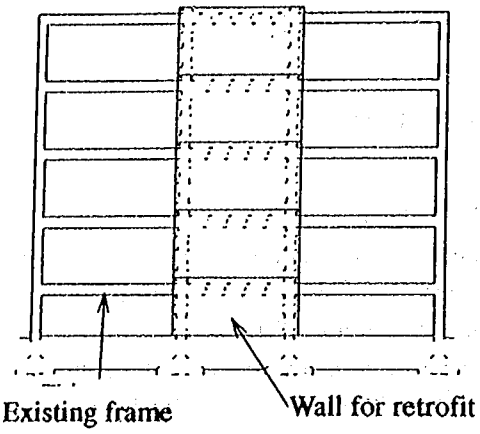


Fig 1 Retrofit of outside wall

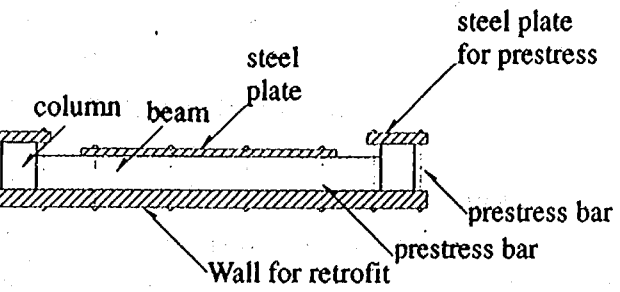


Fig2 Detail of wall and existing frame

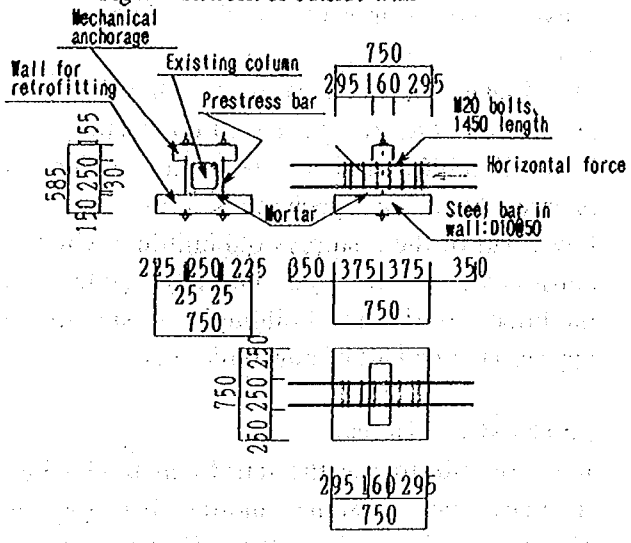


Fig.3-1 Specimen CW-M

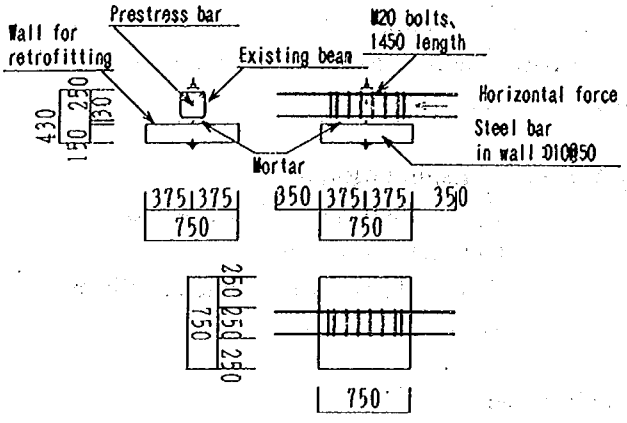


Fig.3-2 Specimen BW-M

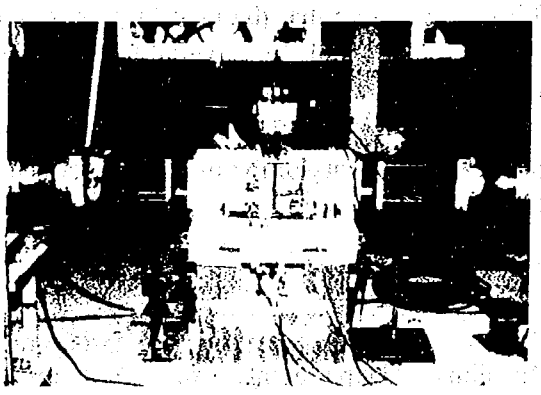


Photo 1 Test of element part specimen CW-M

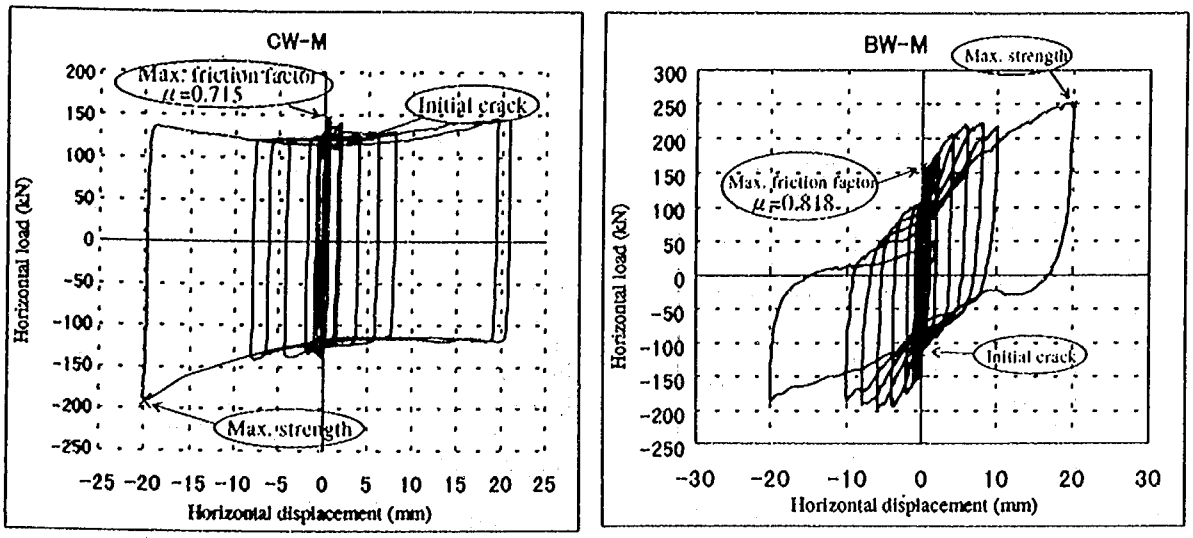
(Depth of a pressure joint:30mm)

Table 1 Material properties of concrete, mortar and grout

Specimen	Part	σc	Ec
CW-M	column	27.4	2.70
	wall	45.3	2.84
	mortar in a pressure joint	16.7	2.83
BW-M	beam	28.4	2.73
	wall	40.7	2.77
	mortar in a pressure joint	24.5	2.69
	grout	5.8	1.74
CW	column	30.7	2.63
	wall	45.1	2.73
BW	beam	30.9	2.58
	wall	45.1	2.55
	grout	6.0	0.71
CW、BW	paste in a pressure joint	51.4	1.76

notes) σc : compressive strength(N/mm^2)

Ec : Young's modulus $\times 10^4$(N/mm^2)



a) Specimen CW-M
(element part of column and wall)
(Pressure by prestress bars:200kN)

b) Speciment BW-M
(element part of beam and wall)
(Pressure by a prestress bar:200kN)

Fig. 4 Relationship between horizontal load and displacement of element part specimens

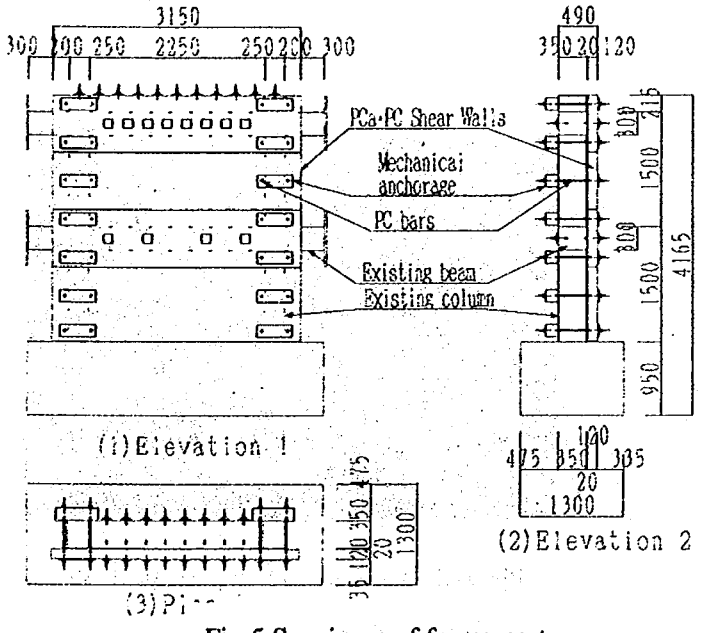


Fig.5 Specimen of frame part

Notes)
(1)Pressure force in horizontal joints of shear walls: 2,040kN
(2)Pressure force between beams and shear walls: 3,170kN
(3)Pressure force between columns and shear walls: 8,000kN

Table 2 Material properties of concrete, mortar and grout

Part	σc	Ec	εc
Concrete of columns and beams	2.7	2.16	2,530
Concrete of PCa·PC shear walls	3.4	2.54	2,300
Mortar in horizontal connections of shear walls	5.3	2.43	2,897
Mortar in prestressed connections between shear walls and a frame	5.7	2.40	3,523
grout	7.3	1.72	5,487

notes) σc : compressive strength(N/mm^2)
Ec : Young's modulus $\times 10^4$(N/mm^2)
εc : stress at compressive strength
$\times 10^{-6}$(mm/mm)

Table 3 Material properties of steel bars and prestress bars

Type	σt	Es	εs	σo
Steel bar D19(SD345)	38	1.81	2147	56
Steel bar D16(SD295)	36	1.79	2087	51
Steel bar D6(SD295)	38	1.93	1979	55
Prestress bar φ23(SBPR 1080/1230)	1154	2.03	5685	1247
Prestress bar φ17 (SBPR 1080/1230)	1150	2.02	5693	1238

notes) σt : yield strength(N/mm^2)
Es : Young's modulus $\times 10^5$(N/mm^2)
εs : stress at yield strength
$\times 10^{-6}$(mm/mm)
σo : tensile strength(N/mm^2)

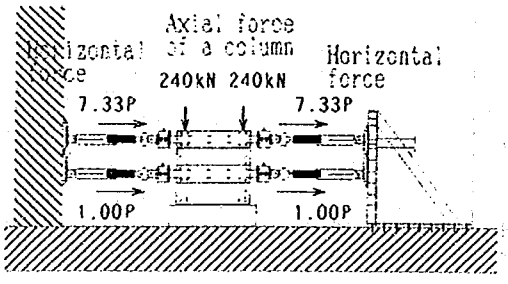


Fig.6 Loading test of Specimen of frame part



Photo 2 Test of the frame part specimen

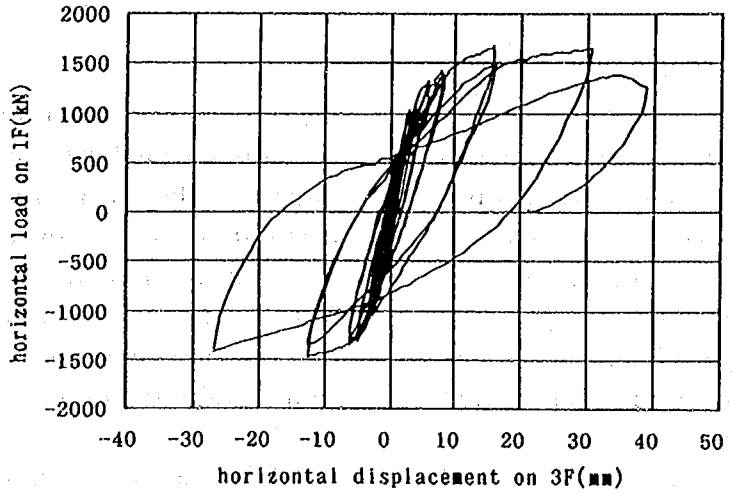


Fig.7 Relationship between load and displacement

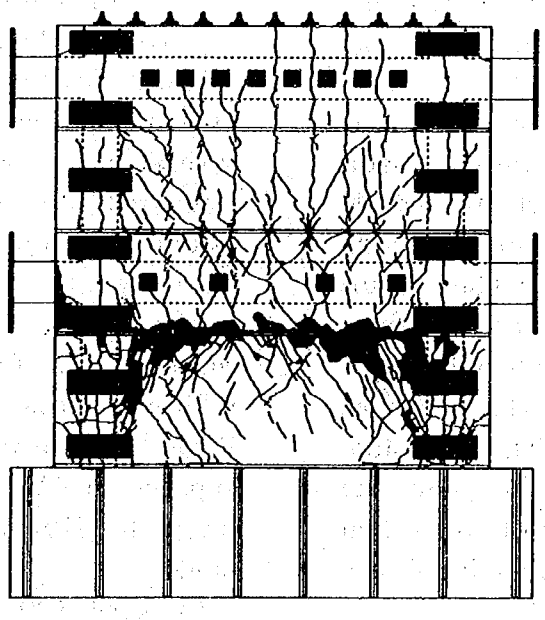


Fig.8 Cracks

Construction of GSI's Nationwide GPS Array

Shin-ichi MIYAZAKI,

ABSTRACT

The Geographical Survey Institute has operated the nationwide GPS array since October 1994. This network is designed both for crustal deformation monitoring and to serve as a highly precise geodetic network in the GPS age. This network has precisely monitored crustal deformation within several millimeters horizontally and several centimeters vertically. Most of the processing is carried out automatically.

This network is the densest GPS array in the world. It consists of 949 observation sites, and data analysis center in GSI campus for daily processing. In this system, three major software, Bernese, GAMIT, and GIPSY are all available. Since we collected more than one-year data, we estimated horizontal crustal velocity field with respect to stable interior of the Eurasian plate by using one-year continuous data. The result suggests that a plate boundary runs from Shizuoka to Niigata. The western half of it moves eastward except for the southern part of Shikoku Island and Kii Peninsula, where interplate coupling between the Eurasian plate and the Philippine Sea plate is observed. On the other hand, the eastern half moves westward.

1. INTRODUCTION

Japan is located on an extremely active tectonic region. As is known, four plates, the Eurasian (or the Amurian) ,the North American (or the Okhotsk) ,the Philippine Sea, and the Pacific plates, are interacting, and crustal strain is continuously accumulating, so it is inevitable that large earthquakes occur in Japan as the strain releases. Such strain accumulation is observed as a crustal deformation in some cases. Therefore, it is important to monitor the crustal deformation using geodetic data in order to understand the tectonic situation of the crust.

Historically, triangulation and triangulation data have been used to study regional tectonics; while VLBI (Very Long Baseline Interferometry) and SLR (Satellite Laser Ranging) are used to investigate global tectonics such as plate motion. In addition to these techniques, GPS (Global Positioning System) and SAR (Synthetic Aparture Rader) are becoming great tools for tectonic study. GPS has several advantages for tectonic study compared to other techniques. For example, data are collected continuously on every site. Also, GPS is cheaper and more compact, and therefore it is easier to construct lots of observation stations than it is with other space geodetic systems. Regarding spatial resolution, GPS is not superior to SAR, so, recently, attempts to integrate GPS and SAR data have been made.

In April 1994, the Crustal Dynamics Department began to operate the COSMOS-G2 (Continuous Strain Monitoring System with GPS by GSI) (Iwata 1994; Sagiya et al, 1995) in order to monitor the crustal deformation in South-Kanto and Tokai areas. After that, in October, 1994, the Geodetic

Department also began to operate the nationwide GPS array, Grapes (GPS Regional Array for Precise Surveying/ Physical Earth Science) (Iimura et al, 1994, Miyazaki et al, 1996) . Both networks successfully detected coseismic and potseismic displacements associated with earthquakes. But, the mean distance of Grapes sites was about 100km, which was not enough to monitor local crustal deformation. Also, to construct active controlling points by GPS, the number of Grapes sites was far from enough. To achieve these purposes, GSI combined COSMOS-G2 and Grapes, and added 739 new sites; the number of sites is now 949 in total. This network is named GEONET (GPS Earth Observation Network).

2. THE OUTLINE OF THE NEW GSI's GPS ARRAY

GEONET consists of 949 permanent GPS observation stations in Japan and a data analysis center at GSI in Tsukuba. The outline of the system is presented in this chapter.

2.1 Observation station

Figure 1 shows a picture of an antenna station pillar at Umaji (Kochi pref) station. Requirements for the observation station are:

(1) stable ground,
(2) wide over-view to avoid cutting off of signal,
(3) electric power supply,
(4) availability of telephone lines, and
(5) accessibility to the point for maintenance.

As a result, most of sites are in school campuses or parks in the suburb.

Each GPS station consists of a tower, an antenna, a GPS receiver, data transfer instruments, and an electric battery for emergencies. The tower is made of stainless steel and is 5m high with a 2m firm ground base. The tower can endure strong winds up to 60m/s. For temperature control in the storage box, a ventilator and a heater are attached. The antenna is mounted on the top, and the GPS receiver and data transfer instruments are placed in the central body of the tower (Figure 2) . The data obtained is transferred to the data analysis center at GSI in Tsukuba through public telephone lines. Since this system uses 24-hour data every day, the digital telephone line ISDN (Integrated Services Digital Network) is used for most of sites to reduce communication costs. Several stations still use analog telephone lines because ISDN is not available. They will be replaced with ISDN as soon as it becomes operational in those areas.

At most sites, sampling rate is 30 seconds, but at 120 sites, the data sampling rate is one second, among which 30 seconds data are usually transferred to Tsukuba. When trigger is pulled by a shake, one second sampling data are stored by the receiver and transferred. We use Trimble 4000 SSi and SSE for 704 sites, TOPCON GP-RIDY (equivalent of Ashtech Z-12) receivers for 211 sites, and , Leica receivers for 34 sites, all of which can receive carrier phase data and P-code data even under the A-S (Anti-Spoofing) condition.

Every receiver has enough internal memory to retain about 10 days of data in case of an emergency situation. Option of data transfer and observation programs can be changed from data analysis center through telephone lines. During an electrical power outage, the electric

battery can supply electricity for five hours.

2. 2 Data analysis center

The data analysis center is located at GSI in Tsukuba. It consists of data management servers, analyzing servers, a data supplying controlling server, a data transferring server, and so on (Figure 3) .

Data management servers download observation data from each site at a certain time every day. The data from each station amounts to 1 MB per day except for 1-second sampling data, which amounts to 30 MB. It takes about 3~20 minutes to transfer the data. Since 32 telephone lines are available, it takes about 3.5 hours to complete data transfer for the entire network every day. Analyzing servers process baseline analysis and display site displacement, strain, and temporal variation of baseline vector component. The data controlling server presents data into an disk array system which can store 420 GB data. Data and solution files are classified into several categories: raw data, RINEX data, solutions of baseline analysis, and solutions of network adjustment. Data stored in disk array are always available online.

3. DATA PROCESSING

3. 1 Overview

Although the precision of one session of GPS observation is, in general, worse than that of VLBI (Very Long Baseline Interferometry) and SLR (Satellite Laser Ranging) , the accuracy is better than them as long as the observation is continuously taking place everyday.

Recently, the repeatability of continuous GPS observation is, typically, 5 mm horizontally and 1. 5 cm vertically.

In addition to that, we can improve the accuracy by using appropriate statistical analysis methods, such as trend estimation or detection of outliers. Thus, it is becoming increasingly feasible to understand both global and regional crustal deformation.

In order to achieve this goal, we have adopted of three major GPS analysis software's for routine processing; one is BERNESE developed by Bern University in Switzerland, the second is GAMIT/ GLOBK developed by MIT (Massachusetts Institute of Technology) and SIO (Scripps Institution of Oceanography, University of California at San Diego) in the U. S., and the third is GIPSY developed by JPL (Jet Propulsion Laboratory) in the U. S.

Since these software's estimate the tropospheric delay of radio waves simultaneously, precision is also getting better in these days: typically 5 mm horizontally and 1.5 cm vertically.

Directory Structure

The directory /DM/NewGard is where the software's and configuration files are stored. There are subdirectories for each software package that store information about the solution types and strategies that have been defined for each software system. There are two subdirectories that store information about what solution types (stif) and strategies (strat) are available to the system. Additional configuration files are stored in /DM/NewGard and /DM/NewGard/ ⟨pkg.⟩ (⟨pkg.⟩ is the name of the selected software package) . The basic structure is displayed in Figure 4.

The stif file is essentially input/

output files (iof) without full session information. GEONET uses the stif file as a template to generate the iof files that are given to the various software packages when an actual session is started. It will be the job of GEONET job submission routine to determine the session information.

The strat file defines what strategies are available. The contents of these files are only the description of what the strategy is and is used by GEONET in order to know what strategies are available. The actual strategy has to be developed and implemented within the native software system.

3. 2 Analyses Strategies

In daily processing, we are currently using both combined ephemerides (rapid/predicted ephemerides) and IGS final ephemerides. The precision of combined ephemerides is worse than IGS final ephemerides. Therefore, in this paper, we will show only the analysis strategy with IGS precise final ephemerides.

3. 2. 1 BERNESE

The basic idea for BERNESE processing is displayed in Figure 5. First, we divide the entire network into two clusters by receiver/antenna types. Both clusters include Tsukuba site, so, at the first stage, ITRF coordinates of these two Tsukuba sites are obtained from Tsukuba-IGS site. Next, two clusters are processed by giving tight constructs to these two sites. Trimble cluster consists of 704 sites. It is still difficult to process as one cluster, so we divided this cluster into a backbone cluster and regional clusters. The backbone cluster, displayed as Figure 6, is a nationwide, sparse cluster, and ITRF coordinates of each site are obtained through Tsukuba-Trimble site. Also, each regional cluster, displayed in Figure 7, is processed, and then, combined with backbone cluster through several sites commonly involved both in backbone and regional clusters.

Ashtech cluster and Leica cluster are processed as one cluster, respectively (Figure 8, Figure 9) , and ITRF coordinates are obtained through Tsukuba-Ashtech, Tsukuba-Leica site, respectively.

Thus, all site coordinates are obtained in ITRF coordinate.

3. 2. 2 GAMIT / GLOBK

GAMIT / GLOBK processing takes place in two steps. In the first step, GAMIT analyzes data from user-specified and automatically determined clusters of stations to create loosely constrained (but ambiguity-resolved) estimates of station coordinates. In the second step, GLOBK combines these GAMIT output files to create solution files in the SINEX format, containing loosely constrained estimates for the entire network. The scheme could be adopted for clusters as small as two stations or as large as the memory and swap allow dimensioning of GAMIT. However, initial testing has been restricted to 20- and 35- Station clusters — large enough to make cleaning and ambiguity resolution robust but small enough to keep GAMIT run times reasonable. Also, the procedure for selecting stations for clusters is currently as follows: stations are first sorted by antenna type and then within each antenna grouping are selected in latitude bands to fill each cluster as evenly as

possible up to its maximum number, with two stations overlaps. This software is now under examination, so a detailed strategy has not been decided yet.

3. 2. 3 GIPSY

Precise Point Positioning (PPP) is adopted as GIPSY processing. PPP is a developed technique for analysis of GPS data for precise geodetic purposes Zumberge et al., (1997) . With PPP, the amount of CPU time increases linearly with the number of stations, rather than geometrically as in conventional multi-station analysis. Hence, it is suitable for precise analysis of large numbers of stations like GEONET, or to rapid analysis of a few stations.

On GEONET, PPP uses both IGS precise and rapid GPS orbital and GPS satellite clock estimates from an analysis by six GSI sites around Japan and IGS or broadcast ephemerides. The GPS orbits and clocks are fixed (not estimated) , and the stations are analyzed one at time. The solution files are then merged at the end in order to obtain the final solution file with all the stations in SINEX format.

When both the GPS satellite orbits and GPS satellite clocks are fixed and not estimated, all correlations between stations are zero. This enables us to break the solution up into N smaller estimation runs (N = number of stations) and obtain the identical estimates and covariances for the bias free station positions.

3. 3 Products

Solution files obtained by Bernese, GAMIT/GLOBK , and GIPSY are translated into SINEX format. Since SINEX format files include full covariance matrix, its size is up to 80 MB for each day routine solution except by GIPSY. However, SINEX format is now the same standard format as GPS solution files. Actually, IGS analysis centers submit their solution files in SINEX format. Three major software's can now treat SINEX format, so it is getting easier to combine several SINEX files into one SINEX file using these software's.

3. 4 Output from GEONET

On the display of GEONET, we can look at several kinds of results obtained by routine analysis. This interface is so convenient that users can look at and print out the results only by selecting menus by a mouse. . Figure 9 is the main menu display of GEONET. We can select displacement vector plot map, time series of each component of each observation site, time series of baseline length, and strain map. Currently, displacement vector map and strain map are displayed by appointing observation site name (velocity or strain rate map are not been supported yet) . Figure 10 shows an example output of displacement vector for southwest Japan. Each vector shows displacement from the 15-day-average from Apr. 1～Apr. 15 in 1996 and the 15-day-average from Dec. 17～Dec. 31 in 1996. The reference point is Nita, marked with an asterisk.

Thus, several kinds of figures are easily printed out without special knowledge about GPS analysis.

4 .VELOCITY FIELD OF JAPAN

We can get site velocities by applying a simple least square method to the time series of site coordinates. Hence, we show the example of the time series (Figure 11).

In the vertical plot, significant annual term is observed for all GEONET sites. On

the other hand, we see much smaller annual term in horizontal plot. Therefore, we estimated only horizontal site velocities using one-year data for the protection to the annual variation. As to the reference frame, we deploy the kinematic reference frame defined through VLBI analysis (Heki, 1996). According to Heki (1996), the site velocity of Tsukuba is 20.5 mm/yr westward and 2.7 mm/yr southward with respect to the stable region of the Eurasian Plate. We fixed the velocity of Tsukuba to this value. Then, we got the velocity field of Tsukuba to this value. Then, we got the velocity field of Japan using one year data (1996/4/6 - 1997/4/19), and display it in Figure 12.

This result demonstrates various tectonic features. First of all, as the whole, the velocity pattern is significantly different among the southwest Japan (SWJ) and northeast Japan (NEJ). The SWJ is basically moving westward with respect to the Eurasian Plate. This result suggests several possibilities. For example, SWJ belongs to the different plate from the Eurasian Plate, the Amurian Plate (Zonnenshain and Savostin, 1983), which is supposed to move eastward with respect to the Eurasian Plate (Ishibashi, 1983). Other possibility is the local deformation such as upwelling of plume in the Yellow Sea, northwest of Kyushu district (Seno, 1997). The velocity structure changes near the Median Tectonic Line (MTL), and the southern site of MTL moves northwestward with respect to the Eurasian Plate. This reflects the interplate coupling between the Eurasian Plate (here, we suppose this area belongs to the EU) and the Philippines Sea Plate. Tabei et al., (1997) estimated the interplate coupling by using this velocity field, and concludes that the coupling is considerably high on the plate boundary off the Kii Peninsula and Shikoku Island. On the contrary, the velocity of Kyushu Island is more complex. We had three earthquakes during the observing period, and at least two of them, Hyuga-nada-oki earthquakes, have significant postseismic deformation. We are now doing the correction of the co- and post- seismic effects.

The velocity field of the NEJ is also complex. This region is considered to belong to the Okhotsuk Plate, the Pacific Plate, and the Eurasian Plate, so sites of the Pacific coast side have large westward velocity, and others of the Japan Sea coast side have small westward velocity. This implies the interplate coupling between the Okhotsuk Plate and the Pacific Plate. However, the northern part of the Tohoku district shows significantly different aspect; that is, the westward velocity is smaller than other part. This suggests that the interplate coupling is much smaller off this area. This weaker plate coupling is attributed to the 1994 Sanriku Haruka Oki earthquake. Heki et al. (1997) analyzed the long-term post-seismic deformation of the earthquake (Figure 13). We suppose that even after the long term after slip, the interplate coupling has not been recovered. This is one of the healing process of large earthquake occurs on plate boundaries (rupture -> relaxation -> decoupling -> coupling). Hokkaido shows more complicated aspect along the southwest coast, like as the Pacific side of Tohoku district, interplate coupling is observed and the norm of velocity vector gets smaller in the central Hokkaido. However, in the southwestern coast,

westward motion becomes larger again. One speculation for this is the viscoelastic effect of the Hokkaido-Nansei-Oki earthquake, occurred in July, 1992. Compared to such complex crustal deformation in the southern Hokkaido, the northern Hokkaido does not reveal any significant deformation. This region may be a relatively stable region of the Okhotsuk Plate.

Like above, we divided Japan into SWJ and NEJ. The boundary between these two regions is considered to be a plate boundary. Traditionally, the Itoigawa-Shizuoka Tectonic Line (ISTL) has been the most possible candidate as the plate boundary. As an anti-these, Tada (1983) proposed a new boundary, which runs from Shizuoka to not Itoigawa but Niigata by analyzing triangulation data. Our velocity field supports his result (Figure 14). Therefore, as long as we look at crustal surveying data, plate boundary runs eastward of the Sado Island.

5. CONCLUSION

GEONET is a powerful system both to monitor spatial temporal crustal deformation and to serve as an active controlling system for GPS surveying.

Three major powerful software's are available for this system. And, crustal displacement velocity field has been obtained.

GEONET deploys more than 900 permanent observation sites. The density of observation sites will be higher than that of the first order triangulation points. Therefore, this system is expected to serve as the backbone survey network of Japan.

REFERENCE

Iimura. Y, K.. Kobayashi, and H.. Morishita (1996) :
Establishment of the nationwide GPS array, Biannual Report of the Geographical Survey Institute, 95, 1- 5. (in Japanese)

Iwata. E. (1995) : Crustal deformation monitoring in southern Kanto-Tokai area using GPS continuous observation network, Biannual Report of the Geographical Survey Institute, 81. (in Japanese)

Miyazaki. S, H. Tsuji, Y. Hatanaka, Y. Abe, A.. Yoshimura, K. Kamada, K. Kobayashi, H. Morishita, and Y. Iimura (1996) : Establishment of the nationwide GPS array (GRAPES) and its initial results on the crustal deformation of Japan, Bulletin of Geographical Survey Institute, 42, 27-41.

Sagiya. T, A. Yoshimura, E. Iwata, K. Abe, I . Kimura, K. Uemura, and T. Tada (1995) : Establishment of permanent GPS observation network and crustal deformation monitoring in the southern Kanto and Tokai areas, Bulletin of Geographical Survey Institute, 41, 105-118.

Zumberge. J. F., M. B. Heflin, D. C. Jefferson, M. M. Watkins, and F. H. Webb (1997) : Precise point positioning for the efficient and robust analysis of GPS data from large networks, Journal of Geophysical Research, 102, 5055-5017.

Figure 1 The antenna station pillar at Umaji (Kochi pref) .

Figure 2 The central body of the tower.

Figure 3 The data analysis center at GSI in Tsukuba.

Figure 4 Directory Structure.

Figure 5 Clustering strategy for New network by BERNESE.

Figure 6 The back-bone cluster of Trimble site network used in Bernese daily processing.

Figure 7 An example of regional Trimble cluster.

Figure 8 Ashtech cluster

Figure 9 The Main Menu display of the new GSI's GPS the system.

Figure 10 Example output of displacement vector.

Figure 11 An example of time series of site coordinates

Figure 12 Horizontal displacement velocity field of Japan derived from one-year continuous GPS data (Apr.6, 1996 – Apr.19, 1997)

Figure 13 Long term post-seismic deformation following 1994 Sanriku Haruka Oki earthquake (after Heki et al., 1997)

Figure 14 Horizontal crustal deformation of the central part of Honshu Island. (Observation period: Oct.1, 1996 – Jun.14, 1997, dot line shows the proposed plate boundary, solid lines show active faults.)

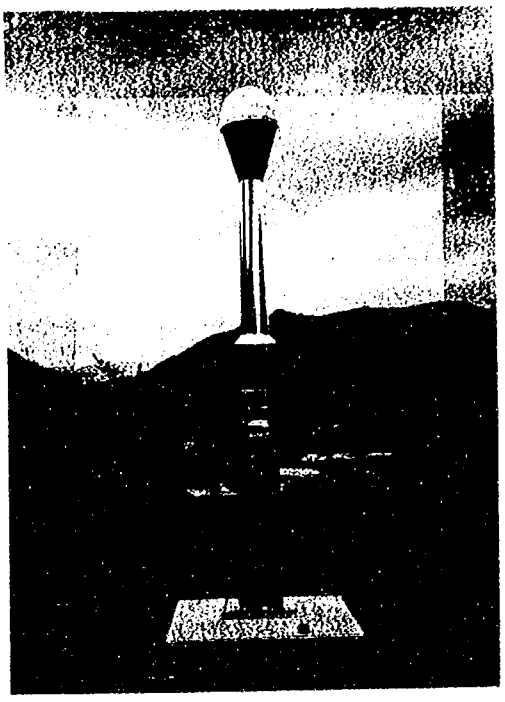


Figure 1 The antenna station pillar at Umaji (Kochi pref) .



Figure 2 The central body of the tower.



Figure 3 The data analysis center at GSI in Tsukuba.

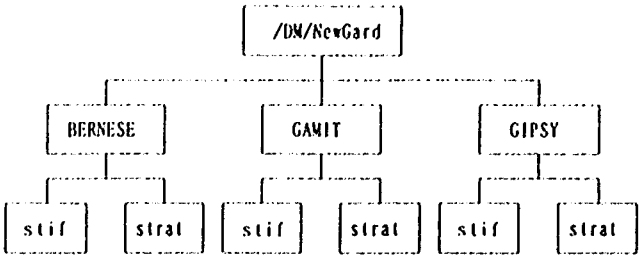


Figure 4 Directory Structure.

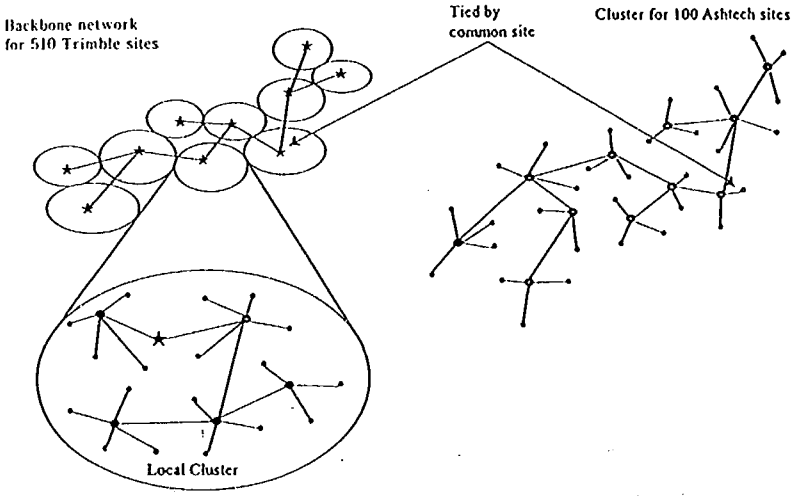


Figure 5 Clustering strategy for New network by BERNESE.



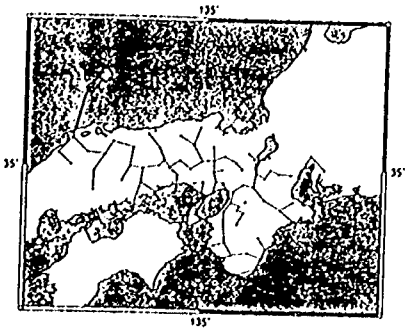


Figure 7 An example of regional Trimble cluster.

Figure 6 The back-bone cluster of Trimble site network used in Bernese daily processing.



Figure 8 Ashtech cluster



Figure 9 The Main Menu display of the new GSI's GPS the system.

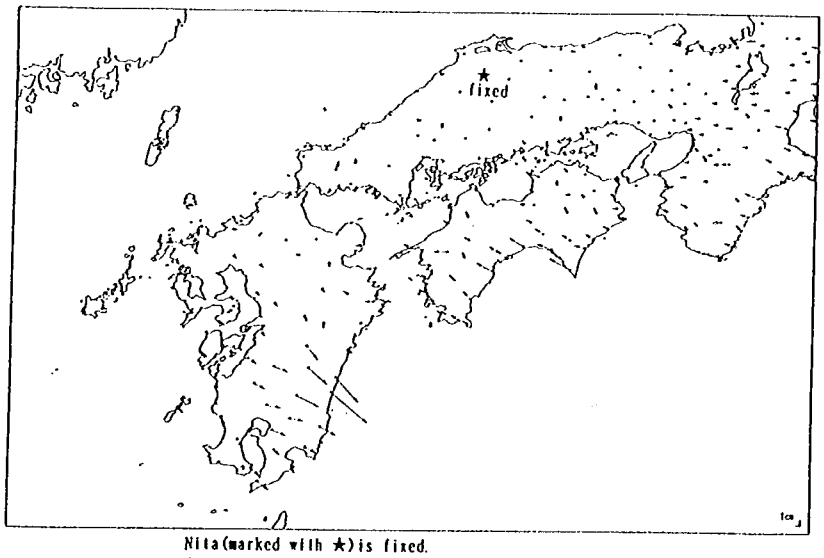


Figure 10 Example output of displacement vector.

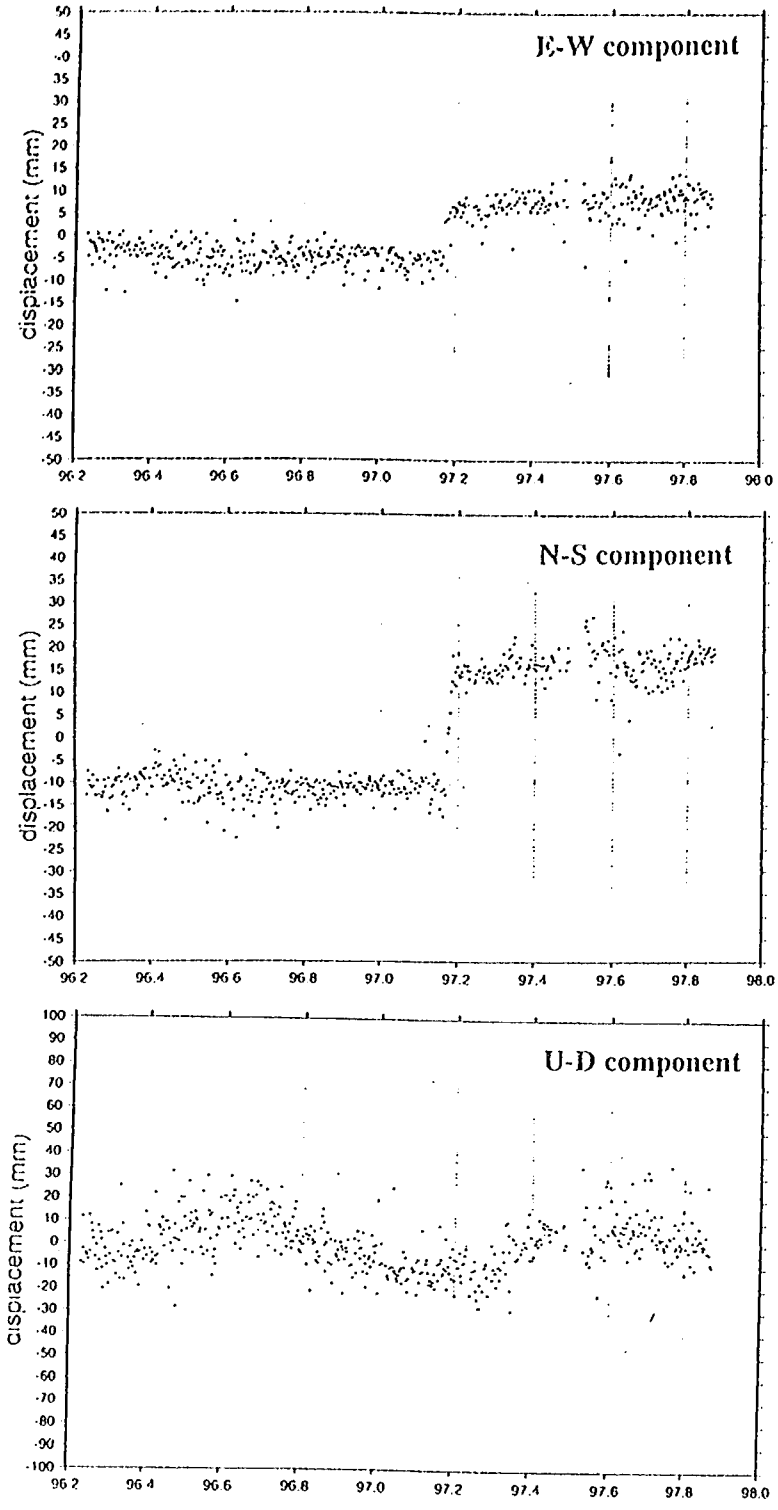
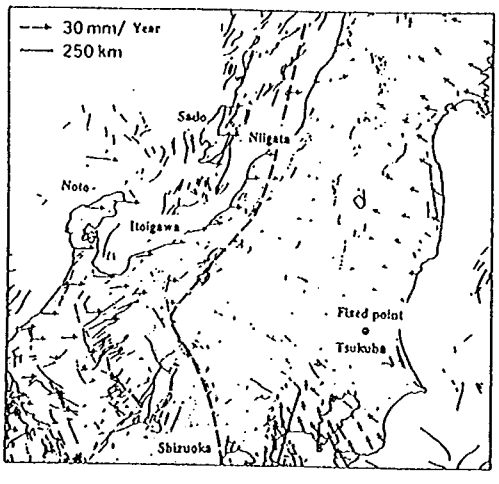


Figure 11 An example of time series of site coordinates



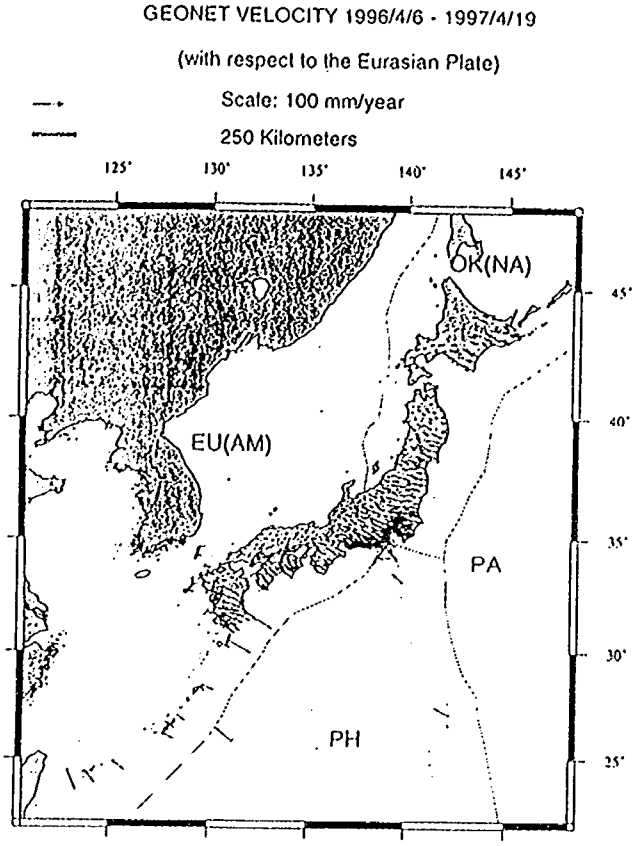


Figure 12 Horizontal displacement velocity field of Japan derived from one-year continuous GPS data (Apr.6, 1996 – Apr.19, 1997)

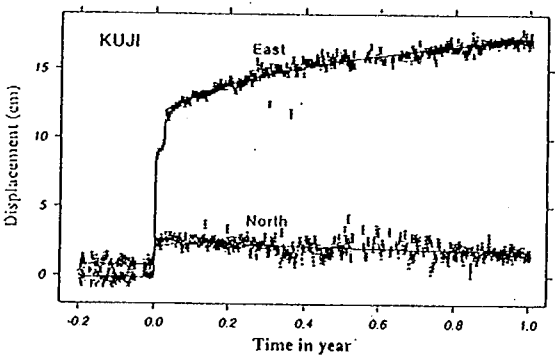


Figure 13 Long term post-seismic deformation following 1994 Sanriku Haruka Oki earthquake (after Heki et al., 1997)

Figure 14 Horizontal crustal deformation of the central part of Honshu Island. (Observation period: Oct.1, 1996 – Jun.14, 1997, dot line shows the proposed plate boundary, solid lines show active faults.)

Appendix

Task Committee Reports

Report of Task Committee A
STRONG MOTION DATA AND APPLICATIONS

Date: 11 May 1999

Place: Public Works Research Institute, Tsukuba, Japan

Attendees:

U. S. side --	R. Borcherdt (Chairman)	USGS
	Mehmet K. Celebi	USGS
	William B. Joyner	USGS
Japan side --	Susumu Iai (Chairman)	PHRI
	Shojiro Kataoka	PWRI
	Takashi Nagao	PHRI
	Izuru Okawa	BRI
	Akio Yoshida	JMA

1. Objective and Scope of Work

To coordinate and promote sharing of strong motion earthquake data among researchers and practicing engineers, and to develop techniques and exchange information for evaluating the destructive effects of earthquake motion.

The scope of work includes:

(1) Instrumentation
(2) Recording, processing, and analyzing strong motion data
(3) Engineering characterization of ground motion
(4) Design applications
(5) Seismic zonation

The activities of the Task Committee include:

(1) Regular exchange of data and publications
(2) Creating procedures for disseminating significant strong motion digital data with regard for the rights and expectations of (a) owner, (b) the users of data and (c) the earthquake engineering community
(3) Planning and conducting T/C workshops and meetings
(4) Coordinating relevant research activities

2. Accomplishments

The 1994 Northridge and 1995 Great Hanshin earthquakes had a tremendous impact on various aspects of the strong motion studies, including characterization of near field motion and site response. Research developments since these earthquakes were very rapid, including proposals and adoption of new seismic guidelines, adoption of new building codes in both U.S. and Japan as well as a new proposal of worldwide seismic hazard map for International Standards Organization (ISO) seismic guidelines for offshore structures. These earthquakes continue to yield improvements in seismic safety guidelines. Committee members have contributed to a number of these important developments. In addition, activities conducted by Task Committee A during 1998 are:

(1) Conducted a workshop entitled "Soil-Structure Interaction"; September 22-23, 1998, Menlo Park, CA; M. Celebi and I. Okawa, Conveners and Editors; Leading Researchers (12 Japan and 20 US) contributed to a very successful workshop; Workshop Proceedings, USGS Open-file report 99-142.
(2) Closely monitored the on-going changes and new proposals for seismic guidelines and codes, including those of UBC97, NEHRP97 in USA and ISO/WG67 in Japan.
(3) Chairmen and members of Task Committee A contributed to International Symposium on "Effects of Surface Geology (ESG 98; December 1998; Yokohama, Japan).
(4) Chairmen and members contributed to Symposium on "Resolution of Site Response Issues from Northridge Earthquake (ROSRINE; December 1998; Los Angeles).
(5) In recognition of the urgent need to improve inadequate sets of strong-motion recordings, US and Japan Task Committee members have contr8ibuted to the development of a vision for strong motion data acquisition for the next millennium (Proceedings of International Workshop entitled "Vision 2005: An Action Plan for Strong-Motion Programs to Mitigate Earthquake Losses in Urbanized Areas", Monterey, Ca, April 1997). COSMOS (Consortium of Organizations for Strong-Motion Observation Systems) was launched by this workshop. During 1998 committee members contributed to the incorporation of COSMOS including election of corporation officers, Board of Directors, establishment of corporation headquarters in conjunction with PEER (Pacific Earthquake Engineering Center-UC Berkeley), and initiation of plans for first meeting in September. Efforts are underway to determine procedures for expanded international participation.
(6) At the suggestion of Task Committee A members, a call for cooperation between U.S. and Japan in strong motion studies was included in the Earthquake Policy Symposium of the Common agenda.
(7) K-net was completed with the effort of Task Committee A members. Its data availability with ease and timely fashion should be a model to both U.S. and Japan strong motion programs for future development. Recently, the fourth and fifth CD-ROM with K-Net data was released in both Japanese and English.
(8) Task committee members contributed to the organization of a workshop on "Strong-motion Instrumentation of Civil Engineering Structure" funded by NATO, NSF, USGS, and others (Istanbul, Turkey; June 2 5, 1999; Web Address: www.boun.tr.edu/natoarw.htm).

1. Future Plans

The future plans include:

(1) Coordinate, where appropriate, ongoing US and Japan developments in strong motion recording programs and data dissemination in conjunction with activities of recently established committees and organizations such as COSMOS, with endorsement to participate in the first meeting of COSMOS in September 1999
(2) Develop recommendations for Common Agenda, possibly in a workshop regarding US an Japan needs for strong-motion measurements in densely urbanized areas to significantly improve pubic earthquake safety.
(3) Coordinate, where appropriate, ongoing developments in seismic hazard map and seismic guidelines to be generalized for worldwide use.
(4) Recognizing the developing emphasis in the engineering and emergency response communities on near-real-time data availability, T/C A will continue to promote and exchange new developments in real-time strong motion data acquisition, processing, and notification. This activity will be in conjunction with the proposed TC on Seismic Information Systems.
(5) Realizing the importance of strong-motion data to earthquake hazard mitigation T/C A suggests the establishment of links on UJNR Web page to the Web pages of major US and Japan agencies with publicly available strong-motion information.
(6) Planning for a combined workshop during the coming year on Real-Time Instrumentation of Densely Urbanized Areas and Instrumentation of Civil Engineering Structures (Japan, S. Iai, I. Okawa; US, R. Borcherdt and M. Celebi).

Report of Task Committee B
TESTING AND EVALUATION PROCEDURES FOR BUILDING SYSTEMS

Date: 12 May 1999

Place: Public Works Research Institute, Tsukuba, Japan

Attendees:	U. S. Side --	H. S. Lew (Chairman)	NIST
		G. Brady	ATC
		R. Hall	WES
		Q. Hossain	LLNL
	Japan Side --	K. Ohtani (Chairman)	NIED
		T. Kaminosono	BRI

1. Objective and Scope of Work

The objective of the Task Committee is to develop and recommend rational test procedures and to collect performance data of the static and dynamic response of structures through both laboratory testing of prototype structures and field testing of structures.

The Task Committee:

(1) Plans and conducts workshops and joint meetings to identify research topics and develop joint research programs.
(2) Coordinates research projects carried out by various laboratories in the U.S. and Japan. Facilitates publication of research results and implementation of findings in codes and standards.
(3) Facilitates exchange of research personnel, the exchange of technical information and the use of available testing facilities.
(4) Develops uniform testing procedures, including loading history, for comparison of results of tests carried out by various researchers, and for establishment of data base.
(5) Develops guidelines for interpretation of test results to improve the design of structures.
(6) Develops methodology for evaluation and interpretation of test results.

2. Accomplishments

(1) The third phase of the U.S. Precast Seismic Structural Systems Program (PRESSS) was initiated in 1995. The design of the five-story full-scale frame was completed.
(2) In Japan, a 3-year program on the development of design guidelines for precast and prestressed buildings was completed in 1998.

(3) The research program on Composite and Hybrid Structures (CHS) in Japan was completed in early 1998. Experimental and analytical work was carried out jointly at the Building Research Institute, several universities and construction companies. The Japan Structural Consultant Association has undertaken an applications study for implementing research results.

(4) The research program on CHS in the U.S. was initiated in 1995 under the sponsorship of the National Science Foundation. Over 16 research projects are in progress. Additional projects on composite wall systems have been underway at several universities.

(5) The Fifth US-Japan Joint Technical Coordinating Committee (JTCC) meeting on CHS was held in October 1998 in Tokyo, Japan. Both sides agreed to continue to coordinate efforts in the development of design guidelines and to transfer technology to the design profession.

(6) The International Symposium to commemorate the 20th Anniversary of the US-Japan Joint Research Program was held in October 1998 in Tokyo, Japan.

(7) The 6th US-Japan Joint Research Program on Smart Structural Systems (Auto-Adoptive Media) was initiated in 1998 and experimental research has been underway.

3. Future Plans

(1) Testing of five-story full scale frame will be carried out at the University of California, San Diego, in August 1999.

(2) The sixth US-Japan Joint Technical Coordinating Committee Meeting on CHS will be held in August 1999 in San Francisco.

(3) Several Technical Coordinating Committee meetings will be scheduled in both countries in the coming year.

(4) In support of the International Decade for Natural Disaster Reduction (IDNDR) Program, avenues will be explored to disseminate findings of completed joint research projects to countries with high seismic risks.

(5) The joint workshop on Test Procedure, Documentation, Retrieval of Test Data, and Experimental Facilities will be planned in the US, in conjunction with the 32nd Joint Panel Meeting.

(6) Future plans for US-Japan joint research programs will consider existing and planned experimental research programs of the three U.S. National Science Foundation Earthquake Engineering Research Centers.

(7) The Task Committee will consider the future U.S.-Japan Joint Research Program using available testing facilities in both countries including the 3-D Full-Scale Earthquake Testing Facility, which is being constructed at Miki, Japan by the National Research Institute for Earth Science and Disaster Prevention.

(8) The task committee will study the feasibility of establishing a network for live transmittal of experimental testing.

(9) The Task Committee will strongly encourage the PRESSS and CHS program coordinators to prepare reports summarizing the experimental and analytical research activities on PRESSS and CHS, respectively, in the U.S. and Japan and discussing their results. This report will also recommend the application and implementation of the results in the design and analysis of PRESSS and CHS.

Report of Task Committee C
HIGH PERFORMANCE STRUCTURAL SYSTEMS; DESIGN, EVALUATION, RETROFIT AND AUTO ADAPTIVE MEDIA

Date: 12 May 1999

Place: Public Work Research Institute, Tsukuba, Japan

Attendees:	U. S. side --	Michel Bruneau (Acting-Chairman)	SUNY, Buffalo
	Japan side --	Hisahiro Hiraishi (Chairman)	BRI
		Takashi Kaminosono	BRI

1. Objective and Scope of Work

The consolidation of the T/Cs(T/C) C on Design, Evaluation, and Improvement of Structures & T/C G on Structural Control and Intelligent Material Systems) was proposed at the U.S.-side Domestic Panel Meeting of September 1997 and was approved by both sides at their respective Domestic Panel Meetings, December 1997. This consolidation T/Cs (C&G) into a new T/C C was approved from the full Panel at the 30th Joint Panel Meeting of May 1998. The objective and scope of work and the future plans of the renewal Task Committee (C) are as follows:

(1) Exchange information and plan, and conduct workshops on new design technologies, evaluation technologies, repair and retrofit techniques.
(2) Study advanced materials and methods for new construction and those for repairing and retrofitting existing structures.
(3) Develop reliable condition assessment systems for new, existing and damaged structures.
(4) Develop and harmonize performance based structural design developed in each country.
(5) Coordinate research projects on design, evaluation and improvement of structures in the U.S. and Japan to minimize duplication and maximize benefits.

Title of T/C C was revised, and objective and scope of work was agreed upon during May 12,1999 meeting of T/C C.

2. Accomplishments

(1) Conducted the 5th U.S.-Japan Technical Coordinating Committee Meeting on Composite and Hybrid Structural Systems in order to exchange each research products and discuss the utilization of research products, October 1998, Tokyo, Japan.
(2) Conducted Workshops on Auto-Adaptive Media (Smart Structural Systems), in May at Sonoma, CA, USA, 1998, and in Jan. at Purdue WL, IN, USA 1999 in order to make US-side research plan.
(3) Conducted a 20 year commemoration symposium on Cooperative Earthquake Engineering Research, October 1998, Tokyo, Japan in order to review 20-years research products and discuss future cooperative research plan.
(4) Japan side started the 6th U.S. Japan Cooperative Research Project on Auto-Adaptive Media (Smart Structural Systems).

3. Future Plans

(1) Conduct 1st U.S-Japan Technical Coordinating Committee Meeting on Auto-Adaptive Media (Smart Structural Systems), fall 1999, Japan in order to coordinate research plan of both countries.

(2) Develop a reliable methodology for screening and analyzing wind and seismic resistant capacity, and advanced instrumentation technology and expert systems to provide condition assessment of existing structures.

(3) Compile a database of advance materials/systems that have potential for improving structural performance of new construction, and for use in rehabilitating and strengthening existing buildings.

(4) Investigate new methodologies based on required structural performance using advanced materials and systems.

(5) Continue to encourage participants by private industry, consulting engineers, universities, national and local government agencies involved in instrumentation, evaluation, condition assessment, and retrofit and strengthening of existing buildings, for seismic and wind resistance.

Report of Task Committee D
EARTHQUAKE ENGINEERING FOR DAMS

Date: May 11, 1999

Place: Public Works Research Institute, Tsukuba, Japan

Attendees:	U. S. Side --	Robert Hall (Chairman)	USAE / WES
	Japan Side --	Hitoshi Yoshida (Chairman)	PWRI
		Tsuneo Uesaka	PWRI
		Isao Nagayama	PWRI
		Yoshikazu Yamaguchi	PWRI

1. Objective and Scope of Work

To develop technical insights into better understanding of the response of dams to seismic effects, the T/C will plan, promote, and develop research initiatives to assist in assuring seismic safety and economical protective countermeasure against earthquake loading for these structures. The scope of work includes:

(1) Methods of analysis for seismic design of dams including outlet works.
Comparison of design methods and criteria between U.S. and Japan.
Development of "Design Earthquake Ground Motions" for analysis and evaluation of dams.
Assessment of investigation and dynamic analysis methods as tools (modeling, calculation codes).
(2) Dynamic characteristics of dam construction materials and site conditions.
Strength and deformation characteristics during earthquakes (concrete, soil and rock).
(3) Analysis of observed behavior of dams and outlet works during earthquakes.
Construction of a database that contains measured ground acceleration and dynamic response of dams and outlet works during earthquakes, and other related information which is necessary to valuate their seismic behavior.
(4) Investigation of the mechanism of damages due to earthquake loading.
Application of the analysis of the observed behavior during earthquake to the earthquake-resistant design.

2. Accomplishments

(1) In the field of seismic design for concrete dams, Mr. Takashi Sasaki, PWRI, finished a one-year (December 1997 December 1998) research at University of California, Berkeley.
(2) In the field of seismic design for embankment dams, Mr. Tomoya Iwashita, PWRI, started a one-year (August 1998 August 1999) research at University of California, Berkeley.
(3) The proceedings of the First Workshop was published and distributed to the T/C members and Panel secretariats.
(4) T/C (D) conducted the Second U.S.-Japan Workshop on Advanced Research on Earthquake Engineering for Dams in Tokyo, Japan on 7-8 May 1999.

3. Future Plans

(1) Exchange of the results of research / investigation and technical information about dam earthquake engineering is encouraged.

(2) Exchange visits to the institutes concerned, of scientists and engineers between U.S. and Japan, is to be extended for the effective communications.

(3) In view of the importance of constructing a database for seismic evaluation of dams and outlet works, cooperative research on the standardization for location and installation of strong motion seismographs, and collection and processing of measured seismic data will be started. Dr. Enrique Mathue, Virginia Polytechnic Institute will complete a six-week joint research with PWRI engineers during the next year at PWRI. Dr. Mathue will work with PWRI engineers in the initial implementation of the database. This discussion will be useful in developing proper format of data, which will be obtained from strong motion instrumentation of dams currently under construction by Ministry of Construction. During the project, he will also work with PWRI engineers in preparing a technical paper on the comparison of U.S. and Japan design standard for concrete dam. A proposal to support this research will be sent to the National Science Foundation during June 1999.

Mr. Michael K. Sharp, WES, will complete a four-week joint research with PWRI during the next year at PWRI to prepare a technical paper on the comparison of U.S. and Japan design standard for embankment dam. A proposal to support this research will be sent to the Japan Science and Technology Agency during 2000.

(4) The proceedings of the Second Workshop will be published and distributed to the T/C members and Panel secretariats.

(5) T/C (D) will hold the Third U.S.-Japan Workshop on Advanced Research on Earthquake Engineering for Dams in about two years in USA. The location and time of the workshop will be determined through correspondence between the chairs of T/D (D). Joint presentations of cooperative research mentioned in (3) will be made at the workshop.

REPORT ON TASK COMMITTEE E
DESIGN FOR WIND AND WIND HAZARD MITIGATION

Date: May 11, 1999

Place: Public Works Research Institute, Tsukuba, Japan

Attendees:

U. S. side --	H. S. Lew (Acting Chair)	NIST
Japan side --	Hisashi Okada (Co-Chairman)	BRI
	Hiroshi Sato (Co-Chairman)	PWRI
	Shoin Yagi	MRI
	Hitomitsu Kikitsu	BRI
	Toshiaki Mabuchi	PWRI

1. Objective and Scope of Work

To exchange technical information and to jointly plan, promote and foster research and dissemination, to improve understanding of wind and its effects on structures, establish more rational wind resistant design methods for structures, and to contribute to wind hazard mitigation.

The scope of work includes:

(1) Characterization of strong wind, especially boundary layer extreme winds.
(2) Wind effects (wind loading on and wind-induced response of structures).
(3) Experimental and analytical methods to predict wind and its effects.
(4) Damage and risk assessment.
(5) Wind hazard assessments and wind hazard mitigation.

2. Accomplishments

(1) Started collaborative research on "Development of Prediction Methods for Wind Response of Long Span Bridges" between PWRI and the University of Washington. Mr. T. Mabuchi of the Structure Division, PWRI stayed at the university in February of 1999, and studied computational fluid dynamics with Profs. D. Reed, G. Turkiyyah and H. Yeh.
(2) Planned the second joint Workshop on Design for Wind and Wind hazard Mitigation that will be held at the PWRI on May 24-26, 1999. The technical site visit to the Honshu-Shikoku Bridges will follow the workshop.

3. Future Plans

(1) Hold the second joint workshop mentioned above.
(2) Pursue the possibility of collaborative research on the following topics recommended at the first workshop.
   a) Application of models and field measurements to determine wind speed-up and turbulence characteristics associated with topographic features
   b) Development and testing of procedures for using comprehensive aerodynamic and/or structural characteristics database to calculate wind loading effects and structural performance
   c) Numerical simulation and measurements
   d) Aerodynamic control

e) Performance evaluations
f) Development of prediction methods for wind response of long span bridges
g) Cooperative efforts in post-storm damage assessment following tropical cyclones

(3) Exchange technical information on the following subjects:
a) Topographical effects on wind and the use of field measurements, numerical models and geographic information systems (GIS) to study these effects.
b) Control of wind-induced response of structures.
c) Computational fluid dynamics and wind tunnel tests.
d) Prediction of wind-induced response of full-scale structures.
e) Investigation of wind hazards, including post-storm damage assessment methodologies.
f) Wind resistant design codes, standards and recommendations.

Report of Task Committee F
DISASTER PREVENTION METHODS FOR LIFELINE SYSTEMS

Date : 11 May 1999

Place : Public Works Research Institute, Tsukuba, Japan

Attendees :

U. S. Side --	James Cooper (Acting Chairman)	FHWA
	Michel Bruneau	MCEER
	Josephine Malilay	CDC
	Phillip Yen	FHWA
Japan Side--	Masahiko Yasuda (Chairman)	PWRI
	Jun-ichi Hoshikuma	PWRI
	Yoshihiro Nakao	PWRI
	Tomofumi Nozaki	PWRI
	Keiichi Tamura	PWRI

1. Objective and Scope of Work

To improve the performance of lifeline systems during earthquakes and extreme winds, and to promote the development and implementation of technical and non-technical countermeasures, including the capability in damage estimation techniques and inspection procedures, through:

(1) Planning and conducting workshops.
(2) Facilitating exchange of technical information and personnel.
(3) Promoting development of design guidelines and standards.

2. Accomplishments

(1) Members of this Task Committee (T/C) participated in the planning and attended the First High-Level U.S.-Japan Earthquake Policy Cooperation Forum held in Seattle, Washington, U.S.A. in October 1998. The Forum was led by the U.S. Federal Emergency Management Agency and the National Land Agency of Japan, under the U.S.-Japan Natural Disaster Reduction Initiative of the U.S.-Japan Framework for New Economic Partnership (Common Agenda).
(2) The Proceedings of the Seventh Joint Workshop on Disaster Prevention for Lifeline Systems have been published and distributed.

3. Future Plans

(1) Encourage collaborative research and development in areas such as: performance prediction and post-earthquake damage assessment of lifeline systems; systems approach to lifeline performance; vulnerability inspection and retrofit techniques; post-earthquake response; and socio-economic impacts of damage to lifeline facilities.
(2) Encourage and strengthen current efforts in both countries for developing seismic design guidelines and standards for lifeline systems. Existing UJNR channels should be fully utilized to facilitate the exchange of relevant information concerning the development of guidelines and standards. Possible collaboration of developing guidelines and standards for lifeline systems should be pursued.

(3) Explore cooperative opportunities to address post-disaster public health issues as a result of disruption to lifeline systems as a part of T/C F. T/C F members will seek interest from appropriate public health counterparts and will make recommendations at the next Joint Panel Meeting on the appropriateness of incorporating this topic within the T/C F scope.

(4) Upon appointment of the U.S.-side Chair, plan and conduct the Eighth Joint Workshop on Disaster Prevention for Lifeline Systems in Japan. Specific location, time, and theme of the workshop will be determined through correspondence between the co-chairs of this task committee.

Report of Task Committee G
SEISMIC INFORMATION SYSTEMS

Date: 12 May 1999

Place: Public Works Research Institute, Tsukuba, Japan

Attendees:			
	U. S. side --	William Roper (Co-chairman)	USACE
		Mehmet Celebi	USGS
		Michael Blackford	NOAA
	Japan side --	Kazuo Okayama (Co-chairman)	NLA
		Hideki Sugita (Co-chairman)	PWRI
		Takaharu Kiriyama	NLA
		Hiroshi Masaharu	GSI
		Tomofumi Nozaki	PWRI
		Toshiaki Yokoi	BRI

1. Objective and Scope of Work

Collaborative activities are planned in the following areas;

(1) Technically assist the earthquake policy cooperation under the U.S.-Japan Framework for New Economic Partnership (Common Agenda).
(2) Improve understanding of earthquakes and social impacts through development of Seismic Information Systems.
(3) Review the principals, objectives, structures and methodologies of existing systems, and facilitate practical application in both countries.

These will be done through a) planning and conducting workshops, b) planning and conducting cooperative researches, c) exchanging information and personnel in administrative and technical fields, d) introducing research accomplishment to guidelines and standards.

2. Accomplishments

(1) The T/C-G members participated in the planning and attended the First High-level U.S.-Japan Earthquake Policy Cooperation Forum (High-level Forum), 20-22 October 1998, Seattle, Washington. The Forum was held under the auspices of FEMA and NLA, and both countries recognized the necessity of closer relationship on Seismic Information Systems. The Second High-level Forum will be held in Japan in 1999.
(2) T/C-G chairmen of both sides discussed the priority areas of cooperative research activities to provide close cooperation with the technical leadership in the Second High-level Forum.

3. Future Plans

(1) The T/C-G encourages cooperative research activities on the areas below.
   a) Earthquake Monitoring/ Notification Systems
   b) Earthquake Damage Estimation/ Emergency Activity Support Systems
   c) Earthquake Damage Estimation Models
(2) The First Workshop on Seismic Information Systems will be held in autumn 1999 in Japan. The date and

place will be proposed by Japan-side chairmen in consideration of the Second High-level Forum program.

(3) The T/C-G encourages exchange information with the other related T/Cs and Panels on common technologies including real-time earthquake ground motion acquisition and remote sensing of earthquake damage.

(4) Enhancing the Seismic Information Systems to the other disasters including wind, storm surge, tsunami and flood will be investigated.

Report of Task Committee H
SOIL BEHAVIOR AND STABILITY DURING EARTHQUAKES

Date: May 12, 1999

Place: PWRI, TSUKUBA, JAPAN

Attendees:

U. S. side --	Mike SHARP (Acting Chairman)	WES
	Richard S. OLSEN	WES
Japan side --	Osamu MATSUO (Chairman)	PWRI
	Kazuhiko FUJIHASHI	NTT
	Hiroshi KOBAYASHI	PWRI
	Chikahiro MINOWA	NIED
	Mitsu OKAMURA	PWRI
	Takahiro SUGANO	PHRI

1. Objective and Scope of Work

Government agencies responsible for public works must assure seismic safety and provide economical protection against earthquake hazards.
The objective of the Task Committee (H) is to assist in meeting these needs by enhancing the availability of technology for predicting the dynamic behavior of soils, foundations and earth structures, and analyzing dynamic soil-structure interaction to assure their safe performance during earthquakes.

In accordance with the objective, the scope of work includes:

(1) Exchange information on technological developments, state-of-the-art and practice related to soil behavior and stability during earthquakes,
(2) Exchange information and technical data related to field performance, research, and methods of practice,
(3) Plan and conduct programs of cooperative research and/or workshops in coordination with the proposed or ongoing programs, and
(4) Make other efforts needed including exchange of researchers between U.S. and Japanese research institutes, and publication of research results and recommended practice.

2. Activities

(1) The National Research Institute for Earth Science and Disaster Prevention (NIED), the Building Research Institute (BRI), and Wayne State University (WSU), have continued to work in their cooperative research program "Physical and Numerical Simulation of Structural Damages Due to Liquefaction and Development of Countermeasure Techniques", 1994-1998.
(2) Port and Harbor Research Institute (PHRI), Colorado School of Mines and the Lovelace Institutes (Albquerque, NM) have continued joint research on application of the Nuclear Magnetic Resonance Imaging (NMRI) method to the study of soil behavior and stability during earthquakes.
(3) The 5th U.S.-Japan Workshop on Geotechnical Earthquake Engineering, subtitled as Soil Dynamics by Use of Centrifuge, was held at PWRI during 28-29 September 1998. A total of 45 researchers, 9 from U.S. side and 36 from Japan side, participated and 17 papers were presented during the workshop. The proceedings of the workshop have been published and distributed.

3. Future Plans

It was agreed by the U.S. and Japan sides that they will put a focus on exchanging research findings and developing cooperative research works in the following two particular areas in which both Japanese and U.S. researchers are currently conducting the studies.

(1) Seismic stability assessment procedures for embankment structures
Japanese researchers are investigating the rationalization of conventional pseudo-static stability analysis procedures and developing predictive procedures of permanent deformation and flow failure.
U.S. researchers are investigating different types of failure mechanisms and the effectiveness of current procedures for liquefaction analysis. Improvement of centrifuge experimentation on embankment structures is a common interest.

(2) Improvement of liquefaction potential assessment procedures
Both the U.S. and Japan currently have procedures for evaluating liquefaction that incorporate many factors. Both sides are currently involved in research to evaluate these factors. In-situ measurement technique by the use of the cone penetrometer is also of common interest for both sides.

The committee also plans an exchange of researchers in the coming year to exchange information and encourage cooperative research activities.

4. Other Activities

Handbook on Liquefaction Remedy was published by the Japanese Geotechnical Society in October 1998. Its English translation and editing of the draft were completed with the assistance of Panel members together with the former members, Prof. Y. Sasaki and Dr. A.G. Franklin.

Report of Task Committee I
STORM SURGES AND TSUNAMI

Date: May 11, 1999

Place: Public Works Research Institute, Tsukuba, Japan

Attendees:	U. S. Side --	Michael E. Blackford (Chairman)	NOAA
	Japan Side --	Kenichi Torii (Chairman)	PWRI
		Masami Okada	MRI
		Yuichiro Tanioka	MRI
		Fuminori Kato	PWRI

1. Objective and Scope of Work

The objective of this Task Committee is to mitigate damage from storm surge and tsunami through cooperative research and shared technology and information. The primary cause of storm surge is considered to be tropical cyclones (hurricanes, typhoons). The primary cause of tsunami is considered to be sudden sea floor deformation due to earthquakes, volcanic activity and landslides. Both hazards may cause disasters along coastal regions.

The scope of work of this T/C is as follows:

(1) Exchange results of research on storm surge and tsunami occurrence, generation, propagation, and coastal effects. This includes observations on historical, current, and theoretical tsunamis. Of particular interest is the effort by U.S. and JAPAN to acquire deep ocean tsunami measurements.
(2) Exchange results and status of storm surge and tsunami mitigation activities including analysis of the problem, planning, warning, and engineering approaches.
(3) Exchange information on development of technologies such as computer programs to predict travel times, land-fall locations, inundation and run-up heights, and wave characteristics, improved instrumentation, and use of satellite communication for detection and warning.
(4) Facilitate dissemination through exchanges of literature, technical reports at joint meetings, special workshops, joint projects, and direct interaction among participants. The storm surge research community which functions through many related societies and international organizations, defines and simulates work in the field. The Task Committee, through its meetings and workshops, encourages exchanges of ideas and joint study by U.S. and Japanese investigators of tsunami events throughout the world.

2. Accomplishments

(1) The Task Committee agreed to support the improvement of the gridded bathymetry and coastal-topography data initiated by International Tsunami Commission.
(2) The Task Committee exchanged ideas on large-scale laboratory experiments on tsunami runup.
(3) Preliminary cooperative experiments on tsunami scouring around a cylinder were performed by using a large wave flume at PWRI.
(4) The Task Committee made a list of large-scale experimental tanks of research institutions in Japan to clarify the roles of large-scale laboratory experiments. The list of facilities in U.S. and Europa will be added.

(5) From July 9 to 11, 1998, the Fifth Tsunami Workshop was held in the City of Sapporo in Hokkaido. During this workshop, the tsunami researchers visited Okushiri Island where they attended a reception to exchange views with people who had experienced the tsunami and observed the state of recovery work in the part of the island it had devastated.

3. Future Plans

The Task Committee exchanges information, and encourages cooperative researches and developments on the following subjects:

(1) Cost reduction of deep ocean tsunami detection systems
(2) Accessibleness of tsunami detection data in deep ocean
(3) Investigation of tsunami detection by artificial satellites
(4) Accessibleness of gridded bathymetry in deep ocean and extension of the database to shallow sea
(5) Development and improvement of numerical model on tsunamis and storm surges
(6) Development of predictive model on scour around structures by tsunamis
(7) Technical support to develop tsunami mitigation program in Pacific nations
(8) Collecting information (tsunami source, run-up height and damages) of historical and current tsunami in Pacific

4. Others

(1) The storm surge research community is small and incorporated into related societies and international organizations which define and stimulate work in the field. The Task Committee "I" encourages these efforts.
(2) Since tsunamis have been less severe in the U.S. than in Japan, the U.S. has fewer researchers in this specialty. The Task Committee, through its meetings and workshops, encourages exchanges of ideas and joint study by U.S. and Japanese investigators of tsunami events throughout the world.

Report of Task Committee J
WIND AND EARTHQUAKE ENGINEERING FOR TRANSPORTATION SYSTEMS

Date: 12 May 1999

Place: Public Works Research Institute, Tsukuba, Japan

Attendees:	U. S. side --	James D. Cooper (Chairman)	FHWA
		W. Phillip Yen	FHWA
	Japan side --	Kazuhiro Nishikawa (Chairman)	PWRI
		Yukio Adachi	PWRI
		Jiro Fukui	PWRI
		Jun-ichi Hoshikuma	PWRI
		Yasushi Josen	PWRI
		Masahiro Nishitani	PWRI
		Keiichi Tamura	PWRI
		Shigeki Unjoh	PWRI
		Masahiko Yasuda	PWRI

1. Objectives and Scope of Work

To:

(1) Plan, promote, and foster research on the behavior of highway bridges when subjected to wind and seismic forces, and

(2) Disseminate research results and provide specifications and guidelines based on the Task Committee's findings. Surface transportation systems play a vital role in the movement of goods and people. Highway bridges are especially influenced by the forces of wind and earthquakes because of their open exposure to those forces.

The scope of work includes:

a) Focus research on highway bridges without limitation on their size and function.

b) Investigate existing and new bridge designs and the behavior of whole bridge systems and/or single components of a bridge.

2. Accomplishments

(1) The 14th U.S.-Japan Bridge Engineering Workshop was held during 3-4 November 1998, in Pittsburgh, Pennsylvania, U.S. The workshop was attended by 34 U.S. and 22 Japanese participants. Since this workshop, it was decided to integrate the Workshop on Seismic Retrofit of Bridges and the Workshop on Earthquake Protective Systems for Bridges into the Bridge Engineering Workshop. The proceedings of the workshop have been published and will be distributed.

(2) Dr. Jun-ichi Hoshikuma, Research Engineer of Earthquake Engineering Division, PWRI started his one-year guest research assignment on seismic design of bridges at University of California, San Diego from March, 1998.

3. Future Plans

(1) The 15th U.S.-Japan Bridge Engineering Workshop will be held in November 1999 at Tsukuba, Japan. The topics of the workshop will include:
   a) Innovative seismic retrofit technology including the application of new materials and new structural systems
   b) Innovative bridge design concept; e.g., bridge types, materials, life cycle cost analysis, etc.

(2) Encourage a coordinated research on the following topics:
   a) Bridge design methodologies which embrace performance based design concepts, limit state design concepts and life cycle cost analyses.
   b) Seismic isolation design methodologies considering the dynamic characteristics of isolation devices and their modeling.

(3) Continue to investigate and exchange technical information on the improved seismic retrofit and strengthening procedures for highway bridges based on experimental, analytical, and field studies, including the development of innovative earthquake protective systems, the evaluation of the seismic performance of total bridge systems, and the development of damage evaluation methods using sensoring systems, etc. This exchange should also include information related to the maintenance of existing bridges.

(4) Continue the coordinated research project to compare the seismic design criteria and seismic retrofit technologies for bridges in Japan and the U.S.

(5) Encourage a research study on seismic, aeroelastic, and aerodynamic response of long span bridges such as cable-supported bridges with emphasis on behavior of composite materials, cable inspection, vibration control, and corrosion protection.

(6) Encourage a coordinated research study on system identification techniques, nondestructive evaluation of bridge structures, use and performance of structural materials including new materials, and performance of jointless bridges.

Report of Task Committee K
WIND AND EARTHQUAKE ENGINEERING FOR OFFSHORE AND COASTAL FACILITIES

Date : 11th May 1999

Place : PWRI,JP

Attendees:	U. S. side --	Charles Smith (Chairman)	MMS
		Gerald Brady	ATC
		Richard Olsen	WES
	Japan side --	Takahiro Sugano (Chairman)	PHRI

1. Objective and Scope of Work

To develop technical insights necessary to mitigate damage to offshore and coastal facilities due to extreme wind and seismic effects. The Task Committee will plan, promote and develop research initiatives to meet this objective and will disseminate the results of its research for incorporation into future specifications and design guidelines. Criteria for the design of offshore and coastal facilities differ from their onshore counterparts. These differences arise due to the unique design or mass distribution of the facilities, to the fluid/structure or wind/structure interaction, to the placement of foundation elements in or on soft, fully saturated soils that can be subject to large hydrodynamic pressures, and to the lack of specific environmental data or engineering experience that has been developed for most Onshore Sites.

The scope of work includes:

(1) Sponsoring and conducting workshops and meetings to identify key areas of research opportunities for cooperation and the exchange of knowledge.
(2) Predicting strong motions for offshore and coastal sites including assessing the effects of basin geometry, and linear and nonlinear local geological effects, using actual seafloor response measurements.
(3) Determining the dynamic response and the interaction of structure/foundation/soil systems to seabed motions and extreme wind forces.
(4) Assessing the dynamic response and behavior of various operational facilities mounted on offshore and coastal structures.
(5) Developing assessment methodologies for earthquakes and other characteristics of potential seismic sources (e.g. faults) for offshore and coastal sites in regards to how these conditions relate to structural design criteria.
(6) Promoting the implementation of new research results into current design and construction processes.
(7) Developing research efforts to include laboratory and field programs to obtain data on the response of offshore and coastal facilities to extreme wind and seismic forces.
(8) Creating performance standards, design specifications, and code recommendations for applications to new construction as well as remedial action for existing facilities

2. Accomplishments

(1) Task Committee K held initial planning phase to conduct a third US-Japan workshop. The theme of this workshop will focus on seismic, wind and hazard mitigation techniques for offshore and coastal facilities. It is to be held in Japan on Dec. 7-8 1999.
(2) Mr. Nozu researcher of PHRI will completed research on earthquake resistant technology for offshore and coastal facilities at California Institute of Technology in Sept. 1999.
(3) Members of Committee K participated in the workshop, "Joint Peer/Industry Workshop on the Seismic Vulnerability of Port Facilities" held by Pacific Earthquake Engineering Research Center, July 1998, San Pedro, California.

3. Future Plans

(1) Develop workshop agenda including invited speakers of the third U.S-Japan Workshop on Wind and Earthquake Engineering for Offshore and Coastal Facilities.
(2) Coordinate, where possible, on-going research on wind and earthquake engineering for offshore and coastal facilities of interest to the members of the Task Committee K. This includes sharing of research reports and publications where possible listed as following.
   a) Japan's port facilities earthquake resistant design standard revised on April 1 1999.
   b) Seismic performance based design concept for onshore and onshore facilities.
   c) Rehabilitation/life extension technologies for offshore and port facility.
   d) Proceedings of International Workshop on Corrosion Control for Marine Facilities, Feb. 1999.
(3) Task Committee K will work within the framework of the U.S.-Japan Common Agenda Program focusing on the issue of acceptable seismic risk guidelines for ports and harbors.
(4) Task Committee K will coordinate activities with the Pacific Earthquake Engineering Research (PEER) Program on ports and harbors centered at the University of Southern California.

Technical Site Visits

SUMMARY OF TECHNICAL SITE VISITS 10 AND 15-20 MAY 1999

During the 31st Joint Panel Meeting of the UJNR Panel on Wind and Seismic Effects, ten locations were visited as part of the Technical Site Visits. In addition to visiting sites in Tsukuba, the delegation traveled to Shizuoka, Kobe, Nagoya, and Tokyo. The delegation is shown in Figure 1, on Awaji Island with the Akashi-Kaikyo Bridge in the background.

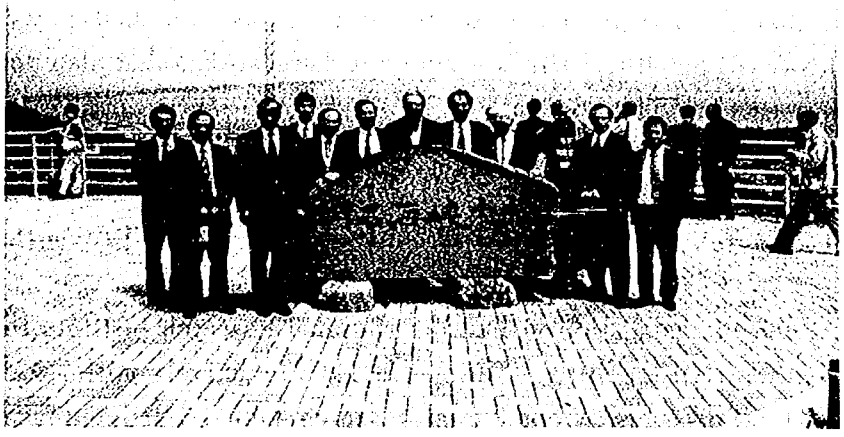


Figure 1 - U.S. and Japanese delegation

Technical aspects of the various sites visited are described below.

1. Geographical Survey Institute

The Geographical Survey Institute is a part of the Ministry of Construction, Japan, and was established in 1869. GSI is the only national organization that conducts basic survey and mapping, instructs related organizations to clarify the conditions of land in Japan, and provides the results of surveys to help improve this land. GSI has four main functions: 1) survey administration, 2) implementation of survey works, 3) research and development of survey and mapping, and 4) international cooperation for survey and mapping. The GSI employs 844 personnel and has its main office located in Tsukuba.

The site visit began at the VLBI Observation Facility. VLBI is an acronym for Very Long Baseline Interferometry and is a technique to measure a distance of thousands of kilometers between two points with an error of a few millimeters using radio waves that come from quasars to the earth traveling several billion light years. Quasars are radio stars that emit radio waves reaching the earth as plane waves. When a signal is received by two antennae at different locations, position can be determined precisely. Antennae that receive these plane waves are

located all over the world and allow for such things as tracking crustal movements and accurately determining sea level.

The second point of the visit at GSI was the nationwide GPS (Global Positioning System) Array in Japan. This is the world's largest permanent GPS array, operating since 1994. There are over 1000 continuous observation stations in the array covering most of the Japanese islands with an average spacing of about 30 Km. The main purpose of this array is the monitoring of deformation to assist in the prediction of large earthquakes and volcanic eruptions. Each station consists of a GPS receiver, a modem or terminal adaptor and a batter. Data from the GPS stations are transmitted via phone line to the GSI in Tsukuba for processing and analysis.

Current work that GSI is involved in to process data was explained as well as results of data from the JERS-SARI Satellite. This system collects radar data that also determines crustal and volcanic movements using interferometry.

2. National Research Institute for Earth Science and Disaster Prevention

On May 10, 1999, the delegation visited the National Research Institute for Earth Science and Disaster Prevention (NIED). It was formed in 1963 to actively mitigate damage and promote recording of natural disasters by conducting research, both applied and basic, and by collecting and distributing data. Its primary functions today are to conduct research in earth science and earthquakes and in understanding other natural disasters. In 1999, NIED had a staff of 120 (of which 40 were administrative and 80 were researchers) and had a research budget of 7.8 billion yen. Two projects of current interest include the development of a high precision seismic network and the building of a new facility to store and distribute disaster data. NIED designs and conducts a wide range of projects to meet its objectives to mitigate the effects of natural disasters. In response to domestic and international needs, NIED is also involved in research that studies future changes in the earth's environment and in research directed at predicting and mitigating natural disasters caused by these changes.

The remainder of the site visit consisted of an introduction to the newly proposed 3-D full scale earthquake testing facility, a visit to the large scale earthquake simulator facility, the super computer system, the observation network for crustal activities of the Kanto-Okai area, and a presentation on the Kyoshin Network (K-NET).

The facility to be constructed in Miki City, on the north of Kobe City in Hyogo Prefecture will be the largest shake table in the world. The basic features of the new facility are as follows: as the worlds largest shake table it will have a dimension of 20m X 15m in size and will be able to test full scale or model structures with a total weight up to 12,000 tons. Failure tests on a full scale model of a 4-story reinforced concrete building can be performed; the shake table will be capable of generating Kobe-class strong motions when loaded with a 1200 ton test structure; it will have three dimensional motions with a maximum acceleration at maximum load of .9 G in

both the X and Y horizontal directions and 1.5 G in the vertical direction; and will be able to produce maximum displacements of +/- 50 cm in the X-axis, +/- 100 cm in the Y-axis and +/- 50 cm in the vertical direction. Operations are scheduled to begin in April 2005. The test facility will be open to research organizations, both national and international. This will be the largest and the most technologically advanced test facility in the world and will require coordination and collaboration of many participants, including academic institutions, government agencies, and private and industrial organizations.

The "Large Scale Earthquake Simulation Facility" was completed in 1970 and enlarged to it present size in 1989. Recently it has been used to study underground water pipes and gas pipes subject to liquefaction. It is also used to test the strength of large-scale structures such as bridges, river embankments and building during earthquakes

The NIED also operates about 100 observation sites to form a network for crustal activities covering the Kanto-Tokai District. These sites are composed of seismometers, strainmeters, tiltmeters and GPS receivers covering an area within an approximately 200-kilometer radius for the Kanto and Tokai region. Some instruments are placed 100 meters deep to gather data. All data are transmitted by using telephone lines to Tsukuba to be analyzed by NIED researchers. This data is stored in a "Super Computer Facility" which consists of several Cray Computer Systems. NIED also uses this facility to simulate a world typhoon model to predict paths as well as wind speeds. An internet site exists at http://www.bosaigo.jp.centers/.

After the Kobe earthquake of 1995, the Japanese government decided to increase the density of strong motion observation stations. NIED was given the responsibility to implement the program. "Kyoshin Net (K-NET)" is the product of this effort. The work Kyoshin stands for strong (kyo) quake (shin). K-NET is a system, which makes available strong-motion data on the Internet. The data are obtained from 1000 observation sites, which are deployed at intervals of about 25 km. Each station has a digital strong-motion seismograph with a wide frequency band (450 Hz) and a wide dynamic range (126dB), having a maximum measurable acceleration of 2000 Gals. The spacing of the instruments sites was done so that the epicentral distance of a magnitude 7 earthquake could be sampled anywhere in Japan. The headquarters of the K-NET is in Tsukuba City. The control center fully monitors the seismographs, acquires data by telemetry, prepares databases and catalogs strong-motion files and releases the information on the Internet. The information from Tsukuba can be accessed as follows: "http://www.k-net.bosai.go.jp". After one year of operation, the K-NET has transmitted over one million data files on the Internet.

3. Construction Site of Nagashima Dam

The Nagashima Dam is a multipurpose dam for flood control, water supply, and irrigation and is part of the General Ohi River Development Plan in the Shizuoka Prefecture, upstream of the Ohi River. Construction of the dam began on 31 October 1987, with the final placement of

mass concrete occurring on 17 March 1998. The reservoir will begin to fill in October 2000 and should reach normal pool elevation within one year.

The Nagashima Dam is a concrete gravity dam with a height of 109 m, and a crest length of 308 m. Roller-compacted concrete (RCC) was used from bedrock up to a height of 15 m. RCC materials were not used for the remainder of the dam because of the six 5.0-m by 6.4-m outlet works being constructed within the body of the dam. The outlet works were modeled with a 1:80-scale model during the design phase to simulate hydraulic flows through the outlet works and to determine safe operations of the gate system to prevent flow-induced vibrations. The dam was designed using the seismic coefficient method, assuming earthquake ground motions of 0.15 g's.

Geologically, the dam is constructed on bedrock consisting of slate with thin layers of tuft. Approximately 10-cm layers of sandstone were found between some of the slate layers. The rock has few faults and is considered satisfactory for a dam foundation.

A 34-m-high check dam is constructed over 4,800 m upstream from the main dam for the purpose of minimizing the amount of sediment entering the main reservoir. The check dam will cause sedimentation to occur upstream of the main dam, and will allow for the removal of sediments with earth-moving equipment. The check dam is being constructed with the new Cemented Sand and Gravel (CSG) method, whereby cement is mixed with locally available material and placed in 50-cm lifts. The CSG material has a 10-MPa compressive strength at 91 days. The CSG material is then covered with unreinforced mass concrete. The spillway section of the check dam is covered with conventional reinforced concrete to prevent scouring of the CSG material. The upstream cofferdam for the check dam is constructed of the CSG material and served as a test section for this new method.

The Sumata Dam is approximately 2,000 m downstream of the Nagashima Dam. The Sumata Dam is a small privately owned hydropower dam. The existence of this and other small hydropower dams in this area resulted in the Nagashima Dam not having any hydropower capability.

4. Construction Site of 2nd Tomei Meishin Highway

The New Tomei Meishin Expressway, currently under construction, is designed to alleviate traffic congestion on the existing Tomei Meishin Expressway and to respond to future traffic demands. It will have six traffic lanes and be constructed to allow high speed driving at approximately 140 km/h. The delegation visited several bridges on the New Tomei Meishin Expressway.

The Meiko Triton is the nickname for the three cable-stayed bridges that are part of the 6.1 km long Ise Bay Highway. Several unique construction techniques were used to build these bridges.

For example, unmanned, remote-controlled excavation techniques were used for the caisson foundations, the seabed subsoil was improved to increase the stability of the towers, and cable-damper systems were used between the towers and the main deck girders. A 3600-ton capacity floating crane was used to erect the girder sections.

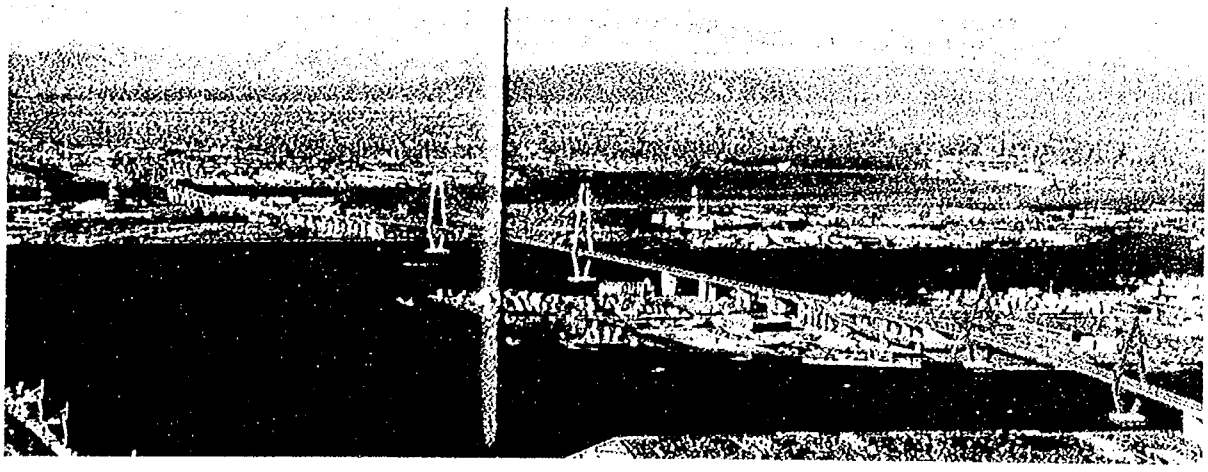


Figure 2 - The Meiko Triton

The bridges individually are:

- Meiko Bridge East (also called Nagoya Port East Bridge) which is 700 meters long with 410 m center span. This bridge is painted blue. The A-frame towers are 125 m tall.
- Meiko Bridge Center (also called Nagoya Port Central Bridge) which is 1170 m long with 590 m center span. This bridge is painted white. The A-frame towers are 190 m tall.
- Meiko Bridge west (also called Nogoya Port West Bridge) which is 758 m long with 425 m center span. This bridge has 122 m tall double A-frames one for each of the two decks and is painted red.

The Kiso River Bridge (also called the Kisogawa) is being constructed where the New Meishin Expressway crosses the Kiso River. The bridge is 1145 meters long with the longest span having a length of 275 meters. The span length is one of the longest of all the bridges crossing the rivers in Japan. The Ibi River Bridge (also called the Ibigawa) is being constructed where the New Meishin Expressway crosses the Ibi River. The bridge length is 1397 meters and the longest span length is 271.5 meters. It has a shape similar to the Kiso River Bridge, but due to its greater length, an additional pier has been added.

Both bridge systems utilize a prestressed concrete (PC)-steel composite. A steel sheet pile foundation is used for both bridges. The substructure of both bridges is composed of wall-type girders.

The Kiso Bridge is a five span continuous, extradosed box girder bridge with a total length of 1145m. The Ibi Bridge is a six span continuous, extradosed box girder bridge with a total length of 1397m.

The New Tomei Meishin Expressway is being constructed by the Japan Highway Public Corporation (JH) which has constructed and operated governmental national expressways throughout Japan since it was founded in 1956. To date, a National network of approximately 6500 km of toll roads and expressways has been completed. The 1999 budget of JH is about $10B. The Nagoya Office, which is responsible for 265 km of the expressway, has a budget of $2B.

5. Phoenix Disaster Prevention Center

On Tuesday morning, May 18, the delegation was shown the Phoenix Disaster Management System of the Hyogo Prefecture Office. Emergency response to the 1995 Great Hanshin-Awagi Earthquake was severely hampered by lack of timely information on disaster conditions. To insure that such difficulties would not occur in future disasters, the Hyogo Prefecture Government established the Phoenix Disaster Management System.

The delegation met in the control room where emergency response decisions will be made. In addition to commercial TV monitors, the room contained 4 small screen monitors for display of information from the fire disaster office, two large-screen monitors, and a telephone bank. The highly-computerized system collects data from seismometers (91 in Hyogo Prefecture), meteorological instruments, video cameras fixed at high elevations, video cameras in helicopters, and digital photographs taken by field workers and transmitted from specially-equipped cars.

The System is based on cooperation among the police, the fire department, the self-defense forces, and other groups. A state of readiness is maintained by periodic system drills. The System is manned 24 hours a day. In case of disaster essential workers are summoned by beeper. There is a three-level response plan depending on initial estimates of damage.

The computer network is part of the Hyogo Prefecture LAN. It is backed up by a satellite communication system and has backup servers located more than 60 km from the headquarters building.

The large-screen monitor in the control room and any computer in the network can display (1) recent earthquakes anywhere in Japan, (2) recent earthquakes in Hyogo Prefecture in greater detail, (3) meteorological data (including satellite pictures) and up-to-date weather forecasts, (4) water level in rivers, (5) maps forecasting earthquake damage in terms of JMA (Japan Meteorological Agency) Intensity, and (6) forecast damage and casualty statistics. Items (5) and (6) were illustrated by simulations based on the 1995 earthquake.

The System is described under the heading Fire and Disaster Management on the English page of the Hyogo Prefecture Home Page URL (http://web.pref.hygo.jp/).

6. Akashi-Kaikyo Bridge

The Akashi-Kaikyo Bridge, which links Kobe City and Awaji Island, both in Hyogo Prefecture, is 3911 m long, with a main span of 1991m. Thus, it has the world's longest bridge span, a title that had been held since 1981 by the 1410 main span of the Humber Bridge in England.

Work began at the site of the Akashi-Kaikyo Bridge in May 1988, and continued until April 1998 while overcoming many difficulties including the Kobe Earthquake in January 1995. During that time, the engineers on the project had to meet a wide range of technical challenges in order to complete the record-breaking bridge structure. It is most noteworthy that no fatal accident was recorded in the 10 years of construction. The average traffic volume is about 15% lower than expected in the first year in service. This may be due to the fact that the industries in the Awaji Island are not fully established yet.

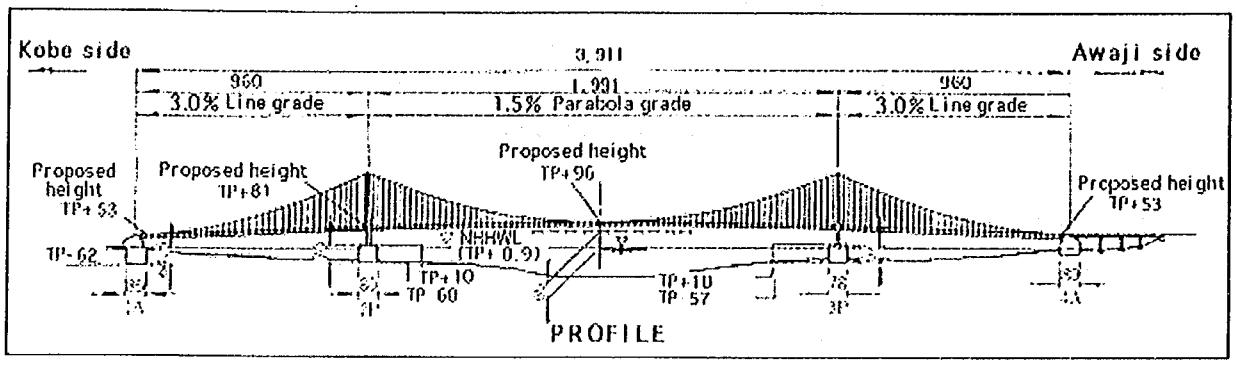


Figure 3 - Akashi-Kaikyo Bridge

The Akashi-Kaikyo Bridge has the following characteristics:

- The bridge has a main span of 1991 m and a total length of 3991 m (There was approximately one meter elongation in each length due to the Kobe Earthquake). The extremely large span was dictated by the waterway and navigation requirements, the topography and geology of the straits, and the land usage at both shores.
- Two main piers were supported on widely spaced caissons that were sunken into position in locations of great water depth and strong tidal currents. Very large deep foundations for the anchorages were constructed on reclaimed land using new technology. All foundations were designed against severe earthquakes. In addition, newly developed low-heat cement and various concrete mixes were used in the foundation.
- The main towers, made of steel, reach 297 m above sea level and were erected with high precision. Strong wind oscillations are carefully suppressed by using tuned-mass dampers.
- The main cables, which were erected by the prefabricated parallel wires strand method, were made of a newly developed high strength galvanized wire, whose breaking strength was improved to 1800 N/mm^2.
- The suspended roadway was designed with a stiffening truss, and its erection was carried out without affecting the heavy marine traffic, which often reached about 1400 ships per day.

Akashi-Kaikyo's aerodynamic stability was experimentally investigated in a newly constructed, boundary layer, large wind tunnel.

7. National Research Institute of Fire and Disaster

The National Research Institute of Fire and Disaster (NRIFD) was founded in 1948 as the Fire Research Institute for the purpose of protecting people and their property from fires and other disasters. Located in Musashino, the NRIFD conducts basic research in fire and its spread, fire prevention, fire-resistant materials, and methods of fire fighting and suppression.

Currently, NRIFD has research programs in the following areas:

- Fire protection plans for residential fires
- Intelligent fire detection system
- Underground fires and tunnel fires
- Extinguishing agents and extinguishing efficiency
- Mechanization of fire-fighting equipment
- Inhibition of full-scale fire spread using small amounts of water
- Aerial attack against urban fires
- Counter measurers to post-earthquake fires
- Strength of oil storage tanks
- Hazardous materials

The delegation visited the Fire Extinguishing Research Building, which contains two test facilities. The main facility is 25m wide × 25m deep × 22m high and has the capability to produce wind velocities up to 10 m/s. The delegation also visited the Fire Test Facility for Large Fires, which contains a fire-resistant laboratory and a blast-proof laboratory. The main test facility is used for experiments on fuel storage tank fires.

Lastly, the delegation was treated to a rich piece of Japanese history in the "Kamakura Kaido" which passes through the NRIFD campus. The Kamakura Kaido is a tree-lined route along which the samurai of the Kanto and surrounding areas traveled to Kamakura, about 800 years ago.

8. Yamaguchi Water Reservoir

The Yamaguchi Reservoir is located in the Saitama prefecture, northwest of Tokyo and is operated by the Bureau of Waterworks, Tokyo Metropolitan Government. The Yamaguchi Reservoir and two smaller interconnected reservoirs, the Murayama-Kami and Murayama-Shimo Reservoirs, serve the population of metropolitan Tokyo. These reservoirs, along with the nearby Ogochi Reservoir, provide 17% of the water supplied to Tokyo. The Yamaguchi Reservoir took six years to build and was completed in 1934. It has an effective storage volume of approximately $19.5 \times 10^6 m^3$.

Following the Kobe earthquake, the earth fill dam was checked for stability using dynamic analysis. Calculations predicted that stability failure would not occur but that settlements in excess of 1.0m would occur. Due to the importance of the reservoir to Tokyo and the urbanization of the downstream side, officials made the decision to reinforce the dam.

Since there were few case histories of reinforcing earthen dams, a technical committee was formed to evaluate five possible countermeasures:

- Simple counterweight embankment
- Facing
- Artificial facing
- Simple counterweight fill + downstream inclined drain
- Simple counterweight fill + vertical drain

As a result of the study, the reinforcing method involving simple counterweight fill plus downstream inclined drain was determined to be the most appropriate. Dynamic analysis carried out to evaluate the seismic safety of the reinforced dam indicated that the target seismic performance would be satisfied.

The existing earth fill dam is approximately 34.6m high, 214.0m at its base and 690m long. It consists of three zones: an impervious core zone, random earth fill shell zone (both upstream and downstream), and downstream counterweight fill zone.

Field and laboratory investigations were carried out to select a suitable material for reinforcing the existing dam. Imokubu Formation was selected for its good engineering properties of compaction density and shear strength and for its availability.

Embankment reinforcing will begin in January of 2000 and will be completed in May of 2002. Two upstream cofferdams will provide sufficient water surface during construction to protect the plants and animals of the natural environment surrounding the reservoir.

9. Mega Float Structure

Mega Float is the name given to a project, begun in 1995, to establish the feasibility of building large floating structures suitable for such uses as airports, offshore distribution bases, or even cities. The project was undertaken because Japan is an island nation with limited land resources; the use of ocean space is an attractive alternative for large facilities. Ultra large floating structures have the advantages of easy expansion of existing facilities, easy relocation, no ocean depth limitations, and they are virtually earthquake proof.

Phase I of the Mega Float project, which was conducted from 1995 to 1998, was devoted to establishing the basic technology for constructing ultra large floating structures. Both the

pontoon and semi-submersible types of structure were studied with the pontoon type being favored. Individual units measuring 100m by 20m by 2m depth were fabricated and four such units were joined at sea in 1995. One year later an additional five units were added to form a floating structure 300m by 60m (18,000m^2). This prototype floating structure is moored in Yokosuka Harbor. During Phase I, research was conducted to establish methods of design and construction of the units, to investigate the offshore technology required for joining the units at sea, and to determine the impact of such structures on the environment.

In Phase II of the Mega Float Project, to be completed in the year 2000, a 1000m model will be constructed. This structure will then be used to study the feasibility of using a floating structure for an offshore airport facility serving small aircraft. Research will be conducted on mooring systems, confirmation of simulations of the behavior of a floating body, environmental assessment and actual take-off and landings.

10. Port and Harbor Research Institute

The Port and Harbor Research Institute (PHRI) is a major research facility of the Japan Ministry of Transportation. Located in Nagase, Yokosuka, PHRI has a total staff of about 200 of which 140 are researchers. The current year operating budget for the institute is about $20m US dollars. The Director General, Masaki Kobayashi, personally gave the overview briefing to our delegation. One of PHRI's important current projects is a study of the expansion of the Kansi Airport and the planning for a new offshore airport. The Director General also noted that PHRI is working with NOAA on coastal environment science and technology.

PHRI is organized into eight major research divisions as follows:

- Special Research Division
- Hydraulic Engineering Division
- Marine Environment Division
- Geotechnical Engineering Division
- Structural Engineering Division
- Planning and Design Standard Division
- Machinery Division
- Information Processing Division

PHRI will begin operating the world's largest underwater shake table this year. Final installation was underway during our visit. The shake table surface is 6m x 6m and has six degrees of movement. Designed to operate in water depths up to 1.5m the pool size is large enough to negate reflected wave effects during shake testing. It's size will allow 1/20 scale caisson testing for major off-shore protective structure projects planned for the future. An image of the shake table during the visit by the U.S. delegation is shown in Figure 4.

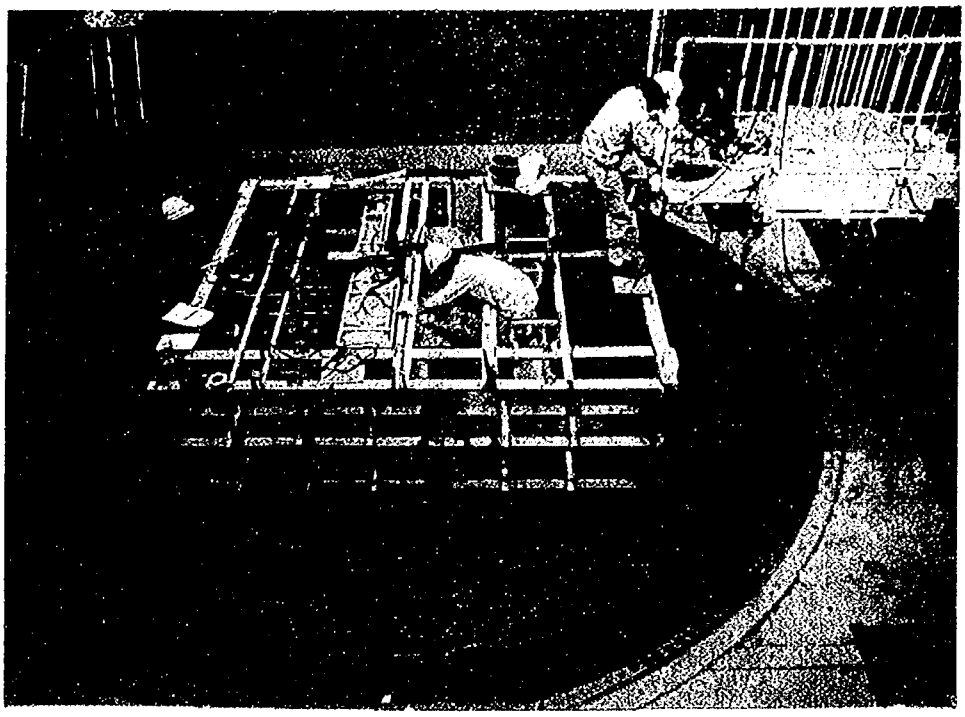


Figure 4 – Underwater Shake Table

Perhaps the most impressive research facility, was the large wave tank that was still under construction during our visit. When completed it will be 184m long, up to 12m deep in some sections, will hold 4m depth of sand, generate 3.5m (6-8 second period) maximum wave height, and introduce 2m/sec side currents. This will be by far the largest wave tank of its kind in the world. The cost of the project is about $15m US and has consumed the entire pooled research facility budget of the Ministry for 1998-99. Getting sufficient operating funding will now be a challenge for PHRI. An image taken inside the wave tank is shown at Figure 5.

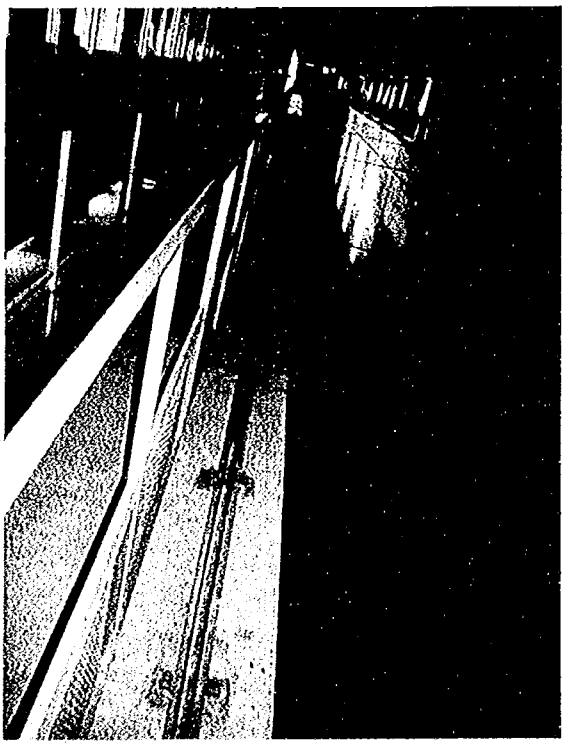


Figure 5 - PHRI Large Wave Tank

Another area of resent development at PHRI is the Navigation Simulator. Several demonstrations of channel navigation design application and tsunami wave inundation simulation were shown to the U.S. delegation. An image of the simulator is shown at Figure 6.

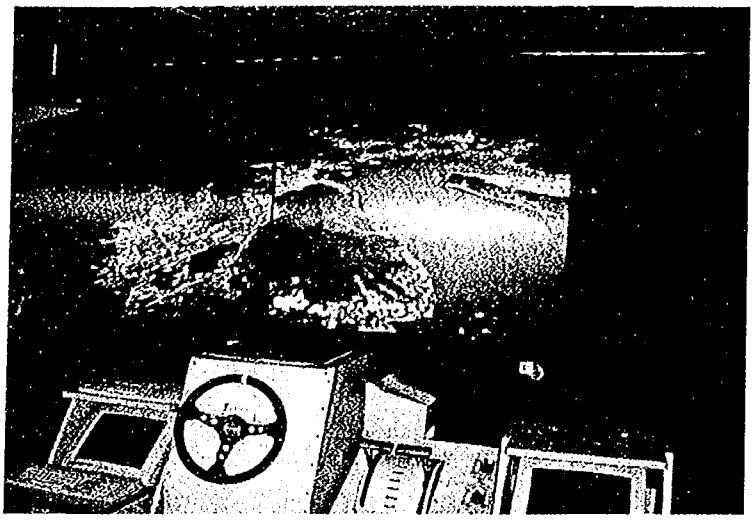


Figure 6 - Navigation Simulator

Other research facilities include a large geotechnical centrifuge which has an effective radius is 3.8m, a maximum payload of 2.71 tons and a maximum acceleration of 113g.